Neuroprotection by Hypoxic Preconditioning - The Role of HIF-1α

DISSERTATION
zur
Erlangung der naturwissenschaftlichen Doktorwürde
(Dr. sc. nat.)

vorgelegt der
Mathematisch-naturwissenschaftlichen Fakultät
der
Universität Zürich

von

Markus Thiersch
aus
Deutschland

Promotionskomitee

Prof. Dr. Stephan Neuhauss (Vorsitz)
Prof. Dr. Christian Grimm (Leitung der Dissertation)
Prof. Dr. Max Gassmann

Zürich, 2009

Blindness

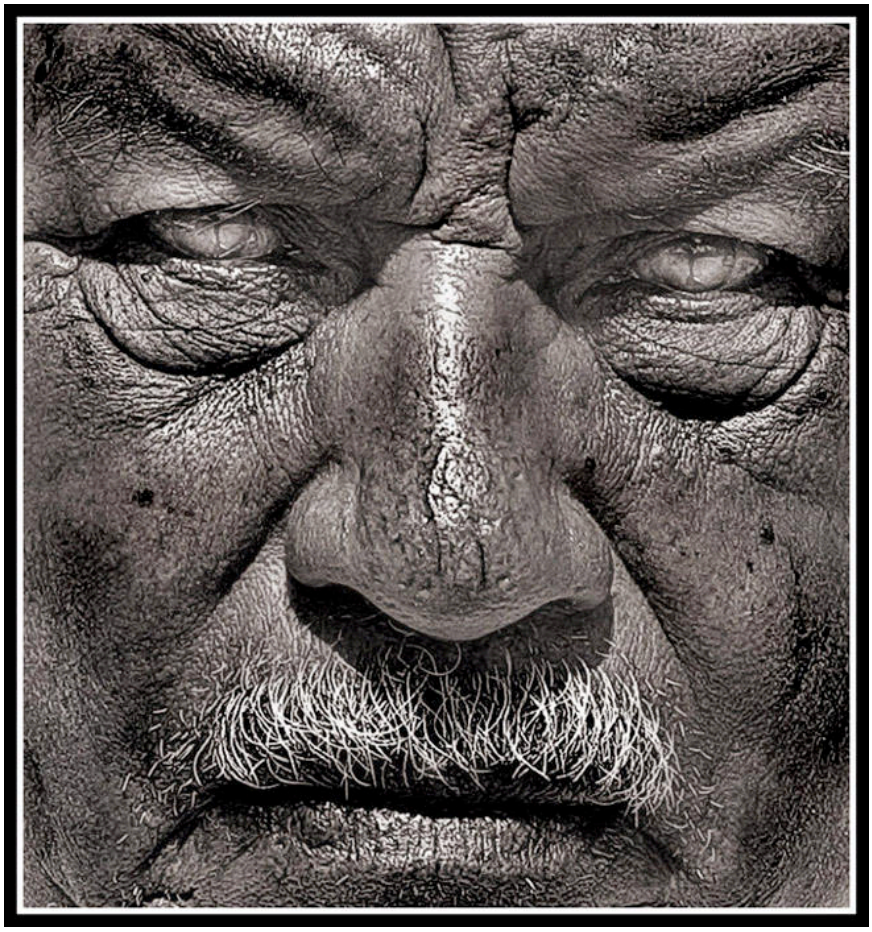

Darren Levant; *"Golden Blind Man"*; 2003; Playa de Carmen near Myan Rivera; Mexico

The World Health Organization (WHO) defines legal blindness as the lack of light perception or a visual acuity less that 3/60 measured by the "Snellen scale" [1].

[1] Snellen Scale consists of a number of rows of letters, which differ in size. The distance to the scale and the font size of recognized characters determine the value of visual acuity (scale-distance/letter-size e.g. 6/6 standard vision; 3/60 poor vision).

Dedication

Gewidmet meinen lieben Eltern Regina und Andreas,
sowie meiner lieben Schwester Stephanie: In Dankbarkeit
für Eure Liebe und Eure Unterstützung in dunklen Zeiten…

SUMMARY

Background:

Blinding diseases like retinitis pigmentosa (RP) or age-related macular degeneration (AMD) share a common feature – the loss of vision due to photoreceptor cell death. To mimic the pathogenesis of retinal degeneration, we employ a model of light-induced retinal degeneration, where photoreceptors undergo apoptosis after extensive exposure to white fluorescent light.

Among several neuroprotective strategies to inhibit or delay neuronal degeneration, hypoxic preconditioning has been shown to successfully prevent photoreceptor cell death. The molecular mechanisms, which are required for retinal cell survival, are largely unknown. However, hypoxia activates various transcription factors, which differentially regulate the expression level of potential neuroprotective genes. Among those transcription factors, hypoxia-inducible factor 1 (HIF-1) responds very specifically to low oxygen levels and alters the gene expression pattern during hypoxia. HIF-1 is a heterodimeric transcription factor, consisting of the constitutively expressed subunit HIF-1β and the oxygen dependent regulated subunit HIF-1α. Upon oxygen deprivation HIF-1α is stabilized, dimerizes with HIF-1β and regulates the expression of genes involved in different pathways like metabolism, angiogenesis or cell survival. Although studies show a correlation of HIF-1α induction and neuroprotection, the role of HIF-1α in retinal neuroprotection after hypoxic preconditioning remains unknown. Here, we analyzed the function of retinal HIF-1α stabilization during hypoxic preconditioning and its impact on neuroprotection in a model of light induced retinal degeneration. Additionally, we investigated the change of retinal gene expression pattern due to hypoxic preconditioning to identify possible neuroprotective target genes.

Results:

To analyze differential gene expression after hypoxic exposure, we isolated retinas of mice immediately, 2 hours, 4 hours and 16 hours after hypoxia and compared their retinal transcriptome to their corresponding normoxic controls by using micro-arrays. Upon hypoxia, we observed a rapid alteration in the retinal transcriptome, which was restored within 16 hours of reoxygenation. A strong induction of cyclin-dependent kinase inhibitor 1a, with a potential role in cell survival, was observed. We challenged hypoxic preconditioned p21 knock out mice with toxic levels of white light

and showed that p21 expression is not essential to protect the retina against light-induced retinal degeneration. Selective clustering of differentially regulated genes suggested additional potential neuroprotective candidate genes like metallothionein1/2, Cebpd or adrenomedullin.

Further, we used conditional HIF-1α knock out mice to elucidate the role of this transcription factor in retinal neuroprotection after hypoxia. The specific deletion of HIF-1α in photoreceptor cells led to a significant reduction of HIF-1α mRNA and protein levels. Accordingly, HIF-1 target gene expression after hypoxia was significantly diminished. Surprisingly, the strong neuroprotective effect of hypoxic preconditioning persisted in conditional knock out mice showing that HIF-1α is not required to protect photoreceptor cells in an autocrine fashion. Additionally, HIF-1α was not required to endure hypoxic preconditioning *per se*. Induction of HIF-2α and pSTAT3 in wild type and in knock out mice suggests that these factors might compensate for the lack of HIF-1α and confer photoreceptor resistance to light damage after hypoxic preconditioning. Furthermore, several potentially neuroprotective genes, detected during micro-array analyses of the hypoxic retinal transcriptome, were similarly induced in knock out and control mice after hypoxia.

Conclusion:

The mechanisms of retinal neuroprotection due to hypoxic preconditioning are largely unknown. The discovery of pathways, transcription factors or specific genes which are required to facilitate retinal neuroprotection should help to understand molecular changes in retinal pathology. Controlling the expression of identified neuroprotective genes or upstream transcription factors, which govern death or survival pathways, provides a possibility to precisely design prospective therapeutic approaches. This study presents an overview of genes, which are differentially regulated in the retina after hypoxia and suggests potential target genes for further investigation. Additionally, we analyzed the role of HIF-1α and it's involvement in retinal neuroprotection by hypoxic preconditioning. We showed that the photoreceptor cell-specific stabilization of HIF-1α during hypoxic preconditioning is not required to protect these cells against toxic light exposure. Therefore, we discuss the potential role of further transcription factors like HIF-2α and STAT3.

ZUSAMMENFASSUNG

Hintergrund:

Alters-abhängige Makula Degeneration (AMD) und Retinitis Pigmentosa (RP) sind Netzhauterkrankungen, die durch den Verlust von Photorezeptorzellen zu einer Beeinträchtigung des Sehvermögens bzw. zur vollständigen Blindheit führen. Um die pathologischen Veränderungen in der erkrankten Netzhaut zu simulieren, verwenden wir ein etabliertes Maus-Modell in dem der Zelltod von Photorezeptoren durch Licht induziert wird.

Neuroprotektion ist eine Strategie, um die Degeneration von Neuronen zu verzögern oder vollständig zu inhibieren. Dabei hat sich gezeigt, dass hypoxisches Präkonditionieren – also eine zeitlich begrenzte artifizielle Reduktion der Sauerstoff-verfügbarkeit – besonders erfolgreich ist. Die Mechanismen, die zu einer Schutzreaktion in der Netzhaut führen, sind jedoch weitgehend unbekannt. Allerdings weiss man, dass während der Hypoxie eine Reihe von Transkriptionsfaktoren aktiviert wird die potentielle neuroprotektive Gene differentiell regulieren. Ein solcher Transkriptionsfaktor ist hypoxic-inducible factor 1 (HIF-1), der sehr spezifisch durch einen geringen Sauerstoffgehalt aktiviert wird und die Expression mehrer Gene reguliert. HIF-1 ist ein Heterodimer, dass aus einer kontinuierlich exprimierten HIF-1β Untereinheit und einer Sauerstoff-abhängig regulierten HIF-1α Untereinheit besteht. Bei geringen Sauerstoffkonzentrationen wird die HIF-1α Untereinheit stabilisiert, dimerisiert mit HIF-1β und reguliert die Expression von Genen mit unterschiedlichen zell-biologischen Funktionen, wie z.B. Energiemetabolismus, Entwicklung von Blutgefässen oder die Induktion von Zellprotektion. Einige Studien haben Hinweise geliefert, dass HIF-1α die treibende Kraft der Netzhautprotektion nach hypoxischen Präkonditionieren sein könnte. Jedoch ist ein HIF-1α abhängiger Schutzmechanismus in der Netzhaut noch nicht vollständig bewiesen worden. Daher haben wir untersucht, ob eine Photorezeptor-spezifische Stabiliserung von HIF-1α während der Hypoxie benötigt wird, um die Netzhaut vor einer Licht-induzierten Degeneration zu schützen. Ausserdem, haben wir mit Hilfe von Micro-arrays die globale Genexpression in der Netzhaut nach hypoxischen Präkonditionieren untersucht, um mögliche neuroprotektive Kandidatengene zu indentifizieren.

Ergebnisse:

Um die globale Genexpression in der Netzhaut nach hypoxischen Präkonditionieren zu analysieren, haben wir Mäuse einer reduzierten Sauerstoffkonzentration ausgesetzt. Anschliessend haben wir Netzhäute direkt oder 2 Stunden, 4 Stunden und 16 Stunden nach Hypoxie isoliert und die Genexpression mit unbehandelten Kontrolltieren verglichen. Dabei haben wir festgestellt, dass es während der Hypoxie zu einer starken Veränderung der Genexpression in der Netzhaut kommt, die sich jedoch innerhalb von 16 Stunden wieder normalisiert. Die Genexpression von Cyclin-dependent kinase inhibitor 1a (p21), welcher möglicherweise protektive Eigenschaften besitzt, war direkt nach der Hypoxie stark induziert. Um zu überprüfen ob p21 tatsächlich eine Rolle bei der Netzhautprotektion spielen könnte, haben wir hypoxisch präkonditionierte p21 “knock out” Mäuse gegen Licht exponiert. Dabei haben wir festgestellt, dass der Hypoxie-induzierte Schutz der Netzhaut unabhängig von einer p21 Expression funktionieren kann. Durch die funktionelle Gruppierung von differentiell regulierten Genen konnten wir weitere mögliche Kandidaten wie Metallothionein 1/2, Cebpd oder Adrenomedullin identifizieren.

Um festzustellen, ob HIF-1α tatsächlich essentiell für die Protektion der Netzhaut ist, haben wir Mäuse mit einem Photorezeptor-spezifischen HIF-1α knock out analysiert. Funktionell führte das sowohl zu einer reduzierten HIF-1α Genexpression in der Retina als auch zu einer reduzierten Proteinakkumulation der HIF-1α Untereinheit unter hypoxischen Bedingungen. Dementsprechend waren nach der Hypoxie auch Gene, die durch HIF-1 reguliert werden, weniger stark induziert. Nachdem wir hypoxisch präkonditionierte HIF-1α knock out Mäuse mit hohen Lichtintensitäten gestresst haben, zeigte sich, dass eine HIF-1α Stabilisierung in Photorezeptoren nicht zwingend notwendig ist, um eine Neuroprotektion zu gewährleisten. Ausserdem war eine Photorezeptor-spezifische HIF-1α Expression nicht erforderlich, um die Netzhaut vor transienter Hypoxie *per se* zu schützen. Die Induktion von HIF-2α und pSTAT3 in knock out und Kontrollmäusen könnte ein Hinweis darauf sein, dass diese Faktoren den Verlust von HIF-1α kompensieren können und somit die Netzhaut weiterhin gegen Lichtschaden schützen. Zusätzlich haben wir beobachtet, dass potentiell neuroprotektive Gene in HIF-1α knock out Mäusen und in Kontrollmäusen vergleichbar exprimiert wurden.

Signifikanz:

Die grundlegeneden Mechanismen, welche die Netzhaut durch hypoxisches Präkonditionieren schützen, sind nicht komplett aufgeklärt. Die Identifizerung von Signalwegen, von Transkriptionsfaktoren oder von spezifischen Genen, die für einen

Schutz der Netzhaut essentiell sind, könnte ebenfalls Aufschluss über grundlegende pathologische Veränderungen in Modellen für Netzhauterkrankungen geben. Die Kontrolle der Expression von identifizierten Genen bzw. die Kontrolle von Transkriptionsfaktoren mit nachgewiesenen Schutzeigenschaften bietet die Möglichkeit einer therapeutischen Strategie, um Netzhauterkrankung einzuschränken oder zu verhindern. In unserer Studie geben wir einerseits einen generellen Überblick über Gene die durch hypoxisches Präkonditionieren differentiell reguliert werden und haben andererseits spezifische Kandidaten-Gene mit potentiell neuroprotektiven Eigenschaften identifiziert. Nachdem wir mit p21 bereits einen ersten Kandidaten selbst analysiert haben, stellt diese Studie weitere Proteine oder Gene zur detaillierten Analyse zur Verfügung. Weiterhin haben wir gezeigt, dass eine Photorezeptor-spezifische Expression von HIF-1α nicht zwingend notwendig ist, um Photorezeptoren gegen toxische Lichtintensitäten zuschützen. In diesem Zusammenhang diskutieren wir die mögliche Beteiligung von anderen Transkriptionsfaktoren wie HIF-2α und pSTAT3.

CONTENTS

SUMMARY **1**

ZUSAMMENFASSUNG **3**

CONTENTS **6**

1 INTRODUCTION **9**

1.1 THE RETINA 9

1.1.1 Architecture of the Retina *9*

1.1.2 Photoreceptor cells *11*

1.1.3 Phototransduction *12*

1.1.4 The Retina as a Part of the Visual Pathway *13*

1.2 RETINAL DISEASES 15

1.2.1 Age-Related Macular Degeneration *16*

1.2.2 Retinitis Pigmentosa (RP) *17*

1.3 MODELS FOR RETINAL DEGENERATION 18

1.3.1 Model for Inherited Retinal Degeneration *19*

1.3.2 Light Exposure – A Model For Induced Retinal Degeneration *20*

1.4 NEUROPROTECTION AND MECHANISMS OF HYPOXIC PRECONDITIONING 21

1.4.1 Retinal Neuroprotection *22*

1.4.2 Hypoxic Preconditioning *22*

1.4.3 Epo Partially Protects the Retina *24*

1.5 THE HIF SYSTEM – MASTER REGULATOR OF HYPOXIA 24

1.5.1 Oxygen-Dependent Regulation of HIF-1α *25*

1.5.2 Oxygen-Independent Regulation of HIF-1α *27*

1.5.3 HIF-1α Regulates Cell Death and Survival *27*

2 AIMS OF THE THESIS **29**

3 RESULTS **31**

3.1 ANALYSIS OF THE RETINAL GENE EXPRESSION PROFILE AFTER HYPOXIC PRECONDITIONING IDENTIFIES CANDIDATE GENES FOR NEUROPROTECTION 31

3.1.1 Supplemental Data for Thiersch et al., 2008, BMC Genomics *46*

3.1.1.1 Quality Control Analyses (Additional File 1) *46*

3.1.1.2 Lists of Differentially Regulated Genes (Additional File 2) *57*

3.1.1.3 Total List of Real-time PCR Results (Additional File 3) *75*

3.1.1.4 List of Genes Functionally Clustered by DAVID (Additional File 4) *76*

3.1.1.5 Hypoxic Preconditioning Gene Networks Discovered by Ingenuity Pathway Analysis (Additional File 5) *100*

3.1.1.6 Primer Sequences and Product Sizes (Additional File 6) *102*

3.2 RETINAL NEUROPROTECTION BY HYPOXIC PRECONDITIONING IS INDEPENDENT OF HIF-1α EXPRESSION IN PHOTORECEPTORS 103

3.2.1 Supplemental Data for accepted manuscript Thiersch et. al (EJN) *138*

3.2.1.1 Supporting information MTF-1 ..... *138*

4 GENERAL DISCUSSION 140

4.1 RETINAL GENE EXPRESSION AFTER HYPOXIC PRECONDITIONING 141

4.1.1 Limitation of the Analysis *141*

4.1.2 Hypoxic and Ischemic Preconditioning *143*

4.1.3 Cell Cycle Inhibitor Cdkn1a (p21) is not Essential for Neuroprotection *144*

4.1.4 Additional Potential Neuroprotective Candidate Genes *146*

4.1.4.1 Cebpd *146*

4.1.4.2 Metallothioneins *146*

4.1.4.3 Vegf *147*

4.1.4.4 Adrenomedullin *148*

4.1.4.5 Paraoxonase *148*

4.1.4.6 Bcl2-like 10 ..... *149*

4.1.4.7 Kif4 ..... *149*

4.1.4.8 Mef2c and Rbm family members *150*

4.2 THE ROLE OF HIF-1α 150

4.2.1 Physiological Role of HIF-1α in the Retina *151*

4.2.2 HIF-1α and Hypoxia *152*

4.2.3 HIF-1α and Retinal Neuroprotection *153*

4.2.4 Possible Alternative Mechanisms for Hypoxia-induced Retinal Neuroprotection *154*

4.3 CONCLUSION 155

5 APPENDIX 158

5.1 UNPUBLISHED DATA 158

5.1.1 Hypoxic Preconditioning Protects Timp3$^{-/-}$ Mice Against Light-induced Retinal Degeneration *158*

5.1.2 Differential Expression of Vegf Isoforms in the Retina After Hypoxia *159*

5.1.3 Expression of Paraoxonase Family Genes in Retina and Eyecup *160*

5.2 REFERENCES FOR INTRODUCTION AND DISCUSSION 161

5.3 LIST OF ABBREVIATIONS 176

6 ADDITIONAL PUBLICATIONS 179

6.1 DIFFERENTIAL ROLE OF JAK-STAT SIGNALING IN RETINAL DEGENERATIONS 179

6.1.1 Author contribution *179*

6.1.2 Summary *179*

6.1.3 Manuscript *180*

6.2 CASPASE-1 ABLATION PROTECTS PHOTORECEPTORS IN A MODEL OF AUTOSOMAL DOMINANT RETINITIS PIGMENTOSA 196
6.2.1 Author contribution 196
6.2.2 Summary 196
6.2.3 Manuscript 198
6.3 THE HYPOXIC TRANSCRIPTOME OF THE RETINA: IDENTIFICATION OF FACTORS WITH POTENTIAL NEUROPROTECTIVE ACTIVITY. 209
6.3.1 Author contribution 209
6.3.2 Summary 209
6.3.3 Manuscript 210
6.4 R91W MUTATION IN RPE65 LEADS TO MILDER EARLY-ONSET RETINAL DYSTROPHY DUE TO THE GENERATION OF LOW LEVELS OF 11-CIS-RETINAL 221
6.4.1 Author contribution 221
6.4.2 Summary 221
6.4.3 Manuscript 222
6.5 LEUKEMIA INHIBITORY FACTOR EXTENDS THE LIFESPAN OF INJURED PHOTORECEPTORS *IN VIVO* 235
6.5.1 Author contribution 235
6.5.2 Summary 235
6.5.3 Manuscript 236
6.6 NONESSENTIAL ROLE OF *B*3 AND *B*5 INTEGRIN SUBUNITS FOR EFFICIENT CLEARANCE OF CELLULAR DEBRIS AFTER LIGHT-INDUCED PHOTORECEPTOR DEGENERATION. 247
6.6.1 Author contribution 247
6.6.2 Summary 247
6.6.3 Manuscript 248
6.7 IN CONDITIONS OF LIMITED CHROMOPHORE SUPPLY RODS ENTRAP 11-*CIS*-RETINAL LEADING TO LOSS OF CONE FUNCTION AND CELL DEATH 259
6.7.1 Author contribution 259
6.7.2 Summary 259
6.7.3 Manuscript 261

7 CURRICULUM VITAE 272

8 ACKNOWLEDGMENT 276

1 INTRODUCTION

1.1 The Retina

1.1.1 Architecture of the Retina

The retina is a heterogeneous neuronal tissue, which lines the inside of the eyeball (Fig.1.A) and consists of the outer nuclear layer (ONL), the inner nuclear layer (INL) and the ganglion cell layer (GCL). The outer and the inner plexiform layers (OPL and IPL), where neurons form synaptic connections, separate the three nuclear layers. Together with the retinal pigment epithelium (PE), which is a non-neuronal single cell layer covering the top of the photoreceptor cells, the retina forms a morphological and functional unit to absorb light and to transform it into an electrical signal [1, 2]. To receive, process and transmit the light-mediated stimulus, different types of cells populate the typical mammalian retina and work closely together (Fig.1B left panel). Photon absorbing photoreceptor cells are located in the ONL – opposite to the retinal surface where the light invades. That means that the light has to penetrate the whole retina to stimulate phototransduction. Photoreceptors connect to bipolar cells, which are located in the INL and transmit the signal vertically to ganglion cells. In addition, horizontal cells and amacrine cells in the INL interact morphologically and functionally with this network to fine-tune the ganglion cell signal [1, 2]. Müller glia cells span the retina radially from the inner limiting membrane close to the GCL to the outer limiting membrane near the ONL. They are essential for the maintenance of the retinal structure and the removal glutamate [3-5] – a neurotransmitter, which causes neuro-toxicity at high concentrations [6-8]. Ganglion cell axons bundle to form the optic nerve, which exits at the centre of the retina to transmit the electro-chemical information to the brain. Because this area is free of photoreceptor cells, it is named “blind spot”. Nutrition and oxygen are provided via two circulatory blood systems. The inner retina is supplied via the central retinal artery, which invades the retina via the blind spot. The retinal blood vessel system consists of three layers – the primary (superficial) vessel plexus at the inner retinal surface, which is connected to two parallel secondary capillary networks: the inner deeper plexus in the IPL and the outer deeper plexus in the OPL (Fig.1.B right panel). Photoreceptor cells are supplied by the choroidal blood system,

which arises from the long and short posterior arteries and lies between retina and sclera [9].

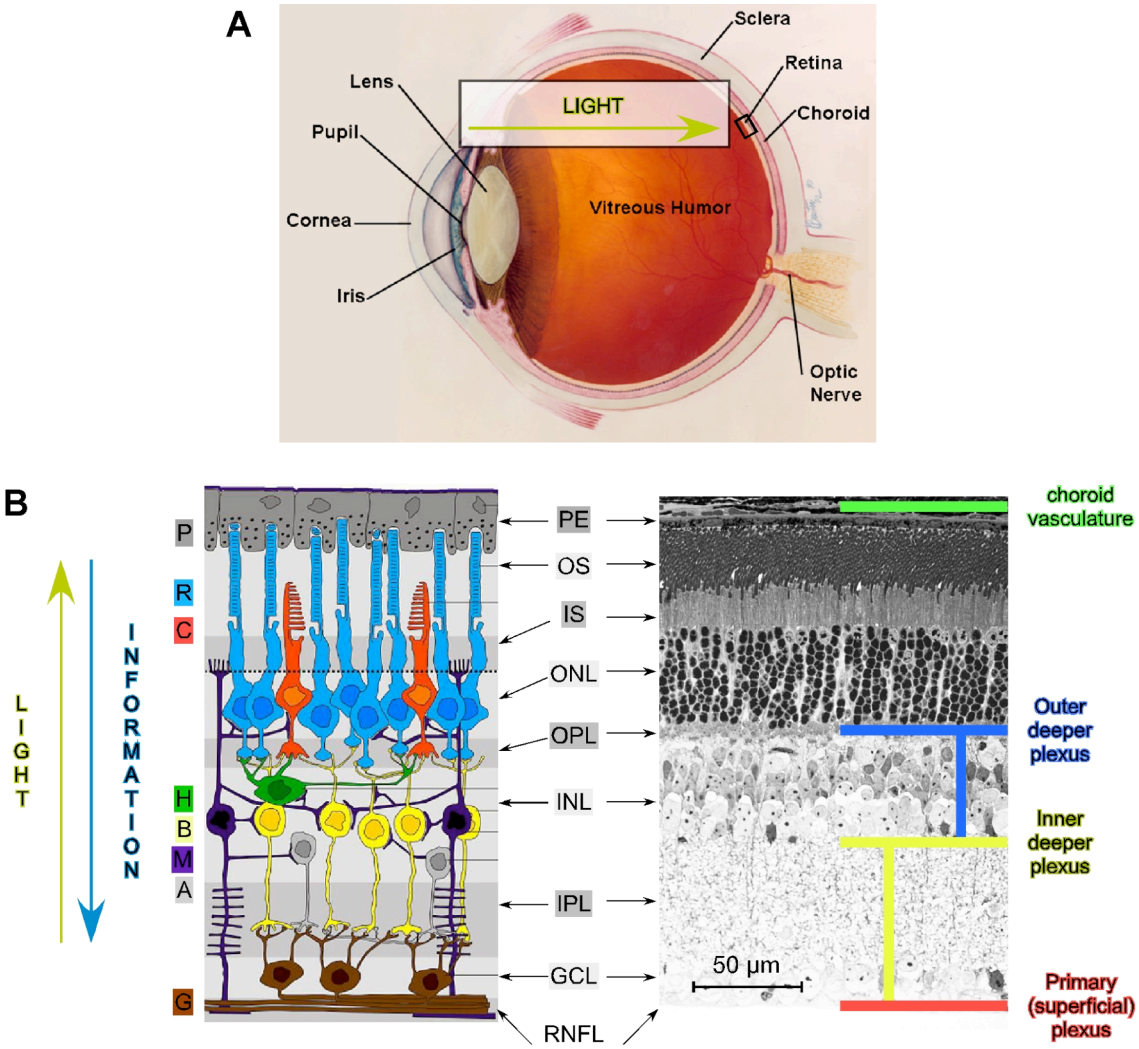

Fig.1 The Retina – the Neural Layer of the Eye. A Schematic structure of the mammalian eye. Sclera and Cornea form the external layer of the eye providing shape and stability. The choroid provides nutrition to the retina. To adapt to different light intensities, the iris forms the pupil and determines the light incidence by contracting and relaxing. The retina is a neuronal tissue, which forms the internal layer of the eye. The eye is filled with the vitreous humor, the lens is required for accommodation to obtain sharp images on the retina and the optic nerve transmits the information from the retina to the brain. **B** Schematic (left panel) and real (right panel) structure of the retina, which consist of three nuclear layers: The outer nuclear layer (ONL) contains rod (R) and cone (C) photoreceptors, which possess inner segments (IS) for energy supply and outer segments (OS) for the photon reception. The tips of the OS are engulfed by pigment epithelium cells (PE), which remove photoreceptor debris. The inner nuclear layer (INL) contains several cell types: horizontal cells (H), bipolar cells (B) and amacrine cells (A) are required for signal transmission from photoreceptors to ganglion cells (G) in the ganglion cell layer (GCL). Müller cells (M) are essential to maintain the retinal integrity. ONL, INL and GCL are separated by the inner (IPL) and outer plexiform layer (OPL) in which synaptic cell-cell contacts are established. The retinal nerve fiber layer (RNFL) bundles ganglion cell axons and transmits information to the optic nerve. The retina is

supplied by two separate blood vessel systems (right panel). Photoreceptor cells receive nutrition and oxygen via the choroidal vasculature (green); the inner retina is supplied by a branched vessel network, which consists of the superficial (red) as well as the inner (yellow) and outer (blue) deeper plexus.
Figure was adapted from http://www.meei.harvard.edu/patient/images/eye.jpg and http://de.wikipedia.org/w/index.php?title=Datei:Retina.jpg&filetimestamp=20080814113451.

1.1.2 Photoreceptor cells

Photoreceptor cells are primary sensory neurons, which absorb light and convert it into an electro-chemical signal. Two distinct types of photoreceptors, differing in size, shape and function are known – rods and cones. Rods are required for dim light vision and are more numerous than cones, which in turn are essential for color and high acuity vision. Mice have a mosaic-like distribution of rods and cones in the entire retina. In contrast, primates have a specialized region within the retina – the macula, an area where cones outnumber rods [10]. The area with the largest concentration of cones near the center of the macula is called fovea and it is required for high acuity vision in bright light conditions.

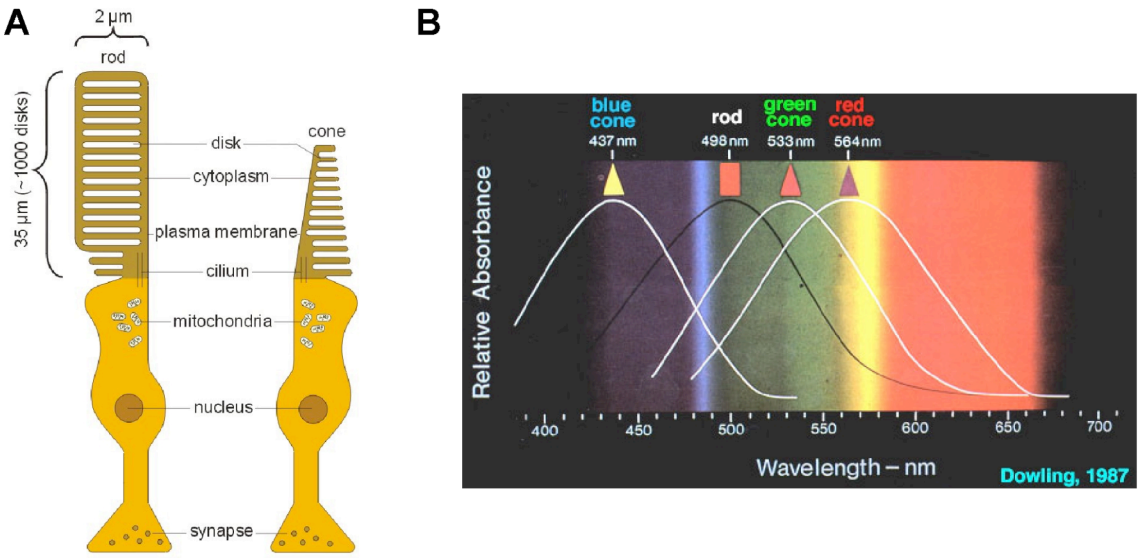

Fig.2 Structural and Functional Features of Photoreceptors. A Schematic views of typical rod and cone photoreceptor morphology. Both types contain outer segments, which are composed of disc membrane like structures. The (connecting) cilium connects the outer segments to the inner segments, which contain mitochondria and synthesize new proteins. The nucleus forms the shape of the cell body and synapses connect to downstream cells. **B** Absorption spectrum of rods and cones. Rods have a maximal absorbance of light at 498 nm. The spectrum of green (533 nm) and red cones (564 nm) is shifted to higher wavelength, whereas blue cones absorb energy-rich light around 437 nm.
Figure was adapted from http://www.fz-juelich.de/inb/inb-1/datapool/page/24/Figure2.jpg and http://webvision.med.utah.edu/imageswv/spectra.jpeg

Morphologically, photoreceptors consist of the synaptic ending, the cell body yielding the nucleus and the inner and outer segments (IS & OS) (Fig.2.A). Mitochondria are located in the IS and guarantee an adequate energy supply for the photoreceptors. Outer segments, which are responsible for the photon uptake, contain disc like double-membrane structures. Embedded within these membrane structures are the visual pigments. The visual pigments are complexes containing the G-protein coupled receptor opsin and the covalently bound vitamin A derivative 11-*cis*-retinal. Opsin molecules integrate into the disc like membranes via their seven membrane spanning helices [11]. The difference of absorption maxima between rods and cones depends on the type of opsin molecule. In rods, opsin and 11-*cis*-retinal form rhodopsin, which has an absorption maximum at 496 nm [12]. Cones express different opsin molecules, which shift the absorption maximum to higher wavelength (green cone, 533 nm) or lower wavelength (blue cone, 437 nm) (Fig.2.B). In contrast to most mammalians, which have blue and green cones, primates possess in addition also red cones (564 nm).

1.1.3 Phototransduction

The first step to convert the light input into a neuronal response in the brain is the phototransduction (Fig.3), which takes place in photoreceptor cells [11]. Unexcited photoreceptors are depolarized due to open cGMP gated sodium channels and a constant influx of sodium and calcium. This causes constant release of the excitatory neurotransmitter glutamate, which stimulates or inhibits different types of downstream bipolar cells.

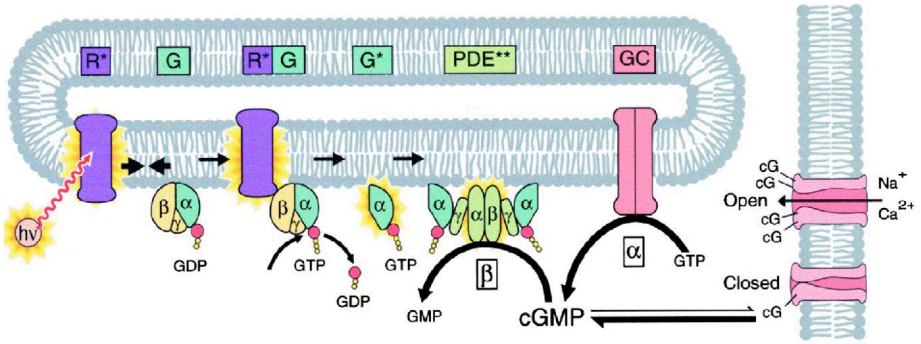

Fig.3 Phototransduction Cascade. Shown is the principle of phototransduction after light reception. When a photon hits rhodopsin (R*) a signalling cascade is activated beginning with GTP mediated activation of the transducin (G) α-subunit. The activated subunit (G*) binds to the γ-subunits phosphodiesterase (PDE**). That causes an activation of the PDE α- and β-subunit and triggers the processing of cGMP to GMP, which finally causes the closure of cGMP-gated cation-channels and thereby the hyperpolarization of the photoreceptor cell. cGMP is restored by the Guanylyl cyclase (GC).

Figure: Leskov et al., 2000 Neuron

Upon light stimulation, 11-*cis* isomerizes into all-*trans*-retinal und thereby induces conformational changes in the rhodopsin structure. Activated rhodopsin (metarhodopsin II) mediates the rapid replacement of GDP by GTP on the α–subunit of transducin, which is a heterotrimeric G-protein. The released GTP-bound α–subunit binds the γ-subunit of a heterotrimeric phosphodiesterase (PDE), which activates its two catalytic α- and β-subunits. The activated PDE induces the cleavage of cGMP to GMP. Thus, cGMP gated sodium channels are closed resulting in a continuing closure of voltage-gated channels. This leads to the hyperpolarization of the cell and the drop of calcium ions stopping the release of glutamate and reversing inhibition or stimulation of bipolar cells [13, 14].

1.1.4 The Retina as a Part of the Visual Pathway

Besides light reception, the retina is required for initial processing of the light-induced flow of information. In general, photoreceptor cells signal to bipolar cells, which transmit the information vertically to ganglion cells. Eventually, the information bundles in the optic nerve and is transmitted to the visual cortex in the brain [11]. The vision in vertebrates depends on the perception of contrasts between images and background. Therefore, two major types of bipolar cells (ON and OFF) respond differently to the glutamate release of cone photoreceptors (Fig.4.A). In order to detect dark images on a light background, bipolar cells having ionotropic glutamate receptors, depolarize and activate the OFF-pathway. In contrast, the ON-pathway is regulated by bipolar cells, which harbor inhibitory metabotropic glutamate receptors and are inactive when glutamate is released from photoreceptors. These cells are required for the recognition of light pattern on dark background. To tune the information, additional cell types are required. Horizontal cells are functional modulators signaling horizontally in the INL to enhance the contrast between ON- and OFF-pathways in a so-called centre surround organization. That means horizontal cells add an opposite signal, surrounding a certain bipolar cell signal, by inhibiting all neighboring bipolar cells. In contrast to cones, only one type of bipolar cell connects to rods, solely transmitting ON-signals. However, unlike cone bipolar cells, rod bipolar cells have no direct connections to ganglion cells but employ amacrine cells to mediate the information (Fig.4.B). Two specialized subtypes of amacrine cells, AII and A17, are required to transmit a signal from rod bipolar cells to ganglion cells. AII amacrine cells signal either directly to ON- and OFF-ganglion cells or they use ON- and OFF-bipolar cells of cones as a relay to signal to ganglion cells. A17 amacrine cells modulate and amplify the AII signals.

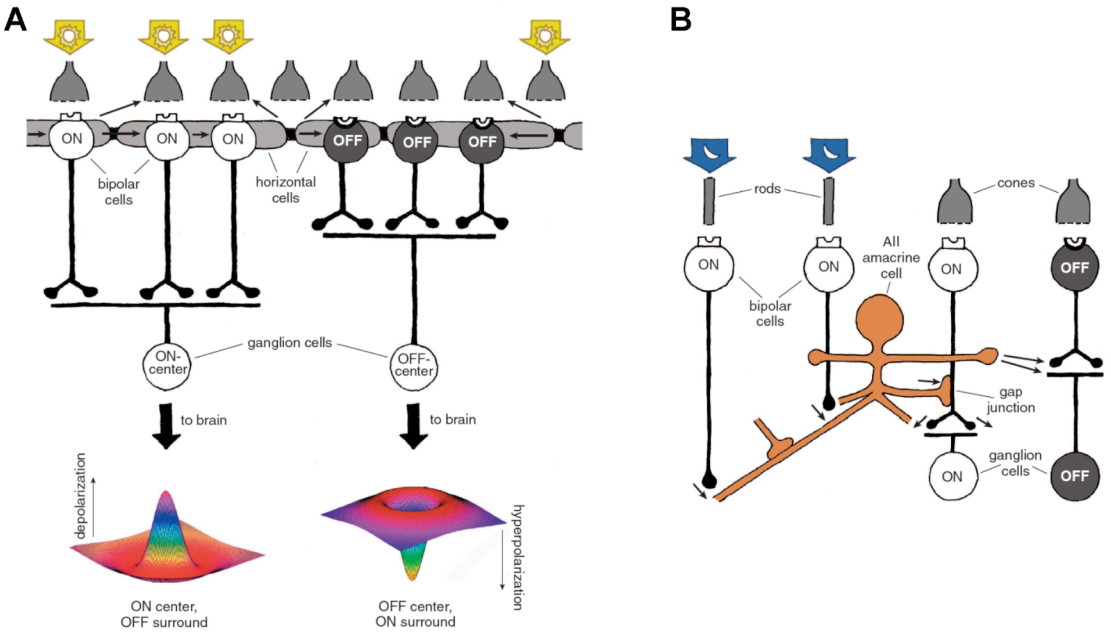

Fig.4 Signaltransmission in the Retina. A Light stimulates cone photoreceptor cells, which are connected to ON- or OFF-bipolar cells. Bipolar cells transmit the signal to ON-centre and to OFF-centre ganglion cells. ON- and OFF-ganglion cells have receptive fields. That means that ON-ganglion cells are activated when light falls into the centre of the receptive field and OFF-ganglion cells are activated, when light falls in the periphery of the receptive filed, leaving their centre dark. To generate a centre-surround like receptive field, horizontal cells generate an antagonistic surround signal to bipolar cells and thereby to ganglion cells. The receptive field of ganglion cells has a “Sombrero-like” structure integrating opposing signals about centre and surround, which helps to sharpen the image boundaries. **B** Rod photoreceptor cells are only connected to ON-bipolar cells and employ AII amacrine cells to mediate the signal to ganglion cells. Thereby, amacrine cells collect the signal from many rods and transmit the information either directly to ON- or OFF-ganglion cells, or they employ the cone-bipolar cells.
Figures: Helga Kolb, 2003 American Scientist

All information leaves the retina via the optic nerve to reach the visual cortex [1, 2] (Fig.5). Visual fibers of both eyes pass the optic chiasm, which is located close to the thalamus and hypothalamus. There, fibers of the nasal half of each retina cross to the contralateral (opposite side) hemisphere of the brain. In contrast, fibers of temporal half of both retinas remain in the ipsilateral (the same side) hemisphere of the brain. Optic fibers form the optic tract, which leads to the lateral geniculate nucleus (LGN). Both hemispheres of the brain contain a LGN, which is located inside the thalamus and acts as the primary processing center for visual information. Typically, the LGN consists of six cell-layers containing different types of cells (magnocellular, parvocellular and koniocellular cells) and receives input from both eyes. Therefore the information is divided alternating among the layers. The LGN signals information to the visual cortex (striate cortex) along fibers of the geniculo-calcarine tract. The primary

visual cortex (V1) consists of six functionally distinct layers, is located in the occipital lobe of the brain and transmits information from the LGN to two separate streams. The dorsal stream goes from V1 to areas called V2 and V5 to the posterior parietal cortex, which integrates sensory and motor portions of the brain. The ventral stream begins with V1 and goes through V2 and V4 to the inferior temporal cortex, which is involved in object feature recognition [11].

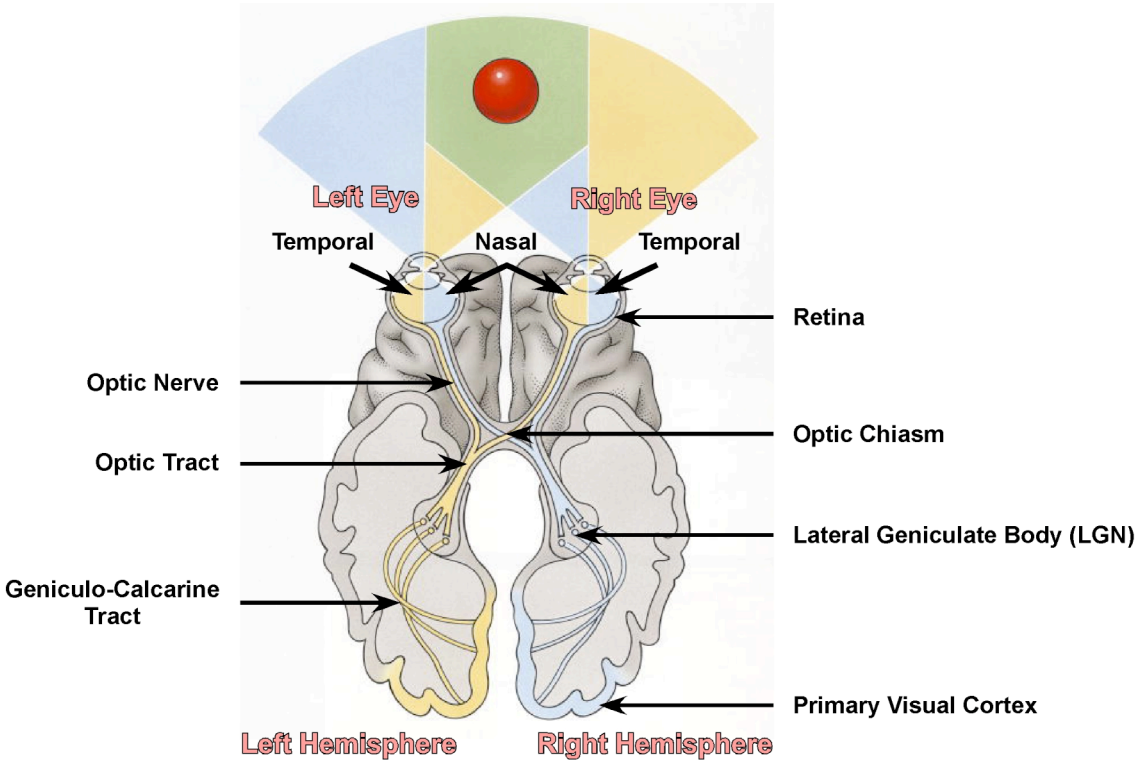

Fig.5 The Visual Pathway. Shown is the visual pathway, which starts in the retina of the eye. After initial signal integration, the information leaves the eye via the optic nerve. In the optic chiasm the optic fibres from the nasal part of the retina cross to the contralateral hemisphere (yellow fibres of the right eye cross to the left hemisphere and blue fibres of the left eye cross to the right hemisphere), whereas optic fibres from the temporal part of the retina are directed to the ipsilateral hemisphere. Nerve fibres are directed along the optic tract to the lateral geniculate body (LGN) and further to the primary visual cortex via the geniculo-calcarine tract.
Figure was adapted from http://pal.pearson.com/teams/PALSearch.do.

1.2 Retinal Diseases

The four most prevalent eye diseases in Europe and North America, which lead to legal blindness, are age-related macular degeneration (AMD), cataract, glaucoma and diabetic retinopathy [15]. Except for cataracts, all diseases severely impair vision or cause blindness by affecting the retina, indicating that retinal degeneration is one of

the major reasons for blindness in human patients. Among the group of retinal diseases, AMD and retinitis pigmentosa (RP) are mainly responsible for the loss of vision by photoreceptor cell death.

1.2.1 Age-Related Macular Degeneration

AMD is a disease usually occurring in patients with the age of over 50 years and impairs or abolishes central vision. During aging, auto fluorescent lipofuscin, which is composed of lipids and proteins from photoreceptor debris, progressively accumulates in PE cells. The pyridinium bis-retinoid A2E is a highly cytotoxic component of lipofuscin and a potent photo-inducible generator of reactive oxygen species (ROS). Additionally, deposits of acellular, polymorphous debris accumulate between PE and Bruch's membrane in healthy subjects to form so-called drusen [11].

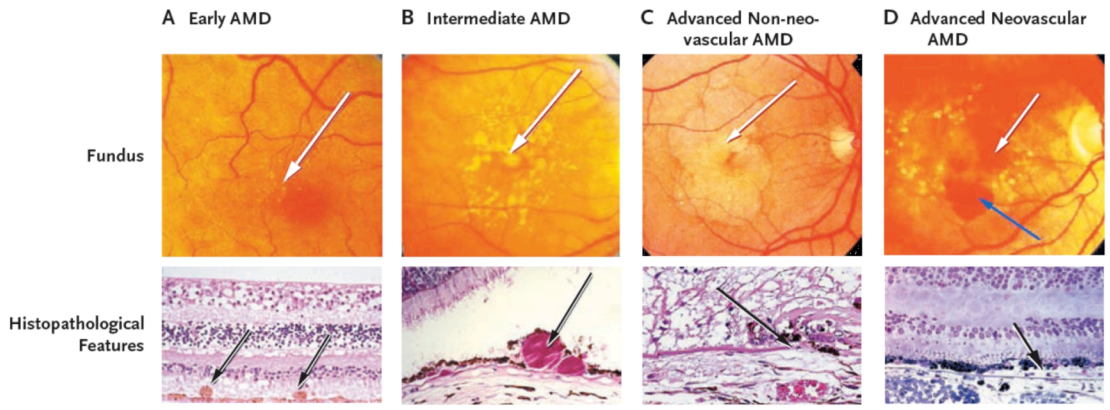

Fig.6 Different Stages of AMD. Shown are different clinical stages of AMD. During early AMD (panel A) small and medium-sized drusen are found by fundus photography and histological analyzes (white and black arrows). During intermediate AMD (panel B) large drusen are present (black arrow), which appear as enlarged yellowish dots in the fundus (white arrow). During this phase geographic atrophy starts but does not extend to the macula centre. The late phase of AMD can be distinguished between dry (non-neovascular) AMD and wet (neovascular) AMD. Dry AMD (panel C) is characterized by geographic atrophy (white arrow) of the macula centre and the loss of Bruch's membrane (black arrow). In wet AMD (panel D) abnormal neovascularization of leaky vessels (white and black arrow) causes haemorrhages (blue arrow).

Figure: Jager et al., 2008 New England Journal of Medicine

The first clinical hallmark of AMD is the abnormal increase of drusen-formation, which can damage the PE (Fig.6). In combination with a chronic aberrant inflammation, this can lead to a geographic atrophy of the retina. Most of the patients develop the atrophic (dry) form of AMD. However, 10 to 15% of AMD patients develop an exudative (wet) form of AMD, featured by abnormal retinal neovascularization. Although wet AMD

is less frequent, it is responsible for 80% of all cases of severe visual impairment and blindness among AMD patients [16]. Wet AMD is accompanied by increased vascular permeability and fragility and can lead to subretinal hemorrhage, fluid exudation, lipid deposition, detachment of the retinal pigment epithelium from the choroid, fibrotic scars or a combination of these findings [16]. Due to hemorrhage, wet AMD can lead to a rapid loss of vision, whereas dry AMD leads to a gradual loss of vision over a time period from month to years. Besides age, several other risk factors like smoking [17-19], ethnical background [20] or obesity [21] are known to accelerate AMD development. Genetically, polymorphisms in factor H [22-25] and in factor B [26] of the complement system are associated with AMD development. Further, a polymorphism in the promoter of HTRA1, a gene encoding a secreted serine protease, increases the risk for AMD development [27, 28]. To reduce the symptoms and the disease progression, several strategies are currently employed. An appropriate nutrition with a low fat diet and antioxidant supplementation may delay the transition into advanced AMD pathology [16]. The intravitreal injection of antiangiogenic components, like antibody fragments raised against human vascular endothelial growth factor (Vegf), is a successful strategy to attenuate progression of neovascularization in wet AMD [29]. Aside from the symptomatic therapy, a cure from the disease is not possible yet.

1.2.2 Retinitis Pigmentosa (RP)

Retinitis pigmentosa (RP), terms a set of hereditary diseases, which are caused by genetic mutations and which are featured by retinal degeneration due to photoreceptor cell death [30, 31]. Statistically, 1 in 4000 humans suffer from RP, which numbers the total affected humans to more than 1.5 million worldwide. RP can be inherited in an autosomal-dominant, an autosomal recessive or in a X-linked manner. 20 – 30% of all patients suffer from associated, non-ocular diseases, which are described by more than 30 different syndromes. The two major forms are Usher and Bardet-Biedl syndrome [30]. In Usher syndrome, a cochlea disease resulting in hearing defects or deafness can accompany RP. In the Bardet-Biedl syndrome, RP can be associated with renal diseases, obesity, polydactyly etc. RP is a variably developing disorder, which can lead to loss of vision between childhood/birth and mid-adulthood. The classical pattern is characterized by an early night blindness during adolescence and the loss of peripheral vision in young adulthood. Typically, intraretinal pigmentation appears in the fundus due to the migration of PE cells into the neural retina (Fig.7). The degeneration starts in the periphery of the retina. As the disease advances, patients

suffer from tunnel vision and eventually from legal blindness – typically in the second decade of life [30, 31].

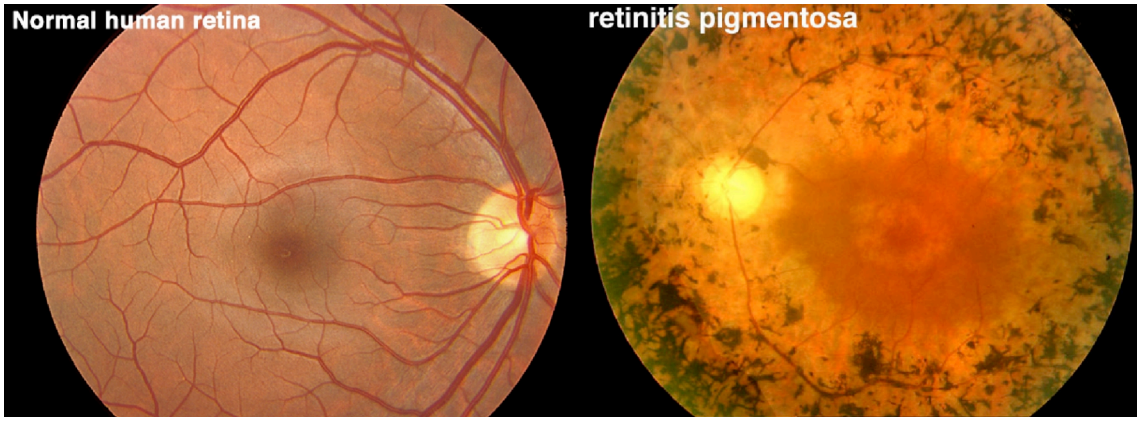

Fig.7 Fundus Photography of a Retinitis Pigmentosa Patient. Shown is the fundus photography of a healthy subject (left panel) in comparison to a retinitis pigmentosa patient (right panel). The dark lesions represent the pigment of the RPE cells, which migrate into the retina in degenerated regions due to the lack of photoreceptor cells. The lesions appear predominantly in the retinal periphery and solely progress to the central retina.
Figure: http://webvision.med.utah.edu/ClinicalERG.html#ERGs%20in%20retinitis%20pigmentosa-like%20diseases

In most forms of RP, loss of rods precedes loss of cones. However, in some cases rods and cones decline is simultaneous and in cone-rod dystrophies cone degeneration precedes loss of rods. This form of RP is characterized by early loss of visual acuity and impaired color vision [32]. Till 2008, approximately 190 disease-related genes were mapped and 130 disease-related genes were identified [31]. These genes belong to different functional groups like transport, metabolism, photoreceptor physiology or ion homeostasis. Mutations in the rhodopsin gene (*RHO*), in the usher syndrome 2A gene (*USH2A*) and in the retinitis pigmentosa GTPase regulator gene (*RPGR*) account for 30% of all RP cases [30]. However, in about 50% of all patients the genes, responsible for RP, are still unknown.

Although some supplemental nutrition like vitamin A and E as well as docosahexaenoic acid (DHA), which is an omega-3 fatty acid, might delay the progress of the disease [30], RP is still incurable and leads to legal blindness.

1.3 Models for Retinal Degeneration

To investigate the pathological changes, the molecular events or possible treatment strategies in retinal degeneration, models are required to focus on specific

problems. Several models are available with certain advantages or disadvantages. In general, two major model systems – inherited and induced – can be distinguished:

1. Inherited retinal degeneration is based on animal models with an artificially introduced or spontaneous genetic modification, which is inherited among the offspring.

2. Induced retinal degeneration requires an exogenous physically or chemically injury stimulus.

1.3.1 Model for Inherited Retinal Degeneration

To mimic retinal degeneration a variety of animal-models harboring either naturally occurring mutations or artificially introduced genetic modifications are available. A variety of different species like cats, dogs, fish, insects, pigs, monkeys or rodents exists to investigate inherited retinal diseases [33]. Due to the availability of many different mutations or genetic modifications specific models may closely resemble a certain human pathology. Mice are excellent tools because they are easily and precisely genetically modifiable. Deleting or mutating specific target genes can resemble genetic conditions of human patients. To date, more than 90 different mouse models exist, which harbor a mutation in a gene relevant for human retinal pathology [33]. A model for autosomal recessive RP is the rd1 mouse [34], which harbors a retroviral insert in the gene encoding the β-subunit of the phosphodiesterase (PDE). This leads to aberrant splicing and a null phenotype causing increased levels of cGMP in photoreceptor cells. As a consequence, ion channels remain constantly open, leading to increased intracellular Ca^{2+} concentrations. This leads to a very rapid degeneration starting at PND11 and resulting in a complete loss of photoreceptors in the central retina with 3 weeks of age. A model for autosomal dominant RP with later onset and slower progression is the transgenic VPP mouse [35, 36]. This mouse expresses additional copies of rhodopsin with 3 different mutations, which lead to 3 amino acid substitutions (V20G, P23H, P27L). Among them, P23H is the most common cause for autosomal dominant RP in human patients.

It is rather difficult to find appropriate models for AMD. Only primates have a human-like macula and AMD is an age related disease, which means animals need to survive a long lifespan. However, there are a couple of mouse models, which feature AMD partially. Among them, $Ccl2^{-/-}$ (chemokine (C-C motif) ligand 2) mice develop drusen-like deposits in the retina after two years and presenting retinal degeneration, which partially resembles AMD pathology [37].

1.3.2 Light Exposure – A Model For Induced Retinal Degeneration

Retinal Degeneration can be induced by a variety of exogenous stimuli like iron, led or calcium overload, by *N*-methyl-*N*-nitrosourea (MNU), by autoantibody treatment, by oxygen deprivation, etc. [33]. A frequently used tool to induce retinal degeneration is light. Light induces photoreceptor cell death, and thereby mimics the key feature of RP pathology [38-40]. Furthermore, it is assumed to accelerate the progression of human retinal diseases [41, 42]. Compared to models of inherited retinal degeneration, light exposure allows a temporal control of induction and a regulation of the severity grad. Two different experimental setups of light exposure, with different kinetics and disease progression, are established. A long-term exposure to low levels of light induces a moderate and slow progression of retinal degeneration [43]. A protocol of short-term exposure to high levels of light rapidly initiates retinal degeneration [44] and provides highly reproducible results (Fig.8). Due to the short and strong death-stimulus, cells respond synchronized either undergoing apoptosis or initiating pro-survival mechanisms. This allows an easy quantification of cell death and might raise certain (apoptosis/cell survival) markers of interest above the detection threshold.

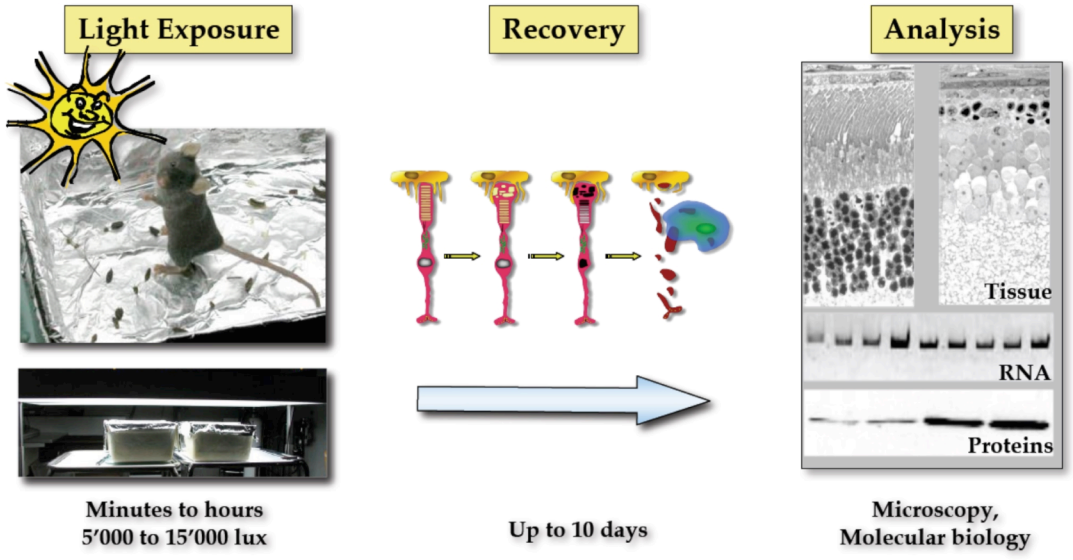

Fig.8 Experimental Setup of Short-Term Light-Induced Retinal Degeneration. Mice are exposed to cytotoxic levels of white light, which triggers photoreceptor cell death. Depending on the genetic background and on the pigmentation of animals (albino vs. pigmented) light intensities between 5'000 and 13'000 lux are employed for 1 to 2 hours. During the recovery phase apoptosis takes place and photoreceptors degenerate. Finally, morphological and biochemical analyses can be performed between 36 hours and 10 days after illumination.

Figure: Courtesy of A. Wenzel, C. Remé and C. Grimm

Photoreceptor cell death after a short-term exposure to a strong light stimulus can be divided into 4 phases [45]. The first step requires repetitive bleaching of rhodopsin [46] and causes an accumulation of retinoid metabolites [47] (e.g. all-trans retinal). Increased oxidative stress may contribute to the pro-apoptotic mechanisms. In the second step – the death-signal transduction-phase I – photoreceptors experience an increased calcium influx [48]. Calcium is known to trigger apoptosis in many neural systems. Although no cytochrome C is released, a swelling of mitochondria marks this phase. In the death-signal transduction-phase II AP-1 is activated 6 – 12 hours after light exposure and confers apoptosis [49-51]. AP-1 is a transcription factor formed by members of the Jun family proteins or of Jun and Fos family members [49, 50]. The termination phase is characterized by DNA fragmentation, cell disintegration and clearance of photoreceptor debris [45]. Progressive photoreceptor cell apoptosis results in released nucleosomes, which can be measured and quantified. Morphologically, photoreceptor cell death can be visualized by disintegration of IS and OS, as well as by the occurrence of pycnotic nuclei. After the peak of apoptosis (1 – 3 days after light exposure) macrophages invade the retina in order to remove photoreceptor debris.

The apoptotic pathways enabled after light exposure are largely unknown and classical pathways like activation of effector-caspases and release of cytochrome c seem to be not induced [52, 53]. However, caspase-1 is induced (but not activated) and might confer apoptosis by an unknown mechanism [51, 52]. Calpains may play a major role and may replace the lacking caspase activity after light exposure [53]. Further, members of the Jak/STAT signaling pathway seem to be involved in models light-induced and inherited retinal degeneration [54].

The limitation of the (light-) induced models is, that induced models only partially feature the pathology of human diseases and the cell-biological mechanisms might severely differ. Nevertheless, these models are easy to handle and might provide interesting candidates, which then can be further tested in appropriate inherited models.

1.4 Neuroprotection and Mechanisms of Hypoxic Preconditioning

In general, neuroprotection can be defined as any therapeutic approach that prevents or retards neuronal cell death. Thereby, the process of cell apoptosis is targeted and not the initial pathogenic stimulus.

1.4.1 Retinal Neuroprotection

Neuroprotective approaches have been successfully tested in a variety of animal models for neurodegenerative diseases like stroke, Parkinson disease, or Alzheimer disease in order to attenuate the pathogenesis and to restore or maintain the function of the affected neuronal system. Among the group of neuroprotective compounds, which are used to treat retinal degeneration, are: anti-inflammatory substances to reduce secondary neuronal cell death, NMDA antagonists to reduce glutamate toxicity, sodium channel blockers, nitric oxide synthase inhibitors or free radical scavengers. Other strategies are corticosteroids, regulators of ion homeostasis like Ca^{2+}-channel blockers or regulators of metabolism [55, 56]. A promising approach to prevent retinal apoptosis is the application or overexpression of growth factors [57] like glial cell derived neurotrophic factor (GDNF) [58], brain-derived neurotrophic factor (BDNF) [59], platelet derived growth factor (PDGF) [60], ciliary neurotrophic factor (CTNF) [61], fibroblast growth factor 2 (FGF2) [62], which is remarkable beneficial in models of glaucoma and inherited or light induced retinal degeneration. However, a neurodegenerative disease includes a complex interplay of several cell types like astrocytes, glia cells and neurons and an activation of multiple pro- and anti-apoptotic cascades. Therefore, most clinical trials were not satisfying when a single factor modulation was tested in brain or in the retina. A multiple drug therapy, which is already applied in cancer therapies, might be a promising alternative. Further, the use of compounds with multiple biological functions like hormones, corticosteroids, progesterone or synthetic drugs like cyclic dipeptides, which protect against oxygen dependent, mechanical injury dependent or free radical dependent neuronal cell death [63] could replace single factor therapies.

1.4.2 Hypoxic Preconditioning

A very successful strategy to attenuate neuro- and retinal degeneration in animal models is preconditioning, which is the exposure of a tissue or an organism to sub-lethal stress conditions. This induces pro-survival pathways to protect against future injury. Preconditioning stimuli like hypothermia [64], endotoxin pretreatment [65, 66] or light [67] have been shown to activate multiple pro-survival pathways and to prevent very efficiently neuronal degeneration. Hypoxic and ischemic preconditioning strongly protect the retina against cell death [68-73]. Whereas hypoxic preconditioning reduces the oxygen availability, ischemic preconditioning additionally inhibits the blood flow preventing nutrition exchange and waste disposal in addition. Although both preconditioning protocols induce a response to low oxygen and have similar protective

effects, they differ in gene regulation and duration of the protective effect [69, 71, 73, 74].

The exact mechanism of neuroprotection after hypoxic preconditioning is still unknown. However, hypoxia causes increased expression of potential neuroprotective genes like Vegf [71], heme oxygenase 1 (HO-1) [74], heat shock protein 27 (Hsp27) [75] or erythropoietin (Epo) [71] and generates a response that protects the retina against high levels of white light – a strong apoptotic stimulus. Photoreceptors of normoxic (21% O_2) control mice undergo apoptosis when exposed to light. In contrast, retinal morphology and function of mice preconditioned by hypoxia (6% O_2) for 6 h are completely maintained when exposed to light after 4 h of reoxygenation (Fig.9.A). Thereby, the level of retinal neuroprotection correlates with the oxygen levels. An oxygen concentration of 6 to 10% provides complete protection against light induced retinal degeneration. 14% oxygen shows an intermediate level of protection and no protection is observed in retinas of mice exposed to 18% oxygen. The protective effect lies within a narrow time window. After 16 h of reoxygenation the retina regains light damage susceptibility and photoreceptors undergo apoptosis again [71, 72]. This implies, that potential neuroprotective factors induced by hypoxic preconditioning are short-lived and rapidly degraded or inactivated during reoxygenation.

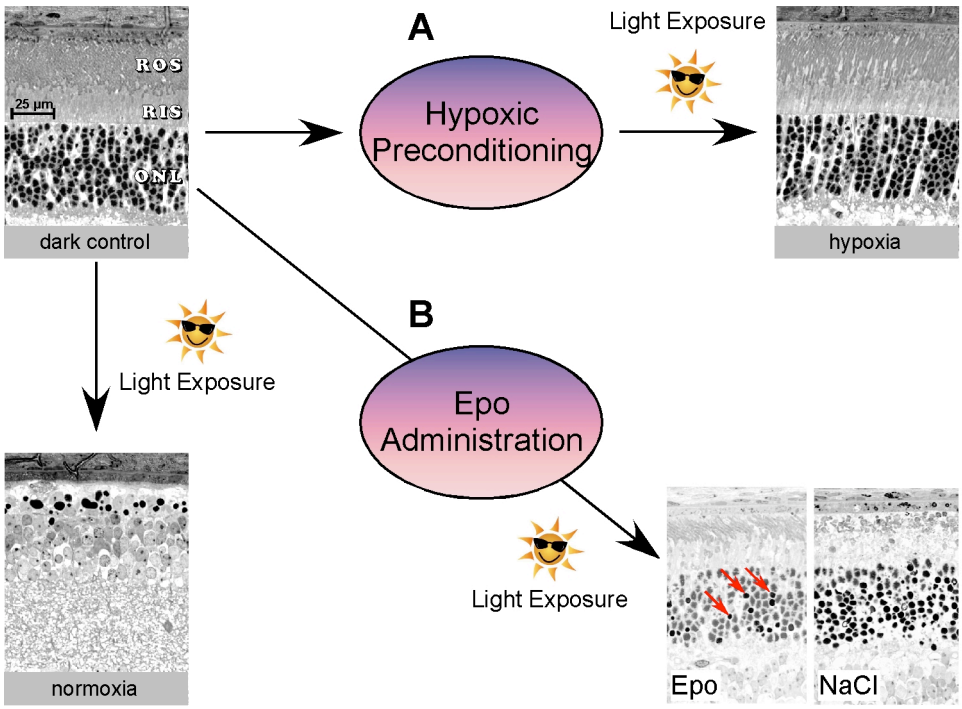

Fig.9 Hypoxic Preconditioning and Epo Administration Protect Against Light-induced Retinal Degeneration. Dark control mice have healthy photoreceptor cells with correctly structured outer and inner segments. Illuminated normoxic mice completely lack photoreceptor cells 10 days after light exposure. **A** Hypoxic preconditioning completely protects the retina against light damage leaving retinal

morphology unimpaired. **B** Epo administration partially protects the retina against light damage. Some pycnotic nuclei (red arrows) are present 36 hours after light exposure. Retinas injected with sodium chloride (NaCl) as control were damaged after illumination.
Figure: M. Thiersch and C. Grimm

1.4.3 Epo Partially Protects the Retina

Epo, one of the most prominent factors differentially regulated by hypoxia, is induced in oxygen-deprived retinas [71]. Epo protects retinal cells from apoptosis in a variety of degeneration models [71, 76-78]. Intraperitoneal application of recombinant human Epo (rhEpo) before and after light exposure reduced light damage susceptibility of mice and protected photoreceptors against toxic light insults (Fig.9.B) [71]. The Epo receptor (EpoR) is localized in the inner segments of photoreceptors and on ganglion cells [71, 79] suggesting that Epo-mediated activation of EpoR directly induces protection of visual cells. The protective effect of rhEpo injections is restricted to a time window of 1h before to 1 h after light exposure and is less complete than after hypoxic preconditioning [71, 72]. Likewise transgenic mice (tg6), which express human Epo and have 20-fold increased retinal Epo levels, are protected to a lower extend against light damage than mice preconditioned by hypoxia [80]. This suggests that pretreatment with low oxygen induces several factors (with Epo being one of them) that may need to act in concert to fully protect photoreceptors against light insult.

Therefore, transcription factors, which control the expression of Epo, Vegf and other potential neuroprotective genes, could be targets for future therapeutic interventions. One promising candidate of such transcription factors may be hypoxia-inducible factor 1 (HIF-1). Similar to the correlation between neuroprotection and oxygen concentration, HIF-1 is dose-dependently activated by decreasing oxygen concentrations.

1.5 The HIF System – Master Regulator of Hypoxia

Hypoxia-inducible factors (HIFs) are transcription factors essential to maintain cellular or systemic oxygen homeostasis. The HIFs are heterodimeric factors consisting of a HIF-α subunit and of a constitutively expressed HIF-β subunit named aryl hydrocarbon receptor nuclear translocator (ARNT). Three different HIF-α subunits are described (HIF-1α, -2α, -3α) [81]. Each α- and β-subunit belongs to the bHLH (basic helix-loop-helix)-PAS (Per/ARNT/SIM) family and contains two PAS domains (PAS-A and PAS-B) and a bHLH domain (Fig.10) [82]. These domains are essential for

DNA binding and for the dimerization of the α- and β-subunits. Additionally, HIF-1α and HIF-2α contain a TAD-N and a TAD-C domain (terminal transactivation domains), which are required for the recruitment of transcriptional co-activators such as p300/CBP [83-85]. The TAD-N domain overlaps with the oxygen-dependent degradation domain (ODD), which is required to regulate the stabilization of the HIF-α subunit depending on the oxygen concentration [81]. In contrast to HIF-1α and HIF-2α, HIF-3α lacks the C-transactivation domain and acts as a suppressor of HIF-1 and HIF-2 in a dominant negative manner [86]. Three out of six known isoforms of HIF-3α even lack the ODD indicating that they might be constantly expressed to counteract HIF-1α.

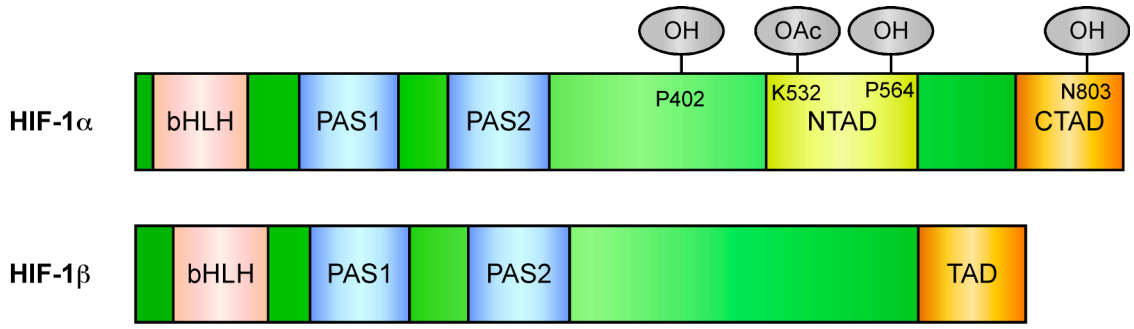

Fig.10 Structure of HIF-1α and HIF-1β subunits. HIF-1α and HIF-1β contain a basic-helix-loop-helix structure (bHLH) and two PER-ARNT-SIM (PAS1 and PAS2) domains. Human HIF-1α is hydroxylated at proline (P) residue 402 and 564 to recruit von Hippel-Lindau tumour suppressor protein (VHL) and to initiate HIF-1α degradation. Hydroxylation of asparagine (N) residue 803 prevents binding of transcriptional co-factors. Additional acetylation at lysine (k) residue 532 enhances the binding of VHL. HIF-1α contains a N- as well as a C- terminal transactivation domains (N/CTAD) and HIF-1β contains one transactivation domain (TAD).

Figure: adapted from Carroll and Ashcroft, 2005 Molecular Medicine

1.5.1 Oxygen-Dependent Regulation of HIF-1α

In order to quickly respond to cellular changes in oxygen concentration, HIF-1α is constitutively expressed but rapidly degraded under normoxic conditions (Fig.11). To target human HIF-1α for proteosomal degradation under normoxic conditions, prolylhydroxylases (PHDs) hydroxylate HIF-1α posttranslationally at two specific proline residues (Pro402 & Pro564) consisting of an LXXLAP aminoacid motive in the ODD [87-90]. Prolyl hydroxylases are Fe(II) dependent dioxygenases, which require oxygen and α-ketoglutarate as co-substrates [90, 91]. Additionally, the acetyltransferase ARD-1 transfers an acetyl group to the Lys-532 residue of the human HIF-1α subunit [92]. The hydroxylation and acetylation steps prepare the binding of the

tumor suppressor von Hippel-Lindau protein (VHL). VHL is a part of an E3 ligase complex, which initiates the binding of ubiquitin eventually leading to proteasomal degradation of HIF-1α [93, 94]. In order to additionally inactivate HIF-α subunits, factor inhibiting HIF (FIH) hydroxylates human HIF-1α subunits at an asparagine residue in the C-terminal transactivation domain (Asn803) [95-97]. This inhibits the binding of the transcriptional co-activators p300 and CBP (CREB binding protein) and reduces the transcription activity of HIF-1.

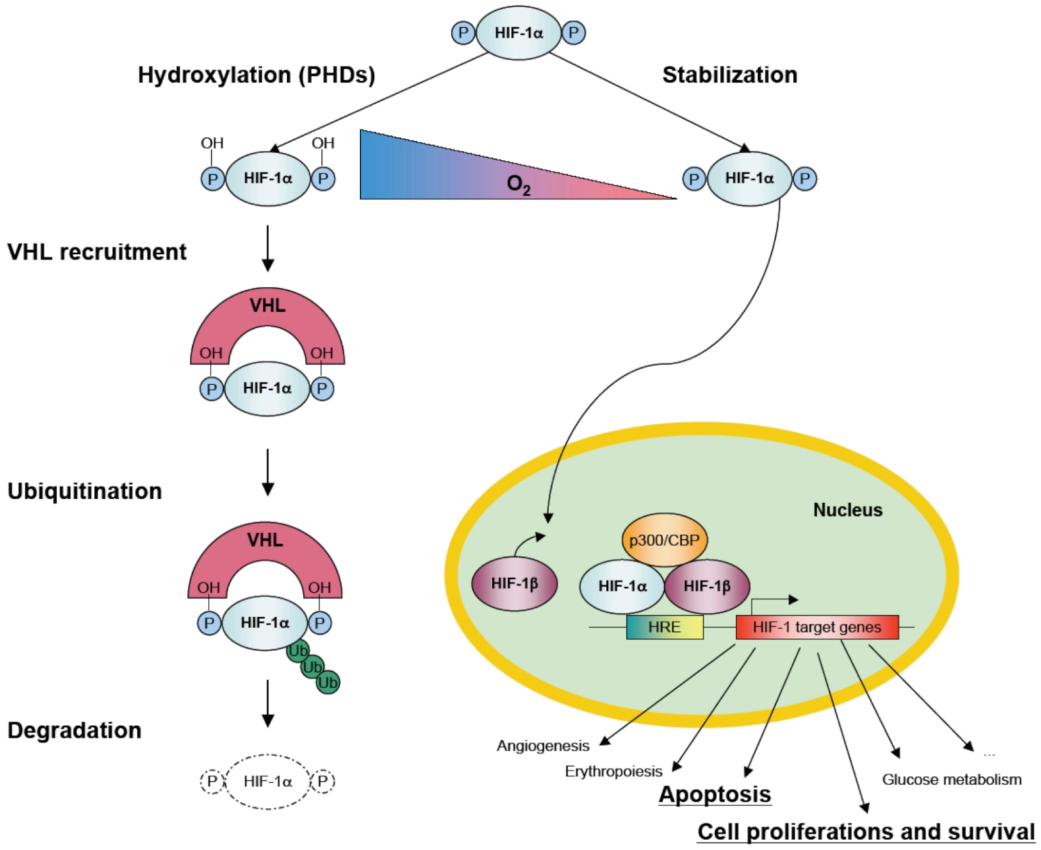

Fig.11 Oxygen-dependent Regulation of HIF-1α. During conditions of normal oxygen (O_2) supply (left side) HIF-1α is hydroxylated at two proline (Pro) residues by prolylhydroxylases (PHDs). The hydroxylation initiates the binding of the von Hippel-Lindau tumour suppressor protein (VHL), which triggers the ligation of ubiquitin (Ub) and results in a rapid degeneration of HIF-1α via the proteosomal degradation pathway. During hypoxia (right side) PHDs fail to hydroxylate HIF-1α, which thereby becomes stabilized. After translocation to the nucleus HIF-1α and HIF-1β dimerize to form HIF-1 and bind to the hypoxia-response element (HRE) in promoter regions of target genes. Due to the recruitment of transcriptional co-activators p300/CBP HIF-1 differentially expresses genes involved in different pathways (e.g. apoptosis or cell survival).

Figure: adapted from http://www.panomics.com/images/hif_celllineflow.gif and from Carroll and Ashcroft, 2005 Molecular Medicine

1.5.2 Oxygen-Independent Regulation of HIF-1α

Besides the oxygen dependent regulation of HIF-1α, other mechanisms are known to regulate the stabilization or activity of HIF-1α under normoxic or hypoxic conditions in an oxygen-independent manner [98].

Negative regulators of HIF-1α are CITED2, CITED4 [99, 100] and p53 [101], which compete with HIF-1α for the binding of p300 to reduce HIF-1 transcriptional activity and/or to facilitate its degradation. HIF-3α4 (IPAS) an isoform of HIF-3α harbors a bHLH-PAS domain but lacks the C-TAD domain and diminishes HIF-1 activity by competing for the binding of HIF-1β [102]. Tumor suppressor, $p14^{ARF}$ binds to the ODD of HIF-1α to inhibit its transcriptional activity without affecting the protein stability [103].

Positive regulators are growth factors and cytokines like epidermal growth factor (EGF) [104], insulin-like growth factor (IGF) 1/2, [105-107] hepatocyte growth factor (HGF) [108] and PDGF [109]. Via the growth factor signaling pathways Ras/Raf/MAPK and PI3K/Akt/PKB they can stabilize HIF-1α under normoxic conditions or boost the HIF-1α activation during hypoxia [110]. The second messenger nitric oxide (NO) regulates HIF-1α in a concentration dependent manner [111]. High levels of NO stimulate HIF-1α accumulation; low levels of NO rather facilitate HIF-1α degradation even under hypoxic conditions. Mitochondria act as oxygen sensors and increase the reactive oxygen species (ROS) generation during hypoxia. In order to endure hypoxia, ROS can activate pathways, which lead to induction of HIF-1α [98].

1.5.3 HIF-1α Regulates Cell Death and Survival

Hypoxia and the stabilization of HIF-1α can induce both, cell death and cell survival [112]. HIF-1 regulates the expression levels of pro-survival genes (like Epo, Vegf, IGF-1, etc. [113-115]) as well as pro-apoptotic genes (p53, Bnip3, caspase-3 etc. [116-118]). The pro-survival or pro-death property of HIF-1 depends on the duration and severity of hypoxia [119], the different types of pathogenic stimuli [120] and on different types of cells [121].

The embryonic vascularization and thereby the whole development of an organism absolutely requires HIF-1α. The ablation of HIF-1α leads to prenatal mortality between embryonic day 8 and 9 due to the complete lack of cephalic vascularization, a severely impaired somatic formation and insufficient neural development [122]. A growing organism or a developing tissue depends on a sufficient nutrition and oxygen

supply, which is warranted via blood vessel networks. HIF-1 induces multiple angiogenic factors like Vegf or angiopoietin, which initiate the development of blood vessels [123, 124]. To optimize the oxygen supply HIFs stimulate the expression of erythropoietin (Epo), which binds to its receptor and enhances the maturation and survival of erythroid progenitor cells in bone marrow and spleen [125]. Additionally, Epo exhibits strong neuroprotective properties (see chapter 1.4.3).

Cellular energy is stored as ATP, which is the key-element for a living cell. Substrates like glucose are required to generate ATP aerobic via electron transport along the respiratory chain in mitochondria (oxidative phosphorylation) or anaerobic via glycolysis during oxygen deprivation. In situations of low intracellular oxygen concentration the ATP generation via oxidative phosphorylation is constricted. HIF-1 can enhance the anaerobic metabolism by the differential regulation of metabolic genes. The induction of glucose transporter 1 (GLUT1) increases the glucose uptake of cells, the expression of glycolytic genes accelerates glucose metabolization to pyruvat and the induced expression of lactate dehydrogenase A (LDHA) leads to an enhanced pyruvat conversion to lactate [126, 127]. Further, HIF-1 optimizes the respiration efficiency under hypoxic conditions by inducing the expression of the COX4-2 subunit, which replaces the COX4-1 subunit in the cytochrome c oxidase [128]. The induction of pyruvat dehydrogenase kinase 1 (PDK) inactivates the pyruvat dehydrogenase (PDH) and thereby prevents the conversion of pyruvat to acetyl coenzyme A, which is the substrate for the Krebs cycle [129]. By contributing to an adequate energy supply HIF-1 can ensure a prolonged cell survival. In fact, the strong pro-survival effects of HIF-1 can be even harmful for an organism. During cancer progression cells grow abnormally. In order to increase beyond microscopic size, tumors need to resist to hypoxia. HIF-1 is stabilized in most of human tumors and is directly correlated to the pathology in human patients [130-133]. A therapeutic strategy is to target the stabilization of HIF-1, which is connected to vascularization and changed expression of metabolism-associated genes – both hallmarks for tumor pathogenesis.

2 AIMS OF THE THESIS

1. Analyses of the retinal transcriptome after hypoxic preconditioning to identify potential neuroprotective factors

Hypoxic preconditioning protects against light induced retinal degeneration. Low oxygen levels result in stabilization of HIF-1α and in induced Epo expression, which protects the retina against light damage. However, systemically applied recombinant human Epo protects the retina only partially against toxic light insults. Therefore, it is likely that additional genes, differentially expressed by hypoxic preconditioning, are required for a complete protection of photoreceptors. The identification of genes, which are differentially expressed during hypoxic preconditioning, should provide a better understanding of the retinal response to hypoxia and of mechanisms of retinal neuroprotection. The aim of this study was to analyze the retinal transcriptome after hypoxia with the focus on the following points:

I. How does the hypoxic transcriptome compare to the normoxic transcriptome in the retina?
II. Are there candidate genes, which potentially contribute to retinal neuroprotection observed after hypoxic preconditioning?
III. Selection and analysis of a first potential target gene to investigate its impact on retinal neuroprotection.

2. The role of HIF-1α in retinal neuroprotection after hypoxic preconditioning

In many systems HIF-1 is associated with cell survival after preconditioning. In the retina HIF-1 is induced during hypoxic preconditioning. HIF-1 controls the expression of genes involved in apoptosis. Therefore HIF-1 should be an excellent candidate for regulating retinal neuroprotection. A systemic knock out of the oxygen dependent regulated component HIF-1α is lethal, and cannot be used as a tool to analyze the role of HIF-1α. However, a conditional photoreceptor cell specific ablation of HIF-1α may help to elucidate its role in retinal neuroprotection against light toxicity. The aim of this project was to delete HIF-1α specifically in photoreceptors using the Cre-lox technology. We employed two different photoreceptor-specific Cre expressing mouse lines (PrpCre and OpnCre) and focused on the following problems:

I. Is photoreceptor-specific HIF-1α required to maintain normal retinal morphology and function?
II. Is photoreceptor-specific HIF-1α required to resist short severe hypoxia?
III. Is photoreceptor-specific HIF-1α the “engine” of retinal neuroprotection after hypoxic preconditioning?
IV. Are there HIF-1α independent mechanisms, which could be responsible for retinal neuroprotection

3 RESULTS

3.1 Analysis of the retinal gene expression profile after hypoxic preconditioning identifies candidate genes for neuroprotection

Markus Thiersch[1], Wolfgang Raffelsberger[2], Rico Frigg[1], Marijana Samardzija[1], Andreas Wenzel[1], Olivier Poch[2] and Christian Grimm[1]

[1]Lab of Retinal Cell Biology, Dept Ophthalmology, University of Zurich, Switzerland
[2]Laboratoire de BioInformatique et Génomique Intégrative, Institut de Genetique et de Biologie Moleculaire et Cellulaire, 67404 Illkirch, France

Published in BMC Genomics 2008, **9**:73 (8 February 2008)

Reference number [134] refers to this paper

BMC Genomics

BioMed Central

Research article

Open Access

Analysis of the retinal gene expression profile after hypoxic preconditioning identifies candidate genes for neuroprotection

Markus Thiersch[1], Wolfgang Raffelsberger[2], Rico Frigg[1], Marijana Samardzija[1], Andreas Wenzel[1], Olivier Poch[2] and Christian Grimm*[1]

Address: [1]Lab of Retinal Cell Biology, Dept Ophthalmology, University of Zurich, Switzerland and [2]Laboratoire de BioInformatique et Génomique Intégrative, Institut de Genetique et de Biologie Moleculaire et Cellulaire, 67404 Illkirch, France

Email: Markus Thiersch - markus.thiersch@usz.ch; Wolfgang Raffelsberger - wraff@titus.u-strasbg.fr; Rico Frigg - enrico.frigg@puk.zh.ch; Marijana Samardzija - marijana.samardzija@opht.uzh.ch; Andreas Wenzel - andreas.wenzel@novartis.com; Olivier Poch - poch@igbmc.u-strasbg.fr; Christian Grimm* - cgrimm@opht.uzh.ch

* Corresponding author

Published: 8 February 2008

BMC Genomics 2008, **9**:73 doi:10.1186/1471-2164-9-73

Received: 22 October 2007
Accepted: 8 February 2008

This article is available from: http://www.biomedcentral.com/1471-2164/9/73

Abstract

Background: Retinal degeneration is a main cause of blindness in humans. Neuroprotective therapies may be used to rescue retinal cells and preserve vision. Hypoxic preconditioning stabilizes the transcription factor HIF-1α in the retina and strongly protects photoreceptors in an animal model of light-induced retinal degeneration. To address the molecular mechanisms of the protection, we analyzed the transcriptome of the hypoxic retina using microarrays and real-time PCR.

Results: Hypoxic exposure induced a marked alteration in the retinal transcriptome with significantly different expression levels of 431 genes immediately after hypoxic exposure. The normal expression profile was restored within 16 hours of reoxygenation. Among the differentially regulated genes, several candidates for neuroprotection were identified like metallothionein-1 and -2, the HIF-1 target gene adrenomedullin and the gene encoding the antioxidative and cytoprotective enzyme paraoxonase 1 which was previously not known to be a hypoxia responsive gene in the retina. The strongly upregulated cyclin dependent kinase inhibitor *p21* was excluded from being essential for neuroprotection.

Conclusion: Our data suggest that neuroprotection after hypoxic preconditioning is the result of the differential expression of a multitude of genes which may act in concert to protect visual cells against a toxic insult.

Background

Retinal blinding diseases like retinitis pigmentosa (RP) and age related macular degeneration (AMD) are characterized by a progressive retinal degeneration which involves the apoptotic loss of photoreceptor cells. Although significant progress in the understanding of the molecular mechanisms leading to AMD and RP has been made in recent years, efficient treatments to successfully prevent loss of vision are still not available.

BMC Genomics 2008, **9**:73 http://www.biomedcentral.com/1471-2164/9/73

Neuroprotection is a strategy to preserve retinal function. It aims at the interference with regulatory mechanisms of cell death to protect photoreceptor cells. To successfully target these mechanisms it is necessary to understand the molecular signalling networks in the degenerating retina. Since neither an extrinsic (activation of caspases via death receptors) nor an intrinsic death pathway (release of cytochrome c from mitochondria) seems to be activated during retinal degeneration [1], mechanisms of photoreceptor cell death are still poorly understood. Several models of inherited [2] and induced [3] retinal degeneration are used to study the molecular events of photoreceptor apoptosis. Inherited models mostly show a slow progression of retinal degeneration resulting in constant but low levels of apoptosis. Models of induced retinal degeneration, like the light damage model [3], are easy to handle and the synchronized response to the apoptotic stimulus may raise apoptotic factors above detection threshold allowing their detailed investigation.

Various preconditioning protocols are used as a strategy to protect tissues from degenerative processes. Especially ischemic and hypoxic preconditioning successfully reduced the severity of induced or inherited degeneration in tissues like brain [4,5] heart [6,7] and the retina [8-12]. Hypoxia describes a state of low oxygen. It appears pathologically during several diseases like cancer, stroke or heart infarction [13] but also physiologically during development in many tissues [14]. In the adult retina, increased oxygen consumption during night time leads to borderline hypoxic conditions [15]. To cope with the reduced oxygen availability cells differentially regulate genes including factors involved in an anti-apoptotic response [16,17]. A key regulator of the tissue response to hypoxia is the transcription factor hypoxia inducible factor 1 (HIF-1), a heterodimeric protein consisting of the constitutively and stably expressed hypoxia inducible factor 1β (HIF-1β) and oxygen regulated subunit hypoxia inducible factor 1α (HIF-1α). During hypoxia HIF-1α is stabilized, enters the nucleus, recruits HIF-1β and regulates the expression of target genes involved in different pathways like apoptosis, metabolism or angiogenesis [18].

Hypoxic preconditioning was shown to stabilize HIF-1α in the retina [9,12]. Stabilization of this transcription factor induces the expression of target genes with neuroprotective properties like vascular endothelial growth factor (*Vegf*) and erythropoietin (*Epo*) suggesting a link between HIF-1 driven gene expression and neuroprotection [9,12]. Exogenous application of Epo not only protects retinal ganglion cells in a model of ischemia-reperfusion injury [19] but also photoreceptors in the model of light induced retinal degeneration [20,21]. However, protection of visual cells from light damage was weaker than after hypoxic preconditioning suggesting that factors in addition to Epo contribute to retinal protection by hypoxia. The identification of these factors is essential for the development of efficient neuroprotective strategies focused on the prevention of retinal degeneration.

We used whole genome microarrays and real-time PCR to detect expression of differentially regulated genes after hypoxic preconditioning in adult mouse retinas. The analysis of the hypoxic transcriptome characterized the response of the retina to low oxygen levels. Cyclin-dependent kinase inhibitor 1a (*p21*) was among the most strongly induced genes and occupied a central position in a differentially regulated gene network affecting cellular growth and proliferation. Using p21 gene knockout animals, we analyzed the impact of this gene on retinal neuroprotection in the model of light induced retinal degeneration.

Results

Time frame of neuroprotection after hypoxic preconditioning

In previous experiments we observed an almost complete protection of photoreceptors against light induced degeneration when exposed at 4 hours after hypoxic preconditioning. Protection, however, was lost after prolonged reoxygenation of 16 hours suggesting a rather short-lived neuroprotective effect of hypoxic preconditioning [9]. To analyze the time frame of hypoxia-induced neuroprotection in more detail, we allowed preconditioned mice to reoxygenate for 4 h, 8 h, 12 h and 16 h, respectively, before they were exposed to high levels of white light. As expected, retinal morphology (Fig. 1A) was almost completely preserved in mice illuminated after a reoxygenation period of 4 h. Only slight disturbances and vesiculations in the rod outer segments but no apoptotic nuclei with condensed chromatin were observed.

Exposure after 8 h of reoxygenation resulted in the appearance of some apoptotic photoreceptor nuclei. 12 h of reoxygenation further reduced the protection against light damage as evidenced by the appearance of many nuclei with condensed chromatin and an almost complete disintegration of rod inner (RIS) and rod outer segments (ROS). Retinas of mice illuminated 16 hours after hypoxic preconditioning were as susceptible to light damage as retinas of normoxic control mice (Fig. 1A).

The retinal response to hypoxic preconditioning

It is well known that hypoxia alters the gene expression profile in a given tissue [22] in an attempt to cope with the unfavourable condition. One of the major factors regulating this response is the transcription factor HIF-1, which is activated in the hypoxic retina (Fig. 1B) [9]. Similarly, the pro-survival transcription factor Stat3 [23], which has been reported to be induced in several hypoxic tissues

BMC Genomics 2008, 9:73 http://www.biomedcentral.com/1471-2164/9/73

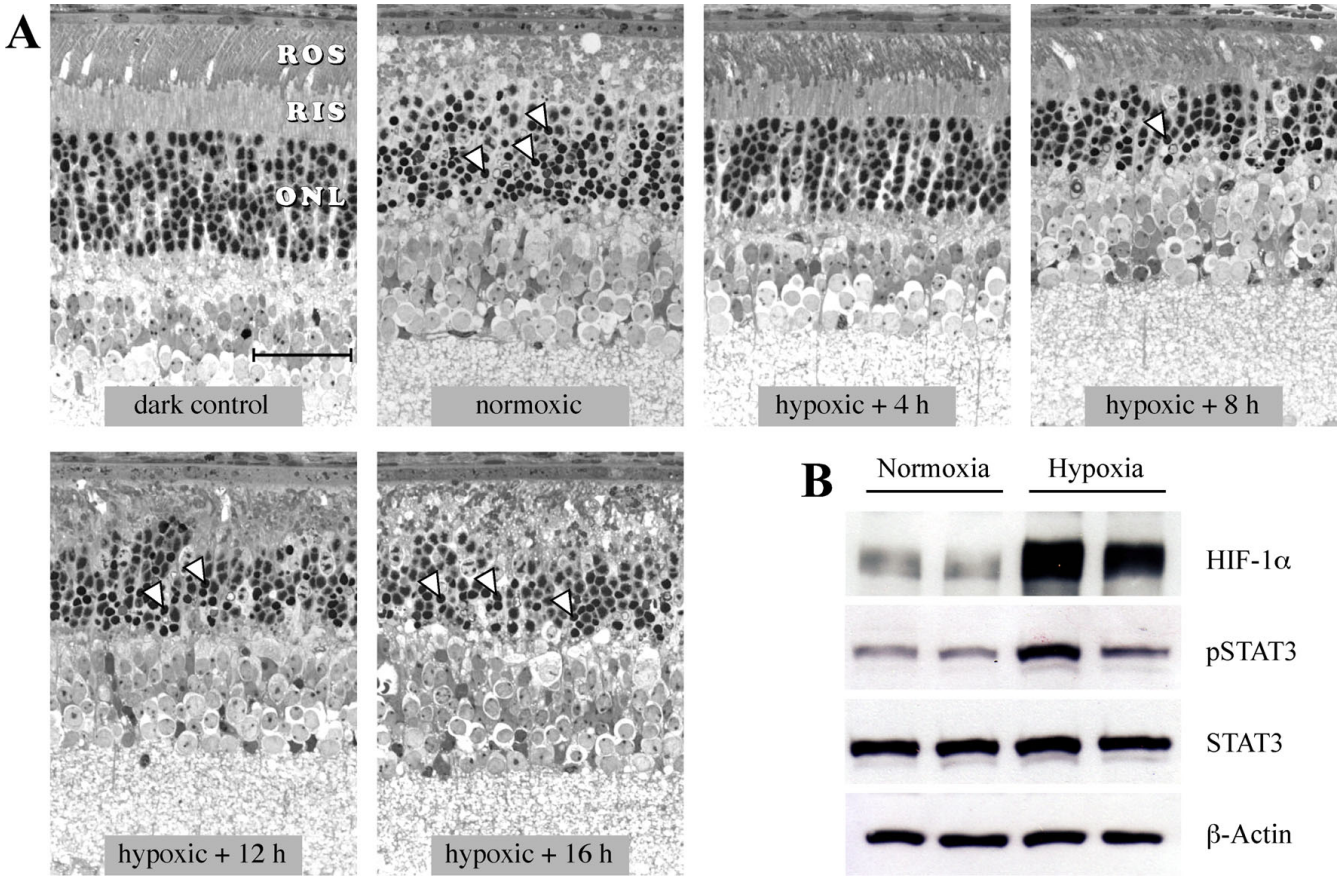

Figure 1

Transient protection of retinal morphology by hypoxic preconditioning. **A)** BALB/c mice were preconditioned by hypoxia for 6 h. After 4 h, 8 h, 12 h or 16 h of reoxygenation in darkness, mice were exposed to 5'000 lux of white light for 1 h. Control animals were not preconditioned and were (normoxic) or were not (dark control) exposed to light. Retinal morphology was analyzed 36 h after light exposure. Normoxic animals exposed to light showed a severe disruption of ROS and RIS with the appearance of many pycnotic photoreceptor nuclei. Mice exposed to light 4 hours after hypoxic preconditioning were almost completely protected and only some ROS vesiculation was observed. The protective effect of hypoxia was progressively weakened with increasing reoxygenation time before illumination as indicated by an increased disruption of ROS and RIS and the increased appearance of pycnotic photoreceptor nuclei. 16 h after preconditioning the protection was completely lost. Hypoxic preconditioning per se did not affect retinal morphology or function even after prolonged survival (data not shown, [9]). Arrowheads: examples of pycnotic nuclei; ROS: rod outer segments; RIS: rod inner segments; ONL: outer nuclear layer, scale bar: 25 μm. **B)** Expression of transcription factors HIF-1α and phospho-STAT3 in the retina was analyzed in normoxic mice or immediately after hypoxic preconditioning by Western blotting. β-actin and STAT3 levels verified equal sample loading. Both transcription factors were induced immediately after hypoxia with some variability between individuals. Shown are results from two normoxic controls and from two mice preconditioned with hypoxia.

[24], was phosphorylated and thus activated in the hypoxic retina (Fig. 1B). The different levels of activation (shown are examples of two mice) point to a certain variability in the response to hypoxia between individual mice. Nevertheless, the activation of these transcription factors suggests a differential regulation of a multitude of potentially neuroprotective genes in the retina by hypoxic preconditioning. Based on the time frame of neuroprotection (Fig. 1A), we analyzed the gene expression pattern in the retina at 0 h, 2 h, 4 h, and at 16 h after hypoxia (see Methods).

Hierarchical clustering of gene chip data showed strong similarities of the three replica-chips of a respective time point after hypoxia [see additional file 1]. Such clustering was not observed in normoxic samples suggesting that hypoxia induced a strong and specific response in the retina. This hypoxic response quickly vanished and at 4 h

after hypoxic preconditioning the retinal transcriptome was similar to normoxic controls.

After normalization of the data by GCRMA algorithm to minimize the theoretical appearance of false positive signals we detected 431 differentially regulated genes immediately after hypoxia, 227 of which had a fold change above 2 (0 h, Fig. 2). The number of regulated genes decreased gradually until 16 h after hypoxia when just 3 genes showed altered expression levels (Fig. 2). The application of our statistical filter for a maximal acceptable FDR suggested that there are (statistically estimated) 25, 23, 6 and 1 false positive genes in the analyzed list of differentially regulated genes at 0 h, 2 h, 4 h and 16 h, respectively.

Prominently regulated genes

The genes with the strongest regulation after hypoxic exposure are listed in Table 1 [for complete gene lists see additional file 2]. The most significantly upregulated gene (>118-fold) was found to be *Obox6*, a homeobox-containing, putative transcriptional activator of unknown function mainly expressed in oocytes [25]. The gene with the strongest downregulation was the cold-inducible RNA binding motif protein 3 (*Rbm3*) with a 19-fold reduced expression immediately after hypoxia (Table 1).

Most interestingly, expression of several genes with a potential capacity to protect photoreceptors against light-induced cell death was upregulated (Table 1). To this group belong *p21* and *Bcl2l10*. In addition, genes belonging to oxidative stress response pathways or lipid metabolism like metallothioneins (*Mt1* and *Mt2*), transthyretin (*Ttr*) and paraoxonase1 (*Pon1*) were induced as was the expression of adrenomedullin (*Adm*) which was previously shown to respond to hypoxic conditions [26] and to have neuroprotective properties [27].

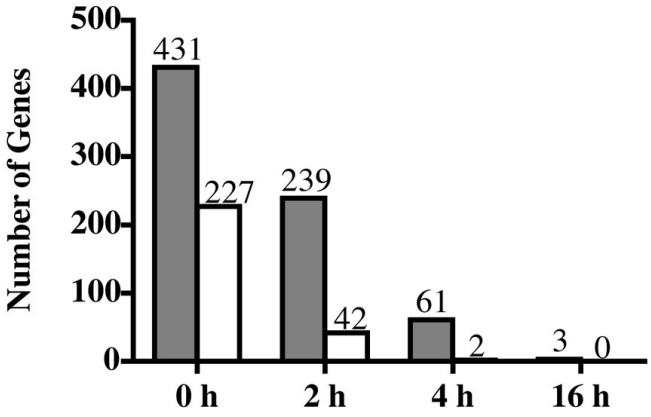

Figure 2
Number of genes differentially expressed immediately (0 h), 2 h, 4 h and 16 h after hypoxic preconditioning. Gray bars: total number of significantly regulated genes. White bars: number of genes regulated at least 2-fold. The number of differentially regulated genes decreased rapidly during reoxygenation, indicating a fast return to the gene expression pattern of normoxic retinas.

Some pro-apoptotic genes were downregulated after hypoxic preconditioning (Table 1) like *Mef2c*, a transcription factor involved in neuronal loss in Parkinson's disease [28] and in the regulation of apoptosis in macrophages [29]. The genes belonging to the Rbm family of genes are also of high interest since some members of this family are known to have an impact on apoptosis regulation [30].

Verification of Affymetrix microarray data

The expression of a total of 32 genes identified by the microarrays was tested by realtime PCR. Differential expression in response to hypoxia was verified for 21 (66%) genes (Fig. 3 and additional file 3). Quality control analysis showed that the integrities of both retinal RNA and chip surfaces were high [QC analysis, see additional file 1] and are thus unlikely to be responsible for the somewhat low confirmation frequency.

Since many of the genes which were not confirmed by real-time PCR to be differentially regulated had a low fold-change on the microarrays, we used only genes with a minimal fold change of 2 for the investigations of functionally related groups (see below). Figure 3 shows the real-time PCR data of 4 selected genes with potential neuroprotective properties (*p21*, *Pon1*, *Ttr*, *Adm*). Consistent with the microarray results, these genes were strongly upregulated immediately after hypoxia and returned quickly to normal expression levels during reoxygenation.

Biological functional groups and pathway analysis

The bioinformatics resource DAVID was used to study the impact of differentially expressed genes on known biological processes [31]. We obtained 39 functional groups for upregulated genes and 8 groups for downregulated genes immediately after hypoxia (H0). Significant functional groups included 'apoptosis', 'cell cycle' or 'negative regulation of transcription' (note that some genes appear in more than one group) were found in the list of upregulated genes (Table 2). Lists of all functional related groups can be found in additional file 4. Gene signalling networks affected by hypoxic preconditioning were identified using Ingenuity Pathway analysis and the complete lists of regulated genes (Fig 4 and see additional file 5). The centre of the strongest affected pathway was occupied by *p21*, one of the most strongly upregulated genes by hypoxia (Fig. 4). All genes belonging to this pathway were differentially regulated. 70% of the genes were induced indicating that the pathway was activated rather than repressed. All genes of

BMC Genomics 2008, **9**:73 http://www.biomedcentral.com/1471-2164/9/73

Table 1: Top 50 differentially regulated genes immediately after hypoxic preconditioning

Affymetrix ID	Gene Symbol	Gene Name	FC	pVal
UPREGULATED				
1440257_at	Obox6	oocyte specific homeobox 6	118.4	2.48E-07
1433837_at	8430408G22Rik	RIKEN cDNA 8430408G22 gene	35.6	6.94E-05
1424638_at	Cdkn1a	cyclin-dependent kinase inhibitor 1A (p21)	30.5	3.00E-05
1454409_at	4833408G04Rik	RIKEN cDNA 4833408G04 gene	24.0	2.07E-06
1418190_at	Pon1	paraoxonase 1	22.5	1.98E-05
1422832_at	Rgr	retinal G protein coupled receptor	22.1	6.20E-05
1454608_x_at	Ttr	transthyretin	20.1	2.67E-04
1455913_x_at	Ttr	transthyretin	20.0	3.11E-04
1458610_at	-	---	17.4	1.95E-04
1416434_at	Bcl2l10	Bcl2-like 10	17.0	2.70E-05
1444487_at	Lrat	lecithin-retinol acyltransferase	16.2	6.54E-06
1441228_at	Apold1	apolipoprotein L domain containing 1	11.7	7.21E-05
1438815_at	Hist2h2aa2	histone 2, H2aa2	10.7	1.01E-04
1416077_at	Adm	adrenomedullin	10.6	2.48E-04
1430197_a_at	Pitpnm2	phosphatidylinositol transfer protein, membrane-associated 2	10.3	5.36E-05
1428942_at	Mt2	metallothionein 2	9.7	5.12E-06
1418808_at	Rdh5	retinol dehydrogenase 5	9.7	9.82E-05
1427221_at	MGI:2143217	X transporter protein 3 similar 1 gene	9.3	1.29E-04
1430817_at	Samd7	sterile alpha motif domain containing 7	8.6	2.66E-04
1447494_at	D7Bwg0826e	DNA segment, Chr 7, Brigham & Women's Genetics 0826 expressed	7.2	5.77E-06
1428352_at	Arrdc2	arrestin domain containing 2	7.1	6.05E-05
1446587_at	-	Transcribed locus	6.9	2.32E-04
1424838_at	A330049M08Ri	RIKEN cDNA A330049M08 gene	6.8	1.21E-04
1426117_a_at	Slc19a2	solute carrier family 19 (thiamine transporter), member 2	6.8	1.80E-04
1430357_at	H3f3b	H3 histone, family 3B	6.3	5.84E-05
1422557_s_at	Mt1	metallothionein 1	6.3	5.42E-06
1454991_at	Slc7a1	solute carrier family 7 (cationic amino acid transporter, y+ system), member 1	6.1	1.39E-04
1429348_at	Sema3c	semaphorin 3C	5.9	3.55E-04
1442366_at	6820408C15Ri	RIKEN cDNA 6820408C15 gene (6820408C15Rik), mRNA	5.6	6.15E-05
1441673_at	C80120	expressed sequence C80120	5.3	1.39E-04
DOWNREGULATED				
1429169_at	Rbm3	RNA binding motif protein 3	19.41	2.54E-04
1435692_at	LOC622320	similar to retinoic acid, EGF, and NGF upregulated	7.02	3.79E-05
1447363_s_at	Bub1b	budding uninhibited by benzimidazoles 1 homolog, beta (S. cerevisiae)	6.36	8.09E-06
1416961_at	Bub1b	budding uninhibited by benzimidazoles 1 homolog, beta (S. cerevisiae)	5.41	1.20E-06
1444172_at	-	Transcribed locus	4.72	2.64E-04
1435158_at	Rbm12b	RNA binding motif protein 12B	4.40	6.09E-05
1425083_at	Otor	otoraplin	4.03	2.21E-04
1445709_at	Mdm1	transformed mouse 3T3 cell double minute 1	3.97	1.64E-04
1450953_at	Wdr39A	WD repeat domain 39	3.70	1.93E-04
1456723_at	Prr14	Proline rich 14	3.49	2.35E-05
1456834_at	Ibrdc2	IBR domain containing 2 (Ibrdc2), mRNA	3.45	1.76E-04
1442051_at	His2h3cl	histone 2, H3c1	3.39	2.63E-04
1437647_at	Dido1	death inducer-obliterator 1	3.38	6.54E-05
1421379_at	Zfp354b	zinc finger protein 354B	3.28	3.41E-04
1424852_at	Mef2c	myocyte enhancer factor 2C	3.22	1.40E-04
1429655_at	Nudcd1	Nudcd1 NudC domain containing 1 3.19 3.84E-04	3.19	3.84E-04
1442249_at	-	Transcribed locus	3.11	1.03E-04
1416920_at	Rbm4	RNA binding motif protein 4	3.11	1.44E-04
1460107_at	1700129I04Rik	RIKEN cDNA 1700129I04 gene	3.11	1.74E-04
1453010_at	Iws1	IWS1 homolog (S. cerevisiae)	2.98	2.80E-04

FC: fold change; pVal: p-value

BMC Genomics 2008, 9:73 http://www.biomedcentral.com/1471-2164/9/73

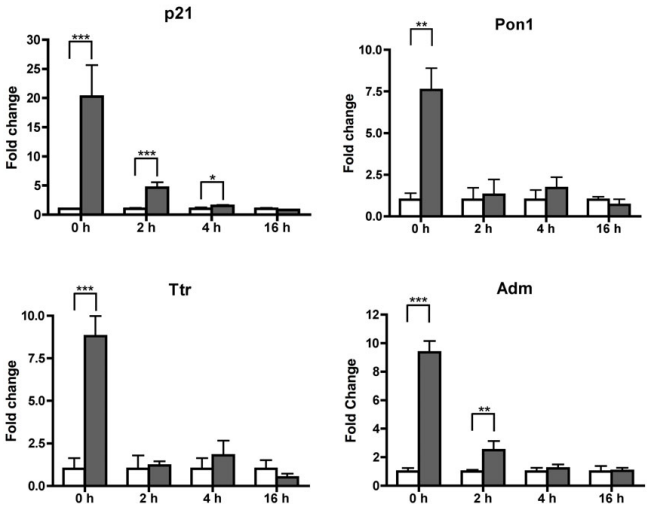

Figure 3
Expression of candidate genes analyzed by real-time PCR. Expression profile of *p21* (*Cdkn1a*), *Pon1* (paraoxonase 1) *Ttr* (transthyretin) and *Adm* (adrenomedullin) immediately after hypoxic exposure (0 h), or after a period of 2 h, 4 h or 16 h of reoxygenation as determined by real-time PCR. Fold-changes are expressed relative to normoxic controls of respective time points, which were set to one. n = 5 for each treatment and time point. White bars: samples of normoxic retinas, grey bars: samples of hypoxic preconditioned retinas; *** $p \geq 0.001$, ** $p \geq 0.01$, * $p \geq 0.05$).

this pathway, which showed at least a two-fold differential regulation on the chip, were tested by real-time PCR. Ten of the 16 tested genes were confirmed to be regulated by hypoxia (Table 3). This suggested that the p21-pathway was indeed strongly affected by the hypoxic preconditioning protocol. Since it is known that p21 not only inhibits cell cycle but can also repress apoptosis [32], it was considered as a strong candidate for the involvement in neuroprotection by hypoxic preconditioning.

The influence of p21 on retinal neuroprotection in the model of light induced degeneration

The hypothesis that p21 is important for neuroprotection in the retina after hypoxic preconditioning was directly tested using p21 knockout animals. Both, normoxic and hypoxic preconditioned $p21^{-/-}$ mice were exposed to high intensity visible light for 2 hours and retinal morphology was analyzed 10 days thereafter (Fig. 5). As expected, normoxic control $p21^{-/-}$ mice showed strong damage after light exposure with the loss of all photoreceptors in the central retina. If p21 was involved in neuroprotection after hypoxic exposure, preconditioned $p21^{-/-}$ mice should show an increased susceptibility to light damage as compared to wild type mice. However, photoreceptors of the p21 knockout mice were completely protected after preconditioning (Fig. 5). The quantification of cell death by biochemical assays (data not shown) supported our conclusion that p21 does not contribute significantly to the neuroprotective effect observed after hypoxic preconditioning. Furthermore, most genes identified by Ingenuity Pathway analysis as being part of the p21 signalling network were similarly regulated in the presence or absence of functional p21. The only exception was Semaphorin 3c (*Sema3c*), which showed no hypoxic upregulation in the absence of p21 (data not shown).

Discussion

Hypoxic preconditioning is strongly neuroprotective and prevents photoreceptor apoptosis after exposure to high levels of visible light [9]. The transcription factors HIF-1 and Stat3 are activated. This suggests differential regulation of the expression of various target genes which was confirmed by the detection of 431 differentially regulated genes immediately after hypoxia. More than 50% of these genes showed at least a 2-fold difference in the expression level as compared to normoxic retinas. Among those were also *Rgr* and *Lrat*, two genes highly expressed in the retinal pigment epithelium. Genes normally not or only barely expressed in the neuronal retina may easily reach a high-fold induction when the tissue is contaminated with neighbouring cells expressing the respective gene at high levels. Low levels of oxygen during hypoxic preconditioning may have altered the physical interaction properties between neuronal retina and retinal pigment epithelium (RPE) leading to an increased contamination rate of the retina by cells of the RPE during tissue isolation. Thus, fold inductions have to be interpreted cautiously.

Reoxygenation caused the rapid return to a normal gene expression pattern. This is in line with a model of hypoxic preconditioning in brain where it was shown that differential gene regulation was low between 12 and 18 hours of reoxygenation [33]. In models of ischemic preconditioning (IPC), however, differential gene expression is observed immediately after the stimulus until up to 7 days after preconditioning [34-36]. This goes together with a long lasting neuroprotective effect of IPC observed in the retina [10] and in brain [37] suggesting that mechanisms of IPC may differ from those of acute hypoxic preconditioning. An extended neuroprotection by hypoxic preconditioning may be achieved by the repetitive exposure to low oxygen [12].

Similarities of hypoxic preconditioning and IPC

Although mechanisms of hypoxic preconditioning and IPC may differ, few genes were found to be differentially regulated in both types of preconditioning protocol. Among those are metallothionein 2 (Mt2), C/ebpd (an apoptosis-related transcription factor) and p21 [35,38]. The identification of these genes makes them strong candidates for playing a role in general retinal neuroprotection.

Table 2: Differentially regulated genes with possible impact on cell survival and neuroprotection; detected and functionally clustered by DAVID.

Affymetrix ID	Gene Symbol	Gene Name	FC
		Up-regulated	
apoptosis ($p \geq 0.032$)			
1424638_at	Cdkn1a	cyclin-dependent kinase inhibitor 1a (p21)	30.5
1416434_at	Bcl2l10	Bcl2-like 10	17.0
1442025_a_at	Zbtb16	zinc finger and btb domain containing 16	3.6
1454109_a_at	Ptdsr	phosphatidylserine receptor	2.4
1420909_at, 1451959_a_at	Vegfa	vascular endothelial growth factor a	2.3
1453851_a_at	Gadd45g	growth arrest and dna-damage-inducible 45 gamma	2.3
1452050_at	Camk1d	calcium/calmodulin-dependent protein kinase id	2.1
1454903_at	Ngfr	nerve growth factor receptor (TNFR superfamily, member 16)	2.0
cell cycle ($p \geq 0.013$)			
1424638_at	Cdkn1a	cyclin-dependent kinase inhibitor 1A (P21)	30.5
1416309_at	Nusap1	nucleolar and spindle associated protein 1	4.4
1454018_at	Tlk2	tousled-like kinase 2 (Arabidopsis)	4.3
1449007_at	Btg3	B-cell translocation gene 3	4.2
1424143_a_at, 1424144_at	Cdt1	retroviral integration site 2	3.4
1419024_at, 1455002_at	Ptp4a1	protein tyrosine phosphatase 4a1	2.7
1453851_a_at	Gadd45g	growth arrest and DNA-damage-inducible 45 gamma	2.3
1420909_at, 1451959_a_at	Vegfa	vascular endothelial growth factor A	2.3
1459978_x_at	-	gene model 877 (NCBI)	2.0
1435870_at	Sycp3	synaptonemal complex protein 3	2.0
negative regulation of transcription ($p \geq 0.031$)			
1442025_a_at	Zbtb16	zinc finger and btb domain containing 16	3.6
1425809_at	Fabp4	Fatty acid binding protein 4, adipocyte (Fabp4), mRNA	3.5
1425895_a_at	Id1	inhibitor of DNA binding 1	3.1
1442397_at	Nfx1	nuclear transcription factor, X-box binding 1	2.7
1425732_a_at	Mxi1	Max interacting protein 1	2.1
		Down-regulated	
regulation of transcription ($p \geq 0.09$)			
1440343_at	Rps6ka5	ribosomal protein S6 kinase, polypeptide 5	0.42
1450034_at	Stat1	signal transducer and activator of transcription 1	0.47
1416826_a_at	Trfp	Trf (TATA binding protein-related factor)-proximal protein homolog (Drosophila)	0.41
1450953_at	Wdr39	WD repeat domain 39	0.27
1421379_at	Zfp354b	zinc finger protein 354B	0.31
1424852_at	Mef2c	myocyte enhancer factor 2C	0.31
1437647_at	Dido1	death inducer-obliterator 1	0.30
1443952_at	Thra	thyroid hormone receptor alpha	0.48
1428760_at	Snapc3	small nuclear RNA activating complex, polypeptide 3	0.40
1456723_at	Prr14	Proline rich 14	0.29

Analysis of the gene expression pattern was immediately after hypoxia; FC: fold change

An involvement of p21 was directly tested using the respective knockout animal. As a HIF-1 target gene [39], p21 was not only very strongly regulated but was also at the center of a highly regulated gene network (Fig. 4). Although p21 can be pro-apoptotic [40] and can trigger non-apoptotic cell death [41], it is also known to have antiapoptotic properties [42]. However, the test of p21 knockout mice in the model of light induced degeneration revealed no significant impact of *p21* on neuroprotection against light damage. Despite the lack of *p21*, all other genes of the p21 pathway (except for *Sema3c*) showed the same response to hypoxic preconditioning as in wild type mice. This raises the possibility that other genes of the p21 network might influence retinal neuroprotection. Specific candidates are *Timp3* which has been reported to be a promoter of apoptosis through the inhibition of metalloproteinases [43] and *Egf* which has proven anti-apoptotic properties [44].

Mt2, as a gene also detected in both preconditioning schemes, may play an important role as a scavenger of free radicals [45]. It is interesting to note that metallothioneins are also induced after ischemic preconditioning of the rat spinal cord [34] and that they have been reported to be neuro- and cardioprotective, respectively, in various degenerative models [46,47]. In addition, metallothioneins have been shown to be induced in light-damaged retinas [48] and to protect retinas from oxidative

BMC Genomics 2008, **9**:73 http://www.biomedcentral.com/1471-2164/9/73

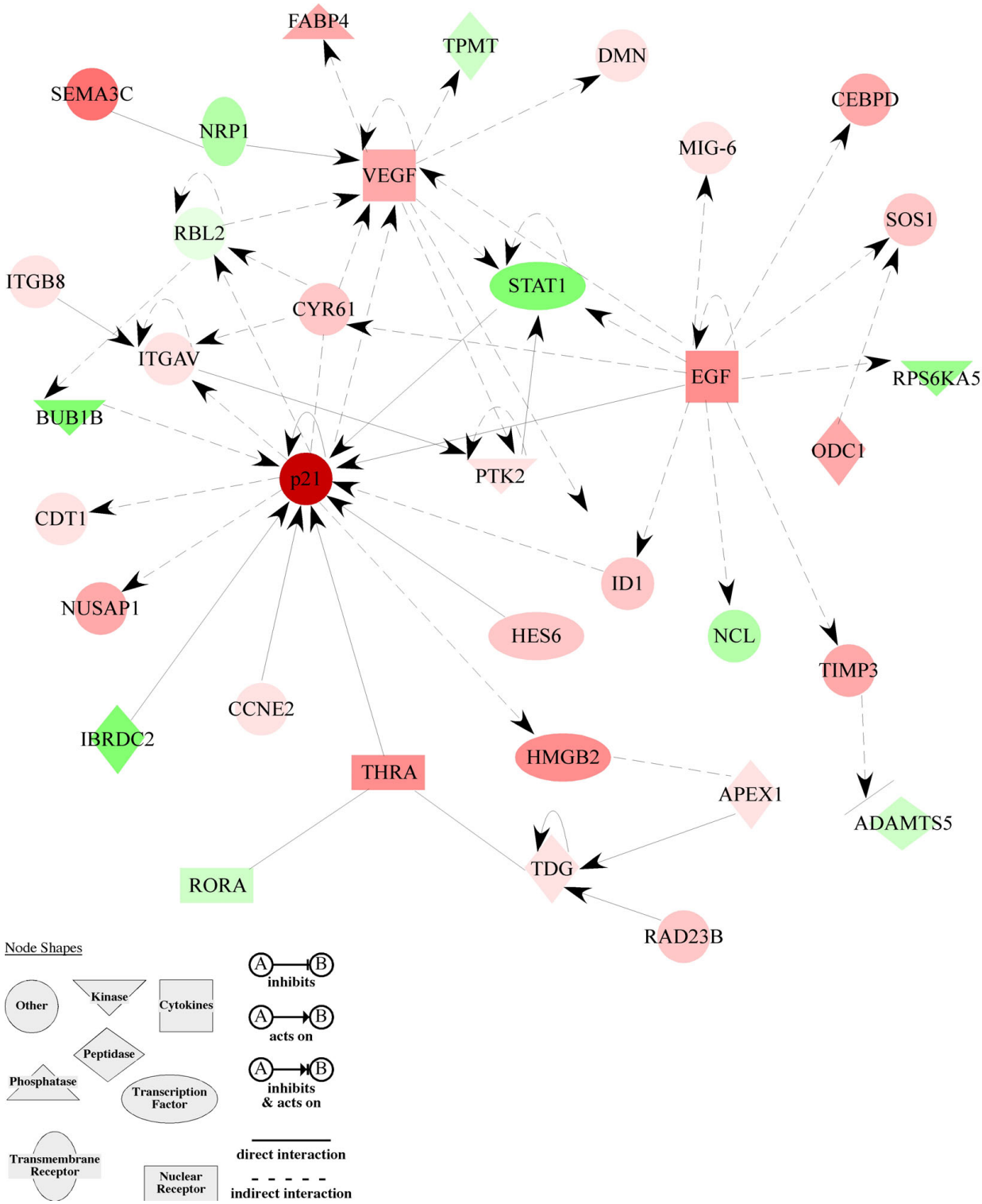

Figure 4

The most prominently affected gene network discovered by Ingenuity Pathway Analysis. Network was classified as: *Cellular growth & proliferation, DNA replication, recombination & repair*. Pathway contains pro survival genes like *Egf*, *Vegf* and *p21*, which occupy central positions in this network. Red: induction; green: repression; white: unaffected; colour intensity correlates with fold change.

Table 3: Real-Time PCR results of 16 genes belonging to the p21 pathway compared to the fold change (FC) detected by Affymetrix microarrays.

Gene symbol	FC Affymetrix Chip	FC PCR
Cdkn1a (p21)	30.5	20.3*
Sema3c	5.9	3.9*
Egf	4.7	2.8*
HMGB2	4.1	3.0*
Fabp4	3.5	5.3*
CEBPd	3.5	3.5*
Timp3	3.3	3.7*
ID1	3.1	1.8*
Rad23b	2.6	1.2
Vegf	2.3	2.0*
Stom	2.0	1.3
Hes6	1.9	1.6*
SOS1	1.9	0.9
Stat1	0.5	1.1
Thra	0.5	0.8
IBRDC2	0.3	0.9

Analysis of gene expression was immediately after hypoxia
FC: fold change. * $p < 0.05$

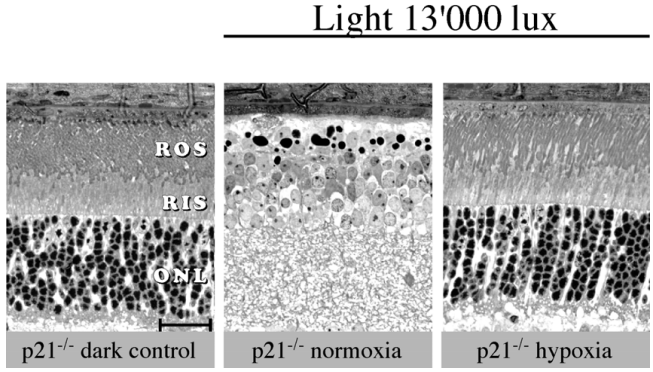

Figure 5
Role of p21 in hypoxic preconditioning. Hypoxic preconditioned (hypoxia) or normoxic (normoxia) $p21^{-/-}$ mice were exposed to 13'000 lux of white light for 2 hours and retinal morphology was analyzed 10 days thereafter. Dark-adapted knockout mice served as controls (dark control). Hypoxic preconditioning almost completely protected the retina of $p21^{-/-}$ mice leading to a retinal morphology indistinguishable from controls. Exposure of normoxic mice led to a complete degeneration of photoreceptors in the central retina. Shown are representative samples of control and light exposed mice. n = 2 (controls); n = 4 (light exposed mice). Abbreviations as in Fig. 1. Scale bar: 25 μm.

stress caused by the glutamate analogue NMDA [49]. Further experiments are clearly needed to evaluate the impact of this protein in retinal neuroprotection.

The low similarity of the transcriptome after IPC and hypoxic preconditioning may be surprising but might be based on the different nature of the preconditioning protocols. Whereas IPC normally uses a very short (minutes) ischemic stimulus followed by reperfusion, our protocol of hypoxic preconditioning uses exposure to 6 hours of low oxygen concentrations followed by the immediate analysis. The different length of exposure to low oxygen and the interrupted supply of nutrients in one (IPC) but not the other protocol might essentially explain the differences in the gene expression patterns.

***Strong candidate genes for neuroprotection:* Adm, Pon1**

Adrenomedullin (*Adm*) is a multifunctional protein involved in angiogenesis, cancer promotion, host defence and neuroprotection [50]. Elevated levels of Adm were found in plasma of patients suffering from retinitis pigmentosa [51]. Previous reports identified *Adm* as a target gene of HIF-1α [52,53] linking it to a possible HIF – mediated protection mechanism.

Interestingly, some genes which so far were not described in the context of hypoxia, like paraoxonase 1 (*Pon1*), were also highly induced. Pon1 is a high-density lipoprotein (HDL) associated enzyme which plays a major role in the prevention of lipid peroxidation [54,55]. Since retinal degeneration involves oxidative stress and inhibition of lipid peroxidation protects against light damage [56] *Pon1* may have an important role in retinal protection after hypoxic preconditioning. Recently, *Pon1* levels were found to be reduced in serum of AMD patients whereas a marker for oxidative stress was elevated [57]. This may suggest that elevated levels of *Pon1* in our model might reduce oxidative stress and prevent photoreceptor degeneration. Interestingly, C57Bl/6 mice which have a reduced sensitivity to light damage show a higher basal expression of *Pon1* than light sensitive strains (data not shown). If the anti-oxidative enzyme Paraoxonase 1 was involved in the protection of the retina against oxidative damage, the different basal expression levels of *Pon1* might contribute to the different light damage susceptibilities of various mouse strains.

Additional genes with potential neuroprotective function

Bcl2-like 10 (*Bcl2l10*) is a anti-apoptotic member of the Bcl2 family [58] acting to suppress cell death by preventing cytochrome c release, casp-3 activation and mitochondrial membrane collapse [59]. However, retinal degeneration induced by acute light exposure may not depend on cytochrome c release or caspase activation [60]. Therefore, upregulation of Bcl2l10 might not be responsible for photoreceptor protection by hypoxic preconditioning.

Induction of the HIF-1 target gene *Vegfa* is an attempt to increase tissue oxygen levels by improving blood circula-

tion through the formation of new vessels [61]. In the retina Vegfa is also recognized as a pro-survival factor protecting retinal neurons against ischemic injury [62]. However, Vegfa is discussed to have also pro-apoptotic properties [63] and its potential role in the preconditioning scheme is unclear. *Ptdsr* encodes a posphatidylserine receptor involved in the clearance of apoptotic cells [64] and it has been shown that lack of Ptdsr activity can increase tissue damage through the stimulation of apoptosis in cells neighbouring apoptotic cells [65]. *Ptdsr* is also involved in the elimination of apoptotic debris of dying photoreceptors by macrophage-mediated phagocytosis which is important for the maintenance of retinal tissue integrity [66].

Downregulated genes with a possible impact on cell death included *Mef2c* and genes of the Rbm family of protein. *Mef2c* triggers apoptosis in macrophages [29] and may be involved in dopaminergic neuron death in Parkinson's disease [28]. Because macrophages seem to play an important role in light induced apoptosis [67,68] a potential influence on neuroprotection may be possible but needs further investigation. This is also true for the identified members of the Rbm family. Although these proteins have been implicated in the modulation of apoptosis [30], and downregulation of *Rbm3* has been specifically connected to the regulation of cell cycle progression [69] and the inhibition of apoptosis [70], their role is still controversial.

Conclusion

Since hypoxia can either lead to adaptation and protection [71] or to apoptosis [72] it may not be surprising that we identified several genes which may rather be involved in promoting apoptosis than in its inhibition. Neuroprotection by hypoxic preconditioning may thus depend on a balance between numerous anti- and proapoptotic factors. The loss of individual proteins like p21 may not be sufficient to shift the balance towards apoptosis. Likewise, it might require several different antiapoptotic factors to fully protect the retina. Full neuroprotection may only be achieved by controlling the central regulators of the hypoxic response like the transcription factors HIF and/or STAT3.

Methods

Animals, hypoxic preconditioning and light damage

Animals were treated in accordance with the regulations of the Veterinary Authority of Zurich and with the statement of 'The Association for Research in Vision and Ophthalmology' for the use of animals in research. BALB/c mice were purchased from Harlan (The Netherlands) and $p21^{-/-}$ mice on a mixed Bl/6;129S2 background were obtained from Jackson Laboratory (Bar Harbor, USA). All mice were homozygous for the light sensitive $Rpe65_{450Leu}$ variant [73]. Hypoxic preconditioning (6% O_2 for 6 hours) was performed as described previously [9]. Reoxygenation was allowed in darkness for 4 h, 8 h, 12 h and 16 h in normal room air. After reoxygenation BALB/c mice were exposed to 5'000 lux of white fluorescent light for 1 h and analyzed at time points as indicated.

Pupils of $p21^{-/-}$ animals (pigmented) were dilated in dim red light using 1% Cyclogyl (Alcon, Cham, Switzerland) and 5% Phenylephrine (Ciba Vision, Niederwangen, Switzerland) 45 minutes prior to illumination. Light dose (13'000 lux) and exposure duration (2 h) was adjusted according to the decreased light damage susceptibility of this mouse strain. After light exposure animals remained in darkness until analyzed or at the most for 36 h.

For morphology mice were sacrificed 36 h or 10 days after light exposure and eyes were enucleated and processed as previously described [74].

RNA isolation and Affymetrix microarrays

Retinas were isolated immediately, 2 h, 4 h and 16 h after hypoxic preconditioning, frozen in liquid nitrogen and stored at -70°C. Normoxic controls were treated in parallel and collected at the same time points. For Affymetrix microarrays 3 retinas of 3 different mice were pooled. This procedure was repeated 3 times to generate independent biological triplicates. RNA was extracted using the RNeasy isolation kit (Qiagen, Hilden, Germany), including a DNase treatment to digest residual genomic DNA. RNA was processed according to standard procedures and hybridized to Affymetrix GeneChip® Mouse Genome 430 2.0 microarrays. The 3 experimental replicates were hybridized independently resulting in three microarray replicates per condition. In total, 24 Affymetrix gene chips were hybridized with RNA from 72 retinas of 72 mice.

Quality control (QC) and Affymetrix microarray analysis

To analyze the quality of the results after gene chip hybridization we employed RReporterGenerator [75] combining Affymetrix-style QC, RMA and residual QC. The complete report is available in additional file 1.

Affymetrix raw gene expression data were summarized and normalized using the GCRMA procedure [76]. The data were filtered in order to remove probe-sets with constant low-level expression. Probe-sets were removed which showed replicate means for a given time-point for both treatments below the threshold separating the two peaks of the bimodal distribution of signal-intensity values. This procedure was performed independently for each of the differential testing procedures. The filtered data-sets were subsequently subjected to t-tests with multiple testing correction and control of the false discovery rate (FDR) using OCplus package [77] available under

Bioconductor [78]. By comparing the plotted number of differentially expressed genes at various FDR levels, corresponding threshold values for the maximum acceptable FDR were chosen with the aim of keeping homogenous groups with similar FDR together.

To group differentially regulated genes according to their biological function the Affymetrix IDs were imported into the Database for Annotation, Visualization and Integrated Discovery (DAVID) from the National Institute of Allergy and Infectious Diseases (NIAID), NIH [31,79] and into Ingenuity Pathway Analyses from Ingenuity Systems [80].

Real-time PCR

cDNA was prepared from equal amounts of total retinal RNA, using oligo(dT) primers and M-MLV reverse transcriptase (Promega, Madison, WI, USA). 10 ng of cDNA was amplified in a LightCycler 480 instrument (Roche Diagnostics AG, Rotkreuz, Switzerland) using LightCycler 480 SYBR Green I Master Mix (Roche Diagnostics AG) and appropriate primer pairs [see additional file 6]. mRNA levels were normalized to β-actin and relative values were calculated using a respective calibrator.

Western blotting

Retinas were homogenized in 0.1 M Tris/HCl (pH 8.0) by sonification at 4°C. The protein content was determined using a Bradford assay (Bio-Rad, Munich, Germany). Protein extracts were mixed with SDS sample buffer and incubated for 10 min at 90°C. Proteins were separated by SDS-PAGE and blotted onto a nitrocellulose membrane. After blocking with 5% non-fat dry milk (Bio-Rad, Munich, Germany) in TBST (Tris/HCl 10 mM, pH 8; 150 mM NaCl; 0.05% Tween-20) membranes were incubated with primary antibodies at 4°C over night. Primary antibodies used were: rabbit anti-HIF-1α (Novus Biologicals NB 100–479; 1:1000), rabbit anti-phospho-STAT3 (Cell Signalling; 1:500), rabbit anti-STAT3 (Cell Signalling 1:1000) and goat anti-β-actin (Santa Cruz; 1:1000). After incubation with horseradish peroxidase labelled secondary antibodies for 1 h at room temperature the protein bands were visualized by the application of a chemiluminescent substrate (PerkinElmer, Boston, USA) and exposure to a Super RX film (Fujifilm, Dielsdorf, Switzerland).

Authors' contributions

MT, RF, MS and CG performed experiments. MT, WR and OP analyzed microarray data. Study was designed by MT, RF, AW and CG. Manuscript was written by MT and CG.

Additional material

Additional file 1

***Fig 1 QC Analyses**. Results of QC analyses using RReporterGenerator. File contains report of QC analyses performed by RReporterGenerator.*
Click here for file
[http://www.biomedcentral.com/content/supplementary/1471-2164-9-73-S1.pdf]

Additional file 2

***Table 1, 2, 3 Gene Lists of differentially regulated genes**. Table 1 List of differentially regulated genes immediately after hypoxia (H0). Table 2 List of differentially regulated genes 2 h after hypoxia (H2). Table 3 List of differentially regulated genes 4 h after hypoxia (H4). File contains all genes found to be differentially regulated immediately after hypoxia (Table 5 H0), 2 h after hypoxia (Table 6, H2) and 4 h after hypoxia (Table 7, H4).*
Click here for file
[http://www.biomedcentral.com/content/supplementary/1471-2164-9-73-S2.xls]

Additional file 3

***Table 4 Real time PCR results**. Table 4 Real-Time PCR results of the expression of genes detected by Affymetrix microarrays as differentially regulated by hypoxic preconditioning. File contains all genes revealed by microarray analyses, which were tested by real time PCR.*
Click here for file
[http://www.biomedcentral.com/content/supplementary/1471-2164-9-73-S3.doc]

Additional file 4

***Table 5,6 List of genes functionally clustered by DAVID**. Table 5 Differentially up-regulated genes functionally clustered by DAVID. Table 6 Differentially down-regulated genes functionally clustered by DAVID. File contains functional clusters of genes found to be differentially regulated immediately after hypoxia (H0 data).*
Click here for file
[http://www.biomedcentral.com/content/supplementary/1471-2164-9-73-S4.xls]

Additional file 5

***Fig 2, 3 Hypoxic preconditioning gene networks discovered by Ingenuity Pathway analysis**. Fig 2 affected gene network discovered by Ingenuity Pathway Analysis and classified as: DNA replication, recombination, cell cycle and cancer. Fig. 3 affected gene network discovered by Ingenuity Pathway Analysis and classified as: Cell death, cellular development, hematological system development & function. File contains schemes of pathways, which are affected by hypoxic preconditioning. Some genes connected to cMyc (Fig. 7) and to TGF-b (Fig. 8) are differentially regulated.*
Click here for file
[http://www.biomedcentral.com/content/supplementary/1471-2164-9-73-S5.doc]

Additional file 6

***Table 7 Primer Sequences and product sizes**. Table 7 Primer pairs used for real time PCR. File contains sequences of Primers used for real time PCR and the expected/obtained product sizes in bp.*
Click here for file
[http://www.biomedcentral.com/content/supplementary/1471-2164-9-73-S6.doc]

Acknowledgements

The authors thank Coni Imsand, Gaby Hoegger, Hedwig Wariwoda, Philipp Huber and the Plate-Forme BioInformatique de Strasbourg for excellent technical assistance. This work was supported by the Swiss National Science Foundation (SNF, grant 3100A0-105793), the Fritz-Tobler-Foundation, the Centre of Integrative Human Physiology (CIHP) of the University of Zurich and the European Union (Evi-GenoRet, LSHG-CT-512036). WR was supported by the European Retinal Research Training Network 'RET-NET' (MRTN-CT-2003-504003), CNRS, INSERM and Université Louis Pasteur de Strasbourg. Prof. Klara Landau is acknowledged for constant support.

References

1. Doonan F, Donovan M, Cotter TG: **Caspase-independent photoreceptor apoptosis in mouse models of retinal degeneration.** *J Neurosci* 2003, **23(13):**5723-5731.
2. Dalke C, Graw J: **Mouse mutants as models for congenital retinal disorders.** *Exp Eye Res* 2005, **81(5):**503-512.
3. Wenzel A, Grimm C, Samardzija M, Reme CE: **Molecular mechanisms of light-induced photoreceptor apoptosis and neuroprotection for retinal degeneration.** *Prog Retin Eye Res* 2005, **24(2):**275-306.
4. Emerson MR, Nelson SR, Samson FE, Pazdernik TL: **A global hypoxia preconditioning model: neuroprotection against seizure-induced specific gravity changes (edema) and brain damage in rats.** *Brain Res Brain Res Protoc* 1999, **4(3):**360-366.
5. Kitagawa K, Matsumoto M, Tagaya M, Hata R, Ueda H, Niinobe M, Handa N, Fukunaga R, Kimura K, Mikoshiba K, Kamada T: **'Ischemic tolerance' phenomenon found in the brain.** *Brain Res* 1990, **528(1):**21-24.
6. Cai Z, Manalo DJ, Wei G, Rodriguez ER, Fox-Talbot K, Lu H, Zweier JL, Semenza GL: **Hearts from rodents exposed to intermittent hypoxia or erythropoietin are protected against ischemia-reperfusion injury.** *Circulation* 2003, **108(1):**79-85.
7. Dong JW, Zhu HF, Zhu WZ, Ding HL, Ma TM, Zhou ZN: **Intermittent hypoxia attenuates ischemia/reperfusion induced apoptosis in cardiac myocytes via regulating Bcl-2/Bax expression.** *Cell Res* 2003, **13(5):**385-391.
8. Gidday JM, Fitzgibbons JC, Shah AR, Park TS: **Neuroprotection from ischemic brain injury by hypoxic preconditioning in the neonatal rat.** *Neurosci Lett* 1994, **168(1–2):**221-224.
9. Grimm C, Wenzel A, Groszer M, Mayser H, Seeliger M, Samardzija M, Bauer C, Gassmann M, Reme CE: **HIF-1-induced erythropoietin in the hypoxic retina protects against light-induced retinal degeneration.** *Nat Med* 2002, **8(7):**718-724.
10. Roth S, Li B, Rosenbaum PS, Gupta H, Goldstein IM, Maxwell KM, Gidday JM: **Preconditioning provides complete protection against retinal ischemic injury in rats.** *Invest Ophthalmol Vis Sci* 1998, **39(5):**777-785.
11. Zhang C, Rosenbaum DM, Shaikh AR, Li Q, Rosenbaum PS, Pelham DJ, Roth S: **Ischemic preconditioning attenuates apoptotic cell death in the rat retina.** *Invest Ophthalmol Vis Sci* 2002, **43(9):**3059-3066.
12. Zhu Y, Zhang Y, Ojwang BA, Brantley MA Jr, Gidday JM: **Long-term tolerance to retinal ischemia by repetitive hypoxic preconditioning: role of HIF-1alpha and heme oxygenase-1.** *Invest Ophthalmol Vis Sci* 2007, **48(4):**1735-1743.
13. Michiels C: **Physiological and pathological responses to hypoxia.** *Am J Pathol* 2004, **164(6):**1875-1882.
14. Fisher SA, Burggren WW: **Role of Hypoxia in the Evolution and Development of the Cardiovascular System.** *Antioxid Redox Signal* 2007.
15. Cringle SJ, Yu DY, Yu PK, Su EN: **Intraretinal oxygen consumption in the rat in vivo.** *Invest Ophthalmol Vis Sci* 2002, **43(6):**1922-1927.
16. Semenza GL: **HIF-1: mediator of physiological and pathophysiological responses to hypoxia.** *J Appl Physiol* 2000, **88(4):**1474-1480.
17. Fruehauf JP, Meyskens FL Jr: **Reactive oxygen species: a breath of life or death?** *Clin Cancer Res* 2007, **13(3):**789-794.
18. Bardos JI, Ashcroft M: **Negative and positive regulation of HIF-1: a complex network.** *Biochim Biophys Acta* 2005, **1755(2):**107-120.
19. Junk AK, Mammis A, Savitz SI, Singh M, Roth S, Malhotra S, Rosenbaum PS, Cerami A, Brines M, Rosenbaum DM: **Erythropoietin administration protects retinal neurons from acute ischemia-reperfusion injury.** *Proc Natl Acad Sci USA* 2002, **99(16):**10659-10664.
20. Grimm C, Wenzel A, Stanescu D, Samardzija M, Hotop S, Groszer M, Naash M, Gassmann M, Reme C: **Constitutive overexpression of human erythropoietin protects the mouse retina against induced but not inherited retinal degeneration.** *J Neurosci* 2004, **24(25):**5651-5658.
21. Rex TS, Allocca M, Domenici L, Surace EM, Maguire AM, Lyubarsky A, Cellerino A, Bennett J, Auricchio A: **Systemic but not intraocular Epo gene transfer protects the retina from light-and genetic-induced degeneration.** *Mol Ther* 2004, **10(5):**855-861.
22. Shih SC, Claffey KP: **Hypoxia-mediated regulation of gene expression in mammalian cells.** *Int J Exp Pathol* 1998, **79(6):**347-357.
23. Stephanou A: **Role of STAT-1 and STAT-3 in ischaemia/reperfusion injury.** *J Cell Mol Med* 2004, **8(4):**519-525.
24. Jung JE, Lee HG, Cho IH, Chung DH, Yoon SH, Yang YM, Lee JW, Choi S, Park JW, Ye SK, Chung MH: **STAT3 is a potential modulator of HIF-1-mediated VEGF expression in human renal carcinoma cells.** *Faseb J* 2005, **19(10):**1296-1298.
25. Rajkovic A, Yan C, Yan W, Klysik M, Matzuk MM: **Obox, a family of homeobox genes preferentially expressed in germ cells.** *Genomics* 2002, **79(5):**711-717.
26. Udono T, Takahashi K, Nakayama M, Yoshinoya A, Totsune K, Murakami O, Durlu YK, Tamai M, Shibahara S: **Induction of adrenomedullin by hypoxia in cultured retinal pigment epithelial cells.** *Invest Ophthalmol Vis Sci* 2001, **42(5):**1080-1086.
27. Xia CF, Yin H, Borlongan CV, Chao J, Chao L: **Adrenomedullin gene delivery protects against cerebral ischemic injury by promoting astrocyte migration and survival.** *Hum Gene Ther* 2004, **15(12):**1243-1254.
28. Smith PD, Mount MP, Shree R, Callaghan S, Slack RS, Anisman H, Vincent I, Wang X, Mao Z, Park DS: **Calpain-regulated p35/cdk5 plays a central role in dopaminergic neuron death through modulation of the transcription factor myocyte enhancer factor 2.** *J Neurosci* 2006, **26(2):**440-447.
29. Fu W, Wei J, Gu J: **MEF2C mediates the activation induced cell death (AICD) of macrophages.** *Cell Res* 2006, **16(6):**559-565.
30. Sutherland LC, Rintala-Maki ND, White RD, Morin CD: **RNA binding motif (RBM) proteins: a novel family of apoptosis modulators?** *J Cell Biochem* 2005, **94(1):**5-24.
31. Dennis G Jr, Sherman BT, Hosack DA, Yang J, Gao W, Lane HC, Lempicki RA: **DAVID: Database for Annotation, Visualization, and Integrated Discovery.** *Genome Biol* 2003, **4(5):**P3.
32. Mahyar-Roemer M, Roemer K: **p21 Waf1/Cip1 can protect human colon carcinoma cells against p53-dependent and p53-independent apoptosis induced by natural chemopreventive and therapeutic agents.** *Oncogene* 2001, **20(26):**3387-3398.
33. Tang Y, Pacary E, Freret T, Divoux D, Petit E, Schumann-Bard P, Bernaudin M: **Effect of hypoxic preconditioning on brain genomic response before and following ischemia in the adult mouse: identification of potential neuroprotective candidates for stroke.** *Neurobiol Dis* 2006, **21(1):**18-28.
34. Carmel JB, Kakinohana O, Mestril R, Young W, Marsala M, Hart RP: **Mediators of ischemic preconditioning identified by microarray analysis of rat spinal cord.** *Exp Neurol* 2004, **185(1):**81-96.
35. Kamphuis W, Dijk F, van Soest S, Bergen AA: **Global gene expression profiling of ischemic preconditioning in the rat retina.** *Mol Vis* 2007, **13:**1020-1030.
36. Kawahara N, Wang Y, Mukasa A, Furuya K, Shimizu T, Hamakubo T, Aburatani H, Kodama T, Kirino T: **Genome-wide gene expression analysis for induced ischemic tolerance and delayed neuronal death following transient global ischemia in rats.** *J Cereb Blood Flow Metab* 2004, **24(2):**212-223.
37. Barone FC, White RF, Spera PA, Ellison J, Currie RW, Wang X, Feuerstein GZ: **Ischemic preconditioning and brain tolerance: temporal histological and functional outcomes, protein synthesis requirement, and interleukin-1 receptor antagonist and early gene expression.** *Stroke* 1998, **29(9):**1937-1950. discussion 1950-1931

38. Kamphuis W, Dijk F, van Soest S, Bergen AA: **Ischemic preconditioning alters the pattern of gene expression changes in response to full retinal ischemia.** *Mol Vis* 2007, **13:**1892-1901.
39. Koshiji M, Kageyama Y, Pete EA, Horikawa I, Barrett JC, Huang LE: **HIF-1alpha induces cell cycle arrest by functionally counteracting Myc.** *Embo J* 2004, **23(9):**1949-1956.
40. Chen T, Turner J, McCarthy S, Scaltriti M, Bettuzzi S, Yeatman TJ: **Clusterin-mediated apoptosis is regulated by adenomatous polyposis coli and is p21 dependent but p53 independent.** *Cancer Res* 2004, **64(20):**7412-7419.
41. Kwon YH, Jovanovic A, Serfas MS, Tyner AL: **The Cdk inhibitor p21 is required for necrosis, but it inhibits apoptosis following toxin-induced liver injury.** *J Biol Chem* 2003, **278(32):**30348-30355.
42. Sharma RR, Ravikumar TS, Raimo D, Yang WL: **Induction of p21WAF1 expression protects HT29 colon cancer cells from apoptosis induced by cryoinjury.** *Ann Surg Oncol* 2005, **12(9):**743-752.
43. Wetzel M, Rosenberg GA, Cunningham LA: **Tissue inhibitor of metalloproteinases-3 and matrix metalloproteinase-3 regulate neuronal sensitivity to doxorubicin-induced apoptosis.** *Eur J Neurosci* 2003, **18(5):**1050-1060.
44. Hicks D, Heidinger V, Mohand-Said S, Sahel J, Dreyfus H: **Growth factors and gangliosides as neuroprotective agents in excitotoxicity and ischemia.** *Gen Pharmacol* 1998, **30(3):**265-273.
45. Andrews GK, Lee DK, Ravindra R, Lichtlen P, Sirito M, Sawadogo M, Schaffner W: **The transcription factors MTF-1 and USF1 cooperate to regulate mouse metallothionein-I expression in response to the essential metal zinc in visceral endoderm cells during early development.** *Embo J* 2001, **20(5):**1114-1122.
46. Ebadi M, Brown-Borg H, El Refaey H, Singh BB, Garrett S, Shavali S, Sharma SK: **Metallothionein-mediated neuroprotection in genetically engineered mouse models of Parkinson's disease.** *Brain Res Mol Brain Res* 2005, **134(1):**67-75.
47. Kang YJ, Chen Y, Yu A, Voss-McCowan M, Epstein PN: **Overexpression of metallothionein in the heart of transgenic mice suppresses doxorubicin cardiotoxicity.** *J Clin Invest* 1997, **100(6):**1501-1506.
48. Chen L, Wu W, Dentchev T, Wong R, Dunaief JL: **Increased metallothionein in light damaged mouse retinas.** *Exp Eye Res* 2004, **79(2):**287-293.
49. Suemori S, Shimazawa M, Kawase K, Satoh M, Nagase H, Yamamoto T, Hara H: **Metallothionein, an endogenous antioxidant, protects against retinal neuron damage in mice.** *Invest Ophthalmol Vis Sci* 2006, **47(9):**3975-3982.
50. Miyashita K, Itoh H, Arai H, Suganami T, Sawada N, Fukunaga Y, Sone M, Yamahara K, Yurugi-Kobayashi T, Park K, Oyamada N, Sawada N, Taura D, Tsujimoto H, Chao TH, Tamura N, Mukoyama M, Nakao K: **The neuroprotective and vasculo-neuro-regenerative roles of adrenomedullin in ischemic brain and its therapeutic potential.** *Endocrinology* 2006, **147(4):**1642-1653.
51. Vingolo EM, Lupo S, Domanico D, Cotesta D, Petramala L, Grenga R, Letizia C: **Adrenomedullin plasma concentrations in patients with retinitis pigmentosa.** *Clin Biochem* 2005, **38(8):**735-738.
52. Garayoa M, Martinez A, Lee S, Pio R, An WG, Neckers L, Trepel J, Montuenga LM, Ryan H, Johnson R, Gassmann M, Cuttitta F: **Hypoxiainducible factor-1 (HIF-1) up-regulates adrenomedullin expression in human tumor cell lines during oxygen deprivation: a possible promotion mechanism of carcinogenesis.** *Mol Endocrinol* 2000, **14(6):**848-862.
53. Leonard MO, Cottell DC, Godson C, Brady HR, Taylor CT: **The role of HIF-1 alpha in transcriptional regulation of the proximal tubular epithelial cell response to hypoxia.** *J Biol Chem* 2003, **278(41):**40296-40304.
54. Ferre N, Marsillach J, Camps J, Mackness B, Mackness M, Riu F, Coll B, Tous M, Joven J: **Paraoxonase-1 is associated with oxidative stress, fibrosis and FAS expression in chronic liver diseases.** *J Hepatol* 2006, **45(1):**51-59.
55. Mackness B, Hine D, Liu Y, Mastorikou M, Mackness M: **Paraoxonase-1 inhibits oxidised LDL-induced MCP-1 production by endothelial cells.** *Biochem Biophys Res Commun* 2004, **318(3):**680-683.
56. Tanito M, Li F, Elliott MH, Dittmar M, Anderson RE: **Protective effect of TEMPOL derivatives against light-induced retinal damage in rats.** *Invest Ophthalmol Vis Sci* 2007, **48(4):**1900-1905.
57. Baskol G, Karakucuk S, Oner AO, Baskol M, Kocer D, Mirza E, Saraymen R, Ustdal M: **Serum paraoxonase 1 activity and lipid peroxidation levels in patients with age-related macular degeneration.** *Ophthalmologica* 2006, **220(1):**12-16.
58. Song Q, Kuang Y, Dixit VM, Vincenz C: **Boo, a novel negative regulator of cell death, interacts with Apaf-1.** *Embo J* 1999, **18(1):**167-178.
59. Zhang H, Holzgreve W, De Geyter C: **Bcl2-L-10, a novel anti-apoptotic member of the Bcl-2 family, blocks apoptosis in the mitochondria death pathway but not in the death receptor pathway.** *Hum Mol Genet* 2001, **10(21):**2329-2339.
60. Donovan M, Cotter TG: **Caspase-independent photoreceptor apoptosis in vivo and differential expression of apoptotic protease activating factor-1 and caspase-3 during retinal development.** *Cell Death Differ* 2002, **9(11):**1220-1231.
61. Argraves WS, Larue AC, Fleming PA, Drake CJ: **VEGF signaling is required for the assembly but not the maintenance of embryonic blood vessels.** *Dev Dyn* 2002, **225(3):**298-304.
62. Nishijima K, Ng YS, Zhong L, Bradley J, Schubert W, Jo N, Akita J, Samuelsson SJ, Robinson GS, Adamis AP, Shima DT: **Vascular endothelial growth factor-A is a survival factor for retinal neurons and a critical neuroprotectant during the adaptive response to ischemic injury.** *Am J Pathol* 2007, **171(1):**53-67.
63. Ferrari G, Pintucci G, Seghezzi G, Hyman K, Galloway AC, Mignatti P: **VEGF, a prosurvival factor, acts in concert with TGF-beta1 to induce endothelial cell apoptosis.** *Proc Natl Acad Sci USA* 2006, **103(46):**17260-17265.
64. Fadok VA, Bratton DL, Rose DM, Pearson A, Ezekewitz RA, Henson PM: **A receptor for phosphatidylserine-specific clearance of apoptotic cells.** *Nature* 2000, **405(6782):**85-90.
65. Hong JR, Lin GH, Lin CJ, Wang WP, Lee CC, Lin TL, Wu JL: **Phosphatidylserine receptor is required for the engulfment of dead apoptotic cells and for normal embryonic development in zebrafish.** *Development* 2004, **131(21):**5417-5427.
66. Hisatomi T, Sakamoto T, Sonoda KH, Tsutsumi C, Qiao H, Enaida H, Yamanaka I, Kubota T, Ishibashi T, Kura S, Susin SA, Kroemer G: **Clearance of apoptotic photoreceptors: elimination of apoptotic debris into the subretinal space and macrophage-mediated phagocytosis via phosphatidylserine receptor and integrin alphavbeta3.** *Am J Pathol* 2003, **162(6):**1869-1879.
67. Gordon WC, Casey DM, Lukiw WJ, Bazan NG: **DNA damage and repair in light-induced photoreceptor degeneration.** *Invest Ophthalmol Vis Sci* 2002, **43(11):**3511-3521.
68. Hoppeler T, Hendrickson P, Dietrich C, Reme C: **Morphology and timecourse of defined photochemical lesions in the rabbit retina.** *Curr Eye Res* 1988, **7(9):**849-860.
69. Baghdoyan S, Dubreuil P, Eberle F, Gomez S: **Capture of cytokin-eresponsive genes (NACA and RBM3) using a gene trap approach.** *Blood* 2000, **95(12):**3750-3757.
70. Baldi A, Battista T, De Luca A, Santini D, Rossiello L, Baldi F, Natali PG, Lombardi D, Picardo M, Felsani A, Paggi MG: **Identification of genes down-regulated during melanoma progression: a cDNA array study.** *Exp Dermatol* 2003, **12(2):**213-218.
71. Liu J, Narasimhan P, Lee YS, Song YS, Endo H, Yu F, Chan PH: **Mild hypoxia promotes survival and proliferation of SOD2-deficient astrocytes via c-Myc activation.** *J Neurosci* 2006, **26(16):**4329-4337.
72. Liu T, Laurell C, Selivanova G, Lundeberg J, Nilsson P, Wiman KG: **Hypoxia induces p53-dependent transactivation and Fas/CD95-dependent apoptosis.** *Cell Death Differ* 2007, **14(3):**411-421.
73. Wenzel A, Grimm C, Samardzija M, Reme CE: **The genetic modifier Rpe65Leu(450): effect on light damage susceptibility in c-Fos-deficient mice.** *Invest Ophthalmol Vis Sci* 2003, **44(6):**2798-2802.
74. Samardzija M, Wenzel A, Aufenberg S, Thiersch M, Reme C, Grimm C: **Differential role of Jak-STAT signaling in retinal degenerations.** *Faseb J* 2006, **20(13):**2411-2413.
75. Raffelsberger W, Krause Y: **RReportGenerator: Automatic reports from routine statistical analysis using R.** *Bioinformatics* 2008, **24(2):**276-278.
76. Wu Z, Rafael A, Irizarry R, Gentleman R, Martinez-Murillo F, Spencer F: **A model-based background adjustment for oligonucleotide expression arrays.** *J Am Stat Assoc* 2004, **99:**909-917.

77. Ploner A, Calza S, Gusnanto A, Pawitan Y: **Multidimensional local false discovery rate for microarray studies.** *Bioinformatics* 2006, **22(5):**556-565.
78. Gentleman RC, Carey VJ, Bates DM, Bolstad B, Dettling M, Dudoit S, Ellis B, Gautier L, Ge Y, Gentry J, Hornik K, Hothorn T, Huber W, Iacus S, Irizarry R, Leisch F, Li C, Maechler M, Rossini AJ, Sawitzki G, Smith C, Smyth G, Tierney L, Yang JY, Zhang J: **Bioconductor: open software development for computational biology and bioinformatics.** *Genome Biol* 2004, **5(10):**R80.
79. **Database for Annotation, Visualization and Integrated Discovery (DAVID)** [http://david.abcc.ncifcrf.gov/home.jsp]
80. **Ingenuity Systems, CA, USA** [http://www.ingenuity.com]

3.1.1 Supplemental Data for Thiersch et al., 2008, BMC Genomics

3.1.1.1 Quality Control Analyses (Additional File 1)

Affymetrix Batch QC using RReportGenerator and R

September 21, 2007

This document was generated by Analysis Type File *automAffyQC2.Rnw'*, Version: 1.0.8
a protocol for automated QC analysis for Affymetrix expression array data.
Written by wolfgang.raffelsberger@igbmc.u-strasbg.fr, LGBI, IGBMC (Strasbourg, France).

QC analysis of 24 cel-files of type Mouse430.2 found in :

```
[1] "/genomics/g6/CELs/retine/Gri_Hypox/all"
```

page 3
The blots address original PM values, either as boxplot or as density estimate for the signal distribution (similar to packages simpleaffy and affyQCReport).

page 4
This figure shows the QC plot from the simpleaffy package. Briefly, these plots show the 3' to 5' ratio for spiked-in and control genes (typically with triangles for b-Actin and squares fro GAPDH). The dot with the vertical line (heading to 0) shows the scaling factor. Finally, the percentage of present calls and value of average background are shown in the left part of the image.

page 5
This pair of graphs shows the RLE (top) and NUSE (bottom) plots from the affyPLM package. The RLE compares expression values on each array against median expression values, for a probeset across all arrays, and the NUSE plot shows the standard errors for each gene standardized across all arrays.

page 6
This page shows false color images for the residuals (from the affyPLM package, with red intensities corresponding to positive residuals and blue to negative residuals).

page 7
MA plots (from affyPLM package) of each array against a synthetic median array (constructed from probe-wise medians). The red line represents a lowess fit to the scatter plot and is helpful in indicating non-linear relationships.

page 8
In the top part the RNA degaradation plot shows the average intensity with respect to the sorted 5' to 3' position of the probes in the target-sequence. Depending on the type of microarray specific patters can be observed (see also Bolstad and Gentleman et al) . The lower figure shows a density estimate for the signal distribution of data resulting from RMA.

page 9
Similarity between GCRMA summarized samples measured as Eucliedean Distance.
Top: Distance matrix for all pairwise comparisons. Red cells indicate very similar samples.
Bottom: Dendrogram from Hierarchical Clustering with Bootstrap p-Values. Approximately Unbiased (AU) p values are shown in red, Bootstrap Probability (BP) in green. AU might be a better approximation to unbiased p-value than BP values (Suzuki et al).

The aim of this report is to provide information on multiple QC aspects for a set of Affymetrix arrays. The interpretation of QC parameters and QC plots should be done with care since this may lead to delicate decisions. For further information and details about the plots shown in this report please look at the references section.

The analysis was run on September 21, 2007 , using R version 2.5.1 on a x86-64-unknown-linux-gnu system.

..total computing time : 417.6 min

Overview of Arrays Used

array index	sample names
1 ...	mz_251105_mz_H0_1
2 ...	mz_251105_mz_H0_2
3 ...	mz_251105_mz_H0_3
4 ...	mz_251105_mz_H16_1
5 ...	mz_251105_mz_H16_2
6 ...	mz_251105_mz_H16_3
7 ...	mz_251105_mz_H2_1
8 ...	mz_251105_mz_H2_2
9 ...	mz_251105_mz_H2_3
10 ...	mz_251105_mz_H4_1
11 ...	mz_251105_mz_H4_2
12 ...	mz_251105_mz_H4_3
13 ...	mz_251105_mz_N0_1
14 ...	mz_251105_mz_N0_2
15 ...	mz_251105_mz_N0_3
16 ...	mz_251105_mz_N16_1
17 ...	mz_251105_mz_N16_2
18 ...	mz_251105_mz_N16_3
19 ...	mz_251105_mz_N2_1
20 ...	mz_251105_mz_N2_2
21 ...	mz_251105_mz_N2_3
22 ...	mz_251105_mz_N4_1
23 ...	mz_251105_mz_N4_2
24 ...	mz_251105_mz_N4_3

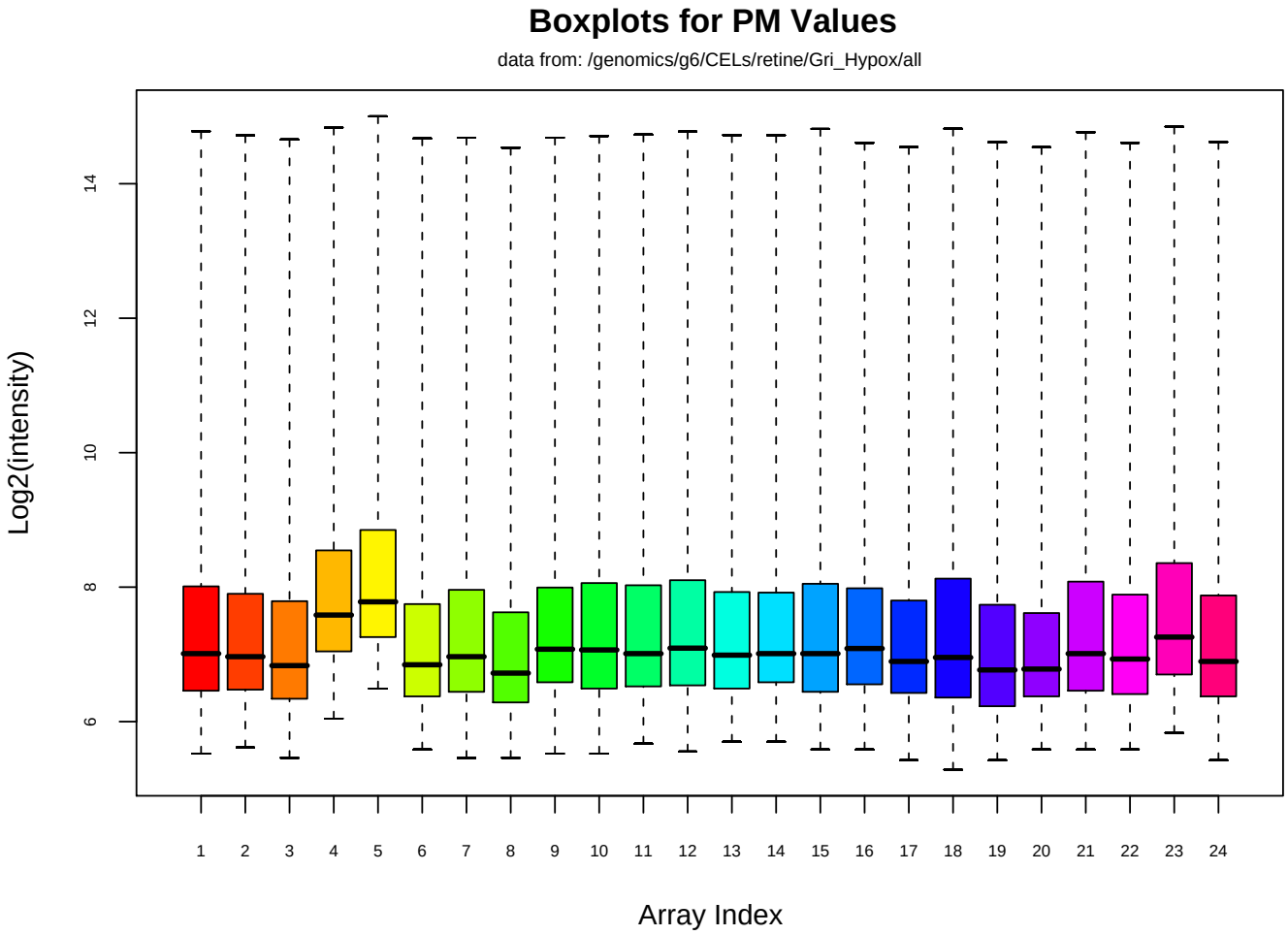
Boxplots for PM Values
data from: /genomics/g6/CELs/retine/Gri_Hypox/all
Log2(intensity)
6
8
10
12
14
1 2 3 4 5 6 7 8 9 10 11 12 13 14 15 16 17 18 19 20 21 22 23 24
Array Index

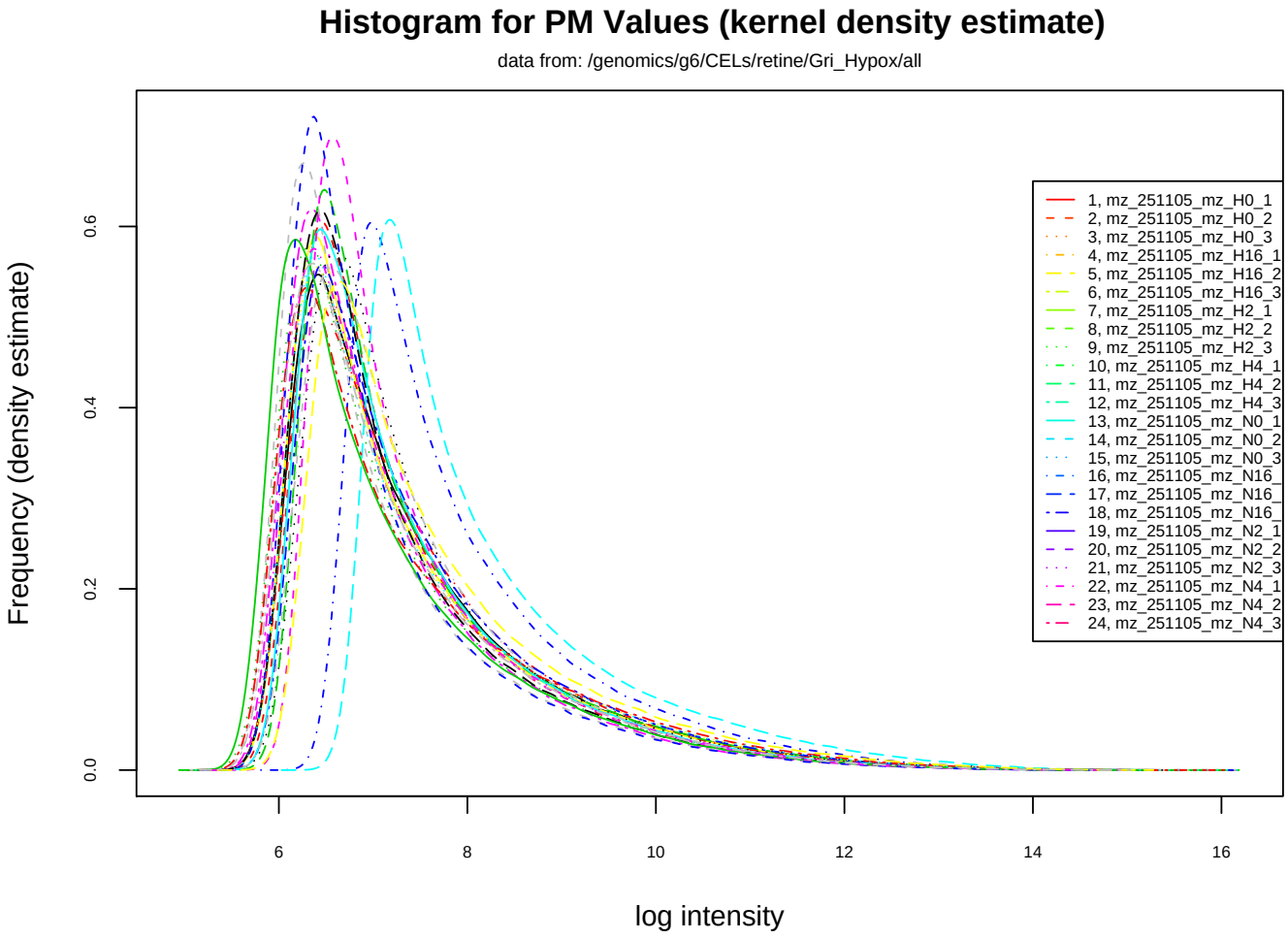
Histogram for PM Values (kernel density estimate)
data from: /genomics/g6/CELs/retine/Gri_Hypox/all
Frequency (density estimate)
0.0
0.2
0.4
0.6
6 8 10 12 14 16
log intensity
1, mz_251105_mz_H0_1
2, mz_251105_mz_H0_2
3, mz_251105_mz_H0_3
4, mz_251105_mz_H16_1
5, mz_251105_mz_H16_2
6, mz_251105_mz_H16_3
7, mz_251105_mz_H2_1
8, mz_251105_mz_H2_2
9, mz_251105_mz_H2_3
10, mz_251105_mz_H4_1
11, mz_251105_mz_H4_2
12, mz_251105_mz_H4_3
13, mz_251105_mz_N0_1
14, mz_251105_mz_N0_2
15, mz_251105_mz_N0_3
16, mz_251105_mz_N16_
17, mz_251105_mz_N16_
18, mz_251105_mz_N16_
19, mz_251105_mz_N2_1
20, mz_251105_mz_N2_2
21, mz_251105_mz_N2_3
22, mz_251105_mz_N4_1
23, mz_251105_mz_N4_2
24, mz_251105_mz_N4_3

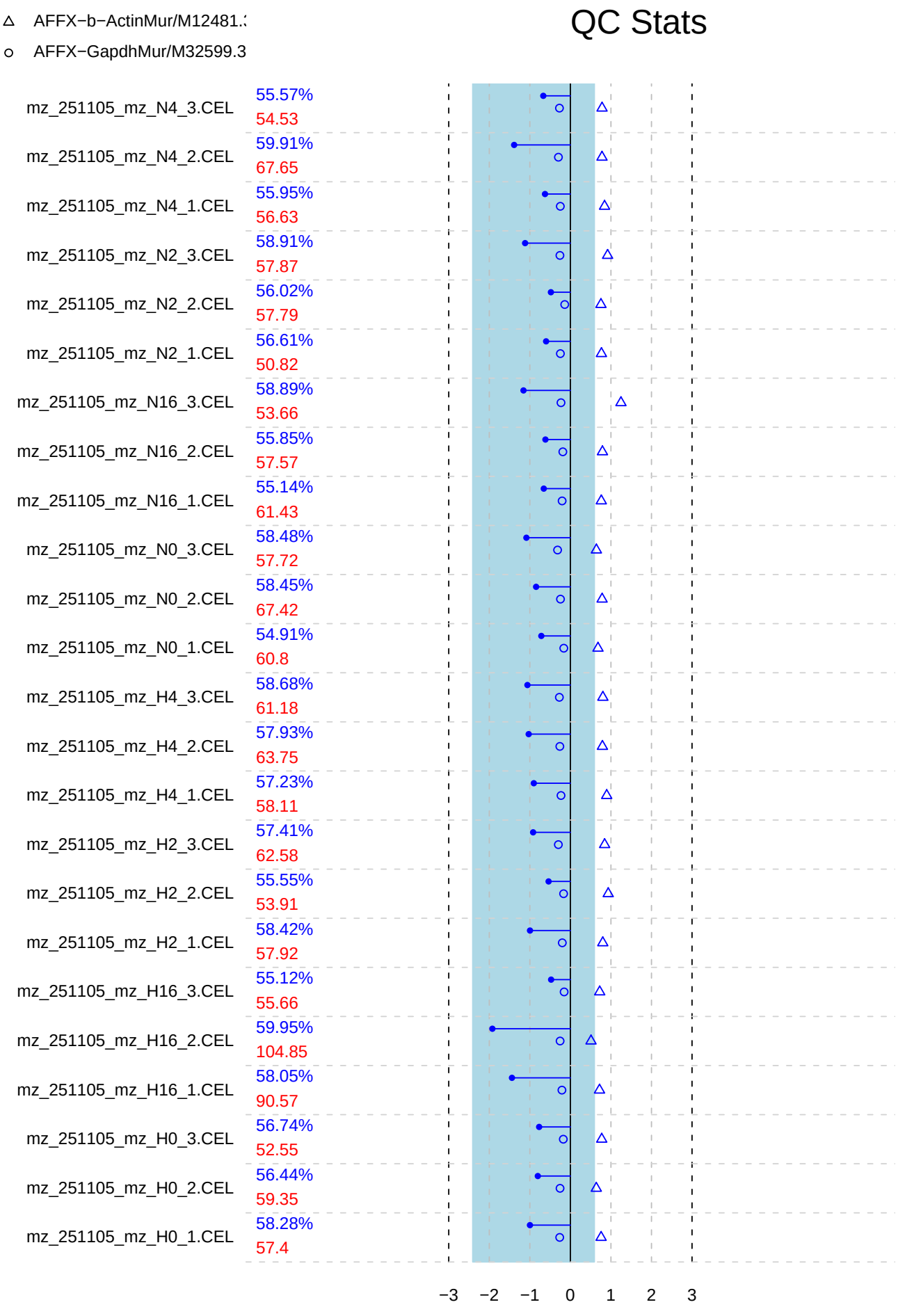
△ AFFX−b−ActinMur/M12481.3
○ AFFX−GapdhMur/M32599.3
QC Stats
mz_251105_mz_N4_3.CEL 55.57% 54.53
mz_251105_mz_N4_2.CEL 59.91% 67.65
mz_251105_mz_N4_1.CEL 55.95% 56.63
mz_251105_mz_N2_3.CEL 58.91% 57.87
mz_251105_mz_N2_2.CEL 56.02% 57.79
mz_251105_mz_N2_1.CEL 56.61% 50.82
mz_251105_mz_N16_3.CEL 58.89% 53.66
mz_251105_mz_N16_2.CEL 55.85% 57.57
mz_251105_mz_N16_1.CEL 55.14% 61.43
mz_251105_mz_N0_3.CEL 58.48% 57.72
mz_251105_mz_N0_2.CEL 58.45% 67.42
mz_251105_mz_N0_1.CEL 54.91% 60.8
mz_251105_mz_H4_3.CEL 58.68% 61.18
mz_251105_mz_H4_2.CEL 57.93% 63.75
mz_251105_mz_H4_1.CEL 57.23% 58.11
mz_251105_mz_H2_3.CEL 57.41% 62.58
mz_251105_mz_H2_2.CEL 55.55% 53.91
mz_251105_mz_H2_1.CEL 58.42% 57.92
mz_251105_mz_H16_3.CEL 55.12% 55.66
mz_251105_mz_H16_2.CEL 59.95% 104.85
mz_251105_mz_H16_1.CEL 58.05% 90.57
mz_251105_mz_H0_3.CEL 56.74% 52.55
mz_251105_mz_H0_2.CEL 56.44% 59.35
mz_251105_mz_H0_1.CEL 58.28% 57.4
−3 −2 −1 0 1 2 3

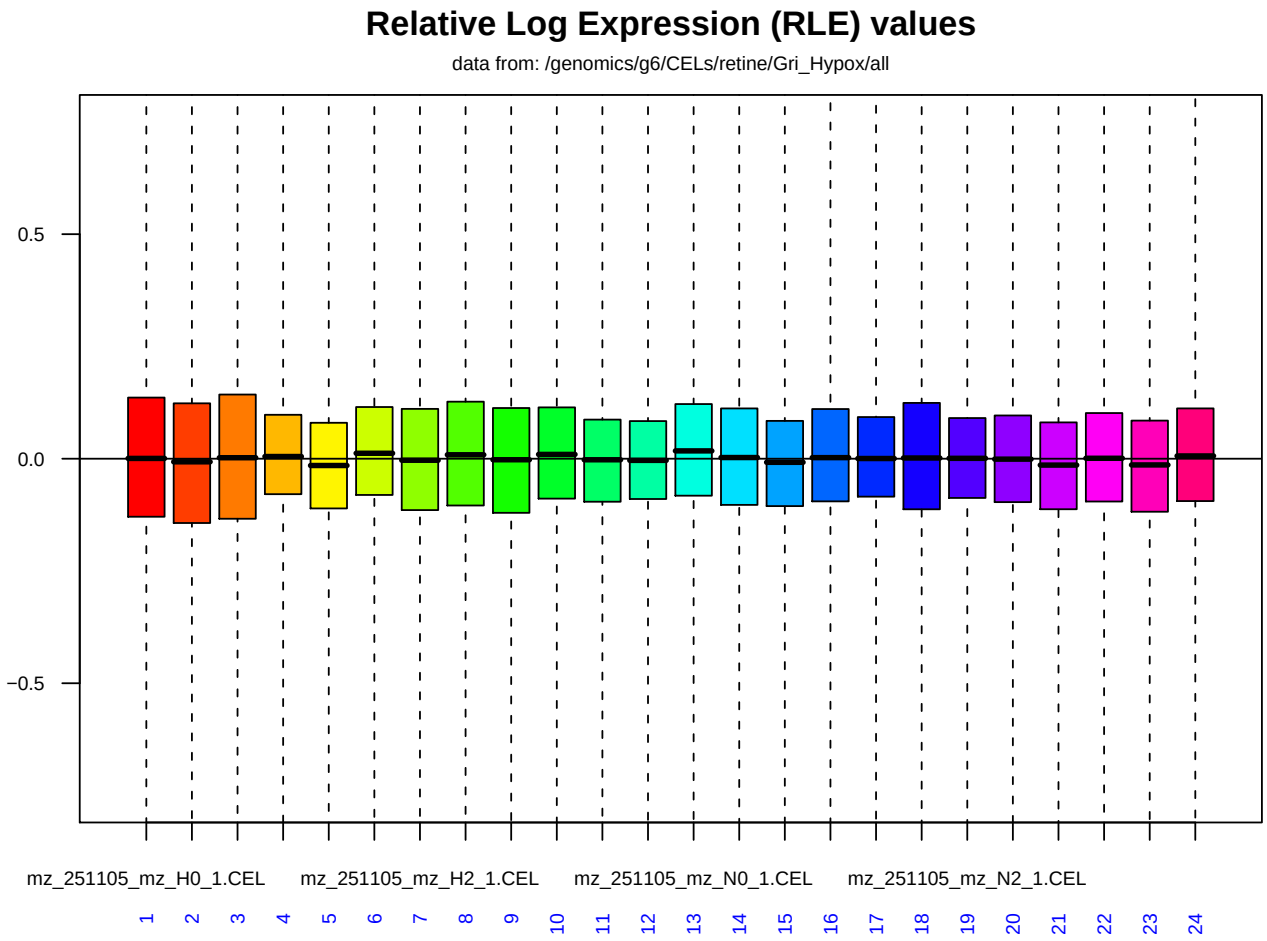
Relative Log Expression (RLE) values
data from: /genomics/g6/CELs/retine/Gri_Hypox/all
0.5
0.0
−0.5
mz_251105_mz_H0_1.CEL
mz_251105_mz_H2_1.CEL
mz_251105_mz_N0_1.CEL
mz_251105_mz_N2_1.CEL
1 2 3 4 5 6 7 8 9 10 11 12 13 14 15 16 17 18 19 20 21 22 23 24

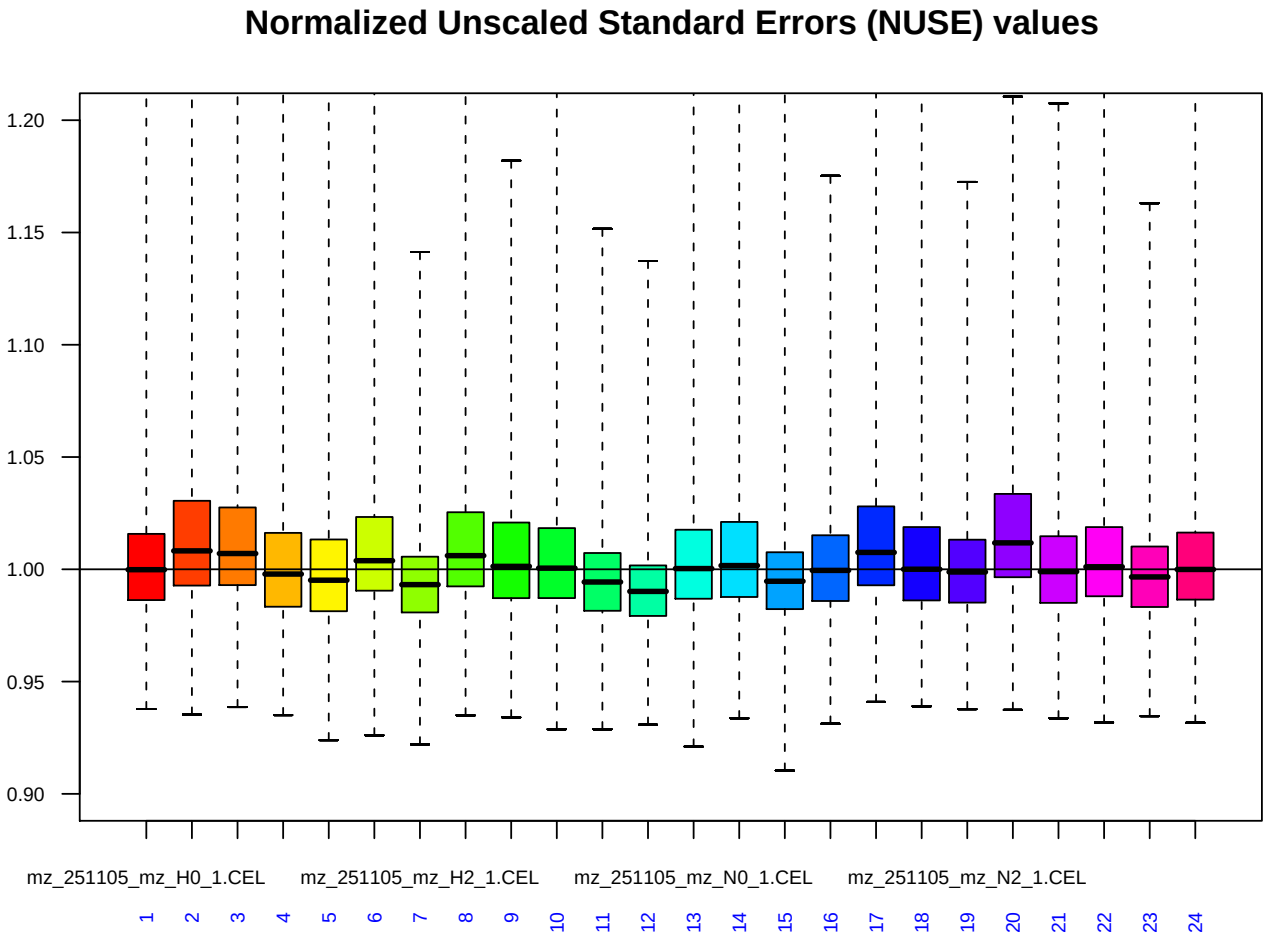
Normalized Unscaled Standard Errors (NUSE) values
1.20
1.15
1.10
1.05
1.00
0.95
0.90
mz_251105_mz_H0_1.CEL
mz_251105_mz_H2_1.CEL
mz_251105_mz_N0_1.CEL
mz_251105_mz_N2_1.CEL
1 2 3 4 5 6 7 8 9 10 11 12 13 14 15 16 17 18 19 20 21 22 23 24

1 mz_2S110S_mz_H0_1

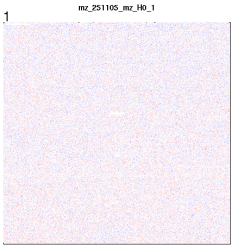

2 mz_2S110S_mz_H0_2

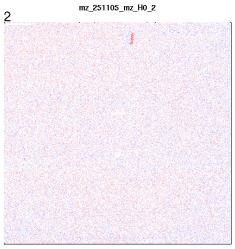

3 mz_2S110S_mz_H0_3

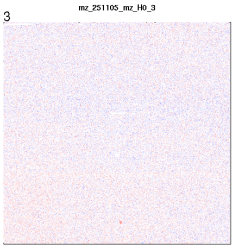

4 mz_2S110S_mz_H16_1

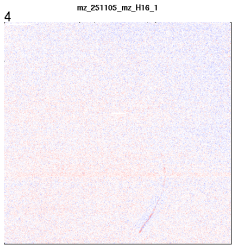

5 mz_2S110S_mz_H16_2

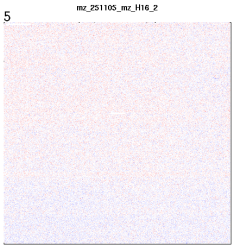

6 mz_2S110S_mz_H16_3

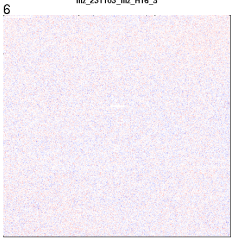

7 mz_2S110S_mz_H2_1

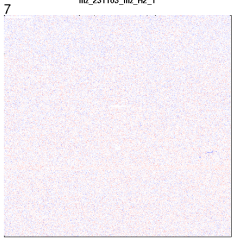

8 mz_2S110S_mz_H2_2

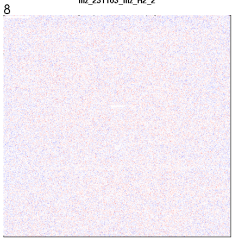

9 mz_2S110S_mz_H2_3

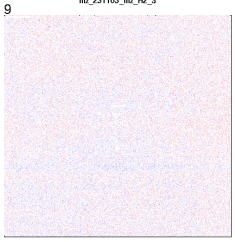

10 mz_2S110S_mz_H4_1

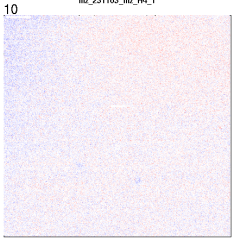

11 mz_2S110S_mz_H4_2

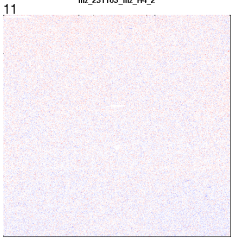

12 mz_2S110S_mz_H4_3

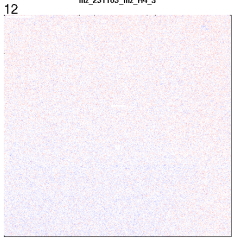

13 mz_2S110S_mz_N0_1

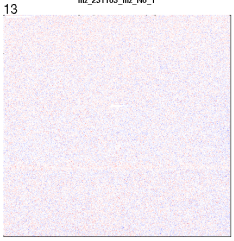

14 mz_2S110S_mz_N0_2

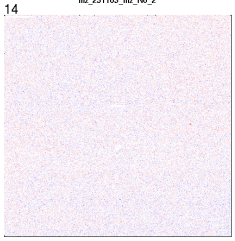

15 mz_2S110S_mz_N0_3

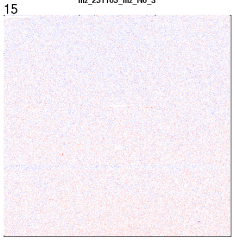

16 mz_2S110S_mz_N16_1

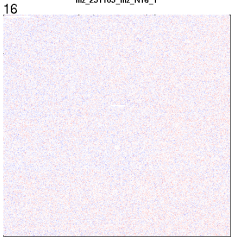

17 mz_2S110S_mz_N16_2

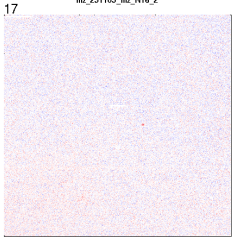

18 mz_2S110S_mz_N16_3

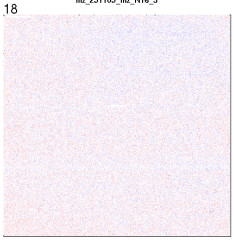

19 mz_2S110S_mz_N2_1

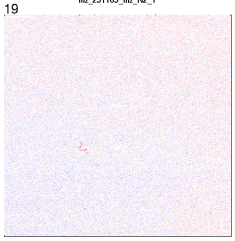

20 mz_2S110S_mz_N2_2

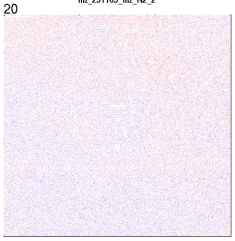

21 mz_2S110S_mz_N2_3

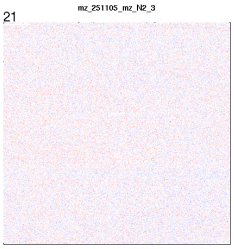

22 mz_2S110S_mz_N4_1

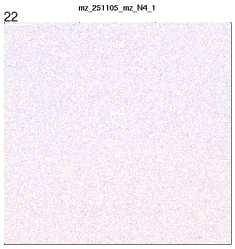

23 mz_2S110S_mz_N4_2

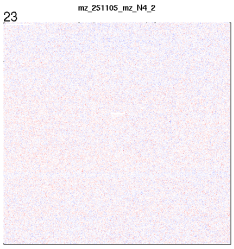

24 mz_2S110S_mz_N4_3

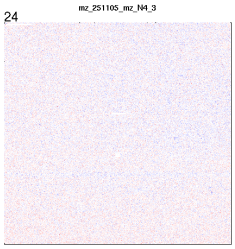


1 mz_251105_mz_H0_1 vs pseudo-median reference chip
2 mz_251105_mz_H0_2 vs pseudo-median reference chip
3 mz_251105_mz_H0_3 vs pseudo-median reference chip
4 mz_251105_mz_H16_1 vs pseudo-median reference chip
5 mz_251105_mz_H16_2 vs pseudo-median reference chip
6 mz_251105_mz_H16_3 vs pseudo-median reference chip
7 mz_251105_mz_H2_1 vs pseudo-median reference chip
8 mz_251105_mz_H2_2 vs pseudo-median reference chip
9 mz_251105_mz_H2_3 vs pseudo-median reference chip
10 mz_251105_mz_H4_1 vs pseudo-median reference chip
11 mz_251105_mz_H4_2 vs pseudo-median reference chip
12 mz_251105_mz_H4_3 vs pseudo-median reference chip
13 mz_251105_mz_N0_1 vs pseudo-median reference chip
14 mz_251105_mz_N0_2 vs pseudo-median reference chip
15 mz_251105_mz_N0_3 vs pseudo-median reference chip
16 mz_251105_mz_N16_1 vs pseudo-median reference chip
17 mz_251105_mz_N16_2 vs pseudo-median reference chip
18 mz_251105_mz_N16_3 vs pseudo-median reference chip
19 mz_251105_mz_N2_1 vs pseudo-median reference chip
20 mz_251105_mz_N2_2 vs pseudo-median reference chip
21 mz_251105_mz_N2_3 vs pseudo-median reference chip
22 mz_251105_mz_N4_1 vs pseudo-median reference chip
23 mz_251105_mz_N4_2 vs pseudo-median reference chip
24 mz_251105_mz_N4_3 vs pseudo-median reference chip

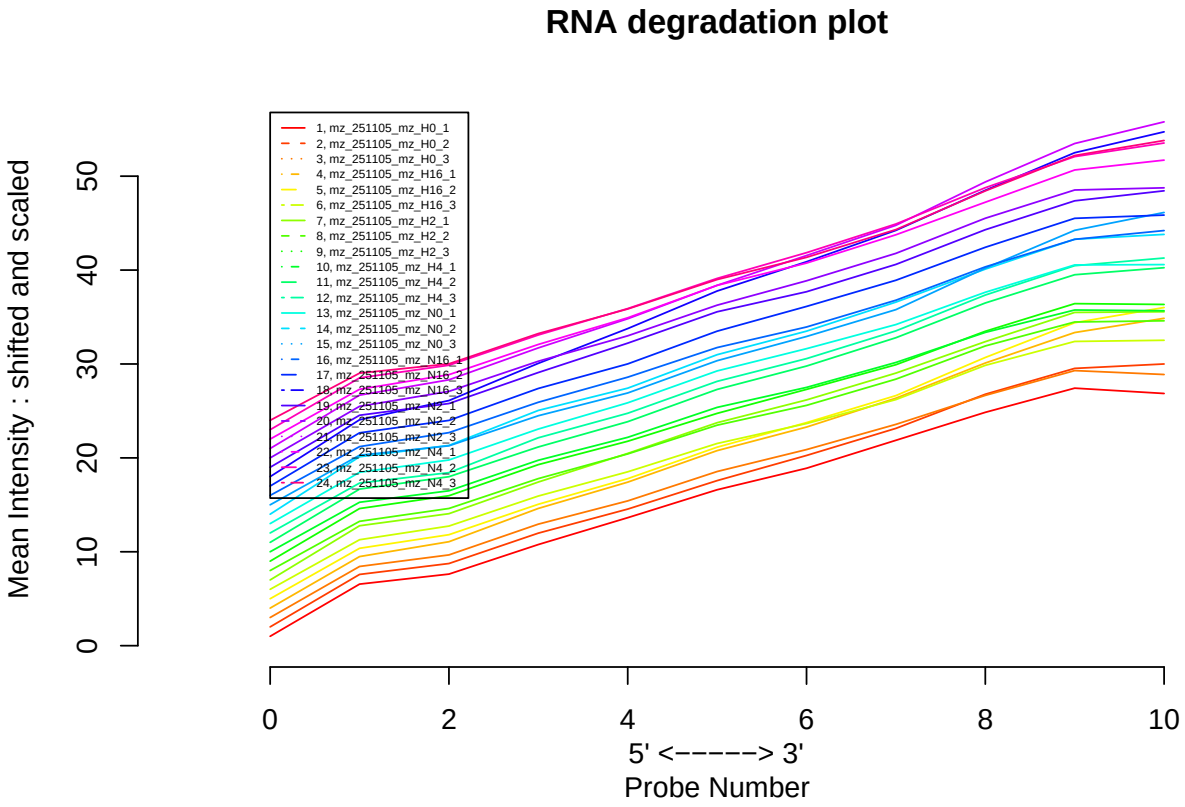
RNA degradation plot
Mean Intensity : shifted and scaled
0
10
20
30
40
50
1, mz_251105_mz_H0_1
2, mz_251105_mz_H0_2
3, mz_251105_mz_H0_3
4, mz_251105_mz_H16_1
5, mz_251105_mz_H16_2
6, mz_251105_mz_H16_3
7, mz_251105_mz_H2_1
8, mz_251105_mz_H2_2
9, mz_251105_mz_H2_3
10, mz_251105_mz_H4_1
11, mz_251105_mz_H4_2
12, mz_251105_mz_H4_3
13, mz_251105_mz_N0_1
14, mz_251105_mz_N0_2
15, mz_251105_mz_N0_3
16, mz_251105_mz_N16_1
17, mz_251105_mz_N16_2
18, mz_251105_mz_N16_3
19, mz_251105_mz_N2_1
20, mz_251105_mz_N2_2
21, mz_251105_mz_N2_3
22, mz_251105_mz_N4_1
23, mz_251105_mz_N4_2
24, mz_251105_mz_N4_3
0
2
4
6
8
10
5' <−−−−−> 3'
Probe Number

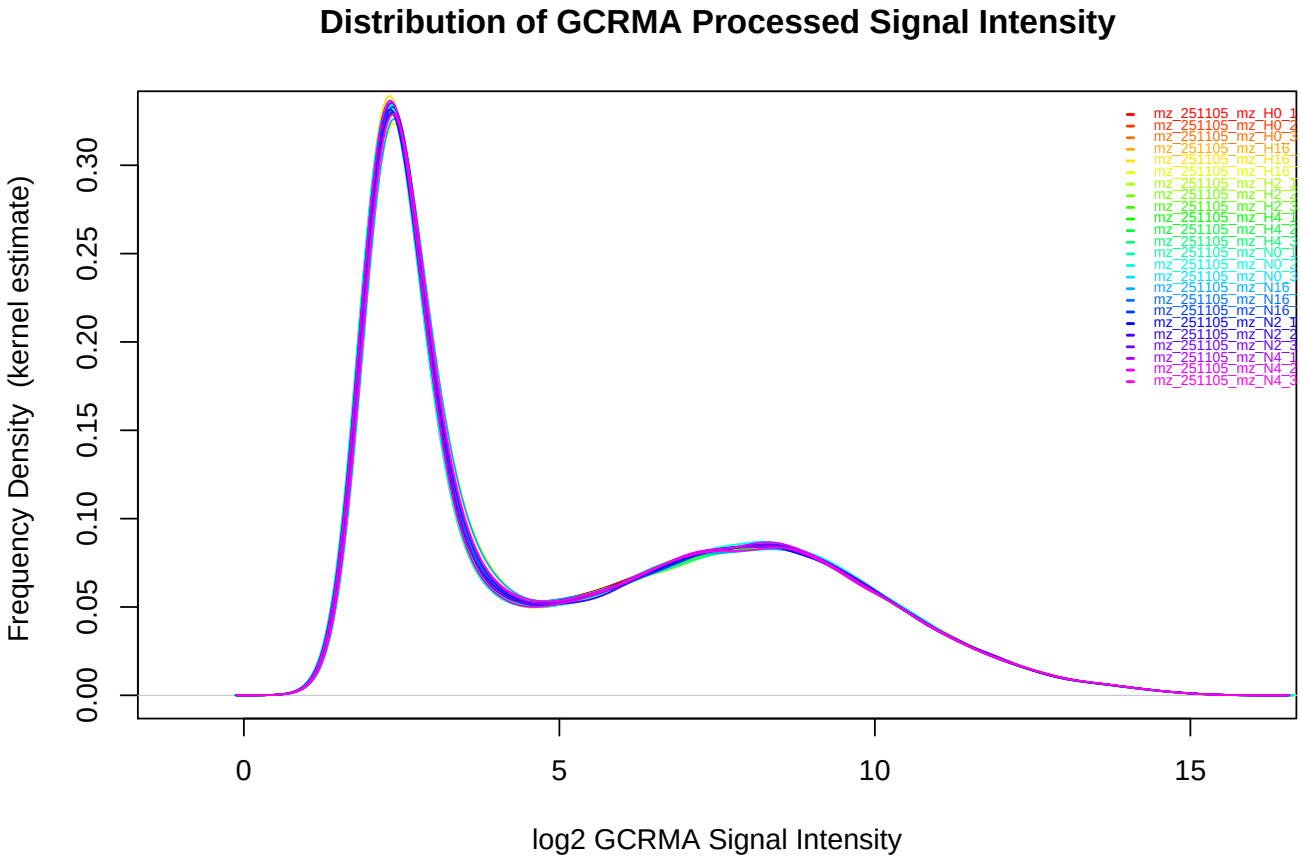
Distribution of GCRMA Processed Signal Intensity
Frequency Density (kernel estimate)
0.00
0.05
0.10
0.15
0.20
0.25
0.30
0
5
10
15
log2 GCRMA Signal Intensity

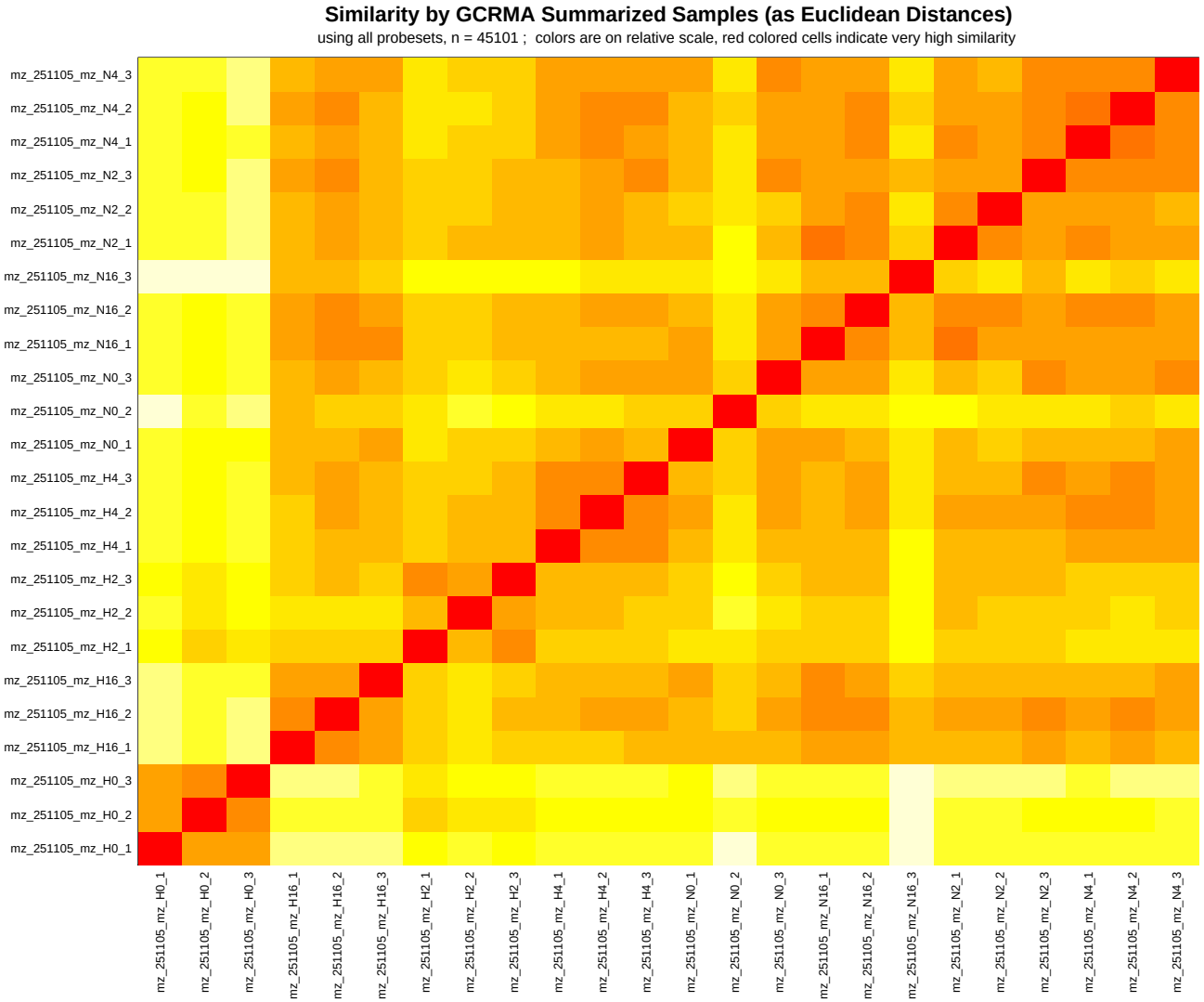

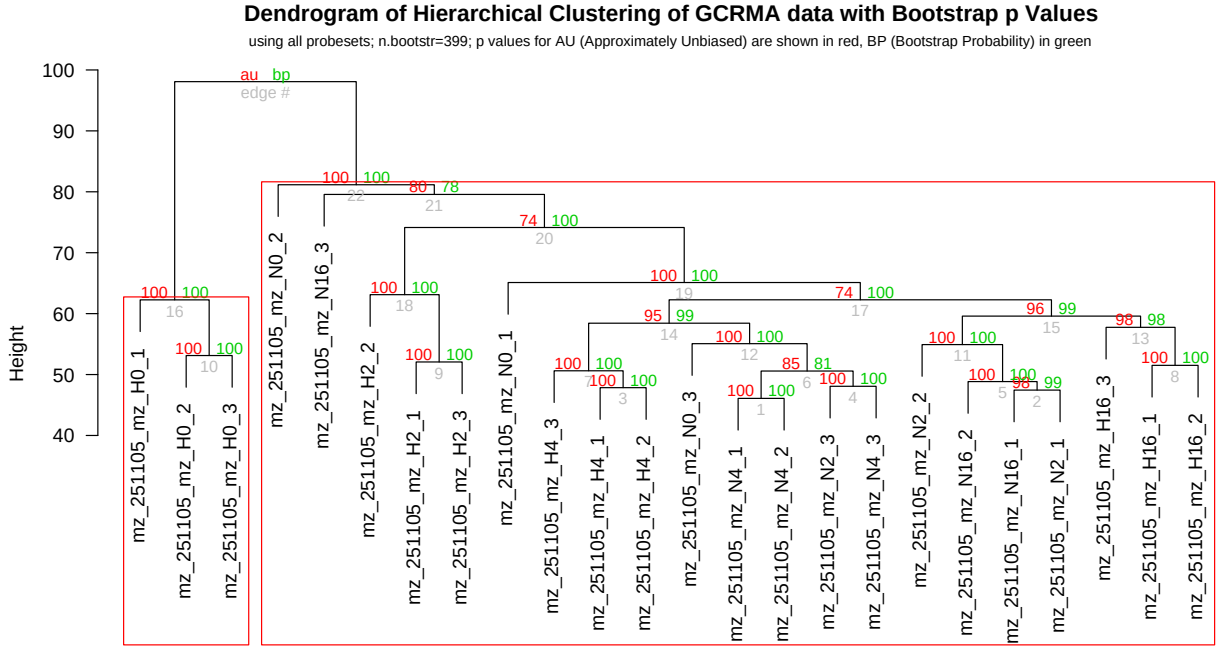

Clusters that 'seem to exist' with p<0.95 are highlighted by red boxes

Distance: euclidean
Cluster method: average

References :

- Raffelsberger W., Krause Y. et al. RReportGenerator : Automatic reports from routine statistical analysis using R. (submitted) and http://www-bio3d-igbmc.u-strasbg.fr/∼wraff
- R Development Core Team (2007). R: A language and environment for statistical computing. R Foundation for Statistical Computing, Vienna, Austria. ISBN 3-900051-07-0, http://www.R-project.org.
- Leisch,F. (2002). Sweave: Dynamic generation of statistical reports using literate data analysis. In: Härdle,W. and Rönz,B. (eds), Proceedings in Computational Statistics, Physica Verlag, Heidelberg, pp.575-580
- Gentleman,R.C. et al. (2004) Bioconductor: open software development for computational biology and bioinformatics. Genome Biol., 5, R80.
- Bolstad BM, Irizarry RA, Astrand M, Speed TP. (2003) A comparison of normalization methods for high density oligonucleotide array data based on variance and bias. Bioinformatics. Jan 22;19(2):185-93.
- Irizarry RA, Bolstad BM, Collin F, Cope LM, Hobbs B, Speed TP. (2003) Summaries of Affymetrix GeneChip probe level data. Nucleic Acids Res. 2003 Feb 15;31(4):e15.
- Gautier L, Cope L, Bolstad BM, Irizarry RA. (2004) affy–analysis of Affymetrix GeneChip data at the probe level. Bioinformatics. 2004 Feb 12;20(3):307-15.
- Rafael A. Irizarry, Laurent Gautier, Benjamin Milo Bolstad, and Crispin Miller with contributions from Magnus Astrand, Leslie M. Cope, Robert Gentleman, Jeff Gentry, Conrad Halling, Wolfgang Huber, James MacDonald, Benjamin I.P. Rubinstein, Christopher Workman and John Zhang (). affy: Methods for Affymetrix Oligonucleotide Arrays. R package.
- Wilson C.L., Miller C.J. (2005) Simpleaffy: a BioConductor package for Affymetrix Quality Control and data analysis. Bioinformatics. 2005 Sep 15;21(18):3683-5.
- Ben Bolstad (2007). affyPLM: Methods for fitting probe-level models. R package. http://bmbolstad.com
- Craig Parman, Conrad Halling and Robert Gentleman (). affyQCReport: QC Report Generation for affyBatch objects. R package
- Reimers M, Weinstein JN. (2005) Quality assessment of microarrays: visualization of spatial artifacts and quantitation of regional biases. BMC Bioinformatics. 2005 Jul 1;6:166.
- Smyth, G. K. (2005). Limma: linear models for microarray data. In: 'Bioinformatics and Computational Biology Solutions using R and Bioconductor'. R. Gentleman, V. Carey, S. Dudoit, R. Irizarry, W. Huber (eds), Springer, New York, pages 397–420.
- Suzuki R, Shimodaira H. (2004) Pvclust: an R package for assessing the uncertainty in hierarchical clustering. Bioinformatics. Jun 15;22(12):1540-2.
- http://www.affymetrix.com

time for reading cel-fiels : 212.46 sec
time for figures QC1 and QC2 : 320.76 sec
time for RNA degradation figure : 25.13 sec
time for plm calculation : 72.62 sec
time for RLE and NUSE figures : 14.75 sec
time for residual images : 603.45 sec
time for MA-plots : 800.85 sec
time for calculating RMA : 252.31 sec
time for plot of Sig Dist of RMA treated data : 2.08 sec
time for hierarchical clustering and bootstrap pValues : 138.9 min

3.1.1.2 Lists of Differentially Regulated Genes (Additional File 2)

TABLE 1 Differentially Regulated Genes by Hypoxic Preconditioning H0

AffymetrixID	p-Value	Fold change	Gene
1440257_at	2.48E-07	118.36	oocyte specific homeobox 6
1433837_at	6.94E-05	35.63	RIKEN cDNA 8430408G22 gene
1424638_at	3.00E-05	30.48	cyclin-dependent kinase inhibitor 1A (P21)
1454409_at	2.07E-06	24.02	RIKEN cDNA 4833408G04 gene
1418190_at	1.98E-05	22.55	paraoxonase 1
1422832_at	6.20E-05	22.09	retinal G protein coupled receptor
1454608_x_at	0.00026744	20.11	transthyretin
1455913_x_at	0.000310957	19.97	transthyretin
1458610_at	0.000195109	17.40	---
1416434_at	2.70E-05	17.02	Bcl2-like 10
1444487_at	6.54E-06	16.17	---
1441228_at	7.21E-05	11.68	PREDICTED: similar to vascular early response gene protein [Mus musculus], mRNA sequence
1438815_at	0.000101469	10.73	histone 2, H2aa2
1416077_at	0.000248019	10.59	adrenomedullin
1430197_a_at	5.36E-05	10.27	phosphatidylinositol transfer protein, membrane-associated 2
1428942_at	5.12E-06	9.72	metallothionein 2
1418808_at	9.82E-05	9.72	retinol dehydrogenase 5
1427221_at	0.000128871	9.33	X transporter protein 3 similar 1 gene
1430817_at	0.000266245	8.60	sterile alpha motif domain containing 7
1447494_at	5.77E-06	7.15	RIKEN cDNA 2600013E07 gene
1428352_at	6.05E-05	7.06	arrestin domain containing 2
1446587_at	0.000232092	6.93	Transcribed locus
1424838_at	0.000120631	6.82	RIKEN cDNA A330049M08 gene
1426117_a_at	0.00018024	6.76	solute carrier family 19 (thiamine transporter), member 2
1430357_at	5.84E-05	6.28	H3 histone, family 3B
1422557_s_at	5.42E-06	6.26	metallothionein 1
1454991_at	0.000139272	6.11	solute carrier family 7 (cationic amino acid transporter, y+ system), member 1
1429348_at	0.00035515	5.86	sema domain, immunoglobulin domain (Ig), short basic domain, secreted, (semaphorin) 3C
1442366_at	6.15E-05	5.61	RIKEN cDNA 6820408C15 gene (6820408C15Rik), mRNA
1441673_at	0.000139215	5.28	expressed sequence C80120
1448231_at	1.89E-06	5.01	FK506 binding protein 5
1435918_at	0.000181976	4.94	cDNA sequence BC055107
1418093_a_at	3.96E-06	4.70	epidermal growth factor
1423785_at	0.00036492	4.44	EGL nine homolog 1 (C. elegans)
1416309_at	0.000163701	4.43	nucleolar and spindle associated protein 1
1455385_at	0.000158024	4.40	SEC15-like 1 (S. cerevisiae)
1454018_at	0.000249767	4.33	tousled-like kinase 2 (Arabidopsis)

1428923_at	3.47E-05	4.28	protein phosphatase 1, regulatory (inhibitor) subunit 3G
1444528_at	7.25E-05	4.25	Zinc finger protein 316 (Zfp316), mRNA
1449007_at	0.000123554	4.21	B-cell translocation gene 3
1455475_at	0.000267688	4.16	RIKEN cDNA 3110057O12 gene
1452534_a_at	7.43E-05	4.06	high mobility group box 2
1422803_at	0.000298361	4.04	follistatin-like 3
1434203_at	0.000193383	3.94	cDNA sequence BC055107
1453303_at	0.000107858	3.93	RIKEN cDNA 4833417J20 gene
1431308_at	0.00036618	3.91	RIKEN cDNA 5730557B15 gene
1427507_at	0.000166537	3.89	tripartite motif protein 17
1416125_at	1.05E-05	3.85	FK506 binding protein 5
1458669_at	0.000151183	3.72	Transcribed locus
1459331_at	0.000195472	3.66	surfeit gene 6
1442025_a_at	0.000106863	3.61	---
1451959_a_at	1.74E-05	3.56	vascular endothelial growth factor A
1456676_a_at	0.000226291	3.56	6-phosphofructo-2-kinase/fructose-2,6-biphosphatase 3
1445443_at	0.000133959	3.52	---
1425809_at	0.00034519	3.50	Fatty acid binding protein 4, adipocyte (Fabp4), mRNA
1423233_at	0.00038307	3.47	CCAAT/enhancer binding protein (C/EBP), delta
1440555_at	1.03E-05	3.45	Ras-related GTP binding D
1436279_at	8.46E-06	3.40	Solute carrier family 26, member 7 (Slc26a7), mRNA
1417887_at	5.87E-05	3.40	RIKEN cDNA 1110055N21 gene
1424143_a_at	0.000174386	3.37	retroviral integration site 2
1424144_at	0.00037672	3.28	retroviral integration site 2
1419089_at	4.49E-05	3.28	tissue inhibitor of metalloproteinase 3
1451325_at	4.70E-05	3.26	forty-two-three domain containing 1
1448359_a_at	7.11E-05	3.23	HIG1 domain family, member 1A
1434202_a_at	0.000112753	3.23	cDNA sequence BC055107
1436006_at	0.00026245	3.18	eukaryotic translation initiation factor 2 alpha kinase 1
1454617_at	5.15E-05	3.15	arrestin domain containing 3
1454623_at	0.00036572	3.13	similar to Carboxypeptidase A2 precursor
1427364_a_at	0.000104267	3.13	ornithine decarboxylase, structural 1 /// similar to Ornithine decarboxylase (ODC) /// similar to Ornithine decarboxylase (ODC)
1425895_a_at	0.000108139	3.10	inhibitor of DNA binding 1
1449335_at	8.21E-05	3.10	tissue inhibitor of metalloproteinase 3
1422885_at	1.33E-05	3.10	small nuclear ribonucleoprotein D3
1436605_at	0.000112507	3.10	transketolase
1419029_at	5.21E-05	3.08	ERO1-like (S. cerevisiae)
1443196_at	5.64E-05	3.03	13 days embryo heart cDNA, RIKEN full-length enriched library, clone:D330001J12 product:unclassifiable, full insert sequence
1437313_x_at	7.81E-05	3.00	high mobility group box 2
1433814_at	0.00037743	2.99	Transcribed locus

1449324_at	2.01E-05	2.98	ERO1-like (S. cerevisiae)
1454949_at	0.00035566	2.97	Ubiquitin specific peptidase 7 (Usp7), mRNA
1437818_at	0.000141517	2.95	RIKEN cDNA 9430016H08 gene
1419030_at	6.69E-06	2.93	ERO1-like (S. cerevisiae)
1423865_at	3.18E-05	2.93	solute carrier family 44, member 1
1429183_at	9.59E-05	2.91	plakophilin 2
1448607_at	0.000262344	2.90	pre-B-cell colony-enhancing factor 1
1429050_at	6.50E-05	2.88	cysteine-rich hydrophobic domain 2
1434570_at	0.000228516	2.84	cDNA sequence AK122525
1440932_at	0.0003692	2.79	---
1457451_at	0.000104526	2.78	---
1416432_at	1.39E-05	2.77	6-phosphofructo-2-kinase/fructose-2,6-biphosphatase 3
1442397_at	6.18E-05	2.74	nuclear transcription factor, X-box binding 1
1436531_at	0.000293193	2.74	methionine aminopeptidase 2
1450725_s_at	0.000171891	2.73	carbonic anhydrase 14
1433674_a_at	0.00011106	2.70	RNA, U22 small nucleolar
1438681_at	7.67E-05	2.69	alkB, alkylation repair homolog (E. coli)
1418370_at	9.16E-05	2.69	troponin C, cardiac/slow skeletal
1452891_at	0.000141048	2.68	RIKEN cDNA 5730568A12 gene
1428544_at	9.38E-05	2.67	RIKEN cDNA 0610007L01 gene
1452414_s_at	0.000300782	2.67	DNA segment, Chr 19, ERATO Doi 678, expressed
1428823_at	0.000153081	2.66	HD domain containing 2
1419024_at	0.00032058	2.66	protein tyrosine phosphatase 4a1
1417149_at	0.000108159	2.65	procollagen-proline, 2-oxoglutarate 4-dioxygenase (proline 4-hydroxylase), alpha II polypeptide
1441315_s_at	0.00032571	2.65	solute carrier family 19 (thiamine transporter), member 2
1430746_at	0.000258587	2.64	RIKEN cDNA 1110050P16 gene
1416039_x_at	0.000107418	2.61	cysteine rich protein 61
1450412_at	8.83E-05	2.60	transducin (beta)-like 2
1430798_x_at	0.000201526	2.60	mitochondrial ribosomal protein L15
1455420_at	5.14E-05	2.59	RAD23b homolog (S. cerevisiae)
1435875_at	3.18E-06	2.57	protein kinase, AMP-activated, beta 2 non-catalytic subunit
1416481_s_at	0.000298381	2.57	HIG1 domain family, member 1A
1429089_s_at	0.00029993	2.55	RIKEN cDNA 2900026A02 gene
1435245_at	5.29E-05	2.53	glutaminase 2 (liver, mitochondrial)
1455002_at	0.000226722	2.53	protein tyrosine phosphatase 4a1
1456748_a_at	3.83E-05	2.52	4-nitrophenylphosphatase domain and non-neuronal SNAP25-like protein homolog 1 (C. elegans)
1437088_at	0.000201662	2.51	SDA1 domain containing 1
1431212_a_at	0.00010318	2.51	RIKEN cDNA 3300001M20 gene
1446769_at	3.20E-05	2.49	RIKEN cDNA 2810439F02 gene
1426417_at	0.00032499	2.46	Yip1 domain family, member 4
1437785_at	3.66E-05	2.46	a disintegrin-like and metallopeptidase (reprolysin type) with thrombospondin type 1 motif, 9
1416512_at	0.000202856	2.44	nucleotide binding protein 2

1454109_a_at	9.54E-05	2.40	phosphatidylserine receptor
1419087_s_at	0.00033316	2.39	splicing factor 3a, subunit 1
1438761_a_at	2.95E-05	2.38	ornithine decarboxylase, structural 1 /// similar to Ornithine decarboxylase (ODC) /// similar to Ornithine decarboxylase (ODC)
1453851_a_at	0.000308457	2.34	growth arrest and DNA-damage-inducible 45 gamma
1455320_at	0.00014932	2.33	expressed sequence AI480535
1439677_at	0.000133355	2.32	epilepsy, progressive myoclonic epilepsy, type 2 gene alpha
1416749_at	0.00038473	2.32	HtrA serine peptidase 1
1434952_at	0.000246056	2.32	Cytochrome c oxidase subunit IV isoform 1 (Cox4i1), mRNA
1438046_at	3.82E-05	2.31	expressed sequence AU019823
1426727_s_at	0.00037587	2.30	protein phosphatase 1, regulatory subunit 10 /// hypothetical protein LOC545202
1455782_at	9.53E-05	2.29	sterile alpha motif domain containing 7
1420909_at	0.000304099	2.25	vascular endothelial growth factor A
1416344_at	0.000278017	2.22	lysosomal membrane glycoprotein 2
1422476_at	0.000116371	2.21	interferon gamma inducible protein 30
1426721_s_at	0.00035377	2.21	TCDD-inducible poly(ADP-ribose) polymerase
1440179_x_at	6.63E-05	2.21	similar to hypothetical protein MGC26996; chromosome 6 open reading frame 172
1438606_a_at	8.03E-05	2.20	chloride intracellular channel 4 (mitochondrial)
1455254_at	0.000205617	2.13	RIKEN cDNA 4833420G11 gene
1459897_a_at	0.000230612	2.13	suprabasin
1425732_a_at	0.00033976	2.12	Max interacting protein 1
1444241_at	0.000144929	2.10	WW domain containing adaptor with coiled-coil
1428529_at	7.11E-06	2.09	RIKEN cDNA 2810026P18 gene
1435351_at	1.85E-06	2.08	RIKEN cDNA 2310026E23 gene
1458046_at	0.00036917	2.08	---
1420138_at	0.000169245	2.07	solute carrier family 19 (sodium/hydrogen exchanger), member 1
1452050_at	6.02E-05	2.06	calcium/calmodulin-dependent protein kinase ID
1425477_x_at	0.00034286	2.06	histocompatibility 2, class II antigen A, beta 1
1448654_at	0.000205405	2.04	mitochondrial carrier homolog 2 (C. elegans)
1438251_x_at	0.000101884	2.04	HtrA serine peptidase 1
1449341_a_at	1.96E-05	2.03	stomatin
1454903_at	0.000234716	1.98	nerve growth factor receptor (TNFR superfamily, member 16)
1426600_at	0.000112368	1.98	solute carrier family 2 (facilitated glucose transporter), member 1
1434012_at	0.000266359	1.96	RIKEN cDNA 1110055N21 gene
1435870_at	0.000120695	1.95	Synaptonemal complex protein 3 (Sycp3), mRNA
1459978_x_at	5.28E-05	1.95	gene model 877, (NCBI)
1421884_at	0.000218307	1.92	Son of sevenless homolog 1 (Drosophila)
1418777_at	0.000267738	1.91	chemokine (C-C motif) ligand 25
1417288_at	3.45E-05	1.90	pleckstrin homology domain-containing, family A (phosphoinositide binding specific) member 2

1428754_at	3.70E-05	1.86	RIKEN cDNA 3300001M20 gene
1436050_x_at	0.000256706	1.86	hairy and enhancer of split 6 (Drosophila)
1454937_at	0.000241224	1.85	RIKEN cDNA B630005N14 gene
1419938_s_at	0.000155818	1.85	---
1433436_s_at	0.00032398	1.85	thiamine triphosphatase
1456005_a_at	3.98E-05	1.85	BCL2-like 11 (apoptosis facilitator)
1426288_at	0.000175909	1.85	low density lipoprotein receptor-related protein 4
1451893_s_at	0.000246465	1.85	membrane associated guanylate kinase, WW and PDZ domain containing 1
1457275_at	0.000234799	1.84	desmuslin
1435448_at	0.000131445	1.83	BCL2-like 11 (apoptosis facilitator)
1455671_at	0.000233252	1.83	COMM domain containing 8
1426594_at	0.00011977	1.82	FERM domain containing 4B
1453344_at	0.000116605	1.82	RIKEN cDNA 1810032O08 gene
1416129_at	0.00035436	1.78	ERBB receptor feedback inhibitor 1
1456355_s_at	6.90E-05	1.77	sensitivity to red light reduced homolog (Arabidopsis)
1451872_a_at	9.59E-06	1.73	neuralized-like homolog (Drosophila)
1424526_a_at	0.000123901	1.73	TDP-glucose 4,6-dehydratase
1423480_at	0.000139804	1.73	nucleolar protein 11
1448276_at	0.000276959	1.72	tetraspanin 4
1418561_at	0.0003567	1.72	splicing factor 3b, subunit 1
1439032_at	9.05E-05	1.71	RIKEN cDNA 2410007P03 gene
1436209_at	5.69E-05	1.71	DnaJ (Hsp40) homolog, subfamily C, member 16
1427171_at	0.000130998	1.70	rearranged L-myc fusion sequence
1434680_at	0.0003249	1.70	pleckstrin homology domain containing, family G (with RhoGef domain) member 3
1422677_at	0.000263535	1.70	diacylglycerol O-acyltransferase 2
1423337_at	0.00035115	1.68	origin recognition complex, subunit 4-like (S. cerevisiae)
1426474_at	0.000202384	1.68	ATP synthase mitochondrial F1 complex assembly factor 2
1455429_at	1.87E-05	1.66	expressed sequence AI450540
1455726_at	0.0002984	1.66	gene model 71, (NCBI)
1437615_s_at	1.06E-05	1.65	Vacuolar protein sorting 37C (yeast), mRNA (cDNA clone MGC:32338 IMAGE:5029143)
1456390_at	7.49E-05	1.64	protein phosphatase 2a, catalytic subunit, alpha isoform
1456775_at	4.29E-05	1.64	RIKEN cDNA 2810013E07 gene
1450425_a_at	0.000288911	1.63	RIKEN cDNA 2700062C07 gene
1425054_a_at	2.23E-05	1.63	RIKEN cDNA 2510006D16 gene
1436100_at	0.000149688	1.62	SH2 domain containing 5
1454802_x_at	2.41E-05	1.62	ariadne homolog 2 (Drosophila)
1424197_s_at	0.000194537	1.61	Fanconi anemia, complementation group E
1451342_at	3.94E-05	1.59	spondin 1, (f-spondin) extracellular matrix protein
1444682_at	8.34E-05	1.58	cDNA Sequence BC037032
1416135_at	7.05E-05	1.58	apurinic/apyrimidinic endonuclease 1
1448769_at	0.000212764	1.57	solute carrier family 35, member B1
1437630_at	0.00035534	1.57	DNA segment, Chr 16, Brigham & Women's

			Genetics 1547 expressed
1434011_a_at	7.33E-05	1.57	RIKEN cDNA 1110055N21 gene
1429080_at	9.62E-05	1.56	M-phase phosphoprotein 10 (U3 small nucleolar ribonucleoprotein)
1417509_at	3.40E-06	1.56	ring finger protein (C3HC4 type) 19
1431423_a_at	1.44E-05	1.55	mediator of RNA polymerase II transcription, subunit 8 homolog (yeast)
1415723_at	7.89E-05	1.54	eukaryotic translation initiation factor 5
1441659_at	0.000294139	1.54	D4, zinc and double PHD fingers, family 3
1449884_at	0.000136622	1.52	EF-hand calcium binding domain 2
1424892_at	0.00034808	1.51	zinc finger protein 95
1426999_at	0.000166058	1.51	RIKEN cDNA 2700069A02 gene
1417900_a_at	0.00037592	1.51	very low density lipoprotein receptor
1456910_at	0.000247631	1.51	Transcribed locus
1429083_at	0.000205794	1.50	amylo-1,6-glucosidase, 4-alpha-glucanotransferase
1448706_at	0.000265081	1.49	Traf and Tnf receptor associated protein
1425966_x_at	0.000237604	1.48	ubiquitin C
1455354_at	8.10E-05	1.47	WD repeat domain 22
1434465_x_at	0.000109228	1.46	very low density lipoprotein receptor
1452771_s_at	4.31E-05	1.46	acyl-CoA synthetase long-chain family member 3
1417508_at	0.000138096	1.44	ring finger protein (C3HC4 type) 19
1421528_a_at	0.000221108	1.43	surfeit gene 5
1449702_at	0.000302957	1.43	zinc finger, AN1-type domain 2A
1452691_at	8.70E-05	1.42	RNA binding motif protein 17
1458218_s_at	0.00032951	1.41	phosphodiesterase 7A
1452693_at	0.00035691	1.41	DEAH (Asp-Glu-Ala-His) box polypeptide 35
1460109_at	0.000163871	1.37	DNA segment, Chr 8, ERATO Doi 325, expressed, mRNA (cDNA clone MGC:36794 IMAGE:3498003)
1435715_x_at	0.00033561	1.37	thymine DNA glycosylase /// similar to Thymine DNA glycosylase /// similar to Thymine DNA glycosylase
1448744_at	0.000114888	1.35	galactosamine (N-acetyl)-6-sulfate sulfatase
1429667_at	8.30E-05	1.35	RIKEN cDNA E130119J07 gene
1423699_at	0.000231602	1.35	DNA segment, Chr 15, ERATO Doi 785, expressed
1452784_at	0.000283203	1.35	integrin alpha V
1423059_at	0.000132421	1.34	PTK2 protein tyrosine kinase 2
1437087_at	0.000198435	1.34	Expressed sequence R75581 (R75581), mRNA
1438446_x_at	9.82E-05	1.34	putative phosphatase
1436223_at	0.00033255	1.34	PREDICTED: integrin beta 8 [Mus musculus], mRNA sequence
1438040_a_at	0.00019203	1.33	tumor rejection antigen gp96
1450015_x_at	0.00037043	1.31	sphingosine-1-phosphate phosphatase 1
1428153_at	7.37E-05	1.30	mitochondrial ribosomal protein S10
1434314_s_at	6.55E-05	1.28	RAB11 family interacting protein 5 (class I)
1423447_at	0.00033514	1.28	caseinolytic peptidase X (E.coli)
1455959_s_at	0.00036529	1.27	glutamate-cysteine ligase, catalytic subunit
1429615_at	0.000124321	1.26	zinc finger protein 91
1423181_s_at	0.000154371	1.26	chloride channel, nucleotide-sensitive, 1A
1417349_at	0.000124108	1.23	pallidin

1423255_at	0.00034569	1.22	ATPase, H+ transporting, V1 subunit G isoform 1
1431826_a_at	1.13E-05	1.22	BR serine/threonine kinase 2
1438218_at	7.22E-05	1.20	zinc finger and BTB domain containing 24
1415749_a_at	3.42E-06	1.19	Ras-related GTP binding C
1434995_s_at	3.30E-05	1.09	death effector domain-containing
1419377_at	0.00032354	1.08	---
1420828_s_at	0.000201853	0.90	tyrosine 3-monooxygenase/tryptophan 5-monooxygenase activation protein, theta polypeptide
1423187_at	4.24E-05	0.86	gamma-aminobutyric acid (GABA-A) receptor-associated protein-like 2
1454641_at	0.00037164	0.85	CGG triplet repeat binding protein 1
1448484_at	6.75E-05	0.85	S-adenosylmethionine decarboxylase 1
1415683_at	0.000165936	0.84	N-myristoyltransferase 1
1423132_a_at	0.000171638	0.83	RIKEN cDNA 5730427N09 gene /// similar to TGF beta-inducible nuclear protein 1 (L-name related LNR42)
1435767_at	0.000102555	0.81	sodium channel, voltage-gated, type III, beta
1420871_at	0.00033192	0.81	guanylate cyclase 1, soluble, beta 3
1456377_x_at	5.70E-05	0.81	RIKEN cDNA 0610025L06 gene
1437309_a_at	0.000193657	0.81	replication protein A1
1424002_at	0.000281601	0.80	phosducin-like 3
1416628_at	0.000123932	0.80	RIKEN cDNA 0610006I08 gene
1422568_at	2.14E-05	0.79	nuclear distribution gene E-like homolog 1 (A. nidulans)
1417206_at	0.000282478	0.79	uroporphyrinogen decarboxylase
1420872_at	0.000272629	0.78	guanylate cyclase 1, soluble, beta 3
1428374_at	0.000193233	0.78	glucuronyl C5-epimerase
1417660_s_at	0.000267853	0.77	vacuolar protein sorting 29 (S. pombe)
1425020_at	2.46E-05	0.77	UBX domain containing 4 /// similar to Ubxd4 protein
1455126_x_at	0.000158685	0.77	RIKEN cDNA 2310028O11 gene
1415772_at	0.000189561	0.77	nucleolin
1416153_at	0.00034836	0.77	signal recognition particle 54
1423709_s_at	0.00038122	0.76	phenylalanine-tRNA synthetase-like, beta subunit
1418792_at	0.000165235	0.76	SH3-domain GRB2-like 2
1448357_at	0.00036854	0.76	small nuclear ribonucleoprotein polypeptide G
1436101_at	0.000178128	0.75	ring finger protein 24
1448761_a_at	0.000231828	0.75	coatomer protein complex, subunit gamma 2
1455940_x_at	0.00020585	0.74	WD repeat domain 6
1448809_at	0.00032438	0.74	chromosome segregation 1-like (S. cerevisiae)
1448203_at	0.000234022	0.74	ATP synthase, H+ transporting, mitochondrial F0 complex, subunit g
1423655_a_at	7.16E-05	0.73	RIKEN cDNA 1500010J02 gene
1452754_at	9.59E-05	0.73	RIKEN cDNA 5730592L21 gene
1434955_at	2.93E-07	0.73	membrane-associated ring finger (C3HC4) 1
1424828_a_at	0.000127627	0.73	fumarate hydratase 1
1450258_a_at	0.000308638	0.73	ELAV (embryonic lethal, abnormal vision, Drosophila)-like 4 (Hu antigen D)

1436889_at	0.00012079	0.73	gamma-aminobutyric acid (GABA-A) receptor, subunit alpha 1
1433794_at	8.85E-05	0.73	amyotrophic lateral sclerosis 4 homolog (human)
1428503_a_at	7.91E-06	0.71	NFKB inhibitor interacting Ras-like protein 1
1451202_at	0.000104819	0.71	RIKEN cDNA C330007P06 gene
1448100_at	0.000112153	0.71	RIKEN cDNA 4833439L19 gene
1418383_at	0.00024715	0.71	adenomatosis polyposis coli down-regulated 1
1426783_at	8.33E-05	0.70	GCN5 general control of amino acid synthesis-like 2 (yeast)
1419522_at	0.00037263	0.70	zinc finger, MYND domain containing 19
1424348_at	0.00036461	0.70	RIKEN cDNA 1110007A13 gene
1448483_a_at	0.000212503	0.70	NADH dehydrogenase (ubiquinone) 1 beta subcomplex, 2
1459749_s_at	0.00033687	0.70	FAT tumor suppressor homolog 4 (Drosophila)
1437742_at	0.000223517	0.69	RAB21, member RAS oncogene family
1455159_at	0.00038107	0.69	RIKEN cDNA 2900057D21 gene
1428331_at	0.00034975	0.69	RIKEN cDNA 2210016F16 gene
1424223_at	0.000149413	0.68	RIKEN cDNA 1700020C11 gene
1455465_at	0.000217527	0.68	Adult male medulla oblongata cDNA, RIKEN full-length enriched library, clone:6330504I23 product:unclassifiable, full insert sequence
1448429_at	0.000157653	0.68	glycogenin 1
1424679_at	0.00017743	0.68	mab-21-like 1 (C. elegans)
1436325_at	6.96E-06	0.68	RAR-related orphan receptor alpha
1426736_at	0.000291976	0.68	G1 to S phase transition 1
1424548_at	4.53E-05	0.67	zinc finger, CCCH-type with G patch domain
1424501_at	0.000266472	0.67	RIKEN cDNA 4732497O03 gene
1428906_at	8.33E-06	0.67	general transcription factor IIH, polypeptide 5
1436266_x_at	1.86E-05	0.67	chromobox homolog 1 (Drosophila HP1 beta)
1420616_at	2.67E-06	0.67	ash2 (absent, small, or homeotic)-like (Drosophila)
1441969_at	5.26E-05	0.66	tripartite motif-containing 36
1418902_at	3.51E-05	0.65	RIKEN cDNA 3110023E09 gene
1424895_at	5.80E-05	0.65	G-protein signalling modulator 2 (AGS3-like, C. elegans)
1416549_at	6.34E-05	0.65	solute carrier family 35, member B4
1454814_s_at	0.000152026	0.65	expressed sequence AU021838
1421882_a_at	0.00034826	0.65	ELAV (embryonic lethal, abnormal vision, Drosophila)-like 2 (Hu antigen B)
1417555_at	0.000157641	0.65	ATPase family, AAA domain containing 1
1425981_a_at	2.28E-05	0.64	retinoblastoma-like 2
1431163_at	0.00011715	0.64	RIKEN cDNA 2700046G09 gene
1429252_at	0.000159177	0.64	RIKEN cDNA 0610010K14 gene (0610010K14Rik), mRNA
1421369_a_at	0.00036578	0.64	mab-21-like 1 (C. elegans)
1423109_s_at	0.000162733	0.64	solute carrier family 25 (mitochondrial carnitine/acylcarnitine translocase), member 20
1434552_at	0.000193604	0.64	WD repeat domain 77
1448672_a_at	0.00037638	0.64	zinc finger protein 289
1425531_at	0.000298986	0.64	zinc finger, HIT domain containing 1

1448372_a_at	4.72E-05	0.64	transmembrane protein 4
1423482_at	4.26E-05	0.63	uroporphyrinogen III synthase
1452284_at	5.62E-05	0.63	protein tyrosine phosphatase, receptor type Z, polypeptide 1
1450966_at	0.000123501	0.63	carnitine O-octanoyltransferase
1423410_at	0.000111604	0.63	meiosis expressed gene 1
1430889_a_at	0.000180387	0.63	thiopurine methyltransferase
1433748_at	9.56E-05	0.63	zinc finger, DHHC domain containing 18
1418148_at	4.54E-05	0.62	abhydrolase domain containing 1
1433953_at	0.000277467	0.62	zinc finger protein 277
1416991_at	3.28E-05	0.61	mitochondrial translation optimization 1 homolog (S. cerevisiae)
1422561_at	0.000150297	0.61	a disintegrin-like and metallopeptidase (reprolysin type) with thrombospondin type 1 motif, 5 (aggrecanase-2)
1429364_at	0.00021382	0.61	RIKEN cDNA 4930579G24 gene
1448287_at	4.32E-05	0.61	RNA polymerase 1-3
1417847_at	0.000216243	0.60	Unc-51 like kinase 2 (C. elegans)
1428620_at	0.000142209	0.60	endosulfine alpha
1425114_at	0.0003375	0.60	retinoblastoma binding protein 6
1460041_at	0.000288987	0.59	RIKEN cDNA D630040I23 gene
1424646_at	8.21E-05	0.59	uridine-cytidine kinase 1-like 1
1452440_at	0.000106035	0.59	tumor necrosis factor (ligand) superfamily, member 12 /// tumor necrosis factor (ligand) superfamily, member 12-member 13
1452883_a_at	0.00038041	0.59	RIKEN cDNA 2310002J21 gene
1426111_x_at	0.00038149	0.58	interferon regulatory factor 3
1427326_at	0.000217915	0.58	RIKEN cDNA 4732471D19 gene
1428636_at	0.0003671	0.58	six transmembrane epithelial antigen of prostate 2
1455337_at	0.000305282	0.58	RIKEN cDNA 9030023J02 gene
1460465_at	0.000145719	0.57	RIKEN cDNA A930038C07 gene
1440215_at	0.000158117	0.57	hypothetical protein C130086A10
1417609_at	0.00035402	0.57	ubiquitin-conjugating enzyme E2A, RAD6 homolog (S. cerevisiae)
1419078_at	1.83E-05	0.56	ninein
1437783_x_at	0.000100968	0.56	transmembrane protein 4
1457708_at	0.000184157	0.56	methyl-CpG binding domain protein 4
1438197_at	0.000141909	0.56	expressed sequence AI854408
1424946_a_at	0.000148187	0.55	mitochondrial fission regulator 1
1418516_at	0.00026168	0.55	metal response element binding transcription factor 2
1422819_at	6.97E-05	0.55	mitochondrial ribosomal protein L36
1450980_at	0.000103876	0.55	GTP binding protein 3
1428975_at	0.000117113	0.55	sushi domain containing 3
1448858_at	0.000303964	0.54	Unc-51 like kinase 2 (C. elegans)
1435096_at	0.000201171	0.54	resistance to inhibitors of cholinesterase 8 homolog B (C. elegans)
1449393_at	0.000311101	0.54	SH2 domain protein 1A
1424575_at	0.000219434	0.54	RAB, member of RAS oncogene family-like 5

1441945_s_at	8.07E-05	0.54	abhydrolase domain containing 14A
1456789_at	3.90E-05	0.54	---
1424896_at	0.0001937	0.54	G protein-coupled receptor 85
1448943_at	0.000273847	0.54	neuropilin 1
1455472_at	0.0003464	0.54	RIKEN cDNA A630071D13 gene
1437872_at	0.000267925	0.53	cDNA sequence AB112350
1426364_at	7.83E-05	0.53	---
1434771_at	0.000186056	0.52	RIKEN cDNA 0610011F06 gene
1427401_at	1.69E-05	0.52	cholinergic receptor, nicotinic, alpha polypeptide 5
1456378_s_at	9.41E-05	0.51	F-box and leucine-rich repeat protein 20
1455906_at	8.18E-05	0.51	RIKEN cDNA 6030446N20 gene
1436833_x_at	0.000289796	0.51	tubulin tyrosine ligase-like 1
1433620_at	0.000189197	0.51	WD repeat domain 41
1433495_at	0.000297816	0.51	glycosyltransferase 25 domain containing 1
1451991_at	0.000237475	0.49	Eph receptor A7
1457686_at	2.88E-05	0.48	RIKEN cDNA B230333C21 gene /// similar to DNA segment on chromosome X and Y (unique) 155 expressed sequence isoform 1
1443952_at	0.000252875	0.48	thyroid hormone receptor alpha
1451271_a_at	2.13E-05	0.47	acetyl-Coenzyme A acetyltransferase 1
1455213_at	7.91E-05	0.47	RIKEN cDNA 4930488E11 gene
1449749_s_at	0.000113813	0.47	transcription factor B1, mitochondrial
1450034_at	3.76E-05	0.47	signal transducer and activator of transcription 1
1418045_at	9.25E-05	0.46	inositol polyphosphate-1-phosphatase
1423923_a_at	0.000211421	0.46	WD repeat domain 8
1418529_at	1.40E-05	0.46	O-sialoglycoprotein endopeptidase
1429059_s_at	0.000231783	0.44	RIKEN cDNA 1110004B13 gene
1416349_at	0.000115826	0.44	mitochondrial ribosomal protein L34
1435668_at	0.00024082	0.44	---
1453128_at	5.34E-05	0.43	extra cellular link domain-containing 1
1448905_at	0.000173644	0.43	expressed in non-metastatic cells 3
1440343_at	0.000189249	0.42	ribosomal protein S6 kinase, polypeptide 5
1433831_at	0.00038315	0.42	RIKEN cDNA 4833418A01 gene
1417859_at	0.00032746	0.42	growth arrest specific 7
1444139_at	0.000174918	0.41	DNA-damage-inducible transcript 4-like
1440485_at	0.00011189	0.41	---
1416826_a_at	6.07E-05	0.41	Trf (TATA binding protein-related factor)-proximal protein homolog (Drosophila)
1417680_at	2.47E-05	0.41	potassium voltage-gated channel, shaker-related subfamily, member 5
1428760_at	1.94E-05	0.40	small nuclear RNA activating complex, polypeptide 3
1438285_at	1.68E-05	0.40	RIKEN cDNA 2210015D19 gene
1438407_at	8.20E-05	0.40	RIKEN cDNA 9330132E09 gene
1457969_at	0.000312548	0.40	RAB interacting factor
1451297_at	0.00037322	0.39	gulonolactone (L-) oxidase
1456904_at	6.14E-05	0.39	Transcribed locus
1417834_at	1.19E-05	0.38	synaptojanin 2 binding protein
1436382_at	4.48E-05	0.38	zinc finger and BTB domain containing 12

1433547_s_at	0.000190494	0.37	NudC domain containing 1
1454681_at	3.80E-05	0.37	RNA binding motif protein 35A
1434837_at	5.81E-05	0.37	mediator of DNA damage checkpoint 1
1423343_at	1.53E-05	0.37	solute carrier organic anion transporter family, member 1c1
1452388_at	7.58E-05	0.35	heat shock protein 1A
1439078_at	4.16E-06	0.34	kelch-like 4 (Drosophila)
1453010_at	0.000279593	0.34	RIKEN cDNA 1700069O15 gene
1460107_at	0.000174203	0.32	RIKEN cDNA 1700129I04 gene
1442249_at	0.000103219	0.32	Transcribed locus
1416920_at	0.000143858	0.32	RNA binding motif protein 4
1429655_at	0.000384	0.31	NudC domain containing 1
1424852_at	0.000140109	0.31	myocyte enhancer factor 2C
1421379_at	0.00034147	0.31	zinc finger protein 354B
1437647_at	6.54E-05	0.30	death inducer-obliterator 1
1442051_at	0.00026252	0.30	histone 2, H3c1
1456834_at	0.000176314	0.29	IBR domain containing 2 (Ibrdc2), mRNA
1456723_at	2.35E-05	0.29	Zinc finger protein 689, mRNA (cDNA clone IMAGE:1263742)
1450953_at	0.000192568	0.27	WD repeat domain 39
1445709_at	0.000163529	0.25	transformed mouse 3T3 cell double minute 1
1425083_at	0.000221231	0.25	otoraplin
1435158_at	6.09E-05	0.23	RNA binding motif protein 12B
1444172_at	0.00026394	0.21	Transcribed locus
1416961_at	1.20E-06	0.18	budding uninhibited by benzimidazoles 1 homolog, beta (S. cerevisiae)
1447363_s_at	8.09E-06	0.16	budding uninhibited by benzimidazoles 1 homolog, beta (S. cerevisiae)
1435692_at	3.79E-05	0.14	Adult male hippocampus cDNA, RIKEN full-length enriched library, clone:C630017C20 product:hypothetical K+ channel tetramerisation/BTB/POZ/BTB domain profile containing protein, full insert sequence
1429169_at	0.000254317	0.05	RNA binding motif protein 3

TABLE 2 Differentially Regulated Genes by Hypoxic Preconditioning H2

AffymetrixID	pValue	Fold change	Gene
1440257_at	0.00041684	22.63	oocyte specific homeobox 6
1450692_at	0.00038942	8.91	kinesin family member 4
1422557_s_at	0.00050407	6.11	metallothionein 1
1454409_at	0.00039689	5.90	RIKEN cDNA 4833408G04 gene
1455385_at	0.00060015	5.55	SEC15-like 1 (S. cerevisiae)
1442366_at	0.00032571	4.35	RIKEN cDNA 6820408C15 gene (6820408C15Rik), mRNA
1441430_at	0.000593	4.25	Transcribed locus
1456653_a_at	0.00076918	3.50	methylenetetrahydrofolate dehydrogenase (NADP+ dependent) 1-like

1449007_at	0.00042528	3.37	B-cell translocation gene 3
1416125_at	2.35508E-05	3.27	FK506 binding protein 5
1417042_at	0.000167361	3.22	solute carrier family 37 (glycerol-6-phosphate transporter), member 4
1448231_at	0.000194797	3.12	FK506 binding protein 5
1441935_at	0.00014658	2.99	ankyrin repeat, family A (RFXANK-like), 2
1422885_at	0.000111381	2.58	small nuclear ribonucleoprotein D3
1436605_at	1.33921E-05	2.54	transketolase
1426389_at	0.000122515	2.53	calcium/calmodulin-dependent protein kinase ID
1427364_a_at	0.000276494	2.47	ornithine decarboxylase, structural 1 /// similar to Ornithine decarboxylase (ODC) /// similar to Ornithine decarboxylase (ODC)
1453522_at	0.00065951	2.47	RIKEN cDNA 6530401N04 gene
1439912_at	0.00059301	2.46	RIKEN cDNA 9430098F02 gene
1452050_at	0.000066249	2.41	calcium/calmodulin-dependent protein kinase ID
1453429_at	0.00065894	2.36	RIKEN cDNA 9530057J20 gene
1425607_at	0.00065431	2.26	holocarboxylase synthetase (biotin- [propriony-Coenzyme A-carboxylase (ATP-hydrolysing)] ligase)
1424834_s_at	0.00062738	2.18	inositol 1,4,5-triphosphate receptor 2
1424149_at	0.000178513	2.02	RIKEN cDNA 1110014D18 gene
1434952_at	0.00057342	1.96	Cytochrome c oxidase subunit IV isoform 1 (Cox4i1), mRNA
1435647_at	0.00054926	1.94	inhibitor of kappaB kinase gamma
1436108_at	0.000088128	1.92	thioredoxin domain containing 9
1450648_s_at	0.00033116	1.82	histocompatibility 2, class II antigen A, beta 1
1417096_at	0.00032979	1.80	RIKEN cDNA 2810430M08 gene
1425024_at	0.00068655	1.80	RIKEN cDNA E430018J23 gene
1423980_at	0.000128141	1.80	solute carrier family 25 (mitochondrial carrier, palmitoylcarnitine transporter), member 29
1437076_at	0.00071934	1.80	RIKEN cDNA A930017M01 gene
1447944_at	0.00034731	1.79	zinc finger with KRAB and SCAN domains 1
1448359_a_at	0.00053321	1.79	HIG1 domain family, member 1A
1460473_at	0.00042559	1.78	RIKEN cDNA 6230400D17 gene
1428832_at	0.000102193	1.77	RIKEN cDNA 1600002H07 gene
1448765_at	0.000039349	1.75	Fyn proto-oncogene
1416155_at	0.00078399	1.73	high mobility group box 3
1435881_at	0.00042308	1.72	poly(rC) binding protein 2
1416595_at	0.00035816	1.71	mitochondrial ribosomal protein S22
1457949_at	0.00069063	1.70	Transcribed locus
1452835_a_at	0.0007643	1.69	polymerase (RNA) mitochondrial (DNA directed)
1417742_a_at	0.00020495	1.63	DNA methyltransferase 1-associated protein 1
1448607_at	0.00059606	1.63	pre-B-cell colony-enhancing factor 1
1429337_at	0.00056578	1.62	RIKEN cDNA 2610301K12 gene
1423981_x_at	2.87152E-06	1.61	solute carrier family 25 (mitochondrial carrier, palmitoylcarnitine transporter), member 29
1455027_at	0.00066007	1.61	DNA segment, Chr 5, Brigham & Women's Genetics 0860 expressed
1436886_x_at	0.00077386	1.61	XPA binding protein 2

1455320_at	0.0007447	1.59	expressed sequence AI480535
1418284_at	0.00075021	1.57	vacuolar protein sorting 72 (yeast)
1449039_a_at	0.000103588	1.56	heterogeneous nuclear ribonucleoprotein D-like
1452515_a_at	0.000239423	1.55	xylosyltransferase II
1454690_at	0.000154256	1.55	inhibitor of kappaB kinase gamma
1416890_at	0.000036626	1.53	WD repeat domain 74
1428375_at	0.000142557	1.53	---
1454913_at	0.000298883	1.52	RIKEN cDNA 9930104L06 gene
1435187_at	0.000247526	1.50	Translocase of outer mitochondrial membrane 20 homolog (yeast) (Tomm20), mRNA
1442002_at	0.00048741	1.49	RIKEN cDNA 7030402D04 gene
1447027_s_at	0.00068279	1.47	lipoic acid synthetase
1432384_a_at	0.00060644	1.47	RIKEN cDNA 1600013P15 gene
1423970_at	0.00054272	1.46	THO complex 3
1428927_at	0.000274764	1.46	SHQ1 homolog (S. cerevisiae)
1451163_at	0.000189693	1.45	Terf1 (TRF1)-interacting nuclear factor 2
1417875_at	0.000114952	1.45	DEAD (Asp-Glu-Ala-Asp) box polypeptide 50
1426510_at	0.000080706	1.44	saccharopine dehydrogenase (putative)
1423811_at	0.000235167	1.44	splicing factor 3a, subunit 3
1423218_a_at	0.000236316	1.44	mitochondrial ribosomal protein L49
1435544_at	0.00065469	1.44	exosome component 6
1418789_at	0.000203658	1.44	syntrophin, gamma 2
1455339_at	0.000191371	1.43	RIKEN cDNA C430014M02 gene
1450172_at	0.0003594	1.42	Pbx/knotted 1 homeobox
1426845_at	0.000090318	1.42	RIKEN cDNA 6030457N17 gene
1426987_at	0.000150698	1.42	RIKEN cDNA 5430417L22 gene
1423197_a_at	0.000046991	1.42	expressed sequence AW011752
1452148_at	0.000211751	1.41	low density lipoprotein receptor-related protein associated protein 1
1428274_s_at	0.000088279	1.41	RIKEN cDNA 1110065L07 gene
1428407_at	1.05742E-05	1.41	heterogeneous nuclear ribonucleoprotein A0 /// similar to heterogeneous nuclear ribonucleoprotein A0
1416110_at	0.00054473	1.40	solute carrier family 35, member A4
1435464_at	0.00032156	1.39	RIKEN cDNA 1110003E01 gene
1427158_at	0.00056069	1.39	mitochondrial ribosomal protein S30
1455354_at	0.00050665	1.38	WD repeat domain 22
1432488_a_at	0.00041313	1.38	splicing factor 3a, subunit 3
1427879_at	0.0001698	1.38	RIKEN cDNA 1810031K17 gene
1425830_a_at	0.00071648	1.37	RIKEN cDNA 2810452K22 gene
1416308_at	0.000067326	1.37	UDP-glucose dehydrogenase
1421756_a_at	0.00039787	1.37	G protein-coupled receptor 19
1438397_a_at	0.00047047	1.37	RNA-binding region (RNP1, RRM) containing 2
1433993_at	0.00047468	1.36	RIKEN cDNA 4931406P16 gene
1423112_at	0.000234545	1.36	ubiquitin-conjugating enzyme E2D 3 (UBC4/5 homolog, yeast)
1426789_s_at	0.000165419	1.35	structure specific recognition protein 1
1433554_at	0.00049141	1.35	expressed sequence AU022870
1431784_a_at	0.000120005	1.34	brix domain containing 5

1415715_at	0.000223839	1.34	RIKEN cDNA 0610039G24 gene
1424887_at	0.00057766	1.33	kelch domain containing 4
1422712_a_at	0.00063827	1.33	ubiquitin-conjugating enzyme E2I
1415985_at	0.00064683	1.32	splicing factor 3b, subunit 3
1452978_at	0.00065586	1.32	RIKEN cDNA 2900055D14 gene
1427080_at	0.0005302	1.32	RIKEN cDNA 2610036D13 gene
1454669_at	0.00076603	1.32	transmembrane protein 11
1426644_at	0.00067247	1.31	TBC1 domain family, member 20
1437071_at	0.00071196	1.31	eukaryotic translation initiation factor 1A, Y-linked
1434088_at	0.00038948	1.31	zinc finger protein 496
1455430_at	0.000201884	1.31	RIKEN cDNA 3200001K10 gene
1424036_at	0.00017426	1.30	RIKEN cDNA 2610031L17 gene
1417264_at	0.000098384	1.30	DNA segment, Chr 5, ERATO Doi 33, expressed
1416866_at	0.00050974	1.29	blocked early in transport 1 homolog (S. cerevisiae)
1416096_at	0.00078368	1.29	expressed sequence AI413782
1450891_at	0.000102644	1.29	signal recognition particle 19
1416341_at	0.00071176	1.29	polymerase (RNA) II (DNA directed) polypeptide C
1451267_at	0.00036524	1.28	SHANK-associated RH domain interacting protein
1424787_a_at	0.00075464	1.28	nuclear respiratory factor 1
1426790_at	0.000302831	1.27	structure specific recognition protein 1
1438771_at	1.91437E-05	1.27	bromodomain containing 1
1451587_a_at	1.79119E-05	1.27	TIP41, TOR signalling pathway regulator-like (S. cerevisiae)
1448711_at	0.000156469	1.27	minichromosome maintenance deficient 3 (S. cerevisiae) associated protein
1435469_at	0.00075773	1.27	quiescin Q6-like 1
1434233_at	0.000263258	1.25	---
1422795_at	0.00035914	1.25	cullin 3
1418648_at	0.0005135	1.25	EGL nine homolog 3 (C. elegans)
1452765_at	0.0000607	1.25	solute carrier family 39 (zinc transporter), member 9
1421135_a_at	0.00025818	1.24	CCR4-NOT transcription complex, subunit 8
1460360_at	0.00042751	1.24	asparaginase like 1
1455898_x_at	0.00056659	1.24	solute carrier family 2 (facilitated glucose transporter), member 3
1427916_at	0.000266575	1.24	suppression of tumorigenicity 7-like
1424251_a_at	0.00067173	1.24	heterogeneous nuclear ribonucleoprotein D-like
1418974_at	0.00032603	1.23	basic leucine zipper nuclear factor 1
1426871_at	0.000084881	1.23	F-box only protein 33
1460171_at	0.00063067	1.23	COP9 (constitutive photomorphogenic) homolog, subunit 5 (Arabidopsis thaliana)
1436828_a_at	0.00072521	1.23	tumor protein D52-like 2
1436028_at	2.20041E-05	1.23	transmembrane protein 33
1435249_at	0.0002232	1.22	BTAF1 RNA polymerase II, B-TFIID transcription factor-associated, 170kDa (Mot1 homolog, S. cerevisiae)
1448970_at	0.00006227	1.22	RIKEN cDNA 1200007B05 gene
1434884_at	0.000103	1.21	Metadherin
1456746_a_at	0.00062566	1.21	Cd99 antigen-like 2
1426939_at	0.00062415	1.20	RIKEN cDNA 2310007F12 gene

1418014_a_at	0.000190135	1.19	UDP-Gal:betaGlcNAc beta 1,4-galactosyltransferase, polypeptide 1
1423573_at	0.00052182	1.19	steroid 5 alpha-reductase 2-like
1447931_at	0.000113849	1.19	Wolf-Hirschhorn syndrome candidate 1-like 1 (human)
1439044_at	0.00055504	1.19	zinc finger protein 354C
1451315_at	0.00057924	1.18	RIKEN cDNA 2610511E22 gene
1426256_at	0.000299568	1.17	translocase of inner mitochondrial membrane 17a
1434289_at	0.00074721	1.17	NOL1/NOP2/Sun domain family, member 5
1453928_a_at	0.00054048	1.16	Sjogren syndrome antigen B
1448488_at	0.00049978	1.14	mitochondrial ribosomal protein S5
1418198_a_at	0.00033672	1.13	transmembrane 9 superfamily member 1
1452039_a_at	0.000307184	1.12	Brca1 associated protein 1
1425572_a_at	0.000078574	1.10	development and differentiation enhancing
1453055_at	0.00068191	0.94	sema domain, transmembrane domain (TM), and cytoplasmic domain, (semaphorin) 6D
1416180_a_at	0.00060015	0.85	radixin
1452603_at	0.000040406	0.85	RIKEN cDNA 5330431N19 gene
1425100_a_at	0.00035585	0.83	phosphodiesterase 6G, cGMP-specific, rod, gamma
1423906_at	0.000062875	0.82	heat shock factor binding protein 1
1455042_at	0.000255739	0.81	Transducin (beta)-like 1 X-linked (Tbl1x), mRNA
1418497_at	0.00048397	0.80	fibroblast growth factor 13
1430713_s_at	0.00033778	0.79	NADH dehydrogenase (ubiquinone) 1 alpha subcomplex, 13
1426716_at	0.000294417	0.78	tudor domain containing 7
1417663_a_at	0.00060094	0.78	N-myc downstream regulated gene 3
1422895_at	0.00042365	0.78	vesicle-associated membrane protein 4
1440795_x_at	0.00068297	0.78	rabaptin, RAB GTPase binding effector protein 2
1448788_at	0.00068826	0.78	Cd200 antigen
1420623_x_at	0.00062057	0.77	heat shock protein 8
1422593_at	0.000017666	0.77	adaptor-related protein complex 3, sigma 1 subunit
1435695_a_at	0.00070538	0.77	RIKEN cDNA A030007L17 gene
1452740_at	0.000051796	0.76	myosin, heavy polypeptide 10, non-muscle
1424089_a_at	0.00071507	0.74	transcription factor 4
1454708_at	0.00035905	0.74	actin-binding LIM protein 1
1424813_at	0.00076327	0.74	expressed sequence AA536717
1434260_at	0.00036935	0.73	FCH and double SH3 domains 2
1426957_at	0.00034571	0.73	transformation related protein 53 binding protein 1
1431593_a_at	3.4515E-06	0.72	tRNA splicing endonuclease 34 homolog (SEN34, S. cerevisiae)
1438664_at	0.000256784	0.72	protein kinase, cAMP dependent regulatory, type II beta
1430583_at	0.00058341	0.72	RIKEN cDNA C130076O07 gene
1416394_at	0.00005655	0.71	Bcl2-associated athanogene 1
1415772_at	0.0001464	0.71	nucleolin
1437533_at	0.000267709	0.71	baculoviral IAP repeat-containing 4
1438477_a_at	0.00050285	0.71	methylmalonyl CoA epimerase
1428540_at	0.00044296	0.71	RIKEN cDNA 3321401G04 gene
1436657_at	0.000251579	0.70	16 days neonate cerebellum cDNA, RIKEN full-

			length enriched library, clone:9630002G20 product:hypothetical protein, full insert sequence
1419449_a_at	0.00075818	0.70	guanine nucleotide binding protein, alpha inhibiting 2
1433583_at	0.000084596	0.70	zinc finger protein 365
1449314_at	0.00052148	0.70	zinc finger protein, multitype 2
1435194_at	0.000195651	0.70	Heat shock protein 4, mRNA (cDNA clone MGC:5961 IMAGE:3494648)
1438430_at	0.000102246	0.69	high mobility group box transcription factor 1
1433482_a_at	0.000276507	0.69	far upstream element (FUSE) binding protein 1
1445850_at	0.00063118	0.69	RIKEN cDNA 9530009M10 gene
1437807_x_at	0.00063803	0.69	catenin (cadherin associated protein), alpha 1
1433504_at	0.000039219	0.69	brain glycogen phosphorylase
1440402_at	0.00064376	0.68	RIKEN cDNA 4831426I19 gene
1451047_at	0.00064808	0.68	integral membrane protein 2A
1436560_at	0.000314327	0.68	expressed sequence AW124694
1416156_at	0.00050387	0.67	vinculin
1455700_at	0.00065476	0.67	MTERF domain containing 3
1436833_x_at	0.000113345	0.67	tubulin tyrosine ligase-like 1
1428487_s_at	0.00042433	0.67	RIKEN cDNA 1500041J02 gene
1418716_at	0.000167078	0.67	mitochondrial ribosomal protein S25
1437657_at	0.00078	0.66	zinc finger protein 291
1452284_at	0.00027223	0.65	protein tyrosine phosphatase, receptor type Z, polypeptide 1
1421883_at	0.000192019	0.65	ELAV (embryonic lethal, abnormal vision, Drosophila)-like 2 (Hu antigen B)
1434674_at	0.0006771	0.65	lysosomal trafficking regulator
1424121_at	0.000159114	0.64	COMM domain containing 1
1417605_s_at	2.79936E-05	0.64	calcium/calmodulin-dependent protein kinase I
1450215_at	0.000261052	0.64	recoverin
1435204_at	0.00068621	0.63	heterogeneous nuclear ribonucleoprotein methyltransferase-like 4 (S. cerevisiae)
1420113_s_at	0.0006	0.63	RIKEN cDNA 2410022L05 gene
1427674_a_at	0.000055249	0.63	seizure related gene 6
1456387_at	0.00046616	0.63	nucleolar protein 4
1417830_at	9.6302E-06	0.62	SMC (structural maintenance of chromosomes 1)-like 1 (S. cerevisiae)
1439815_at	0.00071928	0.62	RIKEN cDNA A230048G03 gene
1429119_at	0.000161092	0.62	RIKEN cDNA 4833421E05 gene
1426090_a_at	0.000258489	0.61	fer (fms/fps related) protein kinase, testis specific 2
1429055_at	0.0005368	0.61	RIKEN cDNA 4930506M07 gene
1448657_a_at	0.00069407	0.61	DnaJ (Hsp40) homolog, subfamily B, member 10
1420886_a_at	0.00064077	0.61	X-box binding protein 1
1453398_at	0.00073895	0.60	RIKEN cDNA A930009A15 gene
1417774_at	0.000143992	0.59	N-acetylneuraminic acid synthase (sialic acid synthase)
1416844_at	0.00078285	0.59	heterogeneous nuclear ribonucleoprotein methyltransferase-like 1 (S. cerevisiae)
1428232_at	0.00044938	0.59	cleavage and polyadenylation specific factor 6

1417970_at	0.00066353	0.57	ATP synthase, H+ transporting, mitochondrial F0 complex, subunit s
1428683_at	0.00077926	0.57	RIKEN cDNA A930016P21 gene
1452955_at	0.00048071	0.57	general transcription factor IIH, polypeptide 5
1452923_at	0.00049036	0.56	RIKEN cDNA 1810058I14 gene
1451063_at	0.00069857	0.55	syntaxin binding protein 4
1425757_a_at	0.00077391	0.54	interphotoreceptor matrix proteoglycan 1
1451822_a_at	0.000255811	0.53	secernin 2
1429036_at	0.00037557	0.53	otopetrin 3
1427126_at	0.00070566	0.52	heat shock protein 1A
1455187_at	0.00070079	0.52	zinc finger and BTB domain containing 40
1434577_at	0.000148256	0.49	cDNA sequence BC052040
1422155_at	0.00057822	0.48	histone 2, H3c2
1452318_a_at	1.02611E-05	0.48	heat shock protein 1A
1430245_at	0.00053063	0.47	---
1417604_at	0.000135427	0.47	calcium/calmodulin-dependent protein kinase I
1440928_at	0.000227124	0.47	RIKEN cDNA D630037F22 gene
1428329_a_at	0.00056601	0.45	WD repeat domain 56
1427127_x_at	0.00048937	0.44	heat shock protein 1A
1436203_a_at	0.00065869	0.44	RIKEN cDNA 1110059G02 gene
1439622_at	0.000086218	0.42	Ras association (RalGDS/AF-6) domain family 4
1428550_at	0.000221568	0.40	RIKEN cDNA 1810015A11 gene
1456532_at	0.000115953	0.39	---
1439078_at	4.4327E-06	0.37	kelch-like 4 (Drosophila)

TABLE 3 Differentially Regulated Genes by Hypoxic Preconditioning H4

AffymetrixID	pValue	Fold change	Gene
1450692_at	0.000070106	13.94	kinesin family member 4
1435234_at	0.000033914	1.49	nuclear receptor coactivator 2
1447500_at	0.000038109	1.48	cut-like 2 (Drosophila)
1417551_at	4.2285E-06	1.43	ceroid lipofuscinosis, neuronal 3, juvenile (Batten, Spielmeyer-Vogt disease)
1416821_at	0.000062761	1.33	expressed sequence 2 embryonic lethal
1452197_at	1.42316E-05	1.29	SMC4 structural maintenance of chromosomes 4-like 1 (yeast)
1456056_a_at	0.000066635	1.20	DNA segment, Chr 6, Wayne State University 116, expressed
1415749_a_at	1.36054E-05	1.18	Ras-related GTP binding C
1418345_at	0.000039922	1.15	tumor necrosis factor (ligand) superfamily, member 13 /// tumor necrosis factor (ligand) superfamily, member 12-member 13
1425265_a_at	2.44588E-05	1.14	prion protein interacting protein 1
1435066_at	0.000055061	0.86	phosphatidylinositol transfer protein, cytoplasmic 1
1428306_at	0.000068874	0.83	DNA-damage-inducible transcript 4
1416064_a_at	2.17324E-05	0.76	heat shock 70kD protein 5 (glucose-regulated protein)
1433444_at	0.000067983	0.75	3-hydroxy-3-methylglutaryl-Coenzyme A synthase 1

1452814_at	2.62974E-05	0.75	copine III
1455265_a_at	3.02218E-05	0.73	regulator of G-protein signaling 16
1438504_x_at	0.000051975	0.71	Transmembrane 7 superfamily member 3 (Tm7sf3), mRNA
1423078_a_at	0.000036291	0.70	sterol-C4-methyl oxidase-like
1439006_x_at	6.7052E-06	0.65	RIKEN cDNA 6430550H21 gene
1419225_at	0.000054204	0.63	calcium channel, voltage-dependent, alpha2/delta subunit 3
1443134_at	0.000068282	0.61	Adult retina cDNA, RIKEN full-length enriched library, clone:A930005G22 product:unclassifiable, full insert sequence
1418186_at	2.53811E-05	0.58	glutathione S-transferase, theta 1
1444603_at	0.000045006	0.51	10, 11 days embryo whole body cDNA, RIKEN full-length enriched library, clone:2810030D12 product:unclassifiable, full insert sequence

3.1.1.3 Total List of Real-time PCR Results (Additional File 3)

TABLE 4 Real-Time PCR results (RT) of genes identified by Affymetrix micro-arrays (Chip) as differentially regulated by hypoxic preconditioning.

Gene Symbol	Gene	H0 Chip	H0 RT	pVal	H2 Chip	H2 RT	pVal	H4 Chip	H4 RT	pVal	H16 Chip	H16 RT	pVal
Adm	adrenomedullin	10.59	9.36	***	-	2.5	**	-	1.21	n.s.	-	1.05	n.s.
Bcl2l10	Bcl2-like 10	17.02	30.44	***	-	n.a.		-	n.a.		-	n.a.	
Cdkn1a (p21)	Cyclin dependent kinase inhibitor 1a	30.48	20.26	**	-	4.64	**	-	1.51	n.s.	-	0.8	n.s.
CEBP/d	CCAAT/enhancer binding protein (C/EBP), delta	3.47	3.47	*	-	n.a.		-	n.a.		-	n.a.	
Dido1 (Iso1/3)	death inducer-obliterator 1	0.3	0.86	n.s.	-	n.a.		-	n.a.		-	n.a.	
Dido1 (Iso2)	death inducer-obliterator 1	0.3	1.21	n.s.	-	n.a.		-	n.a.		-	n.a.	
Egf	epidermal growth factor	4.7	2.46	**	-	1.03	n.s.	-	1	n.s.	-	1.71	*
Egln1	Egl nine homolog 1 (C. elegans)	4.44	5.01	**	-	n.a.		-	n.a.		-	n.a.	
Fabp4	Fatty acid binding protein 4, adipocyte (Fabp4), mRNA	3.5	5.33	*	-	n.a.		-	n.a.		-	n.a.	
H3f3B	H3 histone, family 3B	6.28	1.58	n.s.	-	n.a.		-	n.a.		-	n.a.	
Hes6	hairy and enhancer of split 6 (Drosophila)	1.87	1.59	*	-	n.a.		-	n.a.		-	n.a.	
Hmgb2	high mobility group box 2	4.06	3.05	n.s.	-	n.a.		-	n.a.		-	n.a.	
Ibrdc2	IBR domain containing 2 (Ibrdc2), mRNA	0.29	0.96	n.s.	-	n.a.		-	n.a.		-	n.a.	
Id1	inhibitor of DNA binding 1	3.1	1.75	**	-	n.a.		-	n.a.		-	n.a.	
Kif4	kinesin family member 4A	-	2.94	**	8.91	4.42	**	13.94	6.32	***	-	1.31	n.s.
Mef2c	myocyte enhancer factor 2C	0.31	0.7	*	-	n.a.		-	n.a.		-	n.a.	
Metap2	methionine aminopeptidase 2	2.74	0.81	n.s.	-	0.95	n.s.	-	1.18	n.s.	-	0.95	n.s.
Mt1	metallothionein 1	6.26	6.89	***	6.11	n.a.		-	n.a.		-	n.a.	
Pon1	paraoxonase 1	22.55	7.6	***	-	1.3	n.s.	-	1.7	n.s.	-	0.7	n.s.
Rad23b	RAD23b homolog (S. cerevisiae)	2.6	1.17	n.s.	-	n.a.		-	n.a.		-	n.a.	
Sema3c	Semaphorin 3c	5.86	3.86	*	-	n.a.		-	n.a.		-	n.a.	
Slc2A1 (Glut1)	solute carrier family 2 (facilitated glucose transporter),	1.98	1.73	***	-	n.a.		-	n.a.		-	n.a.	
Sos1	Son of sevenless homolog 1 (Drosophila)	1.92	0.88	n.s.	-	n.a.		-	n.a.		-	n.a.	
Stat1	signal transducer and activator of transcription 1	0.47	1.11	n.s.	-	n.a.		-	n.a.		-	n.a.	
Stom	stomatin	2.03	1.29	n.s.	-	n.a.		-	n.a.		-	n.a.	
Thra	thyroid hormone receptor alpha	0.48	0.78	n.s.	-	n.a.		-	n.a.		-	n.a.	
Timp3	tissue inhibitor of metalloproteinase 3	3.28	2.35	***	-	1.45	n.s.	-	1.24	n.s.	-	1.64	*
Ttr	transthyretin	20.11	8.8	**	-	1.2	n.s.	-	1.7	n.s.	-	0.5	n.s.
Vegfa_all	vascular endothelial growth factor	2.25	2	*	-	0.6	*	-	1.1	n.s.	-	1.5	**
Vegf164 (Iso1)	vascular endothelial growth factor isoform1	2.25	2.5	*	-	0.7	n.s.	-	1.3	n.s.	-	1.1	n.s.
Vegf120 (Iso2)	vascular endothelial growth factor isoform2	2.25	1.9	*	-	1.1	n.s.	-	0.9	n.s.	-	1.3	n.s.
Vegf188 (Iso3)	vascular endothelial growth factor isoform 3	2.25	3	*	-	0.9	n.s.	-	1	n.s.	-	0.9	n.s.

3.1.1.4 List of Genes Functionally Clustered by DAVID (Additional File 4)

TABLE 5 Differentially up-regulated genes functionally clustered by DAVID.

Term Category: cellular physiological process; 75 genes (49.02%); pValue 5.11E-04	
Affymetrix ID	Gene
1426727_s_at	PROTEIN PHOSPHATASE 1, REGULATORY SUBUNIT 10
1453851_a_at	GROWTH ARREST AND DNA-DAMAGE-INDUCIBLE 45 GAMMA
1416432_at, 1456676_a_at	6-PHOSPHOFRUCTO-2-KINASE/FRUCTOSE-2,6-BIPHOSPHATASE 3
1426600_at	SOLUTE CARRIER FAMILY 2 (FACILITATED GLUCOSE TRANSPORTER), MEMBER 1
1430798_x_at	MITOCHONDRIAL RIBOSOMAL PROTEIN L15
1454623_at	SIMILAR TO CARBOXYPEPTIDASE A2 PRECURSOR
1423233_at	CCAAT/ENHANCER BINDING PROTEIN (C/EBP), DELTA
1454018_at	TOUSLED-LIKE KINASE 2 (ARABIDOPSIS)
1435245_at	GLUTAMINASE 2 (LIVER, MITOCHONDRIAL)
1416434_at	BCL2-LIKE 10
1437785_at	A DISINTEGRIN-LIKE AND METALLOPEPTIDASE (REPROLYSIN TYPE) WITH THROMBOSPONDIN TYPE 1 MOTIF, 9
1436006_at	EUKARYOTIC TRANSLATION INITIATION FACTOR 2 ALPHA KINASE 1
1459331_at	SURFEIT GENE 6
1433814_at	F-BOX AND LEUCINE-RICH REPEAT PROTEIN 14
1417149_at	PROCOLLAGEN-PROLINE, 2-OXOGLUTARATE 4-DIOXYGENASE (PROLINE 4-HYDROXYLASE), ALPHA II POLYPEPTIDE
1425895_a_at	INHIBITOR OF DNA BINDING 1
1426721_s_at	TCDD-INDUCIBLE POLY(ADP-RIBOSE) POLYMERASE
1448607_at	PRE-B-CELL COLONY-ENHANCING FACTOR 1
1419087_s_at	SPLICING FACTOR 3A, SUBUNIT 1
1442025_a_at	ZINC FINGER AND BTB DOMAIN CONTAINING 16
1427221_at	X TRANSPORTER PROTEIN 3 SIMILAR 1 GENE
1426117_a_at, 1441315_s_at	SOLUTE CARRIER FAMILY 19 (THIAMINE TRANSPORTER), MEMBER 2
1431212_a_at	RIKEN CDNA 3300001M20 GENE
1425809_at	FATTY ACID BINDING PROTEIN 4, ADIPOCYTE
1454991_at	SOLUTE CARRIER FAMILY 7 (CATIONIC AMINO ACID TRANSPORTER, Y+ SYSTEM), MEMBER 1
1418093_a_at	EPIDERMAL GROWTH FACTOR
1430357_at	H3 HISTONE, FAMILY 3A
1440555_at	RAS-RELATED GTP BINDING D
1430197_a_at	PHOSPHATIDYLINOSITOL TRANSFER PROTEIN, MEMBRANE-ASSOCIATED 2
1424143_a_at, 1424144_at	RETROVIRAL INTEGRATION SITE 2
1425732_a_at	MAX INTERACTING PROTEIN 1
1422832_at	RETINAL G PROTEIN COUPLED RECEPTOR
1416309_at	EXPRESSED SEQUENCE AW547774
1437313_x_at, 1452534_a_at	HIGH MOBILITY GROUP BOX 2
1422885_at	SMALL NUCLEAR RIBONUCLEOPROTEIN D3
1416039_x_at	CYSTEINE RICH PROTEIN 61

1422557_s_at	METALLOTHIONEIN 1
1450725_s_at	CARBONIC ANHYDRASE 14
1447494_at	RIKEN CDNA 2600013E07 GENE
1454949_at	RIKEN CDNA 2210010O09 GENE
1427364_a_at, 1438761_a_at	ORNITHINE DECARBOXYLASE, STRUCTURAL 1
1438606_a_at	CHLORIDE INTRACELLULAR CHANNEL 4 (MITOCHONDRIAL)
1436279_at	SOLUTE CARRIER FAMILY 26, MEMBER 7
1418190_at	PARAOXONASE 1
1419029_at, 1419030_at, 1449324_at	ERO1-LIKE (S. CEREVISIAE)
1416749_at, 1438251_x_at	HTRA SERINE PEPTIDASE 1
1416125_at, 1448231_at	FK506 BINDING PROTEIN 5
1449007_at	B-CELL TRANSLOCATION GENE 3
1429050_at	CYSTEINE-RICH HYDROPHOBIC DOMAIN 2
1439677_at	EPILEPSY, PROGRESSIVE MYOCLONIC EPILEPSY, TYPE 2 GENE ALPHA
1419024_at, 1455002_at	PROTEIN TYROSINE PHOSPHATASE 4A1
1454608_x_at, 1455913_x_at	TRANSTHYRETIN
1454109_a_at	PHOSPHATIDYLSERINE RECEPTOR
1434952_at	CYTOCHROME C OXIDASE SUBUNIT IV ISOFORM 1
1457451_at	ACTIVIN RECEPTOR IIA
1452050_at	CALCIUM/CALMODULIN-DEPENDENT PROTEIN KINASE ID
1459978_x_at	GENE MODEL 877, (NCBI)
1444487_at	LECITHIN-RETINOL ACYLTRANSFERASE (PHOSPHATIDYLCHOLINE-RETINOL-O-ACYLTRANSFERASE)
1455385_at	EXOCYST COMPLEX COMPONENT 6
1424638_at	CYCLIN-DEPENDENT KINASE INHIBITOR 1A (P21)
1436531_at	METHIONINE AMINOPEPTIDASE 2
1435870_at	SYNAPTONEMAL COMPLEX PROTEIN 3
1438815_at	HISTONE 2, H2AA1
1448654_at	MITOCHONDRIAL CARRIER HOMOLOG 2 (C. ELEGANS)
1435875_at	PROTEIN KINASE, AMP-ACTIVATED, BETA 2 NON-CATALYTIC SUBUNIT
1440257_at	OOCYTE SPECIFIC HOMEOBOX 6
1444528_at	ZINC FINGER PROTEIN 316
1420138_at	SOLUTE CARRIER FAMILY 19 (SODIUM/HYDROGEN EXCHANGER), MEMBER 1
1455420_at	RAD23B HOMOLOG (S. CEREVISIAE)
1454903_at	NERVE GROWTH FACTOR RECEPTOR (TNFR SUPERFAMILY, MEMBER 16)
1416344_at	LYSOSOMAL MEMBRANE GLYCOPROTEIN 2
1420909_at, 1451959_a_at	VASCULAR ENDOTHELIAL GROWTH FACTOR A
1423865_at	SOLUTE CARRIER FAMILY 44, MEMBER 1
1442397_at	NUCLEAR X BOX BINDING FACTOR 1
1428942_at	METALLOTHIONEIN 2
Term Category: negative regulation of biological process; 13 genes (8.5%); pValue 0.0015	
Affymetrix ID	Gene
1453851_a_at	GROWTH ARREST AND DNA-DAMAGE-INDUCIBLE 45 GAMMA
1442025_a_at	ZINC FINGER AND BTB DOMAIN CONTAINING 16
1425809_at	FATTY ACID BINDING PROTEIN 4, ADIPOCYTE

1424638_at	CYCLIN-DEPENDENT KINASE INHIBITOR 1A (P21)
1416749_at, 1438251_x_at	HTRA SERINE PEPTIDASE 1
1449007_at	B-CELL TRANSLOCATION GENE 3
1416434_at	BCL2-LIKE 10
1425732_a_at	MAX INTERACTING PROTEIN 1
1436006_at	EUKARYOTIC TRANSLATION INITIATION FACTOR 2 ALPHA KINASE 1
1425895_a_at	INHIBITOR OF DNA BINDING 1
1420909_at, 1451959_a_at	VASCULAR ENDOTHELIAL GROWTH FACTOR A
1442397_at	NUCLEAR X BOX BINDING FACTOR 1
1422803_at	FOLLISTATIN-LIKE 3

Term Category: enzyme linked receptor protein signaling pathway; 7 genes (4.58%); pValue 0.0025

Affymetrix ID	Gene
1418093_a_at	EPIDERMAL GROWTH FACTOR
1425895_a_at	INHIBITOR OF DNA BINDING 1
1419089_at, 1449335_at	TISSUE INHIBITOR OF METALLOPROTEINASE 3
1429348_at	SEMA DOMAIN, IMMUNOGLOBULIN DOMAIN (IG), SHORT BASIC DOMAIN, SECRETED, (SEMAPHORIN) 3C
1416749_at, 1438251_x_at	HTRA SERINE PEPTIDASE 1
1457451_at	ACTIVIN RECEPTOR IIA
1422803_at	FOLLISTATIN-LIKE 3

Term Category: negative regulation of cellular process; 12 genes (7.84%); pValue 0.0025

Affymetrix ID	Gene
1449007_at	B-CELL TRANSLOCATION GENE 3
1416434_at	BCL2-LIKE 10
1442025_a_at	ZINC FINGER AND BTB DOMAIN CONTAINING 16
1425732_a_at	MAX INTERACTING PROTEIN 1
1436006_at	EUKARYOTIC TRANSLATION INITIATION FACTOR 2 ALPHA KINASE 1
1425895_a_at	INHIBITOR OF DNA BINDING 1
1425809_at	FATTY ACID BINDING PROTEIN 4, ADIPOCYTE
1424638_at	CYCLIN-DEPENDENT KINASE INHIBITOR 1A (P21)
1420909_at, 1451959_a_at	VASCULAR ENDOTHELIAL GROWTH FACTOR A
1442397_at	NUCLEAR X BOX BINDING FACTOR 1
1416749_at, 1438251_x_at	HTRA SERINE PEPTIDASE 1
1422803_at	FOLLISTATIN-LIKE 3

Term Category: protein metabolism; 30 genes (19.61%); pValue 0.0037

Affymetrix ID	Gene
1453851_a_at	GROWTH ARREST AND DNA-DAMAGE-INDUCIBLE 45 GAMMA
1454949_at	RIKEN CDNA 2210010O09 GENE
1423785_at	EGL NINE HOMOLOG 1 (C. ELEGANS)
1419029_at, 1419030_at, 1449324_at	ERO1-LIKE (S. CEREVISIAE)
1416749_at, 1438251_x_at	HTRA SERINE PEPTIDASE 1
1416125_at, 1448231_at	FK506 BINDING PROTEIN 5
1430798_x_at	MITOCHONDRIAL RIBOSOMAL PROTEIN L15
1454018_at	TOUSLED-LIKE KINASE 2 (ARABIDOPSIS)
1454623_at	SIMILAR TO CARBOXYPEPTIDASE A2 PRECURSOR
1439677_at	EPILEPSY, PROGRESSIVE MYOCLONIC EPILEPSY, TYPE 2 GENE ALPHA

1437785_at	A DISINTEGRIN-LIKE AND METALLOPEPTIDASE (REPROLYSIN TYPE) WITH THROMBOSPONDIN TYPE 1 MOTIF, 9
1459331_at	SURFEIT GENE 6
1433814_at	F-BOX AND LEUCINE-RICH REPEAT PROTEIN 14
1436006_at	EUKARYOTIC TRANSLATION INITIATION FACTOR 2 ALPHA KINASE 1
1417149_at	PROCOLLAGEN-PROLINE, 2-OXOGLUTARATE 4-DIOXYGENASE (PROLINE 4-HYDROXYLASE), ALPHA II POLYPEPTIDE
1419024_at, 1455002_at	PROTEIN TYROSINE PHOSPHATASE 4A1
1426721_s_at	TCDD-INDUCIBLE POLY(ADP-RIBOSE) POLYMERASE
1457451_at	ACTIVIN RECEPTOR IIA
1419087_s_at	SPLICING FACTOR 3A, SUBUNIT 1
1452050_at	CALCIUM/CALMODULIN-DEPENDENT PROTEIN KINASE ID
1431212_a_at	RIKEN CDNA 3300001M20 GENE
1436531_at	METHIONINE AMINOPEPTIDASE 2
1438815_at	HISTONE 2, H2AA1
1418093_a_at	EPIDERMAL GROWTH FACTOR
1430357_at	H3 HISTONE, FAMILY 3A
1455420_at	RAD23B HOMOLOG (S. CEREVISIAE)
1422832_at	RETINAL G PROTEIN COUPLED RECEPTOR
1437313_x_at, 1452534_a_at	HIGH MOBILITY GROUP BOX 2
1416344_at	LYSOSOMAL MEMBRANE GLYCOPROTEIN 2
1442397_at	NUCLEAR X BOX BINDING FACTOR 1
Term Category: regulation of cell proliferation; 7 genes (4.58%); pValue 0.0038	
Affymetrix ID	Gene
1418093_a_at	EPIDERMAL GROWTH FACTOR
1449007_at	B-CELL TRANSLOCATION GENE 3
1442025_a_at	ZINC FINGER AND BTB DOMAIN CONTAINING 16
1427364_a_at, 1438761_a_at	ORNITHINE DECARBOXYLASE, STRUCTURAL 1
1436006_at	EUKARYOTIC TRANSLATION INITIATION FACTOR 2 ALPHA KINASE 1
1424638_at	CYCLIN-DEPENDENT KINASE INHIBITOR 1A (P21)
1420909_at, 1451959_a_at	VASCULAR ENDOTHELIAL GROWTH FACTOR A
Term Category: positive regulation of physiological process; 10 genes (6.54%); pValue 0.0059	
Affymetrix ID	Gene
1418093_a_at	EPIDERMAL GROWTH FACTOR
1416434_at	BCL2-LIKE 10
1442025_a_at	ZINC FINGER AND BTB DOMAIN CONTAINING 16
1427364_a_at, 1438761_a_at	ORNITHINE DECARBOXYLASE, STRUCTURAL 1
1425809_at	FATTY ACID BINDING PROTEIN 4, ADIPOCYTE
1416309_at	EXPRESSED SEQUENCE AW547774
1424638_at	CYCLIN-DEPENDENT KINASE INHIBITOR 1A (P21)
1454903_at	NERVE GROWTH FACTOR RECEPTOR (TNFR SUPERFAMILY, MEMBER 16)
1419024_at, 1455002_at	PROTEIN TYROSINE PHOSPHATASE 4A1
1420909_at, 1451959_a_at	VASCULAR ENDOTHELIAL GROWTH FACTOR A
Term Category: positive regulation of biological process; 11 genes (7.19%); pValue 0.0078	

Affymetrix ID	Gene
1418093_a_at	EPIDERMAL GROWTH FACTOR
1453851_a_at	GROWTH ARREST AND DNA-DAMAGE-INDUCIBLE 45 GAMMA
1416434_at	BCL2-LIKE 10
1442025_a_at	ZINC FINGER AND BTB DOMAIN CONTAINING 16
1427364_a_at, 1438761_a_at	ORNITHINE DECARBOXYLASE, STRUCTURAL 1
1425809_at	FATTY ACID BINDING PROTEIN 4, ADIPOCYTE
1416309_at	EXPRESSED SEQUENCE AW547774
1424638_at	CYCLIN-DEPENDENT KINASE INHIBITOR 1A (P21)
1454903_at	NERVE GROWTH FACTOR RECEPTOR (TNFR SUPERFAMILY, MEMBER 16)
1419024_at, 1455002_at	PROTEIN TYROSINE PHOSPHATASE 4A1
1420909_at, 1451959_a_at	VASCULAR ENDOTHELIAL GROWTH FACTOR A

Term Category: negative regulation of cellular physiological process; 10 genes (6.54%); pValue 0.0078

Affymetrix ID	Gene
1449007_at	B-CELL TRANSLOCATION GENE 3
1416434_at	BCL2-LIKE 10
1442025_a_at	ZINC FINGER AND BTB DOMAIN CONTAINING 16
1425732_a_at	MAX INTERACTING PROTEIN 1
1436006_at	EUKARYOTIC TRANSLATION INITIATION FACTOR 2 ALPHA KINASE 1
1425895_a_at	INHIBITOR OF DNA BINDING 1
1425809_at	FATTY ACID BINDING PROTEIN 4, ADIPOCYTE
1424638_at	CYCLIN-DEPENDENT KINASE INHIBITOR 1A (P21)
1420909_at, 1451959_a_at	VASCULAR ENDOTHELIAL GROWTH FACTOR A
1442397_at	NUCLEAR X BOX BINDING FACTOR 1

Term Category: transmembrane receptor protein serine/threonine kinase signaling pathway; 4 genes (2.61%); pValue 0.01

Affymetrix ID	Gene
1425895_a_at	INHIBITOR OF DNA BINDING 1
1416749_at, 1438251_x_at	HTRA SERINE PEPTIDASE 1
1457451_at	ACTIVIN RECEPTOR IIA
1422803_at	FOLLISTATIN-LIKE 3

Term Category: negative regulation of physiological process; 10 genes (6.54%); pValue 0.01

Affymetrix ID	Gene
1449007_at	B-CELL TRANSLOCATION GENE 3
1416434_at	BCL2-LIKE 10
1442025_a_at	ZINC FINGER AND BTB DOMAIN CONTAINING 16
1425732_a_at	MAX INTERACTING PROTEIN 1
1436006_at	EUKARYOTIC TRANSLATION INITIATION FACTOR 2 ALPHA KINASE 1
1425895_a_at	INHIBITOR OF DNA BINDING 1
1425809_at	FATTY ACID BINDING PROTEIN 4, ADIPOCYTE
1424638_at	CYCLIN-DEPENDENT KINASE INHIBITOR 1A (P21)
1420909_at, 1451959_a_at	VASCULAR ENDOTHELIAL GROWTH FACTOR A
1442397_at	NUCLEAR X BOX BINDING FACTOR 1

Term Category: BMP signaling pathway; 3 genes (1.96%); pValue 0.01

Affymetrix ID	Gene

1425895_a_at	INHIBITOR OF DNA BINDING 1
1416749_at, 1438251_x_at	HTRA SERINE PEPTIDASE 1
1422803_at	FOLLISTATIN-LIKE 3
Term Category: cell cycle; 10 genes (6.54%); pValue 0.013	
Affymetrix ID	Gene
1454018_at	TOUSLED-LIKE KINASE 2 (ARABIDOPSIS)
1449007_at	B-CELL TRANSLOCATION GENE 3
1453851_a_at	GROWTH ARREST AND DNA-DAMAGE-INDUCIBLE 45 GAMMA
1424143_a_at, 1424144_at	RETROVIRAL INTEGRATION SITE 2
1459978_x_at	GENE MODEL 877, (NCBI)
1416309_at	EXPRESSED SEQUENCE AW547774
1424638_at	CYCLIN-DEPENDENT KINASE INHIBITOR 1A (P21)
1419024_at, 1455002_at	PROTEIN TYROSINE PHOSPHATASE 4A1
1420909_at, 1451959_a_at	VASCULAR ENDOTHELIAL GROWTH FACTOR A
1435870_at	SYNAPTONEMAL COMPLEX PROTEIN 3
Term Category: positive regulation of cellular physiological process; 9 genes (5.88%); pValue 0.014	
Affymetrix ID	Gene
1418093_a_at	EPIDERMAL GROWTH FACTOR
1416434_at	BCL2-LIKE 10
1442025_a_at	ZINC FINGER AND BTB DOMAIN CONTAINING 16
1427364_a_at, 1438761_a_at	ORNITHINE DECARBOXYLASE, STRUCTURAL 1
1416309_at	EXPRESSED SEQUENCE AW547774
1424638_at	CYCLIN-DEPENDENT KINASE INHIBITOR 1A (P21)
1454903_at	NERVE GROWTH FACTOR RECEPTOR (TNFR SUPERFAMILY, MEMBER 16)
1419024_at, 1455002_at	PROTEIN TYROSINE PHOSPHATASE 4A1
1420909_at, 1451959_a_at	VASCULAR ENDOTHELIAL GROWTH FACTOR A
Term Category: negative regulation of cellular metabolism; 6 genes (3.92%); pValue 0.014	
Affymetrix ID	Gene
1442025_a_at	ZINC FINGER AND BTB DOMAIN CONTAINING 16
1425732_a_at	MAX INTERACTING PROTEIN 1
1436006_at	EUKARYOTIC TRANSLATION INITIATION FACTOR 2 ALPHA KINASE 1
1425895_a_at	INHIBITOR OF DNA BINDING 1
1425809_at	FATTY ACID BINDING PROTEIN 4, ADIPOCYTE
1442397_at	NUCLEAR X BOX BINDING FACTOR 1
Term Category: negative regulation of protein kinase activity; 3 genes (1.96%); pValue 0.016	
Affymetrix ID	Gene
1453851_a_at	GROWTH ARREST AND DNA-DAMAGE-INDUCIBLE 45 GAMMA
1425809_at	FATTY ACID BINDING PROTEIN 4, ADIPOCYTE
1424638_at	CYCLIN-DEPENDENT KINASE INHIBITOR 1A (P21)
Term Category: negative regulation of transferase activity; 3 genes (1.96%); pValue 0.017	
Affymetrix ID	Gene
1453851_a_at	GROWTH ARREST AND DNA-DAMAGE-INDUCIBLE 45 GAMMA
1425809_at	FATTY ACID BINDING PROTEIN 4, ADIPOCYTE
1424638_at	CYCLIN-DEPENDENT KINASE INHIBITOR 1A (P21)

Term Category: negative regulation of cell proliferation; 4 genes (2.61%); pValue 0.018	
Affymetrix ID	Gene
1449007_at	B-CELL TRANSLOCATION GENE 3
1442025_a_at	ZINC FINGER AND BTB DOMAIN CONTAINING 16
1436006_at	EUKARYOTIC TRANSLATION INITIATION FACTOR 2 ALPHA KINASE 1
1424638_at	CYCLIN-DEPENDENT KINASE INHIBITOR 1A (P21)
Term Category: negative regulation of enzyme activity; 3 genes (1.96%); pValue 0.019	
Affymetrix ID	Gene
1453851_a_at	GROWTH ARREST AND DNA-DAMAGE-INDUCIBLE 45 GAMMA
1425809_at	FATTY ACID BINDING PROTEIN 4, ADIPOCYTE
1424638_at	CYCLIN-DEPENDENT KINASE INHIBITOR 1A (P21)
Term Category: regulation of progression through cell cycle; 7 genes (4.58%); pValue 0.019	
Affymetrix ID	Gene
1449007_at	B-CELL TRANSLOCATION GENE 3
1453851_a_at	GROWTH ARREST AND DNA-DAMAGE-INDUCIBLE 45 GAMMA
1424143_a_at, 1424144_at	RETROVIRAL INTEGRATION SITE 2
1459978_x_at	GENE MODEL 877, (NCBI)
1416309_at	EXPRESSED SEQUENCE AW547774
1424638_at	CYCLIN-DEPENDENT KINASE INHIBITOR 1A (P21)
1420909_at, 1451959_a_at	VASCULAR ENDOTHELIAL GROWTH FACTOR A
Term Category: regulation of cell cycle; 7 genes (4.58%); pValue 0.019	
Affymetrix ID	Gene
1449007_at	B-CELL TRANSLOCATION GENE 3
1453851_a_at	GROWTH ARREST AND DNA-DAMAGE-INDUCIBLE 45 GAMMA
1424143_a_at, 1424144_at	RETROVIRAL INTEGRATION SITE 2
1459978_x_at	GENE MODEL 877, (NCBI)
1416309_at	EXPRESSED SEQUENCE AW547774
1424638_at	CYCLIN-DEPENDENT KINASE INHIBITOR 1A (P21)
1420909_at, 1451959_a_at	VASCULAR ENDOTHELIAL GROWTH FACTOR A
Term Category: positive regulation of cellular process; 9 genes (5.88%); pValue 0.022	
Affymetrix ID	Gene
1418093_a_at	EPIDERMAL GROWTH FACTOR
1416434_at	BCL2-LIKE 10
1442025_a_at	ZINC FINGER AND BTB DOMAIN CONTAINING 16
1427364_a_at, 1438761_a_at	ORNITHINE DECARBOXYLASE, STRUCTURAL 1
1416309_at	EXPRESSED SEQUENCE AW547774
1424638_at	CYCLIN-DEPENDENT KINASE INHIBITOR 1A (P21)
1454903_at	NERVE GROWTH FACTOR RECEPTOR (TNFR SUPERFAMILY, MEMBER 16)
1419024_at, 1455002_at	PROTEIN TYROSINE PHOSPHATASE 4A1
1420909_at, 1451959_a_at	VASCULAR ENDOTHELIAL GROWTH FACTOR A
Term Category: nitric oxide mediated signal transduction; 2 genes (1.31%); pValue 0.024	
Affymetrix ID	Gene
1428942_at	METALLOTHIONEIN 2

1422557_s_at	METALLOTHIONEIN 1
Term Category: amino acid and derivative metabolism; 6 genes (3.92%); pValue 0.025	
Affymetrix ID	Gene
1418093_a_at	EPIDERMAL GROWTH FACTOR
1435245_at	GLUTAMINASE 2 (LIVER, MITOCHONDRIAL)
1427364_a_at, 1438761_a_at	ORNITHINE DECARBOXYLASE, STRUCTURAL 1
1417149_at	PROCOLLAGEN-PROLINE, 2-OXOGLUTARATE 4-DIOXYGENASE (PROLINE 4-HYDROXYLASE), ALPHA II POLYPEPTIDE
1454608_x_at, 1455913_x_at	TRANSTHYRETIN
1416344_at	LYSOSOMAL MEMBRANE GLYCOPROTEIN 2
Term Category: cell proliferation; 7 genes (4.58%); pValue 0.025	
Affymetrix ID	Gene
1418093_a_at	EPIDERMAL GROWTH FACTOR
1449007_at	B-CELL TRANSLOCATION GENE 3
1442025_a_at	ZINC FINGER AND BTB DOMAIN CONTAINING 16
1427364_a_at, 1438761_a_at	ORNITHINE DECARBOXYLASE, STRUCTURAL 1
1436006_at	EUKARYOTIC TRANSLATION INITIATION FACTOR 2 ALPHA KINASE 1
1424638_at	CYCLIN-DEPENDENT KINASE INHIBITOR 1A (P21)
1420909_at, 1451959_a_at	VASCULAR ENDOTHELIAL GROWTH FACTOR A
Term Category: negative regulation of metabolism; 6 genes (3.92%); pValue 0.026	
Affymetrix ID	Gene
1442025_a_at	ZINC FINGER AND BTB DOMAIN CONTAINING 16
1425732_a_at	MAX INTERACTING PROTEIN 1
1436006_at	EUKARYOTIC TRANSLATION INITIATION FACTOR 2 ALPHA KINASE 1
1425895_a_at	INHIBITOR OF DNA BINDING 1
1425809_at	FATTY ACID BINDING PROTEIN 4, ADIPOCYTE
1442397_at	NUCLEAR X BOX BINDING FACTOR 1
Term Category: zinc ion homeostasis; 2 genes (1.31%); pValue 0.03	
Affymetrix ID	Gene
1428942_at	METALLOTHIONEIN 2
1422557_s_at	METALLOTHIONEIN 1
Term Category: negative regulation of transcription; 5 genes (3.27%); pValue 0.031	
Affymetrix ID	Gene
1442025_a_at	ZINC FINGER AND BTB DOMAIN CONTAINING 16
1425732_a_at	MAX INTERACTING PROTEIN 1
1425895_a_at	INHIBITOR OF DNA BINDING 1
1425809_at	FATTY ACID BINDING PROTEIN 4, ADIPOCYTE
1442397_at	NUCLEAR X BOX BINDING FACTOR 1
Term Category: positive regulation of cell proliferation; 4 genes (2.61%); pValue 0.031	
Affymetrix ID	Gene
1418093_a_at	EPIDERMAL GROWTH FACTOR

1427364_a_at, 1438761_a_at	ORNITHINE DECARBOXYLASE, STRUCTURAL 1
1424638_at	CYCLIN-DEPENDENT KINASE INHIBITOR 1A (P21)
1420909_at, 1451959_a_at	VASCULAR ENDOTHELIAL GROWTH FACTOR A
Term Category: apoptosis; 8 genes (5.23%); pValue 0.032	
Affymetrix ID	Gene
1453851_a_at	GROWTH ARREST AND DNA-DAMAGE-INDUCIBLE 45 GAMMA
1452050_at	CALCIUM/CALMODULIN-DEPENDENT PROTEIN KINASE ID
1416434_at	BCL2-LIKE 10
1442025_a_at	ZINC FINGER AND BTB DOMAIN CONTAINING 16
1424638_at	CYCLIN-DEPENDENT KINASE INHIBITOR 1A (P21)
1454903_at	NERVE GROWTH FACTOR RECEPTOR (TNFR SUPERFAMILY, MEMBER 16)
1454109_a_at	PHOSPHATIDYLSERINE RECEPTOR
1420909_at, 1451959_a_at	VASCULAR ENDOTHELIAL GROWTH FACTOR A
Term Category: programmed cell death; 8 genes (5.23%); pValue 0.035	
Affymetrix ID	Gene
1453851_a_at	GROWTH ARREST AND DNA-DAMAGE-INDUCIBLE 45 GAMMA
1452050_at	CALCIUM/CALMODULIN-DEPENDENT PROTEIN KINASE ID
1416434_at	BCL2-LIKE 10
1442025_a_at	ZINC FINGER AND BTB DOMAIN CONTAINING 16
1424638_at	CYCLIN-DEPENDENT KINASE INHIBITOR 1A (P21)
1454903_at	NERVE GROWTH FACTOR RECEPTOR (TNFR SUPERFAMILY, MEMBER 16)
1454109_a_at	PHOSPHATIDYLSERINE RECEPTOR
1420909_at, 1451959_a_at	VASCULAR ENDOTHELIAL GROWTH FACTOR A
Term Category: macromolecule metabolism; 33 genes (21.57%); pValue 0.035	
Affymetrix ID	Gene
1453851_a_at	GROWTH ARREST AND DNA-DAMAGE-INDUCIBLE 45 GAMMA
1454949_at	RIKEN CDNA 2210010O09 GENE
1423785_at	EGL NINE HOMOLOG 1 (C. ELEGANS)
1416432_at, 1456676_a_at	6-PHOSPHOFRUCTO-2-KINASE/FRUCTOSE-2,6-BIPHOSPHATASE 3
1419029_at, 1419030_at, 1449324_at	ERO1-LIKE (S. CEREVISIAE)
1416749_at, 1438251_x_at	HTRA SERINE PEPTIDASE 1
1430798_x_at	MITOCHONDRIAL RIBOSOMAL PROTEIN L15
1416125_at, 1448231_at	FK506 BINDING PROTEIN 5
1454018_at	TOUSLED-LIKE KINASE 2 (ARABIDOPSIS)
1454623_at	SIMILAR TO CARBOXYPEPTIDASE A2 PRECURSOR
1439677_at	EPILEPSY, PROGRESSIVE MYOCLONIC EPILEPSY, TYPE 2 GENE ALPHA
1437785_at	A DISINTEGRIN-LIKE AND METALLOPEPTIDASE (REPROLYSIN TYPE) WITH THROMBOSPONDIN TYPE 1 MOTIF, 9
1433814_at	F-BOX AND LEUCINE-RICH REPEAT PROTEIN 14
1459331_at	SURFEIT GENE 6
1436006_at	EUKARYOTIC TRANSLATION INITIATION FACTOR 2 ALPHA KINASE 1
1417149_at	PROCOLLAGEN-PROLINE, 2-OXOGLUTARATE 4-DIOXYGENASE (PROLINE 4-HYDROXYLASE), ALPHA II POLYPEPTIDE
1419024_at, 1455002_at	PROTEIN TYROSINE PHOSPHATASE 4A1
1426721_s_at	TCDD-INDUCIBLE POLY(ADP-RIBOSE) POLYMERASE

1457451_at	ACTIVIN RECEPTOR IIA
1419087_s_at	SPLICING FACTOR 3A, SUBUNIT 1
1452050_at	CALCIUM/CALMODULIN-DEPENDENT PROTEIN KINASE ID
1431212_a_at	RIKEN CDNA 3300001M20 GENE
1436531_at	METHIONINE AMINOPEPTIDASE 2
1438815_at	HISTONE 2, H2AA1
1430357_at	H3 HISTONE, FAMILY 3A
1418093_a_at	EPIDERMAL GROWTH FACTOR
1455420_at	RAD23B HOMOLOG (S. CEREVISIAE)
1424143_a_at, 1424144_at	RETROVIRAL INTEGRATION SITE 2
1422832_at	RETINAL G PROTEIN COUPLED RECEPTOR
1437313_x_at, 1452534_a_at	HIGH MOBILITY GROUP BOX 2
1416344_at	LYSOSOMAL MEMBRANE GLYCOPROTEIN 2
1422885_at	SMALL NUCLEAR RIBONUCLEOPROTEIN D3
1442397_at	NUCLEAR X BOX BINDING FACTOR 1
Term Category: negative regulation of nucleobase, nucleoside, nucleotide and nucleic acid metabolism; 5 genes (3.27%); pValue 0.037	
Affymetrix ID	Gene
1442025_a_at	ZINC FINGER AND BTB DOMAIN CONTAINING 16
1425732_a_at	MAX INTERACTING PROTEIN 1
1425895_a_at	INHIBITOR OF DNA BINDING 1
1425809_at	FATTY ACID BINDING PROTEIN 4, ADIPOCYTE
1442397_at	NUCLEAR X BOX BINDING FACTOR 1
Term Category: cellular protein metabolism; 25 genes (16.34%); pValue 0.039	
Affymetrix ID	Gene
1453851_a_at	GROWTH ARREST AND DNA-DAMAGE-INDUCIBLE 45 GAMMA
1454949_at	RIKEN CDNA 2210010O09 GENE
1419029_at, 1419030_at, 1449324_at	ERO1-LIKE (S. CEREVISIAE)
1416749_at, 1438251_x_at	HTRA SERINE PEPTIDASE 1
1416125_at, 1448231_at	FK506 BINDING PROTEIN 5
1430798_x_at	MITOCHONDRIAL RIBOSOMAL PROTEIN L15
1454623_at	SIMILAR TO CARBOXYPEPTIDASE A2 PRECURSOR
1454018_at	TOUSLED-LIKE KINASE 2 (ARABIDOPSIS)
1439677_at	EPILEPSY, PROGRESSIVE MYOCLONIC EPILEPSY, TYPE 2 GENE ALPHA
1437785_at	A DISINTEGRIN-LIKE AND METALLOPEPTIDASE (REPROLYSIN TYPE) WITH THROMBOSPONDIN TYPE 1 MOTIF, 9
1433814_at	F-BOX AND LEUCINE-RICH REPEAT PROTEIN 14
1436006_at	EUKARYOTIC TRANSLATION INITIATION FACTOR 2 ALPHA KINASE 1
1417149_at	PROCOLLAGEN-PROLINE, 2-OXOGLUTARATE 4-DIOXYGENASE (PROLINE 4-HYDROXYLASE), ALPHA II POLYPEPTIDE
1419024_at, 1455002_at	PROTEIN TYROSINE PHOSPHATASE 4A1
1426721_s_at	TCDD-INDUCIBLE POLY(ADP-RIBOSE) POLYMERASE
1457451_at	ACTIVIN RECEPTOR IIA
1419087_s_at	SPLICING FACTOR 3A, SUBUNIT 1
1452050_at	CALCIUM/CALMODULIN-DEPENDENT PROTEIN KINASE ID
1431212_a_at	RIKEN CDNA 3300001M20 GENE

1436531_at	METHIONINE AMINOPEPTIDASE 2
1418093_a_at	EPIDERMAL GROWTH FACTOR
1455420_at	RAD23B HOMOLOG (S. CEREVISIAE)
1422832_at	RETINAL G PROTEIN COUPLED RECEPTOR
1416344_at	LYSOSOMAL MEMBRANE GLYCOPROTEIN 2
1442397_at	NUCLEAR X BOX BINDING FACTOR 1
Term Category: amine metabolism; 6 genes (3.92%); pValue 0.042	
Affymetrix ID	Gene
1418093_a_at	EPIDERMAL GROWTH FACTOR
1435245_at	GLUTAMINASE 2 (LIVER, MITOCHONDRIAL)
1427364_a_at, 1438761_a_at	ORNITHINE DECARBOXYLASE, STRUCTURAL 1
1417149_at	PROCOLLAGEN-PROLINE, 2-OXOGLUTARATE 4-DIOXYGENASE (PROLINE 4-HYDROXYLASE), ALPHA II POLYPEPTIDE
1454608_x_at, 1455913_x_at	TRANSTHYRETIN
1416344_at	LYSOSOMAL MEMBRANE GLYCOPROTEIN 2
Term Category: cell death; 8 genes (5.23%); pValue 0.044	
Affymetrix ID	Gene
1453851_a_at	GROWTH ARREST AND DNA-DAMAGE-INDUCIBLE 45 GAMMA
1452050_at	CALCIUM/CALMODULIN-DEPENDENT PROTEIN KINASE ID
1416434_at	BCL2-LIKE 10
1442025_a_at	ZINC FINGER AND BTB DOMAIN CONTAINING 16
1424638_at	CYCLIN-DEPENDENT KINASE INHIBITOR 1A (P21)
1454903_at	NERVE GROWTH FACTOR RECEPTOR (TNFR SUPERFAMILY, MEMBER 16)
1454109_a_at	PHOSPHATIDYLSERINE RECEPTOR
1420909_at, 1451959_a_at	VASCULAR ENDOTHELIAL GROWTH FACTOR A
Term Category: cellular macromolecule metabolism; 25 genes (16.34%); pValue 0.045	
Affymetrix ID	Gene
1453851_a_at	GROWTH ARREST AND DNA-DAMAGE-INDUCIBLE 45 GAMMA
1454949_at	RIKEN CDNA 2210010O09 GENE
1419029_at, 1419030_at, 1449324_at	ERO1-LIKE (S. CEREVISIAE)
1416749_at, 1438251_x_at	HTRA SERINE PEPTIDASE 1
1416125_at, 1448231_at	FK506 BINDING PROTEIN 5
1430798_x_at	MITOCHONDRIAL RIBOSOMAL PROTEIN L15
1454623_at	SIMILAR TO CARBOXYPEPTIDASE A2 PRECURSOR
1454018_at	TOUSLED-LIKE KINASE 2 (ARABIDOPSIS)
1439677_at	EPILEPSY, PROGRESSIVE MYOCLONIC EPILEPSY, TYPE 2 GENE ALPHA
1437785_at	A DISINTEGRIN-LIKE AND METALLOPEPTIDASE (REPROLYSIN TYPE) WITH THROMBOSPONDIN TYPE 1 MOTIF, 9
1433814_at	F-BOX AND LEUCINE-RICH REPEAT PROTEIN 14
1436006_at	EUKARYOTIC TRANSLATION INITIATION FACTOR 2 ALPHA KINASE 1
1417149_at	PROCOLLAGEN-PROLINE, 2-OXOGLUTARATE 4-DIOXYGENASE (PROLINE 4-HYDROXYLASE), ALPHA II POLYPEPTIDE
1419024_at, 1455002_at	PROTEIN TYROSINE PHOSPHATASE 4A1
1426721_s_at	TCDD-INDUCIBLE POLY(ADP-RIBOSE) POLYMERASE

1457451_at	ACTIVIN RECEPTOR IIA
1419087_s_at	SPLICING FACTOR 3A, SUBUNIT 1
1452050_at	CALCIUM/CALMODULIN-DEPENDENT PROTEIN KINASE ID
1431212_a_at	RIKEN CDNA 3300001M20 GENE
1436531_at	METHIONINE AMINOPEPTIDASE 2
1418093_a_at	EPIDERMAL GROWTH FACTOR
1455420_at	RAD23B HOMOLOG (S. CEREVISIAE)
1422832_at	RETINAL G PROTEIN COUPLED RECEPTOR
1416344_at	LYSOSOMAL MEMBRANE GLYCOPROTEIN 2
1442397_at	NUCLEAR X BOX BINDING FACTOR 1

Term Category: death; 8 genes (5.23%); pValue 0.047

Affymetrix ID	Gene
1453851_a_at	GROWTH ARREST AND DNA-DAMAGE-INDUCIBLE 45 GAMMA
1452050_at	CALCIUM/CALMODULIN-DEPENDENT PROTEIN KINASE ID
1416434_at	BCL2-LIKE 10
1442025_a_at	ZINC FINGER AND BTB DOMAIN CONTAINING 16
1424638_at	CYCLIN-DEPENDENT KINASE INHIBITOR 1A (P21)
1454903_at	NERVE GROWTH FACTOR RECEPTOR (TNFR SUPERFAMILY, MEMBER 16)
1454109_a_at	PHOSPHATIDYLSERINE RECEPTOR
1420909_at, 1451959_a_at	VASCULAR ENDOTHELIAL GROWTH FACTOR A

Term Category: regulation of apoptosis; 6 genes (3.92%); pValue 0.047

Affymetrix ID	Gene
1452050_at	CALCIUM/CALMODULIN-DEPENDENT PROTEIN KINASE ID
1416434_at	BCL2-LIKE 10
1442025_a_at	ZINC FINGER AND BTB DOMAIN CONTAINING 16
1424638_at	CYCLIN-DEPENDENT KINASE INHIBITOR 1A (P21)
1454903_at	NERVE GROWTH FACTOR RECEPTOR (TNFR SUPERFAMILY, MEMBER 16)
1420909_at, 1451959_a_at	VASCULAR ENDOTHELIAL GROWTH FACTOR A

Term Category: regulation of programmed cell death; 6 genes (3.92%); pValue 0.051

Affymetrix ID	Gene
1452050_at	CALCIUM/CALMODULIN-DEPENDENT PROTEIN KINASE ID
1416434_at	BCL2-LIKE 10
1442025_a_at	ZINC FINGER AND BTB DOMAIN CONTAINING 16
1424638_at	CYCLIN-DEPENDENT KINASE INHIBITOR 1A (P21)
1454903_at	NERVE GROWTH FACTOR RECEPTOR (TNFR SUPERFAMILY, MEMBER 16)
1420909_at, 1451959_a_at	VASCULAR ENDOTHELIAL GROWTH FACTOR A

Term Category: nitrogen compound metabolism; 6 genes (3.92%); pValue 0.052

Affymetrix ID	Gene
1418093_a_at	EPIDERMAL GROWTH FACTOR
1435245_at	GLUTAMINASE 2 (LIVER, MITOCHONDRIAL)
1427364_a_at, 1438761_a_at	ORNITHINE DECARBOXYLASE, STRUCTURAL 1
1417149_at	PROCOLLAGEN-PROLINE, 2-OXOGLUTARATE 4-DIOXYGENASE (PROLINE 4-HYDROXYLASE), ALPHA II POLYPEPTIDE
1454608_x_at, 1455913_x_at	TRANSTHYRETIN

1416344_at	LYSOSOMAL MEMBRANE GLYCOPROTEIN 2
Term Category: negative regulation of transcription, DNA-dependent; 4 genes (2.61%); pValue 0.058	
Affymetrix ID	Gene
1442025_a_at	ZINC FINGER AND BTB DOMAIN CONTAINING 16
1425732_a_at	MAX INTERACTING PROTEIN 1
1425895_a_at	INHIBITOR OF DNA BINDING 1
1442397_at	NUCLEAR X BOX BINDING FACTOR 1
Term Category: amino acid derivative metabolism, DNA-dependent; 3 genes (1.96%); pValue 0.058	
Affymetrix ID	Gene
1427364_a_at, 1438761_a_at	ORNITHINE DECARBOXYLASE, STRUCTURAL 1
1417149_at	PROCOLLAGEN-PROLINE, 2-OXOGLUTARATE 4-DIOXYGENASE (PROLINE 4-HYDROXYLASE), ALPHA II POLYPEPTIDE
1454608_x_at, 1455913_x_at	TRANSTHYRETIN
Term Category: positive regulation of programmed cell death; 4 genes (2.61%); pValue 0.06	
Affymetrix ID	Gene
1416434_at	BCL2-LIKE 10
1442025_a_at	ZINC FINGER AND BTB DOMAIN CONTAINING 16
1424638_at	CYCLIN-DEPENDENT KINASE INHIBITOR 1A (P21)
1454903_at	NERVE GROWTH FACTOR RECEPTOR (TNFR SUPERFAMILY, MEMBER 16)
Term Category: primary metabolism; 48 genes (31.37%); pValue 0.061	
Affymetrix ID	Gene
1426727_s_at	PROTEIN PHOSPHATASE 1, REGULATORY SUBUNIT 10
1453851_a_at	GROWTH ARREST AND DNA-DAMAGE-INDUCIBLE 45 GAMMA
1454949_at	RIKEN CDNA 2210010O09 GENE
1427364_a_at, 1438761_a_at	ORNITHINE DECARBOXYLASE, STRUCTURAL 1
1423785_at	EGL NINE HOMOLOG 1 (C. ELEGANS)
1418190_at	PARAOXONASE 1
1416432_at, 1456676_a_at	6-PHOSPHOFRUCTO-2-KINASE/FRUCTOSE-2,6-BIPHOSPHATASE 3
1419029_at, 1419030_at, 1449324_at	ERO1-LIKE (S. CEREVISIAE)
1416749_at, 1438251_x_at	HTRA SERINE PEPTIDASE 1
1430798_x_at	MITOCHONDRIAL RIBOSOMAL PROTEIN L15
1416125_at, 1448231_at	FK506 BINDING PROTEIN 5
1423233_at	CCAAT/ENHANCER BINDING PROTEIN (C/EBP), DELTA
1454623_at	SIMILAR TO CARBOXYPEPTIDASE A2 PRECURSOR
1454018_at	TOUSLED-LIKE KINASE 2 (ARABIDOPSIS)
1435245_at	GLUTAMINASE 2 (LIVER, MITOCHONDRIAL)
1439677_at	EPILEPSY, PROGRESSIVE MYOCLONIC EPILEPSY, TYPE 2 GENE ALPHA
1437785_at	A DISINTEGRIN-LIKE AND METALLOPEPTIDASE (REPROLYSIN TYPE) WITH THROMBOSPONDIN TYPE 1 MOTIF, 9
1436006_at	EUKARYOTIC TRANSLATION INITIATION FACTOR 2 ALPHA KINASE 1
1433814_at	F-BOX AND LEUCINE-RICH REPEAT PROTEIN 14
1459331_at	SURFEIT GENE 6

1417149_at	PROCOLLAGEN-PROLINE, 2-OXOGLUTARATE 4-DIOXYGENASE (PROLINE 4-HYDROXYLASE), ALPHA II POLYPEPTIDE
1425895_a_at	INHIBITOR OF DNA BINDING 1
1419024_at, 1455002_at	PROTEIN TYROSINE PHOSPHATASE 4A1
1454608_x_at, 1455913_x_at	TRANSTHYRETIN
1426721_s_at	TCDD-INDUCIBLE POLY(ADP-RIBOSE) POLYMERASE
1448607_at	PRE-B-CELL COLONY-ENHANCING FACTOR 1
1457451_at	ACTIVIN RECEPTOR IIA
1419087_s_at	SPLICING FACTOR 3A, SUBUNIT 1
1452050_at	CALCIUM/CALMODULIN-DEPENDENT PROTEIN KINASE ID
1442025_a_at	ZINC FINGER AND BTB DOMAIN CONTAINING 16
1444487_at	LECITHIN-RETINOL ACYLTRANSFERASE (PHOSPHATIDYLCHOLINE-RETINOL-O-ACYLTRANSFERASE)
1425809_at	FATTY ACID BINDING PROTEIN 4, ADIPOCYTE
1431212_a_at	RIKEN CDNA 3300001M20 GENE
1436531_at	METHIONINE AMINOPEPTIDASE 2
1438815_at	HISTONE 2, H2AA1
1435875_at	PROTEIN KINASE, AMP-ACTIVATED, BETA 2 NON-CATALYTIC SUBUNIT
1418093_a_at	EPIDERMAL GROWTH FACTOR
1430357_at	H3 HISTONE, FAMILY 3A
1440257_at	OOCYTE SPECIFIC HOMEOBOX 6
1455420_at	RAD23B HOMOLOG (S. CEREVISIAE)
1424143_a_at, 1424144_at	RETROVIRAL INTEGRATION SITE 2
1425732_a_at	MAX INTERACTING PROTEIN 1
1422832_at	RETINAL G PROTEIN COUPLED RECEPTOR
1437313_x_at, 1452534_a_at	HIGH MOBILITY GROUP BOX 2
1454903_at	NERVE GROWTH FACTOR RECEPTOR (TNFR SUPERFAMILY, MEMBER 16)
1416344_at	LYSOSOMAL MEMBRANE GLYCOPROTEIN 2
1422885_at	SMALL NUCLEAR RIBONUCLEOPROTEIN D3
1442397_at	NUCLEAR X BOX BINDING FACTOR 1
Term Category: nucleosome assembly; 3 genes (1.96%); pValue 0.065	
Affymetrix ID	Gene
1430357_at	H3 HISTONE, FAMILY 3A
1437313_x_at, 1452534_a_at	HIGH MOBILITY GROUP BOX 2
1438815_at	HISTONE 2, H2AA1
Term Category: regulation of biological process; 28 genes (18.3%); pValue 0.066	
Affymetrix ID	Gene
1453851_a_at	GROWTH ARREST AND DNA-DAMAGE-INDUCIBLE 45 GAMMA
1427364_a_at, 1438761_a_at	ORNITHINE DECARBOXYLASE, STRUCTURAL 1
1416749_at, 1438251_x_at	HTRA SERINE PEPTIDASE 1
1449007_at	B-CELL TRANSLOCATION GENE 3
1423233_at	CCAAT/ENHANCER BINDING PROTEIN (C/EBP), DELTA
1416434_at	BCL2-LIKE 10

1436006_at	EUKARYOTIC TRANSLATION INITIATION FACTOR 2 ALPHA KINASE 1
1425895_a_at	INHIBITOR OF DNA BINDING 1
1419024_at, 1455002_at	PROTEIN TYROSINE PHOSPHATASE 4A1
1436605_at	TRANSKETOLASE
1452050_at	CALCIUM/CALMODULIN-DEPENDENT PROTEIN KINASE ID
1459978_x_at	GENE MODEL 877, (NCBI)
1442025_a_at	ZINC FINGER AND BTB DOMAIN CONTAINING 16
1431212_a_at	RIKEN CDNA 3300001M20 GENE
1425809_at	FATTY ACID BINDING PROTEIN 4, ADIPOCYTE
1424638_at	CYCLIN-DEPENDENT KINASE INHIBITOR 1A (P21)
1440257_at	OOCYTE SPECIFIC HOMEOBOX 6
1418093_a_at	EPIDERMAL GROWTH FACTOR
1424143_a_at, 1424144_at	RETROVIRAL INTEGRATION SITE 2
1425732_a_at	MAX INTERACTING PROTEIN 1
1416309_at	EXPRESSED SEQUENCE AW547774
1454903_at	NERVE GROWTH FACTOR RECEPTOR (TNFR SUPERFAMILY, MEMBER 16)
1437313_x_at, 1452534_a_at	HIGH MOBILITY GROUP BOX 2
1418370_at	TROPONIN C, CARDIAC/SLOW SKELETAL
1420909_at, 1451959_a_at	VASCULAR ENDOTHELIAL GROWTH FACTOR A
1416039_x_at	CYSTEINE RICH PROTEIN 61
1442397_at	NUCLEAR X BOX BINDING FACTOR 1
1422803_at	FOLLISTATIN-LIKE 3

Term Category: protein complex assembly; 4 genes (2.61%); pValue 0.068

Affymetrix ID	Gene
1430357_at	H3 HISTONE, FAMILY 3A
1459331_at	SURFEIT GENE 6
1437313_x_at, 1452534_a_at	HIGH MOBILITY GROUP BOX 2
1438815_at	HISTONE 2, H2AA1

Term Category: blood vessel development; 4 genes (2.61%); pValue 0.07

Affymetrix ID	Gene
1425895_a_at	INHIBITOR OF DNA BINDING 1
1454109_a_at	PHOSPHATIDYLSERINE RECEPTOR
1420909_at, 1451959_a_at	VASCULAR ENDOTHELIAL GROWTH FACTOR A
1416039_x_at	CYSTEINE RICH PROTEIN 61

Term Category: regulation of physiological process; 36 genes (16.99%); pValue 0.07

Affymetrix ID	Gene
1453851_a_at	GROWTH ARREST AND DNA-DAMAGE-INDUCIBLE 45 GAMMA
1427364_a_at, 1438761_a_at	ORNITHINE DECARBOXYLASE, STRUCTURAL 1
1416749_at, 1438251_x_at	HTRA SERINE PEPTIDASE 1
1449007_at	B-CELL TRANSLOCATION GENE 3
1423233_at	CCAAT/ENHANCER BINDING PROTEIN (C/EBP), DELTA
1416434_at	BCL2-LIKE 10
1436006_at	EUKARYOTIC TRANSLATION INITIATION FACTOR 2 ALPHA KINASE 1
1425895_a_at	INHIBITOR OF DNA BINDING 1

1419024_at, 1455002_at	PROTEIN TYROSINE PHOSPHATASE 4A1
1452050_at	CALCIUM/CALMODULIN-DEPENDENT PROTEIN KINASE ID
1459978_x_at	GENE MODEL 877, (NCBI)
1442025_a_at	ZINC FINGER AND BTB DOMAIN CONTAINING 16
1431212_a_at	RIKEN CDNA 3300001M20 GENE
1425809_at	FATTY ACID BINDING PROTEIN 4, ADIPOCYTE
1424638_at	CYCLIN-DEPENDENT KINASE INHIBITOR 1A (P21)
1418093_a_at	EPIDERMAL GROWTH FACTOR
1440257_at	OOCYTE SPECIFIC HOMEOBOX 6
1424143_a_at, 1424144_at	RETROVIRAL INTEGRATION SITE 2
1425732_a_at	MAX INTERACTING PROTEIN 1
1416309_at	EXPRESSED SEQUENCE AW547774
1454903_at	NERVE GROWTH FACTOR RECEPTOR (TNFR SUPERFAMILY, MEMBER 16)
1437313_x_at, 1452534_a_at	HIGH MOBILITY GROUP BOX 2
1418370_at	TROPONIN C, CARDIAC/SLOW SKELETAL
1420909_at, 1451959_a_at	VASCULAR ENDOTHELIAL GROWTH FACTOR A
1416039_x_at	CYSTEINE RICH PROTEIN 61
1442397_at	NUCLEAR X BOX BINDING FACTOR 1

Term Category: negative regulation of BMP signaling pathway; 2 genes (1.31%); pValue 0.07

Affymetrix ID	Gene
1416749_at, 1438251_x_at	HTRA SERINE PEPTIDASE 1
1422803_at	FOLLISTATIN-LIKE 3

Term Category: vasculature development; 4 genes (2.61%); pValue 0.073

Affymetrix ID	Gene
1425895_a_at	INHIBITOR OF DNA BINDING 1
1454109_a_at	PHOSPHATIDYLSERINE RECEPTOR
1420909_at, 1451959_a_at	VASCULAR ENDOTHELIAL GROWTH FACTOR A
1416039_x_at	CYSTEINE RICH PROTEIN 61

Term Category: regulation of cellular process; 26 Genes (16.99%); pValue 0.078

Affymetrix ID	Gene
1453851_a_at	GROWTH ARREST AND DNA-DAMAGE-INDUCIBLE 45 GAMMA
1427364_a_at, 1438761_a_at	ORNITHINE DECARBOXYLASE, STRUCTURAL 1
1416749_at, 1438251_x_at	HTRA SERINE PEPTIDASE 1
1449007_at	B-CELL TRANSLOCATION GENE 3
1423233_at	CCAAT/ENHANCER BINDING PROTEIN (C/EBP), DELTA
1416434_at	BCL2-LIKE 10
1436006_at	EUKARYOTIC TRANSLATION INITIATION FACTOR 2 ALPHA KINASE 1
1425895_a_at	INHIBITOR OF DNA BINDING 1
1419024_at, 1455002_at	PROTEIN TYROSINE PHOSPHATASE 4A1
1452050_at	CALCIUM/CALMODULIN-DEPENDENT PROTEIN KINASE ID
1459978_x_at	GENE MODEL 877, (NCBI)
1442025_a_at	ZINC FINGER AND BTB DOMAIN CONTAINING 16
1431212_a_at	RIKEN CDNA 3300001M20 GENE
1425809_at	FATTY ACID BINDING PROTEIN 4, ADIPOCYTE
1424638_at	CYCLIN-DEPENDENT KINASE INHIBITOR 1A (P21)

1418093_a_at	EPIDERMAL GROWTH FACTOR
1440257_at	OOCYTE SPECIFIC HOMEOBOX 6
1424143_a_at, 1424144_at	RETROVIRAL INTEGRATION SITE 2
1425732_a_at	MAX INTERACTING PROTEIN 1
1416309_at	EXPRESSED SEQUENCE AW547774
1454903_at	NERVE GROWTH FACTOR RECEPTOR (TNFR SUPERFAMILY, MEMBER 16)
1437313_x_at, 1452534_a_at	HIGH MOBILITY GROUP BOX 2
1420909_at, 1451959_a_at	VASCULAR ENDOTHELIAL GROWTH FACTOR A
1416039_x_at	CYSTEINE RICH PROTEIN 61
1442397_at	NUCLEAR X BOX BINDING FACTOR 1
1422803_at	FOLLISTATIN-LIKE 3
Term Category: regulation of cellular physiological process; 25 genes (16.34%); pValue 0.079	
Affymetrix ID	Gene
1453851_a_at	GROWTH ARREST AND DNA-DAMAGE-INDUCIBLE 45 GAMMA
1427364_a_at, 1438761_a_at	ORNITHINE DECARBOXYLASE, STRUCTURAL 1
1416749_at, 1438251_x_at	HTRA SERINE PEPTIDASE 1
1449007_at	B-CELL TRANSLOCATION GENE 3
1423233_at	CCAAT/ENHANCER BINDING PROTEIN (C/EBP), DELTA
1416434_at	BCL2-LIKE 10
1436006_at	EUKARYOTIC TRANSLATION INITIATION FACTOR 2 ALPHA KINASE 1
1425895_a_at	INHIBITOR OF DNA BINDING 1
1419024_at, 1455002_at	PROTEIN TYROSINE PHOSPHATASE 4A1
1452050_at	CALCIUM/CALMODULIN-DEPENDENT PROTEIN KINASE ID
1459978_x_at	GENE MODEL 877, (NCBI)
1442025_a_at	ZINC FINGER AND BTB DOMAIN CONTAINING 16
1431212_a_at	RIKEN CDNA 3300001M20 GENE
1425809_at	FATTY ACID BINDING PROTEIN 4, ADIPOCYTE
1424638_at	CYCLIN-DEPENDENT KINASE INHIBITOR 1A (P21)
1418093_a_at	EPIDERMAL GROWTH FACTOR
1440257_at	OOCYTE SPECIFIC HOMEOBOX 6
1424143_a_at, 1424144_at	RETROVIRAL INTEGRATION SITE 2
1425732_a_at	MAX INTERACTING PROTEIN 1
1416309_at	EXPRESSED SEQUENCE AW547774
1437313_x_at, 1452534_a_at	HIGH MOBILITY GROUP BOX 2
1454903_at	NERVE GROWTH FACTOR RECEPTOR (TNFR SUPERFAMILY, MEMBER 16)
1420909_at, 1451959_a_at	VASCULAR ENDOTHELIAL GROWTH FACTOR A
1416039_x_at	CYSTEINE RICH PROTEIN 61
1442397_at	NUCLEAR X BOX BINDING FACTOR 1
Term Category: regulation of BMP signaling pathway; 2 genes (1.31%); pValue 0.08	
Affymetrix ID	Gene
1416749_at, 1438251_x_at	HTRA SERINE PEPTIDASE 1
1422803_at	FOLLISTATIN-LIKE 3
Term Category: chromatin assembly; 3 genes (1.96%); pValue 0.084	
Affymetrix ID	Gene

1430357_at	H3 HISTONE, FAMILY 3A
1437313_x_at, 1452534_a_at	HIGH MOBILITY GROUP BOX 2
1438815_at	HISTONE 2, H2AA1
Term Category: metabolism; 52 genes (33.9%); pValue 0.088	
Affymetrix ID	Gene
1426727_s_at	PROTEIN PHOSPHATASE 1, REGULATORY SUBUNIT 10
1453851_a_at	GROWTH ARREST AND DNA-DAMAGE-INDUCIBLE 45 GAMMA
1423785_at	EGL NINE HOMOLOG 1 (C. ELEGANS)
1416432_at, 1456676_a_at	6-PHOSPHOFRUCTO-2-KINASE/FRUCTOSE-2,6-BIPHOSPHATASE 3
1430798_x_at	MITOCHONDRIAL RIBOSOMAL PROTEIN L15
1454018_at	TOUSLED-LIKE KINASE 2 (ARABIDOPSIS)
1423233_at	CCAAT/ENHANCER BINDING PROTEIN (C/EBP), DELTA
1454623_at	SIMILAR TO CARBOXYPEPTIDASE A2 PRECURSOR
1435245_at	GLUTAMINASE 2 (LIVER, MITOCHONDRIAL)
1437785_at	A DISINTEGRIN-LIKE AND METALLOPEPTIDASE (REPROLYSIN TYPE) WITH THROMBOSPONDIN TYPE 1 MOTIF, 9
1459331_at	SURFEIT GENE 6
1433814_at	F-BOX AND LEUCINE-RICH REPEAT PROTEIN 14
1436006_at	EUKARYOTIC TRANSLATION INITIATION FACTOR 2 ALPHA KINASE 1
1417149_at	PROCOLLAGEN-PROLINE, 2-OXOGLUTARATE 4-DIOXYGENASE (PROLINE 4-HYDROXYLASE), ALPHA II POLYPEPTIDE
1425895_a_at	INHIBITOR OF DNA BINDING 1
1426721_s_at	TCDD-INDUCIBLE POLY(ADP-RIBOSE) POLYMERASE
1448607_at	PRE-B-CELL COLONY-ENHANCING FACTOR 1
1419087_s_at	SPLICING FACTOR 3A, SUBUNIT 1
1442025_a_at	ZINC FINGER AND BTB DOMAIN CONTAINING 16
1431212_a_at	RIKEN CDNA 3300001M20 GENE
1425809_at	FATTY ACID BINDING PROTEIN 4, ADIPOCYTE
1430357_at	H3 HISTONE, FAMILY 3A
1418093_a_at	EPIDERMAL GROWTH FACTOR
1430197_a_at	PHOSPHATIDYLINOSITOL TRANSFER PROTEIN, MEMBRANE-ASSOCIATED 2
1424143_a_at, 1424144_at	RETROVIRAL INTEGRATION SITE 2
1425732_a_at	MAX INTERACTING PROTEIN 1
1422832_at	RETINAL G PROTEIN COUPLED RECEPTOR
1437313_x_at, 1452534_a_at	HIGH MOBILITY GROUP BOX 2
1422885_at	SMALL NUCLEAR RIBONUCLEOPROTEIN D3
1450725_s_at	CARBONIC ANHYDRASE 14
1454949_at	RIKEN CDNA 2210010O09 GENE
1418808_at	RETINOL DEHYDROGENASE 5
1427364_a_at, 1438761_a_at	ORNITHINE DECARBOXYLASE, STRUCTURAL 1
1418190_at	PARAOXONASE 1
1419029_at, 1419030_at, 1449324_at	ERO1-LIKE (S. CEREVISIAE)
1416749_at, 1438251_x_at	HTRA SERINE PEPTIDASE 1
1416125_at, 1448231_at	FK506 BINDING PROTEIN 5

1439677_at	EPILEPSY, PROGRESSIVE MYOCLONIC EPILEPSY, TYPE 2 GENE ALPHA
1419024_at, 1455002_at	PROTEIN TYROSINE PHOSPHATASE 4A1
1454608_x_at, 1455913_x_at	TRANSTHYRETIN
1434952_at	CYTOCHROME C OXIDASE SUBUNIT IV ISOFORM 1
1457451_at	ACTIVIN RECEPTOR IIA
1452050_at	CALCIUM/CALMODULIN-DEPENDENT PROTEIN KINASE ID
1444487_at	LECITHIN-RETINOL ACYLTRANSFERASE (PHOSPHATIDYLCHOLINE-RETINOL-O-ACYLTRANSFERASE)
1436531_at	METHIONINE AMINOPEPTIDASE 2
1438815_at	HISTONE 2, H2AA1
1435875_at	PROTEIN KINASE, AMP-ACTIVATED, BETA 2 NON-CATALYTIC SUBUNIT
1440257_at	OOCYTE SPECIFIC HOMEOBOX 6
1455420_at	RAD23B HOMOLOG (S. CEREVISIAE)
1454903_at	NERVE GROWTH FACTOR RECEPTOR (TNFR SUPERFAMILY, MEMBER 16)
1416344_at	LYSOSOMAL MEMBRANE GLYCOPROTEIN 2
1442397_at	NUCLEAR X BOX BINDING FACTOR 1

TABLE 6 Differentially down-regulated genes functionally clustered by DAVID.

Term Category: cellular metabolism; 30 genes (41.67%); pValue 0.002	
Affymetrix ID	Gene
1424852_at	MYOCYTE ENHANCER FACTOR 2C
1428760_at	RIKEN CDNA 4930558A07 GENE
1429169_at	RNA BINDING MOTIF PROTEIN 3
1456723_at	ZINC FINGER PROTEIN 689
1440343_at	RIBOSOMAL PROTEIN S6 KINASE, POLYPEPTIDE 5
1450034_at	SIGNAL TRANSDUCER AND ACTIVATOR OF TRANSCRIPTION 1
1451991_at	EPH RECEPTOR A7
1416349_at	MITOCHONDRIAL RIBOSOMAL PROTEIN L34
1450953_at	WD REPEAT DOMAIN 39
1449749_s_at	TRANSCRIPTION FACTOR B1, MITOCHONDRIAL
1443952_at	THYROID HORMONE RECEPTOR ALPHA
1434837_at	MEDIATOR OF DNA DAMAGE CHECKPOINT 1
1433495_at	GLYCOSYLTRANSFERASE 25 DOMAIN CONTAINING 1
1426364_at	MITOCHONDRIAL RIBOSOME RECYCLING FACTOR
1421379_at	ZINC FINGER PROTEIN 354B
1418529_at	O-SIALOGLYCOPROTEIN ENDOPEPTIDASE
1436833_x_at	TUBULIN TYROSINE LIGASE-LIKE 1
1453128_at	EXTRA CELLULAR LINK DOMAIN-CONTAINING 1
1417859_at	GROWTH ARREST SPECIFIC 7
1451297_at	GULONOLACTONE (L-) OXIDASE
1448905_at	RIKEN CDNA 1810009F08 GENE
1416961_at, 1447363_s_at	BUDDING UNINHIBITED BY BENZIMIDAZOLES 1 HOMOLOG, BETA (S. CEREVISIAE)
1453010_at	RIKEN CDNA 1700069O15 GENE
1416920_at	RNA BINDING MOTIF PROTEIN 4
1416826_a_at	TRF (TATA BINDING PROTEIN-RELATED FACTOR)-PROXIMAL PROTEIN HOMOLOG (DROSOPHILA)

1456378_s_at	F-BOX AND LEUCINE-RICH REPEAT PROTEIN 20
1456834_at	IBR DOMAIN CONTAINING 2
1437647_at	DEATH INDUCER-OBLITERATOR 1
1452388_at	HEAT SHOCK PROTEIN 1B
1442051_at	HISTONE 2, H3C1
Term Category: cellular physiological process; 37 genes (51.39%); pValue 0.003	
Affymetrix ID	Gene
1424852_at	MYOCYTE ENHANCER FACTOR 2C
1428760_at	RIKEN CDNA 4930558A07 GENE
1429169_at	RNA BINDING MOTIF PROTEIN 3
1456723_at	ZINC FINGER PROTEIN 689
1440343_at	RIBOSOMAL PROTEIN S6 KINASE, POLYPEPTIDE 5
1450034_at	SIGNAL TRANSDUCER AND ACTIVATOR OF TRANSCRIPTION 1
1451991_at	EPH RECEPTOR A7
1423343_at	SOLUTE CARRIER ORGANIC ANION TRANSPORTER FAMILY, MEMBER 1C1
1455213_at	RIKEN CDNA 4930488E11 GENE
1416349_at	MITOCHONDRIAL RIBOSOMAL PROTEIN L34
1450953_at	WD REPEAT DOMAIN 39
1449749_s_at	TRANSCRIPTION FACTOR B1, MITOCHONDRIAL
1434837_at	MEDIATOR OF DNA DAMAGE CHECKPOINT 1
1443952_at	THYROID HORMONE RECEPTOR ALPHA
1433495_at	GLYCOSYLTRANSFERASE 25 DOMAIN CONTAINING 1
1457969_at	RAB INTERACTING FACTOR
1417834_at	SYNAPTOJANIN 2 BINDING PROTEIN
1426364_at	MITOCHONDRIAL RIBOSOME RECYCLING FACTOR
1421379_at	ZINC FINGER PROTEIN 354B
1418529_at	O-SIALOGLYCOPROTEIN ENDOPEPTIDASE
1448943_at	NEUROPILIN 1
1451297_at	GULONOLACTONE (L-) OXIDASE
1417859_at	GROWTH ARREST SPECIFIC 7
1436833_x_at	TUBULIN TYROSINE LIGASE-LIKE 1
1453128_at	EXTRA CELLULAR LINK DOMAIN-CONTAINING 1
1448905_at	RIKEN CDNA 1810009F08 GENE
1416961_at, 1447363_s_at	BUDDING UNINHIBITED BY BENZIMIDAZOLES 1 HOMOLOG, BETA (S. CEREVISIAE)
1453010_at	RIKEN CDNA 1700069O15 GENE
1416920_at	RNA BINDING MOTIF PROTEIN 4
1416826_a_at	TRF (TATA BINDING PROTEIN-RELATED FACTOR)-PROXIMAL PROTEIN HOMOLOG (DROSOPHILA)
1456378_s_at	F-BOX AND LEUCINE-RICH REPEAT PROTEIN 20
1456834_at	IBR DOMAIN CONTAINING 2
1437647_at	DEATH INDUCER-OBLITERATOR 1
1452388_at	HEAT SHOCK PROTEIN 1B
1427401_at	CHOLINERGIC RECEPTOR, NICOTINIC, ALPHA POLYPEPTIDE 5
1442051_at	HISTONE 2, H3C1
1417680_at	POTASSIUM VOLTAGE-GATED CHANNEL, SHAKER-RELATED SUBFAMILY, MEMBER 5
Term Category: primary metabolism; 28 genes (38.89%); pValue 0.005	

Affymetrix ID	Gene
1424852_at	MYOCYTE ENHANCER FACTOR 2C
1428760_at	RIKEN CDNA 4930558A07 GENE
1429169_at	RNA BINDING MOTIF PROTEIN 3
1456723_at	ZINC FINGER PROTEIN 689
1440343_at	RIBOSOMAL PROTEIN S6 KINASE, POLYPEPTIDE 5
1450034_at	SIGNAL TRANSDUCER AND ACTIVATOR OF TRANSCRIPTION 1
1451991_at	EPH RECEPTOR A7
1416349_at	MITOCHONDRIAL RIBOSOMAL PROTEIN L34
1450953_at	WD REPEAT DOMAIN 39
1449749_s_at	TRANSCRIPTION FACTOR B1, MITOCHONDRIAL
1443952_at	THYROID HORMONE RECEPTOR ALPHA
1434837_at	MEDIATOR OF DNA DAMAGE CHECKPOINT 1
1433495_at	GLYCOSYLTRANSFERASE 25 DOMAIN CONTAINING 1
1426364_at	MITOCHONDRIAL RIBOSOME RECYCLING FACTOR
1421379_at	ZINC FINGER PROTEIN 354B
1418529_at	O-SIALOGLYCOPROTEIN ENDOPEPTIDASE
1436833_x_at	TUBULIN TYROSINE LIGASE-LIKE 1
1453128_at	EXTRA CELLULAR LINK DOMAIN-CONTAINING 1
1417859_at	GROWTH ARREST SPECIFIC 7
1448905_at	RIKEN CDNA 1810009F08 GENE
1416961_at, 1447363_s_at	BUDDING UNINHIBITED BY BENZIMIDAZOLES 1 HOMOLOG, BETA (S. CEREVISIAE)
1416920_at	RNA BINDING MOTIF PROTEIN 4
1416826_a_at	TRF (TATA BINDING PROTEIN-RELATED FACTOR)-PROXIMAL PROTEIN HOMOLOG (DROSOPHILA)
1456378_s_at	F-BOX AND LEUCINE-RICH REPEAT PROTEIN 20
1456834_at	IBR DOMAIN CONTAINING 2
1437647_at	DEATH INDUCER-OBLITERATOR 1
1452388_at	HEAT SHOCK PROTEIN 1B
1442051_at	HISTONE 2, H3C1

Term Category: metabolism; 30 genes (41.67%); pValue 0.006

Affymetrix ID	Gene
1424852_at	MYOCYTE ENHANCER FACTOR 2C
1428760_at	RIKEN CDNA 4930558A07 GENE
1429169_at	RNA BINDING MOTIF PROTEIN 3
1456723_at	ZINC FINGER PROTEIN 689
1440343_at	RIBOSOMAL PROTEIN S6 KINASE, POLYPEPTIDE 5
1450034_at	SIGNAL TRANSDUCER AND ACTIVATOR OF TRANSCRIPTION 1
1451991_at	EPH RECEPTOR A7
1416349_at	MITOCHONDRIAL RIBOSOMAL PROTEIN L34
1450953_at	WD REPEAT DOMAIN 39
1449749_s_at	TRANSCRIPTION FACTOR B1, MITOCHONDRIAL
1443952_at	THYROID HORMONE RECEPTOR ALPHA
1434837_at	MEDIATOR OF DNA DAMAGE CHECKPOINT 1
1433495_at	GLYCOSYLTRANSFERASE 25 DOMAIN CONTAINING 1
1426364_at	MITOCHONDRIAL RIBOSOME RECYCLING FACTOR
1421379_at	ZINC FINGER PROTEIN 354B

1418529_at	O-SIALOGLYCOPROTEIN ENDOPEPTIDASE
1436833_x_at	TUBULIN TYROSINE LIGASE-LIKE 1
1453128_at	EXTRA CELLULAR LINK DOMAIN-CONTAINING 1
1417859_at	GROWTH ARREST SPECIFIC 7
1451297_at	GULONOLACTONE (L-) OXIDASE
1448905_at	RIKEN CDNA 1810009F08 GENE
1416961_at, 1447363_s_at	BUDDING UNINHIBITED BY BENZIMIDAZOLES 1 HOMOLOG, BETA (S. CEREVISIAE)
1453010_at	RIKEN CDNA 1700069O15 GENE
1416920_at	RNA BINDING MOTIF PROTEIN 4
1416826_a_at	TRF (TATA BINDING PROTEIN-RELATED FACTOR)-PROXIMAL PROTEIN HOMOLOG (DROSOPHILA)
1456378_s_at	F-BOX AND LEUCINE-RICH REPEAT PROTEIN 20
1456834_at	IBR DOMAIN CONTAINING 2
1437647_at	DEATH INDUCER-OBLITERATOR 1
1452388_at	HEAT SHOCK PROTEIN 1B
1442051_at	HISTONE 2, H3C1
Term Category: nucleobase, nucleoside, nucleotide and nucleic acid metabolism; 17 genes (23.61%); pValue 0.006	
Affymetrix ID	Gene
1421379_at	ZINC FINGER PROTEIN 354B
1424852_at	MYOCYTE ENHANCER FACTOR 2C
1428760_at	RIKEN CDNA 4930558A07 GENE
1456723_at	ZINC FINGER PROTEIN 689
1429169_at	RNA BINDING MOTIF PROTEIN 3
1450034_at	SIGNAL TRANSDUCER AND ACTIVATOR OF TRANSCRIPTION 1
1440343_at	RIBOSOMAL PROTEIN S6 KINASE, POLYPEPTIDE 5
1448905_at	RIKEN CDNA 1810009F08 GENE
1416920_at	RNA BINDING MOTIF PROTEIN 4
1416826_a_at	TRF (TATA BINDING PROTEIN-RELATED FACTOR)-PROXIMAL PROTEIN HOMOLOG (DROSOPHILA)
1450953_at	WD REPEAT DOMAIN 39
1437647_at	DEATH INDUCER-OBLITERATOR 1
1452388_at	HEAT SHOCK PROTEIN 1B
1449749_s_at	TRANSCRIPTION FACTOR B1, MITOCHONDRIAL
1443952_at	THYROID HORMONE RECEPTOR ALPHA
1434837_at	MEDIATOR OF DNA DAMAGE CHECKPOINT 1
1442051_at	HISTONE 2, H3C1
Term Category: cartilage condensation; 2 genes (2.78%); pValue 0.028	
Affymetrix ID	Gene
1425083_at	OTORAPLIN
1443952_at	THYROID HORMONE RECEPTOR ALPHA
Term Category: macromolecule metabolism; 18 genes (25%); pValue 0.03	
Affymetrix ID	Gene
1433495_at	GLYCOSYLTRANSFERASE 25 DOMAIN CONTAINING 1
1426364_at	MITOCHONDRIAL RIBOSOME RECYCLING FACTOR
1418529_at	O-SIALOGLYCOPROTEIN ENDOPEPTIDASE

1429169_at	RNA BINDING MOTIF PROTEIN 3
1453128_at	EXTRA CELLULAR LINK DOMAIN-CONTAINING 1
1436833_x_at	TUBULIN TYROSINE LIGASE-LIKE 1
1440343_at	RIBOSOMAL PROTEIN S6 KINASE, POLYPEPTIDE 5
1417859_at	GROWTH ARREST SPECIFIC 7
1416961_at,	BUDDING UNINHIBITED BY BENZIMIDAZOLES 1 HOMOLOG, BETA (S.
1447363_s_at	CEREVISIAE)
1451991_at	EPH RECEPTOR A7
1416920_at	RNA BINDING MOTIF PROTEIN 4
1456378_s_at	F-BOX AND LEUCINE-RICH REPEAT PROTEIN 20
1456834_at	IBR DOMAIN CONTAINING 2
1416349_at	MITOCHONDRIAL RIBOSOMAL PROTEIN L34
1452388_at	HEAT SHOCK PROTEIN 1B
1449749_s_at	TRANSCRIPTION FACTOR B1, MITOCHONDRIAL
1434837_at	MEDIATOR OF DNA DAMAGE CHECKPOINT 1
1442051_at	HISTONE 2, H3C1

Term Category: biopolymer metabolism; 13 genes (18.06%); pValue 0.04

Affymetrix ID	Gene
1433495_at	GLYCOSYLTRANSFERASE 25 DOMAIN CONTAINING 1
1429169_at	RNA BINDING MOTIF PROTEIN 3
1436833_x_at	TUBULIN TYROSINE LIGASE-LIKE 1
1440343_at	RIBOSOMAL PROTEIN S6 KINASE, POLYPEPTIDE 5
1416961_at,	BUDDING UNINHIBITED BY BENZIMIDAZOLES 1 HOMOLOG, BETA (S.
1447363_s_at	CEREVISIAE)
1451991_at	EPH RECEPTOR A7
1416920_at	RNA BINDING MOTIF PROTEIN 4
1456378_s_at	F-BOX AND LEUCINE-RICH REPEAT PROTEIN 20
1456834_at	IBR DOMAIN CONTAINING 2
1452388_at	HEAT SHOCK PROTEIN 1B
1449749_s_at	TRANSCRIPTION FACTOR B1, MITOCHONDRIAL
1434837_at	MEDIATOR OF DNA DAMAGE CHECKPOINT 1
1442051_at	HISTONE 2, H3C1

Term Category: cartilage development; 2 genes (2.78%); pValue 0.078

Affymetrix ID	Gene
1425083_at	OTORAPLIN
1443952_at	THYROID HORMONE RECEPTOR ALPHA

Term Category: cellular macromolecule metabolism; 13 genes (18.06%); pValue 0.08

Affymetrix ID	Gene
1433495_at	GLYCOSYLTRANSFERASE 25 DOMAIN CONTAINING 1
1426364_at	MITOCHONDRIAL RIBOSOME RECYCLING FACTOR
1418529_at	O-SIALOGLYCOPROTEIN ENDOPEPTIDASE
1429169_at	RNA BINDING MOTIF PROTEIN 3
1436833_x_at	TUBULIN TYROSINE LIGASE-LIKE 1
1440343_at	RIBOSOMAL PROTEIN S6 KINASE, POLYPEPTIDE 5
1417859_at	GROWTH ARREST SPECIFIC 7
1416961_at,	BUDDING UNINHIBITED BY BENZIMIDAZOLES 1 HOMOLOG, BETA (S.
1447363_s_at	CEREVISIAE)

1451991_at	EPH RECEPTOR A7
1456378_s_at	F-BOX AND LEUCINE-RICH REPEAT PROTEIN 20
1456834_at	IBR DOMAIN CONTAINING 2
1416349_at	MITOCHONDRIAL RIBOSOMAL PROTEIN L34
1452388_at	HEAT SHOCK PROTEIN 1B
Term Category: regulation of transcription, DNA-dependent; 10 genes (13.89%); pValue 0.09	
Affymetrix ID	Gene
1450034_at	SIGNAL TRANSDUCER AND ACTIVATOR OF TRANSCRIPTION 1
1440343_at	RIBOSOMAL PROTEIN S6 KINASE, POLYPEPTIDE 5
1416826_a_at	TRF (TATA BINDING PROTEIN-RELATED FACTOR)-PROXIMAL PROTEIN HOMOLOG (DROSOPHILA)
1450953_at	WD REPEAT DOMAIN 39
1424852_at	MYOCYTE ENHANCER FACTOR 2C
1421379_at	ZINC FINGER PROTEIN 354B
1437647_at	DEATH INDUCER-OBLITERATOR 1
1428760_at	RIKEN CDNA 4930558A07 GENE
1443952_at	THYROID HORMONE RECEPTOR ALPHA
1456723_at	ZINC FINGER PROTEIN 689
Term Category: transcription, DNA-dependent; 10 genes (13.89%); pValue 0.099	
Affymetrix ID	Gene
1450034_at	SIGNAL TRANSDUCER AND ACTIVATOR OF TRANSCRIPTION 1
1440343_at	RIBOSOMAL PROTEIN S6 KINASE, POLYPEPTIDE 5
1416826_a_at	TRF (TATA BINDING PROTEIN-RELATED FACTOR)-PROXIMAL PROTEIN HOMOLOG (DROSOPHILA)
1450953_at	WD REPEAT DOMAIN 39
1424852_at	MYOCYTE ENHANCER FACTOR 2C
1421379_at	ZINC FINGER PROTEIN 354B
1437647_at	DEATH INDUCER-OBLITERATOR 1
1428760_at	RIKEN CDNA 4930558A07 GENE
1443952_at	THYROID HORMONE RECEPTOR ALPHA
1456723_at	ZINC FINGER PROTEIN 689

3.1.1.5 Hypoxic Preconditioning Gene Networks Discovered by Ingenuity Pathway Analysis (Additional File 5)

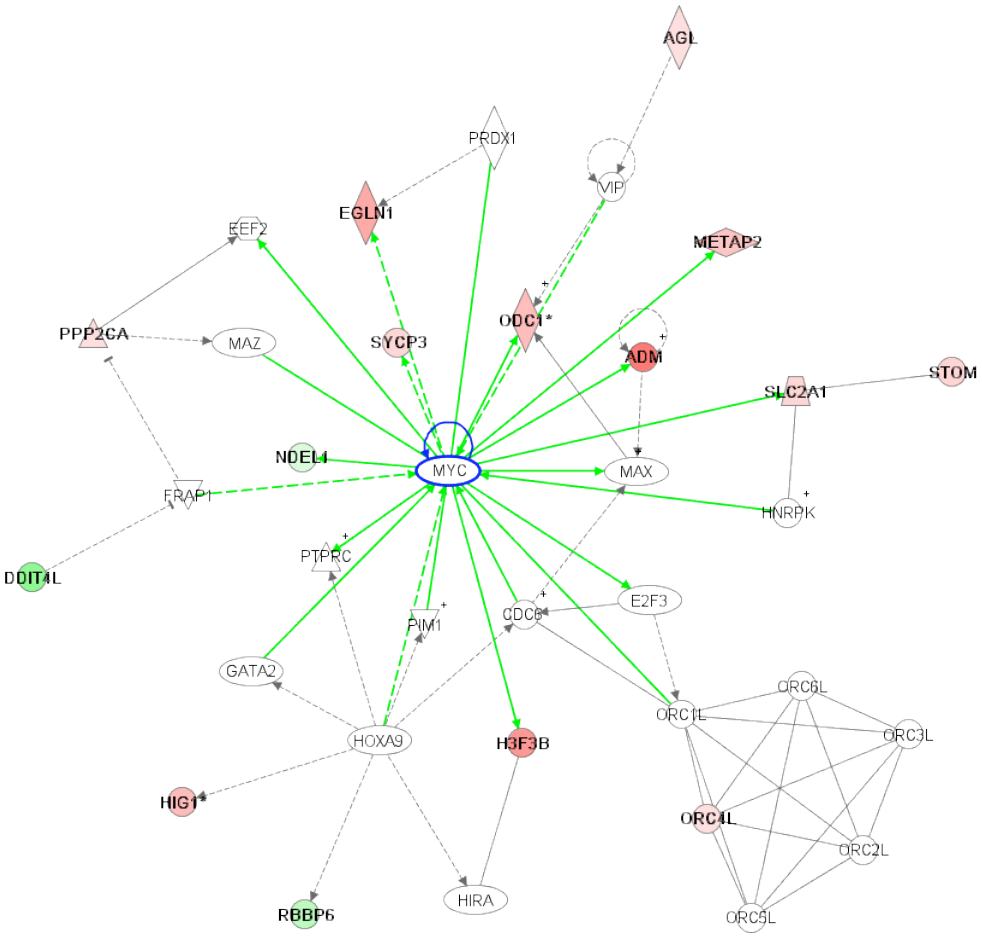

Supplemental Fig.2 A prominent affected gene network discovered by Ingenuity Pathway Analysis. Network was classified as: DNA replication, recombination, cell cycle and cancer. Pathway is centrally occupied by Myc and contains the pro survival gene Adm. Note that Myc itself is not differentially regulated. (red = induction; green = repression; white = unaffected; color intensity correlates with fold change)

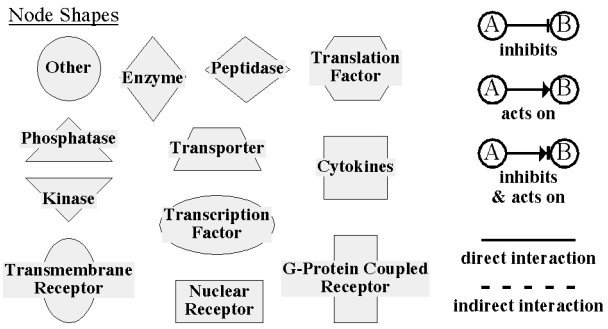

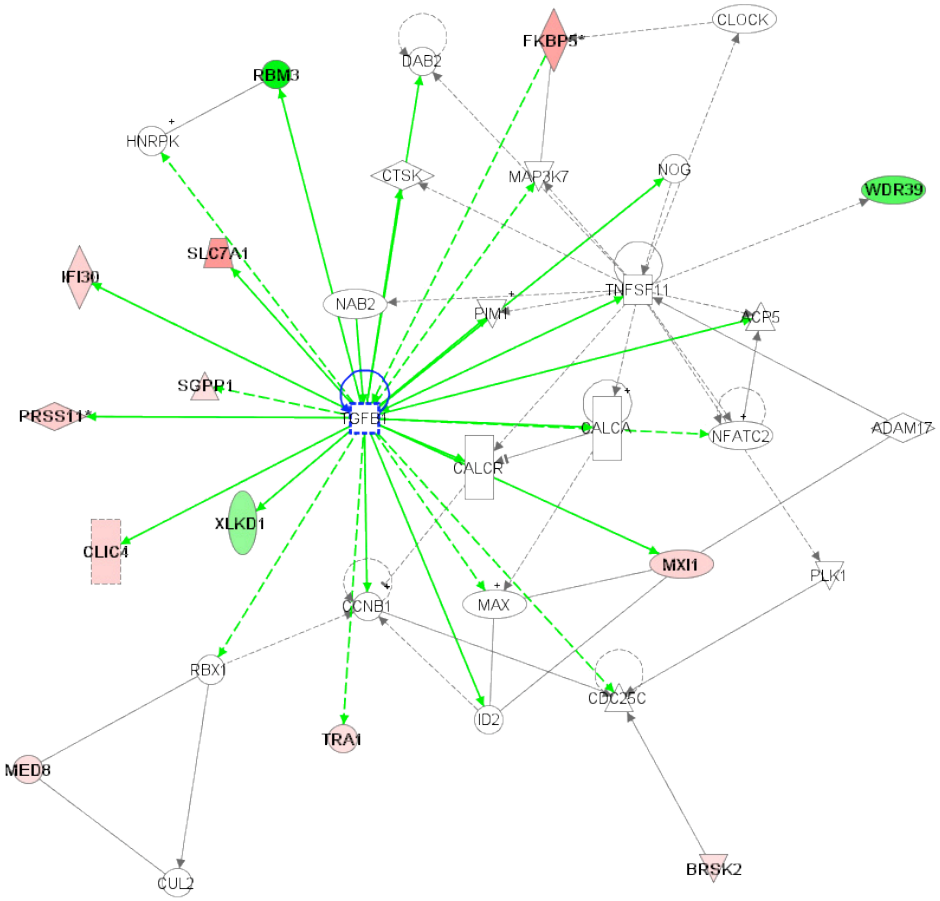

Supplemental Fig.3 An affected gene network discovered by Ingenuity Pathway Analysis. Network was classified as: Cell death, cellular development, hematological system development & function. Some genes related to TGF-b are induced after hypoxic preconditioning (red = Induction; green = repression; white = unaffected; color intensity correlates with fold change)

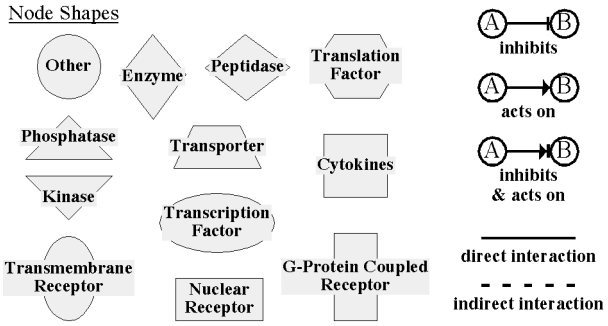

3.1.1.6 Primer Sequences and Product Sizes (Additional File 6)

TABLE 7 Primer pairs used for real time PCR.

Gene	Primer forward	Primer reverse	Product bp
Adm	TTCGCAGTTCCGAAAGAAGT	GGTAGCTGCTGGATGCTTGTA	77
Bcl2l10	GAACTTTCTGTATAATCTGCTCATGG	TGAAGAAGCGGCAAAAGC	89
Cdkn1a	CGGTGTCAGAGTCTAGGGGAATTG	CGTGACGAAGTCAAAGTTCCACC	238
Cebpd	CTTTTAGGTGGTTGCCGAAG	GCAACGAGGAATCAAGTTTCA	70
Dido1 (Iso1/3)	CTCTATATCCGTGGTAGCTCTGG	TGGGGACTGCCTCTTAAACA	76
Dido1 (Iso2)	GACTGAGTTCGAAACGAAGGA	CGAACAACCAAAGGGACAGT	63
Egf	CATGCCCCACAGGATTTG	GGGCAGGAAACAAGTTCGT	64
Egln1	CATTGTTGGCAGAAGGTGTG	CAAAGGACTACAGGGTCTCCA	70
Fabp4	GAAAACGAGATGGTGACAAGC	TTGTGGAAGTCACGCCTTT	60
H3f3B	CGATTGCGGCTCTTGTTC	CTTGGTTCGGGCCATTTT	96
Hes6	GCACGGATCAACGAGAGTC	CGGCGTTCTCTAGCTTGG	76
Hmgb2	GATTGCGTTACGAGAAACCAG	GTCACCCTTGCCCATGAC	126
Ibrdc2	AGGCTGTGGCTCAGACCTTA	ACACTGGAGCCCATCGAC	75
Id1	GCGAGATCAGTGCCTTGG	CTCCTGAAGGGCTGGAGTC	111
Kif4	GCATGACTGCAACCATTGAT	TATCTGGGCTGCTTTGCACT	63
Mef2c	TCTGCCCTCAGTCAGTTGG	CGTGGTGTGTTGTGGGTATC	63
Metap2	GGAGAGAGATGACGACGATGA	CTTCTTCCCAGTTGCACCAT	61
Mt1	GAATGGACCCCAACTGCTC	GCAGCAGCTCTTCTTGCAG	104
Pon1	AATGCTTTCCGTGAAGTAACGC	TCTAACTCTGACACTGCTGGCTCC	218
Rad23b	CCCTGACAGAGCTGTGGAAT	GTCAACCACAGCCTGACTTTC	70
Sema3c	ATGGCCACTCTTGCTCTAGG	CATCTTGTCTTCGGCTCCTC	60
Slc2A1	ATGGATCCCAGCAGCAAG	CCAGTGTTATAGCCGAACTGC	92
Sos1	TCGGCAACTCACTTTACTTGAA	TGTCCACACACTTCCAACTAATTC	76
Stat1	TTGTGTTGAATCCCGAACCT	TCGAACCACTGTGACATCCT	95
Stom	CCAGTGCAGCTCCAGAGAG	CGCATTCATTTCCCCTTC	93
Thra	AAGGTGGAGTGTGGGTCAGA	TTTTTCGCTTTCCATCTGGT	64
Timp3	GCCTCAAGCTAGAAGTCAACAAA	TGTACATCTTGCCTTCATACACG	69
Ttr	AATGTCCTCTGATGGTCAAAGTCC	TGGAACGGGGAAATGCCAAG	238
Vegf_all	ACTTGTGTTGGGAGGAGGATGTC	AATGGGTTTGTCGTGTTTCTGG	171
Vegf164 (Iso1)	CATCTTCAAGCCGTCCTGTGTG	TGACCCTTTCCCTTTCCTCG	240
Vegf120 (Iso2)	GCCAGAAAATCACTGTGAGCC	TCTACAGGAATCCCAGAAACAACC	478
Vegf188 (Iso3)	CAGAAAAATGTGACAAGCCAAGG	TCTACAGGAATCCCAGAAACAACC	344

3.2 Retinal Neuroprotection by Hypoxic Preconditioning is Independent of HIF-1α Expression in Photoreceptors

Markus Thiersch[1], Christina Lange[1], Sandrine Joly[1], Severin Heynen[1], Yun Zheng Le[2], Marijana Samardzija[1] and Christian Grimm[1]

[1]Lab of Retinal Cell Biology, Dept Ophthalmology, University of Zurich, Switzerland

[2]University of Oklahoma, Health Sciences Center, 941 Stanton L. Young Blvd., BSEB 302G, Oklahoma City, OK, USA

European Journal of Neuroscience *accepted for publication*

Reference number [135] refers to this paper

Proposed Journal section: Molecular & Developmental Neuroscience

Proposed Associate Editors: Wim Robberecht

Jean-Marc Fritschy

Retinal neuroprotection by hypoxic preconditioning is independent of HIF-1α expression in photoreceptors

Markus Thiersch[1], Christina Lange[1], Sandrine Joly[1], Severin Heynen[1], Yun Zheng Le[2], Marijana Samardzija[1] and Christian Grimm[1]

[1]Lab of Retinal Cell Biology, Dept Ophthalmology, Center for Integrative Human Physiology and Neuroscience Center Zurich, University of Zurich, Switzerland

[2]University of Oklahoma, Health Sciences Center, 941 Stanton L. Young Blvd., BSEB 302G, Oklahoma City, OK, USA

Corresponding Author:
Christian Grimm
Lab for Retinal Cell Biology
Dept. Ophthalmology
University of Zurich
Frauenklinikstrasse 24
CH-8091 Zurich

Running Title: HIF-1α independent retinal neuroprotection

Number of Pages: 40

Number of Figures: 6

Number of Tables: 1

Number of words: (9581) manuscript; (225) abstract; (615) introduction

Keywords: HIF, Cell survival, Hypoxia, Degeneration, Retina

Abstract

Hypoxic preconditioning stabilizes hypoxia-inducible-factor 1α (HIF-1α) in the retina and protects photoreceptors against light-induced cell death. HIF-1α is one of the major transcription factors responding to low oxygen tension and can differentially regulate a large number of target genes. To analyze whether photoreceptor specific expression of HIF-1α is essential to protect photoreceptors by hypoxic preconditioning, we knocked down expression of HIF-1α specifically in photoreceptor cells using the cre-lox system. The cre-mediated knockdown caused a 20-fold reduced expression of HIF-1α in the photoreceptor cell layer. In the total retina, RNA expression was reduced by 65% and hypoxic preconditioning did only lead to a small increase in HIF-1α protein levels. Accordingly, HIF-1 target gene expression after hypoxia was significantly diminished. Retinas of HIF-1α knockdown animals did not show any pathological alterations and tolerated hypoxic exposure comparable to wild type retinas. Importantly, the strong neuroprotective effect of hypoxic preconditioning against light-induced photoreceptor degeneration persisted in knockdown mice suggesting that hypoxia-mediated survival of light exposure does not depend on an autocrine action of HIF-1α in photoreceptor cells. Hypoxia-mediated stabilization of HIF-2α and phosphorylation of STAT3 was not affected in the retinas of HIF-1α knockdown mice. Thus, these factors are candidates for regulating the resistance of photoreceptors against light damage after hypoxic preconditioning along with several potentially neuroprotective genes which were similarly induced in hypoxic knockdown and control mice.

Introduction

Photoreceptor degeneration is common to many blinding diseases including Retinitis Pigmentosa (RP) and age related macular degeneration (AMD). Whereas RP is a monogenetic disorder affecting primarily photoreceptors, the pathology of AMD is complex and involves death of cells of the retinal pigment epithelium (RPE) and of photoreceptors, changes in the Bruch's membrane, formation of Drusen and – in the wet form of the disease - neovascularization. To mimic photoreceptor degeneration as part of the retinal pathology in these diseases, mice are exposed to cytotoxic levels of white light, which triggers apoptosis in photoreceptors (Wenzel *et al.* 2005). Different strategies such as hypoxic and ischemic preconditioning have been shown to inhibit cell death and to protect non-neuronal as well as neuronal tissues – including the retina – from apoptosis (Gage & Stanton 1996; Barone *et al.* 1998; Roth *et al.* 1998; Gidday *et al.* 1999; Grimm *et al.* 2002; Tanaka *et al.* 2002; Zhang *et al.* 2002; Sharp *et al.* 2004; Zhu *et al.* 2007). The underlying pro-survival mechanisms are not completely understood. However, it is clear that cells respond to hypoxia with the differential regulation of genes driven by several major transcription factors. Among those, hypoxia inducible factors (HIFs) are the most prominent proteins regulating the tissue response to low oxygen levels. The HIF family consists of 3 identified members with HIF-1 being the best-characterized protein (Bruick & McKnight 2002). It is a heterodimeric transcription factor, which consists of the HIF-1α and HIF-1β subunits. Both proteins are ubiquitously expressed with HIF-1α being posttranslationally regulated by oxygen availability (Wang & Semenza 1993; 1995). Under normoxic conditions prolylhydroxylases (PHDs) hydroxylate HIF-1α at specific prolin residues (Bruick & McKnight 2001; Ivan *et al.* 2001; Jaakkola *et al.* 2001) providing the substrate for the von-Hippel-Lindau protein (VHL), which initiates the accumulative binding of ubiquitin to the protein. This finally results in the efficient degradation of HIF-1α via the proteosomal degradation pathway (Salceda & Caro 1997; Huang *et al.* 1998). Additionally, factor inhibiting HIF (FIH) hydroxylates HIF-1α at an asparagine residue in the transactivation domain to inhibit the binding of transcriptional cofactors (Mahon *et al.* 2001). Under hypoxic conditions the hydroxylases fail to hydroxylate HIF-1α resulting in its stabilization and activation. Stabilized HIF-1α is transferred into the nucleus where it binds its partner hypoxia inducible factor-1β (HIF-1β) to form HIF-1, which differentially regulates the expression of many genes involved in apoptosis, cell survival, angiogenesis and metabolism (Bruick & McKnight 2002).

Many reports have connected HIF-1α to tissue- and neuro-protection (Ran *et al.* 2005; Siddiq *et al.* 2005; Hill *et al.* 2008; Rosenberger *et al.* 2008). Recently, it was

reported that cardioprotection against ischemia/reperfusion after ischemic preconditioning requires HIF-1α expression (Cai *et al.* 2008) and that neuronal ablation of HIF-1α enhances pathological effects after cerebral ischemia (Baranova *et al.* 2007). In the retina HIF-1α was found in association with heat shock protein 27 (Hsp27), nitric oxide synthase (NOS) or heme oxygenase-1 (HO-1) to protect from ischemia after ischemic preconditioning (Whitlock *et al.* 2005; Kaur *et al.* 2006; Zhu *et al.* 2007). Additionally, the level of HIF-1α stabilization after hypoxic preconditioning correlated with the degree of photoreceptor protection against light-induced degeneration (Grimm *et al.* 2002). Part of this neuroprotective response was attributed to erythropoietin (Epo) (Grimm *et al.* 2002), which, as newer data indicate, may mainly be regulated by HIF-2 and not by HIF-1 (Rankin *et al.* 2007). This suggests that HIF-2 may have neuroprotective activity affecting cell survival after a toxic insult. To date the impact of HIF-1α on retinal neuroprotection after hypoxic preconditioning has not been analyzed in detail. Using tissue-specific knockdown mice, we analyzed whether photoreceptors require intrinsic activity of HIF-1α to survive light exposure after hypoxic preconditioning.

Material and Methods

Animals

Animals were treated in accordance with the regulations of the Veterinary Authority of Zurich and with the statement of 'The Association for Research in Vision and Ophthalmology' for the use of animals in research. Mice carrying a floxed exon 2 of HIF-1α (HIF-1α$^{F/F}$) (Ryan *et al.* 2000) were kindly provided by Randall Johnson (UCSD San Diego, USA)/Max Gassmann (University of Zurich, Switzerland) and PrP-Cre-ER^{T}(28.4) mice (Weber *et al.* 2001) were obtained from Pierre Chambon (IGBMC, Strasbourg, France). LMOPC1 mice (expressing Cre under the control of the rod opsin promoter) have been published before (Le *et al.* 2006). To generate conditional knockdown mice HIF-1α$^{F/F}$ mice were bred to PrP-Cre-ER^{T}(28.4) mice or to LMOPC1 according to classical breeding schemes. All mouse strains analyzed were maintained on a homozygous Rpe65$_{450Leu}$ background (Wenzel *et al.* 2003). To simplify matters LMOPC1:HIF-1α$^{Δ/Δ}$ mice were named OpnCre$^{(HIF-Δ)}$ and HIF-1α$^{F/F}$ control mice were named OpnCre$^{(HIF-wt)}$. PrP-Cre-ER^{T}(28.4) mice required tamoxifen (TAM) to induce Cre activity. TAM was dissolved in sunflower oil (Sigma-Aldrich, Buchs, Switzerland) to obtain a concentration of 10 mg/ml. TAM (1mg/40g) was injected intraperitoneally in three week old animals twice a day for 5 consecutive days. Control injections were

done with oil only. After injections mice were allowed to recover for 2 weeks before experiments were performed. In keeping with the above nomenclature, TAM treated knockdown animals (PrP-Cre-ER^{T}(28.4):HIF$^{\Delta/\Delta}$) were named PrpCre$^{(HIF-\Delta)}$ and oil treated PrP-Cre-ER^{T}(28.4):HIF$^{F/F}$ control mice were named PrpCre$^{(HIF-wt)}$. For tissue isolation and analysis, mice were sacrificed by CO_2 anesthesia followed by cervical dislocation.

Hypoxic preconditioning and light exposure

Hypoxic preconditioning (6-7% O_2 for 6 hours) was performed as described previously (Grimm *et al.* 2002). After hypoxia, mice were sacrificed at indicated time points for tissue collection or were dark adapted for 4 h before light onset. For light exposure, pupils of mice were dilated in dim red light using 1% Cyclogyl (Alcon, Cham, Switzerland) and 5% Phenylephrine (Ciba Vision, Niederwangen, Switzerland) 45 minutes prior to illumination. After light exposure (13‘000 lux; 2 h) animals remained in darkness over night and were analyzed after 36 h or at the time points indicated.

Morphology and cell death detection

To analyze morphology, mice were sacrificed 36 h after light exposure. Eyes were enucleated and processed for light microscopy as previously described (Samardzija *et al.* 2006). A digitalized Axiovision microscope (Carl Zeiss Microscopy, Jena, Germany) using 40x objective lenses with numerical aperture of 1.3 was used to examine slides. Representative images were taken from the inferior temporal retina. To balance for staining variabilities, contrast and brightness were sometimes slightly adjusted. As semi-quantitative assessment of apoptosis, nucleosomal release was determined at 36 h after light exposure using a cell death detection kit (Roche Diagnostics, Basel, Switzerland) according to the manufacturer’s recommendation.

RNA isolation and real time PCR

Retinas were isolated immediately after hypoxic preconditioning, frozen in liquid nitrogen and stored at -80 °C. Normoxic controls were treated in parallel and collected at the same time points. Total retinal RNA was extracted using the RNeasy isolation kit (Qiagen, Hilden, Germany), including a DNase treatment to digest residual genomic DNA. cDNA was prepared from equal amounts of total retinal RNA using oligo(dT) primers and M-MLV reverse transcriptase (Promega, Madison, WI, USA). 5 ng of cDNA was amplified in a LightCycler 480 instrument (Roche Diagnostics AG, Rotkreuz, Switzerland) using LightCycler 480 SYBR Green I Master Mix (Roche Diagnostics AG,

Rotkreuz, Switzerland) and appropriate primer pairs (Table 1). cDNA levels were normalized to β-actin and relative values were calculated using a respective calibrator. At least eight independent samples were used for each condition in PrpCre mice and five in OpnCre mice.

Western blotting

Retinas were sonified in 0.1 M Tris/HCl (pH 8.0) at 4 °C and protein content was determined using BCA™ Protein Assay Kit (Pierce, Rockford, USA). Protein extracts were mixed with SDS sample buffer and incubated for 10 min at 95 °C. Proteins were separated by SDS-PAGE and blotted onto a nitrocellulose membrane. After blocking with 5% non-fat dry milk (Bio-Rad, Munich, Germany) in TBST (Tris/HCl 10 mM, pH 8; 150 mM NaCl; 0.05% Tween-20) membranes were incubated with primary antibodies at 4 °C overnight. Primary antibodies used were: rabbit anti-HIF-1α (Novus Biologicals NB, Littleton, CA, USA; 100-479; 1:1000), rabbit anti-phospho-STAT3 (Cell Signaling, Danvers, MA, USA; #9131; 1:500), rabbit anti-STAT3 (Cell Signalling, Danvers, MA, USA; #9132; 1:1000), rabbit anti-HIF-2α (Novus Biologicals NB, Littleton, CA, USA; 100-480; 1:500) and goat anti-β-actin (Santa Cruz, Santa Cruz, CA, USA; sc1616; 1:1000). After incubation with horseradish peroxidase labeled secondary antibodies for 1 h at room temperature, the protein bands were visualized by the application of a chemiluminescent substrate (PerkinElmer, Boston, USA) and exposure to a Super RX film (Fujifilm, Dielsdorf, Switzerland).

For protein analyzes at least four individual samples were used for each condition.

Immunofluorescence

Eyes were isolated and incubated for 10 min in PBS containing 4% PFA. Cornea and lens were removed and the remaining tissue including the retina was incubated for another 15 min in 4% PFA. Afterwards, eyecups were kept in 30% sucrose and embedded in cryoprotective medium (Jung, Nussloch, Germany). 12 µm sections were cut and cryoslides were blocked in a humid chamber with PBS containing 3% normal goat serum (NGS) and 0.3% Triton X100. Slides were incubated with rabbit anti HIF-1α antibody (Novus Biologicals NB, Littleton, CA, USA; 100-654; 1:100). After washing with PBS, slides were incubated with Cy3 labeled secondary antibodies (Jackson ImmunoResearch Europe, Suffolk, England), for 1 h at room temperature, washed with PBS, counterstained with 4',6-diamidino-2-phenylindole dilactate (DAPI, Molecular Probes) and mounted with Mowiol 4-88 Reagent (VWR International AG, Lucerna,

Switzerland). Immunofluorescent stainings were analyzed with a digitalized Axiovision microscope (Carl Zeiss Microscopy, Jena, Germany) using 20x objective lenses with a numerical aperture of 0.5. Stainings on normoxic and hypoxic samples were done in parallel on the same slide.

Laser capture microdissection

For laser capture microdissection (LCM) eyes were enucleated, embedded in RNase free cryoprotective medium (Jung, Nussloch, Germany) and stored at -80 °C. Samples were cut (12 µm) and transferred to nuclease and human nucleic acid free membrane slides (Molecular Machines & Industries, Glattbrugg, Switzerland). Prior to LCM samples were incubated with acetone (5 min), 99.9% ethanol (30 sec) and xylol (5 min). After aceton and xylol incubation slides were dried for 5 min and 30 min, respectively. Laser captured tissues were collected in tubes with an adhesive lid (Molecular Machines & Industries, Glattbrugg, Switzerland) and stored at -80 °C. RNA was isolated using the RNeasy Micro Kit (Qiagen, Hilden, Germany) according to the manufacturer's recommendations, including a DNase treatment to digest residual genomic DNA. cDNA synthesis and analyzes were performed as described above.

Statistical Analyzes

For statistical validations of gene expression we used unpaired, two-tailed students t-tests for the individual comparison between wild type and knockdown mice in normoxia or hypoxia, respectively. *F*-value, *t*-ratios (*t*), degrees of freedom (*df*) and number of samples (*n*) are given for each analysis in the body of the main text. One-way analysis of variance (ANOVA) with Bonferroni posttests was used to compare cell death of normoxic and hypoxic wild type or knockdown mice, respectively, to controls. *F*-values, total (treatment plus residual) degrees of freedom (*df*), *t*-ratios (*t*) for each posttest, number of samples (*n*) as well as whether *P* values were above or below level of significance ($P>0.05$ or $P<0.05$) are given within the main text of the results section. All calculations were done using Prism Software (GraphPad Prism Software Inc. San Diego, CA, USA).

Results

HIF-1α is expressed in all retinal cell layers

The HIF-1α gene is ubiquitously expressed in almost all eukaryotic cells. To analyze the mRNA expression of HIF-1α and its family member HIF-2α in the different

layers of the mouse retina we isolated the outer nuclear layer (ONL), the inner nuclear layer (INL) and the ganglion cell layer (GCL) by LCM of normoxic adult PrpCre$^{(HIF\text{-}wt)}$ mice and analyzed gene expression by reverse transcription PCR. Whereas mRNAs of the control genes Gnat1 (ONL), Chx10 (INL) and Opn4 (GCL) were mainly detected in their expected layers, HIF-1α as well as HIF-2α were expressed in all layers of the retina (Fig. 1A).

To analyze protein distribution of HIF-1α we performed immunostaining on normoxic and hypoxic retinas. In normoxic mice HIF-1α protein is rapidly degraded and therefore hardly detectable. Nevertheless, immunostaining for HIF-1α showed some residual protein in the normoxic GCL (Fig. 1B; Normoxia). During hypoxia HIF-1α protein is stabilized and a strong accumulation of HIF-1α was observed in the GCL and INL (Fig. 1B; Hypoxia) as reported previously (Ozaki *et al.* 1999; Zhu *et al.* 2007). In addition, we also observed an intense HIF-1α staining in the ONL supporting our RNA data that HIF-1α is expressed in all retinal cell layers.

Deletion of HIF-1α in photoreceptor cells

The stabilization of HIF-1α in the ONL during hypoxia suggests that it might be needed by photoreceptors to cope with hypoxic stress. To test for the role of HIF-1α in photoreceptor cells, we generated two mouse strains with photoreceptor-specific deletions of HIF-1α (see Materials and Methods). PrpCre mice express tamoxifen (TAM) inducible Cre under the control of the prion protein promoter (Prp) whereas OpnCre mice express Cre under the control of the rod opsin promoter. Both mouse lines were reported to express Cre specifically in photoreceptor cells (Weber *et al.* 2001; Le *et al.* 2006). To generate PrpCre$^{(HIF\text{-}\Delta)}$ mice, PrpCre$^{(HIF\text{-}wt)}$ were treated with TAM to delete HIF-1α in the adult retina leaving postnatal retinal development undisturbed. Oil treated PrpCre$^{(HIF\text{-}wt)}$ mice served as controls. After a recovery phase of 2 weeks after the last TAM (or oil) injection we performed experiments in PrpCre$^{(HIF\text{-}\Delta)}$ and PrpCre$^{(HIF\text{-}wt)}$ mice at 6 weeks of age. Likewise, OpnCre$^{(HIF\text{-}\Delta)}$ mice, which start to delete the floxed target sequence at postnatal day 7 (Le *et al.* 2006) and OpnCre$^{(HIF\text{-}wt)}$ control mice were 6 weeks of age when used for experiments.

To determine the knockdown efficiency in the two strains we isolated total retinal mRNA and protein of at least 5 independent mice. In normoxic OpnCre$^{(HIF\text{-}\Delta)}$ mice HIF-1α mRNA levels were significantly (P=0.019, F=3.409, t=2.919, df=8, n=5 for each strain) reduced to nearly 50% of control mice (Fig. 2A, left panel).

Since this analysis included RNA from cells of the INL and GCL, which do not (or not strongly) express cre recombinase, most of the detected HIF-1α mRNA in retinas of OpnCre$^{(HIF-\Delta)}$ mice was likely to be expressed in cells different from photoreceptors. Under hypoxic conditions HIF-1α RNA levels were not significantly (*P*=0.117, *F*=2.470, *t*=1.756, *df*=8, *n*=5 for each strain) different from controls suggesting an incomplete deletion of the HIF-1α gene in photoreceptors. In PrpCre$^{(HIF-\Delta)}$ mice, HIF-1α RNA levels were strongly and significantly reduced to 35% of controls in both normoxic (*P*=0.0003, *F*=6.263, *t*=4.810, *df*=14, *n*=8 for each strain) and hypoxic (*P*=0.0001, *F*=2.355, *t*=8.655, *df*=14, *n*=8 for each strain) retinas (Fig. 2A, right panel). LCM was used to test the specificity of HIF-1α deletion in retinas of PrpCre$^{(HIF-\Delta)}$ mice. The ONL had 20-fold reduced HIF-1α RNA levels as compared to controls (Fig. 2B). Since expression of HIF-1α is not regulated on the gene level, these data indicate that only between 5% and 10% of the cells in the ONL still express both or one allele of HIF-1α, respectively. Thus, at least 90% of photoreceptors are genuine HIF-1α knockout cells whereas the other cells are either heterozygous or wild type for HIF-1α. In contrast, cells of the INL and GCL of PrpCre$^{(HIF-\Delta)}$ mice showed only a 2-fold reduced expression of HIF-1α mRNA indicating that HIF-1α deletion was restricted mainly but not exclusively to photoreceptor cells. Although most cells in the ONL are knockouts, on a tissue level (whole retina) PrpCre$^{(HIF-\Delta)}$ mice are rather knockdowns for HIF-1α. The reason for the reduced HIF-1α RNA levels in INL and GCL is not known but may be due to cre activity in some cells different from photoreceptors. The general integrity of gene expression in cre expressing PrpCre$^{(HIF-\Delta)}$ mice was not affected as suggested by the normal RNA levels of Chx10 in the INL and Gnat1 in the ONL (data not shown).

To test the effect of the HIF-1α deletion on protein levels we performed Western blotting of normoxic or hypoxic preconditioned PrpCre$^{(HIF)}$ and OpnCre$^{(HIF)}$ mice (Fig. 2C). As expected, we observed only very faint bands in normoxic and a strong stabilization of HIF-1α in hypoxic control animals. The comparison between hypoxic PrpCre$^{(HIF-wt)}$ and PrpCre$^{(HIF-\Delta)}$ mice showed that the HIF-1α protein levels were dramatically reduced in knockdown mice (Fig. 2C). In fact, they seemed to reach almost the basal levels of normoxic mice indicating that the knockdown efficiency was very high on the protein level. In contrast, OpnCre$^{(HIF-\Delta)}$ mice showed a less pronounced reduction of HIF-1α protein expression during hypoxia when compared to control levels.

In conclusion, PrpCre$^{(HIF-\Delta)}$ mice showed a very strong reduction of HIF-1α expression predominantly in photoreceptor cells. OpnCre$^{(HIF-\Delta)}$ mice presented a less

severe reduction with more HIF-1α protein remaining in the retina after hypoxic exposure.

Reduced HIF-1α target gene expression in knockdown mice

HIF-1α regulates the expression of many genes during hypoxia. To analyze the effect of reduced HIF-1α protein levels on HIF-1α target gene expression after hypoxic preconditioning, we determined mRNA expression levels in normoxic and hypoxic retinas (Fig. 3). Egln1 encodes the prolylhydroxylase PHD2, which is required for the oxygen dependent degradation of HIF-1α (Bruick & McKnight 2001; Ivan *et al.* 2001; Jaakkola *et al.* 2001). In PrpCre$^{(HIF\text{-}wt)}$ mice and OpnCre$^{(HIF\text{-}wt)}$ mice Egln1 RNA levels were induced 5-6 times immediately after hypoxia (Fig. 3). The Egln1 induction was significantly suppressed by more than 50% in PrpCre$^{(HIF\text{-}\Delta)}$ (P<0.0001, t=7.142, F=1.501, df=14, n=8 for each strain) and by about 30% in OpnCre$^{(HIF\text{-}\Delta)}$ mice (P=0.0072, F=2.562, t=3.579, df=8, n=5 for each strain), respectively. Similarly reduced mRNA levels after hypoxia were found in the PrpCre$^{(HIF\text{-}\Delta)}$ strain for other HIF-1α target genes like the pro-apoptotic gene Bnip3 (P=0.0001,F=2.981, t=6.261, df=14, n=8 for each strain), the potentially anti-apoptotic genes vascular endothelial growth factor (Vegf; P=0.0011, F=2.980, t=4.085, df=14, n=8 for each strain) and adrenomedullin (Adm; P=0.0002, F=1.284, t=4.884, df=14, n=8 for each strain) as well as the glucose transporter Glut1 (P<0.0001, F=1.157, t=9.052, df=14, n=8 for each strain). RNA levels were also reduced in the hypoxic OpnCre$^{(HIF\text{-}\Delta)}$ mice but reached significance only for Egln1 (see above) and Glut1 (P=0.0362, F=2.023, t=2.514, df=8, n=5 for each strain). The milder reduction of hypoxic mRNA expression in OpnCre$^{(HIF\text{-}\Delta)}$ mice as compared to PrpCre$^{(HIF\text{-}\Delta)}$ mice nicely reflects the different knockdown efficiencies in the two strains.

Normal retinal development and retinal resistance to hypoxia in mice with reduced HIF-1α levels

It has been reported that TAM treatment in patients after breast cancer surgery can very seldom cause mild pathogenic changes in the retina (Heier *et al.* 1994; Tang *et al.* 1997; Bourla *et al.* 2007). On the other hand small dosages of TAM have been shown to promote neuroprotection (Zhang *et al.* 2007; Wakade *et al.* 2008). However, neither TAM nor oil treatment had an obvious effect on retinal morphology in control mice up to 4 months post injections (Fig. 4A). Additionally, oil and TAM treated wild type mice were equally susceptible to light induced retinal degeneration 2 weeks after

TAM application (data not shown) indicating that TAM neither impaired normal retinal morphology nor *per se* protected the retina against a toxic light insult.

Since HIF-1α has been shown to be important to cope with hypoxic conditions in neurons (Vangeison *et al.* 2008) and since the retina becomes borderline hypoxic during dark phases (Cringle *et al.* 2002), we analyzed whether the absence of HIF-1α from photoreceptors in PrpCre$^{(HIF-\Delta)}$ mice during normoxia or hypoxia would be harmful to the retina even without subsequent exposure to damaging light. PrpCre$^{(HIF-wt)}$ and PrpCre$^{(HIF-\Delta)}$ mice were kept in a standard animal facility with a 12:12 hour day-night-cycle for 4 months. During this time no obvious morphological alterations appeared and the retinas of control and knockdown mice were similar (Fig. 4B upper panels). Surprisingly, even a short period of severe hypoxia (6%, 6 h) followed by a recovery period of 4 weeks did not induce any noticable changes in the retina of PrpCre$^{(HIF-\Delta)}$ mice (Fig. 4B lower panels).

During postnatal development HIF-1α is strongly up regulated from PND5 to PND14 (Ozaki *et al.* 1999; Grimm *et al.* 2005). Although excision of a large percentage of floxed sequences by the opsin-driven cre requires several weeks, recombination in OpnCre mice starts already around PND7 (Le *et al.* 2006). We therefore asked whether early loss of HIF-1α in some photoreceptors might influence retinal development. However, we could not observe any changes in the retinal morphology of OpnCre$^{(HIF-\Delta)}$ mice at 6 weeks of age (Fig. 4C). Also retinal susceptibility to light damage seemed to be unimpaired (Fig. 5).

We conclude that photoreceptors can cope with acute (6% oxygen for 6 hours) or mild (normal light-dark-cycle) hypoxic stress in the almost complete absence of their own HIF-1α. We next tested the influence of photoreceptor-specific HIF-1α in a pathological situation by analyzing photoreceptor survival after hypoxic preconditioning and light exposure.

Neuroprotection after hypoxic preconditioning is independent of HIF-1α stabilization in photoreceptor cells

To analyze whether HIF-1α in photoreceptor cells is required to establish the neuroprotective effect of hypoxic preconditioning, we compared light-induced photoreceptor death in hypoxic preconditioned control and knockdown mice. To quantify apoptosis, we measured the release of nucleosomes as indicators of ongoing apoptosis at 36 hours after the toxic light insult (Fig. 5A,B). Non-exposed dark control mice of all strains showed only basal levels of free nucleosomes (Fig. 5A,B). Similarly, retinal morphology was normal (Fig. 5C, upper panels). Normoxic PrpCre$^{(HIF-wt)}$

(P<0.05, F=6.349, df=15, t=2.903, n=3 (control), n=7 (normoxia)) and PrpCre$^{(HIF-\Delta)}$ (P<0.0001, F=264.4, df=12, t=18.18, n=3 (control), n=5 (normoxia)) showed significant cell death when compared to their respective controls. Thus, these mice were susceptible to light damage, as expected (Fig. 5A). Hypoxic preconditioning protected against light-induced apoptosis independently of the presence of HIF-1α in photoreceptors. Cell death in both, light-exposed PrpCre$^{(HIF-wt)}$ (P>0.05, F= 6.349, df=15, t=0.4745, n=3 (control), n=6 (hypoxia)) as well as light-exposed PrpCre$^{(HIF-\Delta)}$ (P>0.05, F=264.4, df=12, t=0.3677, n=3 (control), n=5 (hypoxia)) was not significantly different from dark control. Similar results were obtained with the OpnCre mice. Again, light exposure did not cause significantly elevated levels of free nucleosomes in hypoxic preconditioned OpnCre$^{(HIF-wt)}$ (P>0.05, F=3.541, df=15, t=0.002733, n=3 (control), n=4 (hypoxia)) or OpnCre$^{(HIF-\Delta)}$ (P>0.05, F=2.745, df=13, t=0.008509, n=3 (control), n=4 (hypoxia)) mice as compared to controls (Fig. 5B). These data were morphologically confirmed by the presence of a large number of pycnotic photoreceptor nuclei (Fig. 5C , middle panels, arrowheads) and disintegrated outer and inner segments in light-exposed normoxic wild type and knockdown mice. Hypoxic preconditioning, however, strongly protected retinal morphology against light damage independently of the presence of HIF-1α in photoreceptors. Only few scattered pycnotic nuclei were present leaving the majority of photoreceptor cells unaffected by light exposure (Fig. 5C, lower panels). Analyses of heterozygous HIF-1α knockout mice lacking 50% of total HIF-1α RNA and protein in the retina showed similar results (data not shown).

Although, we successfully deleted HIF-1α from most photoreceptor cells, hypoxic preconditioning still conferred a strong neuroprotective effect rescuing photoreceptors from light damage. This indicates, that protection of visual cells by hypoxic preconditioning does not depend on HIF-1α stabilization in photoreceptors.

Alternative mechanisms for neuroprotection after hypoxic preconditioning

Hypoxia activates several transcription factors in addition to HIF-1α (Kenneth & Rocha 2008) leading to the potential regulation of a variety of HIF-1α independent genes. Here we analyzed selected genes with potential neuroprotective properties, which were found to be differentially regulated during hypoxia in the wild type retina (Thiersch *et al.* 2008). In HIF-1α wild type mice we found a strong, hypoxia-driven induction of the anti-apoptotic gene Bcl2l10 (B-cell lymphoma 2 like 10), of Mt1/2 (metallothionein 1 and 2), Egf (endothelial growth factor) and Epo (erythropoietin) (Fig. 6A, white bars). This induction was not affected in HIF-1α knockdown mice (Fig. 6A,

grey bars). The only exception was Egf, which expression was even slightly induced in hypoxic PrpCre$^{(HIF-\Delta)}$ mice (P=0.0156, F=2.332, t=2.751, df=14, n=8 for each strain). This suggests that these genes might be controlled by transcription factors different from HIF-1. Potential candidates are HIF-2 or STAT3, which were activated by hypoxic exposure in both control and knockdown mice (Fig. 6B). Metal-regulatory transcription factor 1 (Mtf-1), which is strongly expressed in the normoxic and hypoxic retina (supporting information) might be involved in the hypoxic regulation of Mt1 and Mt2 expression (see discussion). The genes not affected by the HIF-1α knockdown included Epo, which was particularly reported to have strong neuroprotective properties (Sakanaka *et al.* 1998; Bernaudin *et al.* 1999; Brines *et al.* 2000; Siren *et al.* 2001; Grimm *et al.* 2002) and to be controlled mainly by HIF-2α (Morita *et al.* 2003; Gruber *et al.* 2007; Rankin *et al.* 2007). Therefore, Epo might function in photoreceptor protection also in the absence of HIF-1α in photoreceptors. In conclusion, the knockdown of HIF-1α in photoreceptors reduced the induction of HIF-1α target genes during hypoxia without affecting the neuroprotective capacity of hypoxic preconditioning. Several genes with neuroprotective potential (e.g. metallothionein 1 and 2; Bcl2l10, Egf; Fig. 6A), which are not affected by the HIF-1α knockdown could potentially participate in the protection of the retina against light induced retinal degeneration.

Discussion

Hypoxic preconditioning is a successful strategy to inhibit tissue degeneration. The reported correlation between HIF-1α stabilization and retinal neuroprotection (Grimm *et al.* 2002; Zhu *et al.* 2007) suggested that the activation of HIF-1α plays an important role in pro-survival mechanisms activated by hypoxic preconditioning. Here we analyzed the impact of the transcription factor HIF-1α on neuroprotection using HIF-1α knockdown mice.

Characterization of photoreceptor specific HIF-1α knockdown mice

Consistent with a previous report (Zhu *et al.* 2007) we found HIF-1α to be expressed and stabilized in all retinal layers during hypoxic preconditioning. To delete HIF-1α predominantly in photoreceptor cells, we employed two different mouse strains expressing Cre recombinase under different promoters. TAM inducible PrpCre deleter mice activate Cre recombinase efficiently and predominantly in photoreceptor cells (Weber *et al.* 2001). In our hands, this strain almost completely deleted HIF-1α in photoreceptors, which was also evidenced by highly reduced HIF-1α target gene transcription after hypoxia. Deletion with the OpnCre line was less effective resulting in

higher HIF-1α levels and less reduced target gene transcription after hypoxia. The knockdown of HIF-1α had no influence on retinal morphology of untreated or hypoxic preconditioned mice. Since different studies showed a correlation of HIF-1α induction and retinal neuroprotection (Grimm *et al.* 2002; Whitlock *et al.* 2005; Zhu *et al.* 2007), we used these mice to analyze the role of HIF-1α in hypoxic preconditioning-mediated protection and survival of photoreceptor cells after exposure to high levels of white light.

HIF-1α in photoreceptor cells is not essential to cope with severe hypoxia or to drive retinal neuroprotection after hypoxic preconditioning

Our experiments show that photoreceptors do not need to express HIF-1α to be protected against light exposure after hypoxic preconditioning. With our approach, however, we cannot exclude the possibility that HIF-1α in cells of the INL and / or GCL might contribute to the protection of photoreceptors through the expression of diffusible factors.

The exact role of HIF-1α in neuronal tissues during severe hypoxia or ischemia is controversial. Two studies with a brain specific deletion of HIF-1α demonstrated somewhat contradictory effects. Whereas Helton (Helton *et al.* 2005) showed that lack of HIF-1α in cortex and hippocampus was rather protective against global ischemia, Baranova (Baranova *et al.* 2007) reported that the reduction of HIF-1α increased the damage after cerebral ischemia. The knockdowns used in these studies differed in the extent of HIF-1α ablation. Baranova used a neuron-specific knockdown, whereas in the mice reported by Helton HIF-1α deletion affected additional cell types, including astrocytes. Of note, a recent report showed that induction of HIF-1α in astrocytes accelerated hypoxia-induced neuronal cell death, whereas an induction of HIF-1α in neurons was beneficial for resistance to severe hypoxia (Vangeison *et al.* 2008).

In contrast to the neuronal HIF-1α deletion in brain, which showed an increased injury after cerebral ischemia (Baranova *et al.* 2007), PrpCre$^{(HIF-\Delta)}$ mice showed no retinal abnormalities after exposure to hypoxia. One explanation for this difference may be that hypoxia is less severe than ischemia/reperfusion. Furthermore, hypoxia allows a substrate exchange and removal of toxic waste products due to the maintained blood flow. Another reason that could explain the retinal resistance to hypoxia is that the retina might have specific mechanisms to deal with low oxygen even in the absence of HIF-1α. The retina is a tissue with a high metabolic rate and becomes borderline hypoxic especially during the night (Cringle *et al.* 2002). The constant exposure to mild

hypoxia during nighttime might activate basic hypoxia-response mechanisms that are not exclusively HIF-1α dependent and that have the potential to protect against severe hypoxia.

Alternative mechanisms for hypoxia induced neuroprotection

Recently, a similar HIF-1α independent protection of brain neurons against cerebral ischemia after hypoxic preconditioning was reported (Baranova *et al.* 2007). In that study HIF-2α was discussed as a possible alternative mechanism to HIF-1α mediated neuroprotection. In the retina, we also found elevated levels of HIF-2α after hypoxia in control and knockdown mice (Fig. 6B). Recently it was shown that HIF-2α and not HIF-1α may regulate the expression of Epo *in vivo* (Morita *et al.* 2003; Gruber *et al.* 2007; Rankin *et al.* 2007) and in cell culture experiments (Chavez *et al.* 2006). In line with these findings, we observed no or only a small decrease in the induction of Epo expression in our knockdown strains after hypoxic preconditioning. Since Epo has proven neuroprotective properties in the brain and the retina (Bernaudin *et al.* 1999; Brines *et al.* 2000; Digicaylioglu & Lipton 2001; Grimm *et al.* 2002; Weishaupt *et al.* 2004), Epo may part of the neuroprotective response in the HIF-1α knockdown strains.

In addition to HIF-2α, other transcription factors like STAT3 and MTF-1 may contribute to the observed protection. STAT3 was strongly phosphorylated after hypoxic preconditioning and is usually connected to anti-apoptotic activities (Stephanou 2004). Recently, Ueki and coworkers suggested a prominent role of STAT3 in LIF-mediated protection of photoreceptors from light induced degeneration (Ueki *et al.* 2008). Mtf-1 controls expression of Mt-1 and Mt-2 (Heuchel *et al.* 1994) which are expressed in all retinal layers (supporting information). Both, Mt-1 and Mt-2 were reported to be upregulated in the hypoxic brain suggesting that expression of these metallothioneins might be part of a general response to hypoxic exposure (Bernaudin *et al.* 2002; Tang *et al.* 2006). Protecting against oxidative stress (Chen *et al.* 2004; Suemori *et al.* 2006; Nachman-Clewner *et al.* 2008), Mt1 and Mt2 may thus participate in the hypoxia-induced resistance against light damage. Interestingly, it has recently been suggested that hypoxic induction of Mt-1 and Mt-2 requires a cooperative interaction between Mtf-1 and HIF-1α (Murphy *et al.* 2008). Since the HIF-1α knockdown did not affect expression of Mt-1 and Mt-2, our results may suggest that Mtf-1 does not strictly depend on HIF-1α but might use alternative factors like HIF-2α for hypoxic gene expression.

In our earlier analysis of the hypoxic transcriptome of the retina (Thiersch *et al.* 2008), we found several additional potential pro-survival factors which have been

connected to cell survival and/or protection of the retina against toxic insults. Among those Bcl2l10 (Song *et al.* 1999), Adm (Garayoa *et al.* 2000; Miyashita *et al.* 2006), Vegf (Jin *et al.* 2000; Nishijima *et al.* 2007) and Egf (Hicks *et al.* 1998) were tested in addition to Epo, Mt1 and Mt2 for their hypoxic regulation in the HIF-1α knockdown retinas. Only the expression of Vegf and Adm was affected in the PrpCre$^{(HIF-\Delta)}$ mouse. However, since both genes encode secreted factors, we cannot exclude that their production in cells of the INL and/or GCL contributed to the protection of photoreceptor cells after hypoxic preconditioning. All of these genes were expressed either independently of HIF-1α or in cell layers where HIF-1α has not been knocked down. Although a detailed investigation of these genes is still needed, these factors are good candidates to play an active role in protecting photoreceptors against light damage.

The cell-type specific deletion of HIF-1α is an excellent tool to address the role and function of HIF-1α exclusively in photoreceptor cells. However, the neuronal retina consists of three cell layers, which form a functional unit with the retinal pigment epithelium. During hypoxia HIF-1α is also strongly stabilized in the GCL and INL where it might drive expression of neuroprotective factors which could directly or indirectly protect photoreceptor cells. Nevertheless, our results demonstrate that photoreceptors do not need to express their own HIF-1α to maintain the structural integrity of the retina despite the borderline hypoxic conditions experienced by retinal cells during each dark period. Photoreceptors do also not need to express and stabilize HIF-1α to survive a toxic light exposure after hypoxic preconditioning. Other factors like HIF-2α, STAT3 and/or Mtf-1 may play a role in photoreceptor protection and it will be of importance to characterize these factors to develop efficient neuroprotective strategies.

Acknowledgements

The authors thank Coni Imsand, Hedwig Wariwoda and Philipp Huber for excellent technical assistance. Randy Johnson, Max Gassmann and Pierre Chambon are acknowledged for kindly providing HIF-1α$^{F/F}$ and PrpCre mice, respectively. This work was supported by the Swiss National Science Foundation (SNF, grant 3100A0-117760), the Fritz-Tobler-Foundation and the European Union (Evi-GenoRet, LSHG-CT-512036).

Abbreviations

Adm adrenomedullin, AMD age-related macular degeneration, Bcl2l10 Bcl2-like 10, Bnip3 BCL2/adenovirus E1B interacting protein 3, CDD cell death detection, CHX10 visual system homeobox 2, Cre cyclization recombinase, DAPI 4',6-diamidino-2-phenylindole, Egf epidermal growth factor, Egln1 EGL nine homolog 1 (C. elegans), Epo erythropoietin, FIH factor inhibiting HIF, GCL ganglion cell layer, Glut1 solute carrier family 2 (facilitated glucose transporter), member 1, Gnat1 transducin, HIF-1/2 hypoxia inducible factor 1/2, HO-1 heme oxygenase (decycling) 1, Hsp27 heat shock protein 27, INL inner nuclear layer, LCM laser capture microdissection, Mt1/2 metallothionein 1/2, MTF-1 metal response element binding transcription factor 1, NGS normal goat serum, NOS nitric oxide synthase, ONL outer nuclear layer, Opn4 melanopsin, PBS phosphate buffered saline, PFA Paraformaldehyde, PHD prolylhydroxylase, PND postnatale day, RP retinitis pigmentosa, RPE retinal pigment epithelium, SDS-PAGE sodium dodecyl sulfate polyacrylamide gel electrophoresis, STAT3 signal transducer and activator of transcription 3, TAM tamoxifen, Vegf vascular endothelial growth factor A, VHL Von Hippel-Lindau disease tumor suppressor

References

Baranova, O., Miranda, L.F., Pichiule, P., Dragatsis, I., Johnson, R.S. & Chavez, J.C. (2007) Neuron-specific inactivation of the hypoxia inducible factor 1 alpha increases brain injury in a mouse model of transient focal cerebral ischemia. *J Neurosci*, **27**, 6320-6332.

Barone, F.C., White, R.F., Spera, P.A., Ellison, J., Currie, R.W., Wang, X. & Feuerstein, G.Z. (1998) Ischemic preconditioning and brain tolerance: temporal histological and functional outcomes, protein synthesis requirement, and interleukin-1 receptor antagonist and early gene expression. *Stroke*, **29**, 1937-1950; discussion 1950-1931.

Bernaudin, M., Marti, H.H., Roussel, S., Divoux, D., Nouvelot, A., MacKenzie, E.T. & Petit, E. (1999) A potential role for erythropoietin in focal permanent cerebral ischemia in mice. *J Cereb Blood Flow Metab*, **19**, 643-651.

Bernaudin, M., Tang, Y., Reilly, M., Petit, E. & Sharp, F.R. (2002) Brain genomic response following hypoxia and re-oxygenation in the neonatal rat. Identification of genes that might contribute to hypoxia-induced ischemic tolerance. *J Biol Chem*, **277**, 39728-39738.

Bourla, D.H., Sarraf, D. & Schwartz, S.D. (2007) Peripheral retinopathy and maculopathy in high-dose tamoxifen therapy. *Am J Ophthalmol*, **144**, 126-128.

Brines, M.L., Ghezzi, P., Keenan, S., Agnello, D., de Lanerolle, N.C., Cerami, C., Itri, L.M. & Cerami, A. (2000) Erythropoietin crosses the blood-brain barrier to protect against experimental brain injury. *Proc Natl Acad Sci U S A*, **97**, 10526-10531.

Bruick, R.K. & McKnight, S.L. (2001) A conserved family of prolyl-4-hydroxylases that modify HIF. *Science*, **294**, 1337-1340.

Bruick, R.K. & McKnight, S.L. (2002) Transcription. Oxygen sensing gets a second wind. *Science*, **295**, 807-808.

Cai, Z., Zhong, H., Bosch-Marce, M., Fox-Talbot, K., Wang, L., Wei, C., Trush, M.A. & Semenza, G.L. (2008) Complete loss of ischaemic preconditioning-induced cardioprotection in mice with partial deficiency of HIF-1 alpha. *Cardiovasc Res*, **77**, 463-470.

Chavez, J.C., Baranova, O., Lin, J. & Pichiule, P. (2006) The transcriptional activator hypoxia inducible factor 2 (HIF-2/EPAS-1) regulates the oxygen-dependent expression of erythropoietin in cortical astrocytes. *J Neurosci*, **26**, 9471-9481.

Chen, L., Wu, W., Dentchev, T., Wong, R. & Dunaief, J.L. (2004) Increased metallothionein in light damaged mouse retinas. *Exp Eye Res*, **79**, 287-293.

Cringle, S.J., Yu, D.Y., Yu, P.K. & Su, E.N. (2002) Intraretinal oxygen consumption in the rat in vivo. *Invest Ophthalmol Vis Sci*, **43**, 1922-1927.

Digicaylioglu, M. & Lipton, S.A. (2001) Erythropoietin-mediated neuroprotection involves cross-talk between Jak2 and NF-kappaB signalling cascades. *Nature*, **412**, 641-647.

Gage, A.T. & Stanton, P.K. (1996) Hypoxia triggers neuroprotective alterations in hippocampal gene expression via a heme-containing sensor. *Brain Res*, **719**, 172-178.

Garayoa, M., Martinez, A., Lee, S., Pio, R., An, W.G., Neckers, L., Trepel, J., Montuenga, L.M., Ryan, H., Johnson, R., Gassmann, M. & Cuttitta, F. (2000) Hypoxia-inducible factor-1 (HIF-1) up-regulates adrenomedullin expression in human tumor cell lines during oxygen deprivation: a possible promotion mechanism of carcinogenesis. *Mol Endocrinol*, **14**, 848-862.

Gidday, J.M., Shah, A.R., Maceren, R.G., Wang, Q., Pelligrino, D.A., Holtzman, D.M. & Park, T.S. (1999) Nitric oxide mediates cerebral ischemic tolerance in a neonatal rat model of hypoxic preconditioning. *J Cereb Blood Flow Metab*, **19**, 331-340.

Grimm, C., Hermann, D.M., Bogdanova, A., Hotop, S., Kilic, U., Wenzel, A., Kilic, E. & Gassmann, M. (2005) Neuroprotection by hypoxic preconditioning: HIF-1 and erythropoietin protect from retinal degeneration. *Semin Cell Dev Biol*, **16**, 531-538.

Grimm, C., Wenzel, A., Groszer, M., Mayser, H., Seeliger, M., Samardzija, M., Bauer, C., Gassmann, M. & Reme, C.E. (2002) HIF-1-induced erythropoietin in the hypoxic retina protects against light-induced retinal degeneration. *Nat Med*, **8**, 718-724.

Gruber, M., Hu, C.J., Johnson, R.S., Brown, E.J., Keith, B. & Simon, M.C. (2007) Acute postnatal ablation of Hif-2alpha results in anemia. *Proc Natl Acad Sci U S A*, **104**, 2301-2306.

Heier, J.S., Dragoo, R.A., Enzenauer, R.W. & Waterhouse, W.J. (1994) Screening for ocular toxicity in asymptomatic patients treated with tamoxifen. *Am J Ophthalmol*, **117**, 772-775.

Helton, R., Cui, J., Scheel, J.R., Ellison, J.A., Ames, C., Gibson, C., Blouw, B., Ouyang, L., Dragatsis, I., Zeitlin, S., Johnson, R.S., Lipton, S.A. & Barlow, C. (2005) Brain-specific knock-out of hypoxia-inducible factor-1alpha reduces rather than increases hypoxic-ischemic damage. *J Neurosci*, **25**, 4099-4107.

Heuchel, R., Radtke, F., Georgiev, O., Stark, G., Aguet, M. & Schaffner, W. (1994) The transcription factor MTF-1 is essential for basal and heavy metal-induced metallothionein gene expression. *Embo J*, **13**, 2870-2875.

Hicks, D., Heidinger, V., Mohand-Said, S., Sahel, J. & Dreyfus, H. (1998) Growth factors and gangliosides as neuroprotective agents in excitotoxicity and ischemia. *Gen Pharmacol*, **30**, 265-273.

Hill, P., Shukla, D., Tran, M.G., Aragones, J., Cook, H.T., Carmeliet, P. & Maxwell, P.H. (2008) Inhibition of hypoxia inducible factor hydroxylases protects against renal ischemia-reperfusion injury. *J Am Soc Nephrol*, **19**, 39-46.

Huang, L.E., Gu, J., Schau, M. & Bunn, H.F. (1998) Regulation of hypoxia-inducible factor 1alpha is mediated by an O2-dependent degradation domain via the ubiquitin-proteasome pathway. *Proc Natl Acad Sci U S A*, **95**, 7987-7992.

Ivan, M., Kondo, K., Yang, H., Kim, W., Valiando, J., Ohh, M., Salic, A., Asara, J.M., Lane, W.S. & Kaelin, W.G., Jr. (2001) HIFalpha targeted for VHL-mediated destruction by proline hydroxylation: implications for O2 sensing. *Science*, **292**, 464-468.

Jaakkola, P., Mole, D.R., Tian, Y.M., Wilson, M.I., Gielbert, J., Gaskell, S.J., Kriegsheim, A., Hebestreit, H.F., Mukherji, M., Schofield, C.J., Maxwell, P.H.,

Pugh, C.W. & Ratcliffe, P.J. (2001) Targeting of HIF-alpha to the von Hippel-Lindau ubiquitylation complex by O2-regulated prolyl hydroxylation. *Science*, **292**, 468-472.

Jin, K.L., Mao, X.O. & Greenberg, D.A. (2000) Vascular endothelial growth factor: direct neuroprotective effect in in vitro ischemia. *Proc Natl Acad Sci U S A*, **97**, 10242-10247.

Kaur, C., Sivakumar, V. & Foulds, W.S. (2006) Early response of neurons and glial cells to hypoxia in the retina. *Invest Ophthalmol Vis Sci*, **47**, 1126-1141.

Kenneth, N.S. & Rocha, S. (2008) Regulation of gene expression by hypoxia. *Biochem J*, **414**, 19-29.

Le, Y.Z., Zheng, L., Zheng, W., Ash, J.D., Agbaga, M.P., Zhu, M. & Anderson, R.E. (2006) Mouse opsin promoter-directed Cre recombinase expression in transgenic mice. *Mol Vis*, **12**, 389-398.

Mahon, P.C., Hirota, K. & Semenza, G.L. (2001) FIH-1: a novel protein that interacts with HIF-1alpha and VHL to mediate repression of HIF-1 transcriptional activity. *Genes Dev*, **15**, 2675-2686.

Miyashita, K., Itoh, H., Arai, H., Suganami, T., Sawada, N., Fukunaga, Y., Sone, M., Yamahara, K., Yurugi-Kobayashi, T., Park, K., Oyamada, N., Sawada, N., Taura, D., Tsujimoto, H., Chao, T.H., Tamura, N., Mukoyama, M. & Nakao, K. (2006) The neuroprotective and vasculo-neuro-regenerative roles of adrenomedullin in ischemic brain and its therapeutic potential. *Endocrinology*, **147**, 1642-1653.

Morita, M., Ohneda, O., Yamashita, T., Takahashi, S., Suzuki, N., Nakajima, O., Kawauchi, S., Ema, M., Shibahara, S., Udono, T., Tomita, K., Tamai, M., Sogawa, K., Yamamoto, M. & Fujii-Kuriyama, Y. (2003) HLF/HIF-2alpha is a key factor in retinopathy of prematurity in association with erythropoietin. *Embo J*, **22**, 1134-1146.

Murphy, B.J., Kimura, T., Sato, B.G., Shi, Y. & Andrews, G.K. (2008) Metallothionein induction by hypoxia involves cooperative interactions between metal-responsive transcription factor-1 and hypoxia-inducible transcription factor-1alpha. *Mol Cancer Res*, **6**, 483-490.

Nachman-Clewner, M., Giblin, F.J., Dorey, C.K., Blanks, R.H., Dang, L., Dougherty, C.J. & Blanks, J.C. (2008) Selective degeneration of central photoreceptors after hyperbaric oxygen in normal and metallothionein-knockout mice. *Invest Ophthalmol Vis Sci*, **49**, 3207-3215.

Nishijima, K., Ng, Y.S., Zhong, L., Bradley, J., Schubert, W., Jo, N., Akita, J., Samuelsson, S.J., Robinson, G.S., Adamis, A.P. & Shima, D.T. (2007) Vascular endothelial growth factor-A is a survival factor for retinal neurons and a critical neuroprotectant during the adaptive response to ischemic injury. *Am J Pathol*, **171**, 53-67.

Ozaki, H., Yu, A.Y., Della, N., Ozaki, K., Luna, J.D., Yamada, H., Hackett, S.F., Okamoto, N., Zack, D.J., Semenza, G.L. & Campochiaro, P.A. (1999) Hypoxia inducible factor-1alpha is increased in ischemic retina: temporal and spatial correlation with VEGF expression. *Invest Ophthalmol Vis Sci*, **40**, 182-189.

Ran, R., Xu, H., Lu, A., Bernaudin, M. & Sharp, F.R. (2005) Hypoxia preconditioning in the brain. *Dev Neurosci*, **27**, 87-92.

Rankin, E.B., Biju, M.P., Liu, Q., Unger, T.L., Rha, J., Johnson, R.S., Simon, M.C., Keith, B. & Haase, V.H. (2007) Hypoxia-inducible factor-2 (HIF-2) regulates hepatic erythropoietin in vivo. *J Clin Invest*, **117**, 1068-1077.

Rosenberger, C., Rosen, S., Shina, A., Frei, U., Eckardt, K.U., Flippin, L.A., Arend, M., Klaus, S.J. & Heyman, S.N. (2008) Activation of hypoxia inducible factors (HIF) ameliorates hypoxic distal tubular injury in the isolated perfused rat kidney. *Nephrol Dial Transplant*.

Roth, S., Li, B., Rosenbaum, P.S., Gupta, H., Goldstein, I.M., Maxwell, K.M. & Gidday, J.M. (1998) Preconditioning provides complete protection against retinal ischemic injury in rats. *Invest Ophthalmol Vis Sci*, **39**, 777-785.

Ryan, H.E., Poloni, M., McNulty, W., Elson, D., Gassmann, M., Arbeit, J.M. & Johnson, R.S. (2000) Hypoxia-inducible factor-1alpha is a positive factor in solid tumor growth. *Cancer Res*, **60**, 4010-4015.

Sakanaka, M., Wen, T.C., Matsuda, S., Masuda, S., Morishita, E., Nagao, M. & Sasaki, R. (1998) In vivo evidence that erythropoietin protects neurons from ischemic damage. *Proc Natl Acad Sci U S A*, **95**, 4635-4640.

Salceda, S. & Caro, J. (1997) Hypoxia-inducible factor 1alpha (HIF-1alpha) protein is rapidly degraded by the ubiquitin-proteasome system under normoxic conditions. Its stabilization by hypoxia depends on redox-induced changes. *J Biol Chem*, **272**, 22642-22647.

Samardzija, M., Wenzel, A., Aufenberg, S., Thiersch, M., Reme, C. & Grimm, C. (2006) Differential role of Jak-STAT signaling in retinal degenerations. *Faseb J*, **20**, 2411-2413.

Sharp, F.R., Ran, R., Lu, A., Tang, Y., Strauss, K.I., Glass, T., Ardizzone, T. & Bernaudin, M. (2004) Hypoxic preconditioning protects against ischemic brain injury. *NeuroRx*, **1**, 26-35.

Siddiq, A., Ayoub, I.A., Chavez, J.C., Aminova, L., Shah, S., LaManna, J.C., Patton, S.M., Connor, J.R., Cherny, R.A., Volitakis, I., Bush, A.I., Langsetmo, I., Seeley, T., Gunzler, V. & Ratan, R.R. (2005) Hypoxia-inducible factor prolyl 4-hydroxylase inhibition. A target for neuroprotection in the central nervous system. *J Biol Chem*, **280**, 41732-41743.

Siren, A.L., Fratelli, M., Brines, M., Goemans, C., Casagrande, S., Lewczuk, P., Keenan, S., Gleiter, C., Pasquali, C., Capobianco, A., Mennini, T., Heumann, R., Cerami, A., Ehrenreich, H. & Ghezzi, P. (2001) Erythropoietin prevents neuronal apoptosis after cerebral ischemia and metabolic stress. *Proc Natl Acad Sci U S A*, **98**, 4044-4049.

Song, Q., Kuang, Y., Dixit, V.M. & Vincenz, C. (1999) Boo, a novel negative regulator of cell death, interacts with Apaf-1. *Embo J*, **18**, 167-178.

Stephanou, A. (2004) Role of STAT-1 and STAT-3 in ischaemia/reperfusion injury. *J Cell Mol Med*, **8**, 519-525.

Suemori, S., Shimazawa, M., Kawase, K., Satoh, M., Nagase, H., Yamamoto, T. & Hara, H. (2006) Metallothionein, an endogenous antioxidant, protects against retinal neuron damage in mice. *Invest Ophthalmol Vis Sci*, **47**, 3975-3982.

Tanaka, H., Calderone, A., Jover, T., Grooms, S.Y., Yokota, H., Zukin, R.S. & Bennett, M.V. (2002) Ischemic preconditioning acts upstream of GluR2 down-regulation to afford neuroprotection in the hippocampal CA1. *Proc Natl Acad Sci U S A*, **99**, 2362-2367.

Tang, R., Shields, J., Schiffman, J., Li, H., Locher, D., Hampton, J., Prager, T. & Pardo, G. (1997) Retinal changes associated with tamoxifen treatment for breast cancer. *Eye*, **11 (Pt 3)**, 295-297.

Tang, Y., Pacary, E., Freret, T., Divoux, D., Petit, E., Schumann-Bard, P. & Bernaudin, M. (2006) Effect of hypoxic preconditioning on brain genomic response before and following ischemia in the adult mouse: identification of potential neuroprotective candidates for stroke. *Neurobiol Dis*, **21**, 18-28.

Thiersch, M., Raffelsberger, W., Frigg, R., Samardzija, M., Wenzel, A., Poch, O. & Grimm, C. (2008) Analysis of the retinal gene expression profile after hypoxic preconditioning identifies candidate genes for neuroprotection. *BMC Genomics*, **9**, 73.

Ueki, Y., Wang, J., Chollangi, S. & Ash, J.D. (2008) STAT3 activation in photoreceptors by leukemia inhibitory factor is associated with protection from light damage. *J Neurochem*, **105**, 784-796.

Vangeison, G., Carr, D., Federoff, H.J. & Rempe, D.A. (2008) The good, the bad, and the cell type-specific roles of hypoxia inducible factor-1 alpha in neurons and astrocytes. *J Neurosci*, **28**, 1988-1993.

Wakade, C., Khan, M.M., De Sevilla, L.M., Zhang, Q.G., Mahesh, V.B. & Brann, D.W. (2008) Tamoxifen neuroprotection in cerebral ischemia involves attenuation of kinase activation and superoxide production and potentiation of mitochondrial superoxide dismutase. *Endocrinology*, **149**, 367-379.

Wang, G.L. & Semenza, G.L. (1993) Characterization of hypoxia-inducible factor 1 and regulation of DNA binding activity by hypoxia. *J Biol Chem*, **268**, 21513-21518.

Wang, G.L. & Semenza, G.L. (1995) Purification and characterization of hypoxia-inducible factor 1. *J Biol Chem*, **270**, 1230-1237.

Weber, P., Metzger, D. & Chambon, P. (2001) Temporally controlled targeted somatic mutagenesis in the mouse brain. *Eur J Neurosci*, **14**, 1777-1783.

Weishaupt, J.H., Rohde, G., Polking, E., Siren, A.L., Ehrenreich, H. & Bahr, M. (2004) Effect of erythropoietin axotomy-induced apoptosis in rat retinal ganglion cells. *Invest Ophthalmol Vis Sci*, **45**, 1514-1522.

Wenzel, A., Grimm, C., Samardzija, M. & Reme, C.E. (2003) The genetic modifier Rpe65Leu(450): effect on light damage susceptibility in c-Fos-deficient mice. *Invest Ophthalmol Vis Sci*, **44**, 2798-2802.

Wenzel, A., Grimm, C., Samardzija, M. & Reme, C.E. (2005) Molecular mechanisms of light-induced photoreceptor apoptosis and neuroprotection for retinal degeneration. *Prog Retin Eye Res*, **24**, 275-306.

Whitlock, N.A., Agarwal, N., Ma, J.X. & Crosson, C.E. (2005) Hsp27 upregulation by HIF-1 signaling offers protection against retinal ischemia in rats. *Invest Ophthalmol Vis Sci*, **46**, 1092-1098.

Zhang, C., Rosenbaum, D.M., Shaikh, A.R., Li, Q., Rosenbaum, P.S., Pelham, D.J. & Roth, S. (2002) Ischemic preconditioning attenuates apoptotic cell death in the rat retina. *Invest Ophthalmol Vis Sci*, **43**, 3059-3066.

Zhang, Y., Milatovic, D., Aschner, M., Feustel, P.J. & Kimelberg, H.K. (2007) Neuroprotection by tamoxifen in focal cerebral ischemia is not mediated by an agonist action at estrogen receptors but is associated with antioxidant activity. *Exp Neurol*, **204**, 819-827.

Zhu, Y., Zhang, Y., Ojwang, B.A., Brantley, M.A., Jr. & Gidday, J.M. (2007) Long-term tolerance to retinal ischemia by repetitive hypoxic preconditioning: role of HIF-1alpha and heme oxygenase-1. *Invest Ophthalmol Vis Sci*, **48**, 1735-1743.

Tables

Table 1 ***Primer pairs used for PCR.***

Gene	Primer forward	Primer reverse	Product bp
β-Actin	CAACGGCTCCGGCATGTGC	CTCTTGCTCTGGGCCTCG	153
Adm	TTCGCAGTTCCGAAAGAAGT	GGTAGCTGCTGGATGCTTGTA	77
Bcl2l10	GAACTTTCTGTATAATCTGCTCATGG	TGAAGAAGCGGCAAAAGC	89
Bnip3	CCTGTCGCAGTTGGGTTC	GAAGTGCAGTTCTACCCAGGAG	93
Chx10	CCAGAAGACAGGATACAGGTG	GGCTCCATAGAGACCATACT	111
Egf	CATGCCCCACAGGATTTG	GGGCAGGAAACAAGTTCGT	64
Egln1	CATTGTTGGCAGAAGGTGTG	CAAAGGACTACAGGGTCTCCA	70
Epo	GCCCTGCTAGCCAATTCC	GGCGACATCAATTCCTTCTG	128
Glut1	ATGGATCCCAGCAGCAAG	CCAGTGTTATAGCCGAACTGC	92
Gnat1	GAGGATGCTGAGAAGGATGC	TGAATGTTGAGCGTGGTCAT	209
HIF-1α	TCATCAGTTGCCACTTCCCCAC	CCGTCATCTGTTAGCACCATCAC	198
HIF-2α	GGAGCTCAAAAGGTGTCAGG	CAGGTAAGGCTCGAACGATG	61
Mt1	GAATGGACCCCAACTGCTC	GCAGCAGCTCTTCTTGCAG	104
Mt2	TCTTCAAACCGATCTCTCGTCG	CAGCAGCTTTTCTTGCAGGAAG	94
Opn4	CCAGCTTCACAACCAGTCCT	CAGCCTGATGTGCAGATGTC	111
Vegf	ACTTGTGTTGGGAGGAGGATGTC	AATGGGTTTGTCGTGTTTCTGG	171

Figure legends

Fig. 1. Distribution of HIF-1α mRNA and protein in the retina.

A) HIF-1α and HIF-2α mRNA expression in the ONL, INL and GCL isolated by laser capture microdissection (LCM). Captured fragments of 3 mice were pooled and analyzed by conventional RT-PCR. HIF-1α and HIF-2α expression was observed in all retinal cell layers. Gnat1 (ONL marker), Chx10 (INL marker) and Opn4 (GCL marker) served as indicators for the purity of the isolated tissue fragments (note that minor cross-contaminations were detected). Total retinal RNA was used as positive control. **B)** Protein distribution of HIF-1α in the retina of normoxic mice and immediately after hypoxia (6% O_2; 6 h). Immunofluorescence staining indicates stable HIF-1α protein in the GCL during normoxia and the stabilization of HIF-1α protein in the whole retina during hypoxia. As a negative control served a normoxic retina, incubated with the secondary antibody (Cy3 anti-rabbit) alone.

ONL: outer nuclear layer; INL: inner nuclear layer; GCL: ganglion cell layer; Scale bar: 25 µm

Fig. 2. Efficiency of HIF-1α knockdown in the ONL.

Gene and protein expression was analyzed in mice held in normoxia or in mice immediately after exposure to hypoxia (6% O_2; 6 h) **A)** Total retinal levels of HIF-1α mRNA was analyzed by real time PCR in Opsin-cre (left panel) and Prp-cre (right panel) mediated HIF-1α knockdowns (grey bars) and compared to their respective wild type controls (white bars). β-actin served as reference and data were normalized to levels of normoxic $Cre^{(HIF\text{-}wt)}$ mice (first bar of each panel). Under normoxic conditions $OpnCre^{(HIF\text{-}\Delta)}$ mice displayed HIF-1α mRNA levels which were significantly (*, *P*=0.0193, *n*=5) reduced by 50%. After hypoxia no significant (*P*=0.117, *n*=5) differences were detectable. HIF-1α deletion in $PrpCre^{(HIF\text{-}\Delta)}$ mice was very efficient and significantly reduced expression of HIF-1α to 35% of control levels under both normoxic (***, *P*=0.0003, *n*=8) and hypoxic (***, *P*=0.0001, *n*=8) conditions. Given are means ± SD. Statistical validations were performed using unpaired, two-tailed t-tests. **B)** HIF-1α RNA expression in normoxic $PrpCre^{(HIF\text{-}\Delta)}$ (grey bars) mice compared to normoxic $PrpCre^{(HIF\text{-}wt)}$ (white bar) mice in ONL, INL and GCL after LCM. For each retinal layer, tissue was pooled from three individual mice. β-Actin expression served as reference and data were normalized to expression levels of $PrpCre^{(HIF\text{-}wt)}$ in each individual layer (set to 1). HIF-1α RNA expression was 20-fold reduced in the ONL of $PrpCre^{(HIF\text{-}\Delta)}$ mice but only 2-fold in INL and GCL. Shown are mean values ± SD of *n*=3. **C)** Western blot analysis of retinal HIF-1α protein expression in normoxic and hypoxic HIF-1α knockdown and wild type mice as indicated. Only faint protein bands were observed under normoxic conditions. After hypoxia, HIF-1α protein expression was increased in retinas of control $OpnCre^{(HIF\text{-}wt)}$ and $PrpCre^{(HIF\text{-}wt)}$ mice. In hypoxic $OpnCre^{(HIF\text{-}\Delta)}$ mice HIF-1α protein levels were only slightly diminished but hypoxic $PrpCre^{(HIF\text{-}\Delta)}$ mice showed severely reduced HIF-1α protein expression. Shown are representative blots of *n*=4.

LCM: laser capture microdissection, other abbreviations as in Figure 1.

Fig. 3. Expression of HIF-1α target genes in total retina.

mRNA levels of HIF-1α target genes were determined immediately after hypoxia or in normoxic controls in total retinal RNA. mRNA expression in $OpnCre^{(HIF\text{-}\Delta)}$ and $PrpCre^{(HIF\text{-}\Delta)}$ mice (grey bars) were compared to $OpnCre^{(HIF\text{-}wt)}$ and $PrpCre^{(HIF\text{-}wt)}$ control mice (white bars). Expression levels of normoxic (N) $Cre^{(HIF\text{-}wt)}$ mice (first bars) were set to "1". β-actin expression served as reference. Expression levels in normoxic $Cre^{(HIF\text{-}wt)}$ and $Cre^{(HIF\text{-}\Delta)}$ mice were comparable. During hypoxia (H) all tested HIF-1α target genes

were induced in control mice. In hypoxic PrpCre$^{(HIF-\Delta)}$ mice the induction of all tested HIF-1α target genes was significantly repressed (***P≤0.0002; **P=0.0011; n=5). Hypoxic OpnCre$^{(HIF-\Delta)}$ mice showed a milder effect and reached significance only for Egln1 (**P=0.0072, n=5) and Glut1 (*P=0.0362, n=5). Shown are means ± SD. Statistical validations were performed using unpaired, two-tailed t-tests.

Fig. 4. Intraperitoneal TAM application and the ablation of HIF-1α in photoreceptor cells has no effect on the retina of normoxic and hypoxic mice.

A) Mice, carrying the floxed exon 2 of HIF-1α without Cre (HIF-1α$^{F/F}$), were intraperitoneally injected with oil or tamoxifen (TAM) as indicated. The treatment did not result in any morphological alterations up to 4 months post-application. **B)** PrpCre-mediated knockdown of HIF-1α did not affect retinal morphology in normoxic mice or after 6 hours of hypoxia (6% O_2). Shown are representative panels of control (PrpCre$^{(HIF-wt)}$) and knockdown (PrpCre$^{(HIF-\Delta)}$) mice kept in normoxia for 4 months after treatment (upper panels) or of mice at 4 weeks after exposure to hypoxia (lower panels).

C) An early but moderate deletion of HIF-1α during development did not interfere with retinal development and mice showed normal retinal morphology at 6 weeks of age. ROS: rod outer segments, RIS: rod inner segments. Other abbreviations as in Figure 1; Scale bar: 25 µm

Fig. 5. Role of HIF-1α in retinal neuroprotection.

Normoxic or hypoxic-pretreated mice were exposed to 13‘000 lux for 2 h and analyzed after 36 h. Dark-adapted, normoxic mice served as negative controls.

A) Relative nucleosomal release was measured as an indicator for apoptotic processes in the retina. Values are expressed relative to PrpCre$^{(HIF-wt)}$ mice, which were set to “1”. Both, normoxic PrpCre$^{(HIF-wt)}$ and normoxic PrpCre$^{(HIF-\Delta)}$ mice were susceptible (*P<0.05, ***P<0.001; n=3 for dark control, n=7 for normoxic PrpCre$^{(HIF-wt)}$ mice, n= 5 for normoxic PrpCre$^{(HIF-\Delta)}$ mice, one-way ANOVA with Bonferroni posttest) to light damage as indicated by the increased release of nucleosomes (grey bars). Hypoxic preconditioned PrpCre$^{(HIF-\Delta)}$ mice showed no increased apoptosis after light exposure. (n.s., P>0.05, n=3 for dark control, n=6 for hypoxic PrpCre$^{(HIF-wt)}$ mice, n= 5 for hypoxic PrpCre$^{(HIF-\Delta)}$ mice, one-way ANOVA with Bonferroni posttest). **B)** OpnCre mice were analyzed as in A. Hypoxic preconditioning resulted in full protection of OpnCre$^{(HIF-wt)}$ and OpnCre$^{(HIF-\Delta)}$ mice (white bars) with no increased cell death as compared to controls (n.s., P>0.05, n=3 for dark control, n=4 for hypoxic OpnCre$^{(HIF-wt)}$

mice, *n*= 4 for hypoxic OpnCre$^{(HIF-\Delta)}$ mice, one-way ANOVA with Bonferroni posttest) **C)** Retinal morphology after light exposure. Dark controls (upper panels) showed normal retinal structure before light exposure. Normoxic PrpCre$^{(HIF-wt)}$, PrpCre$^{(HIF-\Delta)}$ and OpnCre$^{(HIF-\Delta)}$ mice exposed to light (middle panels) showed severe degeneration of photoreceptor cells as indicated by the presence of pycnotic nuclei (arrowheads) and the complete disruption of inner and outer segments. All hypoxic preconditioned mice (lower panel) were strongly protected against light damage.

Shown are means ± SD; number of samples (*n*) are indicated above. Abbreviations as in Figures 1 and 4; Scale Bar 25 µm.

Fig. 6. Hypoxia-mediated upregulation of pro-survival genes and transcription factors in retinas of HIF-1α knockdown retinas.

Mice were (H) or were not (N) exposed to hypoxia and mRNA or protein expression was analyzed immediately after hypoxia.

A) Expression of selected potential pro-survival genes analyzed by real time PCR. Expression levels of normoxic (N) Cre$^{(HIF-wt)}$ mice of each strain were set to "1" (first bar). β-actin served as reference. Expression levels of normoxic Cre$^{(HIF-wt)}$ and Cre$^{(HIF-\Delta)}$ mice were comparable. All genes were strongly induced after hypoxia (H) in control mice as well as in PrpCre$^{(HIF-\Delta)}$ and OpnCre$^{(HIF-\Delta)}$ mice with only slight differences (*, *P*=0.0156, *n*=8; unpaired, two-tailed t-tests). Shown are means ± SD of n=8 (PrpCre strains) or of n=5 (OpnCre strains). **B)** Protein extracts were analyzed by Western blotting. A comparable induction of HIF-2α and pSTAT3 in OpnCre$^{(HIF-\Delta)}$ and PrpCre$^{(HIF-\Delta)}$ mice as well as in OpnCre$^{(HIF-wt)}$ and PrpCre$^{(HIF-\Delta)}$ control mice was observed in hypoxic pretreated mice. β-actin and STAT3 were used as loading controls. Shown are representative blots of n=4.

Figures

Fig.1

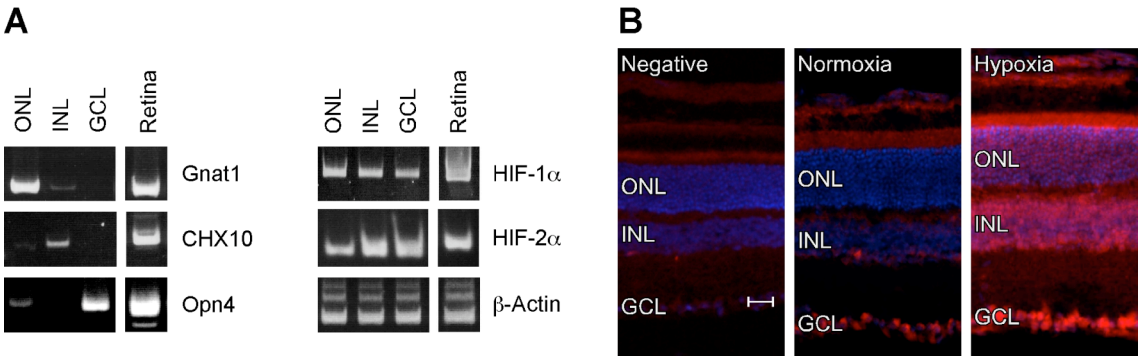

Fig.2

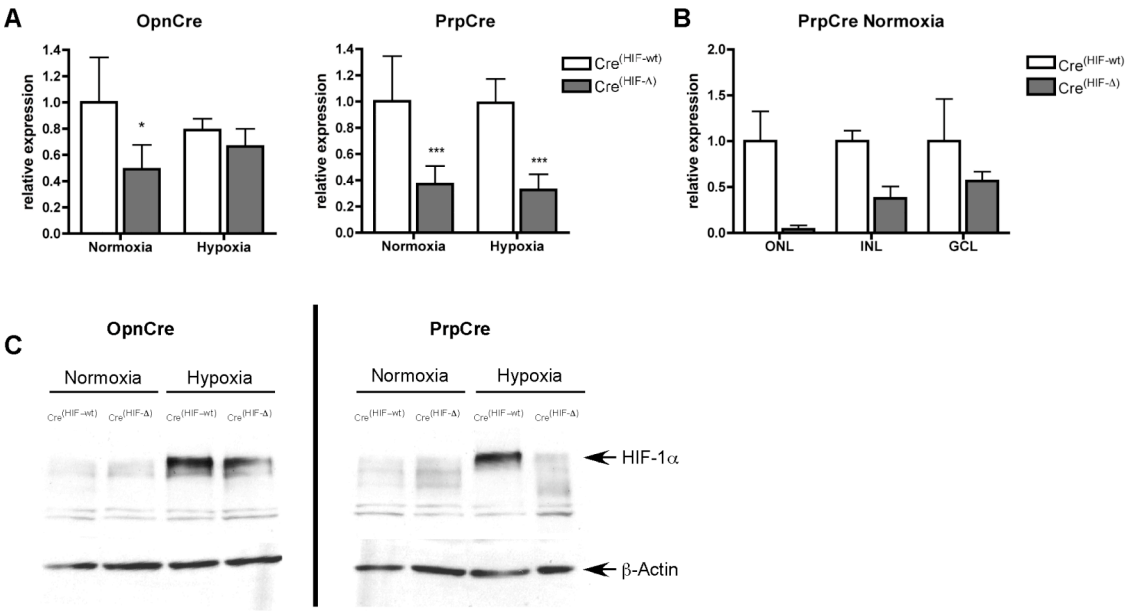
A
OpnCre
PrpCre
relative expression
Normoxia
Hypoxia
Cre(HIF-wt)
Cre(HIF-Δ)
B
PrpCre Normoxia
ONL
INL
GCL
C
OpnCre
PrpCre
HIF-1α
β-Actin

Fig.3

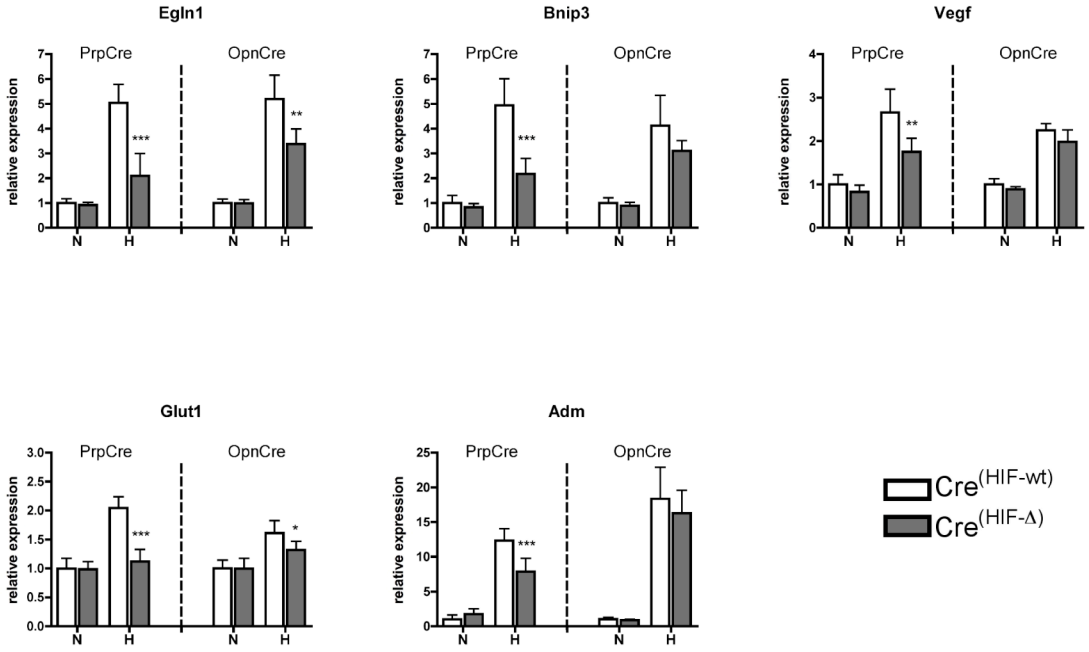
Egln1
Bnip3
Vegf
Glut1
Adm
PrpCre
OpnCre
relative expression
N
H
***
**
*
Cre(HIF-wt)
Cre(HIF-Δ)

Fig.4

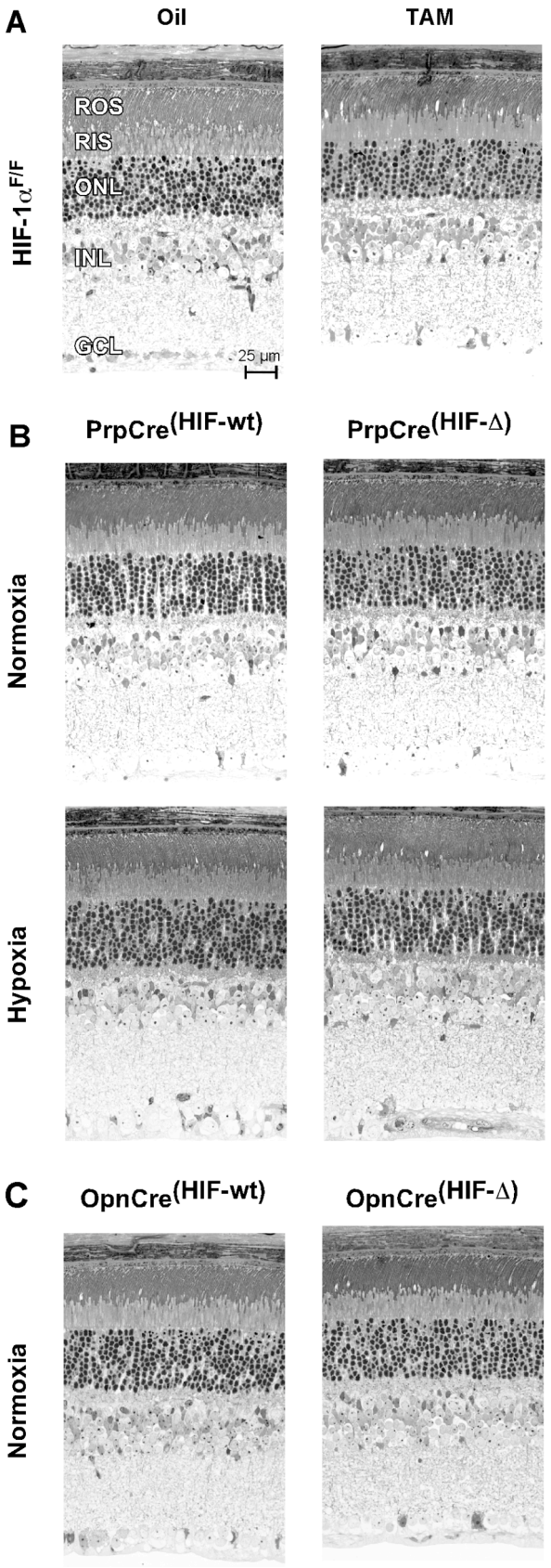
A
Oil
TAM
HIF-1α F/F
ROS
RIS
ONL
INL
GCL
25 µm
B
PrpCre(HIF-wt)
PrpCre(HIF-Δ)
Normoxia
Hypoxia
C
OpnCre(HIF-wt)
OpnCre(HIF-Δ)
Normoxia

Fig.5

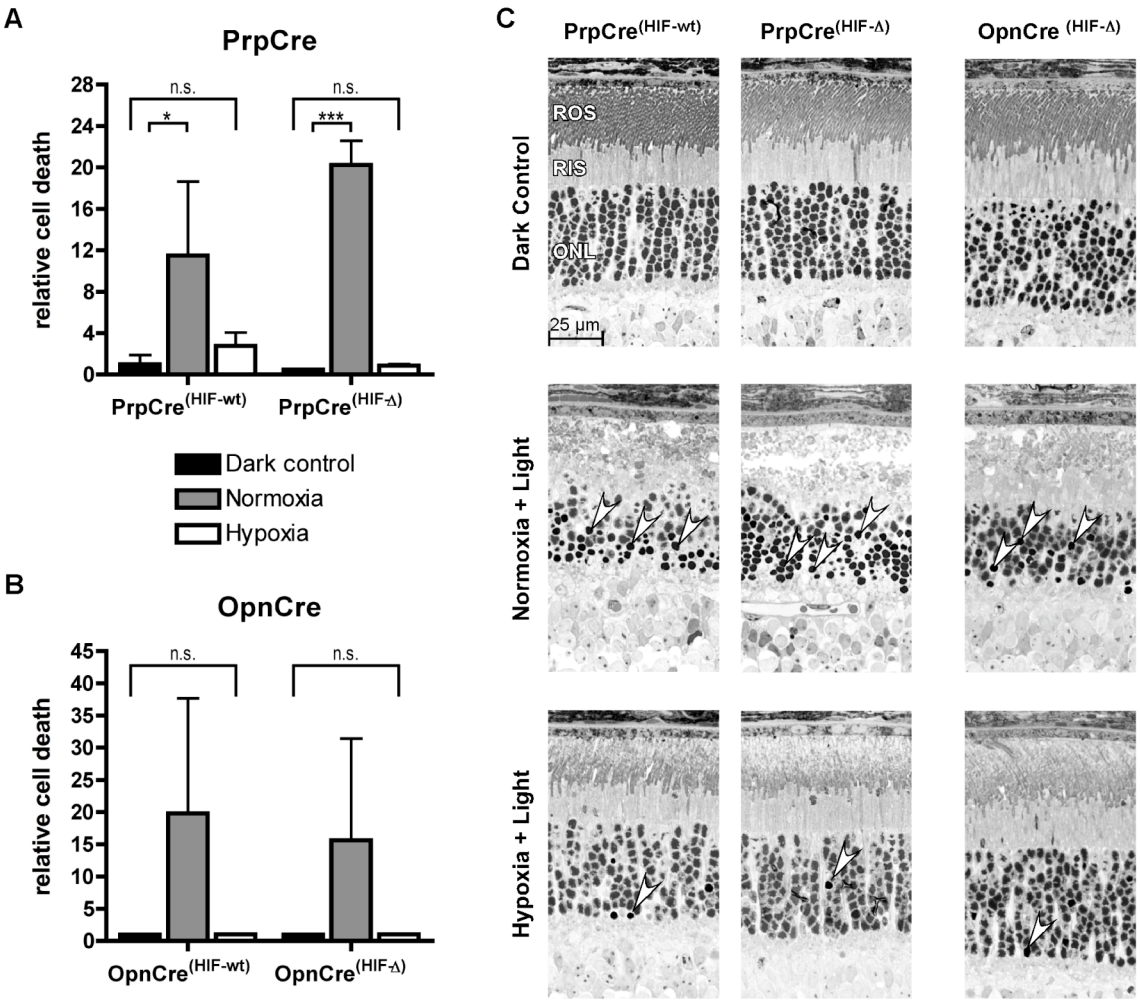
A
PrpCre
relative cell death
28
24
20
16
12
8
4
0
n.s.
*
n.s.
***
PrpCre(HIF-wt)
PrpCre(HIF-Δ)
Dark control
Normoxia
Hypoxia
B
OpnCre
relative cell death
45
40
35
30
25
20
15
10
5
0
n.s.
n.s.
OpnCre(HIF-wt)
OpnCre(HIF-Δ)
C
PrpCre(HIF-wt)
PrpCre(HIF-Δ)
OpnCre (HIF-Δ)
Dark Control
Normoxia + Light
Hypoxia + Light
ROS
RIS
ONL
25 µm

Fig.6

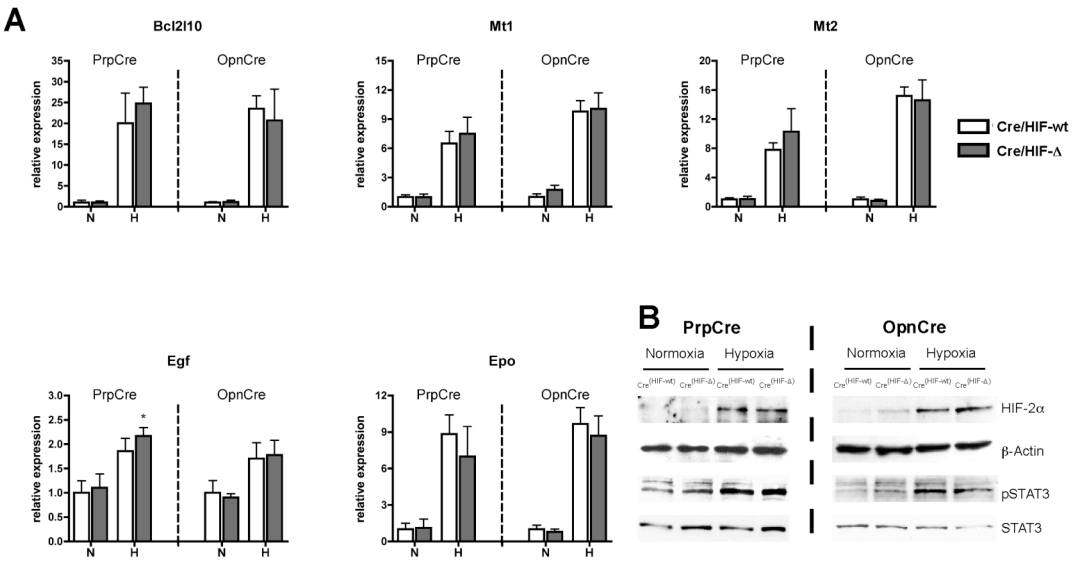
A
Bcl2l10
Mt1
Mt2
Egf
Epo
PrpCre
OpnCre
relative expression
N
H
Cre/HIF-wt
Cre/HIF-Δ
B
PrpCre
OpnCre
Normoxia
Hypoxia
HIF-2α
β-Actin
pSTAT3
STAT3

3.2.1 Supplemental Data for accepted manuscript Thiersch et. al (EJN)

3.2.1.1 Supporting information MTF-1

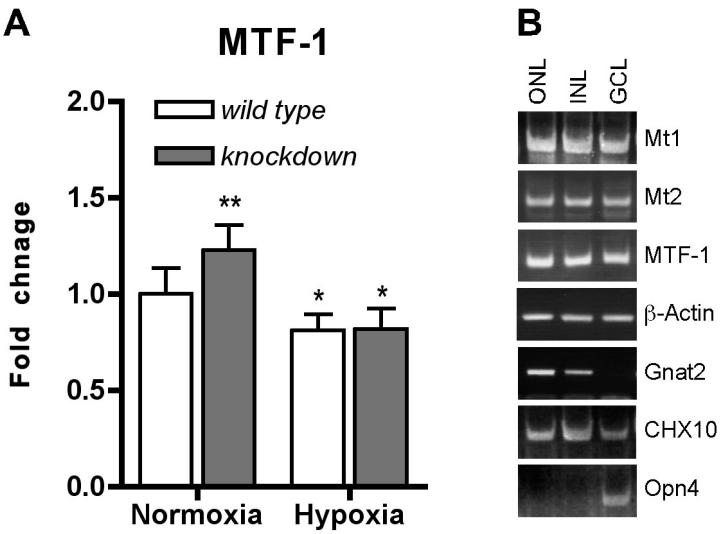

Retinal expression of MTF-1.

A) Expression of MTF-1 was analyzed in retinas of normoxic and hypoxic PrpCre$^{(HIF\text{-}wt)}$ (white bars) and PrpCre$^{(HIF\text{-}\Delta)}$ (grey bars) mice by semi quantitative real-time PCR. Expression levels of normoxic PrpCre$^{(HIF\text{-}wt)}$ mice were set to "1" and β-actin served as reference. The level of MTF-1 expression in PrpCre$^{(HIF\text{-}\Delta)}$ mice was slightly elevated in normoxia (**P<0.01, t=3.884, df=3, n=8). Hypoxia slightly reduced expression of MTF-1 in wild types (*P<0.05, t=3.301, df=3, n=8) and knockdowns (*P<0.05, t=3.172, df=3, n=8) compared to normoxic wild type control mice. Statistical analysis was done using one-way ANOVA (F=22.91, total df=31) with Bonferroni posttests for the comparison between groups.

B) Expression of Mt1, Mt2 and MTF-1 in the different retinal layers of the normoxic mouse retina. Laser capture microdissection was used to isolate the outer nuclear layer (ONL), the inner nuclear layer (INL) and the ganglion cell layer (GCL). RNA was isolated and cDNA prepared (see Material and Methods). cDNA from three individual mice were pooled for PCR amplification. Gnat2 (cone transducin), CHX10 and Opn4 (melanopsin) were used as markers for the ONL, INL and GCL, respectively. Although some cross-contamination from the ONL to the INL (see Gnat2 amplification) and from the INL to the ONL and to the GCL (see CHX10 amplification) was detectable, the uniform intensities of the amplified signals for Mt1, Mt2 and MTF-1 support their expression in all retinal layers.

Reactions were done using specific primer pairs as listed in Table 1. Primers for MTF-1 were: forward: 5'-GTGGGAAAGCGTTTGCAG-3'; reverse: 5'-CAGAAGAAGGGTCTTTCACCA-3'.

4 GENERAL DISCUSSION

Hypoxic preconditioning strongly protects the retina against light induced photoreceptor cell death. Gene expression of the neuroprotective factor Epo is induced during hypoxia and Epo administration protects the retina against toxic light insults [71]. However, in contrast to hypoxic preconditioning, which completely protects the mouse retina against light damage, Epo alone is only partially protective [71]. Therefore, we hypothesized that the neuroprotective effect after hypoxic preconditioning depends on the co-expression of several genes, which might act in concert. To identify further potential neuroprotective target genes, we analyzed the global gene expression pattern of the mouse retina after hypoxic preconditioning by employing micro-array analyzes [134]. The retina responded to the exposure of low oxygen with the differential expression of more than 400 genes. This response involved genes with different biological functions like metabolism, transport etc. but included also cell-survival and apoptosis related genes. Among the large number of potentially protective genes, we selected the strongly induced gene cyclin-dependent kinase inhibitor 1a (*Cdkn1a*), which encodes for p21, to investigate its role in hypoxia mediated retinal neuroprotection. Employing $p21^{-/-}$ mice we showed that p21 is not essential to protect the retina against light damage. Besides p21, our study revealed a potential role of metallothioneins, which might reduce the oxidative stress evoked by light exposure. Additionally, we discovered CCAAT/enhancer binding protein delta (Cebpd), a transcriptional regulator with apoptosis interfering properties.

The large number of differentially regulated genes after hypoxic preconditioning suggested that different transcription factors are activated during hypoxia. Among those transcription factors, HIF-1 was strongly induced in the hypoxic retina [71, 134]. HIF-1 is one of the key-regulators of hypoxia and potentially regulates pro-survival and neuroprotective genes [71, 72, 112, 134]. We hypothesized that activation of HIF-1 in photoreceptor cells is essential to protect the retina against light induced apoptosis in an autocrine fashion. That means that HIF-1 should stimulate the differential expression of neuroprotective factors in photoreceptor cells. The factors may act intrinsically or may be secreted to act on neighboring photoreceptors (or other retinal) cells, respectively. To study the impact of HIF-1 on retinal neuroprotection, HIF-1α (the oxygen dependent regulated component of HIF-1) was efficiently ablated in mouse photoreceptor cells [135]. In accordance with the level of HIF-1α deletion, the HIF-1

target gene expression was clearly reduced after hypoxia. Our results indicate that an activation of HIF-1 in photoreceptor cells is not required to protect the retina against light induced retinal degeneration. In addition, adaptation to short severe hypoxia does not depend on HIF-1 activation in photoreceptor cells.

4.1 Retinal gene expression after hypoxic preconditioning

In our first project [134], we describe the differential regulation of more than 400 genes in the mouse retina immediately after hypoxia. Among them, more than 50% were at least 2-fold regulated. Of interest, the majority of genes (68% of at least 2-fold regulated genes) were induced after hypoxic preconditioning. This suggests, that hypoxic preconditioning induces *de novo* protein synthesis in the retina – an indication, that retinal cells induce mechanisms to resist against future injury (and hypoxia *per se*). The differential gene expression due to hypoxia vanished quickly during reoxygenation to reach normal levels 4 h after hypoxia. This pattern of a strong transcriptional response during hypoxia followed by a fast restoration of normal gene expression levels during reoxygenation is characteristic for hypoxic preconditioned tissues. Hence, hypoxic preconditioning of brain [136, 137] similarly induces a fast differential gene expression and a short-term neuroprotective effect. However, hypoxic preconditioned mice (preconditioning with similar protocol than used here) experienced a second boost of differential gene regulation 24 hours after hypoxia in the brain with an extended protection against ischemic injury [136]. In comparison, ischemic preconditioning of the retina seems to induce a rather mild but longer lasting answer on the transcriptional level (up to 7 days) [138, 139] and a prolonged tissue protection [68-70, 73]. This suggests, that mechanisms of ischemic preconditioning differ from those of hypoxic preconditioning. Nevertheless, it seems possible to extend the duration of retinal neuroprotection after hypoxic preconditioning by repetitive exposure to hypoxia [74] to keep up with the longer-lasting neuroprotective effects of ischemic preconditioning.

4.1.1 Limitation of the Analysis

The analysis of retinal gene expression in hypoxic preconditioned mice by micro-arrays provided an overview of the global transcriptional response. Thereby, we achieved insights into affected gene-networks, which were altered during hypoxia and discovered potentially neuroprotective genes. However, we are aware that

transcriptomic analyses with micro-arrays have certain limitations – functional, technical and statistical.

Functionally, this analysis method is restricted due to the fact that there are many steps like differential splicing, protein synthesis and functional processing regulating cellular physiology and metabolism beyond gene expression. Differential splicing as a posttranscriptional regulatory step is only partially covered by micro-array analyses. Posttranslational modification or regulation includes glycosylation, protein-protein-interactions or phosphorylation etc. that cannot be detected by gene expression analyses. Very recently, microRNAs were discovered to bind mRNAs, forming a hairpin structure and to silence gene expression by repression of protein biosynthesis [140-144]. Therefore, micro-array data reflect the cell response to hypoxia only partially.

Technical, our approach was determined by the micro-array design, the sensitivity of the detection system and the sample preparation. Although an increased retinal expression of Epo was clearly shown after hypoxic preconditioning [71], we did not detect an Epo induction by our micro-array analyzes – simply due to the fact that Epo oligos were not spotted on the chip. That indicates, that it might be possible that other genes may have escaped the detection as well. Additionally, it cannot be completely ruled out that this approach caught up false positive genes. Among the 20 strongest induced genes, Rpe65 and Lrat are not expressed in the neuronal retina but in the retinal pigment epithelium (PE) [145-147] – the single cell layer bordering the retina. This suggests, that tissue cross contamination with PE cells could alter the micro-array output data. Therefore, relevant micro-array raw data were considered carefully and confirmed by real-time PCR.

Furthermore, the detection of a functional subset of genes among 400 differentially regulated genes requires an efficient statistical pre-selection. To identify potential neuroprotective genes, we employed two strategies. On one hand, we used the tool DAVID (Database for Annotation, Visualization and Integrated Discovery) [148-150], which classifies genes according to their known or predicted biological function. Thereby, clustering revealed gene subsets potentially related to apoptosis or other biological functions. However, functional clustering was not sufficient to select appropriate target genes for further analyzes. Many genes can have multiple biological functions complicating the determination of their role in biochemical processes. Additionally, interactions between the gene products were not considered. This might be essential since most biological processes depend on a complex interplay of several factors. In order to complement our target gene screen we additionally performed Ingenuity pathway analysis (IPA) [151] to identify pathways affected by hypoxic

preconditioning. This strategy considered each possible interaction between differentially regulated genes on the level of DNA, mRNA or protein. Among the multitude of discovered pathways, the "*Cellular growth & proliferation, DNA replication, recombination and repair"* network was the most affected by hypoxic preconditioning. Due to the presence of pro-survival genes in this gene network with cyclin-dependent kinase inhibitor 1a (p21) occupying a very central position, this pathway was considered as potentially involved in retinal neuroprotection after hypoxic preconditioning. However, despite its prominent placement in this network, p21 did not play an essential role in neuroprotection (see below 4.1.3). This clearly demonstrates that results of *in silico* analyses do not necessarily reflect the biological situation, even though the algorithms used are quite sophisticated.

4.1.2 Hypoxic and Ischemic Preconditioning

Hypoxic and ischemic preconditioning protects tissues – including the retina – against apoptosis [68-73]. Thereby, both preconditioning protocols provoke somewhat different physiological alterations. Whereas exposure to hypoxia reduces the partial pressure of oxygen and therefore the tissue oxygen concentration, ischemia prevents blood flow partially or completely in a certain tissue. This results not only in tissue hypoxia but also in insufficient nutrient supply and a lack of toxic metabolite removal. However, both protocols share oxygen deprivation as a feature. Although duration and severity differs, tissues respond with the induction of hypoxia inducible factors (HIFs) and differential gene regulation [71, 72, 75, 139, 152] in both preconditioning protocols. It is believed that *de novo* protein synthesis is required for retinal neuroprotection after hypoxic [71, 74, 80, 153] and ischemic preconditioning [69, 70]. Although protein synthesis does not necessarily depend on altered gene expression, genes differentially regulated in both preconditioning strategies might be interesting targets for retinal neuroprotection. Solute carrier family 7, member 1 (Slc7a1), Cebpd, p21 and metallothionein 2 (Mt2) were differentially regulated in retinas of ischemia treated rats [139, 154]. We observed that hypoxic preconditioning caused a comparable regulation of these genes in the mouse retina. Functional clustering identified p21 and Cebpd as potential apoptosis related genes and Mt1/2 as genes responding to oxidative stress. Likewise, we compared our retinal gene expression data to the differential gene expression in brain of mice treated with an identical protocol of hypoxic preconditioning [136] and discovered a comparable regulation of adrenomedullin (Adm), p21, Vegf, Mt2, glucose transporter 1 (Glut1) or Cebpd. The similarity of gene regulation in retina

and brain could be explained by two hypotheses: I.) Comparable types of cells (neurons, glia cells, etc.) populate both – brain and the retina (which itself is a part of the brain) and respond comparable to hypoxia or II.) Hypoxia initiates similar pattern of gene expression in different cells because the adaptation to a critical lack of oxygen requires a specific set of genes and factors. In fact, evidence for both hypotheses can be found: e.g. astrocytes or fibroblasts respond to hypoxia with an induction of genes regulating carbohydrate metabolism [155, 156]. In the retina, such genes were not affected by hypoxia except for a slight induction of 6-Phosphofructo-2-kinase/fructose-2,6-biphosphate-3. Furthermore, expression of collagen and cytoskeletal genes was induced in hypoxia exposed endothelial cells [157, 158] but not detected in the hypoxic retina. This strongly suggests, that distinct cells and tissues respond differently to hypoxic exposure. However, genes like Adm, Vegf, Bnip3 or Cebpd are induced after hypoxia in many tissues [136, 137, 155, 158, 159] including the retina. This indicates that several pathways like the HIF pathway are activated commonly during hypoxia. Since hypoxic and ischemic preconditioning results in cytoprotection in different tissues like brain, retina, heart or kidney [68, 69, 71, 160-165], it is likely that a common hypoxia/ischemia activated pathway is responsible for the pro-survival effect. Hence, to identify appropriate neuroprotective target genes for further analyzes, we selected genes, which were induced after hypoxic and ischemic preconditioning in the retina as well as in brain (Fig.12). Besides Cebpd and Mt2, the cyclin dependent kinase inhibitor p21 was affected in all 3 different experimental setups [136, 154]. Considering that p21 was highly induced in the hypoxic retina and occupied a central role in a mainly affected gene network (as discussed in 4.1.1), it was the first candidate gene to be analyzed for its neuroprotective impact.

4.1.3 Cell Cycle Inhibitor Cdkn1a (p21) is not Essential for Neuroprotection

p21 encodes for a protein, which acts as an inhibitor of the cell cycle by acting on cyclin-dependent kinases (CDKs) 2, 4 and 5 [166-169]. However, besides this biological role in cell nuclei, p21 can act on signaling pathways in the cytosol and has been shown to inhibit apoptosis in a p53 dependent and independent fashion [170-175]. Furthermore, p21 is a target gene of HIF-1α [176, 177], protects cell-cycle independent against oxidative cell damage [178, 179] and was shown to inhibit apoptosis by preventing DNA cleavage [180].

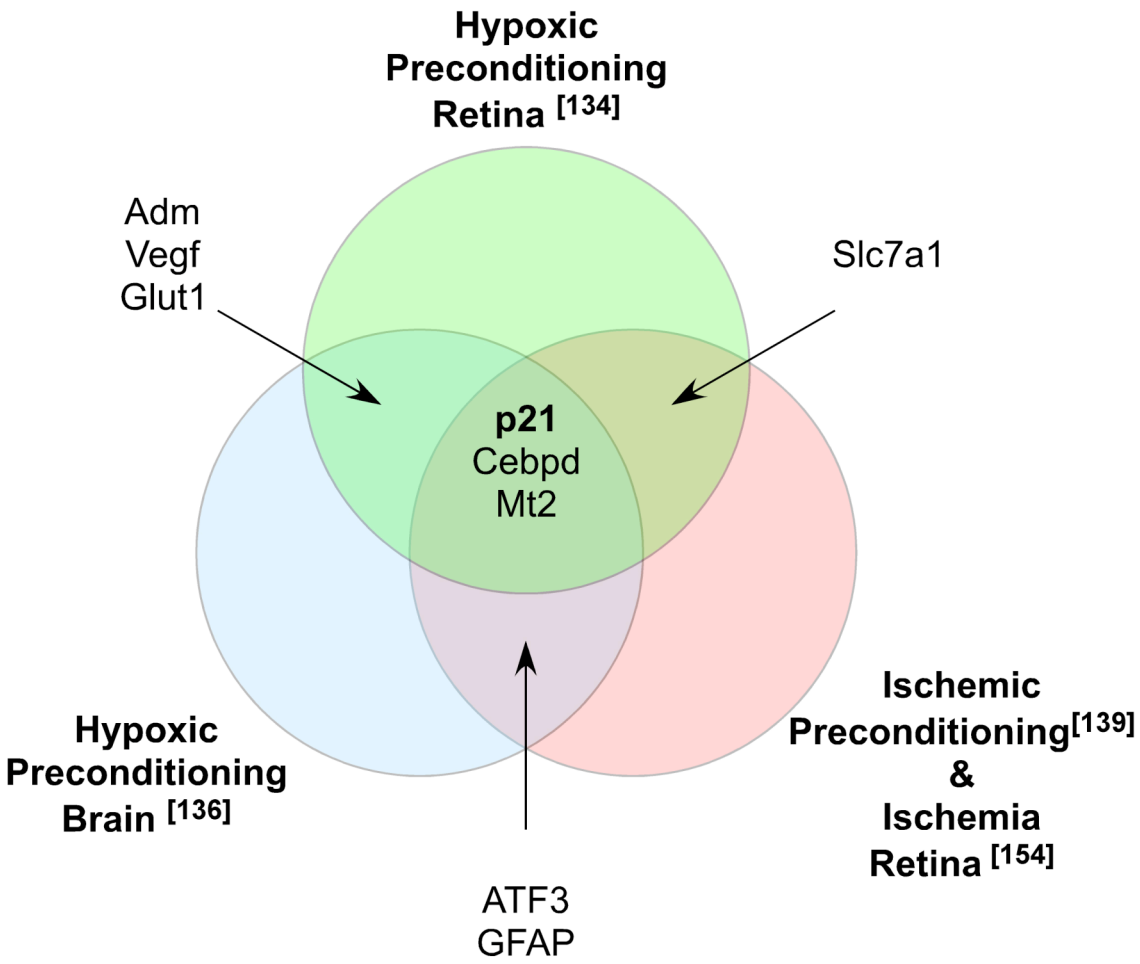

Fig.12 Different Setups of Neuroprotective Preconditioning Partially Induce Expression of Similar Genes. Three different neuroprotective preconditioning setups (hypoxic preconditioning of retina and brain and ischemic preconditioned with or without additional ischemia) show an induction of p21 (cyclin-dependent kinase inhibitor 1A), Cebpd (CCAAT/enhancer binding protein) and Mt2 (metallothionein 2) gene expression. This suggests, that these genes might be part of a general protection response. Further, hypoxic preconditioning triggers the expression of typical HIF-1α target genes like adrenomedullin (Adm), vascular endothelial growth factor (Vegf) and glucose transporter 1 (Glut1) in the retina and in brain. A solute carrier (Slc7a1) is induced in the retina after hypoxic preconditioning or after ischemic preconditioning. Activating transcription factor 3 (ATF3) and glial fibrillary acidic protein (GFAP) are induced in brains of hypoxic preconditioned mice and in retinas of ischemic preconditioned rats; [ ] indicates reference number.

Figure: M. Thiersch

We observed an induction of p21 after hypoxic exposure in the retina and hypothesized that p21 contributes to retinal neuroprotection after hypoxia. Therefore, we analyzed light induced retinal degeneration after hypoxic preconditioning in $p21^{-/-}$ mice. However, hypoxic preconditioned $p21^{-/-}$ mice were completely protected against light induced retinal degeneration, indicating that p21 is not essential for retinal neuroprotection. Nevertheless, this does not exclude the possibility that p21 can

contribute to retinal neuroprotection. Recently it was shown that p21 is induced during HDAC-inhibition but was not essential for HDAC-inhibition mediated neuroprotection of cortical cells [178]. Nevertheless, an over expression of p21 was sufficient to provide a similar protection to these cells [178]. Hypoxic preconditioning of mice activates pro-survival transcription factors like STAT3 and HIF-1 in the retina and leads to the differential expression of more than 400 genes. It could be possible that several overlapping pro-survival pathways are activated in the retina of hypoxic preconditioned mice. Therefore, p21 might be sufficient but not essential to protect the retina against light induced retinal degeneration. Other genes of this pathway could compensate for the lack of p21 and confer retinal neuroprotection. The possible impact on retinal neuroprotection by Timp3, a pro-apoptotic metalloproteinase inhibitor [181, 182] belonging to the p21 network, was tested in Timp3$^{-/-}$ mice (see unpublished data chapter 5.1.1). Similar to p21, Timp3 ablation had no effect on retinal neuroprotection after hypoxic preconditioning.

4.1.4 Additional Potential Neuroprotective Candidate Genes

4.1.4.1 Cebpd

The transcriptional regulator CCAAT/enhancer binding protein delta (Cebpd) can impact on a multitude of biological functions – including pro- and anti-apoptotic processes [183-185] – and is associated to the p21 pathway [134]. Similar to p21, Cebpd is induced in the retina and in brain of hypoxic preconditioned mice [134, 136] as well as in ischemic preconditioned retinas [139]. Furthermore, leukemia inhibitor factor (LIF) or other members of the Il-6 family were shown to differentially regulate Cebpd expression via the gp130-signaling pathway [186]. LIF and the gp130 receptor system provide strong retinal neuroprotection via the Jak/STAT pathway [187, 188]. Especially the pro-survival transcription factor STAT3 [189], which is activated in the retina of hypoxic preconditioned mice [134], seems to be involved in Cebpd gene expression [190]. These evidences suggest that Cebpd might be an interesting candidate gene for retinal neuroprotection as a downstream target of the pro-survival Jak/STAT pathway.

4.1.4.2 Metallothioneins

Retinal metallothionein 2 mRNA levels were elevated after hypoxic preconditioning [134] and after ischemic preconditioning [139, 154]. Additionally, metallothionein 1 was induced in the retina of hypoxic preconditioned mice [134]. Both

metallothioneins are induced in light damaged retinas [191] and protect the retina against NMDA induced toxicity [192]. Furthermore, Mt1 and Mt2 mRNA levels are elevated in spinal cord after ischemic preconditioning and mediate neuro- and cardioprotection [193, 194]. Thereby, Mt1 and Mt2 act as free radical scavengers and counteract oxidative stress [191, 195, 196] – a trigger of light induced retinal degeneration [197-200] and of inherited retinal disorders [201-203]. Although metallothioneins are predominantly regulated by the metal response element-binding transcription factor-1 [204], Mt1 and Mt2 can be also induced by the pro-survival transcription factor STAT3 [205] and are interesting target genes for retinal neuroprotection.

4.1.4.3 Vegf

The vascular endothelial growth factor (Vegf) is a HIF-1 target gene [206-210] and expression levels in the retina are elevated after hypoxic preconditioning of mice [71, 134]. VEGF acts on endothelial cells and stimulates proliferation, migration and tube formation leading to the growth of new blood vessels [211]. However, the role of Vegf in the retina remains controversial. It is considered to be a pro-survival factor for neuronal and endothelial cells [211-216]. Additionally, the development of the retina depends on Vegf signaling [217, 218], which determines neural progenitor cell proliferation and commitment. However, abnormally increased levels of Vegf are connected to retinal diseases like diabetic retinopathy (DR), retinopathy of prematurity (ROP) and wet AMD. Among other symptoms, these retinal disorders are featured by neovascularization, vessel leakiness and retinal degeneration due to hemorrhages [219-230]. It seems that the retinal integrity depends on accurately balanced VEGF levels. Further, three different isoforms (VEGF120, VEGF164, VEGF188 [231]) of VEGF are induced in the retina after hypoxic preconditioning (see unpublished data chapter 5.1.2). Therefore, it is difficult to predict the impact of VEGF (or of a specific isoform) on retinal neuroprotection after hypoxic preconditioning. Mice, which lack HIF-1α in photoreceptor cells, show a significantly lower Vegf induction after hypoxia than respective control mice. Still, these mice are completely protected against light induced retinal degeneration after hypoxic preconditioning [135]. However, cells of the INL and GCL most likely continue to express and secrete VEGF, which might be sufficient to protect photoreceptors against light damage. Certainly, the complex role of VEGF signaling in the retina requires further, detailed analyzes.

4.1.4.4 Adrenomedullin

Adrenomedullin (Adm) is a secreted regulatory peptide with multiple biological impacts. Among other functions, Adm has vasodilatory effects, regulates the water-electrolyte balance in kidneys, stimulates or inhibits cell proliferation or possesses antimicrobial properties [232, 233]. Adm mRNA levels are induced in the retina [134] and the brain [136] of hypoxic preconditioned mice but quickly return to normal expression levels after reoxygenation. Of interest, Adm was reported to offer neuroprotective properties in ischemic brains and to protect neurons against oxygen glucose deprivation [234-236]. Adm is a target gene of HIF-1α [237, 238] and retinal neuroprotection by desferroxamine (DFO) preconditioning was shown to correlate with elevated HIF-1α and Adm levels [239]. Further, elevated Adm serum levels, found in patients suffering from retinitis pigmentosa, could be a response to photoreceptor cell death [240]. Therefore, Adm should be considered as a target gene for retinal neuroprotection.

4.1.4.5 Paraoxonase

Paraoxonase (Pon1) as a member of the paraoxonase gene family, is a high-density lipoprotein (HDL) associated enzyme, which is predominately expressed in liver and secreted into the serum [241]. Pon1 levels seemed to be induced in retinas of hypoxic preconditioned mice [134]. However, the expression pattern analysis of paraoxonase family genes in retina and eyecup indicates that Pon1 is predominantly expressed in the eyecup (see unpublished data chapter 5.1.3). This challenges the observed induction of Pon1 in the retina of hypoxic preconditioned mice and points to possible contamination effects. However, Pon1 is a risk factor for atherosclerosis [242, 243] and has a biological impact on cholesterol transport, on the prevention of lipid peroxidation and on the reduction of oxidative stress [244, 245]. Considering, that retinal degeneration involves oxidative stress and lipid peroxidation [246], Pon1 could play an important role in retinal neuroprotection and in retinal disease progression. Moreover, Pon1 was reported to be reduced in serum of AMD patients as well as in smokers and aged people (both risk factor for AMD) [247-250]. This suggests a potential link of Pon1 to AMD – the most frequent retinal disorder.

4.1.4.6 Bcl2-like 10

Bcl2-like 10 (Bcl2l10), which is also named Diva/Boo, is an apoptosis-regulating member of the Bcl2 family and was strongly induced immediately after hypoxia [134]. It was reported to promote apoptosis by interaction with apoptotic peptidase activating factor 1 (Apaf1), an adapter molecule that activates the initiator caspase-9 [251]. Additionally, it was shown that Bcl2l10 could prevent CD95 ligand dependent apoptosis by interfering with the apoptosome downstream of cytochrome c release [252, 253]. However, light induced retinal apoptosis is independent of classical apoptotic pathways and neither includes cytochrome c release nor caspase activation [45, 48, 52, 53, 254]. Since to little is known about the cell-biological impact of Bcl2l10, it is speculative whether its induction contributes to retinal neuroprotection after hypoxic preconditioning.

4.1.4.7 Kif4

Kinesin family member 4 (Kif4) is an apoptosis-regulating gene, which is induced in the retina after hypoxic preconditioning (see supplemental data 3.1.1.3) peaking 4 h after hypoxia - exactly correlating with the time point of complete protection against light induced retinal degeneration [71]. Kif4 is involved in DNA damage/repair pathways [255, 256] and was shown to regulate neuronal survival by suppressing poly (ADP-ribose) polymerase family, member 1 (Parp1) enzyme activity [257]. Under physiological conditions, Parp1 maintains cell homeostasis through DNA repair, controlling the energy balance and serving as a transcriptional regulator [258, 259]. However, over-stimulation of Parp-1 by excessive oxidant-induced DNA damage induces cell death [45] and pharmacological inhibition of Parp-1 activity protects against cerebral ischemia or myocardial infarction [260]. Recently, it was shown that attenuation of Parp1 activity by Casp3 is essential to mediate neuroprotection against zinc and NMDA toxicity [261]. Whether Kif4 and its target Parp-1 have an impact on retinal neuroprotection after hypoxic preconditioning remains to be analyzed. However, it was shown that Parp-1 inhibition leads to partial retinal protection in an inherited model (rd1 mouse) [262] as well as in different models of induced retinal degeneration (ischemia, NMDA toxicity and N-methyl-N-nitrosourea-induced photoreceptor cell apoptosis) [263-265]. This indicates, that Parp-1 activity may contribute to retinal degeneration and suggests Kif4 as an interesting candidate gene for retinal neuroprotection.

4.1.4.8 Mef2c and Rbm family members

Among the few downregulated genes with potential impact on cell death, Mef2c and members of the Rbm family could be of interest. The role of Mef2c is controversial: On one hand it was shown that the Mef2 transcription factors are required for neuronal development [266] and Mef2c increases the resistance against apoptosis in neuronal progenitor cells [267]. On the other hand, Mef2c might also be involved in dopaminergic neuron death in Parkinson's disease [268] and is an inducer of apoptosis in macrophages [269]. Macrophages play an important role in light induced retinal degeneration [270, 271] to ensure a rapid and efficient clearance of cell debris. This reduces secondary apoptotic effects and pro-inflammatory processes and is required to maintain the retinal integrity. A downregulation of Mef2c could be a response to maintain macrophage activity and to efficiently clear up cells that die after light exposure.

Among the members of the RNA-binding-motif protein family (RBM), gene expression of Rbm3, Rbm4 and Rbm12b was repressed. Members of the Rbm family were shown to be associated with apoptotic processes [272]. Rbm3 has been specifically linked to apoptosis [273] and to proliferation [274]. However, little is known about the biological functions of Rbm proteins in the retina and whether they play a role in retinal degeneration.

4.2 The role of HIF-1α

HIF-1α is expressed in the entire retina [74, 135]. We hypothesized that HIF-1α stabilization is required to protect photoreceptor cells against light induced cell death. To test this, HIF-1α was ablated in photoreceptor cells. We employed a conditional knock out system breeding mice carrying loxP-flanked alleles of HIF-1α [275] with two different Cre-expressing mouse strains. PrpCre deleter mice [276] ablated HIF-1α very efficiently in photoreceptor cells whereas OpnCre mice [277] caused only a partial reduction of HIF-1α in photoreceptor cells. Especially PrpCre mice showed strongly reduced HIF-1α protein levels. Further, typical HIF-1α target genes like Bnip3 [278], Egln1 [279, 280], Vegf [206-210], Adm [237, 238] and Glut1 [281] showed a reduced retinal expression after hypoxic preconditioning especially in PrpCre mice and partially in OpnCre mice. Retinal development and physiology remained normal when HIF-1α was ablated in photoreceptors and no pathological changes were detected in retinas of hypoxic preconditioned knock out mice. Additionally, neuroprotection by hypoxic preconditioning seems to be independent of HIF-1α stabilization in photoreceptors. The

induction of other transcription factors like HIF-2α or STAT3 in control and in knock out mice suggests that other mechanisms might exist to protect photoreceptor cells against toxic insults.

4.2.1 Physiological Role of HIF-1α in the Retina

A systemic knock out of HIF-1α was shown to be lethal between embryonic day 9 and 10 [122, 127]. Thereby, the blood vessel formation is severely impaired in the absence of HIF-1α. That indicates, that HIF-1α stabilization is absolutely required for the embryonic development of mice. In the retina, HIF-1α is induced between postnatal day (PND) 5 and 14, which correlates with an induction of Vegf [72] and the development of the inner retinal blood vessel system [9]. Considering the potential role of HIF-1α in retinal blood vessel formation, a retinal deletion of HIF-1α during eye development might severely impair retinal function and morphology. To avoid potential vascular deficits and a resultant abnormal retinal development, two different photoreceptor specific Cre expressing mouse lines were compared. Cre activity in PrpCre mice [276] can be temporally controlled by tamoxifen (TAM). Inducing Cre activity in adult mice should allow a normal retinal development similarly to wild type mice. In contrast, OpnCre mice activate Cre around PND 7 [277] – the time point when HIF-1α is stabilized in developing retinas of wild type mice [72]. However, the early ablation of HIF-1α did not result in pathological changes of morphology. A possible explanation could be that OpnCre only partially deleted HIF-1α in photoreceptor cells [135]. Furthermore, the three inter-connected blood vessel networks, located in the nerve fiber layer and in both plexiform layers, arise from the inner surface of the retina [9]. HIF-1α expression in ganglion cells and the inner nuclear layer of OpnCre mice might be sufficient to ensure a proper network establishment.

The retina is a high energy demanding tissue with dropping oxygen concentrations during the dark phases [282]. During this phase the retina becomes borderline hypoxic and might require HIF-1α for adaptation. In retinas of adult mice HIF-1α protein is hardly detectable under physiological conditions [71, 134] except for ganglion cells, which show a slight HIF-1α protein signal [135]. In adult PrpCre mice, HIF-1α was efficiently deleted in photoreceptor cells [135]. Nevertheless, no morphological alterations could be observed PrpCre mice over a period of 4 month, suggesting that HIF-1α in photoreceptor cells is not required to maintain retinal integrity of adult mice under physiological conditions.

PrpCre and OpnCre mice deleted HIF-1α photoreceptor cells specific in mature and in developing retinas. Both deleter strains revealed no obvious retinal impairment after HIF-1α ablation and were therefore used for analyzing the impact of HIF-1α deletion during short but severe hypoxia.

4.2.2 HIF-1α and Hypoxia

Almost all types of cells and tissues respond to low levels of oxygen with the stabilization of HIF-1α and differential gene expression [283, 284]. The role of HIF-1α in neuronal tissue during severe hypoxia or ischemia is controversial. Two independent studies showed contradictory effects after brain specific HIF-1α ablation. Baranova et al. showed that a neuron specific deletion of HIF-1α increased brain injury after cerebral ischemia [285]. In contrast, Helton et al. observed even an increased resistance against hypoxic-ischemic damage after HIF-1α ablation in cortex and hippocampus [286]. The difference in both studies could be explained by different extent of HIF-1α ablation. Whereas Baranova reported a neuron specific knock out [285], Helton et al. described mice with HIF-1α deletion in additional cell types, like astrocytes [286]. Interestingly, it was shown that an induction of HIF-1α in astrocytes accelerated hypoxia-induced cell death. In contrast, an induction of HIF-1α in neurons promoted survival and increased the resistance to hypoxia [121]. This suggests a beneficial role for HIF-1α stabilization in neurons. However, the ablation of HIF-1α in photoreceptor cells – the primary neurons within the retina – did not induce retinal degeneration after sever hypoxia (6-7% O_2) in both Cre deleter strains (PrpCre and OpnCre) up to 4 weeks after exposure [135]. The differences between the decreased tolerance against cerebral ischemia in neuron specific HIF-1α deletion in brain [285] and the resistance to severe hypoxia in our model of photoreceptor cell specific HIF-1α ablation [135] could be explained by the different treatments. The oxygen deprivation during hypoxic exposure (6% O_2) of mice as used in our study [135] might be less intense than during ischemia as used by Baranova et al. [285]. Ischemia suppresses blood flow and prevents nutrition supply as well as the removal of toxic metabolites, which might contribute to the cytotoxic effect. Additionally, the retina experiences constant exposure to borderline levels of hypoxia during the night [282]. This might activate general hypoxia-resistance mechanisms, which do not necessarily require HIF-1α in photoreceptor cells and which are sufficient to protect the retina against hypoxia induced damage.

Both, PrpCre and OpnCre mice were protected against hypoxia induced retinal degeneration. Therefore, both mouse models were employed to investigate the role of HIF-1α in retinal neuroprotection after hypoxic preconditioning.

4.2.3 HIF-1α and Retinal Neuroprotection

To analyze the impact of HIF-1α on hypoxia-mediated neuroprotection of the retina, both deleter strains (PrpCre [276] and OpnCre [277]) with photoreceptor cell specific HIF-1α deletion were hypoxic preconditioned and exposed to toxic levels of white light. The results showed that the retinas of mice lacking HIF-1α in photoreceptor cells were (like wild type mice) completely protected against light induced retinal degeneration after hypoxic preconditioning [135]. This finding is perfectly in line with a recent report showing that protection against cerebral ischemia after hypoxic preconditioning is independent from HIF-1α stabilization in neurons [285]. Nevertheless, both findings are somewhat surprising considering that cardio- and nephroprotection after ischemic/hypoxic preconditioning depends on HIF-1α [165, 287-291]. Moreover, several hypoxia-mimicking compounds like the iron-chelators dimethyloxaloylglycine (DMOG), desferroxamine (DFO) etc. or cobalt chloride ($CoCl_2$) were shown to stabilize HIF-1α and to confer cell-, tissue- or neuroprotection [292-298]. Especially the protection of the retina after hypoxic exposure was shown to correlate with the stabilization of HIF-1α and the expression of potentially neuroprotective HIF-1 target genes [71, 74, 75, 134]. Specific HIF-1α deletion in photoreceptor cells – the cells that undergo apoptosis due to light exposure – was used to analyze the impact of HIF-1α on photoreceptor cell survival after hypoxic preconditioning. However, with the employed model we cannot exclude the possibility that remaining HIF-1α in the INL and GCL confers retinal neuroprotection by the expression of secreted factors. Among HIF-1α target genes with a potential neuroprotective impact, Adm [237, 238] and Vegf [206-210] were only partially reduced in HIF-1α ablated mice [135]. This suggests a remaining HIF-1α activity in the INL and GCL and that Adm and Vegf as secreted factors could still contribute to retinal neuroprotection. To date, there are no Cre deleter strains available that express Cre in the entire retina to delete HIF-1α tissue- and not only photoreceptor-specific. Nevertheless, our experiments showed clearly, that an intrinsic activation of the transcription factor HIF-1 in photoreceptor cells is not essential to protect these cells against toxic light insults.

4.2.4 Possible Alternative Mechanisms for Hypoxia-induced Retinal Neuroprotection

Analyzing the retinal transcriptome after hypoxia revealed several potential neuroprotective target genes [134]. Among them, the induction of Bcl2l10, Adm, Vegf, Mt1, Mt2, Epo and Egf was tested in the retina of hypoxic preconditioned HIF-1α knock out mice. Except for Vegf and Adm, which showed reduced expression in hypoxic preconditioned PrpCre mice; all genes seemed to be expressed either in cell layers where HIF-1α was not deleted (INL and GCL) or independently of HIF-1α. This suggests the involvement of other transcription factors. Besides HIF-1α, hypoxia induces or activates additional transcription factors like HIF-2α, STAT3, p53 and members of the Myc- or the NF-κB-family [134, 299-301]. Especially HIF-2α was discussed to mediate neuroprotection in a HIF-1α independent protection of brain neurons against cerebral ischemia after hypoxic preconditioning [285]. Likewise, we observed an induction of HIF-2α after hypoxic preconditioning in the retina of HIF-1α ablated and control mice [135]. Very recently a study suggested that HIF-2α and not HIF-1α is required to mediate neuroprotection against NGF-deprivation-induced cell death in developing neurons [302]. Furthermore, it was shown that HIF-2α instead of HIF-1α regulates the expression of Epo *in vivo* [303-305] and *in vitro* [306]. Epo acts as a strong neuroprotective factor in the brain [114, 307, 308] and in the retina [76, 309] and protects against light induced retinal degeneration [71, 72]. In our conditional HIF-1α knock out mice, Epo mRNA levels were not reduced after hypoxic preconditioning when compared to control animals [135] – an effect, which might be responsible for the sustained strong neuroprotective effect. Several reasons might account for the unaffected Epo expression in the retinas of HIF-1α ablated mice: 1. Retinal Epo expression is indeed regulated by HIF-2α instead of HIF-1α as suggested by Morita et al. [304] and/or 2. Epo is predominantly expressed in cells of the INL and GCL as suggested by García-Ramírez et al. [79]. If Epo is regulated by HIF-2α to confer neuroprotection in the retina, then HIF-2α rather than HIF-1α could be one of the essential components of retinal neuroprotection after hypoxic preconditioning.

In addition to HIF-2α other transcription factors like STAT3, which was phosphorylated (pSTAT3) and thereby activated in retinas of hypoxic preconditioned mice [135], could contribute to retinal neuroprotection. STAT3 is a pro-survival factor [189], which is also activated after light exposure [54] – probably as an attempt to rescue cells. Recently it was suggested that LIF application mediated protection against light induced retinal degeneration in a STAT3 dependent manner [187]. Of

interest, Epo was shown to activate STAT3 via Janus kinase 2 (Jak2) [310] in retinal ganglion cells and it was shown that Jak2/STAT3 promote neuroprotection in a rat model of stroke [311]. This would suggest a link between HIF/Epo induction after hypoxic preconditioning and the activation of the pro-survival transcription factor STAT3. Among potential STAT3 target genes, Mt1 and Mt2 were reported to mediate cardioprotection in a STAT3 dependent fashion [205]. Both metallothioneins act as free radical scavengers [191, 195, 196] and were induced in retinas of both, HIF-1α ablated and control mice after hypoxic preconditioning [135]. This supports the potential impact of STAT3 on retinal neuroprotection. However, metallothioneins are predominately regulated by the metal-regulatory transcription factor 1 (MTF1) [204], which was not analyzed in our model. That indicates, that there are certainly more potential neuroprotective transcription factors activated in the hypoxic retina. To pinpoint the molecular mechanisms of retinal neuroprotection by hypoxic preconditioning further and detailed investigations are clearly required.

4.3 Conclusion

We aimed to analyze mechanisms, which are responsible for retinal neuroprotection after hypoxic preconditioning. Employing micro-arrays we analyzed the retinal transcriptome after hypoxic preconditioning and discovered potential neuroprotective genes. Among them was p21 – the cyclin-dependent kinase inhibitor 1a with potential impact on apoptosis regulation, Cebpd – a downstream target of the strong pro-survival transcription factor STAT3; and Mt2 a free radical scavenger that might counteract oxidative stress. As a first candidate, we selected p21 and analyzed its role by employing $p21^{-/-}$ mice. We showed that p21 is not essential for retinal neuroprotection after hypoxic preconditioning. The persistence of the strong neuroprotective effect after hypoxic preconditioning could be explained by the possibility that hypoxia induces several cell-survival pathways, which partially overlap. If that proves to be true, neuroprotective intervention should not target anti-apoptotic “effector” genes but upstream factors (like transcription factors), which govern the expression of various pro-survival genes or pro-survival pathways. To verify this hypothesis, we specifically investigated the role of HIF-1 – one of the main transcription factors responding to hypoxia – in retinal neuroprotection after hypoxic preconditioning. The photoreceptor-specific deletion of HIF-1α in retinas of developing mice (OpnCre) and retinas of adult mice (PrpCre) impaired neither retinal development nor the maintenance of retinal integrity. Surprisingly, exposure of HIF-1α ablated mice to short,

severe hypoxia caused no functional or morphological abnormalities in the retina. Finally, this study clearly showed that retinal neuroprotection against light damage after hypoxic preconditioning is independent of HIF-1α stabilization in photoreceptor cells. However, the retina is a functional unit consisting of three different neuronal cell layers (ONL, INL and GCL) and a single pigment epithelium cell layer. We discussed the possibility that the remaining HIF-1α protein in INL and GCL might be sufficient to protect the retina by the induction of secreted factors in a paracrine fashion. Further, we observed the activation of additional transcription factors like HIF-2α and the pro-survival transcription factor STAT3. The expression of potentially neuroprotective genes like metallothioneins, Bcl2l10 or Egf was not affected by HIF-1α ablation. Likewise, the induction of the strong neuroprotective factor Epo after hypoxic preconditioning was hardly affected in HIF-1α ablated mice.

Therefore, we hypothesize that HIF-2α rather than HIF-1α regulates the expression of Epo in the retina during hypoxia and as such might be an important factor for retinal neuroprotection. Epo is linked to STAT3 and STAT5 signaling [310-312] and STAT3 has been reported to promote cell survival in the retina [187]. Although Epo-induced STAT5 can provide neuroprotection [312], we observed no phosphorylation of STAT5 after hypoxic preconditioning (not shown). Additionally, Jak2 remained inactive after hypoxic preconditioning (not shown). Nevertheless, Epo might activate STAT3 in retinas of hypoxic preconditioned mice via an unknown mechanism, which could result in the expression of potential STAT3 target genes with neuroprotective properties (Mt1, Mt2 [205] and Cebpd [190]). We assume that retinal neuroprotection could partially depend on a HIF-2α – Epo – STAT3 axis and might require the expression of potential STAT3 target genes – like metallothioneins and Cebpd (Fig.13).

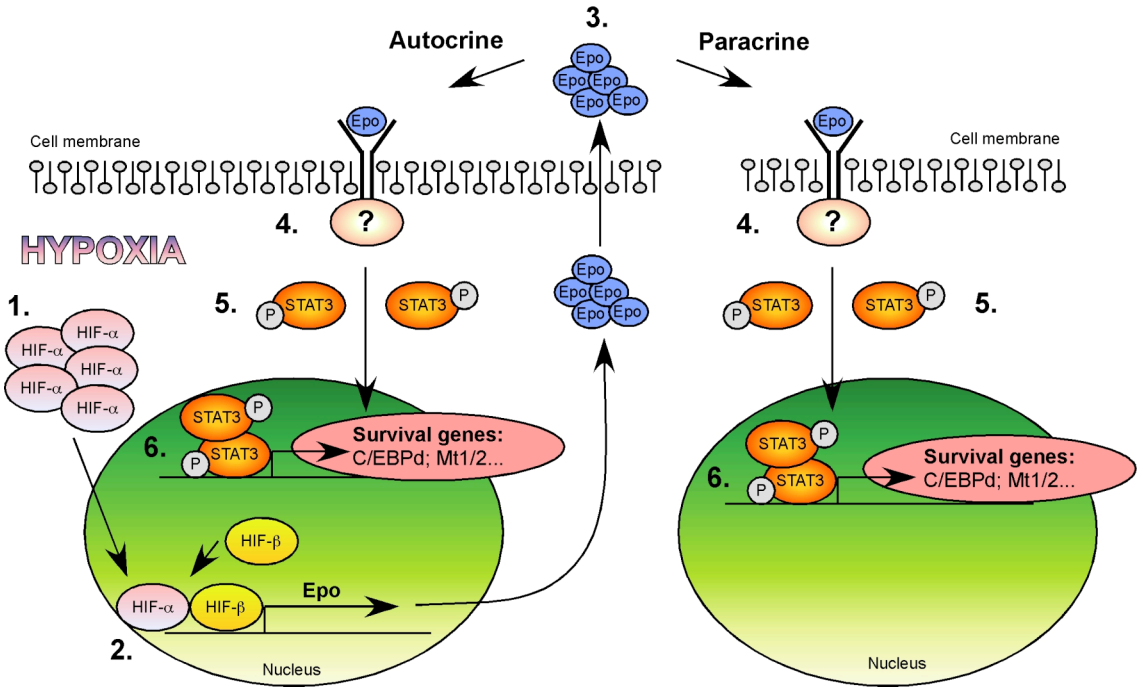

Fig.13 Hypothesized Major Signalling Cascade Induced by Hypoxic Preconditioning to Protect Photoreceptor Cells Against Light-induced Retinal Degeneration. During hypoxia hypoxia-inducible factor alpha subunits (HIFα) accumulate in the retina and dimerize with HIF-β subunits in the nucleus. This induces the gene expression and release of erythropoietin (Epo) (most likely HIF-2α dependent). Epo binds to its receptor, which is localized on photoreceptor cells and mediates neuroprotection in an autocrine fashion (photoreceptor cells produce Epo themselves) or in a paracrine fashion (Epo is not produced by photoreceptor cells but by other cells of the retina). The ligation of Epo to its receptor activates STAT3 via an unknown Jak2-independent mechanism, which induces the expression of neuroprotective genes like metallothionein 2 (Mt2) and CCAAT/enhancer binding protein (Cebpd) and thereby protects the retina against light-induced retinal degeneration.

Figure: M. Thiersch

5 APPENDIX

5.1 Unpublished Data

5.1.1 Hypoxic Preconditioning Protects Timp3$^{-/-}$ Mice Against Light-induced Retinal Degeneration

Analyzing the retinal transcriptome after hypoxic preconditioning suggested that several networks of genes might confer protection against light induced retinal degeneration. Among those genes we tested p21 and showed that it is not essential for retinal neuroprotection. Timp3 belongs to the same gene network and was induced after hypoxic preconditioning. Because Timp3 is a regulator of apoptosis [181, 182], we employed Timp3$^{-/-}$ to analyze the effect of Timp3 ablation on hypoxic preconditioning dependent retinal neuroprotection. The exposure of Timp3$^{+/-}$ control mice and Timp3$^{-/-}$ mice to light caused retinal degeneration, indicated by reduced rhodopsin levels ten days after illumination (Fig.14). Hypoxic preconditioning protected both, Timp3$^{+/-}$ and Timp3$^{-/-}$ mice against light induced retinal degeneration, suggesting that Timp3 is not essential for hypoxia mediated neuroprotection.

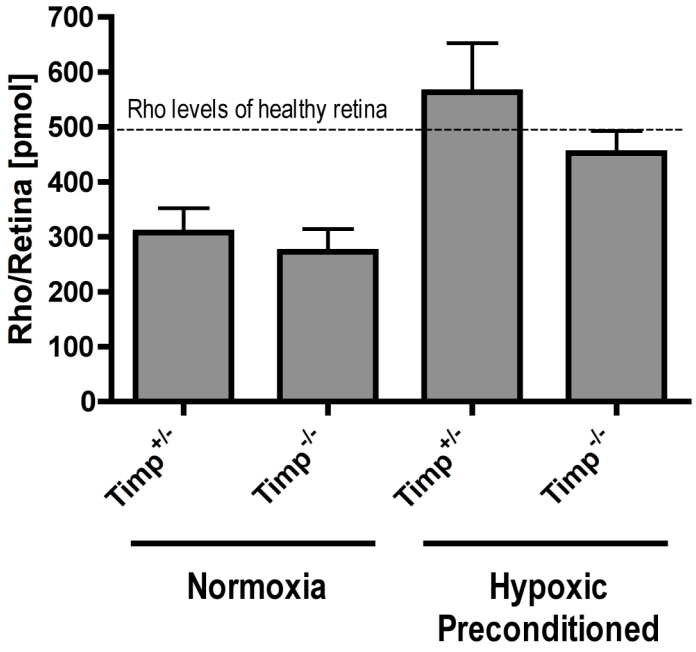

Fig.14 Rhodopsin levels in normoxic or hypoxic preconditioned Timp3$^{-/-}$ mice and Timp3$^{+/-}$ control mice ten days after light exposure. Shown are levels of rhodopsin as indicator for the presence

of photoreceptor cells. A physiological normal retina contains approximately 500 pmol of rhodopsin per retina (indicated by dashed line). Both $Timp3^{+/-}$ and $Timp3^{-/-}$ mice showed reduced levels of rhodopsin after illumination, suggesting that they were susceptible to light and underwent retinal degeneration. Hypoxic preconditioned $Timp3^{+/-}$ and $Timp3^{-/-}$ mice were completely protected against light induced retinal degeneration and reveal normal levels of rhodopsin. Shown are means ±SD of n=3

5.1.2 Differential Expression of Vegf Isoforms in the Retina After Hypoxia

Hypoxic preconditioning induces the expression of Vegf [71, 134]. However, at least three different isoforms of Vegf (VEGF120, VEGF164, VEGF188 [231]) are expressed in the retina. It might be possible that the induction of a specific isoform confers to retinal neuroprotection. Therefore, we used real time PCR and isoform specific primer to analyze whether the Vegf isoforms in the retina were similarly induced by hypoxia or whether alternative splicing preferentially activated a specific isoform during hypoxia. Real time PCR confirmed the general expression of Vegf and a rapid return to normal expression levels. Further we observed that all isoforms (Vegf 164, 120 and 188) showed a similar pattern of induction between 2 – 3 fold and a quick restoration of the normoxic gene expression levels (Fig.15). This suggests that Vegf isoforms are similarly regulated in the hypoxic retina.

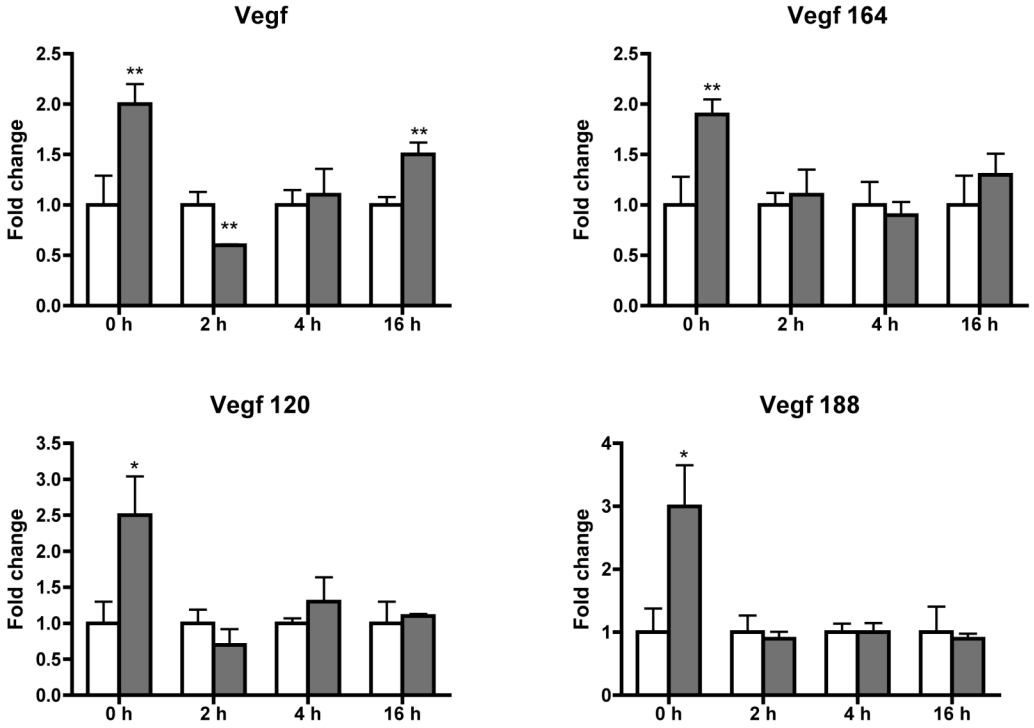

Fig.15 Differential Expression of Vegf Isoforms after Hypoxic Preconditioning in the Retina. Expression levels of total Vegf mRNA and of the isoforms Vegf 164, 120 and 188 in normoxic mice (white

bar) and after 0, 2, 4 and 16 hours of hypoxia (grey bars). Data were normalized to normoxic mice which were set to "1" for each time point. Statistical significance was estimated with student's t-test (n = 4): *p ≤ 0.05; **p ≤ 0.01.

5.1.3 Expression of Paraoxonase Family Genes in Retina and Eyecup

Analyzing the retinal transcriptome in response to hypoxia revealed a few interesting candidate genes, which could be implicated in retinal neuroprotection. Among those genes, we found Paraoxonase 1 (Pon1), which could be potentially involved in oxidative stress response of the retina. Further it was shown, that reduced Pon1 activity is correlated with the development of AMD [247-250]. In order to estimate retinal expression levels of all three paraoxonase family genes, we analyzed mRNA of the retina and compared it to eyecup and liver (the major Pon1 producing tissue) (Fig.16).

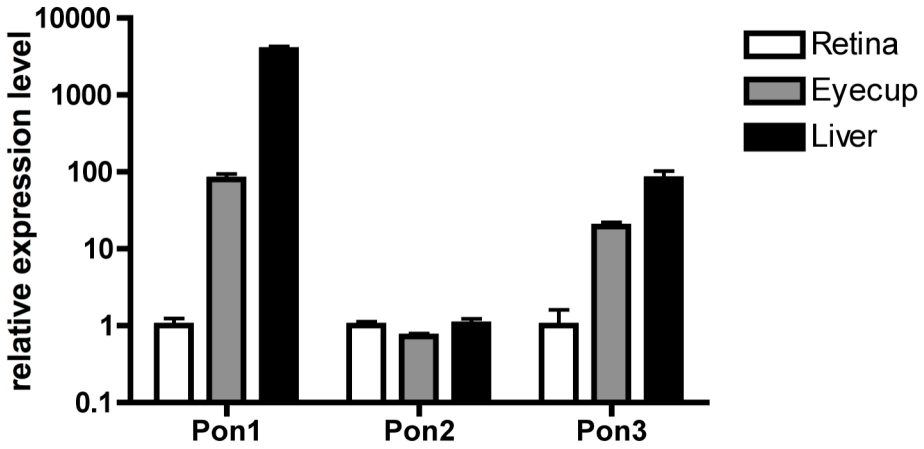

Fig.16 Pon1 Expression in Retina compared to Eyecup and Liver. Relative expression levels of paraoxonase 1, 2, 3 (Pon1, 2, 3) mRNA in the retina (white bar), eyecup (grey bar) and liver (black bar) are logarithmically presented. Data were normalized to retinal expression levels, which were set to "1". (n=4)

Pon2 was equally expressed in retina, eyecup and liver. In contrast, Pon1 and Pon3 were predominantly expressed in the liver. Of note, the gene expression levels of Pon1 and Pon3 in eyecup strongly exceeded the retinal expression levels, suggesting a potential biological role in the eyecup or even in RPE cells.

5.2 References for Introduction and Discussion

1. Masland RH: **The fundamental plan of the retina**. *Nat Neurosci* 2001, **4**(9):877-886.
2. Kolb H: **How the Retina Works**. *American Scientist* 2003, **91**(1):28-35.
3. Ross CD, Bowers M, Godfrey DA: **Distribution of glutaminase activity in retinal layers of rat and guinea pig**. *Brain Res* 1987, **401**(1):168-172.
4. Heidinger V, Hicks D, Sahel J, Dreyfus H: **Ability of retinal Muller glial cells to protect neurons against excitotoxicity in vitro depends upon maturation and neuron-glial interactions**. *Glia* 1999, **25**(3):229-239.
5. Bringmann A, Pannicke T, Grosche J, Francke M, Wiedemann P, Skatchkov SN, Osborne NN, Reichenbach A: **Muller cells in the healthy and diseased retina**. *Prog Retin Eye Res* 2006, **25**(4):397-424.
6. Lucas DR, Newhouse JP: **The toxic effect of sodium L-glutamate on the inner layers of the retina**. *AMA Arch Ophthalmol* 1957, **58**(2):193-201.
7. Haberecht MF, Mitchell CK, Lo GJ, Redburn DA: **N-methyl-D-aspartate-mediated glutamate toxicity in the developing rabbit retina**. *J Neurosci Res* 1997, **47**(4):416-426.
8. Choi DW: **Glutamate neurotoxicity and diseases of the nervous system**. *Neuron* 1988, **1**(8):623-634.
9. Fruttiger M: **Development of the retinal vasculature**. *Angiogenesis* 2007, **10**(2):77-88.
10. Dowling JE, Boycott BB: **Organization of the primate retina: electron microscopy**. *Proc R Soc Lond B Biol Sci* 1966, **166**(2):80-111.
11. Kolb H, Fernandez E, Nelson R, Jones BW: **WEBVISION The Organization of the Retina and Visual System**. *http://webvisionmedutahedu/*.
12. Dartnall HJ, Bowmaker JK, Mollon JD: **Human visual pigments: microspectrophotometric results from the eyes of seven persons**. *Proc R Soc Lond B Biol Sci* 1983, **220**(1218):115-130.
13. Burns ME, Baylor DA: **Activation, deactivation, and adaptation in vertebrate photoreceptor cells**. *Annu Rev Neurosci* 2001, **24**:779-805.
14. Arshavsky VY, Lamb TD, Pugh EN, Jr.: **G proteins and phototransduction**. *Annu Rev Physiol* 2002, **64**:153-187.
15. Rosenberg EA, Sperazza LC: **The visually impaired patient**. *Am Fam Physician* 2008, **77**(10):1431-1436.
16. Jager RD, Mieler WF, Miller JW: **Age-related macular degeneration**. *N Engl J Med* 2008, **358**(24):2606-2617.
17. Vingerling JR, Hofman A, Grobbee DE, de Jong PT: **Age-related macular degeneration and smoking. The Rotterdam Study**. *Arch Ophthalmol* 1996, **114**(10):1193-1196.
18. Seddon JM, Willett WC, Speizer FE, Hankinson SE: **A prospective study of cigarette smoking and age-related macular degeneration in women**. *Jama* 1996, **276**(14):1141-1146.
19. Christen WG, Glynn RJ, Manson JE, Ajani UA, Buring JE: **A prospective study of cigarette smoking and risk of age-related macular degeneration in men**. *Jama* 1996, **276**(14):1147-1151.
20. Friedman DS, Katz J, Bressler NM, Rahmani B, Tielsch JM: **Racial differences in the prevalence of age-related macular degeneration: the Baltimore Eye Survey**. *Ophthalmology* 1999, **106**(6):1049-1055.
21. Klein BE, Klein R, Lee KE, Jensen SC: **Measures of obesity and age-related eye diseases**. *Ophthalmic Epidemiol* 2001, **8**(4):251-262.
22. Klein RJ, Zeiss C, Chew EY, Tsai JY, Sackler RS, Haynes C, Henning AK, SanGiovanni JP, Mane SM, Mayne ST, Bracken MB, Ferris FL, Ott J, Barnstable C, Hoh J: **Complement factor H polymorphism in age-related macular degeneration**. *Science* 2005, **308**(5720):385-389.
23. Haines JL, Hauser MA, Schmidt S, Scott WK, Olson LM, Gallins P, Spencer KL, Kwan SY, Noureddine M, Gilbert JR, Schnetz-Boutaud N, Agarwal A, Postel EA, Pericak-Vance MA: **Complement factor H variant increases the risk of age-related macular degeneration**. *Science* 2005, **308**(5720):419-421.
24. Hageman GS, Anderson DH, Johnson LV, Hancox LS, Taiber AJ, Hardisty LI, Hageman JL, Stockman HA, Borchardt JD, Gehrs KM, Smith RJ, Silvestri G, Russell SR, Klaver CC, Barbazetto I, Chang S, Yannuzzi LA, Barile GR, Merriam JC, Smith RT, Olsh AK, Bergeron J, Zernant J, Merriam JE, Gold B, Dean M, Allikmets R: **A common haplotype in the complement regulatory gene factor H (HF1/CFH) predisposes individuals to age-related macular degeneration**. *Proc Natl Acad Sci U S A* 2005, **102**(20):7227-7232.

25. Edwards AO, Ritter R, 3rd, Abel KJ, Manning A, Panhuysen C, Farrer LA: **Complement factor H polymorphism and age-related macular degeneration**. *Science* 2005, **308**(5720):421-424.
26. Gold B, Merriam JE, Zernant J, Hancox LS, Taiber AJ, Gehrs K, Cramer K, Neel J, Bergeron J, Barile GR, Smith RT, Hageman GS, Dean M, Allikmets R: **Variation in factor B (BF) and complement component 2 (C2) genes is associated with age-related macular degeneration**. *Nat Genet* 2006, **38**(4):458-462.
27. Yang Z, Camp NJ, Sun H, Tong Z, Gibbs D, Cameron DJ, Chen H, Zhao Y, Pearson E, Li X, Chien J, Dewan A, Harmon J, Bernstein PS, Shridhar V, Zabriskie NA, Hoh J, Howes K, Zhang K: **A variant of the HTRA1 gene increases susceptibility to age-related macular degeneration**. *Science* 2006, **314**(5801):992-993.
28. Gibbs D, Yang Z, Constantine R, Ma X, Camp NJ, Yang X, Chen H, Jorgenson A, Hau V, Dewan A, Zeng J, Harmon J, Buehler J, Brand JM, Hoh J, Cameron DJ, Dixit M, Tong Z, Zhang K: **Further mapping of 10q26 supports strong association of HTRA1 polymorphisms with age-related macular degeneration**. *Vision Res* 2008, **48**(5):685-689.
29. Rosenfeld PJ, Brown DM, Heier JS, Boyer DS, Kaiser PK, Chung CY, Kim RY: **Ranibizumab for neovascular age-related macular degeneration**. *N Engl J Med* 2006, **355**(14):1419-1431.
30. Hartong DT, Berson EL, Dryja TP: **Retinitis pigmentosa**. *Lancet* 2006, **368**(9549):1795-1809.
31. Daiger SP, Bowne SJ, Sullivan LS: **Perspective on genes and mutations causing retinitis pigmentosa**. *Arch Ophthalmol* 2007, **125**(2):151-158.
32. Birch DG, Anderson JL, Fish GE: **Yearly rates of rod and cone functional loss in retinitis pigmentosa and cone-rod dystrophy**. *Ophthalmology* 1999, **106**(2):258-268.
33. Samardzija M, Neuhauss SCF, Joly S, Kurz-Levin M, Grimm C: **Animal Models for Retinal Degeneration.** *Neuromethods; Animal Models of Retinal Disease; Iok-Hou Pang and Abbot F Clark (Edts); The Humana Press Inc, Totowa, NJ, USA* submitted.
34. Bowes C, Li T, Danciger M, Baxter LC, Applebury ML, Farber DB: **Retinal degeneration in the rd mouse is caused by a defect in the beta subunit of rod cGMP-phosphodiesterase**. *Nature* 1990, **347**(6294):677-680.
35. Samardzija M, Wenzel A, Naash M, Reme CE, Grimm C: **Rpe65 as a modifier gene for inherited retinal degeneration**. *Eur J Neurosci* 2006, **23**(4):1028-1034.
36. Naash MI, Ripps H, Li S, Goto Y, Peachey NS: **Polygenic disease and retinitis pigmentosa: albinism exacerbates photoreceptor degeneration induced by the expression of a mutant opsin in transgenic mice**. *J Neurosci* 1996, **16**(24):7853-7858.
37. Ambati J, Anand A, Fernandez S, Sakurai E, Lynn BC, Kuziel WA, Rollins BJ, Ambati BK: **An animal model of age-related macular degeneration in senescent Ccl-2- or Ccr-2-deficient mice**. *Nat Med* 2003, **9**(11):1390-1397.
38. Reme CE, Grimm C, Hafezi F, Wenzel A, Williams TP: **Apoptosis in the Retina: The Silent Death of Vision**. *News Physiol Sci* 2000, **15**:120-124.
39. Reme CE, Grimm C, Hafezi F, Marti A, Wenzel A: **Apoptotic cell death in retinal degenerations**. *Prog Retin Eye Res* 1998, **17**(4):443-464.
40. Reme CE, Grimm C, Hafezi F, Iseli HP, Wenzel A: **Why study rod cell death in retinal degenerations and how?** *Doc Ophthalmol* 2003, **106**(1):25-29.
41. Wu J, Seregard S, Algvere PV: **Photochemical damage of the retina**. *Surv Ophthalmol* 2006, **51**(5):461-481.
42. Paskowitz DM, LaVail MM, Duncan JL: **Light and inherited retinal degeneration**. *Br J Ophthalmol* 2006, **90**(8):1060-1066.
43. Organisciak DT, Darrow RM, Barsalou L, Darrow RA, Kutty RK, Kutty G, Wiggert B: **Light history and age-related changes in retinal light damage**. *Invest Ophthalmol Vis Sci* 1998, **39**(7):1107-1116.
44. Hao W, Wenzel A, Obin MS, Chen CK, Brill E, Krasnoperova NV, Eversole-Cire P, Kleyner Y, Taylor A, Simon MI, Grimm C, Reme CE, Lem J: **Evidence for two apoptotic pathways in light-induced retinal degeneration**. *Nat Genet* 2002, **32**(2):254-260.
45. Wenzel A, Grimm C, Samardzija M, Reme CE: **Molecular mechanisms of light-induced photoreceptor apoptosis and neuroprotection for retinal degeneration**. *Prog Retin Eye Res* 2005, **24**(2):275-306.

46. Grimm C, Wenzel A, Hafezi F, Yu S, Redmond TM, Reme CE: **Protection of Rpe65-deficient mice identifies rhodopsin as a mediator of light-induced retinal degeneration**. *Nat Genet* 2000, **25**(1):63-66.
47. Saari JC, Garwin GG, Van Hooser JP, Palczewski K: **Reduction of all-trans-retinal limits regeneration of visual pigment in mice**. *Vision Res* 1998, **38**(10):1325-1333.
48. Donovan M, Carmody RJ, Cotter TG: **Light-induced photoreceptor apoptosis in vivo requires neuronal nitric-oxide synthase and guanylate cyclase activity and is caspase-3-independent**. *J Biol Chem* 2001, **276**(25):23000-23008.
49. Wenzel A, Grimm C, Marti A, Kueng-Hitz N, Hafezi F, Niemeyer G, Reme CE: **c-fos controls the "private pathway" of light-induced apoptosis of retinal photoreceptors**. *J Neurosci* 2000, **20**(1):81-88.
50. Hafezi F, Marti A, Grimm C, Wenzel A, Reme CE: **Differential DNA binding activities of the transcription factors AP-1 and Oct-1 during light-induced apoptosis of photoreceptors**. *Vision Res* 1999, **39**(15):2511-2518.
51. Grimm C, Wenzel A, Hafezi F, Reme CE: **Gene expression in the mouse retina: the effect of damaging light**. *Mol Vis* 2000, **6**:252-260.
52. Samardzija M, Wenzel A, Thiersch M, Frigg R, Reme C, Grimm C: **Caspase-1 ablation protects photoreceptors in a model of autosomal dominant retinitis pigmentosa**. *Invest Ophthalmol Vis Sci* 2006, **47**(12):5181-5190.
53. Donovan M, Cotter TG: **Caspase-independent photoreceptor apoptosis in vivo and differential expression of apoptotic protease activating factor-1 and caspase-3 during retinal development**. *Cell Death Differ* 2002, **9**(11):1220-1231.
54. Samardzija M, Wenzel A, Aufenberg S, Thiersch M, Reme C, Grimm C: **Differential role of Jak-STAT signaling in retinal degenerations**. *Faseb J* 2006, **20**(13):2411-2413.
55. Osborne NN, Casson RJ, Wood JP, Chidlow G, Graham M, Melena J: **Retinal ischemia: mechanisms of damage and potential therapeutic strategies**. *Prog Retin Eye Res* 2004, **23**(1):91-147.
56. Barkana Y, Belkin M: **Neuroprotection in ophthalmology: a review**. *Brain Res Bull* 2004, **62**(6):447-453.
57. Chaum E: **Retinal neuroprotection by growth factors: a mechanistic perspective**. *J Cell Biochem* 2003, **88**(1):57-75.
58. Leveillard T, Mohand-Said S, Lorentz O, Hicks D, Fintz AC, Clerin E, Simonutti M, Forster V, Cavusoglu N, Chalmel F, Dolle P, Poch O, Lambrou G, Sahel JA: **Identification and characterization of rod-derived cone viability factor**. *Nat Genet* 2004, **36**(7):755-759.
59. Hojo M, Abe T, Sugano E, Yoshioka Y, Saigo Y, Tomita H, Wakusawa R, Tamai M: **Photoreceptor protection by iris pigment epithelial transplantation transduced with AAV-mediated brain-derived neurotrophic factor gene**. *Invest Ophthalmol Vis Sci* 2004, **45**(10):3721-3726.
60. Cayouette M, Smith SB, Becerra SP, Gravel C: **Pigment epithelium-derived factor delays the death of photoreceptors in mouse models of inherited retinal degenerations**. *Neurobiol Dis* 1999, **6**(6):523-532.
61. MacDonald IM, Sauve Y, Sieving PA: **Preventing blindness in retinal disease: ciliary neurotrophic factor intraocular implants**. *Can J Ophthalmol* 2007, **42**(3):399-402.
62. O'Driscoll C, O'Connor J, O'Brien CJ, Cotter TG: **Basic fibroblast growth factor-induced protection from light damage in the mouse retina in vivo**. *J Neurochem* 2008, **105**(2):524-536.
63. Faden AI, Stoica B: **Neuroprotection: challenges and opportunities**. *Arch Neurol* 2007, **64**(6):794-800.
64. Yenari M, Kitagawa K, Lyden P, Perez-Pinzon M: **Metabolic downregulation: a key to successful neuroprotection?** *Stroke* 2008, **39**(10):2910-2917.
65. Rosenzweig HL, Minami M, Lessov NS, Coste SC, Stevens SL, Henshall DC, Meller R, Simon RP, Stenzel-Poore MP: **Endotoxin preconditioning protects against the cytotoxic effects of TNFalpha after stroke: a novel role for TNFalpha in LPS-ischemic tolerance**. *J Cereb Blood Flow Metab* 2007, **27**(10):1663-1674.
66. Rosenzweig HL, Lessov NS, Henshall DC, Minami M, Simon RP, Stenzel-Poore MP: **Endotoxin preconditioning prevents cellular inflammatory response during ischemic neuroprotection in mice**. *Stroke* 2004, **35**(11):2576-2581.
67. Liu C, Peng M, Laties AM, Wen R: **Preconditioning with bright light evokes a protective response against light damage in the rat retina**. *J Neurosci* 1998, **18**(4):1337-1344.

68. Zhang C, Rosenbaum DM, Shaikh AR, Li Q, Rosenbaum PS, Pelham DJ, Roth S: **Ischemic preconditioning attenuates apoptotic cell death in the rat retina**. *Invest Ophthalmol Vis Sci* 2002, **43**(9):3059-3066.
69. Roth S, Li B, Rosenbaum PS, Gupta H, Goldstein IM, Maxwell KM, Gidday JM: **Preconditioning provides complete protection against retinal ischemic injury in rats**. *Invest Ophthalmol Vis Sci* 1998, **39**(5):777-785.
70. Roth S: **Endogenous neuroprotection in the retina**. *Brain Res Bull* 2004, **62**(6):461-466.
71. Grimm C, Wenzel A, Groszer M, Mayser H, Seeliger M, Samardzija M, Bauer C, Gassmann M, Reme CE: **HIF-1-induced erythropoietin in the hypoxic retina protects against light-induced retinal degeneration**. *Nat Med* 2002, **8**(7):718-724.
72. Grimm C, Hermann DM, Bogdanova A, Hotop S, Kilic U, Wenzel A, Kilic E, Gassmann M: **Neuroprotection by hypoxic preconditioning: HIF-1 and erythropoietin protect from retinal degeneration**. *Semin Cell Dev Biol* 2005, **16**(4-5):531-538.
73. Casson RJ, Wood JP, Melena J, Chidlow G, Osborne NN: **The effect of ischemic preconditioning on light-induced photoreceptor injury**. *Invest Ophthalmol Vis Sci* 2003, **44**(3):1348-1354.
74. Zhu Y, Zhang Y, Ojwang BA, Brantley MA, Jr., Gidday JM: **Long-term tolerance to retinal ischemia by repetitive hypoxic preconditioning: role of HIF-1alpha and heme oxygenase-1**. *Invest Ophthalmol Vis Sci* 2007, **48**(4):1735-1743.
75. Whitlock NA, Agarwal N, Ma JX, Crosson CE: **Hsp27 upregulation by HIF-1 signaling offers protection against retinal ischemia in rats**. *Invest Ophthalmol Vis Sci* 2005, **46**(3):1092-1098.
76. Zhong L, Bradley J, Schubert W, Ahmed E, Adamis AP, Shima DT, Robinson GS, Ng YS: **Erythropoietin promotes survival of retinal ganglion cells in DBA/2J glaucoma mice**. *Invest Ophthalmol Vis Sci* 2007, **48**(3):1212-1218.
77. Zhang J, Wu Y, Jin Y, Ji F, Sinclair SH, Luo Y, Xu G, Lu L, Dai W, Yanoff M, Li W, Xu GT: **Intravitreal injection of erythropoietin protects both retinal vascular and neuronal cells in early diabetes**. *Invest Ophthalmol Vis Sci* 2008, **49**(2):732-742.
78. Yamasaki M, Mishima HK, Yamashita H, Kashiwagi K, Murata K, Minamoto A, Inaba T: **Neuroprotective effects of erythropoietin on glutamate and nitric oxide toxicity in primary cultured retinal ganglion cells**. *Brain Res* 2005, **1050**(1-2):15-26.
79. Garcia-Ramirez M, Hernandez C, Simo R: **Expression of erythropoietin and its receptor in the human retina: a comparative study of diabetic and nondiabetic subjects**. *Diabetes Care* 2008, **31**(6):1189-1194.
80. Grimm C, Wenzel A, Stanescu D, Samardzija M, Hotop S, Groszer M, Naash M, Gassmann M, Reme C: **Constitutive overexpression of human erythropoietin protects the mouse retina against induced but not inherited retinal degeneration**. *J Neurosci* 2004, **24**(25):5651-5658.
81. Bruick RK, McKnight SL: **Transcription. Oxygen sensing gets a second wind**. *Science* 2002, **295**(5556):807-808.
82. Wang GL, Jiang BH, Rue EA, Semenza GL: **Hypoxia-inducible factor 1 is a basic-helix-loop-helix-PAS heterodimer regulated by cellular O2 tension**. *Proc Natl Acad Sci U S A* 1995, **92**(12):5510-5514.
83. O'Rourke JF, Tian YM, Ratcliffe PJ, Pugh CW: **Oxygen-regulated and transactivating domains in endothelial PAS protein 1: comparison with hypoxia-inducible factor-1alpha**. *J Biol Chem* 1999, **274**(4):2060-2071.
84. Jiang BH, Zheng JZ, Leung SW, Roe R, Semenza GL: **Transactivation and inhibitory domains of hypoxia-inducible factor 1alpha. Modulation of transcriptional activity by oxygen tension**. *J Biol Chem* 1997, **272**(31):19253-19260.
85. Ema M, Hirota K, Mimura J, Abe H, Yodoi J, Sogawa K, Poellinger L, Fujii-Kuriyama Y: **Molecular mechanisms of transcription activation by HLF and HIF1alpha in response to hypoxia: their stabilization and redox signal-induced interaction with CBP/p300**. *Embo J* 1999, **18**(7):1905-1914.
86. Lee JW, Bae SH, Jeong JW, Kim SH, Kim KW: **Hypoxia-inducible factor (HIF-1)alpha: its protein stability and biological functions**. *Exp Mol Med* 2004, **36**(1):1-12.

87. Masson N, Willam C, Maxwell PH, Pugh CW, Ratcliffe PJ: **Independent function of two destruction domains in hypoxia-inducible factor-alpha chains activated by prolyl hydroxylation**. *Embo J* 2001, **20**(18):5197-5206.

88. Jaakkola P, Mole DR, Tian YM, Wilson MI, Gielbert J, Gaskell SJ, Kriegsheim A, Hebestreit HF, Mukherji M, Schofield CJ, Maxwell PH, Pugh CW, Ratcliffe PJ: **Targeting of HIF-alpha to the von Hippel-Lindau ubiquitylation complex by O2-regulated prolyl hydroxylation**. *Science* 2001, **292**(5516):468-472.

89. Ivan M, Kondo K, Yang H, Kim W, Valiando J, Ohh M, Salic A, Asara JM, Lane WS, Kaelin WG, Jr.: **HIFalpha targeted for VHL-mediated destruction by proline hydroxylation: implications for O2 sensing**. *Science* 2001, **292**(5516):464-468.

90. Bruick RK, McKnight SL: **A conserved family of prolyl-4-hydroxylases that modify HIF**. *Science* 2001, **294**(5545):1337-1340.

91. Epstein AC, Gleadle JM, McNeill LA, Hewitson KS, O'Rourke J, Mole DR, Mukherji M, Metzen E, Wilson MI, Dhanda A, Tian YM, Masson N, Hamilton DL, Jaakkola P, Barstead R, Hodgkin J, Maxwell PH, Pugh CW, Schofield CJ, Ratcliffe PJ: **C. elegans EGL-9 and mammalian homologs define a family of dioxygenases that regulate HIF by prolyl hydroxylation**. *Cell* 2001, **107**(1):43-54.

92. Jeong JW, Bae MK, Ahn MY, Kim SH, Sohn TK, Bae MH, Yoo MA, Song EJ, Lee KJ, Kim KW: **Regulation and destabilization of HIF-1alpha by ARD1-mediated acetylation**. *Cell* 2002, **111**(5):709-720.

93. Salceda S, Caro J: **Hypoxia-inducible factor 1alpha (HIF-1alpha) protein is rapidly degraded by the ubiquitin-proteasome system under normoxic conditions. Its stabilization by hypoxia depends on redox-induced changes**. *J Biol Chem* 1997, **272**(36):22642-22647.

94. Huang LE, Gu J, Schau M, Bunn HF: **Regulation of hypoxia-inducible factor 1alpha is mediated by an O2-dependent degradation domain via the ubiquitin-proteasome pathway**. *Proc Natl Acad Sci U S A* 1998, **95**(14):7987-7992.

95. Mahon PC, Hirota K, Semenza GL: **FIH-1: a novel protein that interacts with HIF-1alpha and VHL to mediate repression of HIF-1 transcriptional activity**. *Genes Dev* 2001, **15**(20):2675-2686.

96. Lando D, Peet DJ, Whelan DA, Gorman JJ, Whitelaw ML: **Asparagine hydroxylation of the HIF transactivation domain a hypoxic switch**. *Science* 2002, **295**(5556):858-861.

97. Lando D, Peet DJ, Gorman JJ, Whelan DA, Whitelaw ML, Bruick RK: **FIH-1 is an asparaginyl hydroxylase enzyme that regulates the transcriptional activity of hypoxia-inducible factor**. *Genes Dev* 2002, **16**(12):1466-1471.

98. Bardos JI, Ashcroft M: **Negative and positive regulation of HIF-1: a complex network**. *Biochim Biophys Acta* 2005, **1755**(2):107-120.

99. Braganca J, Eloranta JJ, Bamforth SD, Ibbitt JC, Hurst HC, Bhattacharya S: **Physical and functional interactions among AP-2 transcription factors, p300/CREB-binding protein, and CITED2**. *J Biol Chem* 2003, **278**(18):16021-16029.

100. Bhattacharya S, Michels CL, Leung MK, Arany ZP, Kung AL, Livingston DM: **Functional role of p35srj, a novel p300/CBP binding protein, during transactivation by HIF-1**. *Genes Dev* 1999, **13**(1):64-75.

101. Blagosklonny MV, An WG, Romanova LY, Trepel J, Fojo T, Neckers L: **p53 inhibits hypoxia-inducible factor-stimulated transcription**. *J Biol Chem* 1998, **273**(20):11995-11998.

102. Makino Y, Kanopka A, Wilson WJ, Tanaka H, Poellinger L: **Inhibitory PAS domain protein (IPAS) is a hypoxia-inducible splicing variant of the hypoxia-inducible factor-3alpha locus**. *J Biol Chem* 2002, **277**(36):32405-32408.

103. Fatyol K, Szalay AA: **The p14ARF tumor suppressor protein facilitates nucleolar sequestration of hypoxia-inducible factor-1alpha (HIF-1alpha) and inhibits HIF-1-mediated transcription**. *J Biol Chem* 2001, **276**(30):28421-28429.

104. Jiang BH, Jiang G, Zheng JZ, Lu Z, Hunter T, Vogt PK: **Phosphatidylinositol 3-kinase signaling controls levels of hypoxia-inducible factor 1**. *Cell Growth Differ* 2001, **12**(7):363-369.

105. Fukuda R, Hirota K, Fan F, Jung YD, Ellis LM, Semenza GL: **Insulin-like growth factor 1 induces hypoxia-inducible factor 1-mediated vascular endothelial growth factor expression, which is dependent on**

MAP kinase and phosphatidylinositol 3-kinase signaling in colon cancer cells. *J Biol Chem* 2002, **277**(41):38205-38211.

106. Feldser D, Agani F, Iyer NV, Pak B, Ferreira G, Semenza GL: **Reciprocal positive regulation of hypoxia-inducible factor 1alpha and insulin-like growth factor 2**. *Cancer Res* 1999, **59**(16):3915-3918.
107. Bardos JI, Ashcroft M: **Hypoxia-inducible factor-1 and oncogenic signalling**. *Bioessays* 2004, **26**(3):262-269.
108. Tacchini L, Dansi P, Matteucci E, Desiderio MA: **Hepatocyte growth factor signalling stimulates hypoxia inducible factor-1 (HIF-1) activity in HepG2 hepatoma cells**. *Carcinogenesis* 2001, **22**(9):1363-1371.
109. Gorlach A, Diebold I, Schini-Kerth VB, Berchner-Pfannschmidt U, Roth U, Brandes RP, Kietzmann T, Busse R: **Thrombin activates the hypoxia-inducible factor-1 signaling pathway in vascular smooth muscle cells: Role of the p22(phox)-containing NADPH oxidase**. *Circ Res* 2001, **89**(1):47-54.
110. Semenza G: **Signal transduction to hypoxia-inducible factor 1**. *Biochem Pharmacol* 2002, **64**(5-6):993-998.
111. Mateo J, Garcia-Lecea M, Cadenas S, Hernandez C, Moncada S: **Regulation of hypoxia-inducible factor-1alpha by nitric oxide through mitochondria-dependent and -independent pathways**. *Biochem J* 2003, **376**(Pt 2):537-544.
112. Chen W, Ostrowski RP, Obenaus A, Zhang JH: **Prodeath or prosurvival: two facets of hypoxia inducible factor-1 in perinatal brain injury**. *Exp Neurol* 2009, **216**(1):7-15.
113. Bergeron M, Gidday JM, Yu AY, Semenza GL, Ferriero DM, Sharp FR: **Role of hypoxia-inducible factor-1 in hypoxia-induced ischemic tolerance in neonatal rat brain**. *Ann Neurol* 2000, **48**(3):285-296.
114. Digicaylioglu M, Lipton SA: **Erythropoietin-mediated neuroprotection involves cross-talk between Jak2 and NF-kappaB signalling cascades**. *Nature* 2001, **412**(6847):641-647.
115. Shrivastava K, Ram MS, Bansal A, Singh SS, Ilavazhagan G: **Cobalt supplementation promotes hypoxic tolerance and facilitates acclimatization to hypobaric hypoxia in rat brain**. *High Alt Med Biol* 2008, **9**(1):63-75.
116. Althaus J, Bernaudin M, Petit E, Toutain J, Touzani O, Rami A: **Expression of the gene encoding the pro-apoptotic BNIP3 protein and stimulation of hypoxia-inducible factor-1alpha (HIF-1alpha) protein following focal cerebral ischemia in rats**. *Neurochem Int* 2006, **48**(8):687-695.
117. Halterman MW, Miller CC, Federoff HJ: **Hypoxia-inducible factor-1alpha mediates hypoxia-induced delayed neuronal death that involves p53**. *J Neurosci* 1999, **19**(16):6818-6824.
118. Van Hoecke M, Prigent-Tessier AS, Garnier PE, Bertrand NM, Filomenko R, Bettaieb A, Marie C, Beley AG: **Evidence of HIF-1 functional binding activity to caspase-3 promoter after photothrombotic cerebral ischemia**. *Mol Cell Neurosci* 2007, **34**(1):40-47.
119. Halterman MW, Federoff HJ: **HIF-1alpha and p53 promote hypoxia-induced delayed neuronal death in models of CNS ischemia**. *Exp Neurol* 1999, **159**(1):65-72.
120. Aminova LR, Chavez JC, Lee J, Ryu H, Kung A, Lamanna JC, Ratan RR: **Prosurvival and prodeath effects of hypoxia-inducible factor-1alpha stabilization in a murine hippocampal cell line**. *J Biol Chem* 2005, **280**(5):3996-4003.
121. Vangeison G, Carr D, Federoff HJ, Rempe DA: **The good, the bad, and the cell type-specific roles of hypoxia inducible factor-1 alpha in neurons and astrocytes**. *J Neurosci* 2008, **28**(8):1988-1993.
122. Ryan HE, Lo J, Johnson RS: **HIF-1 alpha is required for solid tumor formation and embryonic vascularization**. *Embo J* 1998, **17**(11):3005-3015.
123. Vincent KA, Shyu KG, Luo Y, Magner M, Tio RA, Jiang C, Goldberg MA, Akita GY, Gregory RJ, Isner JM: **Angiogenesis is induced in a rabbit model of hindlimb ischemia by naked DNA encoding an HIF-1alpha/VP16 hybrid transcription factor**. *Circulation* 2000, **102**(18):2255-2261.
124. Yamakawa M, Liu LX, Date T, Belanger AJ, Vincent KA, Akita GY, Kuriyama T, Cheng SH, Gregory RJ, Jiang C: **Hypoxia-inducible factor-1 mediates activation of cultured vascular endothelial cells by inducing multiple angiogenic factors**. *Circ Res* 2003, **93**(7):664-673.
125. Richmond TD, Chohan M, Barber DL: **Turning cells red: signal transduction mediated by erythropoietin**. *Trends Cell Biol* 2005, **15**(3):146-155.

126. Iliopoulos O, Levy AP, Jiang C, Kaelin WG, Jr., Goldberg MA: **Negative regulation of hypoxia-inducible genes by the von Hippel-Lindau protein**. *Proc Natl Acad Sci U S A* 1996, **93**(20):10595-10599.

127. Iyer NV, Kotch LE, Agani F, Leung SW, Laughner E, Wenger RH, Gassmann M, Gearhart JD, Lawler AM, Yu AY, Semenza GL: **Cellular and developmental control of O2 homeostasis by hypoxia-inducible factor 1 alpha**. *Genes Dev* 1998, **12**(2):149-162.

128. Fukuda R, Zhang H, Kim JW, Shimoda L, Dang CV, Semenza GL: **HIF-1 regulates cytochrome oxidase subunits to optimize efficiency of respiration in hypoxic cells**. *Cell* 2007, **129**(1):111-122.

129. Kim JW, Tchernyshyov I, Semenza GL, Dang CV: **HIF-1-mediated expression of pyruvate dehydrogenase kinase: a metabolic switch required for cellular adaptation to hypoxia**. *Cell Metab* 2006, **3**(3):177-185.

130. Semenza GL: **Targeting HIF-1 for cancer therapy**. *Nat Rev Cancer* 2003, **3**(10):721-732.

131. Semenza GL: **Evaluation of HIF-1 inhibitors as anticancer agents**. *Drug Discov Today* 2007, **12**(19-20):853-859.

132. Semenza GL: **Hypoxia and cancer**. *Cancer Metastasis Rev* 2007, **26**(2):223-224.

133. Semenza GL: **Hypoxia-inducible factor 1 and cancer pathogenesis**. *IUBMB Life* 2008, **60**(9):591-597.

134. Thiersch M, Raffelsberger W, Frigg R, Samardzija M, Wenzel A, Poch O, Grimm C: **Analysis of the retinal gene expression profile after hypoxic preconditioning identifies candidate genes for neuroprotection**. *BMC Genomics* 2008, **9**:73.

135. Thiersch M, Lange C, Joly S, Heynen S, Le ZL, Samardzija M, Grimm C: **Retinal Neuroprotection by Hypoxic Preconditioning is Independent of HIF-1a Expression in Photoreceptors**. *European Journal of Neuroscience* submitted.

136. Tang Y, Pacary E, Freret T, Divoux D, Petit E, Schumann-Bard P, Bernaudin M: **Effect of hypoxic preconditioning on brain genomic response before and following ischemia in the adult mouse: identification of potential neuroprotective candidates for stroke**. *Neurobiol Dis* 2006, **21**(1):18-28.

137. Bernaudin M, Tang Y, Reilly M, Petit E, Sharp FR: **Brain genomic response following hypoxia and re-oxygenation in the neonatal rat. Identification of genes that might contribute to hypoxia-induced ischemic tolerance**. *J Biol Chem* 2002, **277**(42):39728-39738.

138. Li Y, Roth S, Laser M, Ma JX, Crosson CE: **Retinal preconditioning and the induction of heat-shock protein 27**. *Invest Ophthalmol Vis Sci* 2003, **44**(3):1299-1304.

139. Kamphuis W, Dijk F, van Soest S, Bergen AA: **Global gene expression profiling of ischemic preconditioning in the rat retina**. *Mol Vis* 2007, **13**:1020-1030.

140. Bartel DP: **MicroRNAs: target recognition and regulatory functions**. *Cell* 2009, **136**(2):215-233.

141. Lau NC, Lim LP, Weinstein EG, Bartel DP: **An abundant class of tiny RNAs with probable regulatory roles in Caenorhabditis elegans**. *Science* 2001, **294**(5543):858-862.

142. Lee RC, Ambros V: **An extensive class of small RNAs in Caenorhabditis elegans**. *Science* 2001, **294**(5543):862-864.

143. Reinhart BJ, Slack FJ, Basson M, Pasquinelli AE, Bettinger JC, Rougvie AE, Horvitz HR, Ruvkun G: **The 21-nucleotide let-7 RNA regulates developmental timing in Caenorhabditis elegans**. *Nature* 2000, **403**(6772):901-906.

144. Wightman B, Ha I, Ruvkun G: **Posttranscriptional regulation of the heterochronic gene lin-14 by lin-4 mediates temporal pattern formation in C. elegans**. *Cell* 1993, **75**(5):855-862.

145. Saari JC, Bredberg DL, Farrell DF: **Retinol esterification in bovine retinal pigment epithelium: reversibility of lecithin:retinol acyltransferase**. *Biochem J* 1993, **291 (Pt 3)**:697-700.

146. Batten ML, Imanishi Y, Maeda T, Tu DC, Moise AR, Bronson D, Possin D, Van Gelder RN, Baehr W, Palczewski K: **Lecithin-retinol acyltransferase is essential for accumulation of all-trans-retinyl esters in the eye and in the liver**. *J Biol Chem* 2004, **279**(11):10422-10432.

147. Redmond TM, Yu S, Lee E, Bok D, Hamasaki D, Chen N, Goletz P, Ma JX, Crouch RK, Pfeifer K: **Rpe65 is necessary for production of 11-cis-vitamin A in the retinal visual cycle**. *Nat Genet* 1998, **20**(4):344-351.

148. **Database for Annotation, Visualization and Integrated Discovery (DAVID)**. *http://davidabccncifcrfgov/*.

149. Huang da W, Sherman BT, Lempicki RA: **Systematic and integrative analysis of large gene lists using DAVID bioinformatics resources**. *Nat Protoc* 2009, **4**(1):44-57.

150. Dennis G, Jr., Sherman BT, Hosack DA, Yang J, Gao W, Lane HC, Lempicki RA: **DAVID: Database for Annotation, Visualization, and Integrated Discovery**. *Genome Biol* 2003, **4**(5):P3.
151. **Ingenuity Systems, CA, USA**. *http://wwwingenuitycom*.
152. Eckle T, Kohler D, Lehmann R, El Kasmi K, Eltzschig HK: **Hypoxia-inducible factor-1 is central to cardioprotection: a new paradigm for ischemic preconditioning**. *Circulation* 2008, **118**(2):166-175.
153. Peng PH, Huang HS, Lee YJ, Chen YS, Ma MC: **Novel role for the delta-opioid receptor in hypoxic preconditioning in rat retinas**. *J Neurochem* 2009, **108**(3):741-754.
154. Kamphuis W, Dijk F, Bergen AA: **Ischemic preconditioning alters the pattern of gene expression changes in response to full retinal ischemia**. *Mol Vis* 2007, **13**:1892-1901.
155. Mense SM, Sengupta A, Zhou M, Lan C, Bentsman G, Volsky DJ, Zhang L: **Gene expression profiling reveals the profound upregulation of hypoxia-responsive genes in primary human astrocytes**. *Physiol Genomics* 2006, **25**(3):435-449.
156. Greijer AE, van der Groep P, Kemming D, Shvarts A, Semenza GL, Meijer GA, van de Wiel MA, Belien JA, van Diest PJ, van der Wall E: **Up-regulation of gene expression by hypoxia is mediated predominantly by hypoxia-inducible factor 1 (HIF-1)**. *J Pathol* 2005, **206**(3):291-304.
157. Ning W, Chu TJ, Li CJ, Choi AM, Peters DG: **Genome-wide analysis of the endothelial transcriptome under short-term chronic hypoxia**. *Physiol Genomics* 2004, **18**(1):70-78.
158. Manalo DJ, Rowan A, Lavoie T, Natarajan L, Kelly BD, Ye SQ, Garcia JG, Semenza GL: **Transcriptional regulation of vascular endothelial cell responses to hypoxia by HIF-1**. *Blood* 2005, **105**(2):659-669.
159. Leonard MO, Cottell DC, Godson C, Brady HR, Taylor CT: **The role of HIF-1 alpha in transcriptional regulation of the proximal tubular epithelial cell response to hypoxia**. *J Biol Chem* 2003, **278**(41):40296-40304.
160. Lee HT, Emala CW: **Protective effects of renal ischemic preconditioning and adenosine pretreatment: role of A(1) and A(3) receptors**. *Am J Physiol Renal Physiol* 2000, **278**(3):F380-387.
161. Kitagawa K, Matsumoto M, Tagaya M, Hata R, Ueda H, Niinobe M, Handa N, Fukunaga R, Kimura K, Mikoshiba K, et al.: **'Ischemic tolerance' phenomenon found in the brain**. *Brain Res* 1990, **528**(1):21-24.
162. Gidday JM, Fitzgibbons JC, Shah AR, Park TS: **Neuroprotection from ischemic brain injury by hypoxic preconditioning in the neonatal rat**. *Neurosci Lett* 1994, **168**(1-2):221-224.
163. Emerson MR, Nelson SR, Samson FE, Pazdernik TL: **A global hypoxia preconditioning model: neuroprotection against seizure-induced specific gravity changes (edema) and brain damage in rats**. *Brain Res Brain Res Protoc* 1999, **4**(3):360-366.
164. Dong JW, Zhu HF, Zhu WZ, Ding HL, Ma TM, Zhou ZN: **Intermittent hypoxia attenuates ischemia/reperfusion induced apoptosis in cardiac myocytes via regulating Bcl-2/Bax expression**. *Cell Res* 2003, **13**(5):385-391.
165. Cai Z, Manalo DJ, Wei G, Rodriguez ER, Fox-Talbot K, Lu H, Zweier JL, Semenza GL: **Hearts from rodents exposed to intermittent hypoxia or erythropoietin are protected against ischemia-reperfusion injury**. *Circulation* 2003, **108**(1):79-85.
166. Gartel AL, Serfas MS, Tyner AL: **p21--negative regulator of the cell cycle**. *Proc Soc Exp Biol Med* 1996, **213**(2):138-149.
167. Brugarolas J, Moberg K, Boyd SD, Taya Y, Jacks T, Lees JA: **Inhibition of cyclin-dependent kinase 2 by p21 is necessary for retinoblastoma protein-mediated G1 arrest after gamma-irradiation**. *Proc Natl Acad Sci U S A* 1999, **96**(3):1002-1007.
168. Waga S, Hannon GJ, Beach D, Stillman B: **The p21 inhibitor of cyclin-dependent kinases controls DNA replication by interaction with PCNA**. *Nature* 1994, **369**(6481):574-578.
169. LaBaer J, Garrett MD, Stevenson LF, Slingerland JM, Sandhu C, Chou HS, Fattaey A, Harlow E: **New functional activities for the p21 family of CDK inhibitors**. *Genes Dev* 1997, **11**(7):847-862.
170. Gartel AL, Tyner AL: **The role of the cyclin-dependent kinase inhibitor p21 in apoptosis**. *Mol Cancer Ther* 2002, **1**(8):639-649.
171. Liu S, Bishop WR, Liu M: **Differential effects of cell cycle regulatory protein p21(WAF1/Cip1) on apoptosis and sensitivity to cancer chemotherapy**. *Drug Resist Updat* 2003, **6**(4):183-195.

172. Coqueret O: **New roles for p21 and p27 cell-cycle inhibitors: a function for each cell compartment?** *Trends Cell Biol* 2003, **13**(2):65-70.

173. Seoane J, Le HV, Massague J: **Myc suppression of the p21(Cip1) Cdk inhibitor influences the outcome of the p53 response to DNA damage**. *Nature* 2002, **419**(6908):729-734.

174. Suzuki A, Tsutomi Y, Akahane K, Araki T, Miura M: **Resistance to Fas-mediated apoptosis: activation of caspase 3 is regulated by cell cycle regulator p21WAF1 and IAP gene family ILP**. *Oncogene* 1998, **17**(8):931-939.

175. Dotto GP: **p21(WAF1/Cip1): more than a break to the cell cycle?** *Biochim Biophys Acta* 2000, **1471**(1):M43-56.

176. Koshiji M, Kageyama Y, Pete EA, Horikawa I, Barrett JC, Huang LE: **HIF-1alpha induces cell cycle arrest by functionally counteracting Myc**. *Embo J* 2004, **23**(9):1949-1956.

177. Lim JH, Park JW, Kim MS, Park SK, Johnson RS, Chun YS: **Bafilomycin induces the p21-mediated growth inhibition of cancer cells under hypoxic conditions by expressing hypoxia-inducible factor-1alpha**. *Mol Pharmacol* 2006, **70**(6):1856-1865.

178. Langley B, D'Annibale MA, Suh K, Ayoub I, Tolhurst A, Bastan B, Yang L, Ko B, Fisher M, Cho S, Beal MF, Ratan RR: **Pulse inhibition of histone deacetylases induces complete resistance to oxidative death in cortical neurons without toxicity and reveals a role for cytoplasmic p21(waf1/cip1) in cell cycle-independent neuroprotection**. *J Neurosci* 2008, **28**(1):163-176.

179. Zaman K, Ryu H, Hall D, O'Donovan K, Lin KI, Miller MP, Marquis JC, Baraban JM, Semenza GL, Ratan RR: **Protection from oxidative stress-induced apoptosis in cortical neuronal cultures by iron chelators is associated with enhanced DNA binding of hypoxia-inducible factor-1 and ATF-1/CREB and increased expression of glycolytic enzymes, p21(waf1/cip1), and erythropoietin**. *J Neurosci* 1999, **19**(22):9821-9830.

180. O'Reilly MA: **Redox activation of p21Cip1/WAF1/Sdi1: a multifunctional regulator of cell survival and death**. *Antioxid Redox Signal* 2005, **7**(1-2):108-118.

181. Wetzel M, Rosenberg GA, Cunningham LA: **Tissue inhibitor of metalloproteinases-3 and matrix metalloproteinase-3 regulate neuronal sensitivity to doxorubicin-induced apoptosis**. *Eur J Neurosci* 2003, **18**(5):1050-1060.

182. Wetzel M, Li L, Harms KM, Roitbak T, Ventura PB, Rosenberg GA, Khokha R, Cunningham LA: **Tissue inhibitor of metalloproteinases-3 facilitates Fas-mediated neuronal cell death following mild ischemia**. *Cell Death Differ* 2008, **15**(1):143-151.

183. Vinson C, Myakishev M, Acharya A, Mir AA, Moll JR, Bonovich M: **Classification of human B-ZIP proteins based on dimerization properties**. *Mol Cell Biol* 2002, **22**(18):6321-6335.

184. Ramji DP, Foka P: **CCAAT/enhancer-binding proteins: structure, function and regulation**. *Biochem J* 2002, **365**(Pt 3):561-575.

185. Johnson P: **Molecular stop signs: regulation of cell-cycle arrest by C/EBP transcription factors.** *J Cell Sci* 2005, **118**(Pt 12):2545-2555.

186. Hogan JC, Stephens JM: **Effects of leukemia inhibitory factor on 3T3-L1 adipocytes**. *J Endocrinol* 2005, **185**(3):485-496.

187. Ueki Y, Wang J, Chollangi S, Ash JD: **STAT3 activation in photoreceptors by leukemia inhibitory factor is associated with protection from light damage**. *J Neurochem* 2008, **105**(3):784-796.

188. Joly S, Lange C, Thiersch M, Samardzija M, Grimm C: **Leukemia inhibitory factor extends the lifespan of injured photoreceptors in vivo**. *J Neurosci* 2008, **28**(51):13765-13774.

189. Stephanou A: **Role of STAT-1 and STAT-3 in ischaemia/reperfusion injury**. *J Cell Mol Med* 2004, **8**(4):519-525.

190. Cantwell CA, Sterneck E, Johnson PF: **Interleukin-6-specific activation of the C/EBPdelta gene in hepatocytes is mediated by Stat3 and Sp1**. *Mol Cell Biol* 1998, **18**(4):2108-2117.

191. Chen L, Wu W, Dentchev T, Wong R, Dunaief JL: **Increased metallothionein in light damaged mouse retinas**. *Exp Eye Res* 2004, **79**(2):287-293.

192. Suemori S, Shimazawa M, Kawase K, Satoh M, Nagase H, Yamamoto T, Hara H: **Metallothionein, an endogenous antioxidant, protects against retinal neuron damage in mice**. *Invest Ophthalmol Vis Sci* 2006, **47**(9):3975-3982.

193. Kang YJ, Chen Y, Yu A, Voss-McCowan M, Epstein PN: **Overexpression of metallothionein in the heart of transgenic mice suppresses doxorubicin cardiotoxicity**. *J Clin Invest* 1997, **100**(6):1501-1506.

194. Ebadi M, Brown-Borg H, El Refaey H, Singh BB, Garrett S, Shavali S, Sharma SK: **Metallothionein-mediated neuroprotection in genetically engineered mouse models of Parkinson's disease**. *Brain Res Mol Brain Res* 2005, **134**(1):67-75.

195. West AK, Hidalgo J, Eddins D, Levin ED, Aschner M: **Metallothionein in the central nervous system: Roles in protection, regeneration and cognition**. *Neurotoxicology* 2008, **29**(3):489-503.

196. Lazo JS, Kondo Y, Dellapiazza D, Michalska AE, Choo KH, Pitt BR: **Enhanced sensitivity to oxidative stress in cultured embryonic cells from transgenic mice deficient in metallothionein I and II genes**. *J Biol Chem* 1995, **270**(10):5506-5510.

197. Yamashita H, Horie K, Yamamoto T, Nagano T, Hirano T: **Light-induced retinal damage in mice. Hydrogen peroxide production and superoxide dismutase activity in retina**. *Retina* 1992, **12**(1):59-66.

198. Sakaguchi H, Miyagi M, Darrow RM, Crabb JS, Hollyfield JG, Organisciak DT, Crabb JW: **Intense light exposure changes the crystallin content in retina**. *Exp Eye Res* 2003, **76**(1):131-133.

199. Rohrer B, Matthes MT, LaVail MM, Reichardt LF: **Lack of p75 receptor does not protect photoreceptors from light-induced cell death**. *Exp Eye Res* 2003, **76**(1):125-129.

200. Miyagi M, Sakaguchi H, Darrow RM, Yan L, West KA, Aulak KS, Stuehr DJ, Hollyfield JG, Organisciak DT, Crabb JW: **Evidence that light modulates protein nitration in rat retina**. *Mol Cell Proteomics* 2002, **1**(4):293-303.

201. Shen J, Yang X, Dong A, Petters RM, Peng YW, Wong F, Campochiaro PA: **Oxidative damage is a potential cause of cone cell death in retinitis pigmentosa**. *J Cell Physiol* 2005, **203**(3):457-464.

202. Dong A, Xie B, Shen J, Yoshida T, Yokoi K, Hackett SF, Campochiaro PA: **Oxidative stress promotes ocular neovascularization**. *J Cell Physiol* 2009.

203. Ahuja-Jensen P, Johnsen-Soriano S, Ahuja S, Bosch-Morell F, Sancho-Tello M, Romero FJ, Abrahamson M, van Veen T: **Low glutathione peroxidase in rd1 mouse retina increases oxidative stress and proteases**. *Neuroreport* 2007, **18**(8):797-801.

204. Heuchel R, Radtke F, Georgiev O, Stark G, Aguet M, Schaffner W: **The transcription factor MTF-1 is essential for basal and heavy metal-induced metallothionein gene expression**. *Embo J* 1994, **13**(12):2870-2875.

205. Oshima Y, Fujio Y, Nakanishi T, Itoh N, Yamamoto Y, Negoro S, Tanaka K, Kishimoto T, Kawase I, Azuma J: **STAT3 mediates cardioprotection against ischemia/reperfusion injury through metallothionein induction in the heart**. *Cardiovasc Res* 2005, **65**(2):428-435.

206. Wenger RH: **Cellular adaptation to hypoxia: O2-sensing protein hydroxylases, hypoxia-inducible transcription factors, and O2-regulated gene expression**. *Faseb J* 2002, **16**(10):1151-1162.

207. Shima DT, Kuroki M, Deutsch U, Ng YS, Adamis AP, D'Amore PA: **The mouse gene for vascular endothelial growth factor. Genomic structure, definition of the transcriptional unit, and characterization of transcriptional and post-transcriptional regulatory sequences**. *J Biol Chem* 1996, **271**(7):3877-3883.

208. Laughner E, Taghavi P, Chiles K, Mahon PC, Semenza GL: **HER2 (neu) signaling increases the rate of hypoxia-inducible factor 1alpha (HIF-1alpha) synthesis: novel mechanism for HIF-1-mediated vascular endothelial growth factor expression**. *Mol Cell Biol* 2001, **21**(12):3995-4004.

209. Ikeda E, Achen MG, Breier G, Risau W: **Hypoxia-induced transcriptional activation and increased mRNA stability of vascular endothelial growth factor in C6 glioma cells**. *J Biol Chem* 1995, **270**(34):19761-19766.

210. Forsythe JA, Jiang BH, Iyer NV, Agani F, Leung SW, Koos RD, Semenza GL: **Activation of vascular endothelial growth factor gene transcription by hypoxia-inducible factor 1**. *Mol Cell Biol* 1996, **16**(9):4604-4613.

211. Penn JS, Madan A, Caldwell RB, Bartoli M, Caldwell RW, Hartnett ME: **Vascular endothelial growth factor in eye disease**. *Prog Retin Eye Res* 2008, **27**(4):331-371.

212. Witmer AN, Vrensen GF, Van Noorden CJ, Schlingemann RO: **Vascular endothelial growth factors and angiogenesis in eye disease**. *Prog Retin Eye Res* 2003, **22**(1):1-29.

213. Sakamoto T, Sakamoto H, Murphy TL, Spee C, Soriano D, Ishibashi T, Hinton DR, Ryan SJ: **Vessel formation by choroidal endothelial cells in vitro is modulated by retinal pigment epithelial cells**. *Arch Ophthalmol* 1995, **113**(4):512-520.

214. Saint-Geniez M, Maldonado AE, D'Amore PA: **VEGF expression and receptor activation in the choroid during development and in the adult**. *Invest Ophthalmol Vis Sci* 2006, **47**(7):3135-3142.

215. Blaauwgeers HG, Holtkamp GM, Rutten H, Witmer AN, Koolwijk P, Partanen TA, Alitalo K, Kroon ME, Kijlstra A, van Hinsbergh VW, Schlingemann RO: **Polarized vascular endothelial growth factor secretion by human retinal pigment epithelium and localization of vascular endothelial growth factor receptors on the inner choriocapillaris. Evidence for a trophic paracrine relation**. *Am J Pathol* 1999, **155**(2):421-428.

216. Maharaj AS, Saint-Geniez M, Maldonado AE, D'Amore PA: **Vascular endothelial growth factor localization in the adult**. *Am J Pathol* 2006, **168**(2):639-648.

217. Yang X, Cepko CL: **Flk-1, a receptor for vascular endothelial growth factor (VEGF), is expressed by retinal progenitor cells**. *J Neurosci* 1996, **16**(19):6089-6099.

218. Hashimoto T, Zhang XM, Chen BY, Yang XJ: **VEGF activates divergent intracellular signaling components to regulate retinal progenitor cell proliferation and neuronal differentiation**. *Development* 2006, **133**(11):2201-2210.

219. Wang F, Rendahl KG, Manning WC, Quiroz D, Coyne M, Miller SS: **AAV-mediated expression of vascular endothelial growth factor induces choroidal neovascularization in rat**. *Invest Ophthalmol Vis Sci* 2003, **44**(2):781-790.

220. Roberts WG, Palade GE: **Increased microvascular permeability and endothelial fenestration induced by vascular endothelial growth factor**. *J Cell Sci* 1995, **108 (Pt 6)**:2369-2379.

221. Qaum T, Xu Q, Joussen AM, Clemens MW, Qin W, Miyamoto K, Hassessian H, Wiegand SJ, Rudge J, Yancopoulos GD, Adamis AP: **VEGF-initiated blood-retinal barrier breakdown in early diabetes**. *Invest Ophthalmol Vis Sci* 2001, **42**(10):2408-2413.

222. Okamoto N, Tobe T, Hackett SF, Ozaki H, Vinores MA, LaRochelle W, Zack DJ, Campochiaro PA: **Transgenic mice with increased expression of vascular endothelial growth factor in the retina: a new model of intraretinal and subretinal neovascularization**. *Am J Pathol* 1997, **151**(1):281-291.

223. Madan A, Penn JS: **Animal models of oxygen-induced retinopathy**. *Front Biosci* 2003, **8**:d1030-1043.

224. Lopez PF, Sippy BD, Lambert HM, Thach AB, Hinton DR: **Transdifferentiated retinal pigment epithelial cells are immunoreactive for vascular endothelial growth factor in surgically excised age-related macular degeneration-related choroidal neovascular membranes**. *Invest Ophthalmol Vis Sci* 1996, **37**(5):855-868.

225. Ishida S, Usui T, Yamashiro K, Kaji Y, Ahmed E, Carrasquillo KG, Amano S, Hida T, Oguchi Y, Adamis AP: **VEGF164 is proinflammatory in the diabetic retina**. *Invest Ophthalmol Vis Sci* 2003, **44**(5):2155-2162.

226. Hammes HP, Lin J, Bretzel RG, Brownlee M, Breier G: **Upregulation of the vascular endothelial growth factor/vascular endothelial growth factor receptor system in experimental background diabetic retinopathy of the rat**. *Diabetes* 1998, **47**(3):401-406.

227. Duh E, Aiello LP: **Vascular endothelial growth factor and diabetes: the agonist versus antagonist paradox**. *Diabetes* 1999, **48**(10):1899-1906.

228. Bates DO, Curry FE: **Vascular endothelial growth factor increases microvascular permeability via a Ca(2+)-dependent pathway**. *Am J Physiol* 1997, **273**(2 Pt 2):H687-694.

229. Aiello LP, Avery RL, Arrigg PG, Keyt BA, Jampel HD, Shah ST, Pasquale LR, Thieme H, Iwamoto MA, Park JE, et al.: **Vascular endothelial growth factor in ocular fluid of patients with diabetic retinopathy and other retinal disorders**. *N Engl J Med* 1994, **331**(22):1480-1487.

230. Adamis AP, Miller JW, Bernal MT, D'Amico DJ, Folkman J, Yeo TK, Yeo KT: **Increased vascular endothelial growth factor levels in the vitreous of eyes with proliferative diabetic retinopathy**. *Am J Ophthalmol* 1994, **118**(4):445-450.

231. Ferrara N, Houck K, Jakeman L, Leung DW: **Molecular and biological properties of the vascular endothelial growth factor family of proteins**. *Endocr Rev* 1992, **13**(1):18-32.

232. Hinson JP, Kapas S, Smith DM: **Adrenomedullin, a multifunctional regulatory peptide**. *Endocr Rev* 2000, **21**(2):138-167.

233. Eto T: **A review of the biological properties and clinical implications of adrenomedullin and proadrenomedullin N-terminal 20 peptide (PAMP), hypotensive and vasodilating peptides**. *Peptides* 2001, **22**(11):1693-1711.

234. Xia CF, Yin H, Borlongan CV, Chao J, Chao L: **Adrenomedullin gene delivery protects against cerebral ischemic injury by promoting astrocyte migration and survival**. *Hum Gene Ther* 2004, **15**(12):1243-1254.

235. Tixier E, Leconte C, Touzani O, Roussel S, Petit E, Bernaudin M: **Adrenomedullin protects neurons against oxygen glucose deprivation stress in an autocrine and paracrine manner**. *J Neurochem* 2008, **106**(3):1388-1403.

236. Miyashita K, Itoh H, Arai H, Suganami T, Sawada N, Fukunaga Y, Sone M, Yamahara K, Yurugi-Kobayashi T, Park K, Oyamada N, Sawada N, Taura D, Tsujimoto H, Chao TH, Tamura N, Mukoyama M, Nakao K: **The neuroprotective and vasculo-neuro-regenerative roles of adrenomedullin in ischemic brain and its therapeutic potential**. *Endocrinology* 2006, **147**(4):1642-1653.

237. Garayoa M, Martinez A, Lee S, Pio R, An WG, Neckers L, Trepel J, Montuenga LM, Ryan H, Johnson R, Gassmann M, Cuttitta F: **Hypoxia-inducible factor-1 (HIF-1) up-regulates adrenomedullin expression in human tumor cell lines during oxygen deprivation: a possible promotion mechanism of carcinogenesis**. *Mol Endocrinol* 2000, **14**(6):848-862.

238. Cormier-Regard S, Nguyen SV, Claycomb WC: **Adrenomedullin gene expression is developmentally regulated and induced by hypoxia in rat ventricular cardiac myocytes**. *J Biol Chem* 1998, **273**(28):17787-17792.

239. Zhu Y, Zhang L, Gidday JM: **Deferroxamine preconditioning promotes long-lasting retinal ischemic tolerance**. *J Ocul Pharmacol Ther* 2008, **24**(6):527-535.

240. Vingolo EM, Lupo S, Domanico D, Cotesta D, Petramala L, Grenga R, Letizia C: **Adrenomedullin plasma concentrations in patients with retinitis pigmentosa**. *Clin Biochem* 2005, **38**(8):735-738.

241. James RW: **A long and winding road: defining the biological role and clinical importance of paraoxonases**. *Clin Chem Lab Med* 2006, **44**(9):1052-1059.

242. Shih DM, Gu L, Xia YR, Navab M, Li WF, Hama S, Castellani LW, Furlong CE, Costa LG, Fogelman AM, Lusis AJ: **Mice lacking serum paraoxonase are susceptible to organophosphate toxicity and atherosclerosis**. *Nature* 1998, **394**(6690):284-287.

243. Mackness B, Quarck R, Verreth W, Mackness M, Holvoet P: **Human paraoxonase-1 overexpression inhibits atherosclerosis in a mouse model of metabolic syndrome**. *Arterioscler Thromb Vasc Biol* 2006, **26**(7):1545-1550.

244. Mackness B, Hine D, Liu Y, Mastorikou M, Mackness M: **Paraoxonase-1 inhibits oxidised LDL-induced MCP-1 production by endothelial cells**. *Biochem Biophys Res Commun* 2004, **318**(3):680-683.

245. Ferre N, Marsillach J, Camps J, Mackness B, Mackness M, Riu F, Coll B, Tous M, Joven J: **Paraoxonase-1 is associated with oxidative stress, fibrosis and FAS expression in chronic liver diseases**. *J Hepatol* 2006, **45**(1):51-59.

246. Tanito M, Li F, Elliott MH, Dittmar M, Anderson RE: **Protective effect of TEMPOL derivatives against light-induced retinal damage in rats**. *Invest Ophthalmol Vis Sci* 2007, **48**(4):1900-1905.

247. Solak ZA, Kabaroglu C, Cok G, Parildar Z, Bayindir U, Ozmen D, Bayindir O: **Effect of different levels of cigarette smoking on lipid peroxidation, glutathione enzymes and paraoxonase 1 activity in healthy people**. *Clin Exp Med* 2005, **5**(3):99-105.

248. Mackness B, Durrington PN, Abuashia B, Boulton AJ, Mackness MI: **Low paraoxonase activity in type II diabetes mellitus complicated by retinopathy**. *Clin Sci (Lond)* 2000, **98**(3):355-363.

249. Isik B, Ceylan A, Isik R: **Oxidative stress in smokers and non-smokers**. *Inhal Toxicol* 2007, **19**(9):767-769.

250. Baskol G, Karakucuk S, Oner AO, Baskol M, Kocer D, Mirza E, Saraymen R, Ustdal M: **Serum paraoxonase 1 activity and lipid peroxidation levels in patients with age-related macular degeneration**. *Ophthalmologica* 2006, **220**(1):12-16.

251. Inohara N, Gourley TS, Carrio R, Muniz M, Merino J, Garcia I, Koseki T, Hu Y, Chen S, Nunez G: **Diva, a Bcl-2 homologue that binds directly to Apaf-1 and induces BH3-independent cell death**. *J Biol Chem* 1998, **273**(49):32479-32486.

252. Song Q, Kuang Y, Dixit VM, Vincenz C: **Boo, a novel negative regulator of cell death, interacts with Apaf-1**. *Embo J* 1999, **18**(1):167-178.

253. Naumann U, Weit S, Wischhusen J, Weller M: **Diva/Boo is a negative regulator of cell death in human glioma cells**. *FEBS Lett* 2001, **505**(1):23-26.

254. Doonan F, Donovan M, Cotter TG: **Caspase-independent photoreceptor apoptosis in mouse models of retinal degeneration**. *J Neurosci* 2003, **23**(13):5723-5731.

255. Wu G, Zhou L, Khidr L, Guo XE, Kim W, Lee YM, Krasieva T, Chen PL: **A novel role of the chromokinesin Kif4A in DNA damage response**. *Cell Cycle* 2008, **7**(13):2013-2020.

256. Mazumdar M, Lee JH, Sengupta K, Ried T, Rane S, Misteli T: **Tumor formation via loss of a molecular motor protein**. *Curr Biol* 2006, **16**(15):1559-1564.

257. Midorikawa R, Takei Y, Hirokawa N: **KIF4 motor regulates activity-dependent neuronal survival by suppressing PARP-1 enzymatic activity**. *Cell* 2006, **125**(2):371-383.

258. Tulin A, Spradling A: **Chromatin loosening by poly(ADP)-ribose polymerase (PARP) at Drosophila puff loci**. *Science* 2003, **299**(5606):560-562.

259. Griesenbeck J, Ziegler M, Tomilin N, Schweiger M, Oei SL: **Stimulation of the catalytic activity of poly(ADP-ribosyl) transferase by transcription factor Yin Yang 1**. *FEBS Lett* 1999, **443**(1):20-24.

260. Pieper AA, Verma A, Zhang J, Snyder SH: **Poly (ADP-ribose) polymerase, nitric oxide and cell death**. *Trends Pharmacol Sci* 1999, **20**(4):171-181.

261. Lee JY, Kim YJ, Kim TY, Koh JY, Kim YH: **Essential role for zinc-triggered p75NTR activation in preconditioning neuroprotection**. *J Neurosci* 2008, **28**(43):10919-10927.

262. Paquet-Durand F, Silva J, Talukdar T, Johnson LE, Azadi S, van Veen T, Ueffing M, Hauck SM, Ekstrom PA: **Excessive activation of poly(ADP-ribose) polymerase contributes to inherited photoreceptor degeneration in the retinal degeneration 1 mouse**. *J Neurosci* 2007, **27**(38):10311-10319.

263. Miki K, Uehara N, Shikata N, Matsumura M, Tsubura A: **Poly (ADP-ribose) polymerase inhibitor 3-aminobenzamide rescues N-methyl-N-nitrosourea-induced photoreceptor cell apoptosis in Sprague-Dawley rats through preservation of nuclear factor-kappaB activity**. *Exp Eye Res* 2007, **84**(2):285-292.

264. Goebel DJ, Winkler BS: **Blockade of PARP activity attenuates poly(ADP-ribosyl)ation but offers only partial neuroprotection against NMDA-induced cell death in the rat retina**. *J Neurochem* 2006, **98**(6):1732-1745.

265. Chiang SK, Lam TT: **Post-treatment at 12 or 18 hours with 3-aminobenzamide ameliorates retinal ischemia-reperfusion damage**. *Invest Ophthalmol Vis Sci* 2000, **41**(10):3210-3214.

266. Gregoire S, Yang XJ: **Association with class IIa histone deacetylases upregulates the sumoylation of MEF2 transcription factors**. *Mol Cell Biol* 2005, **25**(6):2273-2287.

267. Li Z, McKercher SR, Cui J, Nie Z, Soussou W, Roberts AJ, Sallmen T, Lipton JH, Talantova M, Okamoto S, Lipton SA: **Myocyte enhancer factor 2C as a neurogenic and antiapoptotic transcription factor in murine embryonic stem cells**. *J Neurosci* 2008, **28**(26):6557-6568.

268. Smith PD, Mount MP, Shree R, Callaghan S, Slack RS, Anisman H, Vincent I, Wang X, Mao Z, Park DS: **Calpain-regulated p35/cdk5 plays a central role in dopaminergic neuron death through modulation of the transcription factor myocyte enhancer factor 2**. *J Neurosci* 2006, **26**(2):440-447.

269. Fu W, Wei J, Gu J: **MEF2C mediates the activation induced cell death (AICD) of macrophages**. *Cell Res* 2006, **16**(6):559-565.

270. Hoppeler T, Hendrickson P, Dietrich C, Reme C: **Morphology and time-course of defined photochemical lesions in the rabbit retina**. *Curr Eye Res* 1988, **7**(9):849-860.

271. Gordon WC, Casey DM, Lukiw WJ, Bazan NG: **DNA damage and repair in light-induced photoreceptor degeneration**. *Invest Ophthalmol Vis Sci* 2002, **43**(11):3511-3521.

272. Sutherland LC, Rintala-Maki ND, White RD, Morin CD: **RNA binding motif (RBM) proteins: a novel family of apoptosis modulators?** *J Cell Biochem* 2005, **94**(1):5-24.

273. Kita H, Carmichael J, Swartz J, Muro S, Wyttenbach A, Matsubara K, Rubinsztein DC, Kato K: **Modulation of polyglutamine-induced cell death by genes identified by expression profiling**. *Hum Mol Genet* 2002, **11**(19):2279-2287.

274. Baghdoyan S, Dubreuil P, Eberle F, Gomez S: **Capture of cytokine-responsive genes (NACA and RBM3) using a gene trap approach**. *Blood* 2000, **95**(12):3750-3757.

275. Ryan HE, Poloni M, McNulty W, Elson D, Gassmann M, Arbeit JM, Johnson RS: **Hypoxia-inducible factor-1alpha is a positive factor in solid tumor growth**. *Cancer Res* 2000, **60**(15):4010-4015.

276. Weber P, Metzger D, Chambon P: **Temporally controlled targeted somatic mutagenesis in the mouse brain**. *Eur J Neurosci* 2001, **14**(11):1777-1783.

277. Le YZ, Zheng L, Zheng W, Ash JD, Agbaga MP, Zhu M, Anderson RE: **Mouse opsin promoter-directed Cre recombinase expression in transgenic mice**. *Mol Vis* 2006, **12**:389-398.

278. Sowter HM, Ratcliffe PJ, Watson P, Greenberg AH, Harris AL: **HIF-1-dependent regulation of hypoxic induction of the cell death factors BNIP3 and NIX in human tumors**. *Cancer Res* 2001, **61**(18):6669-6673.

279. del Peso L, Castellanos MC, Temes E, Martin-Puig S, Cuevas Y, Olmos G, Landazuri MO: **The von Hippel Lindau/hypoxia-inducible factor (HIF) pathway regulates the transcription of the HIF-proline hydroxylase genes in response to low oxygen**. *J Biol Chem* 2003, **278**(49):48690-48695.

280. Berra E, Benizri E, Ginouves A, Volmat V, Roux D, Pouyssegur J: **HIF prolyl-hydroxylase 2 is the key oxygen sensor setting low steady-state levels of HIF-1alpha in normoxia**. *Embo J* 2003, **22**(16):4082-4090.

281. Chen C, Pore N, Behrooz A, Ismail-Beigi F, Maity A: **Regulation of glut1 mRNA by hypoxia-inducible factor-1. Interaction between H-ras and hypoxia**. *J Biol Chem* 2001, **276**(12):9519-9525.

282. Cringle SJ, Yu DY, Yu PK, Su EN: **Intraretinal oxygen consumption in the rat in vivo**. *Invest Ophthalmol Vis Sci* 2002, **43**(6):1922-1927.

283. Wang GL, Semenza GL: **General involvement of hypoxia-inducible factor 1 in transcriptional response to hypoxia**. *Proc Natl Acad Sci U S A* 1993, **90**(9):4304-4308.

284. Maxwell PH, Pugh CW, Ratcliffe PJ: **Inducible operation of the erythropoietin 3' enhancer in multiple cell lines: evidence for a widespread oxygen-sensing mechanism**. *Proc Natl Acad Sci U S A* 1993, **90**(6):2423-2427.

285. Baranova O, Miranda LF, Pichiule P, Dragatsis I, Johnson RS, Chavez JC: **Neuron-specific inactivation of the hypoxia inducible factor 1 alpha increases brain injury in a mouse model of transient focal cerebral ischemia**. *J Neurosci* 2007, **27**(23):6320-6332.

286. Helton R, Cui J, Scheel JR, Ellison JA, Ames C, Gibson C, Blouw B, Ouyang L, Dragatsis I, Zeitlin S, Johnson RS, Lipton SA, Barlow C: **Brain-specific knock-out of hypoxia-inducible factor-1alpha reduces rather than increases hypoxic-ischemic damage**. *J Neurosci* 2005, **25**(16):4099-4107.

287. Cai Z, Zhong H, Bosch-Marce M, Fox-Talbot K, Wang L, Wei C, Trush MA, Semenza GL: **Complete loss of ischaemic preconditioning-induced cardioprotection in mice with partial deficiency of HIF-1 alpha**. *Cardiovasc Res* 2008, **77**(3):463-470.

288. Bernhardt WM, Warnecke C, Willam C, Tanaka T, Wiesener MS, Eckardt KU: **Organ protection by hypoxia and hypoxia-inducible factors**. *Methods Enzymol* 2007, **435**:221-245.

289. Bernhardt WM, Campean V, Kany S, Jurgensen JS, Weidemann A, Warnecke C, Arend M, Klaus S, Gunzler V, Amann K, Willam C, Wiesener MS, Eckardt KU: **Preconditional activation of hypoxia-inducible factors ameliorates ischemic acute renal failure**. *J Am Soc Nephrol* 2006, **17**(7):1970-1978.

290. Bernhardt WM, Schmitt R, Rosenberger C, Munchenhagen PM, Grone HJ, Frei U, Warnecke C, Bachmann S, Wiesener MS, Willam C, Eckardt KU: **Expression of hypoxia-inducible transcription factors in developing human and rat kidneys**. *Kidney Int* 2006, **69**(1):114-122.

291. Park AM, Nagase H, Kumar SV, Suzuki YJ: **Effects of intermittent hypoxia on the heart**. *Antioxid Redox Signal* 2007, **9**(6):723-729.

292. Yao SY, Soutto M, Sriram S: **Preconditioning with cobalt chloride or desferrioxamine protects oligodendrocyte cell line (MO3.13) from tumor necrosis factor-alpha-mediated cell death**. *J Neurosci Res* 2008, **86**(11):2403-2413.

293. Mu D, Chang YS, Vexler ZS, Ferriero DM: **Hypoxia-inducible factor 1alpha and erythropoietin upregulation with deferoxamine salvage after neonatal stroke**. *Exp Neurol* 2005, **195**(2):407-415.

294. Liu XB, Wang JA, Ogle ME, Wei L: **Prolyl hydroxylase inhibitor dimethyloxalylglycine enhances mesenchymal stem cell survival**. *J Cell Biochem* 2009.

295. Li YX, Ding SJ, Xiao L, Guo W, Zhan Q: **Desferoxamine preconditioning protects against cerebral ischemia in rats by inducing expressions of hypoxia inducible factor 1 alpha and erythropoietin**. *Neurosci Bull* 2008, **24**(2):89-95.

296. Jones NM, Kardashyan L, Callaway JK, Lee EM, Beart PM: **Long-term functional and protective actions of preconditioning with hypoxia, cobalt chloride, and desferrioxamine against hypoxic-ischemic injury in neonatal rats**. *Pediatr Res* 2008, **63**(6):620-624.

297. Hamrick SE, McQuillen PS, Jiang X, Mu D, Madan A, Ferriero DM: **A role for hypoxia-inducible factor-1alpha in desferoxamine neuroprotection**. *Neurosci Lett* 2005, **379**(2):96-100.

298. Chen W, Jadhav V, Tang J, Zhang JH: **HIF-1alpha inhibition ameliorates neonatal brain injury in a rat pup hypoxic-ischemic model**. *Neurobiol Dis* 2008, **31**(3):433-441.

299. Pugh CW, Ratcliffe PJ: **Regulation of angiogenesis by hypoxia: role of the HIF system**. *Nat Med* 2003, **9**(6):677-684.

300. Patel SA, Simon MC: **Biology of hypoxia-inducible factor-2alpha in development and disease**. *Cell Death Differ* 2008, **15**(4):628-634.

301. Kenneth NS, Rocha S: **Regulation of gene expression by hypoxia**. *Biochem J* 2008, **414**(1):19-29.

302. Lomb DJ, Desouza LA, Franklin JL, Freeman RS: **Prolyl hydroxylase inhibitors depend on extracellular glucose and HIF-2a to inhibit cell death caused by NGF deprivation: evidence that HIF-2a has a role in NGF-promoted survival of sympathetic neurons**. *Mol Pharmacol* 2009.

303. Rankin EB, Biju MP, Liu Q, Unger TL, Rha J, Johnson RS, Simon MC, Keith B, Haase VH: **Hypoxia-inducible factor-2 (HIF-2) regulates hepatic erythropoietin in vivo**. *J Clin Invest* 2007, **117**(4):1068-1077.

304. Morita M, Ohneda O, Yamashita T, Takahashi S, Suzuki N, Nakajima O, Kawauchi S, Ema M, Shibahara S, Udono T, Tomita K, Tamai M, Sogawa K, Yamamoto M, Fujii-Kuriyama Y: **HLF/HIF-2alpha is a key factor in retinopathy of prematurity in association with erythropoietin**. *Embo J* 2003, **22**(5):1134-1146.

305. Gruber M, Hu CJ, Johnson RS, Brown EJ, Keith B, Simon MC: **Acute postnatal ablation of Hif-2alpha results in anemia**. *Proc Natl Acad Sci U S A* 2007, **104**(7):2301-2306.

306. Chavez JC, Baranova O, Lin J, Pichiule P: **The transcriptional activator hypoxia inducible factor 2 (HIF-2/EPAS-1) regulates the oxygen-dependent expression of erythropoietin in cortical astrocytes**. *J Neurosci* 2006, **26**(37):9471-9481.

307. Brines ML, Ghezzi P, Keenan S, Agnello D, de Lanerolle NC, Cerami C, Itri LM, Cerami A: **Erythropoietin crosses the blood-brain barrier to protect against experimental brain injury**. *Proc Natl Acad Sci U S A* 2000, **97**(19):10526-10531.

308. Bernaudin M, Marti HH, Roussel S, Divoux D, Nouvelot A, MacKenzie ET, Petit E: **A potential role for erythropoietin in focal permanent cerebral ischemia in mice**. *J Cereb Blood Flow Metab* 1999, **19**(6):643-651.

309. Weishaupt JH, Rohde G, Polking E, Siren AL, Ehrenreich H, Bahr M: **Effect of erythropoietin axotomy-induced apoptosis in rat retinal ganglion cells**. *Invest Ophthalmol Vis Sci* 2004, **45**(5):1514-1522.

310. Kretz A, Happold CJ, Marticke JK, Isenmann S: **Erythropoietin promotes regeneration of adult CNS neurons via Jak2/Stat3 and PI3K/AKT pathway activation**. *Mol Cell Neurosci* 2005, **29**(4):569-579.

311. Shyu WC, Lin SZ, Chiang MF, Chen DC, Su CY, Wang HJ, Liu RS, Tsai CH, Li H: **Secretoneurin promotes neuroprotection and neuronal plasticity via the Jak2/Stat3 pathway in murine models of stroke**. *J Clin Invest* 2008, **118**(1):133-148.

312. Liu J, Narasimhan P, Yu F, Chan PH: **Neuroprotection by hypoxic preconditioning involves oxidative stress-mediated expression of hypoxia-inducible factor and erythropoietin**. *Stroke* 2005, **36**(6):1264-1269.

5.3 List of Abbreviations

(N/C)TAD	N/C-terminal transactivation domain
(rh)Epo	recombinant human Epo
A	amacrine cell
Adm	adrenomedullin
AMD	age related macular degeneration
Apaf-1	apoptotic peptidase activating factor 1
ARNT	aryl hydrocarbon receptor nuclear translocator
ATP	adenosine triphosphate
Bcl2l10	Bcl2-like 10
BDNF	brain-derived neurotrophic factor
bHLH	basic-helix-loop-helix domain
Bnip3	BCL2/adenovirus E1B 19 kDa interacting protein 3
C	cone
Ccl2	chemokine C-C motif ligand 2
CDK	cycline dependent kinase
Cdkn1a / p21	cycline dependent kinase inhibitor 1a
Cebpd	CCAAT/enhancer binding protein (C/EBP), delta
cGMP	cyclic guanosine monophosphate
Cox2/4	cytochrome c oxidase subunit 2/4
CTNF	ciliary neurotrophic factor
DAVID	Database for Annotation, Visualization and Integrated Discovery
DFO	desferroxamine
DHA	docosahexaenoic acid
DMOG	dimethyloxaloylglycine
DNA	deoxyribonucleic acid
DR	diabetic retinopathy
EGF	epidermal growth factor
Epo	erythropoietin
EpoR	erythropoietin receptor
FGF-2	fibroblast growth factor 2
FIH	factor inhibiting HIF
G	ganglion cell
GCL	ganglion cell layer
GDNF	glial cell derived neurotrophic factor

GDP	guanosine diphosphate
Glut1	glucose transporter 1
GTP	guanosine triphosphate
H	horizontal cell
HDL	high density lipoprotein
HGF	hepatocyte growth factor
HIF	hypoxia inducible factor
HO-1	heme oxygenase 1
Hsp27	heat shock protein 2
IGF 1/2	insulin-like growth facto 1/2
INL	inner nuclear layer
IPA	Ingenuity Pathway Analysis
IPAS	hypoxia inducible factor 3
IPL	inner plexiform layer
IS	inner segments
Jak2	janus kinase 2
Kif-4	kinesin family member 4
LdhA	lactate dehydrogenase A
LGN	laterale geniculate nucleus
LIF	leukemia inhibitor factor
M	müller cell
MNU	*N*-methyl-*N*-nitrosourea
Mt1/2	metallothionein 1/2
MTF-1	metal response element binding transcription factor 1
Myc	myelocytomatosis oncogene
NMDA	*N*-methyl-*D*-aspartic acid
NO	nitric oxide
O_2	oxygen
ODD	oxygen-dependent degradation domain
ONL	outer nuclear layer
OPL	outer plexiform layer
OS	outer segments
p53	transformation related protein 53
Parp1	poly (ADP-ribose) polymerase family, member 1
PAS1/2	Per-Arnt-Sim domain
PDE	phosphodiesterase / transducin
PDGF	platelet derived growth factor
PDH	pyruvat dehydrogenase
PDK	pyruvat dehydrogenase kinase
PE	retinal pigment epithelium

PHD	prolylhydroxylase
PND	postnatal day
Pon1 /2/3	paraoxonase 1/2/3
Pro	proline
R	rod
Rbm	RNA binding motif protein
RNA	ribonucleic acid
Rho	rhodopsin
RMA	robust multi-array average
RNFL	retinal nerve fiber layer
ROP	retinopathy of prematurity
ROS	reactive oxygen species
RP	retinitis pigmentosa
Rpgr	retinitis pigmentosa GTPase regulator
Slc7a1	solute carrier family 7, member 1
STAT3	signal transducer and activator of transcription 3
TAM	tamoxifen
Ush2a	usher syndrome 2a homolog
Vegf	vascular endothelial growth factor
VHL	von Hippel-Lindau disease tumor suppressor

6 ADDITIONAL PUBLICATIONS

6.1 Differential Role of Jak-STAT Signaling in Retinal Degenerations

Marijana Samardzija, Andreas Wenzel, Svenja Aufenberg, **Markus Thiersch**, Charlotte Remé, and Christian Grimm

Laboratory for Retinal Cell Biology, Department Ophthalmology, Center for Integrative Human Physiology (CIHP) and Neuroscience Center Zurich (ZNZ), University Hospital, Zurich, Switzerland

Published in FASEB *J.* 20, E1790–E1801 (2006)

6.1.1 Author contribution

Design:	MS and CG
Experiments:	MS, SA, **MT** (assisted in animal treatment; western blot, histology) and CG
Interpretation:	MS, AW, **MT**, CR and CG
Manuscript:	MS, AW and CG
Manuscript Correction:	MS, AW, **MT** and CG

6.1.2 Summary

The mechanisms of retinal degeneration are largely unknown. In this paper signaling pathways were analyzed in light induced retinal degeneration and in inherited models for autosomal recessive (*rd1* mouse) and for autosomal dominant (VPP mouse) retinitis pigmentosa. Expression and activation of proteins was death-stimulus specific. Erk1/2 was induced in light damaged retinas. In contrast, Akt was specifically activated in the inherited models. Nevertheless, as a common response to retinal injury, all models differentially expressed LIF and CLC – members of the interleukin (IL)-6 family – in the degenerating retina. These cytokines are known to signal via the Jak/STAT pathway, which is potentially involved in the regulation neurodegeneration

and neuroprotection. Indeed, in all models of degeneration Jak2, STAT1 and STAT3 were activated and cytokine-signaling suppressors CIS, SOCS1 and SOCS3 were induced as a negative feedback loop. In the model of light induced retinal degeneration, the cytokines LIF and CLC as well as the Jak/STAT signaling was activated between 6 and 24 h after illumination – prior to retinal apoptosis (peaks 36 h after light exposure). Further we showed, that a sub-lethal exposure to light was not sufficient to activate the Jak/STAT signaling, which suggests a potential role of the Jak/STAT pathway in retinal apoptosis. Application of AG-490 – a Jak family specific tyrosine kinase inhibitor – protected the retina against light induced retinal degeneration but failed to protect the retina against inherited retinal degeneration in the VPP mouse. AG-490 inactivated Jak2 in the protected, light exposed retinas and the degenerating retinas of the VPP mouse. Likewise, the potential Jak2 downstream target STAT1 remained inactive in both models. In contrast, STAT3 was activated in the degenerating VPP mouse but not in the protected retinas after light exposure. We concluded that Jak2 and the activation of the pro-apoptotic transcription factor STAT1 might be involved in light induced retinal degeneration but not in the inherited models. Further, we speculated that the activation of STAT3 – presumably a pro-survival factor – might occur via a different, Jak2 independent pathway and is an attempt to protect the retina. Because AG-490 treated mice were protected against light induced retinal degeneration, STAT3 activation might have been not required under these circumstances. Because Jak2, STAT1 and STAT3 were predominantly expressed in the INL and GCL, we hypothesized that photoreceptor injury initiates a response in the INL or GCL, which attempts to either minimize and/or accelerates photoreceptor cell death.

6.1.3 Manuscript

The FASEB Journal • FJ Express Full-Length Article

Differential role of Jak-STAT signaling in retinal degenerations

Marijana Samardzija, Andreas Wenzel, Svenja Aufenberg, Markus Thiersch, Charlotte Remé, and Christian Grimm[1]

Laboratory for Retinal Cell Biology, Department Ophthalmology, Center for Integrative Human Physiology (CIHP) and Neuroscience Center Zurich (ZNZ), University Hospital, Zürich, Switzerland

ABSTRACT **Retinal degeneration is a major cause of severe visual impairment or blindness. Understanding the underlying molecular mechanisms is a prerequisite to develop therapeutic approaches for human patients. We show in three mouse models that induced and inherited retinal degeneration induces LIF and CLC as members of the interleukin (IL)-6 family of proteins, activates proteins of the Jak-STAT signaling pathway, and up-regulates suppressors of cytokine signaling as a negative feedback loop. Inhibition of Jak2 leads to protection of photoreceptors in a model of induced but not in a model of inherited retinal degeneration. Differential activation of Akt suggests alternative pathways for cell death and/or survival in different models. Proteins induced during photoreceptor degeneration are not mainly expressed in photoreceptors but in cells of other retinal layers. This suggests a model in which photoreceptor injury is signaled to cells of the inner retina, which in turn initiate a response either to support viability or accelerate death of injured cells.—Samardzija, M., Wenzel, A., Aufenberg, S., Thiersch, M., Remé, C., Grimm, C. Differential role of Jak-STAT signaling in retinal degenerations. *FASEB J.* 20, E1790–E1801 (2006)**

Key Words: apoptosis · neuroprotection · photoreceptor

The neuronal retina is designed to absorb photons and convert the information into electrical signals that are transmitted to the brain. Due to their high specialization, photoreceptors are highly vulnerable to any endogenous or exogenous disturbances. So far more than 150 genes are known to cause some form of retinal disorder when mutated (http://www.sph.uth.tmc.edu/Retnet/). Retinitis pigmentosa (RP) and age-related macular degeneration (AMD), two frequent causes of severe visual impairment or blindness in patients, are characterized by the progressive loss of visual cells by apoptosis. Various animal models have been generated and used to investigate the molecular mechanisms of disease induction and progression. Besides genetically modified animals, the model of light-induced photoreceptor apoptosis is widely used to analyze signaling pathways during retinal cell death and to test the efficacy of neuroprotective substances (1–8).

Inhibition of photoreceptor apoptosis is one possible strategy to protect morphology and function of the retina and to prolong the period of useful vision in patients. Several compounds, including cytokines like fibroblast growth factor-2 (FGF-2), pigment epithelium-derived factor (PEDF), and ciliary neurotrophic factor (CNTF), have been shown to be protective in light damage and in models of inherited retinal degeneration; other factors protect photoreceptors only in induced but not inherited models (2, 5, 9–13). The mechanisms of protection are still largely unknown but may involve differential intracellular signaling cascades. CNTF, for example, is suggested to activate the Janus kinase signal transducer and activator of transcription (Jak-STAT) signaling pathway in ganglion cells and Muller cells. Such activated Muller cells may initiate a secondary, neuroprotective activity to preserve photoreceptor viability (14). FGF-2 and glial-derived neurotrophic factor (GDNF) might be such factors produced and released by Muller cells upon proper stimulation (15). In addition to Jak-STAT signaling, CNTF may also stimulate cell survival through phosphatidylinositol-3 phosphate kinase (PI3K)-mediated Akt signaling (16, 17).

Upon binding to the heterodimeric receptor complex containing gp130, members of the IL-6 family of cytokines induce autophosphorylation of cytoplasmic Jak kinases, which then phosphorylate downstream molecules such as transcription factors of the signal transducer and activator of transcription (STAT) family of proteins. In addition to the IL-6 family of cytokines that consists of seven members (leukemia inhibitory factor, LIF; cardiotrophin-1, CT-1; CNTF; cardiotrophin-like cytokine, CLC; oncostatin M, OSM; neuropoetin, NP; interleukin-6 (IL-6), IFN alpha and gamma are similarly strong activators of the Jak-STAT pathway (18). Of particular interest is the fact that Jak-STAT signaling has been implicated in both pro- and anti-apoptotic mechanisms. STAT1 is frequently described as being proapoptotic whereas STAT3 is often found in proliferating tumor cells and is suspected to be anti-

[1] Correspondence: Laboratory for Retinal Cell Biology, Department Ophthalmology, University Hospital, Frauenklinikstrasse 24, 8091 Zürich, Switzerland. E-mail: cgrimm@opht.unizh.ch

doi: 10.1096/fj.06-5895fje

apoptotic (19–21). This signaling cascade is controlled by a negative feedback loop involving members of the suppressor of cytokine signaling (SOCS) family of proteins (22).

Here we show that retinal degeneration in three different mouse models of induced and inherited photoreceptor apoptosis activates expression of several proteins of the IL-6 family of cytokines. This leads to the phosphorylation of members of the Jak-STAT signaling pathway and to the activation of a negative feedback loop by the increased expression of several members of the SOCS family. Interference with this pathway protects the retinal tissue against an acute toxic insult but not against photoreceptor degeneration in an inherited model. Our results suggest that Jak-STAT-mediated regulation of an intracellular response to photoreceptor degeneration is of differential importance for the retina depending on the nature of the insult.

RESULTS

Induction of LIF and CLC by acute light exposure

Injury or stress to the retina or to the optic nerve induces the expression of several neurotrophic factors, including CNTF and FGF-2. These molecules may act as survival factors protecting photoreceptors and other retinal cells from further damage (23–28). In the search for additional factors relevant for retinal injury, we tested expression of cytokines of the IL-6 family in BALB/c mice after exposure to high levels of white light, a treatment that represents a strong retinal insult leading to rapid photoreceptor apoptosis. Whereas CLC and LIF where highly up-regulated, peaking 12 h after light exposure, expression CNTF showed a slow response with a slight increase after 36 h (**Fig. 1*A*, *B***; Supplemental Table 1). CT-1 remained unchanged throughout the period investigated. TGF-β, another cytokine involved in many regulatory and inflammatory processes in the retina, increased slightly 48 h after light exposure. Increased expression of LIF and CLC well preceded the light-induced release of free nucleosomes, which peaks ~ 36 h after exposure and indicates a late stage of apoptosis (Fig. 1*B*) (2). Increased CNTF expression largely coincided with the apoptotic wave as detected by the biochemical detection of free nucleosomes.

Induction of the janus-activated kinase (JAK)-STAT pathway by acute light exposure

Upon binding to their respective receptors, members of the IL-6 family of cytokines activate the Jak/STAT signaling pathway. Functional receptors are heterodimeric complexes consisting of a common gp130 protein and of specific proteins like CNTF receptor or LIF receptor, all of which are expressed in the mammalian retina (**Fig. 2**; see Fig. 6) (29). In extracts of untreated retinas, activated (phosphorylated) Jak2, STAT1, and STAT3 were not or were only barely (p-STAT3) detectable, in contrast to p-Akt_{473} and p-Erk1,2 (Fig. 2). After light exposure, phosphorylation of Jak2, STAT1, STAT3, and Erk1,2 strongly increased, peaking ~ 6 to 12 h postillumination. The level of p-Akt_{473} remained largely unchanged, as did expression of gp130. GFAP expression, a marker for activated Muller glia cells, increased slightly over time as it was observed earlier (30). Total levels of individual proteins remained largely constant, although STAT1 and STAT3 showed a slight increase with time.

Not only activation of proteins by a specific stimulus but also a timely controlled attenuation of the response

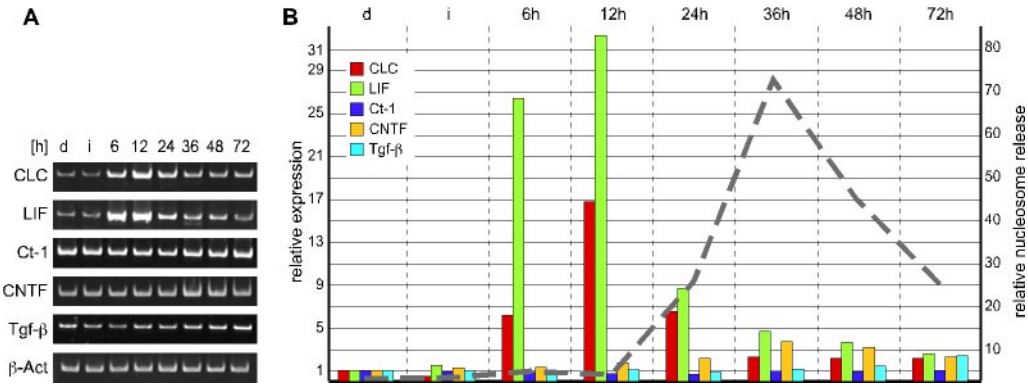

Figure 1. Members of the IL-6 family of cytokines are induced upon exposure to damaging light. BALB/c mice were not (dark control, d) or were exposed to 5000 lux of white light for 1 h and retinal RNA was prepared immediately (i) or 6 to 72 h after light exposure, as indicated. After isolation, identical amounts of RNA were reverse transcribed. Equal amounts of cDNAs from three different animals of a particular condition were pooled and used for exponential PCR. PCR amplifications were done in triplicate. Thus, each signal represents the average RNA level of three mice. *A)* Radiolabeled products after exponential RT-PCR were separated by nondenaturing PAGE. *B)* Signal intensities were determined on a PhosphorImager. Gene expression is shown semiquantitatively and relative to β-Act RNA levels. Dark control levels were set to 1. The dotted line represents the time course of apoptosis (release of nucleosomes) after light treatment. These data were published before (2) and are shown here for informative purposes.

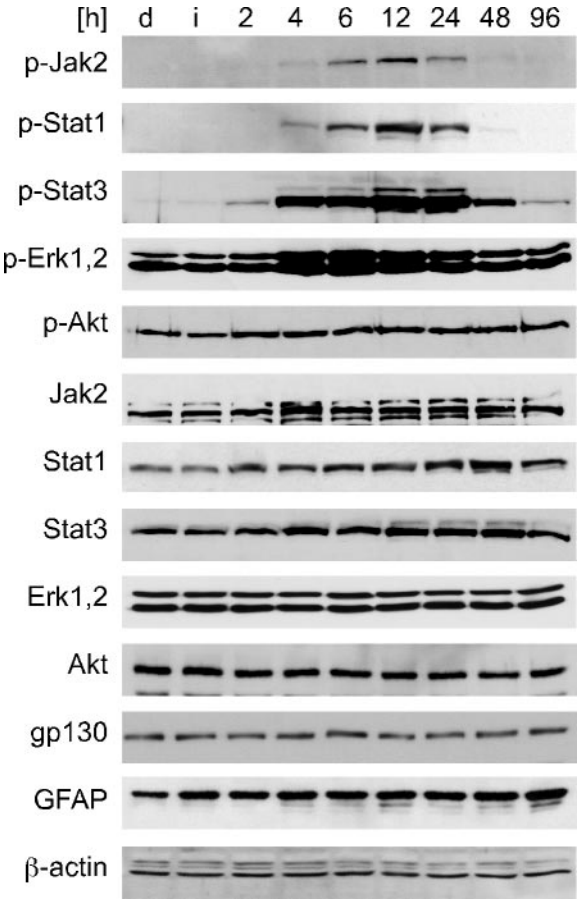

Figure 2. Induction of the Jak-STAT pathway in the retina after acute light exposure. *A)* BALB/c mice were not (dark control, d) or were exposed to 5000 lux of white light for 1 h. After light exposure, mice were sacrificed immediately (i) or after 2 to 96 h in darkness, as indicated. Proteins were extracted from isolated retinas and detected by Western blot.

is essential for an appropriate cellular reaction. The SOCS family of inhibitory proteins consists of eight members (CIS and SOCS1–7). CIS, SOCS1, and SOCS3 showed a distinct induction at the gene expression level, peaking ~6 (SOCS1) or 12 h after illumination, respectively. Expression of SOCS4, SOCS5, SOCS6, and SOCS7 was slightly (2-fold) and transiently reduced. Levels of SOCS2 RNA remained constant throughout the experiment (**Fig. 3*A*, *B***; Supplemental Table 1).

Correlation with photoreceptor injury

Light-induced phosphorylation of the Jak-STAT proteins in the retina might be a physiological response to the light pulse after dark adaptation or it might be associated with retinal injury. We tested these possibilities by analyzing three mouse strains that are differentially susceptible to light damage. The mice exposed to high levels of light were *1)* mice deficient for c-Fos expressing the $RPE65_{450Met}$ variant (resistant to light damage, ref. 31), *2)* mice deficient for c-Fos expressing the $RPE65_{450Leu}$ variant (susceptible to light damage, ref. 32), and *3)* control mice expressing the $RPE65_{450Met}$ variant (susceptible to light damage, ref. 33). A comparison of the phosphorylation pattern in these three mouse strains should reveal whether Jak-STAT activation is a general response to light (if so, activation should be detected in all three lines) or whether activation is associated with damage (up-regulation in strains 2 and 3 only). The influence of c-Fos can be assessed by comparing strains 1 and 3, and a potential role for the leucine-methionine variant in RPE65 can be analyzed by a comparison of strains 1 and 2 (**Fig. 4**). Exposure to excessive light-induced phosphorylation of Jak2, STAT1, STAT3 in strains susceptible to light damage (strains 2 and 3) but not in the resistant strain 1, as shown by the phosphorylation pattern at 6 h after light exposure. This demonstrates that activation of Jak/STAT correlates with light dam-

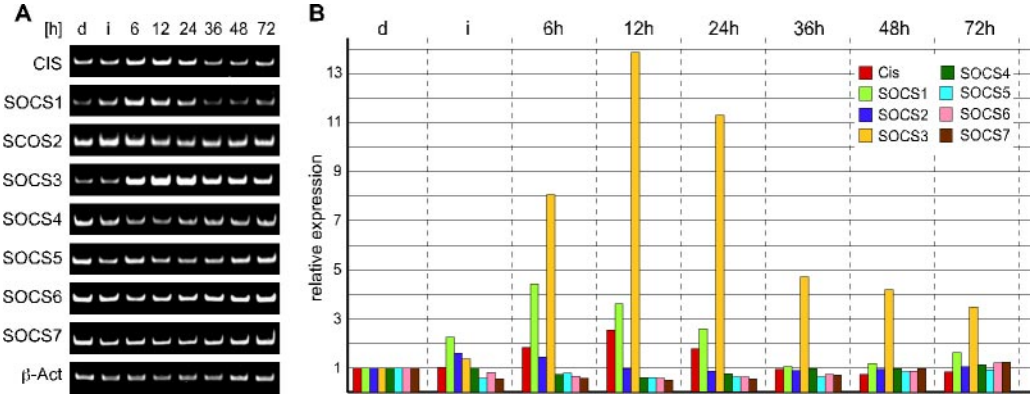

Figure 3. Members of the suppressor of cytokine signaling family are induced upon exposure to damaging light. BALB/c mice were not (dark control, d) or were exposed to 5000 lux of white light for 1 h and retinal RNA was prepared immediately (i) or after 6 to 72 h, as indicated. After isolation, identical amounts of RNA were reverse transcribed. Equal amounts of cDNAs from three different animals of a particular condition were pooled and used for exponential PCR. PCR amplifications were done in triplicate. Thus, each signal represents the average RNA level of three mice. *A)* Radiolabeled products after exponential RT-PCR were separated by nondenaturing PAGE. *B)* Signal intensities were determined on a PhosphorImager. Gene expression is shown semiquantitatively and relative to β-Act RNA levels. Dark control levels were set to 1. See also Supplemental Table 1.

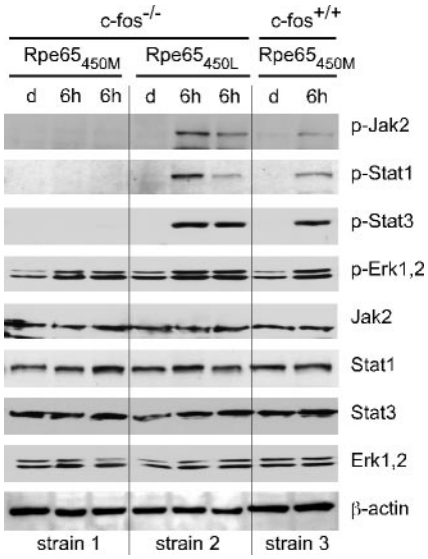

Figure 4. Induction of the Jak-STAT signaling pathway is associated with retinal damage. Three strains of mice were or were not (dark control, d) exposed to 13,000 lux of white fluorescent light for 2 h. Retinal proteins were isolated at 6 h after illumination and analyzed by Western blot, as indicated. Retinas of c-fos$^{-/-}$ mice on the Rpe65$_{450M}$ background (strain 1) are resistant to light exposure whereas retinas of c-fos$^{-/-}$ mice on the Rpe65$_{450L}$ genetic background (strain 2) are susceptible. WT mice (SV129BL/6) on the Rpe65$_{450M}$ background (strain 3) are susceptible. Phosphorylation of Jak-STAT was only induced in mice susceptible to light damage. ERK1,2 was induced in all strains of mice on light exposure. The phosphorylation pattern of one dark control and of one (strain 3) or of two different animals exposed to light (strains 1 and 2) is shown.

age and not with light absorption *per se*. Furthermore, activation is not directly influenced by the presence or absence of c-Fos and/or the Leu450Met variant in RPE65. In contrast, increased phosphorylation of Erk1,2 was detected in all mouse strains after light exposure. Thus, activation of Jak2, STAT1, and STAT3 may be part of the degenerative pathway induced by excessive light whereas phosphorylation of Erk1,2 is not, and may represent a physiological response of the retina to light or perhaps be part of a protective pathway.

The Jak-STAT pathway in inherited retinal degenerations

We used a model for autosomal recessive RP (rd1; ref. 34) and a model for autosomal dominant RP (VPP; ref. 35) to test whether the signaling pathway activated in the light-induced model of photoreceptor apoptosis might also play a role in inherited retinal degeneration. Since the degeneration in VPP mice proceeds slower than in rd1 mice (12), the time frame of analysis was adjusted accordingly. As in the light damage model, p-STAT3 levels were up-regulated during the phase of photoreceptor degeneration in both inherited models (**Fig. 5**), as were levels of total STAT3 protein. Similarly, total levels of STAT1 protein were elevated although p-STAT1 was not (rd1, Fig. 5*A*) or barely (VPP, Fig. 5*B*) detectable. In contrast to the induced model, levels of phosphorylated Jak2 were not or were only marginally elevated, and levels of p-Erk1,2 remained constant. Instead, levels of p-Akt$_{473}$ remained high in the inherited models and declined at the end of postnatal retinal development in wild-type (WT) mice. The strong induction of GFAP may reflect activation of Muller glia cells and the process of retinal remodeling (36, 37). At PND 37, when there are hardly any photoreceptors left in the rd1 retina (12, 38), all analyzed proteins were expressed at higher or at similar levels as in WT mice. This argues that these proteins are not predominantly expressed in photoreceptors, an interpretation that is in line with the results of the immunofluorescent stainings for Jak2, STAT1, and STAT3 (**Fig. 7*A***).

As in the light damage model, expression of LIF, CLC, and SOCS3 was robustly induced in the two inherited models of retinal degeneration. SOCS1 was up-regulated slightly in both models and CIS was induced in VPP mice only during the initial phase of degeneration (**Fig. 6*A, B***). CNTF was up-regulated late in the light damage model (Fig. 1) and was moderately induced in the rd1 mouse retina. FGF-2 was strongly up-regulated in the VPP mouse but not or only marginally in the rd1 retina. Again, expression of these genes did not decline with loss of photoreceptors, whereas expression of the rod-specific gene rhodopsin did (Fig. 6*A*). These results suggest that different models of retinal degeneration differentially activate members of the Jak-STAT signaling pathway.

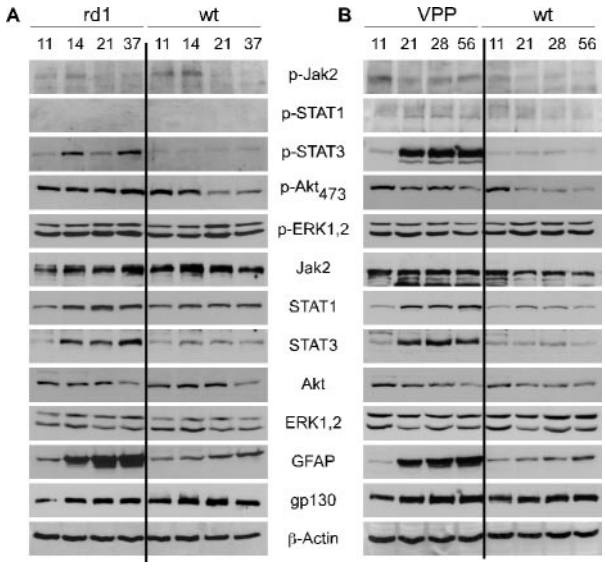

Figure 5. Members of the Jak-STAT signaling pathway are differentially induced in inherited retinal degeneration. *A)* Retinal proteins of rd1 and corresponding WT (wt) mice were extracted at indicated postnatal days and analyzed by Western blot. *B)* Same analysis as in panel *A*, but using VPP mice as an autosomal dominant model for retinal degeneration. Time points for analysis were chosen according to the different time frame of degeneration in the two models.

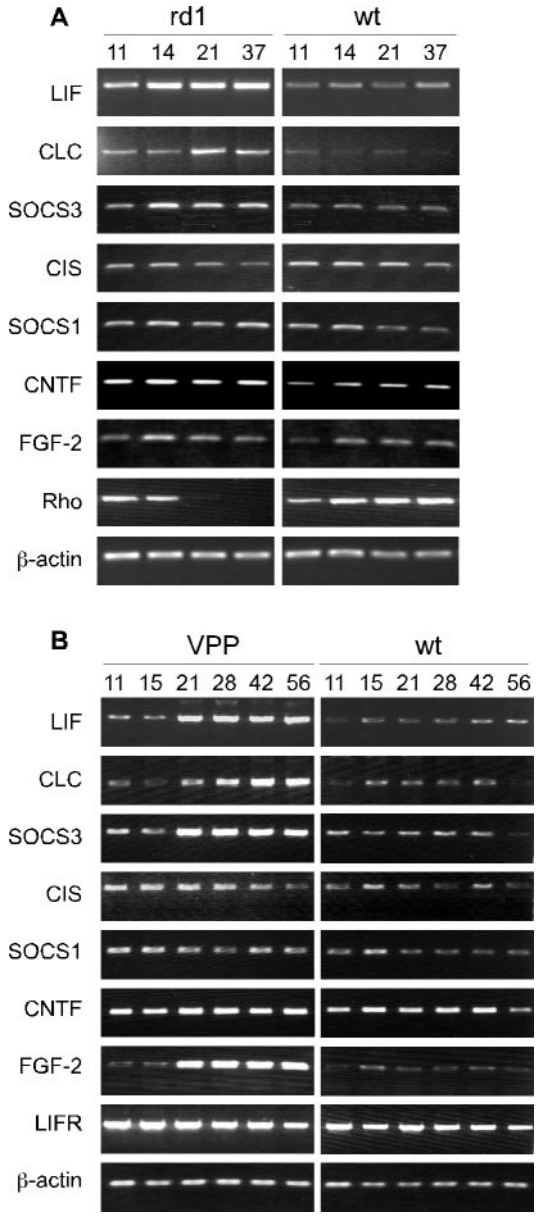

Figure 6. Expression of members of the IL-6 family of cytokines and of the SOCS family is induced in models of inherited retinal degeneration. *A)* Retinal RNA of rd1 and corresponding WT (wt) mice was isolated at indicated postnatal days. After isolation, identical amounts of RNA from three different animals were pooled, reverse transcribed and the resulting cDNA was used for exponential PCR. Thus, each signal represents the average RNA level of three mice. *B)* Same as in panel *A*, but using VPP mice as an autosomal dominant model for retinal degeneration.

Retinal localization of Jak/STAT proteins and photoreceptor degeneration

We used immunofluorescence to investigate the retinal localization of Jak/STAT proteins in the models of induced (light damage) and inherited (VPP) retinal degeneration (Fig. 7*A*). In untreated mice, Jak2 and STAT3 localized to some but not all cells of the inner nuclear layer and of the ganglion cell layer. Some STAT3 staining could also be detected in inner segments of photoreceptor cells and in the outer plexiform layer (OPL). STAT1 localized mainly to the inner plexiform layer (IPL) and OPL as well as to the ganglion cells. The pattern of the STAT1 staining in the IPL may reflect stratification within the layer and therefore the synaptic complexes between bipolar, amacrine, and ganglion cells. Light treatment of the retinas did not alter the distribution of STAT1 and STAT3 but seemed to have caused a shift of Jak2 localization mainly to the IPL and OPL (between ONL and INL). Note that a similar shift of Jak2 localization to the IPL was detected in degenerating VPP retinas. Most important, however, no increased localization to the ONL was found in light-damaged retinas even though light exposure induced cell death exclusively in this cell layer (Fig. 7*B*).

An increased immunofluorescence for STAT3 was detected in the ONL of 28-day-old VPP mice whereas STAT1 staining remained largely unaffected. STAT3 was also the main protein that was differentially expressed in the VPP mice when analyzed by Western blot (Fig. 5). However, increased immunofluorescence did not seem to correlate with the few apoptotic photoreceptors present in the ONL at the time point analyzed (Fig. 7*B*).

Inhibition of Jak-STAT signaling pathway protects against induced but not inherited retinal degeneration

The differential activation of members of the Jak-STAT pathway in the induced and inherited models of retinal degeneration may suggest that interference with this signaling may lead to different effects. We used AG-490, a tyrosine kinase inhibitor specific for the Jak family kinases (39–41), in an attempt to dissect the role of the Jak/STAT signaling pathway in the different models of retinal degeneration. AG-490 was injected intraperitoneally (i.p.) immediately before onset of light exposure. The phosphorylation pattern of Jak2, STAT1, and STAT3 was analyzed 18 h thereafter (**Fig. 8*A***). In contrast to mice injected with carrier or to uninjected mice, AG-490-treated mice did not show increased protein phosphorylation. Furthermore, AG-490 treatment, and thus interference with the Jak-STAT pathway, significantly reduced light damage susceptibility of photoreceptors as indicated by reduced internucleosomal DNA cleavage (Fig. 8*B*). AG-490-treated mice had only few scattered photoreceptor nuclei showing condensed chromatin (pyknotic nuclei) as a classical sign of apoptosis (Fig. 8*C*, middle panel), whereas mice treated with carrier showed a highly increased number of pyknotic nuclei (Fig. 8*C*, bottom panel).

To assess a potential role for Jak2 in STAT3 activation and retinal degeneration in the VPP mouse as a model for inherited retinal degeneration, we treated VPP mice with daily injections of AG-490, starting at PND 15 and ending at PND 27. Analysis was at PND 28. The retina of 15-day-old VPP mice had 7 to 9 rows of photoreceptor nuclei and distinct (but shortened) inner and outer segments (not shown). AG-490 treatment slightly re-

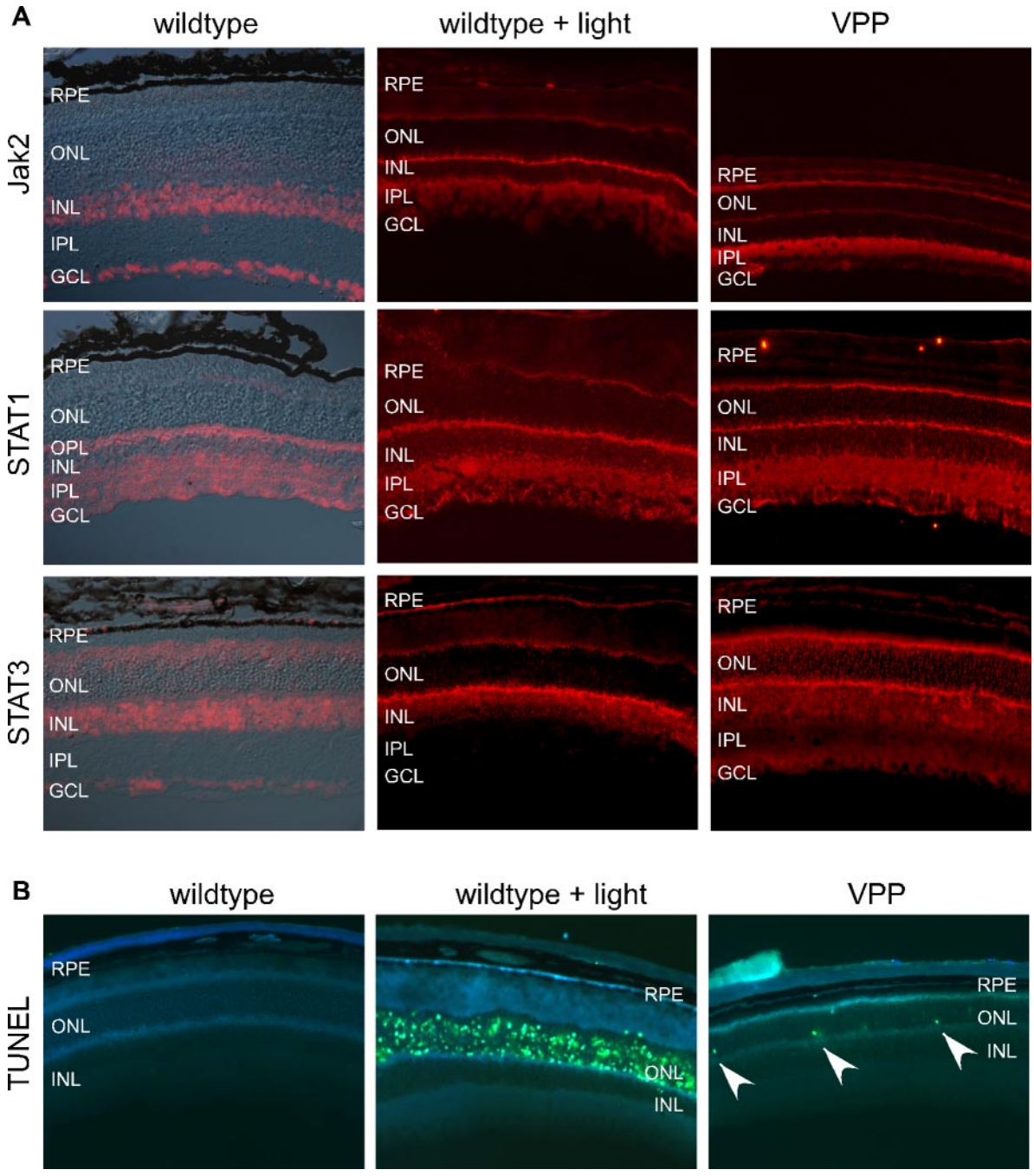

Figure 7. Immunofluorescent stainings detecting Jak-STAT proteins (*A*) or apoptotic cells (*B*). *A)* Cryosections of WT (left column), light-exposed WT mice at 12 h after exposure (middle column) and VPP mice at 28 days of age (right column) were stained with antibodies, as indicated. The panels in the left column are merged pictures of fluorescent (antibody staining, red) and Nomarski images (for a better visualization of retinal structures). The middle and right columns show fluorescent images only. *B)* Staining for apoptotic cells (TUNEL staining). No TUNEL-positive cells are detected in WT control retinas. Light exposure of WT cells induced apoptosis and TUNEL-positive stainings in a large number of cells in the ONL but not in other cell layers. Arrowheads point to TUNEL-positive cells in the ONL of VPP mice. RPE: retinal pigment epithelium; ONL: outer nuclear layer; INL: inner nuclear layer; IPL: inner plexiform layer; GCL: ganglion cell layer.

duced phosphorylation levels of Jak2. Levels of p-STAT3, however, were still elevated and comparable to untreated VPP mice (**Fig. 9*A***). The amount of rhodopsin per retina was measured to quantify photoreceptor degeneration. Four-wk-old WT mice had 0.43 ± 0.083 (n=3) nmol rhodopsin whereas untreated VPP mice of the same age had only 0.071 ± 0.015 (n=3) nmol and AG-490-treated mice had 0.065 ± 0.014 (n=4) rhodopsin left. Thus, despite AG-490 treatment, >80% of the photoreceptors were lost (Fig. 9*B*). Morphological evaluation of retinas from 4-wk-old animals showed that control VPP and AG-490-treated VPP mice had retained about three rows of photoreceptor nuclei compared with 12 rows in a WT retina (Fig. 9*C*).

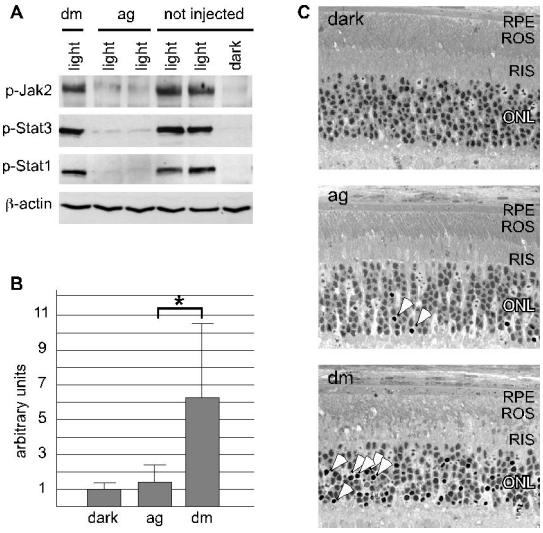

Figure 8. Inhibition of Jak signaling prevents retinal degeneration after bright light exposure. *A)* BALB/c mice received immediately before light exposure no (not injected) or a single injection of 800 μg AG-490 (ag) or of carrier DMSO (dm), as indicated. Mice were not (dark) or were subsequently exposed for 1 h to 5000 lux and phosphorylation of proteins was tested 18 h after exposure. Retinal proteins from separate animals were loaded in each lane. *B)* Retinas of animals not exposed to light (dark) or of animals pretreated either with AG-490 (ag) or DMSO (dm) and exposed for 1 h to 5000 lux were used to quantify apoptosis by ELISA. $*P = 0.003$, two-tailed t test; $n = 10$ mice for each condition. *C)* Light microscopy 18 h after light exposure. Retinas of dark control mice showed regular photoreceptors (upper panel). Retinas of AG-490 (ag) -treated mice exhibited few apoptotic photoreceptor nuclei (arrowheads, middle panel) and retinas of carrier (DMSO, dm) -treated mice had significantly more dying photoreceptors (arrowheads, lower panel). ROS: rod outer segments; RIS: rod inner segments. Other abbreviations as in Fig. 7.

To test whether the lack of an effect of AG-490 treatment on STAT3 phosphorylation was due to an adaptational response of the retina to the long-term treatment, we analyzed phosphorylation pattern 19 h after the injection of a single dose of AG-490. The timing and treatment are comparable to the experimental protocol of AG-490 application and analysis in the light damage experiments (Fig. 8). However, STAT3 phosphorylation was not reduced after this treatment (Fig 9*D*). In addition, there was no obvious reduction in Jak2 phosphorylation. Thus, the continuously present stimulus in the VPP mouse (the mutant protein) may require several repetitive applications of AG-490 to establish an effect on Jak2 phosphorylation.

MATERIALS AND METHODS

Mice and light exposure

Animals were treated in accordance with the regulations of the Veterinary Authority of Zurich and with the statement of 'The Association for Research in Vision and Ophthalmology' for the use of animals in research. c-fos WT and c-fos knockout (c-fos$^{-/-}$) mice were on mixed SV129BL/6 background. Genotyping for c-fos and for the Rpe65 variant at position 450 was done as described (12, 32). VPP mice were kept on a mixed SV129BL/6 background and genotyped using upstream primer 5′-AGA CTG ACA TGG GGA GGA ATT CCC AGA-3′ and downstream primer 5′-CAG CTG CTC GAA GTG ACT CCG ACC-3. Rd1 (C3H) and BALB/c mice were from Harlan (Netherlands). Six to 8-wk-old male BALB/c mice were dark-adapted overnight (16 h) and exposed to 5000 lux of white fluorescent light for 1 h. After exposure, mice were returned to darkness for 24 h before they were returned to cyclic (12 h:12 h) light. Pigmented c-fos$^{-/-}$ or c-fos$^{+/+}$ mice were dark adapted as above, their pupils dilated (1% Cyclogyl, Alcon, Cham, Switzerland; and

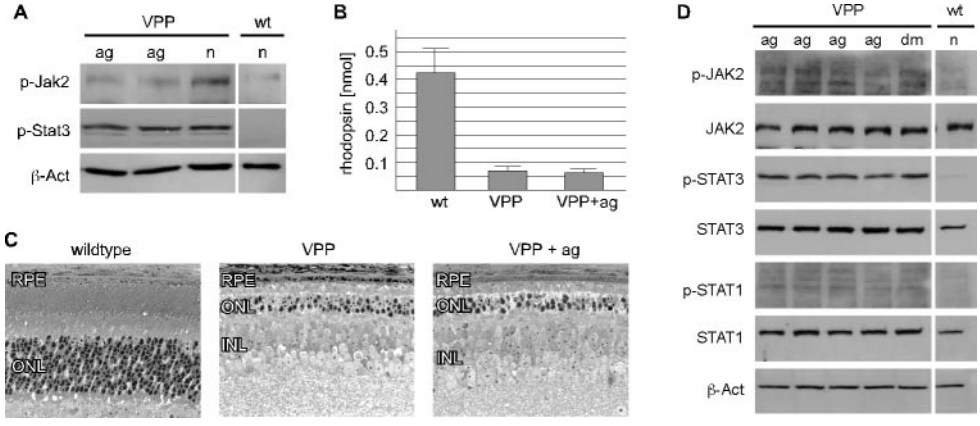

Figure 9. AG-490 treatment does not prevent photoreceptor degeneration in the VPP mouse. VPP mice received 12 i.p. injections on 12 consecutive days (*A–C*) or one single (*D*) injections of 800 μg AG-490. Daily injected mice were treated starting at PND15 and ending at PND 27. Mice were sacrificed for analysis at PND 28. *A)* Western blot analysis of total retinal protein of VPP or WT (wt) mice that were (ag) or were not (n) repetitively treated with AG-490. AG-490 treatment reduced Jak2 phosphorylation in VPP mice to similar levels as in wt mice. Phosphorylation of STAT3 was still prominent. Shown are two different mice treated with AG-490. *B)* Photoreceptor loss at PND 28 was quantified by measurement of retinal rhodopsin in wt (n=3), VPP (n=3) and AG-490-treated VPP mice (n=4). *C)* Morphological evaluation of retinal degeneration in WT (left panel), VPP (middle panel) and AG-490-treated VPP mice (right panel) at PND 28. Abbreviations as in Fig. 7. *D)* Western blot analysis of total retinal protein of 28-day-old VPP or WT (wt) mice that were not treated (n) or were treated with either DMSO (dm) or a single injection of 800 μg AG-490 (ag). Analysis was 19 h after injection. Shown are four different mice treated with AG-490 and a single mouse for each control.

5% phenylephrine, Ciba Vision, Niederwangen, Switzerland) 1 h prior to light exposure, and exposed to 13,000 lux of white light for 2 h.

Microscopy, immunofluorescence, and TUNEL staining

For light microscopy, eyes were fixed in 2.5% glutaraldehyde in 0.1 M cacodylate buffer, pH 7.3, at 4°C overnight. For each eye, the superior and inferior retina were prepared, washed in cacodylate buffer, incubated in osmium tetroxide for 1 h, dehydrated, and embedded in Epon 812. Sections (0.5 μm) were prepared from the lower central retina (most affected in our light damage model) and counterstained with methylene blue.

For immunofluorescence and TUNEL staining, eyes of adult WT control or light exposed (2 h at 13,000 lux, analysis was at+12 h) mice, respectively, or of 28-day-old VPP mice of the $Rpe65_{450M}$ background (64) were enucleated, embedded in Tissue Tec OCT compound (Mioles Inc., Elkhart, IN, USA), and frozen in liquid nitrogen. Sections (10 μ) were dried and fixed in acetone for 10 min at 4°C. Sections were washed in PBST (PBS+0.05% Triton X-100) for 2 × 5 min at room temperature. After blocking in PBST + 10% normal goat serum (NGS) for 1 h at room temperature, sections were incubated with the respective primary antibodies (anti-Jak2, Biosource; Camarillo, CA, USA; anti-STAT1 and anti-STAT3, Cell Signaling; Beverly, MA, USA). Sections were washed 3 × 10 min in PBST and Cy3-conjugated secondary anti-rabbit antibodies (Jackson ImmunoResesarch, Soham, UK) were added in PBST + 3% NGS (dilution 1/500) for 1–2 h at room temperature. Sections were washed 2 × 10 min in PBST and 1 × in PBS. TUNEL staining was done according to the manufacturer's recommendation (Roche diagnostics, Basel, Switzerland).

Western blot

Retinas were homogenized in 100 mM Tris/HCl, pH 8.0, and analyzed for protein content using Bradford reagent. Standard SDS-PAGE and Western blot were performed. For immunodetection, the following antibodies were used: anti-Jak2 (#44–406, Biosource), anti-STAT1 (#9172, Cell Signaling), anti-STAT3 (#9132, Cell Signaling), anti-ERK1,2 (#9102, NEB), anti-Akt (#9272, Cell Signaling), anti-gp130 (sc-656, Santa Cruz), anti-GFAP (G-3893, Sigma), anti-β-actin (sc-1616, Santa Cruz), anti-phospho-$Jak2_{pYpY1007/1008}$ (#44–426, Biosource), anti-phospho-$STAT1_{Tyr701}$ (#9171, Cell Signaling), anti-phospho-$STAT3_{Tyr705}$ (#9131, Cell Signaling), anti-phospho-$ERK1,2_{Thr202/Tyr204}$ (#9101, NEB), anti-phospho-Akt_{Tyr473} (#9271, Cell Signaling). Blots were incubated overnight at 4°C with primary antibodies followed by a 1 h incubation at room temperature with HRP-conjugated secondary antibodies. Immunoreactivity was visualized using the Renaissance-Western blot detection kit (Perkin Elmer Life Sciences, Emeryville, CA, USA).

RNA preparation and RT-polymerase chain reaction (RT-PCR)

Retinas were removed through a slit in the cornea and immediately frozen in liquid nitrogen. Total retinal RNA was prepared using the RNeasy RNA isolation kit (Qiagen, Hilden, Germany), including DNase treatment to digest residual genomic DNA. Identical amounts of RNA were used for reverse transcription using oligo(dT) and M-MLV reverse transcriptase (Promega, Madison, WI, USA). cDNAs from three different animals were pooled and amplified with specific primers (**Table 1**). Amplification was stopped at cycle numbers ensuring analysis of products in the linear amplification phase of the polymerase chain reaction (PCR) (numbers of cycles were determined in pre-experiments). Downstream primers were ^{32}P-end-labeled. Amplification products were resolved on a 6% native polyacrylamide gel, quantified on a PhosphorImager, and normalized to β-actin expression. In experiments without quantification, PCR products were resolved on a 1.5% agarose gel.

AG-490 injections, ELISA cell death assay, rhodopsin measurements

AG-490 (LC Laboratories, Woburn, MA, USA) was dissolved in 56% DMSO. AG-490 (40 μg/g) (65, 66) was injected i.p. immediately before light exposure or daily ~ 10 AM, respectively. Control animals were injected with 56% DMSO. Cell death was quantified 18 h after light exposure using the ELISA-based Cell Death Detection Kit (Roche Diagnostics, Basel, Switzerland) according to the manufacturer's recommendation. The rhodopsin content was determined as described (67).

TABLE 1. *PCR primers used for amplifications*

Gene	Upstream	Downstream	Product
CIS	GCTACCTGTTCACACTGTCA	GACTAGCCGACACAGATGTT	350 bp
SOCS1	CTCCGTGACTACCTGAGTTC	CCAGACACAAGCTGCTACAA	278 bp
SOCS2	CTGTTCACCTGTACCTGACCA	CACATAGCTGCATTCGGAGA	240 bp
SOCS3	GGAGACAGATGAGGCTGGTGA	GGACCTACTGACCGAGAGAT	349 bp
SOCS4	GTCATAACTGCCAACAGTGC	CTGAAGGAGGTCTGGAACAAG	252 bp
SOCS5	GCGAGAGAAGACGGCTTAGT	GACCTGTTGTAGCGGCGGAA	481 bp
SOCS6	CCTTGCTGGTGACTTCGTGA	CACTCGCATCTCCATCTTGA	361 bp
SOCS7	GCCTCAGCCTCCTAGATGAT	CACCACCGACTGACAGCGAT	473 bp
CLC	GCATCAACTCCGCAGCTTAG	CTGAACGCCATAGCCAGGTCT	443 bp
LIF	AATGCCACCTGTGCCATACG	CAACTTGGTCTTCTCTGTCCCG	216 bp
Ct-1	TTTCTGTCTCTCCATCTGTGTCCTG	GTGGGAAGGTCCTAAGGTGAATG	492 bp
CNTF	AGCCTTGACTCAGTGGATGGTG	ATCAGCCTCTTTTTCAGGGACC	276 bp
FGF-2	TGTGTCTATCAAGGGAGTGTGTGC	ACCAACTGGAGTATTTCCGTGACCG	158 bp
Tgf-β	GCAACAATTCCTGGCGTTAC	CTGTGGAGCTGAAGCAATAG	345 bp
β-Actin	CAACGGCTCCGGCATGTGC	CTCTTGCTCTGGGCCTCG	153 bp
LIFR	TGGCTGTCATTGTTGGCGTG	CTTACCCTCTTCATCTTCTGCTGC	536 bp
Rho	TTTTATGTGCCCTTCTCCAACG	TTTTATGTGCCCTTCTCCAACG	440 bp

DISCUSSION

Retinal degeneration is a leading cause of blindness in human patients. Here we investigated signaling pathways in an induced, an autosomal recessive, and an autosomal dominant model for the disease in humans. We show that proteins of the Jak-STAT pathway were induced in all models but that the individual activation patterns were death stimulus-specific. Differentially activated proteins include cytokine ligands, STAT transcription factors, and molecules of a negative feedback loop. The neuroprotective effect of the inhibition of Jak2 in induced but not in inherited cell death suggests that this signaling cascade is of differential importance depending on the death stimulus.

The Jak-STAT signaling pathway, and especially STAT1 and STAT3 proteins have been implicated in neurodegenerative as well as neuroprotective mechanisms (42). In the light-treated retina, STAT1 and STAT3 proteins were both activated, suggesting that cell death as well as cell survival pathways were induced. We speculate that the retina generates death factors promoting apoptosis of photoreceptors that are damaged beyond rescue and survival factors that help to rescue damaged photoreceptors that are still viable. The nature of such factors remains to be determined, but their production may be differentially controlled by STAT1 and STAT3, respectively.

Jak2, STAT1, and STAT3 proteins were found mainly in the INL, GCL, IPL, and OPL but rarely in photoreceptors (Fig. 7), which agrees with previous reports (14, 43, 44). However, photoreceptors are the cells primarily affected in all models of retinal degeneration used here. Thus, the fate of photoreceptors might be determined by other cell types through STAT1/STAT3-regulated production and release of growth factors and/or cytokines. Recently, injection of CT-1 (a member of the IL-6 family of cytokines) into the eyes of a rat model for inherited retinal disease increased phosphorylation of STAT3 and STAT1 and protected photoreceptors. Increased phosphorylation colocalized with Muller cells, implicating these cells in the regulation of photoreceptor apoptosis in a paracrine fashion (45). Evidence suggests that the neuroprotective effect of CNTF on photoreceptors and ganglion cells may be mediated through induction of STAT3 (14, 46). Our results here are in line with such a conclusion.

Peak activation of the Jak-STAT pathway was at 12 h postillumination whereas the peak of apoptotic release of nucleosomes was found ~ 36 h after exposure (2), supporting the notion that Jak-STAT signaling is an early event that may regulate the fate of photoreceptor cells. Thus, it is conceivable that interference with such an early event can influence the progression of the degeneration. The tyrosine kinase inhibitor AG-490 interferes with Jak kinases, including Jak2 (39–41). Thus, reduced activation of STAT1 and STAT3 may have been through inhibition of Jak2, although we cannot completely rule out an involvement of other AG-490-responsive kinases. Since the presumable proapoptotic pathway (STAT1) was blocked, the simultaneous reduction of the presumable antiapoptotic STAT3 pathway was not disastrous for the retina, and the net result of the treatment was protection of photoreceptors.

In the case of the analyzed models for inherited photoreceptor degeneration, mainly STAT3 but not STAT1 was activated throughout the degenerative period. Although STAT1 may be an important death mediator in the light damage model, it may not be involved in the inherited models. Also, phosphorylation of Jak2 was at best slightly increased in the VPP mouse and remained at basal levels in the rd1 retina. Since cell death in the inherited models stretches over an extended period, activation of the proteins may only occur in a small number of cells simultaneously and may therefore go undetected in Western blot experiments. However, the immunofluorescent stainings did not give evidence that the proteins colocalize with dying (TUNEL-positive) cells. This suggests that photoreceptor degeneration in the inherited models may be independent of Jak2, a conclusion corroborated by the ineffectiveness of AG-490 treatment of VPP mice. The strong activation of STAT3 in these mice therefore may be by an alternative pathway, which may include, for example, an oxidative stress response (47, 48). Nevertheless, activation of the (presumably) protective STAT3 signaling obviously is not sufficient for rescuing photoreceptors in the inherited model. Although STAT3 is activated in induced and inherited models, the signaling system through which STAT3 is activated may be different. The differential effectiveness of many factors on induction and progression of induced or inherited retinal degeneration (2) also argues for the existence of multiple signaling systems that lead to photoreceptor cell death. To develop therapeutic strategies for a large variety of diseases, it will be important to identify and understand these signaling events.

The sustained phosphorylation of Akt in both models of inherited retinal degeneration argues for molecular mechanisms in addition to STAT3 signaling. The PI3K-Akt pathway has been shown to be important for the survival of several neuronal cell types (49–51), and Akt has been suggested to be part of a retinal defense mechanism in response to toxic insults (52), perhaps through the activation of CNTF expression (17). At least in the rd1 retina, steady-state levels of CNTF mRNA were moderately elevated in the late phase of degeneration, as has been reported by others (53). In the rd1 retina, Akt and pAkt expression did not decline at P37, a time point when the rd1 mouse has lost almost all photoreceptors. This indicates that the majority of Akt is not expressed in photoreceptors. The same holds true for the other genes tested (Figs. 5, 6) as judged by their expression pattern during aging. The immunofluorescent studies (Fig. 7) support this conclusion. Therefore, induction of the genes and proteins shown here might be a response of cells in the INL and/or GCL to photoreceptor injury. The protection of photoreceptors against light damage by inhibition of Jak2

may thus suggest a model in which photoreceptors signal injury to cells in the INL, which then initiate the appropriate response to either support survival or promote death of the injured photoreceptors. In addition, induction of a general defense mechanism may ensure survival of cells not directly damaged by the applied toxic stimulus. Such a defense mechanism may involve CNTF in the rd1 mouse and FGF-2 in the VPP mouse. Chronic up-regulation of FGF-2 may slow down the progression of photoreceptor degeneration in the VPP mouse as has been suggested for other models (54).

It is tempting to speculate that the cells that "rule" over the fate of other cells might be the Muller glia cells. These cells have been shown to react strongly to retinal injury and they seem to release neurotrophic factors, including the protective cytokines FGF-2 and CNTF, in protocols of preconditioning and neuroprotection (14, 15, 26, 55–58).

The role of LIF

The role of CLC and LIF, the two members of the IL-6 family of cytokines that were induced in all models of retinal degeneration, is unclear. They may act in an autocrine or paracrine fashion. In the rd1 mouse, expression of CLC and LIF was still up-regulated even after most photoreceptors had died and were cleared from the subretinal space. The same long-lasting stimulation was observed for p-STAT3, p-Akt_{473}, and GFAP. This may suggest that these factors play a role in the retina even after photoreceptor degeneration—for example, in the remodeling of second order neurons, which begins as early as PND10 in the rd1 retina (36, 37). LIF may be of particular interest in this respect since this factor was shown to keep cells in an undifferentiated state to modulate stem cell renewal (59, 60). In the postnatal retina, LIF blocks expression of Nrl and Crx transcription factors (61), disrupts synaptic organization (62), and arrests developing photoreceptors in a pre-rod stage (63). Increased expression of LIF in a degenerating retina may therefore be required for the adjustment of the remaining cells of the INL and GCL to the new retinal architecture.

In summary, we show the differential regulation of the IL-6 family of cytokines and of the Jak-STAT signaling pathway in different models of retinal degeneration. Interference with this signaling protects a model of induced but not a model of inherited photoreceptor apoptosis, suggesting that regulation/execution of cell death of visual cells strongly depends on the particular apoptotic stimulus. The expression pattern of the various factors supports a pivotal regulatory role of the INL and/or GCL in photoreceptor apoptosis. Treatment strategies to prevent photoreceptor degeneration in human blinding diseases may thus need to target the regulatory molecular response of cells apart from photoreceptors. FJ

The authors wish to thank Coni Imsand, Gaby Hoegger, and Hedwig Wariwoda for excellent technical assistance and Muna Naash for providing the VPP transgenic mouse line. This work was supported by the Swiss National Science Foundation (3100A0–105793), the Novartis Foundation, the German Research Council (SP1088), and by a grant from the European Community (EVI-GenoRet; LSHG-computed tomography-512036). The authors are especially thankful for the generous support by the H. Messerli Fonds. The Laboratory of Retinal Cell Biology is a member of the Center of Integrative Human Physiology (CIHP) and of the Neuroscience Center Zurich (ZNZ) of the University of Zurich.

REFERENCES

1. Reme, C. E., Grimm, C., Hafezi, F., Marti, A., and Wenzel, A. (1998) Apoptotic cell death in retinal degenerations. *Prog. Retin. Eye Res.* **17,** 443–464
2. Wenzel, A., Grimm, C., Samardzija, M., and Reme, C. E. (2005) Molecular mechanisms of light-induced photoreceptor apoptosis and neuroprotection for retinal degeneration. *Prog. Retin. Eye Res.* **24,** 275–306
3. Grimm, C., Wenzel, A., Groszer, M., Mayser, H., Seeliger, M., Samardzija, M., Bauer, C., Gassmann, M., and Reme, C. E. (2002) HIF-1-induced erythropoietin in the hypoxic retina protects against light-induced retinal degeneration. *Nat. Med.* **8,** 718–724
4. Wenzel, A., Grimm, C., Seeliger, M. W., Jaissle, G., Hafezi, F., Kretschmer, R., Zrenner, E., and Reme, C. E. (2001) Prevention of photoreceptor apoptosis by activation of the glucocorticoid receptor. *Invest Ophthalmol. Vis. Sci.* **42,** 1653–1659
5. Imai, D., Yoneya, S., Gehlbach, P. L., Wei, L. L., and Mori, K. (2005) Intraocular gene transfer of pigment epithelium-derived factor rescues photoreceptors from light-induced cell death. *J. Cell. Physiol.* **202,** 570–578
6. Organisciak, D. T., Darrow, R. A., Barsalou, L., Darrow, R. M., and Lininger, L. A. (1999) Light-induced damage in the retina: differential effects of dimethylthiourea on photoreceptor survival, apoptosis and DNA oxidation. *Photochem. Photobiol.* **70,** 261–268
7. Ranchon, I., Chen, S., Alvarez, K., and Anderson, R. E. (2001) Systemic administration of phenyl-N-tert-butylnitrone protects the retina from light damage. *Invest. Ophthalmol. Vis. Sci.* **42,** 1375–1379
8. Zhang, C., Lei, B., Lam, T. T., Yang, F., Sinha, D., and Tso, M. O. (2004) Neuroprotection of photoreceptors by minocycline in light-induced retinal degeneration. *Invest. Ophthalmol. Vis. Sci.* **45,** 2753–2759
9. LaVail, M. M., Unoki, K., Yasumura, D., Matthes, M. T., Yancopoulos, G. D., and Steinberg, R. H. (1992) Multiple growth factors, cytokines, and neurotrophins rescue photoreceptors from the damaging effects of constant light. *Proc. Natl. Acad. Sci. U. S. A.* **89,** 11249–11253
10. Tao, W., Wen, R., Goddard, M. B., Sherman, S. D., O'Rourke, P. J., Stabila, P. F., Bell, W. J., Dean, B. J., Kauper, K. A., and Budz, V. A., *et al.* (2002) Encapsulated cell-based delivery of CNTF reduces photoreceptor degeneration in animal models of retinitis pigmentosa. *Invest Ophthalmol. Vis. Sci.* **43,** 3292–3298
11. Cao, W., Tombran-Tink, J., Elias, R., Sezate, S., Mrazek, D., and McGinnis, J. F. (2001) In vivo protection of photoreceptors from light damage by pigment epithelium-derived factor. *Invest. Ophthalmol. Vis. Sci.* **42,** 1646–1652
12. Grimm, C., Wenzel, A., Stanescu, D., Samardzija, M., Hotop, S., Groszer, M., Naash, M., Gassmann, M., and Reme, C. (2004) Constitutive overexpression of human erythropoietin protects the mouse retina against induced but not inherited retinal degeneration. *J. Neurosci.* **24,** 5651–5658
13. Kaldi, I., Dittmar, M., Pierce, P., and Anderson, R. E. (2003) L-NAME protects against acute light damage in albino rats, but not against retinal degeneration in P23H and S334ter transgenic rats. *Exp. Eye Res.* **76,** 453–461
14. Peterson, W. M., Wang, Q., Tzekova, R., and Wiegand, S. J. (2000) Ciliary neurotrophic factor and stress stimuli activate the Jak-STAT pathway in retinal neurons and glia. *J. Neurosci.* **20,** 4081–4090

15. Harada, T., Harada, C., Kohsaka, S., Wada, E., Yoshida, K., Ohno, S., Mamada, H., Tanaka, K., Parada, L. F., and Wada, K. (2002) Microglia-Muller glia cell interactions control neurotrophic factor production during light-induced retinal degeneration. *J. Neurosci.* **22,** 9228–9236
16. Alonzi, T., Middleton, G., Wyatt, S., Buchman, V., Betz, U. A., Muller, W., Musiani, P., Poli, V., and Davies, A. M. (2001) Role of STAT3 and PI 3-kinase/Akt in mediating the survival actions of cytokines on sensory neurons. *Mol. Cell. Neurosci.* **18,** 270–282
17. Ikeda, K., Tatsuno, T., Noguchi, H., and Nakayama, C. (2004) Ciliary neurotrophic factor protects rat retina cells in vitro and in vivo via PI3 kinase. *Curr. Eye Res.* **29,** 349–355
18. Platanias, L. C. (2005) Mechanisms of type-I- and type-II-interferon-mediated signalling. *Nat. Rev. Immunol.* **5,** 375–386
19. Stephanou, A. (2004) Role of STAT-1 and STAT-3 in ischaemia/reperfusion injury. *J. Cell. Mol. Med.* **8,** 519–525
20. Calo, V., Migliavacca, M., Bazan, V., Macaluso, M., Buscemi, M., Gebbia, N., and Russo, A. (2003) STAT proteins: from normal control of cellular events to tumorigenesis. *J. Cell. Physiol.* **197,** 157–168
21. Aaronson, D. S., and Horvath, C. M. (2002) A road map for those who don't know JAK-STAT. *Science* **296,** 1653–1655
22. Krebs, D. L., and Hilton, D. J. (2000) SOCS: physiological suppressors of cytokine signaling. *J. Cell Sci.* **113,** 2813–2819
23. Cao, W., Wen, R., Li, F., Lavail, M. M., and Steinberg, R. H. (1997) Mechanical injury increases bFGF and CNTF mRNA expression in the mouse retina. *Exp. Eye Res.* **65,** 241–248
24. Casson, R. J., Chidlow, G., Wood, J. P., Vidal-Sanz, M., and Osborne, N. N. (2004) The effect of retinal ganglion cell injury on light-induced photoreceptor degeneration. *Invest. Ophthalmol. Vis. Sci.* **45,** 685–693
25. Nir, I., Liu, C., and Wen, R. (1999) Light treatment enhances photoreceptor survival in dystrophic retinas of Royal College of Surgeons rats. *Invest. Ophthalmol. Vis. Sci.* **40,** 2383–2390
26. Walsh, N., Valter, K., and Stone, J. (2001) Cellular and subcellular patterns of expression of bFGF and CNTF in the normal and light stressed adult rat retina. *Exp. Eye Res.* **72,** 495–501
27. Wen, R., Song, Y., Cheng, T., Matthes, M. T., Yasumura, D., LaVail, M. M., and Steinberg, R. H. (1995) Injury-induced upregulation of bFGF and CNTF mRNAS in the rat retina. *J. Neurosci.* **15,** 7377–7385
28. Valter, K., Bisti, S., Gargini, C., Di Loreto, S., Maccarone, R., Cervetto, L., and Stone, J. (2005) Time course of neurotrophic factor upregulation and retinal protection against light-induced damage after optic nerve section. *Invest. Ophthalmol. Vis. Sci.* **46,** 1748–1754
29. Beltran, W. A., Rohrer, H., and Aguirre, G. D. (2005) Immunolocalization of ciliary neurotrophic factor receptor alpha (CNTFRalpha) in mammalian photoreceptor cells. *Mol. Vis.* **11,** 232–244
30. De Raad, S., Szczesny, P. J., Munz, K., and Reme, C. E. (1996) Light damage in the rat retina: glial fibrillary acidic protein accumulates in Muller cells in correlation with photoreceptor damage. *Ophthal. Res.* **28,** 99–107
31. Hafezi, F., Steinbach, J. P., Marti, A., Munz, K., Wang, Z. Q., Wagner, E. F., Aguzzi, A., and Reme, C. E. (1997) The absence of c-fos prevents light-induced apoptotic cell death of photoreceptors in retinal degeneration in vivo. *Nat. Med.* **3,** 346–349
32. Wenzel, A., Grimm, C., Samardzija, M., and Reme, C. E. (2003) The genetic modifier Rpe65Leu(450): effect on light damage susceptibility in c-Fos-deficient mice. *Invest. Ophthalmol. Vis. Sci.* **44,** 2798–2802
33. Wenzel, A., Reme, C. E., Williams, T. P., Hafezi, F., and Grimm, C. (2001) The Rpe65 Leu450Met variation increases retinal resistance against light-induced degeneration by slowing rhodopsin regeneration. *J. Neurosci.* **21,** 53–58
34. Bowes, C., Li, T., Danciger, M., Baxter, L. C., Applebury, M. L., and Farber, D. B. (1990) Retinal degeneration in the rd mouse is caused by a defect in the beta subunit of rod cGMP-phosphodiesterase. *Nature* **347,** 677–680
35. Naash, M. I., Ripps, H., Li, S., Goto, Y., and Peachey, N. S. (1996) Polygenic disease and retinitis pigmentosa: albinism exacerbates photoreceptor degeneration induced by the expression of a mutant opsin in transgenic mice. *J. Neurosci.* **16,** 7853–7858
36. Strettoi, E., Pignatelli, V., Rossi, C., Porciatti, V., and Falsini, B. (2003) Remodeling of second-order neurons in the retina of rd/rd mutant mice. *Vision Res.* **43,** 867–877
37. Marc, R. E., Jones, B. W., Watt, C. B., and Strettoi, E. (2003) Neural remodeling in retinal degeneration. *Prog. Retin. Eye Res.* **22,** 607–655
38. Bowes, C., Li, T., Frankel, W. N., Danciger, M., Coffin, J. M., Applebury, M. L., and Farber, D. B. (1993) Localization of a retroviral element within the rd gene coding for the β subunit of cGMP phosphodiesterase. *Proc. Natl. Acad. Sci. U. S. A.* **90,** 2955–2959
39. Burdelya, L., Catlett-Falcone, R., Levitzki, A., Cheng, F., Mora, L. B., Sotomayor, E., Coppola, D., Sun, J., Sebti, S., and Dalton, W. S., *et al.* (2002) Combination therapy with AG-490 and interleukin 12 achieves greater antitumor effects than either agent alone. *Mol. Cancer Ther.* **1,** 893–899
40. Meydan, N., Grunberger, T., Dadi, H., Shahar, M., Arpaia, E., Lapidot, Z., Leeder, J. S., Freedman, M., Cohen, A., and Gazit, A., *et al.* (1996) Inhibition of acute lymphoblastic leukaemia by a Jak-2 inhibitor. *Nature* **379,** 645–648
41. Wang, L. H., Kirken, R. A., Erwin, R. A., Yu, C. R., and Farrar, W. L. (1999) JAK3, STAT, and MAPK signaling pathways as novel molecular targets for the tyrphostin AG-490 regulation of IL-2-mediated T cell response. *J. Immunol.* **162,** 3897–3904
42. Battle, T. E., and Frank, D. A. (2002) The role of STATs in apoptosis. *Curr. Mol. Med.* **2,** 381–392
43. Zhang, S. S., Wei, J. Y., Li, C., Barnstable, C. J., and Fu, X. Y. (2003) Expression and activation of STAT proteins during mouse retina development. *Exp. Eye Res.* **76,** 421–431
44. Rhee, K. D., and Yang, X. J. (2003) Expression of cytokine signal transduction components in the postnatal mouse retina. *Mol. Vis.* **9,** 715–722
45. Song, Y., Zhao, L., Tao, W., Laties, A. M., Luo, Z., and Wen, R. (2003) Photoreceptor protection by cardiotrophin-1 in transgenic rats with the rhodopsin mutation s334ter. *Invest. Ophthalmol. Vis. Sci.* **44,** 4069–4075
46. Ji, J. Z., Elyaman, W., Yip, H. K., Lee, V. W., Yick, L. W., Hugon, J., and So, K. F. (2004) CNTF promotes survival of retinal ganglion cells after induction of ocular hypertension in rats: the possible involvement of STAT3 pathway. *Eur. J. Neurosci.* **19,** 265–272
47. Dikdan, G. S., Saba, S. C., Dela Torre, A. N., Roth, J., Wang, S., and Koneru, B. (2004) Role of oxidative stress in the increased activation of signal transducers and activators of transcription-3 in the fatty livers of obese Zucker rats. *Surgery* **136,** 677–685
48. Carballo, M., Conde, M., El Bekay, R., Martin-Nieto, J., Camacho, M. J., Monteseirin, J., Conde, J., Bedoya, F. J., and Sobrino, F. (1999) Oxidative stress triggers STAT3 tyrosine phosphorylation and nuclear translocation in human lymphocytes. *J. Biol. Chem.* **274,** 17580–17586
49. Brunet, A., Datta, S. R., and Greenberg, M. E. (2001) Transcription-dependent and -independent control of neuronal survival by the PI3K-Akt signaling pathway. *Curr. Opin. Neurobiol.* **11,** 297–305
50. Barber, A. J., Nakamura, M., Wolpert, E. B., Reiter, C. E., Seigel, G. M., Antonetti, D. A., and Gardner, T. W. (2001) Insulin rescues retinal neurons from apoptosis by a phosphatidylinositol 3-kinase/Akt-mediated mechanism that reduces the activation of caspase-3. *J. Biol. Chem.* **276,** 32814–32821
51. Datta, S. R., Brunet, A., and Greenberg, M. E. (1999) Cellular survival: a play in three Akts. *Genes Dev.* **13,** 2905–2927
52. Johnson, L. E., van Veen, T., and Ekstrom, P. A. (2005) Differential Akt activation in the photoreceptors of normal and rd1 mice. *Cell Tissue Res.* **320,** 213–222
53. Jomary, C., Cullen, J., and Jones, S. E. (2006) Inactivation of the Akt survival pathway during photoreceptor apoptosis in the retinal degeneration mouse. *Invest. Ophthalmol. Vis. Sci.* **47,** 1620–1629
54. Yu, D. Y., Cringle, S., Valter, K., Walsh, N., Lee, D., and Stone, J. (2004) Photoreceptor death, trophic factor expression, retinal oxygen status, and photoreceptor function in the P23H rat. *Invest. Ophthalmol. Vis. Sci.* **45,** 2013–2019
55. Wang, Y., Smith, S. B., Ogilvie, J. M., McCool, D. J., and Sarthy, V. (2002) Ciliary neurotrophic factor induces glial fibrillary acidic protein in retinal Muller cells through the JAK/STAT signal transduction pathway. *Curr. Eye Res.* **24,** 305–312

56. Chun, M. H., Ju, W. K., Kim, K. Y., Lee, M. Y., Hofmann, H. D., Kirsch, M., and Oh, S. J. (2000) Upregulation of ciliary neurotrophic factor in reactive Muller cells in the rat retina following optic nerve transection. *Brain Res.* **868,** 358–362
57. Harada, T., Harada, C., Nakayama, N., Okuyama, S., Yoshida, K., Kohsaka, S., Matsuda, H., and Wada, K. (2000) Modification of glial-neuronal cell interactions prevents photoreceptor apoptosis during light-induced retinal degeneration. *Neuron* **26,** 533–541
58. Harada, C., Harada, T., Quah, H. M., Maekawa, F., Yoshida, K., Ohno, S., Wada, K., Parada, L. F., and Tanaka, K. (2003) Potential role of glial cell line-derived neurotrophic factor receptors in Muller glial cells during light-induced retinal degeneration. *Neuroscience* **122,** 229–235
59. Murray, P., and Edgar, D. (2001) The regulation of embryonic stem cell differentiation by leukaemia inhibitory factor (LIF). *Differentiation* **68,** 227–234
60. Cartwright, P., McLean, C., Sheppard, A., Rivett, D., Jones, K., and Dalton, S. (2005) LIF/STAT3 controls ES cell self-renewal and pluripotency by a Myc-dependent mechanism. *Development* **132,** 885–896
61. Graham, D. R., Overbeek, P. A., and Ash, J. D. (2005) Leukemia inhibitory factor blocks expression of Crx and Nrl transcription factors to inhibit photoreceptor differentiation. *Invest. Ophthalmol. Vis. Sci.* **46,** 2601–2610
62. Sherry, D. M., Mitchell, R., Li, H., Graham, D. R., and Ash, J. D. (2005) Leukemia inhibitory factor inhibits neuronal development and disrupts synaptic organization in the mouse retina. *J. Neurosci. Res.* **82,** 316–332
63. Neophytou, C., Vernallis, A. B., Smith, A., and Raff, M. C. (1997) Muller-cell-derived leukaemia inhibitory factor arrests rod photoreceptor differentiation at a postmitotic pre-rod stage of development. *Development* **124,** 2345–2354
64. Samardzija, M., Wenzel, A., Naash, M., Reme, C. E., and Grimm, C. (2006) Rpe65 as a modifier gene for inherited retinal degeneration. *Eur. J. Neurosci.* **23,** 1028–1034
65. Xuan, Y. T., Guo, Y., Han, H., Zhu, Y., and Bolli, R. (2001) An essential role of the JAK-STAT pathway in ischemic preconditioning. *Proc. Natl. Acad. Sci. U. S. A.* **98,** 9050–9055
66. Yamauchi, K., Osuka, K., Takayasu, M., Usuda, N., Nakazawa, A., Nakahara, N., Yoshida, M., Aoshima, C., Hara, M., and Yoshida, J. (2006) Activation of JAK/STAT signalling in neurons following spinal cord injury in mice. *J. Neurochem.* **96,** 1060–1070
67. Kueng-Hitz, N., Grimm, C., Lansel, N., Hafezi, F., He, L., Fox, D. A., Reme, C. E., Niemeyer, G., and Wenzel, A. (2000) The retina of c-fos-/- mice: electrophysiologic, morphologic and biochemical aspects. *Invest. Ophthalmol. Vis. Sci.* **41,** 909–916

Received for publication February 16, 2006.
Accepted for publication June 12, 2006.

The FASEB Journal • FJ Express Summary

Differential role of Jak-STAT signaling in retinal degenerations

Marijana Samardzija, Andreas Wenzel, Svenja Aufenberg, Markus Thiersch, Charlotte Remé, and Christian Grimm[1]

Laboratory for Retinal Cell Biology, Department Ophthalmology, Center for Integrative Human Physiology (CIHP) and Neuroscience Center Zurich (ZNZ), University Hospital, Zürich, Switzerland

To read the full text of this article, go to http://www.fasebj.org/cgi/doi/10.1096/fj.06-5895fje

SPECIFIC AIMS

Photoreceptor apoptosis is a hallmark of blinding diseases caused by retinal degeneration. Neuroprotective strategies may protect photoreceptors from cell death and thus prolong the period of useful vision in patients. For the development of such strategies it is essential to understand the molecular signaling pathways involved in the degeneration of the retina. Molecules of the Jak-STAT pathway have been implicated in the control of cell survival, cell progression, and cell death. We analyzed a potential role of Jak-STAT signaling in three models of induced and inherited retinal degeneration. Using an inhibitor of Jak2, we tested whether the Jak-STAT pathway might be a potential target for therapeutic approaches, with the goal to prevent photoreceptor apoptosis.

PRINCIPAL FINDINGS

1. Induction of the Jak-STAT signaling pathway in a model of light-induced retinal degeneration

Retinal expression of leukemia inhibitory factor (LIF) and cardiotrophin like cytokine (CLC), members of the interleukin (IL)-6 family of cytokines, was strongly up-regulated during photoreceptor degeneration induced by exposure to bright white light. Peak expression of LIF and CLC occurred 12 h after light exposure, declining to near-basal levels in 3 days.

Concomitant with the induction of the cytokines, Janus kinase-2 (Jak2) as well as signal transducer and activator of transcription-1 (STAT1) and STAT3, both targets of Jak2, were activated by phosphorylation (**Fig. 1**). Extracellular-regulated kinase 1,2 (ERK1,2) was phosphorylated but Akt was not. This suggests that LIF and/or CLC were binding to their respective membrane receptors, leading to the activation of the intracellular Jak-STAT signaling pathway.

Jak2 and STAT-3 localized mainly to cells of the inner nuclear layer (INL) and the ganglion cell layer (GCL) with a weaker signal of STAT-3 in the inner segments of photoreceptors. STAT-1 localized mainly to the inner and outer plexiform layers (IPL and OPL) as well as to the GCL. This localization agrees with earlier publications and suggests that cells of the INL and GCL may respond to photoreceptor cell death.

The family of suppressors of cytokine signaling (SOCS) constitute a negative feedback loop for the regulation of Jak-STAT signaling. Expression analysis of all eight members of the SOCS family revealed a strong induction of SOCS3 (>13-fold) and, to a lesser extent, of SOCS1 (>6-fold) and of CIS (>2-fold).

2. Light-induced activation of the Jak-STAT pathway is damage dependent

To evaluate the significance of the activation of the Jak-STAT pathway for retinal degeneration, we tested phosphorylation of Jak2, STAT1, STAT3, and ERK1,2 in mouse strains differentially susceptible to light-induced retinal degeneration. Retinas of mice lacking the c-Fos protein on a genetic background expressing the methionine variant of the Rpe65 gene (c-fos$^{-/-}$; Rpe65$_{450M}$) are not susceptible to light damage whereas photoreceptors of c-fos$^{-/-}$ mice expressing the leucine variant of the Rpe65 gene (Rpe65$_{450L}$) undergo rapid apoptosis after acute light exposure.

Phosphorylation of ERK1,2 was increased after exposure in all strains, suggesting that ERK1,2 is activated by light *per se* and so may be involved in a physiological response to increased lighting conditions. In contrast, Jak2, STAT1, and STAT3 were activated exclusively in strains that are susceptible to light damage. No activation could be detected in the resistant strain. Thus, the Jak-STAT signaling pathway may be important for the induction of cell death after the light stimulus, an interpretation supported by the peak of activation at 12 h postillumination, 24 h before the maximal release

[1] Correspondence: Laboratory for Retinal Cell Biology, Department Ophthalmology, University Hospital, Frauenklinikstrasse 24, 8091 Zürich, Switzerland. E-mail: cgrimm@opht.unizh.ch

doi: 10.1096/fj.06-5895fje

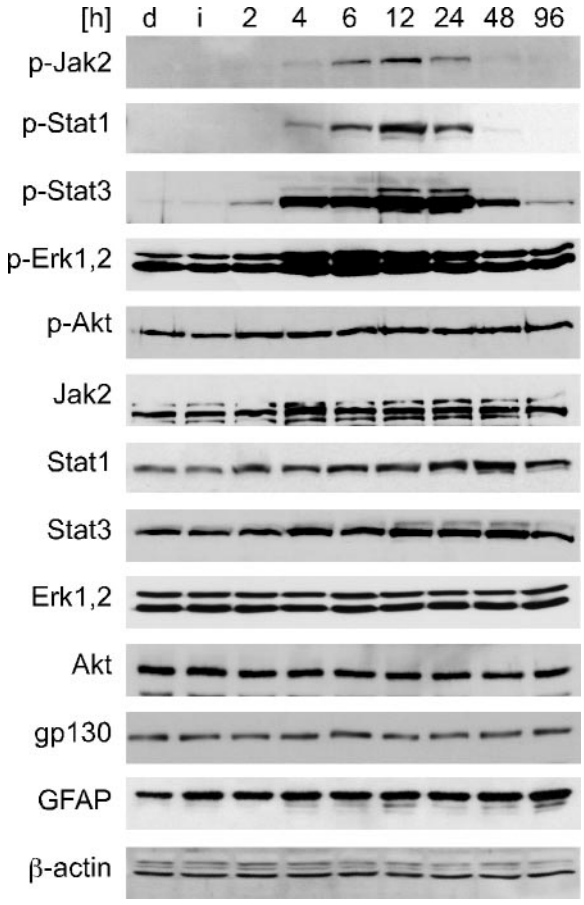

Figure 1. Induction of the Jak-STAT pathway in the retina after acute light exposure. BALB/c mice were not (dark control, d) or were exposed to 5000 lux of white light for 1 h. After light exposure, mice were sacrificed immediately (i) or after two 96 h of recovery in darkness as indicated. Proteins were extracted from isolated retinas and tested by Western blot.

of free nucleosomes, which was analyzed as a biochemical marker for apoptosis.

3. Induction of members of the Jak-STAT pathway in inherited retinal degeneration

We used the rd1 mouse as a model for autosomal recessive retinitis pigmentosa (arRP) and the transgenic VPP mouse as a model for autosomal dominant RP (adRP) to test whether the pathway activated by acute light exposure may also be involved in photoreceptor apoptosis in inherited retinal degeneration. A mutation in the β-subunit of phosphodiesterase causes the rapid degeneration of photoreceptors in the rd1 mouse, with an early onset around postnatal day (PND) 11 and almost complete degeneration at 3 wk of age. The transgene in the VPP mouse expresses a mutant rhodopsin protein with three amino acid substitutions. Degeneration induced by the transgene has a later onset and is slowly progressing. As in the light damage model, p-STAT3 levels were up-regulated during the phase of photoreceptor degeneration in both inherited models. Although levels of total STAT1 protein were elevated in both inherited models, p-STAT1 was not (rd1) or was only barely (VPP) detectable. In contrast to the induced model, p-Jak2 was not (rd1) or only marginally (VPP) activated, and levels of p-ERK1,2 remained constant. Instead, levels of p-Akt were elevated in the adult retinas of both models.

Exponential RT-polymerase chain reaction (RT-PCR) showed that LIF and CLC cytokines were also induced in both inherited models, as was SOCS3. CIS was slightly elevated in the VPP model but not in the rd1 mouse. SOCS1, however, remained at basal levels in both models. These results suggest that a degeneration-inducing stimulus causes a specific expression and/or activation of members of the Jak-STAT pathway. This is further supported by our observation that ciliary neurotrophic factor (CNTF) was moderately induced in the rd1 mouse retina and that fibroblast growth factor-2 (FGF-2) was strongly up-regulated in the VPP mouse but only marginally in the rd1 retina.

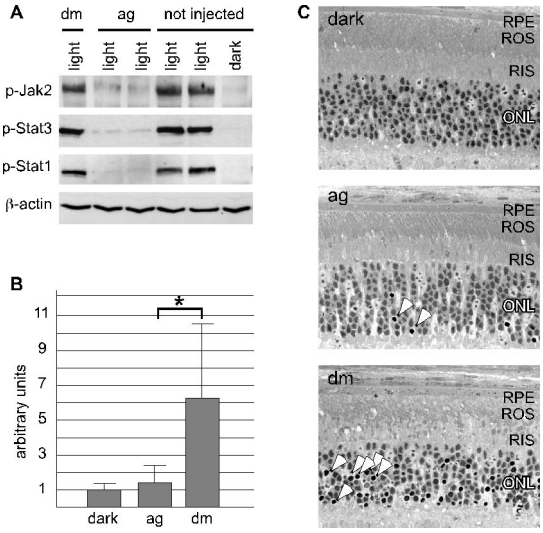

Figure 2. Inhibition of Jak signaling prevents retinal degeneration after bright light exposure. *A)* Immediately before light exposure, BALB/c mice received a single injection of 800 μg AG-490 (ag) or carrier DMSO (dm) or were not injected. Mice were subsequently exposed for 1 h to 5′000 lux or not (dark) and phosphorylation of proteins was tested 18 h postexposure. Retinal proteins from separate animals were loaded in each lane. *B)* Retinas of animals not exposed to light (dark) or of animals pretreated with AG-490 (ag) of DMSO (dm) and exposed for 1 h to 5′000 lux were used to quantify apoptosis by ELISA. $*P = 0.003$, 2-tailed t test; $n = 10$ mice for each condition. *C)* Light microscopy 18 h after light exposure. Retinas of dark control mice showed regular photoreceptors (upper panel). Retinas of AG-490 (ag)-treated mice exhibited few apoptotic photoreceptor nuclei (arrowheads, middle panel); retinas of carrier (DMSO, dm)-treated mice had significantly more dying photoreceptors (arrowheads, lower panel). RPE: retinal pigment epithelium; reactive oxygen species (ROS): rod outer segments; RIS: rod inner segments; ONL outer nuclear layer.

4. Inhibition of Jak-STAT signaling protects against induced but not inherited retinal degeneration

AG-490, an inhibitor of Jak2 activity, was injected i.p. immediately before the onset of light exposure. In contrast to control mice injected with carrier or ones that did not receive an injection, AG-490-treated mice did not show increased protein phosphorylation (**Fig. 2**). Furthermore, AG-490 treatment, and thus interference with the Jak-STAT pathway, significantly reduced light damage susceptibility of photoreceptors as indicated by reduced internucleosomal DNA cleavage (Fig. 2*B*). AG-490-treated mice had only a few scattered photoreceptor nuclei showing condensed chromatin as a classical sign of apoptosis (Fig. 2*C*, middle panel), whereas mice treated with carrier only showed a highly increased number of pyknotic nuclei (Fig. 2*C*, bottom panel).

To assess the potential role of Jak2 in STAT3 activation and retinal degeneration in the VPP mouse, we treated VPP mice with daily injections of AG-490, starting at PND 15 and ending at PND 27. Analysis was at PND 28. The retina of 15-day-old VPP mice had 7 to 9 rows of photoreceptor nuclei and distinct (but shortened) inner and outer segments. AG-490 treatment reduced phosphorylation of Jak2 to levels found in wild-type (WT) animals. Levels of p-STAT3, however, were still elevated and clearly above WT levels. The amount of rhodopsin per retina was measured to quantify photoreceptor degeneration. Four-wk-old WT mice had 0.43 ± 0.083 ($n=3$) nmol rhodopsin, whereas untreated VPP mice of the same age had only 0.071 ± 0.015 ($n=3$) nmol and AG-490-treated mice had 0.065 ± 0.014 ($n=4$) rhodopsin left. Thus, regardless of the AG-490 treatment, >80% of the photoreceptors were lost.

CONCLUSIONS AND SIGNIFICANCE

In this work we show that members of the Jak-STAT pathway are induced in three different models of retinal degeneration. The individual activation patterns, however, are death stimulus specific. Differentially activated proteins include cytokine ligands, STAT transcription factors, and molecules of a negative feedback loop. The neuroprotective effect of the inhibition of Jak2 in induced but not in inherited cell death, supports the conclusion of different molecular pathways in retinal degenerations.

The Jak-STAT signaling pathway has been implicated in neurodegenerative as well as neuroprotective mechanisms. Activation of STAT1 is mostly proapoptotic whereas phosphorylation of STAT3 is commonly accepted as antiapoptotic. In the light-treated retina, STAT1 and STAT3 proteins were both activated, implying that cell death as well as cell survival mechanisms were induced. We speculate that the retina responds to an insult by generating both death factors promoting apoptosis of photoreceptors that are damaged beyond rescue and survival factors which help to rescue damaged photoreceptors that are still viable (**Fig. 3**). The production of such factors may be differentially controlled by STAT1 and STAT3, respectively. Jak2, STAT1, and STAT3 proteins were found mainly in cells of the INL and GCL and in the inner and outer plexiform layers. However, photoreceptors are the cells primarily affected in all models of retinal degeneration used here. Thus, the fate of photoreceptors might be determined by other cell types through STAT1/STAT3-regulated production and release of growth factors and/or cytokines.

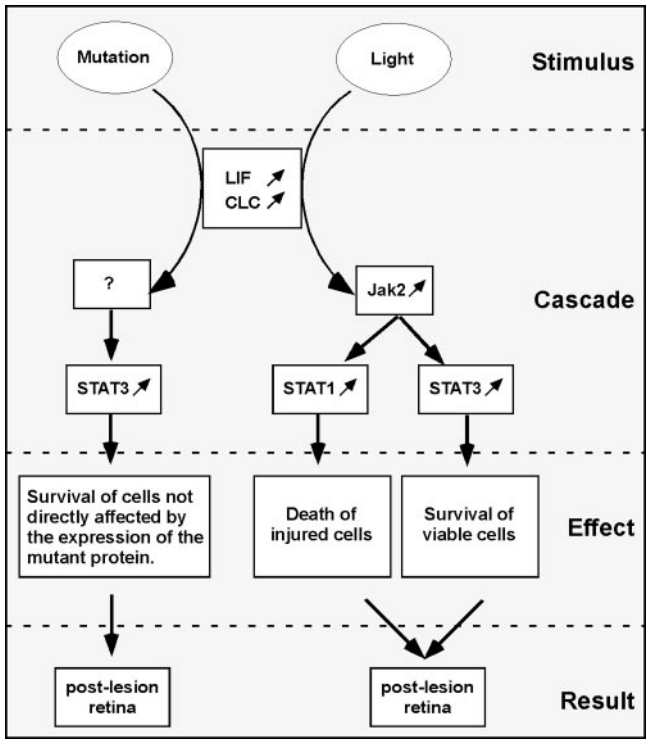

Figure 3. Schematic representation of the signaling pathways involved in the models of retinal degeneration.

Treatment with AG-490 did not rescue photoreceptors in the VPP mouse, which suggests that different mechanisms are involved in inherited retinal degenerations. The differential activation of STAT3 and STAT1 proteins, and especially the sustained phosphorylation of Akt in both inherited but not the induced model, support this conclusion. To find treatment strategies for a broad range of retinal degeneration, it is of outmost importance to analyze the different signaling cascades in order to identify common molecules as potential treatment targets. FJ

6.2 Caspase-1 Ablation Protects Photoreceptors in a Model of Autosomal Dominant Retinitis Pigmentosa

Marijana Samardzija, Andreas Wenzel, **Markus Thiersch**, Rico Frigg, Charlotte Remé, and Christian Grimm

Laboratory for Retinal Cell Biology, Department Ophthalmology, Center for Integrative Human Physiology (CIHP) and Neuroscience Center Zurich (ZNZ), University Hospital, Zurich, Switzerland

Published in IOVS, Vol. 47, No. 12, 5181–5190 (2006)

6.2.1 Author contribution

Design:	MS, AW and CG
Experiments:	MS, RF, **MT** (assisted in animal treatment, histology) and CG
Interpretation:	MS, AW, **MT**, CR and CG
Manuscript:	MS and CG
Manuscript Correction:	MS, AW and CG

6.2.2 Summary

In this paper we investigated the role of caspase-1 (Casp-1), which was induced on the transcriptional level during light-induced retinal degeneration. We assumed that caspase-1 might trigger apoptosis and tested our hypothesis in a model for light induced retinal degeneration and in inherited models for autosomal recessive (*rd1* mouse) and for autosomal dominant (VPP mouse) retinal degeneration. Apoptosis induced by light was measured by nucleosomal release, which peaked 36 h after illumination. The uncleaved pro-from of caspase-1 started to accumulate 6 h after light. In correlation with the nucleosomal release, pro-caspase-1 protein levels reached a plateau between 36 h and 72 h after light exposure. In a second boost, it peaked again 5 days after light and reached basal levels 20 days after light exposure. In contrast, protein levels of initiator caspase-9 and effector-caspase-3, -6 and –7 pro-forms were not induced. IL-1β encodes for a precursor protein, which has to be proteolytic processed to the mature form by activated Casp-1. IL-1β mRNA levels were

upregulated after light exposure with a maximal induction 12 h after illumination. However, neither was IL-1β processed nor was the pro-form of Casp-1 cleaved and thereby activated. We observed a similar induction of Casp-1 pro-form but no cleavage or Casp-1 activity in *rd1* and VPP mice – both models for inherited retinal degeneration. Nevertheless, we speculated that the pro-form of Casp-1 might initiate apoptosis via an unknown mechanism. Therefore, we compared the light susceptibility of Casp-$1^{-/-}$ mice to wild type control mice. The ablation of Casp-1 did not notably influence light induced retinal degeneration. IL-1R$1^{-/-}$ mice lack the IL-1 receptor type 1, which is the target receptor for Casp-1-activated IL-1β. However, IL-1R$1^{-/-}$ mice and control mice similarly degenerated after light exposure – supporting the finding of a Casp-1 independent apoptosis mechanism. To test a potential Casp-1 impact in models for inherited retinal degeneration, we generated double-mutant *rd1*/Casp-$1^{-/-}$ and VPP/Casp-$1^{-/-}$ mice. Casp-1 ablation neither impaired progression nor severity of retinal pathogenesis in *rd1* mice. In contrast, Casp-1 ablation substantially protected retinal morphology in VPP mice. VPP/Casp-$1^{-/-}$ mice had twice as high rhodopsin levels (a marker for the survival of photoreceptor cells) as single mutant VPP mice. To test, whether Casp-1 facilitates cell death via its classical downstream target IL-1β in VPP mice, we analyzed VPP/IL-1R$1^{-/-}$ double-mutant mice. However, the lack of IL-1R1 did not influence retinal degeneration, suggesting a role of Casp-1 independent from its classical function as an IL-1β processor. We assumed that cytokine and chemokine signaling might be required for a non-conventional Casp-1 function. Therefore, we analyzed Casp-1, speck-like protein (asc), CNTF, FGF-2 and monocyte chemoattractant protein (MCP-1) gene expression in wild type, Casp-$1^{-/-}$, VPP and VPP/Casp-$1^{-/-}$ mice (Note: primers for Casp-1 aligned upstream the neomycin cassette and therefore detected expression levels of the disrupted, nonfunctional Casp-1 gene). Casp-1 gene expression remained steady state during postnatal development (PND11 – PND56) but was induced in VPP mice, which correlated with the Casp-1 protein expression. Nonfunctional Casp-1 gene expression was induced in Casp-$1^{-/-}$ mice and even more pronounced in VPP/Casp-$1^{-/-}$ mice. We speculated that Casp-1 might regulates its own gene activity in a feedback loop. Expression levels of asc – a CARD (caspase recruiting domain) containing protein, involved in Casp-1 activation – declined in wild type mice but were elevated in VPP mice. This further supports an impact of Casp-1 in retinal degeneration of VPP mice. However, Casp-$1^{-/-}$ and VPP/Casp-$1^{-/-}$ mice showed hardly any asc expression, suggesting that asc is Casp-1 dependent regulated. CNTF was elevated in VPP and VPP/Casp-$1^{-/-}$ mice during the late phase of retinal degeneration (PND42 – PND56). FGF-2 was strongly induced in

VPP and VPP/Casp-1$^{-/-}$ mice. However, FGF-2 expression was slightly reduced in VPP/Casp-1$^{-/-}$ mice compared to VPP mice, which possibly reflects the milder and/or delayed retinal degeneration in Casp-1 ablated mice. MCP-1 is involved in the recruitment of macrophages to the side of injury, which is essential to minimize secondary apoptosis or necrosis. Because MCP-1 expression levels were induced in VPP mice and even more in VPP/Casp-1$^{-/-}$ mice, we suggested that it might be required for the improved retinal maintenance in Casp-1 ablated VPP mice. In conclusion, we discovered that light-induced retinal degeneration and inherited retinal degeneration in *rd1* mice is caspase-1 independent. In VPP mice, casp-1 is partially involved in retinal degeneration via a non-classical pathway. However, ablation of Casp-1 did not completely protect the retina of VPP mice, suggesting further pro-apoptotic pathways.

6.2.3 Manuscript

Caspase-1 Ablation Protects Photoreceptors in a Model of Autosomal Dominant Retinitis Pigmentosa

Marijana Samardzija, Andreas Wenzel, Markus Thiersch, Rico Frigg, Charlotte Remé, and Christian Grimm

Purpose. Caspase-1 gene expression has been reported to be upregulated during light-induced retinal degeneration and to be reduced after neuroprotective treatments. Thus, caspase-1 may be proapoptotic in the retina. To test directly the role of caspase-1 in photoreceptor apoptosis, three mouse models were analyzed for retinal degeneration in the presence or absence of caspase-1.

Methods. Photoreceptor apoptosis was monitored in one model of induced (exposure to light) and in two models of inherited (*rd1*, VPP) retinal degeneration. Retinal degeneration was assessed qualitatively by light microscopy and quantitatively by the determination of free nucleosomes with ELISA or by rhodopsin measurements. Gene expression and protein levels were assessed by real-time RT-PCR and by Western blot analysis, respectively.

Results. Levels of caspase-1 proenzyme increased in all models of retinal degeneration concomitantly with the onset of cell death. Maturation or classic activity of caspase-1 was not detected in the retina. Ablation of caspase-1 was protective in the model of adRP (VPP mouse), but not in the two other models. Ablation of interleukin-1 receptor type 1 was without effect. Expression of monocyte chemoattractant protein (MCP)-1 increased in the model protected by caspase-1 ablation.

Conclusions. Increased retinal expression of caspase-1 proenzyme may be a common marker for photoreceptor degeneration. The differential effects of caspase-1 ablation suggests a modulatory role of caspase-1 for photoreceptor apoptosis in some but not all models. Such a modulatory activity may involve a caspase-1 function different from the classic activation of interleukin-1β. (*Invest Ophthalmol Vis Sci.* 2006;47: 5181–5190) DOI:10.1167/iovs.06-0556

Photoreceptor cell death is a hallmark of most retinal dystrophies. Dying photoreceptors share all the major morphologic features of apoptosis including nuclear condensation and nucleosomal DNA fragmentation, cytosolic condensation, and cell shrinkage as well as the formation of apoptotic bodies. Apoptosis has been considered as the final common pathway of cell death in retinal degenerations.[1–3] The intracellular signals that lead to apoptosis of the visual cells are still far from conclusive. The caspases, a family of cysteine proteases, have been implicated in the regulation of apoptotic cell death in a variety of systems. Caspase-dependent cell death is regulated via one of three major pathways: the receptor- or the mitochondria-mediated cell signaling pathway or by an endoplasmic reticulum stress response. One of the key events triggering caspase-dependent apoptosis is the activation of initiator caspases by oligomerization of the inactive cellular precursors in response to death stimuli. Once activated, initiator caspases induce a tightly regulated cascade of events propagating the death signal by activation of downstream effector caspases leading to cleavage of various cellular substrates in a process that culminates in cell death (reviewed in Ref. 4).

In experimental models developed to study cell death in the retina, several different caspases—in particular, caspase-3—have been reported to be activated during apoptosis. These models include cell death induced by ischemia,[5] excitotoxicity,[6] treatment with autoantibodies,[7] and lead and calcium overload.[8] Caspase activation has also been demonstrated in some animal models of inherited retinal degeneration such as rhodopsin S334ter rats,[9] Royal College of Surgeon (RCS) rats,[10] tubby mice,[11] and *rds* mice.[12] For retinal degeneration in the *rd1* mouse, which carries a mutation in the gene encoding the phosphodiesterase β-subunit (PDE6β)[13] contradictory data regarding the involvement of caspase-3 have been reported. Both caspase-dependent[14–17] and -independent[18] photoreceptor cell death have been described.

Caspase (Casp)-1 has been identified as the mammalian homologue to the nematode *ced-3* gene[19] and has been implicated in programmed cell death. Today, Casp-1 is mainly associated with inflammation, for its ability to cleave the inactive 31-kDa cytokine pro-interleukin-1-β (pro-IL-1β) into an active 17-kDa mature form.[20,21] However, evidence of an involvement of Casp-1 also in apoptosis has been demonstrated in several in vitro and in vivo systems.[22–25] Using the model of light-induced retinal degeneration, we and others have shown that Casp-1 gene expression is increased in retinas injured by exposure to light[26–28] and that treatments that increase the resistance against light-induced damage (e.g., hypoxic preconditioning) prevent increased Casp-1 expression.[29] These findings suggest that Casp-1 is involved in the mediation or regulation of photoreceptor apoptosis after a light-induced insult.

In the present study, we tested whether Casp-1 was induced in other models of retinal degeneration as well and whether ablation of Casp-1 would influence the degenerative process. For this purpose, we used the *rd1* mouse as a model for autosomal recessive retinitis pigmentosa (arRP) and the VPP mouse, representing a model for autosomal dominant RP (adRP). The *rd1* mouse develops a fast and light-independent degeneration of photoreceptors starting around postnatal day (PND)10.[13] The VPP mouse expresses a mutant rhodopsin transgene encoding a protein with three amino acid substitutions (V20G, P23H, and P27L)[30] one of which (P23H) repre-

From the Laboratory for Retinal Cell Biology, Department of Ophthalmology, the Center for Integrative Human Physiology (CIHP), and the Neuroscience Center Zürich (ZNZ), University of Zürich, Zürich, Switzerland.

Supported by Grant 3100A0-105793 from the Swiss National Science Foundation and a grant from the European Community (EVI-GenoRet; LSHG-CT-512036) and the H. Messerli Fonds. The Laboratory of Retinal Cell Biology is a member of the Center of Integrative Human Physiology (CIHP) and of the Neuroscience Center Zürich (ZNZ) of the University of Zürich.

Submitted for publication May 19, 2006; revised August 2, 2006; accepted September 20, 2006.

Disclosure: **M. Samardzija**, None; **A. Wenzel**, None; **M. Thiersch**, None; **R. Frigg**, None; **C. Remé**, None; **C. Grimm**, None

The publication costs of this article were defrayed in part by page charge payment. This article must therefore be marked "*advertisement*" in accordance with 18 U.S.C. §1734 solely to indicate this fact.

Corresponding author: Christian Grimm, Lab for Retinal Cell Biology, Department of Ophthalmology, University Hospital Zürich, Frauenklinikstrasse 24, 8091 Zürich, Switzerland; cgrimm@opht.unizh.ch.

TABLE 1. Primer Sequences

Gene	Forward Primer	Reverse Primer
Genotyping		
Casp1 wt	CTGTGGTGACTAACCGATAA	CATGCCTGAATAATGATCACC
Casp1$^{-/-}$	CTGTGGTGACTAACCGATAA	GCGCCTCCCCTACCCGG
rd1	CATCCCACCTGAGCTCACAGAAAG	GCCTACAACAGAGGAGCTTCTAGC
IL-1R1 wt	GAGTTACCCGAGGTCCAG	GAAGAAGCTCACGTTGTC
IL-1R1$^{-/-}$	GAGTTACCCGAGGTCCAG	GCGAATGGGCTGACCCGCT
VPP	AGACTGACATGGGGAGGAATTCCCAGA	CAGCTGCTCGAAGTGACTCCGACC
RT-PCR		
β-Actin	CAACGGCTCGGCATGTG	CTCTTGCTCTGGGCCTCG
Casp-1	GGCAGGAATTCTGGAGCTTCAA	GTCAGTCCTGGAAATGTGCC
IL-1β	GCAGGCAGTATCACTCATTG	CGTTGCTTGGTTCTCCTTGT
Asc	ACGCCATAGATCTCACTGAC	CACAGCTCCAGACTCTTCTT
FGF-2	TGTGTCTATCAAGGGAGTGTGTGC	ACCAACTGGAGTATTTCCGTGACCG
MCP-1	GGCTCAGCCAGATGCAGTTA	CTGCTGCTGGTGATCCTCTT
CNTF	CTCTGTAGCCGCTCTATCTG	GGTACACCATCCACTGAGTC

sents the most common cause for adRP in the United States. The expression of the transgene leads to photoreceptor death with loss of function.[30,31] Retinal degeneration in the VPP mouse is accelerated by light[32,33] but proceeds slower than in the *rd1* mouse. We analyzed the course of retinal degeneration in the light-induced and the two inherited models in the presence and absence of functional Casp-1 and showed that the lack of Casp-1 activity affected the retina differentially in the three models.

MATERIALS AND METHODS

Animals

All procedures concerning animals were in accordance with the regulations of the Veterinary Authority of Zurich and with the ARVO Statement for the use of Animals in Ophthalmic and Vision Research. All animals were raised in cyclic light (12:12 hours; 60 lux at cage level).

BALB/c mice were purchased from Harlan (Horst, The Netherlands). Casp-1-deficient mice (Casp1$^{-/-}$) are described elsewhere[34] and were generously provided by Winnie Wong (BASF Bioresearch, Worcester, MA). VPP mice (generously provided by Muna Naash, University of Oklahoma, Oklahoma City, OK) and wild-type mice (both on a 129.B6 background) and *rd1* mice (C3H/HeJ) were maintained at the University Hospital Zurich. The IL-1R1$^{-/-}$ mice, backcrossed onto BALB/c background for more than eight generations,[35,36] were kindly provided by Manfred Kopf (ETH, Zurich, CH). The double mutants *rd1*/Casp1$^{-/-}$, VPP/Casp1$^{-/-}$, and VPP/IL-1R1$^{-/-}$ were generated by classic breeding schemes. Genotyping was performed by PCR on genomic DNA, using the primers shown in Table 1. For *rd1* genotyping, PCR products were digested with *Dde*I, as described elsewhere.[37] All mouse strains were homozygous for the $Rpe65_{450Leu}$ variant.[38]

Exposure to Light and Assessment of Retinal Damage

Light damage was induced in dark-adapted 6- to 8-week-old mice placed in cages with reflective interior by exposure to 5 klux/1 hour (albino strains) or to 13 klux/2 hours (pigmented, with dilated pupils) of diffuse white fluorescent light, as described elsewhere.[39] The extent of light-induced damage in the retinas after different recovery periods in darkness was quantified by the ELISA-based determination of free nucleosomes in the cytoplasm (generated after internucleosomal cleavage of genomic DNA during the course of apoptosis), with a cell viability kit (Cell Death Detection Kit no. 1920685; Roche Diagnostics, Basel, Switzerland) according to the manufacturer's recommendation or by the determination of the rhodopsin content after 16 hours of dark adaptation as described.[40]

Qualitative assessment of retinal tissue was performed by light microscopic viewing of sections from the lower temporal retina of 2.5% glutaraldehyde-fixed and Epon 812-embedded eyes, as has been described.[39]

Semiquantitative RT-PCR Analysis

RNA isolation from retinas and cDNA synthesis were performed as described previously.[26] Primer pairs used for specific amplifications were designed to span intronic sequences or cover exon–intron boundaries (Table 1). Gene expression was analyzed by real-time RT-PCR with a polymerase ready mix (SYBR Green JumpStart *Taq* ReadyMix; Sigma-Aldrich, Munich, Germany) and a thermocycler (LightCycler; Roche Diagnostics). Amplification specificity was controlled by performing a melting curve analysis of the amplified PCR fragments and by visualizing amplified products on agarose gels. For relative quantification of gene expression, mRNA levels were normalized to β-actin using the $\Delta\Delta^{CT}$ (comparative threshold cycle) method and relative values were calculated with a respective control sample used for calibration, as indicated in the Results section. Each reaction was run in triplicate.

Western Blot Analysis

Retinas were homogenized in 100 mM Tris/HCl (pH 8.0) and analyzed for protein content by using the Bradford method. Standard SDS-PAGE and Western blot analysis were performed. Polyclonal rabbit anti-casp-1, -3, -6, -7, (kindly provided by Peter Vandenabeele, Ghent University, Belgium), anti-casp-1 (p10) (sc-514; Santa Cruz Biotechnology, Santa Cruz, CA), anti-casp-9 (no. 9504; Cell Signaling, Danvers, MA) and sheep anti-IL1β (S329/B4b, kind gift from Stephen Poole; NIBSC [Institute for Biological Standards and Control], Potters Bar, UK) antibodies were applied, followed by a horseradish peroxidase (HRP)-conjugated secondary anti-rabbit (no. NA934; GE Healthcare, Munich, Germany) or anti-sheep/goat (STAR88P; Serotec, Oxford, UK) antibody. To control for equal protein loading, membranes were reprobed with goat anti-actin antibody (sc-1616; Santa Cruz Biotechnology). Immunoreactivity was visualized using a Western blot detection kit (Renaissance; PerkinElmer Life Sciences, Emeryville, CA).

Determination of WEHD-pNA Cleavage

Retinas were dissected and homogenized in 120 μL of cold lysis buffer (BF14100; R&D Systems, Minneapolis, MN) followed by incubation on ice for 30 minutes. The retinal homogenates were centrifuged at 15,000*g* for 10 minutes at 4°C. The protein content of supernates was determined by a protein assay (Bio-Rad, Hercules, CA) using bovine serum albumin as the standard. An equal quantity (150 μg) of retinal protein was loaded into each well of a microtiter plate. Lysates were incubated with an equal volume of 1× reaction buffer and Casp-1

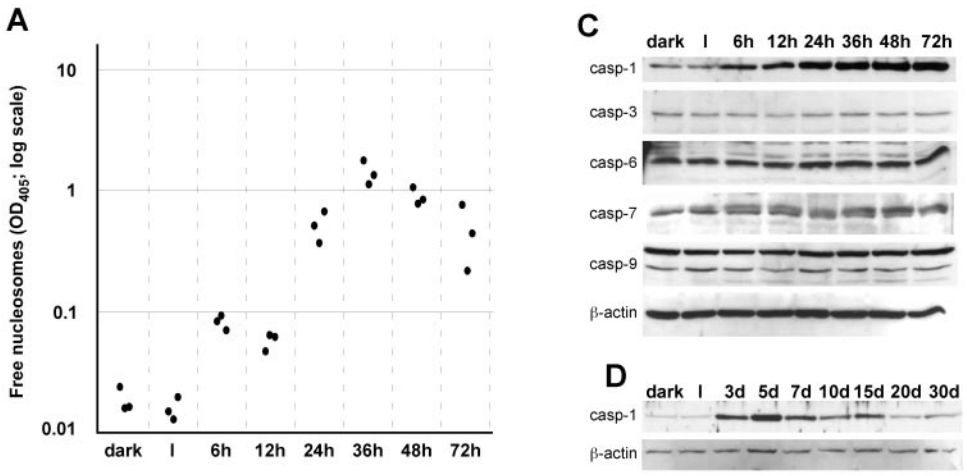

FIGURE 1. Retinal apoptosis and expression of caspases after exposure to light. Dark-adapted BALB/c (**A**, **C**, **D**) or 129.B6 (**B**) mice were not exposed (dark) or were exposed to 5 klux of white fluorescent light for 1 hour (**A**, **C**, **D**) or to 13 klux for 2 hours (**B**). Retinas were harvested immediately (I) or at different time points as indicated. (**A**) Cell death in the retina was detected by ELISA-based measurement of free nucleosomes in cytoplasmic extracts. Release of nucleosomes was detected as early as 6 hours after exposure and peaked at 36 hours. Data points represent the OD_{405} of retinas of individual mice. Note the logarithmic scale on the *y*-axis. (**B**) Retinal morphology of 129.B6 mice at the indicated time points before (dark) or after exposure to light. (**C**) Apoptotic cell death was associated with accumulation of the Casp-1 proform. Western blots show proforms of individual caspases at different time points after exposure to light as indicated. Levels of Casp-1 increased steadily, whereas expression of other tested caspases remained constant. Representative Western blot analyses from at least three independent experiments are shown. Membranes were reprobed with β-actin to control for equal protein load. (**D**) Long-term follow-up of Casp-1 expression after exposure to light. Expression of Casp-1 peaked at 5 days after illumination before basal levels were reached after 20 days. β-Actin was tested as loading control.

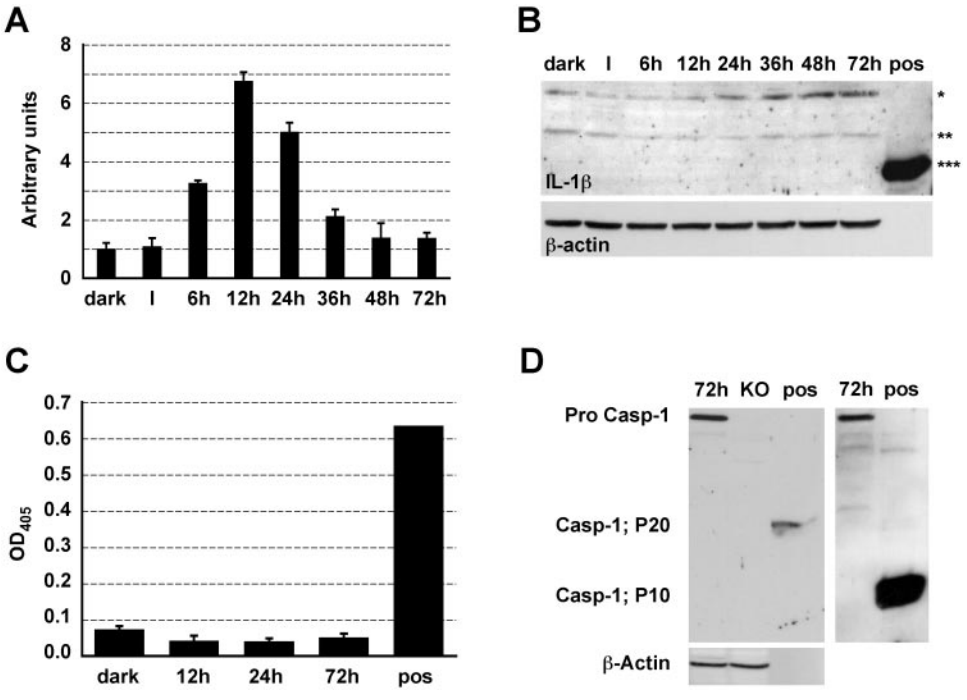

FIGURE 2. Caspase-1 activity was not detected after exposure to light. Dark-adapted BALB/c mice were not exposed (dark) or were exposed for 1 hour to 5 klux, and retinas were harvested immediately (I) or at different time points thereafter as indicated. (**A**) Levels of IL-1β mRNA increased after exposure and peaked at 12 hours after illumination. Relative mRNA levels were assessed by exponential RT-PCR (mean ± SD of three reactions performed on a pool of RNAs from three retinas isolated from three different animals per time point). (**B**) Il-1β was not processed after light-induced damage. Increasing pro-IL-1β levels were detected by Western blot analysis with increasing time (as indicated) after exposure to light (*top*). Mouse recombinant mature IL-1β (17 kDa) was used as a positive control (pos) for immunoblot analysis. Mature IL-1β was not detected in retinal extracts. *31 kDa proform of Il-1β, **unspecific signal, ***mature form of Il-1β. β-Actin served as the loading control (*bottom*). (**C**) Casp-1 was not enzymatically active after light-induced damage. WEHD-pNA cleavage was determined spetrophotometrically in vitro using an ELISA-based method on retinal extracts prepared from control (dark) or from retinas isolated at different time points after exposure to light, as indicated. pos: recombinant active Casp-1 as the positive control (the mean ± SD of three retinas from three different animals). (**D**) Pro-Casp-1 was not processed after exposure to light. Retinal extracts prepared at 72 hours after exposure to light were tested with two antibodies recognizing the Casp-1 proform and p20 active form (*left*) or the Casp-1 proform and the p10 active form (*rigbt*). Extract of Casp-1 knockout mice (KO) was loaded for specificity control, and β-actin served as the loading control (*bottom*). pos: recombinant active Casp-1 as positive control for antibodies.

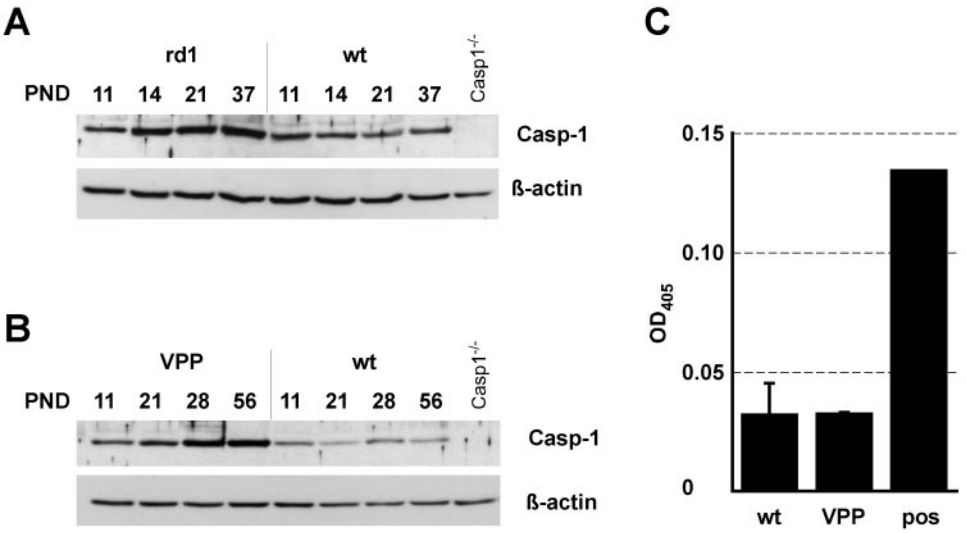

FIGURE 3. Induction of Casp-1 expression in inherited models of retinal degeneration. *rd1* (**A**) and VPP (**B**) mice were raised in dim cyclic light, and retinas were harvested on different postnatal days, as indicated. Each time point was compared with age-matched wild-type mice. Casp-1 expression was tested in total retinal homogenates by Western blot analysis. Extracts from $Casp1^{-/-}$ mice served as the control for antibody specificity. Casp-1 activation was monitored by the WEHD-pNA substrate cleavage assay as in Fig. 2C. (**A**) Casp-1 levels increased in retinas of *rd1* mice starting at ~PND14. (**B**) Casp-1 levels increased in retinas of VPP mice starting at ~PND21. Mature Casp-1 was not detected at any age in any genotype tested (not shown). (**C**) No classic Casp-1 activity was detected in extracts from retinas of VPP mice. WEHD-pNA cleavage was measured spectrophotometrically in retinal extracts from 4-week-old VPP mice and corresponding wild-type control animals. pos: activity of recombinant active Casp-1 as positive control. The mean ± SD of three independent retinas from three different animals.

substrate, according to the manufacturer's instructions at 37°C for 18 hours. Cleavage of the peptide substrate WEHD-pNA was monitored by liberation of the chromogenic pNA measuring absorption at 405 nm. Three animals were analyzed per condition.

RESULTS

To establish the time course of light-induced photoreceptor apoptosis, we used two different methods. To quantify the amount of cells, which irreversibly entered the process of apoptotic cell death, that is cells in the phase of internucleosomal DNA cleavage, we measured the release of free nucleosomes in retinal cell lysates by ELISA. To assess cell loss and morphologic changes by apoptosis in the retina, we used classic histologic methods.

Nucleosomal release above background was detectable at 6 hours after illumination and peaked at 36 hours after exposure to light (Fig. 1A) as described earlier.[41] Signal intensity declined slowly thereafter, but relatively high levels remained up to 3 days after illumination (the last time point tested). Morphologic changes in light-exposed retinas were detectable by light microscopy at 1 day after exposure (Fig. 1B). Rod outer segments (ROS) and rod inner segments (RIS) were severely disturbed, and many photoreceptor nuclei in the outer nuclear layer (ONL) showed condensed chromatin. At 2 days after illumination, the ONL was thinned and contained predominantly nuclei with condensed chromatin. The area of ROS and RIS showed complete devastation. The gap between ONL and pigment epithelium (PE) at days 2 and 5 may be preparation artifacts resulting from the weakened retinal structures. Between 2 and 5 days after exposure, most photoreceptor nuclei were lost. Between 5 and 10 days, debris of dead cells was removed, and no further change was obvious up to day 30 after the exposure.

DNA cleavage, as detected by the cell death detection ELISA assay, precedes the removal of the affected cell. Its peak was detected between 1 and 3 days after the insult, whereas physical loss of cells followed after a delay of approximately 1 day (peak between 2 and 5 days). Accordingly, we focused on the first 3 days after exposure to light for the analysis of biochemical events in the signaling cascades leading to cell death.

Expression and Activity of Caspase-1 in Retinal Degeneration

In many systems, apoptotic cell death is mediated by caspases. In the light-induced damage system, however, Western blot analysis revealed that the amount of the proenzymatic forms of caspase-3, -6, -7, and -9 remained unchanged over a period of 3 days after the exposure to light (Fig. 1C). In addition, cleaved (activated) fragments of these caspases remained undetectable. Together with results from others,[18,42] this suggests that light-induced damage is independent of these caspases. In contrast, increasing Casp-1 proenzyme levels were detected after light treatment (Fig 1C). Induction of Casp-1 followed the initial time course of nucleosomal release (Fig. 1A) starting at 6 hours after illumination. In contrast to the release of nucleosomes, Casp-1 proenzyme increased continuously, reaching a maximum at 5 days. Thereafter, pro-Casp-1 levels declined to baseline (Figs. 1C, 1D). Thus, elevated Casp-1 levels were present beyond the peak of apoptosis.

The major known role of active Casp-1 is proteolytic processing of IL-1β from a 33-kDa precursor protein to the 17-kDa mature form. Light exposure induced expression of IL-1β, with peak mRNA levels at 12 hours (Fig. 2A) and maximum protein (proform) levels at 24 to 72 hours after illumination (Fig. 2B). Although both Casp-1 protease and IL-1β substrate were induced and present in high amounts at 72 hours after illumination, we did not observe mature IL-1β by Western blot analysis (Fig. 2B) or ELISA (not shown). Using an in vitro assay for WEHD-pNA substrate cleavage, we also did not detect increased Casp-1 activity in retinal extracts after exposure to light (Fig. 2C). Because Casp-1 has to be cleaved to become active, we tested for the presence of the mature form of Casp-1 in retinal extracts prepared 72 hours after illumination. Using two different antibodies that recognized cleaved Casp-1 products in control experiments (p20 and p10, respectively), we did not detect any cleaved products of Casp-1 in retinal extracts (Fig. 2D). The lack of IL-1β substrate cleavage and of the cleaved Casp-1 mature form suggests that Casp-1 did not mature and was therefore not activated, despite the increased expression of the proform.

To test whether increased Casp-1 levels is be a general phenomenon of retinal degeneration, we also analyzed its expression in two models of inherited retinal degeneration.

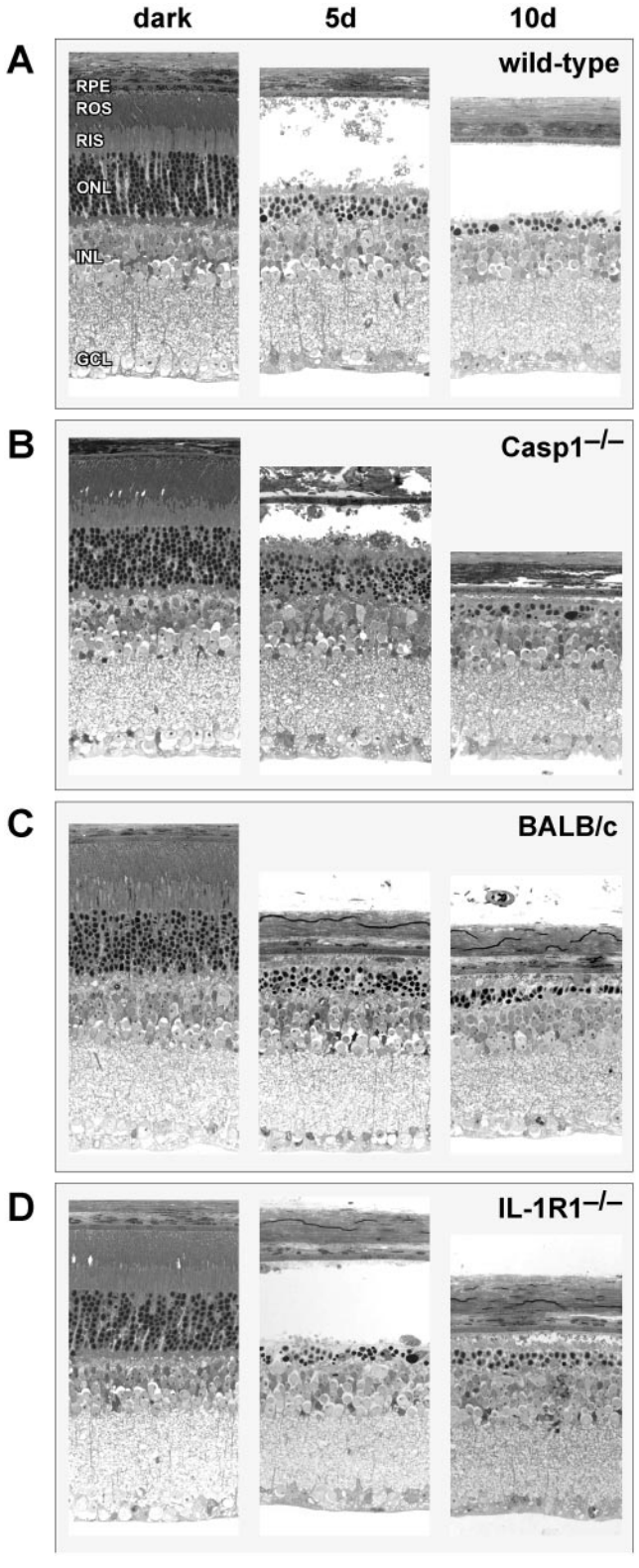

FIGURE 4. Ablation of Casp-1 did not protect retinal morphology against light-induced damage. Dark-adapted, pigmented (wild-type, Casp1$^{-/-}$), and albino (BALB/c, IL-1R1$^{-/-}$) mice were exposed for 2 hours to13 klux or for 1 hour to 5 klux of light, respectively. Retinal morphology of mice not exposed to light (dark, *left*) or of mice exposed to light and analyzed after 5 (5d, *middle*) or 10 (10d, *right*) d was analyzed by light microscopy. Shown are images of light-induced retinal degeneration in (**A**) pigmented wild-type animals, (**B**) pigmented Casp1$^{-/-}$ animals, (**C**) albino wild-type (BALB/c) mice, and (**D**) IL-1R1$^{-/-}$ knockout mice on an BALB/c genetic background. All mouse strains analyzed showed severe loss of photoreceptor nuclei and destruction of outer and inner segments at 5 days after exposure. At 10 days after exposure, most photoreceptor nuclei were lost. Shown are representative sections of the most affected retinal regions of two to four animals per time point and genotype. The large gap between ONL and RPE in some sections is due to a preparational artifact of the injured tissue.

The *rd1* mouse is characterized by fast photoreceptor degeneration, beginning at approximately postnatal day 10 (PND10) and peaking at ~PND13,[43] whereas retinal degeneration in the transgenic VPP mouse[30,31] has a later onset, and degeneration proceeds more slowly[44] (compare the images in Figs. 5A and 5B). Although retinal degeneration in the *rd1* mouse may[14–17] or may not[18] involve Casp-3, the molecular pathways of photoreceptor apoptosis in the VPP mouse have not been investigated so far. Whereas wild-type animals expressed low amounts of Casp-1 protein that remained unchanged at all time-points, increased levels of Casp-1 were found early after onset of degeneration in *rd1* and VPP retinas (Figs. 3A, 3B). In both models of inherited retinal degeneration, Casp-1 levels increased further with age. Of note, Casp-1 levels in the *rd1* retina where highest at PND37, at a time point when loss of photoreceptors was nearly complete (see Fig. 5A). This suggests that Casp-1 was expressed in cells different from photoreceptors.

Similar to the light-damage model, we did not observe cleaved mature Casp-1 (not shown). Furthermore, in vitro cleavage assays using retinal extracts from wild-type and VPP mice at PND28 again pointed to the absence of classic Casp-1 activity (Fig 3C).

In each of the three models of retinal degeneration, increased levels of Casp-1 coincided with the onset of photoreceptor apoptosis. Levels of Casp-1 remained high, at least until the degenerative process was completed.

Role of Casp-1 in Retinal Degeneration

Previously, we have shown that hypoxic preconditioning suppresses transcriptional upregulation of Casp-1 after exposure to light and protects photoreceptors from light-induced damage. These findings suggest that pretreatment may protect retinal morphology and function by interfering with a Casp-1–dependent pathway.[29] To test the suggested role of Casp-1 in light-induced photoreceptor apoptosis, we exposed Casp1$^{-/-}$ and wild-type control mice, both on a mixed 129/Sv-B6 genetic background, to high levels of white light (2 hours, 13 klux) and analyzed their retinal morphology at 5 and 10 days after exposure. Absence of Casp-1 did not notably influence light-induced retinal degeneration, as progression and extent of degeneration was comparable to wild-type mice (Figs. 4A, 4B). Retinas of both genotypes, analyzed 5 days after exposure to light, were characterized by a thinned ONL and a complete disintegration of RIS and ROS. Most of the remaining photoreceptor nuclei were pyknotic, indicating ongoing cell death. Photoreceptor cells were mostly cleared from the retina 10 days after illumination. During all times, the inner retinal structures were well preserved.

As the biochemical assays used to detect mature Casp-1 and IL-1β (Figs. 1, 2) may not have been sensitive enough to detect small amounts of active proteins, we addressed a potential role of IL-1β in retinal degeneration by using IL-1 receptor type 1 knockout mice (IL-1R1$^{-/-}$) on a BALB/c background. BALB/c wild-type mice served as the control. As IL-1R1 is the only identified signaling receptor mediating the effects of IL-1β,[45,46] its absence should completely prevent any IL-1β signaling,

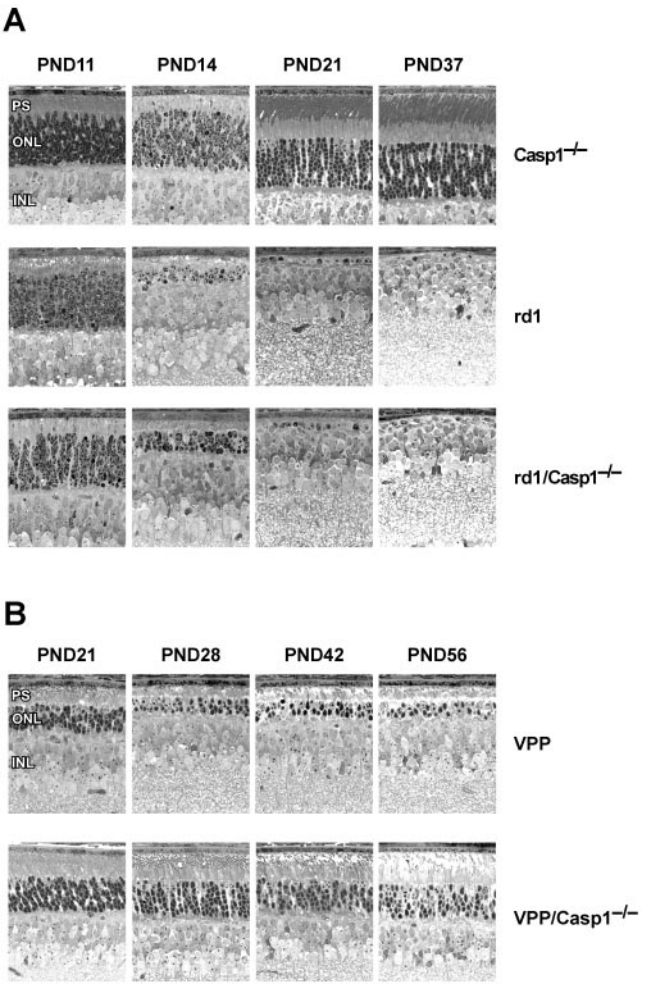

FIGURE 5. Differential effect of Casp-1 gene ablation in models of inherited retinal degeneration. (**A**) Absence of Casp-1 in *rd1* mice did not alter the progression of photoreceptor degeneration. Retinal morphology was assessed at the PNDs indicated. Casp1$^{-/-}$ mice had a normal retinal morphology (*top*). Photoreceptor degeneration proceeded similarly in *rd1* and *rd1*/Casp$^{-/-}$ retinas (*middle* and *bottom*). Both showed thinning of the ONL at PND14 and almost complete loss of photoreceptors at PND21 and -37. (**B**) Ablation of Casp-1 delayed retinal degeneration in VPP mice. VPP and VPP/Casp1$^{-/-}$ double-mutant were analyzed at the PNDs indicated. Compared with VPP retinas (*top*), the VPP/Casp1$^{-/-}$ mice (*bottom*) showed an increased number of photoreceptor nuclei in the ONL and better preservation of photoreceptor segments. Representative sections of the most affected areas of two to four animals per time point and genotype are presented.

although the potential existence of alternative signaling mechanisms has been discussed.[47,48] Wild-type and IL-1R1$^{-/-}$ mice were exposed to 5 klux of light for 1 hour and analyzed 5 and 10 days after exposure. Retinal degeneration was comparably severe in both types of mice (Figs. 4C, 4D).

These experiments show that lack of Casp-1 did not prevent light-induced photoreceptor degeneration and suggest that IL-1β signaling may not be involved in the degenerative process.

Several molecular pathways exist for cell death in different forms of retinal degeneration.[2,41] Therefore, we also tested the potential effect of Casp-1 ablation in the two models of inherited retinal degeneration. For this purpose, we generated *rd1*/Casp1$^{-/-}$ and VPP/Casp1$^{-/-}$ double-mutant mice and investigated retinal morphology at different postnatal days. Retinas of Casp1$^{-/-}$ mice, used as controls in this experiment, showed a normal morphologic appearance (Fig. 5A, top). Ablation of Casp-1 did not affect the course of retinal degeneration in *rd1* mice, as the process proceeded without notable differences in *rd1* (Fig. 5A, middle) and *rd1*/Casp1$^{-/-}$ double-mutant mice (Fig. 5A, bottom). Both *rd1* and *rd1*/Casp1$^{-/-}$ retinas showed scattered apoptotic nuclei at PND11 and almost complete loss of photoreceptors by PND21.

In contrast, ablation of Casp-1 substantially protected retinal morphology in VPP mice (Fig. 5B). At PND21, the ONL thickness in retinas of VPP mice was about half that of Casp1$^{-/-}$ (compare top rows of Figs. 5A and 5B) or of wild-type mice. Most of the outer segments were severely disturbed. Accordingly, reduced levels of rhodopsin (17% compared with wild-type or Casp1$^{-/-}$) were detected at this age (Table 2). VPP/Casp1$^{-/-}$ double mutant mice, however, had more photoreceptor nuclei, better preserved outer segments and higher levels of rhodopsin (twice as much) than VPP mice. Preservation of retinal morphology and higher rhodopsin contents persisted until at least PND42 (Fig. 5B, Table 2). At PND56, the ONL was still thicker in double-mutant mice, but the structure of the outer segments was severely disturbed, which was reflected by a rhodopsin content similar to that of VPP mice. Although lack of Casp-1 protected the retina of VPP mice, morphology and rhodopsin content did not reach the quality or the amount, respectively, of wild-type or Casp1$^{-/-}$ animals. The continuous expression of mutant rhodopsin obviously prevented a complete protection.

Because lack of Casp-1 protected the VPP retina even though we did not observe Casp-1 cleavage activity in VPP mice in in vitro assays (Fig. 3C), we also analyzed VPP/IL-1R1$^{-/-}$ double mutant animals to address a potential role IL-1β signaling for VPP mediated retinal degeneration. Lack of IL-1R1 did not influence the degeneration in the VPP mouse retina as judged by the amount of rhodopsin at PND21 and PND42 (Table 2) and retinal morphology (not shown). This finding supports the conclusion that Casp-1 may influence retinal degeneration in the VPP mouse independent from its classic function as activator of IL-1β signaling.

Signaling Mechanisms

To address potential signaling mechanisms involved in such a nonconventional Casp-1 function, we tested expression of several genes involved in cytokine or chemokine signaling by real-time PCR. In retinas of wild-type animals, Casp-1 gene expression remained stable and at low levels during postnatal development and aging (Fig. 6). In VPP mice, however, increased Casp-1 gene expression was detected from PND21 (4-fold) to PND56 (10-fold), which is in line with the increased levels of Casp-1 protein detected by Western blot analysis (Fig. 3B). The oligonucleotides used for real-time PCR hybridize upstream of the neomycin insertion (exon 6,[34]) in the Casp-1 knockout allele and can therefore detect its expression. Expression of the disrupted gene in the Casp1$^{-/-}$ retinas was increased compared with that in wild-type. This elevated expression was even more pronounced in the VPP/Casp1$^{-/-}$ mice (Fig. 6). Obviously, lack of Casp-1 protein caused an increased transcription rate of the Casp-1 gene. This increase could be because of the lack of a negative feedback inhibition that may normally be imposed by the Casp-1 protein. The highly increased Casp-1 gene expression in the VPP/Casp1$^{-/-}$ retina may be an attempt to produce the protease in response to the injury (as in the VPP mouse with wild-type Casp-1). Because the protein cannot be generated, the putative regulatory feedback signal may be missing, resulting in a vicious cycle and a steady increase of gene expression.

Apoptosis-associated speck-like protein (asc) is a CARD (caspase recruiting domain) containing protein that is mainly

TABLE 2. Rhodopsin Content in Retinas of Dark-Adapted Mice with Different Genotypes

Mouse Strain	PND21	PND28	PND42	PND56
wt	0.43 ± 0.02 nmol 100% 3/3	0.43 ± 0.08 nmol 100% 3/3	0.47 ± 0.05 nmol 100% 7/5	0.50 ± 0.02 nmol 100% 3/3
Casp1$^{-/-}$	0.41 ± 0.03 nmol 95% 6/6	0.42 ± 0.02 nmol 96% 4/2	ND	0.48 ± 0.04 nmol 96% 3/3
VPP	0.07 ± 0.01 nmol 17% 3/3	0.07 ± 0.02 nmol 16% 3/3	0.06 ± 0.04 nmol 12% 17/10	0.08 ± 0.04 nmol 16% 7/5
VPP/Casp1$^{-/-}$	0.14 ± 0.01 nmol 32% 3/3	0.14 ± 0.04 nmol 33% 8/4	0.14 ± 0.02 nmol 31% 16/8	0.11 ± 0.04 nmol 23% 9/6
VPP/IL-1R$^{-/-}$	0.08 ± 0.02 nmol 19% 4/4	ND	0.05 ± 0.03 nmol 10% 12/8	ND

Data for each retina are given as the mean ± SD. Data for wild-type mice were set to 100%, and rhodopsin levels of the different genotypes were calculated as percentages of wild-type levels at a particular age. Numbers divided by virgules represent the number of retinas analyzed and the number of different animals used, respectively. Differences in rhodopsin content were significant between VPP and VPP/Casp1$^{-/-}$ mice at PND21, -28, and -42 (unpaired *t*-test with Welch correction, $P \leq 0.05$). ND, not determined.

involved in the activation of pro-Casp-1.[49] Recently, asc has also been implicated in the activation of Casp-8.[50] In contrast to the decreasing expression in wild-type mice, VPP mice show a two-fold increase of asc expression with time (Fig. 6). In mice lacking functional Casp-1, asc expression is almost undetectable (Fig. 6) suggesting that Casp-1 protein is necessary to stimulate asc gene expression. The increase of asc in VPP mice also further supports an involvement of Casp-1 in the degenerative process.

Ciliary neurotrophic factor (CNTF) and fibroblast growth factor (FGF)-2 have been implicated in retinal neuroprotection (reviewed in Ref. 41). Expression levels of CNTF were similar in all four strains tested (Fig. 6). Only at PND56, both VPP and

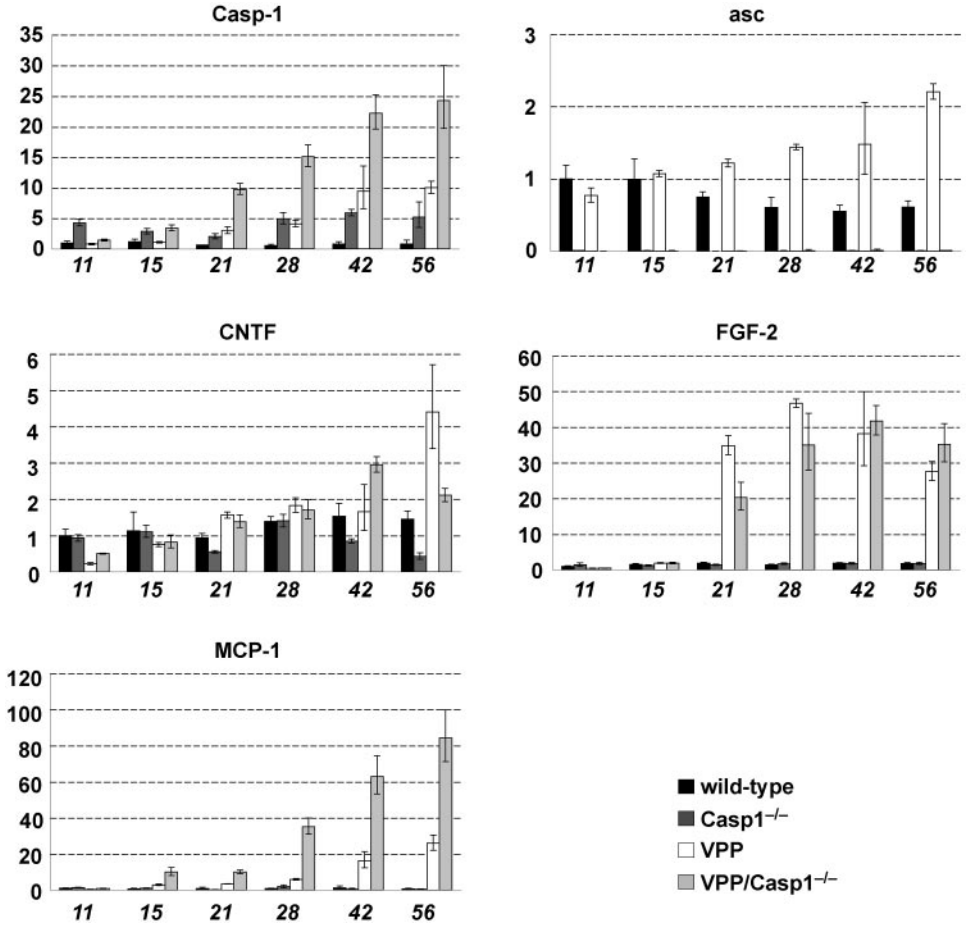

FIGURE 6. Gene expression in wild-type and single- and double-mutant mice. Relative levels of indicated RNAs in retinas of wild-type, Casp1$^{-/-}$, VPP, and VPP/Casp1$^{-/-}$ at PNDs 11, 15, 21, 28, 42, and 56, as determined by real-time RT-PCR. mRNA levels are expressed relative to those of the 11-day-old wild-type samples, which was set to 1. RNAs isolated from three independent retinas per time point and genotype were pooled, and amplifications were performed in triplicate (means ± SD).

VPP/Casp1$^{-/-}$ showed a tendency of increased CNTF expression. Because expression increased similarly in both strains, especially at the earlier time points, CNTF may not be a factor responsible for the observed protection by ablation of Casp-1. In contrast to CNTF, expression of FGF-2 responded strongly to the presence of the VPP transgene: Expression was induced 30- to 50-fold beginning at PND21, concomitantly with the onset of the degeneration (Fig. 6). At PND21 and PND28, expression in double-mutant mice was slightly reduced compared with that in VPP mice. This finding may reflect the reduced severity of retinal injury at this time point in these mice.

Monocyte chemoattractant protein (MCP)-1 has been implicated in the recruitment of macrophages to the site of injury.[51] Because the lack of MCP-1 has been reported to cause an AMD-like phenotype in aged mice,[52] MCP-1 may be needed to maintain normal retinal morphology. Whereas expression of MCP-1 was at basal levels in wild-type and Casp1$^{-/-}$ animals at all time points tested, its expression strongly increased in VPP (from PND21) and especially in VPP/Casp1$^{-/-}$ mice (from PND15; Fig. 6). At all time-points tested (except PND11), expression of MCP-1 was stronger in the VPP/Casp1$^{-/-}$ animals. Such an increased expression was not detected in Casp1$^{-/-}$ animals but occurred only in combination with the disease-causing transgene. Therefore, lack of Casp-1 did not result in an increased MCP-1 expression per se, suggesting that MCP-1 could be one factor, which may play a role in the protective effect of Casp-1 ablation in VPP mice.

Discussion

We show that Casp-1 RNA and protein are upregulated in three different models of retinal degeneration (light-induced, *rd1*, VPP). Our data suggest that an injured retina increases expression of the proform of Casp-1 and that this proform may exhibit a nonclassic activity different from IL-1β cleavage. Ablation of Casp-1 slowed the disease progression only in the model with the mildest form of retinal degeneration (VPP). However, the protection observed in VPP/Casp$^{-/-}$ animals was only transient suggesting that additional pathways, independent of Casp-1, are involved in the regulation of retinal degeneration.

Lack of Casp-1 did not protect photoreceptors after acute light damage, in which cell death is synchronous and proceeds quickly and after which most photoreceptors are cleared from the subretinal space within 10 days. Also in the *rd1* model, loss and clearance of photoreceptors occurs roughly in the same time frame, and photoreceptors are not protected by the ablation of Casp-1. In contrast, apoptosis of visual cells in the VPP mouse proceeds slowly over an extended period. In addition and contrary to light damage, cell death in the VPP mouse depends on phototransduction but not on c-Fos.[33,53] Thus, significant differences in the signaling of apoptosis exist between these two models, and it appears that Casp-1 rather affects death pathways causing retinal degeneration of a milder phenotype with a slow progression. This is in line with results showing that lack of Casp-1 renders neonatal mice resistant to moderate but not to severe cerebral hypoxia–ischemia insults.[54]

Even though degeneration of the ONL may proceed at different speeds in the various models, the death process may nevertheless be similar on the single cell level once apoptosis is induced. Therefore, the amount of dying cells at any given time may be critical for the protective effect observed by the ablation of Casp-1. Recent theoretical and mathematical evaluations of neuronal cell death in several models of inherited retinal degeneration and other neurologic disorders suggested that a mutation imposes a mutant steady state and that a single event randomly induces cell death.[55] This model has been refined by the inclusion of diffusible death factors to explain patchy cell death as it often is observed in patients with RP and in animal models.[56] Such diffusible factors or at least cell–cell interactions between dying and neighboring cells have been postulated earlier[57] and bystander effects were suggested to play an important role in neuronal cell death in the retina as well.[58] Similarly, the magnitude of the cell death stimulus is a determining factor deciding over an acute or a chronic fate.[59] Based on these reflections, we propose that lack of Casp-1 may influence a bystander effect and/or may play a role in the production, release or activity of potential death factors. The nature of the cells that may be involved in such an effect remains to be determined, but the high expression of Casp-1 in *rd1* retinas at PND37 (Fig. 3A) when most photoreceptors have been cleared from the retina (Fig. 5A) suggests strong Casp-1 expression in cells different from photoreceptors. In contrast, recent reports rather convincingly demonstrate high expression of Casp-1 in the ONL in several models of retinal injury.[27,28] Clearly, a careful and more elaborate study of retinal Casp-1 expression is needed to unravel the complete role of Casp-1 in disease induction and progression.

In models with almost synchronous cell death as in the light-damage model and the *rd1* mouse, such effects and/or factors may be of such concentrations that lack of Casp-1 may not be able to influence their activity sufficiently. In models of slow photoreceptor degeneration, however, the reduced amount of dying cells per time may allow protection by the lack of Casp-1.

The initial analysis of factors that could be involved in the protection observed in the VPP/Casp1$^{-/-}$ double mutant mice revealed a striking difference in the expression of MCP-1. Expression of this chemokine is induced in the degenerating VPP retina, and lack of Casp-1 seems to stimulate its mRNA production even further (Fig. 6). Whether MCP-1 may be involved in the protection of photoreceptors in VPP/Casp1$^{-/-}$ double-mutant mice remains to be shown, but it is interesting to note that lack of MCP-1 has been reported to lead to an AMD-like phenotype, including photoreceptor atrophy.[52] Even though such a phenotype manifests itself only in aged animals, MCP-1 may nevertheless play a role in the survival of retinal cells, as has been suggested for central nervous system neurons,[60] and/or MCP-1 may be involved in maintaining the integrity of the retinal structure.

VPP mice express a human transgene encoding a mutant rhodopsin with three amino acid substitutions (V20G, P23H, P27L), one of which (P23H) is the most prevalent mutation in patients with RP. The proposed mechanism of P23H-mediated degeneration involves formation of protein aggregations and proteasome-processing defects.[61] This mechanism links this form of RP to a broad class of neurodegenerative diseases characterized by accumulation of misfolded protein aggregates such as Alzheimer disease, Parkinson disease, Huntington disease, prion encephalopathies, and amyotrophic lateral sclerosis (ALS).[24,62–64] Casp-1–mediated pathways and –increased expression of MCP-1 have been suggested to play a role in a variety of these acute and chronic neurologic disorders,[65,66] similar to the results presented herein.

It has been generally accepted that the common event for caspase activation is proteolysis of the proenzyme at internal aspartate residues producing, in the case of Casp-1, mature p20 and p10 forms. However, four lines of evidence suggests that in the retina, Casp-1 may not exhibit classic activity: First, p10 and p20 cleavage products were not detected with two different antibodies, as reported earlier by others[42]; second, we did not detect any cleavage activity in retinal extracts; third, we did not observe any mature IL-1β, although all models showed increased Il-1β mRNA levels; and fourth, lack of IL-1R1 did not influence retinal degeneration, suggesting that mature IL-1β,

the product of classic Casp-1 activity, is not involved in initiation and/or progression of the degeneration. Instead of mature Casp-1, we detected overaccumulation of the Casp-1 proform. Based on these data and the neuroprotective effect of Casp-1 ablation in the VPP mouse, we speculate that Casp-1 may orchestrate mechanisms of cell death independent of IL-1β maturation. It has been reported for example that the CARD domain of the proenzyme interacts with RIP2 and activates NFκB independently of enzymatic activity.[67,68] Other mechanisms are possible as well.

Recent work has revealed that initiator caspases may be activated through oligomerization and a conformational change independent of a cleavage activity.[69,70] Similarly, pro-Casp-1 can be activated through oligomerization in vitro[71] a process facilitated in vivo by asc.[72] Overexpression of asc can lead to apoptotic cell death, and asc is silenced in human breast carcinoma and glioblastoma cells.[73–75] In the retina of VPP mice, asc is expressed at higher levels compared with controls, whereas asc expression is almost completely silenced in mice lacking functional Casp-1 (Fig. 6).

In summary, we showed that increased expression of Casp-1 may be a common marker for retinal degeneration, and that ablation of Casp-1 is neuroprotective, at least in a model of a comparably mild form of photoreceptor degeneration. It is important to establish the generality of these observations and to test whether interference with classic or nonclassic Casp-1 function may be an option to protect retinal cells in slowly progressing retinal degenerations.

Acknowledgments

The authors thank Coni Imsand, Gaby Hoegger, and Hedwig Wariwoda for excellent technical assistance. Winnie Wong, Muna Naash, Manfred Kopf, Peter Vandenabeele and Stephen Poole generously provided mice or antibodies for this study.

References

1. Milam AH, Li ZY, Fariss RN. Histopathology of the human retina in retinitis pigmentosa. *Prog Retin Eye Res*. 1998;17:175–205.
2. Pierce EA. Pathways to photoreceptor cell death in inherited retinal degenerations. *Bioessays*. 2001;23:605–618.
3. Reme CE, Grimm C, Hafezi F, Marti A, Wenzel A. Apoptotic cell death in retinal degenerations. *Prog Retin Eye Res*. 1998;17:443–464.
4. Chang HY, Yang X. Proteases for cell suicide: functions and regulation of caspases. *Microbiol Mol Biol Rev*. 2000;64:821–846.
5. Katai N, Yoshimura N. Apoptotic retinal neuronal death by ischemia-reperfusion is executed by two distinct caspase family proteases. *Invest Ophthalmol Vis Sci*. 1999;40:2697–2705.
6. Cascio C, Guarneri R, Russo D, et al. A caspase-3-dependent pathway is predominantly activated by the excitotoxin pregnenolone sulfate and requires early and late cytochrome c release and cell-specific caspase-2 activation in the retinal cell death. *J Neurochem*. 2002;83:1358–1371.
7. Shiraga S, Adamus G. Mechanism of CAR syndrome: anti-recoverin antibodies are the inducers of retinal cell apoptotic death via the caspase 9- and caspase 3-dependent pathway. *J Neuroimmunol*. 2002;132:72–82.
8. He L, Poblenz AT, Medrano CJ, Fox DA. Lead and calcium produce rod photoreceptor cell apoptosis by opening the mitochondrial permeability transition pore. *J Biol Chem*. 2000;275:12175–12184.
9. Liu C, Li Y, Peng M, Laties AM, Wen R. Activation of caspase-3 in the retina of transgenic rats with the rhodopsin mutation s334ter during photoreceptor degeneration. *J Neurosci*. 1999;19:4778–4785.
10. Yamazaki H, Ohguro H, Maeda T, et al. Preservation of retinal morphology and functions in royal college surgeons rat by nilvadipine, a Ca(2+) antagonist. *Invest Ophthalmol Vis Sci*. 2002;43:919–926.
11. Bode C, Wolfrum U. Caspase-3 inhibitor reduces apoptotic photoreceptor cell death during inherited retinal degeneration in tubby mice. *Mol Vis*. 2003;9:144–150.
12. Hughes EH, Schlichtenbrede FC, Murphy CC, et al. Minocycline delays photoreceptor death in the rds mouse through a microglia-independent mechanism. *Exp Eye Res*. 2004;78:1077–1084.
13. Bowes C, Li T, Danciger M, Baxter LC, Applebury ML, Farber DB. Retinal degeneration in the rd mouse is caused by a defect in the beta subunit of rod cGMP-phosphodiesterase. *Nature*. 1990;347:677–680.
14. Jomary C, Neal MJ, Jones SE. Characterization of cell death pathways in murine retinal neurodegeneration implicates cytochrome c release, caspase activation, and bid cleavage. *Mol Cell Neurosci*. 2001;18:335–346.
15. Yoshizawa K, Kiuchi K, Nambu H, et al. Caspase-3 inhibitor transiently delays inherited retinal degeneration in C3H mice carrying the rd gene. *Graefes Arch Clin Exp Ophthalmol*. 2002;240:214–219.
16. Sharma AK, Rohrer B. Calcium-induced calpain mediates apoptosis via caspase-3 in a mouse photoreceptor cell line. *J Biol Chem*. 2004;279:35564–35572.
17. Zeiss CJ, Neal J, Johnson EA. Caspase-3 in postnatal retinal development and degeneration. *Invest Ophthalmol Vis Sci*. 2004;45:964–970.
18. Doonan F, Donovan M, Cotter TG. Caspase-independent photoreceptor apoptosis in mouse models of retinal degeneration. *J Neurosci*. 2003;23:5723–5731.
19. Yuan J, Shaham S, Ledoux S, Ellis HM, Horvitz HR. The C. elegans cell death gene ced-3 encodes a protein similar to mammalian interleukin-1 beta-converting enzyme. *Cell*. 1993;75:641–652.
20. Black RA, Kronheim SR, Merriam JE, March CJ, Hopp TP. A pre-aspartate-specific protease from human leukocytes that cleaves pro-interleukin-1 beta. *J Biol Chem*. 1989;264:5323–5326.
21. Kostura MJ, Tocci MJ, Limjuco G, et al. Identification of a monocyte specific pre-interleukin 1 beta convertase activity. *Proc Natl Acad Sci USA*. 1989;86:5227–5231.
22. Li M, Ona VO, Guegan C, et al. Functional role of caspase-1 and caspase-3 in an ALS transgenic mouse model. *Science*. 2000;288:335–339.
23. Li M, Ona VO, Chen M, et al. Functional role and therapeutic implications of neuronal caspase-1 and -3 in a mouse model of traumatic spinal cord injury. *Neuroscience*. 2000;99:333–342.
24. Ona VO, Li M, Vonsattel JP, et al. Inhibition of caspase-1 slows disease progression in a mouse model of Huntington's disease. *Nature*. 1999;399:263–267.
25. Zhang WH, Wang X, Narayanan M, et al. Fundamental role of the Rip2/caspase-1 pathway in hypoxia and ischemia-induced neuronal cell death. *Proc Natl Acad Sci USA*. 2003;100:16012–16017.
26. Grimm C, Wenzel A, Hafezi F, Reme CE. Gene expression in the mouse retina: the effect of damaging light. *Mol Vis*. 2000;6:252–260.
27. Wu T, Chiang SK, Chau FY, Tso MO. Light-induced photoreceptor degeneration may involve the NF kappa B/caspase-1 pathway in vivo. *Brain Res*. 2003;967:19–26.
28. Lohr HR, Kuntchithapautham K, Sharma AK, Rohrer B. Multiple, parallel cellular suicide mechanisms participate in photoreceptor cell death. *Exp Eye Res*. 2006;83:380–389.
29. Grimm C, Wenzel A, Groszer M, et al. HIF-1-induced erythropoietin in the hypoxic retina protects against light-induced retinal degeneration. *Nat Med*. 2002;8:718–724.
30. Naash MI, Hollyfield JG, al-Ubaidi MR, Baehr W. Simulation of human autosomal dominant retinitis pigmentosa in transgenic mice expressing a mutated murine opsin gene. *Proc Natl Acad Sci USA*. 1993;90:5499–5503.
31. Goto Y, Peachey NS, Ripps H, Naash MI. Functional abnormalities in transgenic mice expressing a mutant rhodopsin gene. *Invest Ophthalmol Vis Sci*. 1995;36:62–71.
32. Naash MI, Ripps H, Li S, Goto Y, Peachey NS. Polygenic disease and retinitis pigmentosa: albinism exacerbates photoreceptor degeneration induced by the expression of a mutant opsin in transgenic mice. *J Neurosci*. 1996;16:7853–7858.

33. Samardzija M, Wenzel A, Naash M, Reme CE, Grimm C. Rpe65 as a modifier gene for inherited retinal degeneration. *Eur J Neurosci*. 2006;23:1028–1034.
34. Li P, Allen H, Banerjee S, et al. Mice deficient in IL-1 beta-converting enzyme are defective in production of mature IL-1 beta and resistant to endotoxic shock. *Cell*. 1995;80:401–411.
35. Eriksson U, Kurrer MO, Sonderegger I, et al. Activation of dendritic cells through the interleukin 1 receptor 1 is critical for the induction of autoimmune myocarditis. *J Exp Med*. 2003;197:323–331.
36. Schmitz N, Kurrer M, Kopf M. The IL-1 receptor 1 is critical for Th2 cell type airway immune responses in a mild but not in a more severe asthma model. *Eur J Immunol*. 2003;33:991–1000.
37. Hafezi F, Abegg M, Grimm C, et al. Retinal degeneration in the rd mouse in the absence of c-fos. *Invest Ophthalmol Vis Sci*. 1998; 39:2239–2244.
38. Grimm C, Wenzel A, Stanescu D, et al. Constitutive overexpression of human erythropoietin protects the mouse retina against induced but not inherited retinal degeneration. *J Neurosci*. 2004;24: 5651–5658.
39. Wenzel A, Grimm C, Marti A, et al. c-fos controls the "private pathway" of light-induced apoptosis of retinal photoreceptors. *J Neurosci*. 2000;20:81–88.
40. Wenzel A, Oberhauser V, Pugh EN Jr, et al. The retinal G protein-coupled receptor (RGR) enhances isomerohydrolase activity independent of light. *J Biol Chem*. 2005;280:29874–29884.
41. Wenzel A, Grimm C, Samardzija M, Reme CE. Molecular mechanisms of light-induced photoreceptor apoptosis and neuroprotection for retinal degeneration. *Prog Retin Eye Res*. 2005;24:275–306.
42. Donovan M, Cotter TG. Caspase-independent photoreceptor apoptosis in vivo and differential expression of apoptotic protease activating factor-1 and caspase-3 during retinal development. *Cell Death Differ*. 2002;9:1220–1231.
43. Rich KA, Zhan Y, Blanks JC. Aberrant expression of c-Fos accompanies photoreceptor cell death in the rd mouse. *J Neurobiol*. 1997;32:593–612.
44. Goto Y, Peachey NS, Ziroli NE, et al. Rod phototransduction in transgenic mice expressing a mutant opsin gene. *J Opt Soc Am A Opt Image Sci Vis*. 1996;13:577–585.
45. Sims JE, Gayle MA, Slack JL, et al. Interleukin 1 signaling occurs exclusively via the type I receptor. *Proc Natl Acad Sci USA*. 1993;90:6155–6159.
46. Leon LR. Invited review: cytokine regulation of fever: studies using gene knockout mice. *J Appl Physiol*. 2002;92:2648–2655.
47. Parker LC, Luheshi GN, Rothwell NJ, Pinteaux E. IL-1 beta signalling in glial cells in wildtype and IL-1RI deficient mice. *Br J Pharmacol*. 2002;136:312–320.
48. Touzani O, Boutin H, LeFeuvre R, et al. Interleukin-1 influences ischemic brain damage in the mouse independently of the interleukin-1 type I receptor. *J Neurosci*. 2002;22:38–43.
49. Mariathasan S, Newton K, Monack DM, et al. Differential activation of the inflammasome by caspase-1 adaptors ASC and Ipaf. *Nature*. 2004;430:213–218.
50. Parsons MJ, Vertino PM. Dual role of TMS1/ASC in death receptor signaling. *Oncogene*. Published online May 22, 2006.
51. Corrigall VM, Arastu M, Khan S, et al. Functional IL-2 receptor beta (CD122) and gamma (CD132) chains are expressed by fibroblast-like synoviocytes: activation by IL-2 stimulates monocyte chemoattractant protein-1 production. *J Immunol*. 2001;166:4141–4147.
52. Ambati J, Anand A, Fernandez S, et al. An animal model of age-related macular degeneration in senescent Ccl-2- or Ccr-2-deficient mice. *Nat Med*. 2003;9:1390–1397.
53. Hao W, Wenzel A, Obin MS, et al. Evidence for two apoptotic pathways in light-induced retinal degeneration. *Nat Genet*. 2002; 32:254–260.
54. Xu H, Barks JD, Schielke GP, Silverstein FS. Attenuation of hypoxia-ischemia-induced monocyte chemoattractant protein-1 expression in brain of neonatal mice deficient in interleukin-1 converting enzyme. *Brain Res Mol Brain Res*. 2001;90:57–67.
55. Clarke G, Collins RA, Leavitt BR, et al. A one-hit model of cell death in inherited neuronal degenerations. *Nature*. 2000;406:195–199.
56. Burns J, Clarke G, Lumsden CJ. Photoreceptor death: spatiotemporal patterns arising from one-hit death kinetics and a diffusible cell death factor. *Bull Math Biol*. 2002;64:1117–1145.
57. Huang PC, Gaitan AE, Hao Y, Petters RM, Wong F. Cellular interactions implicated in the mechanism of photoreceptor degeneration in transgenic mice expressing a mutant rhodopsin gene. *Proc Natl Acad Sci USA*. 1993;90:8484–8488.
58. Zhang M, Atherton SS. Apoptosis in the retina during MCMV retinitis in immunosuppressed BALB/c mice. *J Clin Virol*. 2002; 25(suppl 2):S137–S147.
59. Friedlander RM. Apoptosis and caspases in neurodegenerative diseases. *N Engl J Med*. 2003;348:1365–1375.
60. Eugenin EA, D'Aversa TG, Lopez L, Calderon TM, Berman JW. MCP-1 (CCL2) protects human neurons and astrocytes from NMDA or HIV-tat-induced apoptosis. *J Neurochem*. 2003;85:1299–1311.
61. Illing ME, Rajan RS, Bence NF, Kopito RR. A rhodopsin mutant linked to autosomal dominant retinitis pigmentosa is prone to aggregate and interacts with the ubiquitin proteasome system. *J Biol Chem*. 2002;277:34150–34160.
62. Friedlander RM, Brown RH, Gagliardini V, Wang J, Yuan J. Inhibition of ICE slows ALS in mice (published correction appears in *Nature*. 1998;392:560). *Nature*. 1997;388:31.
63. Zhu SG, Sheng JG, Jones RA, et al. Increased interleukin-1beta converting enzyme expression and activity in Alzheimer disease. *J Neuropathol Exp Neurol*. 1999;58:582–587.
64. Mogi M, Togari A, Kondo T, et al. Caspase activities and tumor necrosis factor receptor R1 (p55) level are elevated in the substantia nigra from parkinsonian brain. *J Neural Transm*. 2000;107: 335–341.
65. Henkel JS, Beers DR, Siklos L, Appel SH. The chemokine MCP-1 and the dendritic and myeloid cells it attracts are increased in the mSOD1 mouse model of ALS. *Mol Cell Neurosci*. 2006;31:427–437.
66. Grammas P, Ovase R. Inflammatory factors are elevated in brain microvessels in Alzheimer's disease. *Neurobiol Aging*. 2001;22: 837–842.
67. Lamkanfi M, Kalai M, Saelens X, Declercq W, Vandenabeele P. Caspase-1 activates nuclear factor of the kappa-enhancer in B cells independently of its enzymatic activity. *J Biol Chem*. 2004;279: 24785–24793.
68. Lamkanfi M, Declercq W, Vanden Berghe T, Vandenabeele P. Caspases leave the beaten track: caspase-mediated activation of NF-kappaB. *J Cell Biol*. 2006;173:165–171.
69. Boatright KM, Renatus M, Scott FL, et al. A unified model for apical caspase activation. *Mol Cell*. 2003;11:529–541.
70. Rodriguez J, Lazebnik Y. Caspase-9 and APAF-1 form an active holoenzyme. *Genes Dev*. 1999;13:3179–3184.
71. Yang X, Chang HY, Baltimore D. Autoproteolytic activation of pro-caspases by oligomerization. *Mol Cell*. 1998;1:319–325.
72. Srinivasula SM, Poyet JL, Razmara M, Datta P, Zhang Z, Alnemri ES. The PYRIN-CARD protein ASC is an activating adaptor for caspase-1. *J Biol Chem*. 2002;277:21119–21122.
73. Conway KE, McConnell BB, Bowring CE, Donald CD, Warren ST, Vertino PM. TMS1, a novel proapoptotic caspase recruitment domain protein, is a target of methylation-induced gene silencing in human breast cancers. *Cancer Res*. 2000;60:6236–6242.
74. Stone AR, Bobo W, Brat DJ, Devi NS, Van Meir EG, Vertino PM. Aberrant methylation and down-regulation of TMS1/ASC in human glioblastoma. *Am J Pathol*. 2004;165:1151–1161.
75. McConnell BB, Vertino PM. TMS1/ASC: the cancer connection. *Apoptosis*. 2004;9:5–18.

6.3 The hypoxic transcriptome of the retina: identification of factors with potential neuroprotective activity.

Markus Thiersch[1], Wolfgang Raffelsberger[2], Rico Frigg[1], Marijana Samardzija[1], Patricia Blank[1], Olivier Poch[2] and Christian Grimm[1*]

[1]Lab of Retinal Cell Biology, Dept Ophthalmology, University of Zurich, Switzerland
[2]Laboratoire de BioInformatique et Génomique Intégrative, Institut de Genetique et de Biologie Moleculaire et Cellulaire, 67404 Illkirch, France

Book chapter, published in Adv Exp Med Biol. 2008 ;613 :75-85 18188931

6.3.1 Author contribution

Design:	**MT**, WR, RF, and CG
Experiments:	**MT** (major contribution to experiments), WR, RF, MS, PB and CG
Interpretation:	**MT**, WR, MS, OP and CG
Manuscript:	**MT** and CG
Manuscript Correction:	**MT**, WR, MS, and CG

6.3.2 Summary

Within this book chapter we briefly described the retinal response to hypoxic preconditioning of mice. We used micro-arrays and analyzed them with the Mas5.0 algorithm to identify differentially regulated genes 0, 2, 4 and 16 hours after hypoxic preconditioning (Note: in Thiersch et al., 2008, BMC Genomics we employed the advanced GCRMA algorithm, which is a specific modification of the robust multi-array average (RMA) algorithm). Depending on the applied statistical filters we observed a differential regulation of 83 genes (stringent filtering) or 772 genes (less stringent filtering). For biological classification of differentially regulated genes we used ONTO-Express (http://vortex.cs.wayne.edu/ontoexpress/). Hypoxic preconditioning seemed to affect genes involved in transport and apoptosis. With focus on neuroprotection, which involves a suppression of apoptosis, we particularly analyzed the expression of apoptosis regulating genes and observed the induction cyclin-dependent kinase

inhibitor 1a (p21), Bcl2-like 10 and vascular endothelial growth factor (Vegf) among the induced anti-apoptotic genes. The functional group of pro-apoptotic genes contained BCL2/adenovirus E1B interacting protein 3 (Bnip3) and Bcl2-like 11 etc. In order to verify our micro-array data, we selected three apoptosis-related genes (Vegf, p21 and Bcl2-like 10) and confirmed their induction by real-time PCR. We hypothesized, that p21 could be an important gene for retinal neuroprotection after hypoxic preconditioning. We described preliminary results of $p21^{-/-}$ mice, which were hypoxic preconditioned and illuminated 4 hours after hypoxia. Our data, suggested that p21 might not be essential for retinal neuroprotection.

6.3.3 Manuscript

THE HYPOXIC TRANSCRIPTOME OF THE RETINA: IDENTIFICATION OF FACTORS WITH POTENTIAL NEUROPROTECTIVE ACTIVITY

Markus Thiersch[1*], Wolfgang Raffelsberger[2], Enrico Frigg[1], Marijana Samardzija[1], Patricia Blank[1], Olivier Poch[2], and Christian Grimm[1]

1. INTRODUCTION

Most blinding diseases of the retina share a common feature – the loss of photoreceptor cells by apoptosis. Although degenerative diseases like age-related macular degeneration (AMD) and Retinitis Pigmentosa (RP) are among the main causes for severe visual impairment and blindness, no effective therapeutical treatments are available to prevent loss of vision in human patients. Protection of retinal cells against cell death is a promising strategy to develop therapies aiming at the rescue of retinal function. For the successful design of neuroprotective strategies, it is essential to understand the molecular events leading to the degeneration of retinal cells. To study signaling pathways and molecular mechanisms during the degenerative processes, several mouse models of inherited retinal degeneration are used (Fauser et al. 2002). These models are complemented by models of induced photoreceptor apoptosis like the model of light-induced degeneration (Wenzel et al. 2005). The advantage of the induced models is the synchronized apoptotic response of many photoreceptor cells to the death stimulus. This might raise the activation of regulatory factors above detection threshold allowing their detailed investigation.

Recently, we showed that hypoxic preconditioning protects photoreceptor cells against light-induced cell death by preserving retinal function and morphology (Grimm et al. 2002). Similarly, hypoxic pretreatment can also protect other tissues like heart or brain against various toxic insults (Gidday et al. 1994; Emerson et al. 1999; Cai et al. 2003; Dong et al. 2003) suggesting that hypoxic preconditioning might induce a general protective response. Such a response might involve hypoxia-inducible-factor 1a (HIF-1a) which is stabilized in the retina after hypoxic exposure (Grimm et al. 2002). As a

[1]Lab for Retinal Cell Biology, Dept Ophthalmology, CIHP, University of Zurich, Switzerland
[2] Laboratoire de BioInformatique et Génomique Intégrative (IGBMC), Strasbourg, France
*email address of corresponding author: markus.thiersch@usz.ch

transcription factor, HIF-1a (together with HIF-2a) is a key element of the hypoxic response regulating expression of many target genes. Such genes are involved in different physiological functions like angiogenesis, general metabolism and apoptosis. One target gene of HIF-1a and/or HIF-2a has been identified in erythropoietin (Epo). Epo was shown to prevent death of precursor cells of erythrocytes in bone marrow and was thus recognized as a potent anti-apoptotic factor (Koury et al. 2002). Since expression of Epo is strongly induced after hypoxic preconditioning in the retina and Epo receptor expression was localized mainly to photoreceptor and ganglion cells (Bocker-Meffert et al. 2002; Grimm et al. 2002; Grimm et al. 2004), Epo was considered to be a factor protecting the retina against degeneration. Supporting this conclusion, application of recombinant Epo protected photoreceptor cells against light-induced degeneration. However, protection was not as complete as after hypoxic preconditioning suggesting that exposure to reduced oxygen levels may differentially regulate expression of additional genes involved in the protection of photoreceptor cells (Grimm et al. 2002; Grimm et al. 2004).

The goal of the present study was to analyze the retinal response to hypoxia and to identify differentially regulated genes that might be involved in retinal neuroprotection.

2. MATERIAL AND METHODS

2.1. Hypoxic preconditioning and Affymetrix microarrays

Animals were treated in accordance with the regulations of the Veterinary Authority of Zurich and with the statement of 'The Association for Research in Vision and Ophthalmology' for the use of animals in research. BALB/c mice (Harlan, The Netherlands) were exposed to 6% oxygen for 6 h. Retinas were isolated at 0 h, 2 h, 4 h or 16 h after the period of hypoxic preconditioning. Normoxic controls were treated in parallel and collected at the same time points. For each condition three retinas of three different mice were pooled. Total RNA was prepared, processed according to standard procedures and hybridized to Affymetrix GeneChip® Mouse Genome 430 2.0 microarrays. The experiment was conducted three times independently resulting in three microarray replicates per condition and a total number of 9 retinas per condition.

2.2. Quality control and Affymetrix chip analyzes

To analyze the quality of the results after gene chip hybridization the online tool RACE (Remote Analysis Computation for gene Expression data) of the University of Lausanne was used.

To analyze gene expression profiles and to identify differentially regulated genes, we used Genespring 7.0 (Agilent Technologies) software based on the Mas5.0 algorithm. In brief, hypoxic samples (H, hypoxic) were compared to their corresponding normoxic controls (N, normoxic) resulting in 4 different analyzes: N0 vs. H0, N2 vs. H2, N4 vs. H4 and N16 vs. H16. In the first step, genes were tested for their presence or absence in the samples. Genes were considered to be expressed and allowed to pass the filter only when all 3 replicates of a particular condition (normoxic, hypoxic) got a present call. Genes that passed the first filter were then analyzed and filtered according to their fold change (at least factor 2) and to their p-value (≤ 0.05). Additionally, a statistical correction

according to Benjamini/Hochberg (Benjamini and Hochberg 1995) was applied. To sort differentially regulated genes according to their biological function the online tool Onto-Express from Intelligent Systems and Bioinformatics Laboratory (Draghici et al. 2003a; Draghici et al. 2003b; Draghici et al. 2003c) was used (http://vortex.cs.wayne.edu/projects.htm).

2.3. Real-time PCR

Gene regulation was confirmed by real-time PCR on cDNA prepared from total retinal RNA, using a LightCycler 480 instrument (Roche Diagnostics AG, Rotkreuz, Switzerland) and LightCycler 480 SYBR Green I Master Mix (Roche Diagnostics AG). Primers were designed using the Universal ProbeLibrary Assay Design Centre (Roche Diagnostics AG) *https://www.roche-applied-science.com*. Relative expression was calculated according to the expression of b-actin using the LightCycler software package.

2.4. Light exposure and quantification of cell death

$p21^{-/-}$ mice on a mixed Bl/6;129S2 background were purchased from Jackson Laboratory (Bar Harbor, USA). Mice homozygous for the light sensitive $Rpe65_{450Leu}$ variant (Wenzel et al. 2001; Samardzija et al. 2006) were used to establish the breeding colony. After hypoxic preconditioning (see 2.1.) mice were reoxygenated in darkness (dark adaptation) for 4 hours prior to illumination. 45 minutes prior to illumination, pupils were dilated in dim red light using 1% Cyclogyl (Alcon, Cham, Switzerland) and 5% Phenylephrine (Ciba Vision, Niederwangen, Switzerland). Mice were exposed to 13'000 lux of white fluorescent light for 2 hours.

36 hours after light exposure apoptotic cell death was quantified in isolated retinas using a sandwich ELISA system (Cell Death Detection ElisaPlus, Roche Diagnostics, Basel, Switzerland, used according to the manufacturer's recommendation) to determine the relative amount of free nucleosomes in the cytosolic fraction of isolated retinas.

2.5. Morphology

Eyes were removed and fixed in 2.5% glutaraldehyde in 0.1 M cacodylate buffer, pH 7.3 at 4°C overnight. For each eye, the superior central and the inferior central retina adjacent to the optic nerve were trimmed and embedded in Epon 812. Sections (0.5 µm) were prepared from the inferior central retina, stained with toluidine blue and analyzed using an Axioplan microscope (Zeiss, Oberkochen, Germany).

3. RESULTS

3.1. Statistical Analyzes

Hypoxic preconditioning was shown to completely protect photoreceptor cells against light–induced cell death when the light stimulus was given after a reoxygenation period of 4 h (Grimm et al. 2002). In contrast, mice exposed to light at 16 h after hypoxic preconditioning were not protected suggesting that the protective effect of hypoxia is transient and short-lived. Based on these findings we decided to analyze the retinal transcriptome at 4 different time points after hypoxic preconditioning. The first three time points were within the frame of full neuroprotection (0 h, +2 h, +4 h) whereas the last

Table 1. Total number of genes differentially regulated at 0 h, 2 h, 4 h and 16 h after hypoxia.

Condition	Altered Genes with Benjamini/Hochberg	False positive	Altered Genes without Benjamini/Hochberg	False positive
H0 vs. N0	83	4	772	96
H2 vs. N2	7	-	189	24
H4 vs. N4	0	-	74	9
H16 vs. N16	0	-	24	3

Shown are the numbers of genes passing the stringent Benjamini/Hochberg correction in comparison to a normal t-test. The columns 'false positive' show the expected number of genes which have passed the respective test but which are nevertheless not differentially regulated. H0, H2, H4, H16: retinas at 0h, 2h, 4h and 16h, respectively, after hypoxic preconditioning. N0, N2, N4, N16: control normoxic retinas.

time point was taken after neuroprotection has ceased (+16 h). Quality controls were used to confirm the successful performance of the experiment. Analyzes, which compare the global similarity of all gene chips indicated that hypoxic replicates were very similar within their groups and highly different to their normoxic controls (data not shown).

Genespring 7.0 software was used to detect genes that were differentially regulated by hypoxic exposure. In this first statistical analysis without mathematical correction 772 genes appeared to be differentially regulated immediately after hypoxia. This number decreased during reoxygenation to 189 genes after 2 h, 74 genes after 4 h and 24 genes 16 h after hypoxia (Table 1). After application of the highly stringent statistical method of Benjamini/Hochberg (Benjamini and Hochberg 1995), we identified a total of 83 genes as significantly regulated immediately after hypoxic preconditioning. Already at 2 h after hypoxia, only 7 genes remained to have significantly different expression levels and at 4 h and 16 h after hypoxia the retinal transcriptome of preconditioned mice was indistinguishable from normoxic controls (Table 1). Both statistical methods indicated that differential regulation of gene expression is strongest immediately after hypoxia. During reoxygenation, the retinal transcriptome quickly returned to the normoxic gene expression pattern suggesting a short-lived molecular effect of hypoxic preconditioning.

3.2. Biological classification

It is eminent to sort differentially regulated genes according to their biological relevance. Using the statistical online tool "Onto express" we classified the identified genes with respect to their various biological functions like apoptosis, transport, cell cycle and others (Fig. 1). The highest number of regulated genes was sorted into the group of transport-related genes followed by apoptosis-related processes. This may be of high relevance since hypoxic preconditioning induces a neuroprotective response in the retina, which most likely involves a number of genes related to the control of apoptotic events. Having in mind, that genes can be present in more than one biological group, the number of sorted genes does not reflect the real number of genes identified as differentially regulated. Individual genes of the group of 'anti-apoptotic' or the group of 'induction of apoptosis' were also found in the group 'apoptosis'. Table 2 summarizes differentially regulated genes that are considered anti-apoptotic. Note that some of these genes are repressed by the hypoxic pretreatment. Table 3 shows the most prominently regulated pro-apoptotic genes. In total, 13 genes with a known anti-apoptotic function

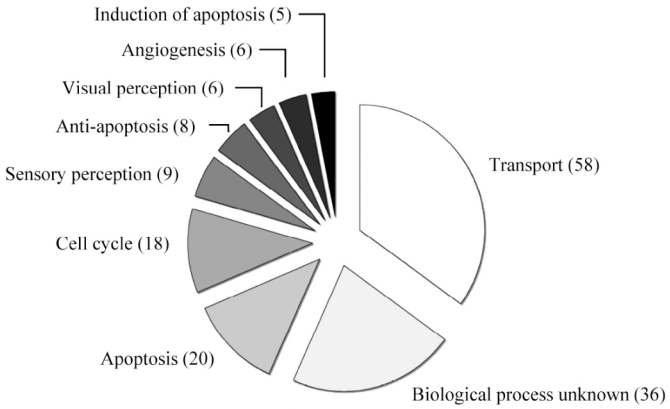

Figure 1. Classification of differentially expressed genes according to their biological function. Genes regulated immediately after hypoxia (0 h) without statistical correction were classified using Onto-Express. Only most prominent and statistically significant ($p \leq 0.05$) groups are shown. Numbers of genes in each group are given in brackets.

Table 2. Differentially regulated genes with anti-apoptotic functions.

Gene	FC 0 h	FC 2 h	FC 4 h	FC 16 h
p21	34.4	-	-	-
Bcl2-like 10	6.3	-	-	-
Snai2	-	3.1	-	-
Vegfa	2.6	-	-	-
Bhlhb4	2.3	-	-	-
Bfar	2.2	-	-	-
Camk1d	-	2.2	2.0	-
Birc6	-	2.1	-	-
C/EBP	2.0	2.3	-	-
p21-activated kinase 7	0.46	-	-	-
Apoptosis inhibitor 5	0.34	-	-	-
Glutaminyl-tRNA-Synthetase	0.32	-	-	-
Birc4	0.22	-	-	-

Shown are the gene-chip deduced fold-changes (FC) at 0h, 2h, 4h and 16h after hypoxic preconditioning. p21 is the most prominently up-regulated gene within this group. -; not detected

Table 3. Differentially regulated genes with pro-apoptotic functions.

Gene	FC 0 h	FC 2 h	FC 4 h	FC 16 h
Pmaip1	12.9	-	-	-
Sh3glb1 (endophilin)	5	4.7	-	-
Bnip3	2.3	-	-	-
BCL2-like 11	2.2	-	-	-
Foxo3a	2.1	-	-	-

Shown are the gene-chip deduced fold-changes (FC) at 0h, 2h, 4h and 16h after hypoxic preconditioning. . -; not detected

were differentially regulated by hypoxia. Nine genes were induced whereas 4 genes were repressed (Table 2). Test of VEGF, p21 and Bcl2l10 gene expression by real-time PCR confirmed the chip data and their up-regulation in response to the hypoxic pretreatment (Fig. 2). In addition to the anti-apoptotic genes, expression of 5 genes expected to be pro-apoptotic was induced during hypoxia (Table 3).

Having both, pro- and anti-apoptotic genes regulated by hypoxia suggests that the preconditioning protocol induces a complex response priming the tissue to resist a toxic insult but also preparing the cells to induce apoptotic cell death if needed. We hypothesize that reducing the number of cells may be required in case of prolonged hypoxic exposure to ensure that at least some cells can be supplied with sufficient oxygen to function.

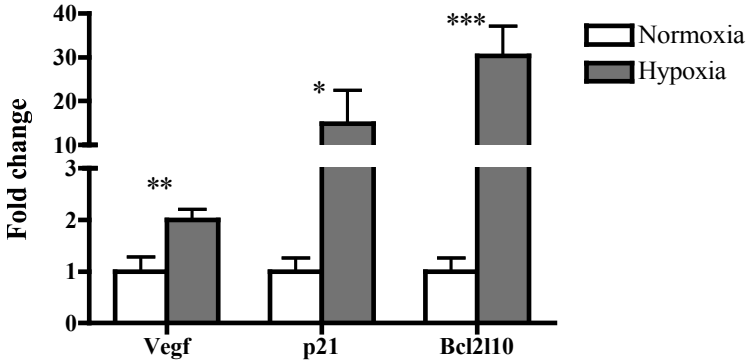

Figure 2. Expression of apoptosis-related genes immediately after hypoxic preconditioning relative to normoxic controls as determined by real-time PCR. Expression of Vegf, p21 and Bcl2l10 (as indicated) was determined in three normoxic and three hypoxic retinas. Amplifications were done in duplicates. Normoxic samples were set to 1 and hypoxic samples represent the relative fold change due to hypoxia.

3.3. The neuroprotective impact of p21

One of the most prominently induced genes with reported anti-apoptotic properties was p21, a cyclin-dependent kinase inhibitor. To analyze its role in neuroprotection by hypoxic preconditioning, p21 knockout mice were exposed to hypoxia, reoxygenated for 4 hours and exposed to 2 hours of 13,000 lux of white light. As controls, $p21^{-/-}$ mice were kept in normoxic conditions before light exposure. Light-induced photoreceptor apoptosis was analyzed 36 hours after exposure by light microscopy (Fig. 3A) and by the semi-quantitative determination of free nucleosomes (Fig. 3B). In contrast to normoxic control mice, hypoxic preconditioned p21 knockout animals did not produce a significant amount of free nucleosomes after light-exposure suggesting that lack of p21 did not interfere with the neuroprotection by hypoxic preconditioning. These findings were confirmed by the morphological analysis of retinal tissue after light exposure (Fig. 3A). In contrast to normoxic controls where light exposure induced the formation of pyknotic nuclei and a severe disruption of rod inner and outer segments, retinal morphology of preconditioned knockout mice was completely protected.

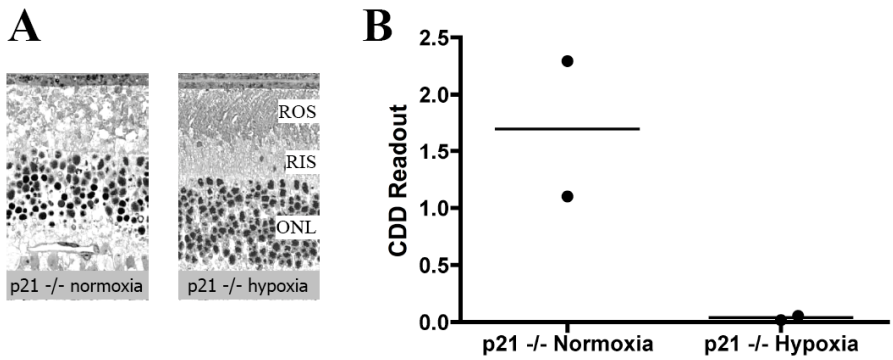

Figure 3. Analysis of the role of p21 in retinal neuroprotection by hypoxic preconditioning. $p21^{-/-}$ mice were either kept in normoxia or were preconditioned with 6% O_2 for 6 hours before light exposure. A) Retinal morphology was analyzed 36 hours after exposure. Normoxic mice (left panel) showed strong signs of degeneration with many pyknotic photoreceptor nuclei and severe destruction of inner and outer segments. Retinas of hypoxic preconditioned mice (right panel) were completely protected against light-induced degeneration. B) Cell death detection (CDD) assay to analyze the amount of free nucleosomes in the cytoplasmic fraction 36 h after light exposure. Normoxic mice showed a high content of free nucleosomes whereas hypoxic preconditioned mice showed no detectable release of nucleosomes. Shown are data points of two individual mice (dots) with the respective average (line). ROS: rod outer segments; RIS: rod inner segments; ONL: outer nuclear layer.

4. DISCUSSION

Photoreceptor cells are among the cells with the highest need for oxygen. Highest oxygen concentrations are measured at the level of the outer segments which are closest to the choroidal blood vessels. With increasing distance from the RPE and the choroidea, oxygen concentrations drop rapidly and photoreceptor cells can experience borderline hypoxic conditions at night, the time of highest energy consumption (Yu and Cringle 2005). To react and/or adapt to such conditions, the retina needs a system that can sense oxygen levels and induce appropriate endogenous mechanisms in response to varying conditions. In a normal physiological situation, such a response may include an adaptation of the metabolism reducing or increasing the consumption of energy. In harsher conditions, the retina may prepare the cells to survive by the induction of an endogenous neuroprotective response. If unfavorable conditions persist, the sacrifice of some individual cells may be required in order to safe the function of the retinal tissue as a whole. Understanding the retinal response to hypoxia may lead to the identification of potent endogenous neuroprotective mechanisms. Artificial and controlled stimulation of such mechanisms may be beneficial for human patients suffering from loss of vision due to retinal degeneration. Furthermore, hypoxia is one of the driving forces for neovascularization, a major complication of many retinal diseases including diabetic retinopathy and AMD (Zhang and Ma 2007). Identification of the molecular mechanisms controlling the hypoxia-related production of angiogenic factors like VEGF may lead to the development of new and efficient treatments for these diseases.

Recently we showed that a transient period of strong hypoxia induces a molecular response in the retina which protects photoreceptors from the otherwise deleterious effect of light exposure (Grimm et al. 2002). A central regulator of this response might be the transcription factor HIF-1a which is stabilized and therefore activated in hypoxic conditions in several tissues including the retina (Grimm et al. 2002; Maxwell 2003; Sharp and Bernaudin 2004). However, since HIF-1a and other transcription factors modulate the expression of a large amount of genes (Ke and Costa 2006), the molecular mechanisms involved in the tissue response to hypoxia are still poorly understood and the molecular basis for hypoxia-induced neuroprotection remains unclear. Our study was therefore designed to increase our knowledge of hypoxia-dependent gene regulation and neuroprotection by analyzing the retinal transcriptome after hypoxic preconditioning.

The highest number of differentially regulated genes was found immediately after hypoxia. At this time, HIF-1a is present at high levels suggesting that HIF-1a may indeed be one of the major factors controlling the hypoxic response in the retina. This is further supported by the rapid decline of HIF-1a levels (Grimm et al. 2002) and of differentially expressed genes during reoxygenation.

The most prominent functional group affected by hypoxia was “transport” which includes genes of general metabolic activity like Slc37a4 (glucose-6phosphate transporter) or FABP4 (fatty acid binding protein 4). This may reflect an adaptational response of the retina, which may normally occur to a rather mild change in oxygen levels. Despite the strong neuroprotective capacity of hypoxic preconditioning, we also detected a number of differentially regulated genes that are pro-apoptotic and may therefore promote cell death. As discussed above, these factors may be produced to reduce the number of oxygen-consuming cells if low levels of oxygen persist. This might secure sufficient oxygen supply and therefore energy for a smaller cell population which may thus survive and function even in unfavorable conditions. Although this may reduce the general sensitivity of the retina, it may nevertheless rescue some (reduced) function. It might be interesting to analyze whether less severe hypoxic conditions would increase the differential regulation of genes involved in general metabolism and decrease the number of pro-apoptotic genes.

Our focus, however, is the elucidation of the neuroprotective mechanisms in response to a harsh but transient hypoxic period. Therefore, we concentrated during our initial analysis on genes which might be involved in an anti-apoptotic response of the retina. Because p21 was one of the most prominently induced genes with known anti-apoptotic functions (Zaman et al. 1999; Mahyar-Roemer and Roemer 2001), we focused on its potential role in neuroprotection after hypoxic preconditioning. We hypothesized that lack of p21 would reduce the neuroprotective effect if the gene was indeed involved in the protective response. However, mice with a functional knockout of p21 were highly protected against a toxic light insult when preconditioned with hypoxia. This suggests that this Cyclin dependent kinase inhibitor is at least not a major contributor to the neuroprotective response induced by hypoxic preconditioning.

We will continue the analysis of individual genes identified in our screen. Future studies will focus on genes like Bcl2l10 or C/EBP which were up-regulated during hypoxia and which are known to be anti-apoptotic (Song et al. 1999; Naumann et al. 2001; Buck and Chojkier 2003). Additionally, strongly up-regulated genes (not shown) like Paraoxonase 1, which is involved in oxidative stress response and lipid oxidation (Aviram et al. 1998) or Adrenomedullin, which was reported to be neuroprotective in

ischemia models (Miyashita et al. 2006) will be studied for their relevance to retinal neuroprotection after hypoxic preconditioning.

5. ACKNOWLEDGEMENTS

The authors thank Coni Imsand, Gaby Hoegger, Hedwig Wariwoda and Philipp Huber for excellent technical assistance. This work was supported by the Swiss National Science Foundation (SNF), the Fritz-Tobler-Foundation, the Centre of Integrative Human Physiology (CIHP) and the European Union (Evi-GenoRet).

6. REFERENCES

Aviram, M., Rosenblat, M., Bisgaier, C.L., Newton, R.S., Primo-Parmo, S.L., and La Du, B.N. 1998. Paraoxonase inhibits high-density lipoprotein oxidation and preserves its functions. A possible peroxidative role for paraoxonase. *J Clin Invest* **101**(8): 1581-1590.

Benjamini, Y. and Hochberg, Y. 1995. Controlling the false discovery rate - a practical and powerful approach to multiple testing. *J Roy Stat Soc* **57**: 289-300.

Bocker-Meffert, S., Rosenstiel, P., Rohl, C., Warneke, N., Held-Feindt, J., Sievers, J., and Lucius, R. 2002. Erythropoietin and VEGF promote neural outgrowth from retinal explants in postnatal rats. *Invest Ophthalmol Vis Sci* **43**(6): 2021-2026.

Buck, M. and Chojkier, M. 2003. Signal transduction in the liver: C/EBPbeta modulates cell proliferation and survival. *Hepatology* **37**(4): 731-738.

Cai, Z., Manalo, D.J., Wei, G., Rodriguez, E.R., Fox-Talbot, K., Lu, H., Zweier, J.L., and Semenza, G.L. 2003. Hearts from rodents exposed to intermittent hypoxia or erythropoietin are protected against ischemia-reperfusion injury. *Circulation* **108**(1): 79-85.

Dong, J.W., Zhu, H.F., Zhu, W.Z., Ding, H.L., Ma, T.M., and Zhou, Z.N. 2003. Intermittent hypoxia attenuates ischemia/reperfusion induced apoptosis in cardiac myocytes via regulating Bcl-2/Bax expression. *Cell Res* **13**(5): 385-391.

Draghici, S., Khatri, P., Bhavsar, P., Shah, A., Krawetz, S.A., and Tainsky, M.A. 2003a. Onto-Tools, the toolkit of the modern biologist: Onto-Express, Onto-Compare, Onto-Design and Onto-Translate. *Nucleic Acids Res* **31**(13): 3775-3781.

Draghici, S., Khatri, P., Martins, R.P., Ostermeier, G.C., and Krawetz, S.A. 2003b. Global functional profiling of gene expression. *Genomics* **81**(2): 98-104.

Draghici, S., Khatri, P., Shah, A., and Tainsky, M.A. 2003c. Assessing the functional bias of commercial microarrays using the onto-compare database. *Biotechniques* **Suppl**: 55-61.

Emerson, M.R., Nelson, S.R., Samson, F.E., and Pazdernik, T.L. 1999. A global hypoxia preconditioning model: neuroprotection against seizure-induced specific gravity changes (edema) and brain damage in rats. *Brain Res Brain Res Protoc* **4**(3): 360-366.

Fauser, S., Luberichs, J., and Schuttauf, F. 2002. Genetic animal models for retinal degeneration. *Surv Ophthalmol* **47**(4): 357-367.

Gidday, J.M., Fitzgibbons, J.C., Shah, A.R., and Park, T.S. 1994. Neuroprotection from ischemic brain injury by hypoxic preconditioning in the neonatal rat. *Neurosci Lett* **168**(1-2): 221-224.

Grimm, C., Wenzel, A., Groszer, M., Mayser, H., Seeliger, M., Samardzija, M., Bauer, C., Gassmann, M., and Reme, C.E. 2002. HIF-1-induced erythropoietin in the hypoxic retina protects against light-induced retinal degeneration. *Nat Med* **8**(7): 718-724.

Grimm, C., Wenzel, A., Stanescu, D., Samardzija, M., Hotop, S., Groszer, M., Naash, M., Gassmann, M., and Reme, C. 2004. Constitutive overexpression of human erythropoietin protects the mouse retina against induced but not inherited retinal degeneration. *J Neurosci* **24**(25): 5651-5658.

Ke, Q. and Costa, M. 2006. Hypoxia-inducible factor-1 (HIF-1). *Mol Pharmacol* **70**(5): 1469-1480.

Koury, M.J., Sawyer, S.T., and Brandt, S.J. 2002. New insights into erythropoiesis. *Curr Opin Hematol* **9**(2): 93-100.

Mahyar-Roemer, M. and Roemer, K. 2001. p21 Waf1/Cip1 can protect human colon carcinoma cells against p53-dependent and p53-independent apoptosis induced by natural chemopreventive and therapeutic agents. *Oncogene* **20**(26): 3387-3398.

Maxwell, P. 2003. HIF-1: an oxygen response system with special relevance to the kidney. *J Am Soc Nephrol* **14**(11): 2712-2722.

Miyashita, K., Itoh, H., Arai, H., Suganami, T., Sawada, N., Fukunaga, Y., Sone, M., Yamahara, K., Yurugi-Kobayashi, T., Park, K., Oyamada, N., Sawada, N., Taura, D., Tsujimoto, H., Chao, T.H., Tamura, N., Mukoyama, M., and Nakao, K. 2006. The neuroprotective and vasculo-neuro-regenerative roles of adrenomedullin in ischemic brain and its therapeutic potential. *Endocrinology* **147**(4): 1642-1653.

Naumann, U., Weit, S., Wischhusen, J., and Weller, M. 2001. Diva/Boo is a negative regulator of cell death in human glioma cells. *FEBS Lett* **505**(1): 23-26.

Samardzija, M., Wenzel, A., Naash, M., Reme, C.E., and Grimm, C. 2006. Rpe65 as a modifier gene for inherited retinal degeneration. *Eur J Neurosci* **23**(4): 1028-1034.

Sharp, F.R. and Bernaudin, M. 2004. HIF1 and oxygen sensing in the brain. *Nat Rev Neurosci* **5**(6): 437-448.

Song, Q., Kuang, Y., Dixit, V.M., and Vincenz, C. 1999. Boo, a novel negative regulator of cell death, interacts with Apaf-1. *Embo J* **18**(1): 167-178.

Wenzel, A., Grimm, C., Samardzija, M., and Reme, C.E. 2005. Molecular mechanisms of light-induced photoreceptor apoptosis and neuroprotection for retinal degeneration. *Prog Retin Eye Res* **24**(2): 275-306.

Wenzel, A., Reme, C.E., Williams, T.P., Hafezi, F., and Grimm, C. 2001. The Rpe65 Leu450Met variation increases retinal resistance against light-induced degeneration by slowing rhodopsin regeneration. *J Neurosci* **21**(1): 53-58.

Yu, D.Y. and Cringle, S.J. 2005. Retinal degeneration and local oxygen metabolism. *Exp Eye Res* **80**(6): 745-751.

Zaman, K., Ryu, H., Hall, D., O'Donovan, K., Lin, K.I., Miller, M.P., Marquis, J.C., Baraban, J.M., Semenza, G.L., and Ratan, R.R. 1999. Protection from oxidative stress-induced apoptosis in cortical neuronal cultures by iron chelators is associated with enhanced DNA binding of hypoxia-inducible factor-1 and ATF-1/CREB and increased expression of glycolytic enzymes, p21(waf1/cip1), and erythropoietin. *J Neurosci* **19**(22): 9821-9830.

Zhang, S.X. and Ma, J.X. 2007. Ocular neovascularization: Implication of endogenous angiogenic inhibitors and potential therapy. *Prog Retin Eye Res* **26**(1): 1-37.

6.4 R91W Mutation in Rpe65 Leads to Milder Early-onset Retinal Dystrophy Due to the Generation of Low Levels of 11-cis-retinal

Marijana Samardzija[1], Johannes von Lintig[2], Naoyuki Tanimoto[3], Vitus Oberhauser[2], **Markus Thiersch[1]**, Charlotte Reme[1], Mathias Seeliger[3], Christian Grimm[1] and Andreas Wenzel[1]

[1]Laboratory for Retinal Cell Biology, Department Ophthalmology, University of Zurich
[2]Institute of Biology I, Animal Physiology and Neurobiology, University of Freiburg
[3]Ocular Neurodegeneration Research Group, Institute for Ophthalmic Research, University of Tuebingen

Published in Human Molecular Genetics, Vol. 17, No. 2, 281–292 (2008)

6.4.1 Author contribution

Design:	MS, CR, JvL, MSe and AW
Experiments:	MS, JvL, NT, VO, **MT** (assisted in animal treatment; real-time PCR), MSe, CG and AW
Interpretation:	MS, JvL, **MT**, CR, MSe, CG and AW
Manuscript:	MS and AW
Manuscript Correction:	MS, JvL, **MT**, MSe, CG and AW

6.4.2 Summary

RPE65 is a protein expressed in retinal pigment epithelium cells and is essential for the restoration of the photoreceptor-chromophore 11-*cis*-retinal after rhodopsin bleaching. Mutations in RPE65 cause retinal dystrophies and we generated a knock in mouse with the most frequent RPE65 mutation in human patients – an amino acid substitution at position 91 (R91W). Affected patients have cone vision during childhood, but progressively lose sight during adolescence. We characterized the new mouse model and compared it to wild type mice and *RPE65* null mice ($Rpe65^{-/-}$). RPE65 mRNA was slightly reduced in R91W mice, when compared to wild type mice and no mRNA was found in $Rpe65^{-/-}$ mice. Western blot analyzes and immunohistochemistry showed that RPE65 protein expression was largely reduced in

R91W mice but that the protein was correctly localized in the retinal pigment epithelium. In contrast to Rpe65$^{-/-}$ mice, were no 11-*cis*-retinal was detected, retinas of 4, 8, 12, 24 and 40-week old R91W mice contained very low amounts of 11-*cis*-retinal, proving that the mutant RPE65 protein possessed biological activity *in vivo*. However, retinyl esters, which are the substrate for RPE65, accumulated comparably in R91W and in Rpe65$^{-/-}$ mice leading to a similar formation of lipid-like inclusions in the RPE. That suggested that RPE65 activity in R91W mice processed retinyl esters to slow – either because of the reduced protein levels and/or an impaired enzyme activity. Further, in dark-adapted R91W mice only 6% - 10% of wild type rhodopsin levels could be measured. Because the RPE65 protein determines the kinetics of rhodopsin regeneration, we assumed a reduced regeneration rate. After bleaching wild type mice regenerated approximately 90% of rhodopsin within one hour. However, R91W mice reached even after 5 days only 44% of the pre-bleach value. Photoreceptor function was assessed by electroretinography (ERG), which employs light flashes to induce an electrical response in the retina. Scotopic ERG measures rod and mixed rod/cone responses and showed a reduced electrical response in R91W mice compared to wild type mice. During aging (8 to 40 weeks) light sensitivity remained unaltered in R91W mice but the amplitude of the b-wave (response of secondary neurons) declined progressively. Photopic ERG measures the function of cones and shows a comparable light sensitivity between wild type and R91W mice. However, the shape of the waves was altered in R91W mice and we hypothesized that rods remained active in these mice, suggesting an overlapping response of the rod and the cone system even under photopic conditions. Similar to the scotopic ERG, the b-wave declined during aging. Photoreceptor cells in Rpe65$^{-/-}$ mice slowly undergo apoptosis. The morphology of R91W mice indicated, that the retina degenerates as well. However, up to 12 weeks of age R91W mice showed a better preservation of OS and contained more cone nuclei than respective Rpe65$^{-/-}$ mice. R91W mice were clearly distinct from Rpe65$^{-/-}$ mice and showed the formation of 11-*cis*-retinal, the presence of rhodopsin and a better residual function of the retina. Our results indicated that we generated a mouse model for a specific RPR65 mutation, which genetically reflects the human disease and which provides a tool to test therapeutic approaches for human patients with RPE65 missense mutations.

6.4.3 Manuscript

Human Molecular Genetics, 2008, Vol. 17, No. 2 **281–292**
doi:10.1093/hmg/ddm304
Advance Access published on October 12, 2007

R91W mutation in Rpe65 leads to milder early-onset retinal dystrophy due to the generation of low levels of 11-*cis*-retinal

Marijana Samardzija[1,*], Johannes von Lintig[2], Naoyuki Tanimoto[3], Vitus Oberhauser[2], Markus Thiersch[1], Charlotte E. Remé[1], Mathias Seeliger[3], Christian Grimm[1] and Andreas Wenzel[1,†]

[1]Laboratory for Retinal Cell Biology, Department of Ophthalmology, University of Zurich, Frauenklinikstr. 24, 8091 Zurich, Switzerland, [2]Institute of Biology I, Animal Physiology and Neurobiology, University of Freiburg, Hauptstr. 1, D-79104 Freiburg, Germany and [3]Ocular Neurodegeneration Research Group, Institute for Ophthalmic Research, University of Tuebingen, Schleichstr. 4/3, D-72076 Tuebingen, Germany

Received September 18, 2007; Revised and Accepted October 10, 2007

RPE65 is a retinal pigment epithelial protein essential for the regeneration of 11-*cis*-retinal, the chromophore of cone and rod visual pigments. Mutations in *RPE65* lead to a spectrum of retinal dystrophies ranging from Leber's congenital amaurosis to autosomal recessive retinitis pigmentosa. One of the most frequent missense mutations is an amino acid substitution at position 91 (R91W). Affected patients have useful cone vision in the first decade of life, but progressively lose sight during adolescence. We generated R91W knock-in mice to understand the mechanism of retinal degeneration caused by this aberrant *Rpe65* variant. We found that in contrast to *Rpe65* null mice, low but substantial levels of both RPE65 and 11-*cis*-retinal were present. Whereas rod function was impaired already in young animals, cone function was less affected. Rhodopsin metabolism and photoreceptor morphology were disturbed, leading to a progressive loss of photoreceptor cells and retinal function. Thus, the consequences of the R91W mutation are clearly distinguishable from an *Rpe65* null mutation as evidenced by the production of 11-*cis*-retinal and rhodopsin as well as by less severe morphological and functional disturbances at early age. Taken together, the pathology in R91W knock-in mice mimics many aspects of the corresponding human blinding disease. Therefore, this mouse mutant provides a valuable animal model to test therapeutic concepts for patients affected by *RPE65* missense mutations.

INTRODUCTION

The vitamin A derivative 11-*cis*-retinal is the chromophore of rod and cone visual pigments. Absorption of light leads to an 11-*cis* to all-*trans* isomerization followed by dissociation of all-*trans*-retinal from the protein moiety (opsin) of the visual pigment holo-complex. The regeneration of the visual chromophore is a complex protein-mediated process termed the visual cycle (1). The crucial all-*trans* to 11-*cis*-retinoid isomerization reaction step takes place in the retinal pigment epithelium (RPE) and is catalyzed by RPE65 (2–4). Rpe65-deficient mice lack 11-*cis*-retinal and consequently no rhodopsin is detectable in their eyes (5,6). Instead, these animals show in the RPE an over-accumulation of retinyl esters, retinoid intermediates of the visual cycle (5).

More than 60 disease-associated mutations have been identified in the human *RPE65* gene [summarized in http://www.retina-international.com/sci-news/rpe65mut.htm; see also Zernant *et al*. (7)]. The broad spectrum of mutations includes point mutations, splice-site defects, deletions and insertions. Mutations in *RPE65* are estimated to account for ~11% of all autosomal recessive childhood-onset retinal dystrophy cases (8). Patients suffering from mutations in the *RPE65* gene are alternatively diagnosed as autosomal recessive retinitis pigmentosa, autosomal recessive retinal dystrophy, early-onset severe retinal dystrophy (EOSRD) or Leber's

*To whom correspondence should be addressed at Tel: +41 442553872; Fax: +41 442554385; E-mail: samam@opht.uzh.ch
†Present address: Novartis Pharma Schweiz AG—BU Ophthalmics, Monbijoustrasse 118, CH-3007 Bern, Switzerland.

282 Human Molecular Genetics, 2008, Vol. 17, No. 2

congenital amaurosis type II (LCAII) (8–10). These rather diverse diagnoses reflect the phenotypic heterogeneity of the underlying disease. Most patients suffering from mutations in the *RPE65* gene are diagnosed early in childhood as severely visually impaired, with night blindness, distinctly restricted visual fields and nystagmus, but no photophobia (summarized in 11). Retinal function (ERG) is undetectable after dark adaptation and is severely impaired following light adaptation. However, many of these patients have sufficient vision to attend elementary school. Vision is then gradually lost, resulting in blindness almost invariably in the third decade of life (11).

Two naturally occurring models (rd12 mouse and Briard dog) and the genetically engineered Rpe65 knock-out mouse ($Rpe65^{-/-}$) have been useful for the delineation of RPE65 protein function in the visual cycle (5,12,13). These models have meanwhile been used in pre-clinical gene replacement therapy experiments to restore rod and cone photoreceptor function [rd12 (14), $Rpe65^{-/-}$ (15–18), dog (19–22)]. All of the above models represent a 'null situation' for RPE65, in which the visual cycle has never been functional. However, current literature indicates that more than 50% of *RPE65* mutations in patients are missense mutations. Some of these missense mutations presumably produce mutant versions of RPE65 with some residual enzymatic activity. Recently, we characterized three consanguineous families carrying the R91W mutation in *RPE65* (23). All affected family members had useful cone-mediated vision in the first decade of life, suggesting that the mutant RPE65 protein is expressed and possesses residual function. The consequences of a partial loss of RPE65 activity caused by a missense mutation have not yet been studied in an *in vivo* animal model and little is known about the pathology of LCA/EOSRD under such conditions.

To assess this specific pathology, we generated the Rpe65-R91W knock-in mouse as a model for the human disease and analyzed the effect of the mutation on retinal function, visual cycle and morphology.

RESULTS

Generation of R91W knock-in mice

Gene targeting in mouse ES cells was used to modify exon 4 of the Rpe65 gene such that codon 91 changed from arginine to tryptophan (R91W) (Fig. 1A). In humans, the R91W mutation is caused by a single point mutation (TGA>TGG). However, in mice, arginine 91 is encoded by a CGA codon; therefore, two point mutations were introduced into codon 91 (CGA>TGG). The introduction of these two mutations resulted in the loss of a *Taq*I restriction site, facilitating the genotype analysis (Fig. 1A–C).

The gene targeting strategy is shown in Figure 1B. In addition to mouse Rpe65 genomic DNA carrying the R91W mutation, the targeting vector contained a floxed neo resistance and a diphtheria toxin (DT) cassette as selection markers. Sequencing of the full genomic DNA insert of the targeting vector confirmed the presence of the R91W mutation and the selection markers in an otherwise wild-type sequence (Fig. 1A). The linearized construct was electroporated into coisogenic TC1 ES cells, and correctly targeted ES cell clones were identified and characterized in detail by Southern blotting, PCR and PCR restriction digestion analysis (Fig. 1C; data not shown).

These clones were used to generate germ-line competent chimeric mice. A chimeric male was mated with coisogenic 129S6 females to propagate the line. The resulting heterozygous ($Rpe65^{R91Wneo}$) F1 mice were bred with a germ-line Cre-deleter mouse line [129S6-Tg(Prnp-GFP/Cre)1Blw/J)] (24) to excise the neo cassette (Fig. 1B). The resulting offspring was heterozygous for the R91W mutation (R91W/wt). The only foreign sequence in addition to the R91W substitution was a single intronic *lox*P site. Finally, we interbred the heterozygous R91W/wt mice to obtain pure homozygous 129S6/SvEvTac-$Rpe65^{tm1Lrcb}$ (R91W) knock-in mice. Of note, these mice were coisogenic to 129S6 control mice, except for codon 91 and the above-mentioned *lox*P site.

Rpe65 expression in mutant mice

Quantitative RT–PCR, immunoblotting and immunohistochemistry showed that the mutant protein is expressed in R91W knock-in but not in $Rpe65^{-/-}$ mice (Fig. 2A–C). Whereas the expression of Rpe65 mRNA was only slightly reduced in R91W mice (Fig. 2A), immunoblotting revealed that the steady-state protein levels of the $RPE65^{R91W}$ mutant variant were reduced by 95% when compared with wild-type mice (Fig. 2B; data not shown). The mutant protein was detected in the RPE and thus was correctly localized (Fig. 2C).

Lecithin retinol acyltransferase (LRAT) and cellular retinaldehyde binding protein (CRALBP) are functionally connected to RPE65 and the visual cycle (25–28). Expression of both proteins was comparable in eyecups of 8-week-old wild-type, R91W knock-in and $Rpe65^{-/-}$ animals with a tendency of increased LRAT levels in knock-out mice (Fig. 2B). Levels of rod opsin were slightly reduced in retinas of R91W mice and—as previously reported (5)—in retinas of $Rpe65^{-/-}$ animals.

Retinoid analysis

The absence of RPE65 results in the arrest of the visual cycle, causing an accumulation of retinyl esters in the RPE and visual chromophore deficiency (5). On the basis of this observation, we expected that the dramatically reduced protein levels of the $RPE65^{R91W}$ variant (Fig. 2B) would also result in a disturbance of the visual cycle. Therefore, we analyzed the retinoid composition in dark-adapted wild-type, R91W/wt heterozygous, R91W homozygous and $Rpe65^{-/-}$ mice at different ages. HPLC analysis of whole eye preparations of 4, 8, 12, 24 and 40-week-old animals demonstrated the presence of 11-*cis*-retinal in R91W homozygous mice, though at low levels between 2.5 and 6.3% when compared with age-matched wild-type animals (Table 1). As expected, no 11-*cis*-retinal was detectable in $Rpe65^{-/-}$ mice at any age (Table 1) (5,29). All-*trans*-retinal, all-*trans*-retinol and 9-*cis*-retinal levels were comparable between R91W and $Rpe65^{-/-}$ mice. The retinoid content and composition in R91W/wt heterozygous animals did not differ from wild-type mice at all tested ages (Table 1).

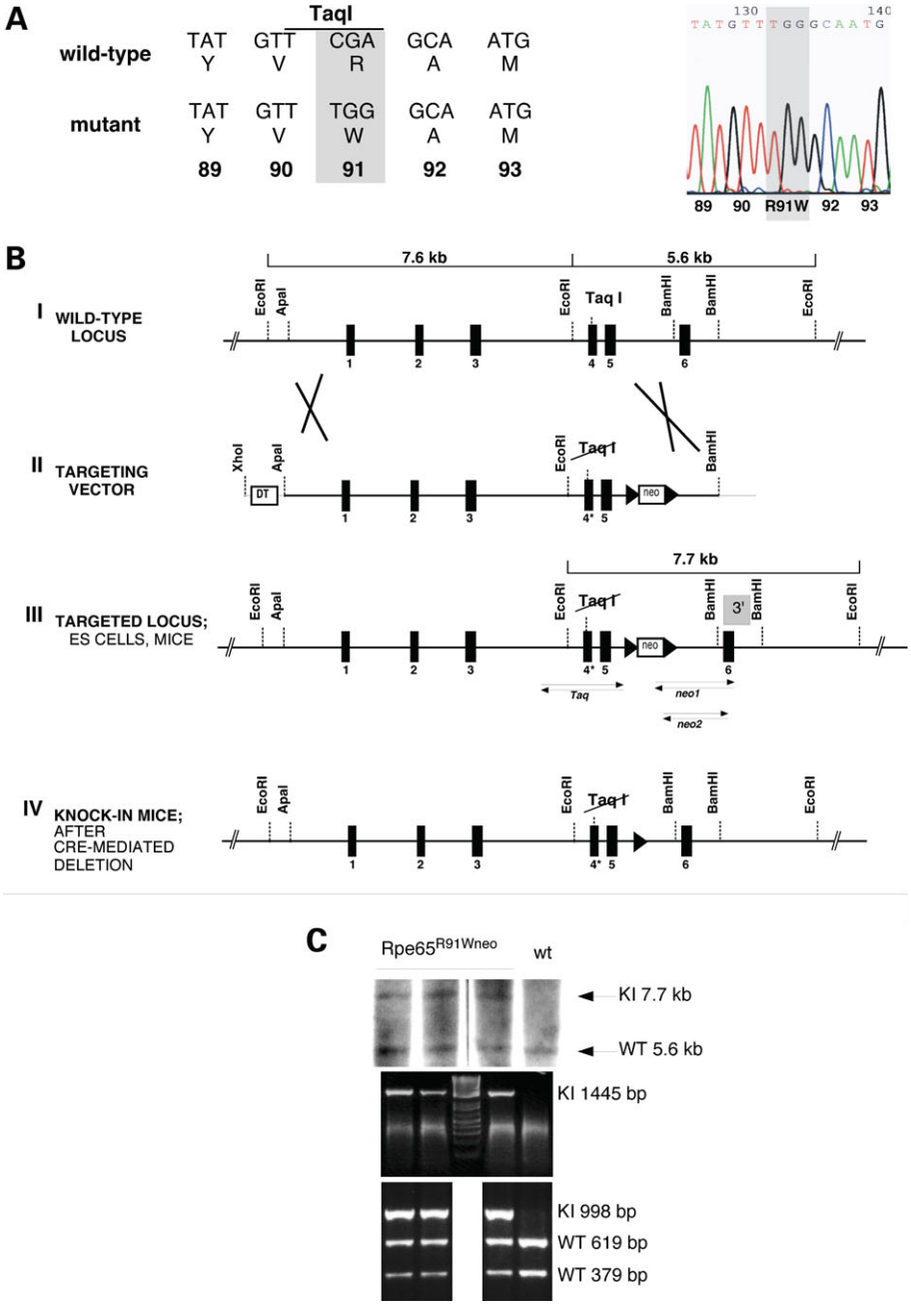

Figure 1. Generation of R91W knock-in mice. (**A**) Partial sequence of exon 4 wild-type and mutated R91W DNA. Note that two point mutations were introduced in the codon for arginine (R) at position 91 to obtain tryptophan (W). This resulted in the loss of a *Taq*I restriction site in the mutated DNA (right panel). Sequence data of the targeting vector showing the mutant TGG triplet at position 91 (left panel). (**B**) Schematic representation of the R91W targeting strategy I: partial wild-type *Rpe65* allele, with restriction enzyme sites and location of first six exons (boxes). II: targeting construct containing R91W mutation (indicated as lost *Taq*I restriction site in mutated exon 4*), neomycin (neo)-resistant gene flanked by *lox*P sites (indicated as triangles) suitable for cre-medated excision, and diphtheria resistance cassette (DT). Note the unique *Xho*I restriction site used for linearization of the targeting vector. III: genomic *Rpe65* DNA after integration of targeting vector carrying the neomycin cassette ($Rpe65^{R91Wneo}$). Positions of PCR primer pairs and Southern blot probe (gray box) for PCR are indicated. Neo1 and neo2 are nested primer pairs designed to read from the selection cassette into the 3′ short arm outside of targeting area. These primers were used to confirm the HR. The *Taq* primer pair was used to confirm the presence of R91W mutation (see Materials and Methods). IV: the partial R91W mutant allele after the removal of the neo cassette by crossing $Rpe65^{R91Wneo}$ mice with the Cre-deleter mice. (**C**) Genotyping of R91W mutants. Upper panel: DNA was isolated from neomycin-resistant ES cell colonies and analyzed by Southern blotting, after digestion with *Eco*RI, and using 3′external probe as indicated in (B). Signal from the genomic DNA from wild-type (wt) allele is 5.6 kb. A heterozygous $Rpe65^{R91Wneo}$ knock-in (KI) allele gives rise to additional 7.7 kb due to the presence of the neomycin cassette. Middle panel: PCR analysis of the same DNA using neo1 and neo2 nested primer pair. A PCR fragment of 1445 bp detected in heterozygous $Rpe65^{R91Wneo}$ knock-in due to the presence of the neomycin cassette. Lower panel: RFLP-PCR analysis of the same DNA using the *Taq* primer pair [see (B)]. A PCR fragment of 998 bp was digested with the *Taq*I restriction enzyme. In wild-type animals, this results in a 379 and a 619 bp fragment. Heterozygous $Rpe65^{R91Wneo}$ knock-in DNA contains an additional 998 bp fragment due to the loss of the *Taq*I restriction site. This protocol was used for genotyping of the final R91W knock-in mice. Asterisk indicates mutated exon 4.

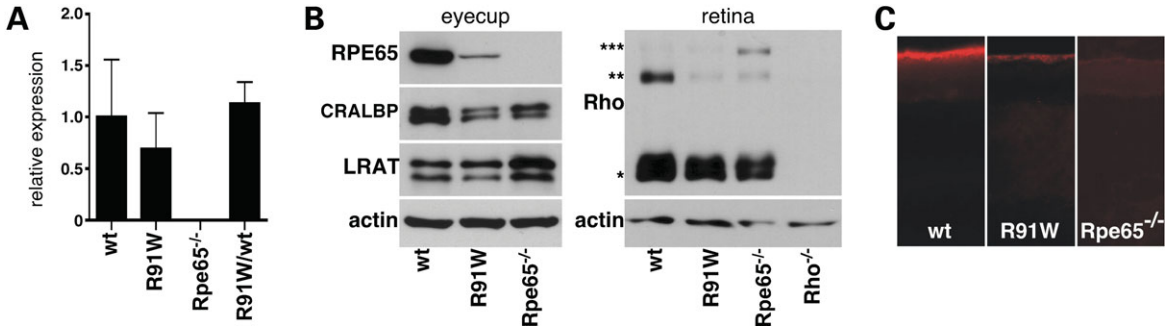

Figure 2. R91W mutation causes reduced levels of RPE65. (**A**) Relative mRNA levels of Rpe65 expressed in eyecups of wild-type, R91W (homozygous), $Rpe65^{-/-}$ and R91W/wt (heterozygous) mice at 8 weeks of age as determined by real-time RT–PCR. mRNA levels, normalized to β-actin, are expressed relative to wild-type control, which was set to 1. RNA isolated from three independent retinas per age and genotype was amplified in triplicates (means ± SD). (**B**) Western blotting of eyecup or retinal proteins from 8-week-old wild-type, R91W or $Rpe65^{-/-}$ mice. The presence of the R91W mutation resulted in reduced amounts of RPE65 immunoreactivity. Note similar levels of LRAT and CRALBP in the eyecups of all strains with a tendency of increased LRAT levels in $Rpe65^{-/-}$ mice. Slightly reduced amounts of rod opsin (Rho) were detected in retinas of mutant mice (asterisk indicates Rho monomer, dimer or trimer, respectively). Shown are the representative blots from at least three different animals per genotype. (**C**) Immunolabeling with a polyclonal antibody to RPE65, demonstrating that the $RPE65^{R91W}$ mutant protein is expressed only in RPE cells. Note the reduced immunoreactivity when compared with animals expressing wild-type RPE65 protein. The $Rpe65^{-/-}$ animals served as negative controls.

Table 1. Retinoid analysis

	Age	11-*cis*-retinal	All-*trans*-retinal	All-*trans*-retinol	Retinyl ester	9-*cis*-retinal
Wild-type	4	380.2 ± 60.1	39.0 ± 11.3	4.2 ± 3.6	30.6 ± 5.6	n.d.
	8	336.1 ± 21.8	34.7 ± 1.6	5.4 ± 9.4	39.2 ± 5.0	n.d.
	12	336.7 ± 32.4	62.6 ± 12.9	n.d.	34.9 ± 4.6	n.d.
	24	373.6 ± 75.5	47.9 ± 3.7	2.2 ± 3.8	106.2 ± 27.2	n.d.
R91W/wt	4	394.7 ± 22.6	53.4 ± 7.1	6.0 ± 0.8	44.3 ± 5.4	n.d.
	8	371.8 ± 22.1	87.1 ± 4.7	n.d.	55.7 ± 8.4	3.7 ± 0.3
	12	454.8 ± 42.0	52.4 ± 5.5	3.0 ± 3.7	89.6 ± 17.9	n.d.
	24	337.4 ± 49.0	86.4 ± 15.3	n.d.	108.9 ± 23.3	n.d.
R91W	4	24.0 ± 3.0	3.6 ± 0.6	10.4 ± 1.9	420.7 ± 34.5	7.6 ± 0.8
	8	15.4 ± 0.2	4.8 ± 1.5	9.2 ± 5.2	651.9 ± 127.4	9.9 ± 0.9
	12	13.5 ± 0.2	2.7 ± 0.4	13.9 ± 2.7	1542.7 ± 271.8	9.2 ± 1.2
	24	9.4 ± 8.2	1.9 ± 1.7	20.2 ± 17.7	2186.1 ± 160.1	4.3 ± 3.7
	40	18.2 ± 4.8	2.2 ± 1.0	12.4 ± 3.4	2107.9 ± 138.9	10.6 ± 3.2
$Rpe65^{-/-}$	4	n.d.	n.d.	8.6 ± 2.5	271.4 ± 22.8	4.8 ± 1.5
	8	n.d.	1.3 ± 1.2	5.4 ± 1.0	474.9 ± 49.1	8.5 ± 0.7
	12	n.d.	1.9 ± 0.4	14.9 ± 4.1	805.9 ± 57.5	6.7 ± 0.9
	24	n.d.	2.1 ± 0.3	8.5 ± 4.8	1160.6 ± 529.0	10.3 ± 3.8
	40	n.d.	2.8 ± 1.0	15.6 ± 5.1	2622.9 ± 531.3	13.1 ± 11.2

All values are given in pmol/eye ± SD ($n = 3$). Age in weeks, as indicated. n.d., not detectable.

The presence of 11-*cis*-retinal indicated that the visual cycle is functional in R91W animals. Nevertheless, we detected a strong and almost linear (13 pmol/day; $R^2 = 0.93$) accumulation of retinyl esters during the first 24 weeks of life. Between 24 and 40 weeks, no further increase was detected (2186 and 2108 pmol/eye, respectively; Table 1) suggesting that a plateau was reached in R91W mice. In $Rpe65^{-/-}$ animals retinyl ester levels increased linearly (9 pmol/day; $R^2 = 0.96$) throughout 40 weeks (Table 1). Electron microscopy revealed that this accumulation of retinyl esters was accompanied by the formation of lipid droplets in the RPE of R91W and, as previously reported, in $Rpe65^{-/-}$ mice (5) (Fig. 3).

Rhodopsin content and regeneration

We next determined dark-adapted rhodopsin levels, which reached 30 pmol/retina (Fig. 4A) in R91W mice representing 6% of wild-type rhodopsin. This percentage was comparable to the amount of 11-*cis*-retinal observed in 4-week-old R91W mice, which corresponded likewise to 6% of wild-type levels (Table 1).

The expression levels of RPE65 protein govern the kinetics of rhodopsin regeneration (30,31). Given the reduced amount of RPE65 in R91W mice (Fig. 2), we expected that rhodopsin would regenerate with a much slower rate. To allow a maximal rhodopsin production, we kept R91W mice in darkness for 4, 10 and 22 days. By the time of analysis, the mice were 6–7-weeks old. Maximal rhodopsin levels detected after 22 days in darkness were 42 pmol, which was still <10% of wild-type animals (Fig. 4A; see Fig. 4C for the wild-type levels).

In order to test rhodopsin regeneration kinetics, 6–7-week-old animals were dark-adapted for 24 h and exposed for 10 min to 5000 lux, which bleaches 90% of rhodopsin in

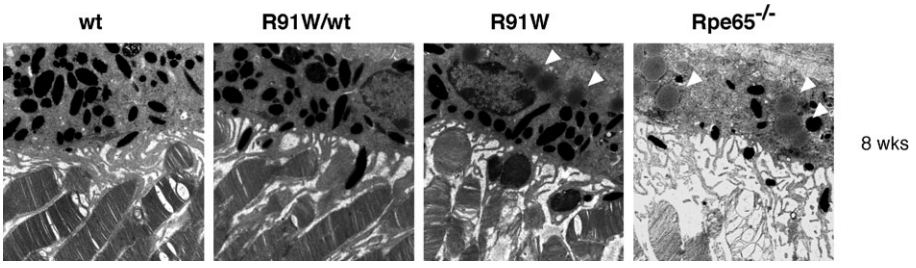

Figure 3. Lipid-like inclusions in R91W mice. Electron microscopy of the RPE-photoreceptor interface in 8-week-old wt, R91W/wt, R91W and Rpe65$^{-/-}$ mice. Note that lipid-like inclusions (arrowheads) are present in R91W and Rpe65$^{-/-}$ mice only, and the better preservation of OS morphology in R91W mice when compared with Rpe65$^{-/-}$.

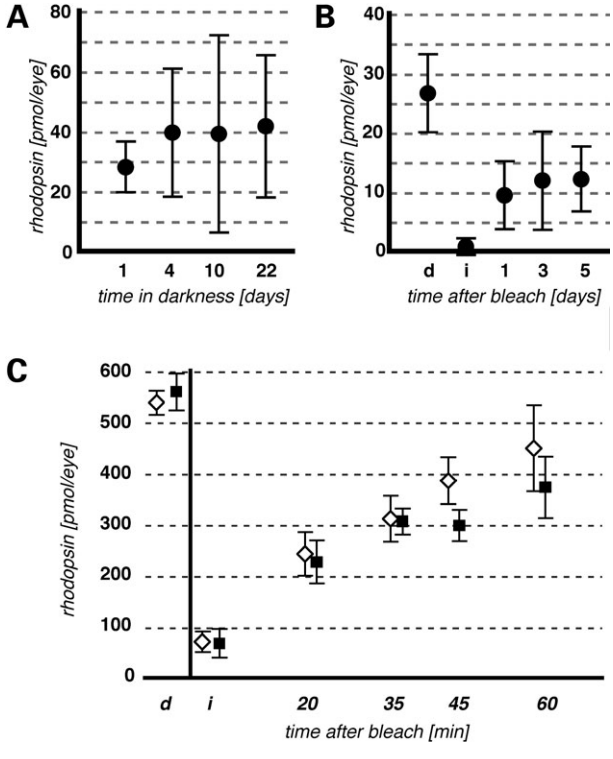

Figure 4. Rhodopsin content and regeneration kinetics. (**A**) Rhodopsin levels in 6–7-week-old R91W animals kept in darkness for 1 day or up to 22 days (as indicated). (**B**) Rhodopsin regeneration of R91W and wild-type mice. Following 24 h dark-adaptation, R91W mice were exposed to 5000 lux for 10 min and the rhodopsin content was analyzed either immediately (i) or after different periods of recovery in darkness (as indicated). Unexposed, dark-adapted mice (d) served as controls. (**C**) Rhodopsin regeneration of wild-type and R91W/wt heterozygous mice. Experimental protocol and abbreviations are as in (B). Note the slightly slower regeneration kinetics in R91W/wt mice. Filled squares, R91W/wt; open squares, wild-type. All values are given in pmol/eye ± SD. At least three animals per condition and genotype were analyzed.

wild-type mice (27). Animals were returned to darkness to allow regeneration of the visual pigment. Non-exposed R91W mice contained 27 pmol of rhodopsin (Fig. 4B), which was bleached by light exposure, reducing it to 1 pmol. Even after prolonged dark-adaptation (5 days) only 44% (12 pmol) of the pre-bleach value (27 pmol) was detectable. Thus, following a strong bleach, regeneration of rhodopsin was inefficient and reached a plateau at about half the maximal level of non-bleached, dark-adapted animals. Maximal dark-adapted rhodopsin levels were similar in R91W/wt heterozygous (538 pmol/retina) and wild-type (560 pmol/retina) (Fig. 4C). The calculated regeneration rates following a strong bleach were 6.3 pmol/min in wild-type and 4.9 pmol/min in R91W/wt mice, indicating slightly slower rhodopsin regeneration kinetics in the heterozygous situation.

Photoreceptor function in R91W mutant mice

Next, we studied the consequences of the reduced 11-*cis*-retinal levels on retinal function. Scotopic ERG recordings revealed that higher flash intensities were needed to induce an electrical response in R91W when compared with wild-type mice (Fig. 5A, top panel). By assessing the luminance required to generate a half maximal b-wave amplitude (32), the reduction in light sensitivity in 8-week-old R91W mice was determined to be ~2.5 log units when compared with wild-type. Therefore, R91W mice are about one log unit more sensitive to light than Rpe65$^{-/-}$ animals (6). In age series testing of 8, 12, 24 and 40-week-old animals, the sensitivity threshold remained unaltered, whereas the b-wave amplitude was reduced with increasing age in R91W, this being especially prominent between 12 and 24 weeks (Fig. 5A, top and bottom panels). From 24 to 40 weeks of age, no further reduction in b-wave amplitude was detected. Thus, the sensitivity of the retina was not prone to age-related reduction, whereas the maximal response size was.

In order to test cone function, ERG responses were recorded under photopic conditions (Fig. 5B). Notably, there was no difference in threshold sensitivity or in amplitude of the b-wave between 8-week-old R91W and wild-type control animals (Fig. 5B, top and bottom panels). Given the low amount of chromophore available (Table 1), cone responses should be somehow affected. In addition, the waveforms were altered in a way similar to that observed in *Rpe65* null mice (6), indicating that rods are active under those conditions. Therefore, it appears that the photopic signals are mixed responses containing both rod and cone system components.

A comparison of wild-type and R91W/wt heterozygous animals resulted, as expected, in no difference between the genotypes under scotopic or photopic conditions (data not shown).

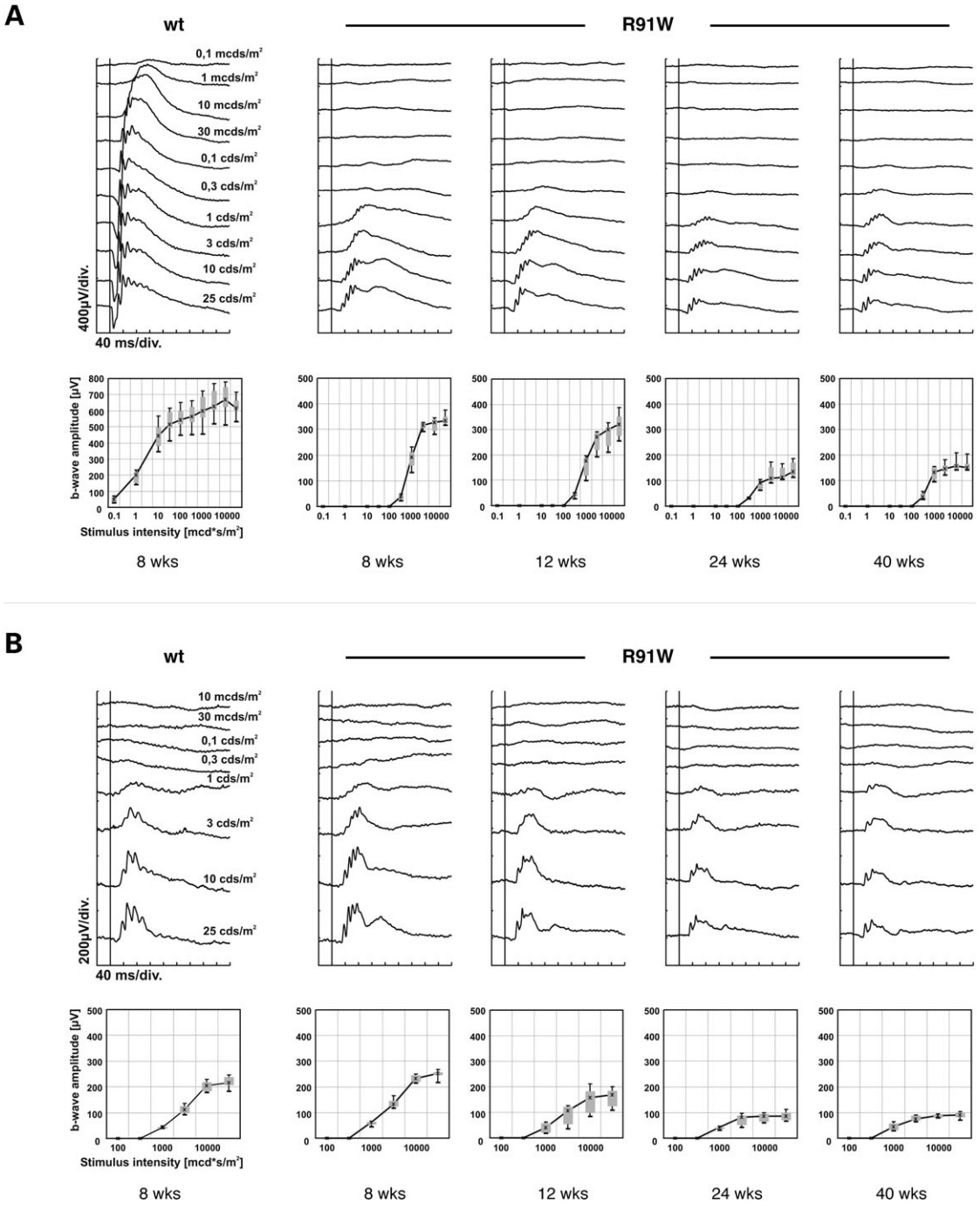

Figure 5. ERG responses to single-flash stimuli with increasing intensities in 8, 12, 24 and 40-week-old R91W and wild-type animals. (**A**) Scotopic single-flash ERG intensity series indicating loss of sensitivity in mutant mice. (**B**) Photopic single-flash ERG intensity series reflecting a similar sensitivity of wild-type and R91W animals at 8 weeks of age. Note the decline of the b-wave amplitude with increasing age. Upper panels in (A) and (B) are recordings from representative animals for a given genotype and age and in lower panels group statistics are presented ($n = 3$). Boxes in group statistic graphs indicate the 25 and 75% quantile range, whiskers indicate the 5 and 95% quantile, and the black line connects the medians of the data.

Assessment of retinal morphology

The results of the tests for retinal function, both scotopic and photopic ERG responses, in R91W mice suggested an age-related retinal degenerative process (Fig. 5). To analyze the consequences of the R91W mutation on retinal morphology, we compared the three different genotypes (wild-type, R91W and Rpe65$^{-/-}$) at various ages (from 4 weeks to 1 year; Fig. 6). Already at 4 weeks of age, the outer segments (OS) of R91W and Rpe65$^{-/-}$ mice showed signs of disorganization (Fig. 6, top row). The reduced compactness and shortening of OS became more obvious as mice grew older. Although the thickness of the outer nuclear layer (ONL) at earlier time-points was comparable with wild-type,

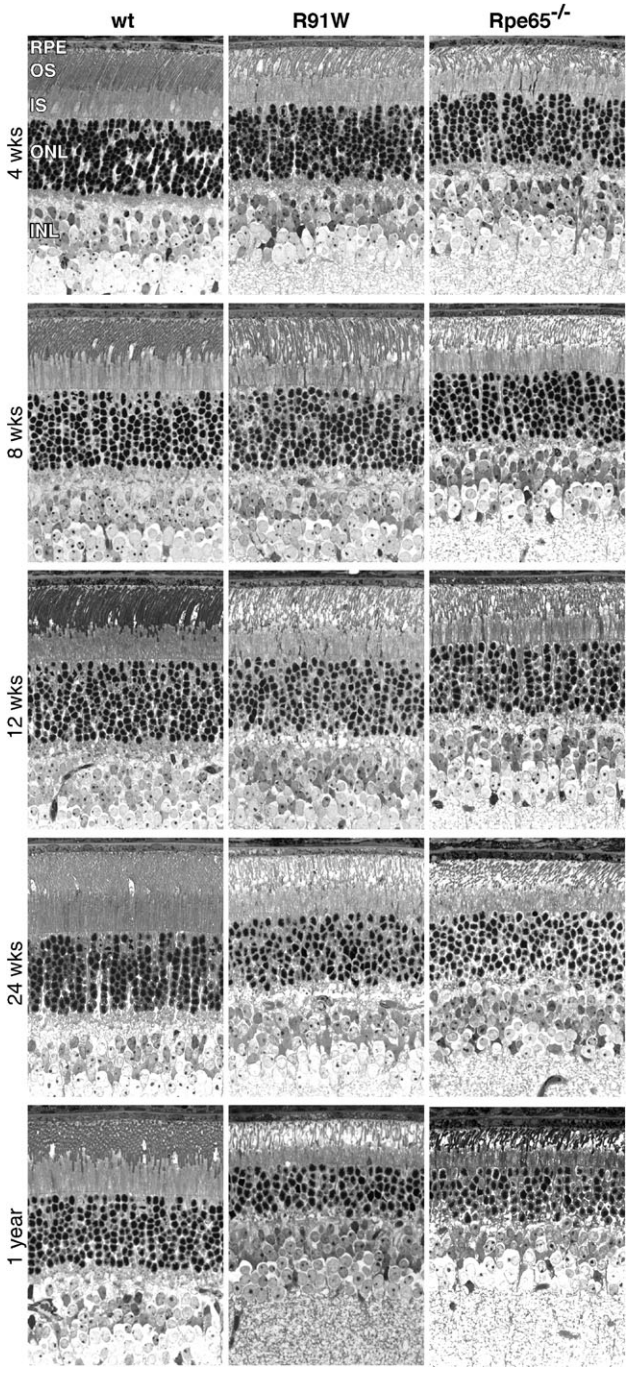

Figure 6. Light microscopic changes in R91W retinas in comparison to wild-type and Rpe65$^{-/-}$ mice at various ages. Disorganization of OS was evident in R91W mice already at 4 weeks and became more pronounced with aging. By 8 weeks, more voids were visible in the ONL accompanied by the appearance of pycnotic nuclei. By 1 year, only five to six rows of nuclei remained in the ONL. When compared with Rpe65$^{-/-}$ mice, R91W mice showed better retinal preservation (longer OS and higher density) and more cone nuclei were visible in younger animals. RPE, retinal pigment epithelium; OS, outer segments; IS, inner segments; ONL, outer nuclear layer; INL, inner nuclear layer.

only five rows of nuclei remained in the central area of 1-year-old mutant animals, when compared with nine to 10 rows in 1-year-old wild-types. In comparison to Rpe65$^{-/-}$ animals, R91W mice showed a better preservation of OS, at least up to 12 weeks of age (Fig. 6). Notably, R91W mice contained more cone nuclei than respective age-matched Rpe65$^{-/-}$ mice, particularly at early age.

At all ages, we found no differences between the retinal morphology of wild-type and R91W/wt heterozygous mice (data not shown), which is in line with a recessive inheritance of the phenotype caused by the R91W mutation. Furthermore, no morphological differences between genotypes were detectable in inner retinal structures upon examination by light microscopy.

DISCUSSION

R91W knock-in mice phenocopy human disease

In humans, about half of the identified mutations in *RPE65* are missense mutations [http://www.retina-international.com/sci-news/rpe65mut.htm; see also Zernant *et al*. (7)]. The newly generated Rpe65 R91W knock-in mice represent the analogous animal model to human patients carrying a missense mutation in *RPE65*. In patients, the different mutations in *RPE65* are associated with variable degrees of severity of retinal dysfunction (10,33). This is likely explained by the different functional consequences of these mutations. All presently available animal models, however, carry either null mutations having no residual function or a variant (L450M) which causes only a mild disturbance of the visual cycle without retinal degeneration (34).

We found that the rod system in R91W knock-in mice is severely desensitized, although not as much as in mice lacking RPE65 (6). Cones, however, are better preserved and appear to be functional at least in young animals. Similarly, R91W patients diagnosed with EOSRD are typically night-blind (desensitized rod system) but retain cone-mediated vision in the first decade (23). Reports on patients carrying other missense mutations in *RPE65* demonstrate functional cone vision early in life (summarized in 35). Another distinct group of patients affected by *RPE65* mutations is characterized as legally blind from birth or severely visually impaired in infancy. These patients are diagnosed as LCAII. The corresponding mouse model, Rpe65$^{-/-}$ mice, clearly has no cone function, and the minimal residual visual function is due to desensitized rods using isorhodopsin with 9-*cis*-retinal as a chromophore (6,36). The R91W knock-in mice, like patients suffering from EORSD, possess a phenotype clearly distinguishable from the null situation in both mice and humans. Thus, our analysis suggests that for an understanding of a particular disease, reproducing the real mutation is superior to a 'simple' knock-out mouse model.

Metabolic changes induced by R91W mutation

Very recently, the role of RPE65 as the isomerohydrolase in the visual cycle was demonstrated by studies in cell culture systems (2–4,37). In these experiments, a minimal visual cycle has been restored in cell lines different from RPE and only cells transfected with RPE65 vectors produced 11-*cis*-retinal from precursor molecules. Further studies using the same experimental paradigm aimed at the understanding of

the consequences caused by missense mutations in *RPE65* related to human disease (4,38,39). In particular, a study on *RPE65*^{R91W} showed that this mutation causes decreased protein levels due to a decreased protein stability and/or protein mislocalization (39). Additionally, in this report no isomerohydrolase activity of the RPE65^{R91W} protein variant was detected. To circumvent the limitations of the *in vitro* cell culture system and to analyze the consequences of RPE65 missense mutations in a more 'natural' environment, Chen *et al*. (17) employed a different strategy: they delivered mutant Rpe65 genes to the RPE of RPE65-deficient mice by means of an adenoviral vector. This strategy reproduced the results of the *in vitro* cell culture system. In particular, the expression of Rpe65^{R91W} did not result in detectable RPE65 immunostaining in the RPE and accordingly was not accompanied by 11-*cis*-retinal production or a gain of retinal function.

In contrast, R91W knock-in mice showed: (i) detectable protein expression with a correct localization to the RPE and (ii) metabolic activity as evidenced by the generation of 11-*cis*-retinal. Thus, not surprisingly, the *in vivo* situation represents the most accurate model to assess the consequences of a mutation. This study also validates our hypothesis that the RPE65 protein with an R91W amino acid substitution possesses residual activity in human patients.

R91W knock-in mice have an altered visual cycle

Like the wild-type protein, the mutant RPE65^{R91W} was detected exclusively in the RPE, but at highly reduced levels (5% of wild-type levels). Since RNA levels were less affected (-40%), translational or post-translational mechanisms may contribute to the reduction in the protein levels of the RPE65^{R91W} variant. Comparison of Rpe65 knock-out with Rpe65 R91W knock-in mice revealed important differences with regard to biochemical function, the most important one being the limited, but measurable ability of R91W knock-in mice to generate 11-*cis*-retinal. In order to form functional rhodopsin, 11-*cis*-retinal has to be incorporated into rod opsin. In wild-type mice, the levels of 11-*cis*-retinal and rod opsin are linearly correlated (27). In R91W mice, rod opsin was only slightly reduced in comparison to wild-type animals (Fig. 2B). Thus, low amounts of rod opsin are not the reason for reduced 11-*cis*-retinal and rhodopsin levels ($<10\%$ of wild-type). Another limitation of the visual cycle in R91W knock-in mice was revealed in bleaching experiments. Wild-type mice recovered their rhodopsin within 1–3 h after a bleach (27,34). R91W mice did not recover rhodopsin to dark-adapted levels within days. Thus, in addition to the limitation in rhodopsin production as outlined above, a strong bleach impaired rhodopsin regeneration.

Our data suggest that large amounts of unliganded rod opsin must be present in photoreceptors of R91W knock in mice, despite the fact that R91W mice can produce 11-*cis*-retinal. As 11-*cis*-retinal acts as an inverse agonist, its low availability could cause increased spontaneous activity of the chromophore-free opsin molecule, leading to a constitutive activation of the phototransduction cascade (40,41). It has been hypothesized that in the presence of unliganded opsin the retina sends a signal that results in vitamin A uptake from the circulation (26). Thus, an insufficient supply of opsin with 11-*cis*-retinal in R91W mice may be the cause of the observed accumulation of retinyl esters.

One might speculate that 11-*cis*-retinal in R91W mice does not originate from RPE, but from the recently proposed cone visual cycle (42). In this alternate pathway, the cone pigment is regenerated in Müller glia cells, independently of the RPE. Hypothetically, such a cone visual cycle could be less affected, or even may be fully operational despite the R91W mutation. But how would the rods acquire 11-*cis*-retinal under this condition? 11-*cis*-retinal is covalently bound to rod opsin via a protonated Schiff base and this binding is tight. The cone opsin/11-*cis*-retinal holocomplex is less stable, and it has been recently shown to dissociate spontaneously (43). Thus, 11-*cis*-retinal might be 'stolen' by rods from cones due to this spontaneous dissociation of the visual chromophore. This scenario might also explain why rhodopsin regeneration kinetics is inefficient. Even though RPE65 has been reported to be detected in cones (44,45) and this disputed (6,46), there is no experimental evidence that RPE65 is directly involved in the proposed cone visual cycle. However, contradictory to this hypothesis, almost equal amounts of 11-*cis*-retinal were retained up to 40 weeks of age, the time when the cones in R91W animals are almost completely lost (unpublished data).

Retinal degeneration

Constant activation of the phototransduction cascade due to chromophore starvation has been implicated in rod degeneration in Rpe65$^{-/-}$ mice and consequently rod degeneration can be prevented by blocking rod specific G-protein transducin (Gnat1) signaling (47). Nevertheless, Rpe65$^{-/-}$; Gnat1$^{-/-}$ double mutant animals accumulate similar amounts of retinyl esters as Rpe65$^{-/-}$ mice, indicating that unliganded opsin, and not the accumulation of retinyl esters, is the primary cause of degeneration (47). This concept is reinforced by the observation that systemic supplementation with 9-*cis*-retinal preserves photoreceptor structure, despite continuing accumulation of retinyl esters (26). Accordingly, a better preservation and slower degeneration of retinal morphology in R91W in comparison to Rpe65$^{-/-}$ animals might be attributable to the presence of small amounts of 11-*cis*-retinal. Nevertheless, also in R91W mice, the phototransduction cascade may be permanently activated, finally causing retinal degeneration. This possibility will be further investigated in R91W; Gnat1$^{-/-}$ double mutant mice.

Conclusion

We generated a novel mouse model for retinal dystrophy caused by a missense mutation in RPE65. There are striking functional differences to the knock-out situation, which are not only important for basic research but also for understanding the pathology and for clinical diagnosis in patients. Furthermore, our results indicate that the therapeutic window for gene therapy—the first tests of which are being carried out these very days—is likely to differ between patients with

Human Molecular Genetics, 2008, Vol. 17, No. 2 289

null and missense mutations. Thus, preclinical trials for gene replacement are underway for the R91W knock-in mouse.

MATERIALS AND METHODS

Generation of R91W knock-in mice

A classical strategy using homologous recombination (HR) in embryonic stem (ES) cells has been employed to replace the wild-type with a modified Rpe65 allele; 13.3 kb of Rpe65 genomic DNA (derived from the 129/Sv mouse strain) divided into two contiguous subclones: E1-12 containing exons 1–3 and clone E2-8 containing exons 4–6 cloned into *Eco*RI restriction site of pBluescriptII SK(−) vector were kindly provided by M.T. Redmond (National Eye Institute, Bethesda, USA) (48).

Clone E2-8 containing exon 4 served as template for the PCR targeted site-directed mutagenesis. Two point mutations were introduced into the mouse R91 codon (CGA > TGG) using a respective reverse primer (C AGT CAT TGC CCA AAC ATA AGC ATC AGT GCG GAT GAA TCT GAA GAC TAT TGA GAA ATG GA; underlined codon denotes position 91) to obtain the R91W mutation. The forward primer (GCG CGT AAT ACG ACT CAC TA) was designed to hybridize in the plasmid backbone. The presence of the R91W mutation was confirmed by sequencing. The neomycin (neo) resistance cassette flanked by *lox*P sites (floxed-neo) in the direct repeat orientation was integrated into the *Nhe*I site downstream exon 5. The 3′ site of the vector was truncated by *Bam*HI digestion resulting in the creation of the short arm of the targeting construct. In the final step, the DT cassette was introduced at the 5′ site of the vector (upstream of exon 1) to serve as a negative selection marker. The final targeting construct carrying the R91W mutation was sequenced.

The *Xho*I-linearized targeting vector was electroporated into coisogenic TC1 ES cells derived from 129S6/SvEvTac (129S6) mouse strain (49). Genomic DNA from G418-resistant ES clones was analyzed for correct vector integration by PCR and Southern blotting as described below.

The positive ES clones were injected into blastocysts originating from C57BL/6 mice to obtain chimeric mice. Two chimeric males were born. Germ-line transmission was confirmed in one male. This was done by breeding the chimeric males with C57BL/6 females where positive selection was performed by coat colour assessment and PCR genotyping form tail genomic DNA using neo1, neo2 and *Taq* primer pairs (Table 2).

Following the confirmation of germ-line transmission, the chimeric male was bred to 129S6 females to propagate the line on a coisogenic background. This breeding resulted in the generation of a heterozygous $Rpe65^{R91Wneo}$ line. The genotype was confirmed by PCR using neo1, neo2 and *Taq* primer pairs (Table 2).

For *in vivo* removal of the neo resistance cassette, $Rpe65^{R91Wneo}$ mice were bred with deleter mice expressing cre recombinase in their germ-line [129S6-Tg(Prnp-GFP/Cre)1Blw/J (24)]. The $Rpe65^{R91Wneo}$ mice were kept on a cre-deleter background for two generations to ensure complete excision of the floxed-neo cassette. The deletion of the neo cassette was confirmed by PCR genotyping using neo1, neo2 and cre primer pairs (Table 2). Finally, the resulting heterozygous (R91W/wt) offspring was intercrossed to obtain R91W homozygous mice. The R91W knock-in mice analyzed herein were therefore on a coisogenic 129S6 background. The genotyping of the final R91W knock-in mice was performed by PCR on tail genomic DNA using the *Taq* primer pair as described in Table 2.

Genotype assessment

DNA from G418-resistant ES cells was analyzed by Southern blotting. An external 3′ *Bam*HI probe (759 bp) was random-labeled using the DIG labeling kit (#1585614, Roche Diagnostics, Mannheim, Germany). Genomic ES cell DNA was digested overnight with *Eco*RI and electrophoresed on a 0.8% agarose gel. DNA samples were transferred onto a nylon membrane by a capillary method. The membrane was incubated with the DIG-labeled probe. Fragments corresponding to wild-type and, knock-in alleles (5.6 and 7.7 kb, respectively) were detected by enhanced chemiluminescence.

For the detection of the correctly integrated neo cassette, two primer pairs have been selected to allow a nested PCR approach (Table 2). For the neo1 primer pair, the forward primer was designed within the neo cassette and the reverse primer was positioned outside of the targeted DNA sequence. To further minimize any false-positive result, a nested neo2 primer pair was created within the same area, thus only correctly integrated DNA should be detectable by PCR (Table 2).

A *Taq* primer pair (Table 2) was used to detect the presence of the R91W mutation. This pair produced a 998 bp fragment from both wild-type and mutant DNA. Only the wild-type DNA amplicon included a *Taq*I restriction site, resulting in 619 and 379 bp fragments after incubation with *Taq*I restriction enzyme.

Animals

All procedures concerning animals were in accordance with the regulations of the Veterinary Authority of Zurich and with the statement of 'The Association for Research in Vision and Ophthalmology' for the use of animals in research. All animals were raised in cyclic light (12:12 h; 60 lux at cage level). The cre expressing mice 129S6-Tg(Prnp-GFP/Cre)1Blw/J (24) and corresponding wild-type mice (129S6) were purchased from the Jackson Laboratory (Bar Harbor, USA). Rpe65 deficient mice ($Rpe65^{-/-}$) were maintained at the University Hospital Zurich (5). Genotyping was performed by PCR on tail genomic DNA, using the primers shown in Table 2.

RNA isolation, reverse transcription and real-time PCR

RNA isolation and reverse transcription from eyecup tissue were performed as previously described (50). cDNA quantification was carried out by real-time PCR using the LightCycler 480 Sybr Green I Master kit and a LightCycler 480 instrument (Roche). cDNAs were amplified with primers for Rpe65 and β-actin described elsewhere (5,51), and normalization was done using the ΔΔCT (comparative threshold cycle) method. Relative values were calculated using a suitable calibrator

Table 2. PCR primers used for genotyping

Primer	Forward (5′–3′)	Reverse (5′–3′)	Size (bp)
neo1[a]	AGCAGCCTCTGTTCCACATAC	GATGAGCAGTGGCACCATTG	1513
neo2[a]	CTCAGTATTGTTTTGCCAAG	GATCAACCTGTAGAATGAAAG	1445
Cre	GGACATGTTCAGGGATCGCCAGGCG	GCATAACCAGTGAAACAGCATTGCTG	268
Taq[b]	GCTGGTCTTGCCTGTATCA	GTCAGAGACAGTGCTGTGTT	998

[a]The genotyping using neo1 and neo2 included: a first PCR using the neo1 primer pair amplified for 20 cycles followed by the nested PCR using neo2 primer pair amplified for 35 cycles.
[b]*Taq* primer pair used to genotype R91W mice. Genotyping included digestion of the 998 bp PCR product by *Taq*I restriction. This digestion results in generation of 619 and 379 bp fragments in wild-type animals, or no cleavage in R91W knock-in animals.

sample as indicated in the results. Three animals were analyzed per genotype and each reaction was run in triplicate.

Western blotting

The retina or the remaining eyecup tissue was separately isolated and processed for immunoblotting as previously described (27). The primary antibodies used were: rabbit anti-RPE65 (pin5; 1:2000); mouse anti-LRAT (1:1000, gift from K. Palczewski, University of Washington, Seattle, USA); rabbit anti-CRALBP (UW55; 1:10 000, gift from J.C. Saari, University of Washington, Seattle, USA); mouse anti-Rho (4D2) (1:8000, gift from D. Hicks, Université Louis Pasteur, Strasbourg, France) and β-actin as standard (1: 1000, Santa Cruz, USA). At least three animals were analyzed per genotype.

Rhodopsin steady-state levels and rhodopsin regeneration kinetics

Mice were dark adapted for 24 h, sacrificed under dim red light, and retinas were isolated through a slit in the cornea. Rhodopsin content was analyzed as described earlier (27). The kinetics of rhodopsin regeneration after bleaching was analyzed as previously described in detail (27). Briefly, mice were dark adapted for 24 h and pupils were dilated 30–60 min prior to light exposure. Animals were exposed for 10 min to 5000 lux of fluorescent white light. Following illumination, mice were placed in darkness for the times indicated in the results and rhodopsin content was analyzed as described above. Non-exposed mice served as dark controls. At least three animals were analyzed per condition and genotype.

Histology

Animals were sacrificed and the superior part of the eye was marked for orientation. The enucleated eyes were fixed overnight in 2.5% glutaraldehyde prepared in 0.1 M cacodylate buffer and processed as described previously (50). Semi-thin sections (0.5 μm) of Epon-embedded tissue were prepared from the inferior central retina, counterstained with Methylene blue and analyzed using a microscope (Axiovision, Zeiss, Jena, Germany). For electron microscopy, thin sections were analyzed using a Hitachi 7000 electron microscope (Hitachi, Tokyo, Japan).

Immunofluorescence

Enucleated eyes were immersed in cryoprotective medium (Jung, Nussloch, Germany) and processed for immunofluorescence as described recently (29). For detection, rabbit anti-RPE65 primary antibody (1:500) and Cy3 conjugated anti-rabbit secondary antibody (Jackson ImmunoResesarch, Soham, UK) were applied. Immunofluorescence was analyzed on a microscope (Axiovision, Zeiss) and documented using a digital imaging system.

HPLC determination of retinoids

Mice were dark-adapted for 24 h. All steps were carried out under dim red light. Animals were sacrificed, and lens and vitreous were removed from the eye through a slit in the cornea. The rest of the tissue including the retina and eyecup was snap frozen in liquid nitrogen until further analysis. Retinoid extraction and HPLC analysis was performed as previously described (27).

ERG functional tests

ERGs were recorded binocularly according to previously described procedures (6) in anesthetized mice with dilated pupils using a Ganzfeld bowl, a DC amplifier and a PC-based control and recording unit (Toennies Multiliner Vision; Viasys Healthcare, Höchberg, Germany). Recordings were obtained in both scotopic (dark-adapted overnight) and photopic (light-adapted 10 min at 30 cd s/m^2) conditions.

Single white-flash stimulus intensity ranged from −4 to 1.5 log cd s/m^2 under scotopic and from −2 to 4 log cd s/m^2 under photopic conditions, divided into 10 and 13 steps, respectively. Ten responses per intensity were averaged with an inter-stimulus interval of either 5 or 17 s (>1 cd s/m^2). At least three animals per genotype and age were analyzed.

ACKNOWLEDGEMENTS

The authors thank Coni Imsand, Gaby Hoegger, Philipp Huber and Hedwig Wariwoda for excellent technical assistance. Dr Birgit Lederman (University of Zurich) is acknowledged for help with generation of R91W knock-in animals, Sarah Habegger (Nagerzentrum) for assistance in propagation of the mutant line and Dr Andreas Zurlinden (University of Zurich) for providing Neo and DT plasmid vectors. We

thank Professor Klara Landau (Department of Opthalmology) for constant support.

Conflict of Interest statement. None declared.

FUNDING

This study was supported by the Swiss National Science Foundation (3100A0-105793) and the German Research Foundation (DFG) (RE318/2; Se837/4-1, 5-1, and 6-1, Li956-2).

REFERENCES

1. Lamb, T.D. and Pugh, E.N., Jr. (2004) Dark adaptation and the retinoid cycle of vision. *Prog. Retin. Eye Res.*, **23**, 307–380.
2. Jin, M., Li, S., Moghrabi, W.N., Sun, H. and Travis, G.H. (2005) Rpe65 is the retinoid isomerase in bovine retinal pigment epithelium. *Cell*, **122**, 449–459.
3. Moiseyev, G., Chen, Y., Takahashi, Y., Wu, B.X. and Ma, J.X. (2005) RPE65 is the isomerohydrolase in the retinoid visual cycle. *Proc. Natl Acad. Sci. USA*, **102**, 12413–12418.
4. Redmond, T.M., Poliakov, E., Yu, S., Tsai, J.Y., Lu, Z. and Gentleman, S. (2005) Mutation of key residues of RPE65 abolishes its enzymatic role as isomerohydrolase in the visual cycle. *Proc. Natl Acad. Sci. USA*, **102**, 13658–13663.
5. Redmond, T.M., Yu, S., Lee, E., Bok, D., Hamasaki, D., Chen, N., Goletz, P., Ma, J.X., Crouch, R.K. and Pfeifer, K. (1998) Rpe65 is necessary for production of 11-*cis*-vitamin A in the retinal visual cycle. *Nat. Genet.*, **20**, 344–351.
6. Seeliger, M.W., Grimm, C., Stahlberg, F., Friedburg, C., Jaissle, G., Zrenner, E., Guo, H., Reme, C.E., Humphries, P., Hofmann, F., Biel, M., Fariss, R.N., Redmond, T.M. and Wenzel, A. (2001) New views on RPE65 deficiency: the rod system is the source of vision in a mouse model of Leber congenital amaurosis. *Nat. Genet.*, **29**, 70–74.
7. Zernant, J., Kulm, M., Dharmaraj, S., den Hollander, A.I., Perrault, I., Preising, M.N., Lorenz, B., Kaplan, J., Cremers, F.P., Maumenee, I., Koenekoop, R.K. and Allikmets, R. (2005) Genotyping microarray (disease chip) for leber congenital amaurosis: detection of modifier alleles. *Invest. Ophthalmol. Vis. Sci.*, **46**, 3052–3059.
8. Thompson, D.A., Gyurus, P., Fleischer, L.L., Bingham, E.L., McHenry, C.L., Apfelstedt-Sylla, E., Zrenner, E., Lorenz, B., Richards, J.E., Jacobson, S.G., Sieving, P.A. and Gal, A. (2000) Genetics and phenotypes of RPE65 mutations in inherited retinal degeneration. *Invest. Ophthalmol. Vis. Sci.*, **41**, 4293–4299.
9. Morimura, H., Fishman, G.A., Grover, S.A., Fulton, A.B., Berson, E.L. and Dryja, T.P. (1998) Mutations in the RPE65 gene in patients with autosomal recessive retinitis pigmentosa or leber congenital amaurosis. *Proc. Natl Acad. Sci. USA*, **95**, 3088–3093.
10. Lorenz, B., Gyurus, P., Preising, M., Bremser, D., Gu, S., Andrassi, M., Gerth, C. and Gal, A. (2000) Early-onset severe rod-cone dystrophy in young children with RPE65 mutations. *Invest. Ophthalmol. Vis. Sci.*, **41**, 2735–2742.
11. Thompson, D.A. and Gal, A. (2003) Vitamin A metabolism in the retinal pigment epithelium: genes, mutations, and diseases. *Prog. Retin. Eye Res.*, **22**, 683–703.
12. Pang, J.J., Chang, B., Hawes, N.L., Hurd, R.E., Davisson, M.T., Li, J., Noorwez, S.M., Malhotra, R., McDowell, J.H., Kaushal, S., Hauswirth, W.W., Nusinowitz, S., Thompson, D.A. and Heckenlively, J.R. (2005) Retinal degeneration 12 (rd12): a new, spontaneously arising mouse model for human Leber congenital amaurosis (LCA). *Mol. Vis.*, **11**, 152–162.
13. Aguirre, G.D., Baldwin, V., Pearce-Kelling, S., Narfstrom, K., Ray, K. and Acland, G.M. (1998) Congenital stationary night blindness in the dog: common mutation in the *RPE65* gene indicates founder effect. *Mol. Vis.*, **4**, 23.
14. Pang, J.J., Chang, B., Kumar, A., Nusinowitz, S., Noorwez, S.M., Li, J., Rani, A., Foster, T.C., Chiodo, V.A., Doyle, T., Li, H., Malhotra, R., Tusner, J., McDowell, J.H., Min, S.H., Li, Q., Kaushal, S. and Hauswirth, W.W. (2005) Gene therapy restores vision-dependent behavior as well as retinal structure and function in a mouse model of RPE65 Leber congenital amaurosis. *Mol. Ther.*, **13**, 565–572.
15. Dejneka, N.S., Surace, E.M., Aleman, T.S., Cideciyan, A.V., Lyubarsky, A., Savchenko, A., Redmond, T.M., Tang, W., Wei, Z., Rex, T.S., Glover, E., Maguire, A.M., Pugh, E.N., Jr., Jacobson, S.G. and Bennett, J. (2004) *In utero* gene therapy rescues vision in a murine model of congenital blindness. *Mol. Ther.*, **9**, 182–188.
16. Lai, C.M., Yu, M.J., Brankov, M., Barnett, N.L., Zhou, X., Redmond, T.M., Narfstrom, K. and Rakoczy, P.E. (2004) Recombinant adeno-associated virus type 2-mediated gene delivery into the Rpe65$^{-/-}$ knockout mouse eye results in limited rescue. *Genet. Vaccines Ther.*, **2**, 3.
17. Chen, Y., Moiseyev, G., Takahashi, Y. and Ma, J.X. (2006) RPE65 gene delivery restores isomerohydrolase activity and prevents early cone loss in Rpe65−/− mice. *Invest. Ophthalmol. Vis. Sci.*, **47**, 1177–1184.
18. Bemelmans, A.P., Kostic, C., Crippa, S.V., Hauswirth, W.W., Lem, J., Munier, F.L., Seeliger, M.W., Wenzel, A. and Arsenijevic, Y. (2006) Lentiviral gene transfer of RPE65 rescues survival and function of cones in a mouse model of Leber congenital amaurosis. *PLoS Med.*, **3**, e347.
19. Acland, G.M., Aguirre, G.D., Ray, J., Zhang, Q., Aleman, T.S., Cideciyan, A.V., Pearce-Kelling, S.E., Anand, V., Zeng, Y., Maguire, A.M., Jacobson, S.G., Hauswirth, W.W. and Bennett, J. (2001) Gene therapy restores vision in a canine model of childhood blindness. *Nat. Genet.*, **28**, 92–95.
20. Narfstrom, K., Katz, M.L., Bragadottir, R., Seeliger, M., Boulanger, A., Redmond, T.M., Caro, L., Lai, C.M. and Rakoczy, P.E. (2003) Functional and structural recovery of the retina after gene therapy in the RPE65 null mutation dog. *Invest. Ophthalmol. Vis. Sci.*, **44**, 1663–1672.
21. Acland, G.M., Aguirre, G.D., Bennett, J., Aleman, T.S., Cideciyan, A.V., Bennicelli, J., Dejneka, N.S., Pearce-Kelling, S.E., Maguire, A.M., Palczewski, K., Hauswirth, W.W. and Jacobson, S.G. (2005) Long-term restoration of rod and cone vision by single dose rAAV-mediated gene transfer to the retina in a canine model of childhood blindness. *Mol. Ther.*, **12**, 1072–1082.
22. Narfstrom, K., Vaegan, Katz, V.M., Bragadottir, R., Rakoczy, E.P. and Seeliger, M. (2005) Assessment of structure and function over a 3-year period after gene transfer in RPE65−/− dogs. *Doc. Ophthalmol.*, **111**, 39–48.
23. El Matri, L., Ambresin, A., Schorderet, D.F., Kawasaki, A., Seeliger, M.W., Wenzel, A., Arsenijevic, Y., Borruat, F.X. and Munier, F.L. (2006) Phenotype of three consanguineous Tunisian families with early-onset retinal degeneration caused by an R91W homozygous mutation in the RPE65 gene. *Graefes Arch. Clin. Exp. Ophthalmol.*, **244**, 1104–1112.
24. Scheel, J.R., Garrett, L.J., Allen, D.M., Carter, T.A., Randolph-Moore, L., Gambello, M.J., Gage, F.H., Wynshaw-Boris, A. and Barlow, C. (2003) An inbred 129SvEv GFPCre transgenic mouse that deletes *lox*P-flanked genes in all tissues. *Nucleic Acids Res.*, **31**, e57.
25. Saari, J.C. (2000) Biochemistry of visual pigment regeneration: the Friedenwald lecture. *Invest. Ophthalmol. Vis. Sci.*, **41**, 337–348.
26. Van Hooser, J.P., Liang, Y., Maeda, T., Kuksa, V., Jang, G.F., He, Y.G., Rieke, F., Fong, H.K., Detwiler, P.B. and Palczewski, K. (2002) Recovery of visual functions in a mouse model of Leber congenital amaurosis. *J. Biol. Chem.*, **277**, 19173–19182.
27. Wenzel, A., Oberhauser, V., Pugh, E.N., Jr., Lamb, T.D., Grimm, C., Samardzija, M., Fahl, E., Seeliger, M.W., Reme, C.E. and von Lintig, J. (2005) The retinal G protein-coupled receptor (RGR) enhances isomerohydrolase activity independent of light. *J. Biol. Chem.*, **280**, 29874–29884.
28. Chen, P., Hao, W., Rife, L., Wang, X.P., Shen, D., Chen, J., Ogden, T., Van Boemel, G.B., Wu, L., Yang, M. and Fong, H.K. (2001) A photic visual cycle of rhodopsin regeneration is dependent on Rgr. *Nat. Genet.*, **28**, 256–260.
29. Wenzel, A., von Lintig, J., Oberhauser, V., Tanimoto, N., Grimm, C. and Seeliger, M.W. (2007) RPE65 is essential for the function of cone photoreceptors in NRL-deficient mice. *Invest. Ophthalmol. Vis. Sci.*, **48**, 534–542.
30. Wenzel, A., Grimm, C., Samardzija, M. and Reme, C.E. (2003) The genetic modifier Rpe65Leu(450): effect on light damage susceptibility in c-Fos-deficient mice. *Invest. Ophthalmol. Vis. Sci.*, **44**, 2798–2802.
31. Lyubarsky, A.L., Savchenko, A.B., Morocco, S.B., Daniele, L.L., Redmond, T.M. and Pugh, E.N., Jr. (2005) Mole quantity of RPE65 and its productivity in the generation of 11-*cis*-retinal from retinyl esters in the living mouse eye. *Biochemistry*, **44**, 9880–9888.

32. Machida, S., Kondo, M., Jamison, J.A., Khan, N.W., Kononen, L.T., Sugawara, T., Bush, R.A. and Sieving, P.A. (2000) P23H rhodopsin transgenic rat: correlation of retinal function with histopathology. *Invest. Ophthalmol. Vis. Sci.*, **41**, 3200–3209.
33. Hamel, C., Marlhens, F., Griffoin, J., Bareil, C., Claustres, M. and Arnaud, B. (1999) Different mutations in RPE65 are associated with variability in the severity of retinal dystrophy. In Hollyfield, J., Anderson, R. and LaVail, M. (eds), *Retinal Degenerative Diseases and Experimental Therapy*. Kluwer Academic/Plenum, New York, pp. 27–33.
34. Wenzel, A., Reme, C.E., Williams, T.P., Hafezi, F. and Grimm, C. (2001) The Rpe65 Leu450Met variation increases retinal resistance against light-induced degeneration by slowing rhodopsin regeneration. *J. Neurosci.*, **21**, 53–58.
35. Paunescu, K., Wabbels, B., Preising, M.N. and Lorenz, B. (2005) Longitudinal and cross-sectional study of patients with early-onset severe retinal dystrophy associated with RPE65 mutations. *Graefes Arch. Clin. Exp. Ophthalmol.*, **243**, 417–426.
36. Fan, J., Rohrer, B., Moiseyev, G., Ma, J.X. and Crouch, R.K. (2003) Isorhodopsin rather than rhodopsin mediates rod function in RPE65 knock-out mice. *Proc. Natl Acad. Sci. USA*, **100**, 13662–13667.
37. Takahashi, Y., Moiseyev, G., Chen, Y. and Ma, J.X. (2005) Identification of conserved histidines and glutamic acid as key residues for isomerohydrolase activity of RPE65, an enzyme of the visual cycle in the retinal pigment epithelium. *FEBS Lett.*, **579**, 5414–5418.
38. Chen, Y., Moiseyev, G., Takahashi, Y. and Ma, J.X. (2006) Impacts of two point mutations of RPE65 from Leber's congenital amaurosis on the stability, subcellular localization and isomerohydrolase activity of RPE65. *FEBS Lett.*, **580**, 4200–4204.
39. Takahashi, Y., Chen, Y., Moiseyev, G. and Ma, J.X. (2006) Two point mutations of RPE65 from patients with retinal dystrophies decrease the stability of RPE65 protein and abolish its isomerohydrolase activity. *J. Biol. Chem.*, **281**, 21820–21826.
40. Bond, R.A., Leff, P., Johnson, T.D., Milano, C.A., Rockman, H.A., McMinn, T.R., Apparsundaram, S., Hyek, M.F., Kenakin, T.P., Allen, L.F. and Lefkowitz, R.J. (1995) Physiological effects of inverse agonists in transgenic mice with myocardial overexpression of the beta 2-adrenoceptor. *Nature*, **374**, 272–276.
41. Kefalov, V.J., Carter Cornwall, M. and Crouch, R.K. (1999) Occupancy of the chromophore binding site of opsin activates visual transduction in rod photoreceptors. *J. Gen. Physiol.*, **113**, 491–503.
42. Mata, N.L., Radu, R.A., Clemmons, R.C. and Travis, G.H. (2002) Isomerization and oxidation of vitamin a in cone-dominant retinas: a novel pathway for visual-pigment regeneration in daylight. *Neuron*, **36**, 69–80.
43. Kefalov, V.J., Estevez, M.E., Kono, M., Goletz, P.W., Crouch, R.K., Cornwall, M.C. and Yau, K.W. (2005) Breaking the covalent bond–a pigment property that contributes to desensitization in cones. *Neuron*, **46**, 879–890.
44. Ma, J., Xu, L., Othersen, D.K., Redmond, T.M. and Crouch, R.K. (1998) Cloning and localization of RPE65 mRNA in salamander cone photoreceptor cells1. *Biochim. Biophys. Acta*, **1443**, 255–261.
45. Znoiko, S.L., Crouch, R.K., Moiseyev, G. and Ma, J.X. (2002) Identification of the RPE65 protein in mammalian cone photoreceptors. *Invest. Ophthalmol. Vis. Sci.*, **43**, 1604–1609.
46. Hemati, N., Feathers, K.L., Chrispell, J.D., Reed, D.M., Carlson, T.J. and Thompson, D.A. (2005) RPE65 surface epitopes, protein interactions, and expression in rod- and cone-dominant species. *Mol. Vis.*, **11**, 1151–1165.
47. Woodruff, M.L., Wang, Z., Chung, H.Y., Redmond, T.M., Fain, G.L. and Lem, J. (2003) Spontaneous activity of opsin apoprotein is a cause of Leber congenital amaurosis. *Nat. Genet.*, **35**, 158–164.
48. Boulanger, A., Liu, S., Yu, S. and Redmond, T.M. (2001) Sequence and structure of the mouse gene for RPE65. *Mol. Vis.*, **7**, 283–287.
49. Deng, C., Wynshaw-Boris, A., Zhou, F., Kuo, A. and Leder, P. (1996) Fibroblast growth factor receptor 3 is a negative regulator of bone growth. *Cell*, **84**, 911–921.
50. Samardzija, M., Wenzel, A., Aufenberg, S., Thiersch, M., Reme, C. and Grimm, C. (2006) Differential role of Jak-STAT signaling in retinal degenerations. *FASEB J.*, **20**, 2411–2413.
51. Samardzija, M., Wenzel, A., Thiersch, M., Frigg, R., Reme, C. and Grimm, C. (2006) Caspase-1 ablation protects photoreceptors in a model of autosomal dominant retinitis pigmentosa. *Invest. Ophthalmol. Vis. Sci.*, **47**, 5181–5190.

6.5 Leukemia Inhibitory Factor Extends the Lifespan of Injured Photoreceptors *In Vivo*

Sandrine Joly, Christina Lange, **Markus Thiersch**, Marijana Samardzija, and Christian Grimm

Laboratory for Retinal Cell Biology, Department Ophthalmology, Center for Integrative Human Physiology (CIHP) and Neuroscience Center Zurich (ZNZ), University Hospital, Zurich, Switzerland

Published in The Journal of Neuroscience, 28(51), 13765–13774 (2008)

6.5.1 Author contribution

Design:	SJ and CG
Experiments:	SJ, CL, **MT** (real time PCR), MS and CG
Interpretation:	SJ, CL, **MT**, MS and CG
Manuscript:	CG
Manuscript Correction:	SJ, CL, **MT**, MS and CG

6.5.2 Summary

In this paper we show that photoreceptor injury induces the expression of the IL-6 family member LIF in the retina initiating protective response mechanisms. We showed that degenerating retinas of VPP mice have increased levels of LIF mRNA beginning with PND21 and peaking at PND42. In correlation, the lack of LIF in double mutant VPP/LIF$^{-/-}$ mice caused an acceleration of retinal degeneration between PND28 and PND42 but not at early time points, which suggested a pro-survival role of LIF. Of note, LIF$^{-/-}$ mice developed normal retina and protein expression as well as localization of typical markers for horizontal cells (calbindin), bipolar cells (CHX10), Müller cells (glutamine synthetase (GS)) and ganglion cell (Brn3a) was not affected when compared to wild type animals. To identify the cells, which expressed LIF in degenerating retinas, we combined *in situ* hybridization and immunofluorescene. In contrast to wild type controls, VPP mice and light exposed mice showed a specific LIF mRNA staining in a few scattered cells within the INL. That signal correlated with the staining of the Müller cell marker GS. However, only a subset of Müller cells seemed to

express LIF whereby the GS intensity correlated inversely with the LIF staining intensity. Further, we showed that the lack of LIF in VPP/LIF$^{-/-}$ mice prevented the activation of STAT3 and Akt. GFAP as a marker for Müller cell activation was induced during retinal degeneration. However, VPP/LIF$^{-/-}$ mice had no elevated GFAP levels, suggesting that injury stimuli might require LIF to activate Müller cells. LIF ablation caused a disturbance of proper retinal signaling in response to stress or injury. As a response to retinal degeneration in VPP mice and light-exposed mice photoreceptor cells expressed increased levels of endothelin 2 (Edn2) mRNA. Additionally, Casp-1, GFAP, FGF2, Jak3 and SOCS3 mRNA levels were induced in those retinas. However, these genes were not induced or even repressed in VPP/LIF$^{-/-}$ mice. The intravitreal application of recombinant LIF to LIF$^{-/-}$ mice completely restored the signaling in the retina and caused a STAT3 reactivation as well as an induction of Edn2, GFAP and FGF-2 mRNA expression. To test our hypothesis that Edn2 signaling in response to retinal injury requires LIF to initiates the signaling cascade; we injected an End2 receptor (Ednrb) agonist (BQ-3020) intravitreally. In wild type mice BQ-3020 indeed induced the mRNA expression of LIF, FGF2 and Edn2. However, in LIF$^{-/-}$ mice BQ-3020 failed to induce FGF-2 expression and hardly induced End2 expression, showing that LIF is indeed required to mediate Edn2 signaling. Further, we showed that the application of BQ-3020 diminished retinal apoptosis after light exposure. In contrast, application of the Ednrb antagonist BQ-788 enhanced apoptosis in the VPP mouse supporting an important role of the Ednrb signaling system in retinal degeneration. To analyze, whether LIF signaling requires photoreceptor cells, we employed photoreceptor cell devoid *rd1* mice and cone only NRL$^{-/-}$ mice. Application of recombinant LIF did not significantly induce the LIF signaling cascade when compared to PBS-injected controls. This suggests that the LIF mediated signaling cascade requires not only LIF expression in Müller cells but also the presence of rod photoreceptors. Finally, we proposed a model pathway in which LIF is induced in a subset of Müller cells after photoreceptor cell injury. LIF induces via an unknown pathway the expression of Edn2 in photoreceptor cells, which signals back to the INL in order to activate Müller cells and to stimulate the expression of the pro-survival factor FGF-2.

6.5.3 Manuscript

The Journal of Neuroscience, December 17, 2008 • 28(51):13765–13774 • 13765

Neurobiology of Disease

Leukemia Inhibitory Factor Extends the Lifespan of Injured Photoreceptors *In Vivo*

Sandrine Joly, Christina Lange, Markus Thiersch, Marijana Samardzija, and Christian Grimm

Laboratory for Retinal Cell Biology, Department of Ophthalmology, Center for Integrative Human Physiology and Neuroscience Center Zurich, University of Zurich, 8091 Zurich, Switzerland

Survival and death of photoreceptors in degenerative diseases of the retina is controlled by a multitude of genes and endogenous factors. Some genes may be involved in the degenerative process itself whereas others may be part of an endogenous defense system. We show in two models of retinal degeneration that photoreceptor death strongly induces expression of leukemia inhibitory factor (LIF) in a subset of Muller glia cells in the inner nuclear layer of the retina. LIF expression is essential to induce an extensive intraretinal signaling system which includes Muller cells and photoreceptors and is characterized by an upregulation of Edn2, STAT3, FGF2 and GFAP. In the absence of LIF, Muller cells remain quiescent, the signaling system is not activated and retinal degeneration is strongly accelerated. Intravitreal application of recombinant LIF induces the full molecular pathway including the activation of Muller cells in wild-type and *Lif*$^{-/-}$ mice. Interruption of the signaling cascade by an Edn2 receptor antagonist increases whereas activation of the receptor decreases photoreceptor cell death. Thus, LIF is essential and sufficient to activate an extensive molecular defense response to photoreceptor injury. Our data establish LIF as a Muller cell derived neuronal survival factor which controls an intrinsic protective mechanism that includes Edn2 signaling to support photoreceptor cell survival and to preserve vision in the injured retina.

Key words: **leukemia inhibitory factor; Edn2; retina; photoreceptor degeneration; neuroprotection; endogenous rescue pathway**

Introduction

Human vision depends on the absorption of photons by rod and cone photoreceptors which convert the light information into a signal which is transported by connecting neurons to the brain. This highly specialized process requires sophisticated molecular interactions between a variety of intra- and intercellular retinal components. Thus, the retina has to maintain a high integrity of its cellular architecture and of the molecular machinery of visual cells. Mutations and/or exogenous stimuli disturb the retinal integrity and may lead to photoreceptor apoptosis and retinal degeneration (Remé et al., 1998). Cells of the retina can react to unfavorable (stress) conditions or to injury with the production of various cytokines and growth factors in an attempt to protect neurons and to preserve retinal function. This might best be seen in experimental paradigms of preconditioning in which a subtoxic stimulus induces the differential expression of specific genes. This increases the resistance of the tissue to a subsequent stronger stress and thus promotes cell survival (Kamphuis et al., 2007; Zhu et al., 2007; Thiersch et al., 2008). Ischemic or hypoxic exposure are classical preconditioning schemes but light exposure below damaging threshold has also been successfully applied (O'Driscoll et al., 2008) demonstrating the existence of several activatable survival pathways in the retina.

Exposure to high levels of white light induces photoreceptor degeneration (Remé et al., 1998) and activates a signaling cascade which includes leukemia inhibitory factor (LIF), Janus kinase 2 (Jak2), signal transducer and activator of transcription 1 (STAT1) and STAT3 (Samardzija et al., 2006a). A similar retinal response has been observed in models of inherited retinal degeneration (Samardzija et al., 2006a). Since recombinant LIF can protect photoreceptor cells against light-induced degeneration (Ueki et al., 2008), the increased expression of endogenous LIF in response to damaging light suggests that LIF might be part of a retinal defense mechanism to increase survival of visual cells. Such an endogenous protective response has recently been postulated by Rattner and Nathans. In their study, they propose that injured photoreceptors produce endothelin 2 (Edn2) which signals onto Muller cells. Activated Muller cells and/or other cells may then produce and release fibroblast growth factor 2 (FGF2) to support survival of viable photoreceptors (Rattner and Nathans, 2005).

Here we focused on the role of LIF in the degenerating retina of the VPP mouse, a model for autosomal dominant retinitis pigmentosa (Naash et al., 1993; Grimm et al., 2004). We show that lack of LIF prevents Edn2 expression, STAT3 phosphorylation, FGF2 production and activation of Muller glia cells and strongly accelerates retinal degeneration. This suggests that LIF is the key factor regulating an endogenous defense mechanism to ensure survival and function of retinal cells. Since LIF expression

Received Oct. 23, 2008; revised Oct. 31, 2008; accepted Nov. 1, 2008.

This work was supported by the Swiss National Science Foundation (Grant 3100A0-117760), a grant from the European Community (EVI-GenoRet; LSHG-CT-512036), the Fritz Tobler Foundation, the Vontobel Foundation, and the H. Messerli Foundation. We thank Coni Imsand, Hedwig Wariwoda, and Philipp Huber for excellent technical assistance and Muna Naash (VPP), Bettina Holtmann, and Michael Sendtner (*Lif*$^{-/-}$) for providing transgenic mouse lines.

Correspondence should be addressed to Christian Grimm, Laboratory for Retinal Cell Biology, Department of Ophthalmology, University of Zurich, Frauenklinikstrasse 24, 8091 Zurich, Switzerland. E-mail: cgrimm@opht.uzh.ch.

DOI:10.1523/JNEUROSCI.5114-08.2008

 0270-6474/08/2813765-10$15.00/0

Table 1. Primers used for genotyping and real-time PCR

Gene/allele	Forward	Reverse
Genotyping		
VPP	AGACTGACATGGGGAGGAATTCCCAGA	CAGCTGCTCGAAGTGACTCCGACC
Lif/wt	AAATGCCACCTGTGCCATACGC	CAACTTGGTCTTCTCTGTCCCG
Lif/KO	CTCTAAGCCTGAACTCTCTCATCC	GATTCGCAGCGCAGCGCATCGCCTT
Ccl-2/wt	GGAGCATCCACGTGTTGGC	ACAGCTTCTTTGGGACACC
Ccl-2/KO	CTTGGGTGGAGAGGCTATTC	AGGTGAGATGACAGGAGATC
Rd1	CATCCCACCTGAGCTCACAGAAAG	GCCTACAACAGAGGAGCTTCTAGC
Nrl/wt	GTGTTCCTTGGCTGGAAAGA	CTGTTCACTGTGGGCTTTCA
Nrl/KO	TGAATACAGGGACGACACCA	GTTCTAATTCCATCAGAAGCTGAC
Real-time PCR		
Edn1	TCCCGTGATCTTCTCTCTGC	AGTTCGGCTCCCAAGACAG
Edn2	AGACCTCCTCCGAAAGCTG	CTGGCTGTAGCTGGCAAAG
Ednrb	ACCTACAAGTTGCTCGCAGAGG	AAAACCTATGGCTTCGGGGAC
Smad1	TGGTTCCAAGCAGAAGGAGGTC	GCTCATTTTGTCCCAGGTTGC
Gfap	CCACCAAACTGGCTGATGTCTAC	TTCTCTCCAAATCCACACGAGC
Mcl1	GTGACTCTTATTTCTTTCGGTGCC	CATCCCAGCCTCTTTGTTTGAC
Casp-1	GGCAGGAATTCTGGAGCTTCAA	GTCAGTCCTGGAAATGTGCC
Fgf2	TGTGTCTATCAAGGGAGTGTGTGC	ACCAACTGGAGTATTTCCGTGACCG
Cntf	CTCTGTAGCCGCTCTATCTG	GGTACACCATCCACTGAGTC
Bdnf	CAAAGCCACAATGTTCCACCAG	GATGTCGTCGTCAGACCTCTCG
Gdnf	AGATGAAGTTATGGGATGTCGTGG	GGCATATTGGAGTCACTGGTCAG
Bcl-2	TTGTGGCCTTCTTTGAGTTCG	ATTTCTACTGCTTTAGTGAACC
Survivin	AACTACCGCATCGCCACCTTCAAG	AGCCAGGGGAGTGCTTTCTATG
Jak1	TGAGCTTTGATCGGATCCTT	GCAGGGTCCCAGAATAGATATG
Jak2	GAACCTACAGATACGGAGTGTCC	CAAAATCATGCCGCCACT
Jak3	CACAGTGCATGGCCTATGAT	AGGTGTGGGGTCTGAGAGG
Tyk2	CCTGTGTCACCTTGCTCTCA	GGAATGAGGGATGCAGTTCT
Socs3	GGAGACAGATGAGGCTGGTGA	GGACCTACTGACCGAGAGAT
Stat3	CAAAACCCTCAAGAGCCAAGG	TCACTCACAATGCTTCTCCGC
Lif-R	ACTGAAGTGGAACGACAGAGG	CTTTACCACTCAGCATTGTGTTG
Gnat1	GAGGATGCTGAGAAGGATGC	TGAATGTTGAGCGTGGTCAT
Lif	AATGCCACCTGTGCCATACG	CAACTTGGTCTTCTCTGTCCCG
Mcp-1	GGCTCAGCCAGATGCAGTTA	CTGCTGCTGGTGATCCTCTT

Primers for *Gnat1* were from Znoiko et al. (2005).

is specifically induced in a subset of Muller glia cells, Muller cells may coordinate the molecular response to injury and initiate an elaborate and LIF-dependent crosstalk between various retinal cells of the INL and ONL.

Materials and Methods

Mice, light exposure, intravitreal injections, and detection of cell death. Animals were treated in accordance with the regulations of the Veterinary Authority of Zurich and with the statement of "The Association for Research in Vision and Ophthalmology" for the use of animals in research. VPP mice [generous gift from Muna Naash (Naash et al., 1993)] were on a mixed SV129BL/6 background. $Lif^{-/-}$ mice (Escary et al., 1993) were kindly provided by Bettina Holtmann and Michael Sendtner (University of Wuerzburg, Germany). $Ccl\text{-}2^{-/-}$ (Jackson Laboratory), BALB/c mice (Harlan) and 129S6/SvEvTac (Taconic) were purchased from commercial suppliers. All mice except BALB/c and 129S6/SvEvTac (both $Rpe65_{450Leu}$) expressed the $Rpe65_{450Met}$ variant (Samardzija et al., 2006b). Double mutant mice were generated by classical breeding schemes. Primer pairs for genotyping are listed in Table 1. For rd1 genotyping, PCR products were digested with *Dde*I to detect presence or absence of the mutation as described earlier (Hafezi et al., 1998).

For light exposure, 8-week-old wild-type mice were dark-adapted overnight and their pupils were dilated with 1% Cyclogyl (Alcon) and 5% phenylephrine (Ciba Vision) 45 min before exposure to 5000 lux of white fluorescent light for 2 h. After exposure, mice were returned to darkness for 12 h.

Intravitreal injections were performed on anesthetized animals with a 34G needle mounted on a 10 μl Hamilton syringe. Injection site was just behind the limbus on the superior part of the eye. Intravitreal placement of the needle was observed through the pupil. One microliter of rLIF in PBS (10 ng/μl; Millipore), BQ-3020 in H_2O (1 μg/μl; American Peptide), BQ-788 in 10%DMSO in PBS (2 μg/μl; American Peptide) or of vehicle alone was injected within 5–10 s and the empty needle was kept in place for additional 30 s before it was slowly withdrawn. BQ-3020 injections were done in 129S6/SvEvTac mice ($n = 21$) 24 h before exposure to 2 h of 13,000 lux of white light. Analysis of cell death was 24 h after exposure. BQ-788 injections were done in VPP mice ($n = 9$) at PND 35 and analysis of cell death was 48 h thereafter. Cell death was analyzed by measuring free nucleosomes in each (total) retina individually using the cell death detection kit (Roche) according to the manufacturer's recommendations. Retinal cell death in compound injected eyes was expressed as fold-difference to cell death in the sham injected contralateral eyes of the same animal.

Microscopy and immunofluorescence. For light microscopy, eyes were fixed in 2.5% glutaraldehyde in 0.1 M cacodylate buffer, pH 7.3, at 4°C overnight. For each eye, the superior and the inferior retina were prepared, washed in cacodylate buffer, incubated in osmium tetroxide for 1 h, dehydrated, and embedded in Epon 812. Sections (0.5 μm) were prepared from the lower central retina and counterstained with methylene blue.

For immunofluorescence, mice were perfused with 4% paraformaldehyde in PBS. Eyes were removed and post fixed for 10 min in 4% paraformaldehyde. Cornea and lens were removed and eyecups were postfixed in 4% paraformaldehyde for additional 15 min at room temperature. The tissue was then incubated in 10% sucrose (in PBS) for 10 min, 20% sucrose for 30 min and 30% sucrose overnight at 4°C. Eyecups were embedded in Tissue Tec OCT (Mioles), frozen in liquid nitrogen and stored at −70°C until further use. Twelve micrometer sections were cut, dried and washed in PBST (PBS + 1% Triton X-100) for 3 × 5 min at room temperature (RT). After blocking in PBS + 10% horse serum (HS) for 1 h at RT, sections were incubated with the respective primary antibodies anti-Calbindin (AB1778), anti Brn-3a (MAB1585), anti-CHX10 (AB9014), anti-glutamine synthetase (MAB302; all Millipore), anti-Iba-1 (#019-19741, Wako), anti-PKCβ (sc-209, Santa Cruz; kindly provided by S. Neuhauss, University of Zurich, Zurich, Switzerland), anti-Calretinin or anti-Disabled-3 (both kindly provided by E. Strettoi, Neuroscience Institute, Italian National Research Council, Pisa, Italy). Sections were washed 3 × 10 min in PBS and Cy3- or Cy2-conjugated secondary antibodies (Jackson ImmunoResearch) were applied in PBS + 10% HS (dilution 1:500) for 1–2 h at RT. Sections were washed 3 × 10 min in PBS, mounted and analyzed using a Zeiss fluorescent microscope.

In situ *hybridization.* For *in situ* hybridization, nonfixed tissue was frozen in Tissue Tec OCT (Mioles). Twelve micrometer sections were cut and air dried for 20 min at room temperature and 10 min at 50°C. Sections were post-fixed for 10 min at room temperature in 4% paraformaldehyde (in PBS) followed by 3 washing steps with PBS (5 min each). Samples were acetylated for 20 min at room temperature in 100 mM triethanolamine, 2.5 μl/ml acetic anhydride followed by 3 washing steps with PBS (5 min each). Prehybridization was done at room temperature for 2 h in 50% formamide, 5xSSC, 1xDenhardt's, 1 mg/ml yeast tRNA, 0.1% Tween 20, 0.1% CHAPS, 5 mM EDTA. Hybridization was done for 16 h at 65°C in 15 ml of the same solution including 7–15 μg of DIG-labeled sense or antisense RNA probe. Slides were washed 5 times in SSC with increasing stringency and blocked in 100 mM Tris, pH 7.5, 150 mM NaCl and 1% blocking reagent (Roche # 1096176) for 1 h at room temperature. Incubation with anti-DIG antibody (Roche) in blocking buffer was for 16 h at 4°C. Slides were washed twice in 100 mM Tris, 150 mM NaCl at room temperature for 20 min each, equilibrated for 5 min in 100 mM Tris, pH 9.5, 150 mM NaCl, 50 mM $MgCl_2$, 0.25 mg/ml levamisole (Sigma, L9756) and incubated in the same solution including 1 μl/ml NBT and 3.5 μl/ml BCIP for up to 16 h at room temperature. After color had developed, reaction was stopped in 10 mM Tris (pH 8.0)/1 mM EDTA, slides were mounted and analyzed.

Combined in situ *hybridization/immunofluorescence. In situ* hybridization was performed as described above on perfused (4% PFA) and cryopreserved tissue (see Microscopy and immunofluorescence) using RNase free reagents. After color development slides were washed 2 × in PBS for 5 min each. Slides were then postfixed in 4% PFA for 10 min at RT, washed 2 × in PBS (5 min each) and the primary antibodies were applied in 5% HINGS (heat inactivated goat serum) for 3 h at RT. Slides were

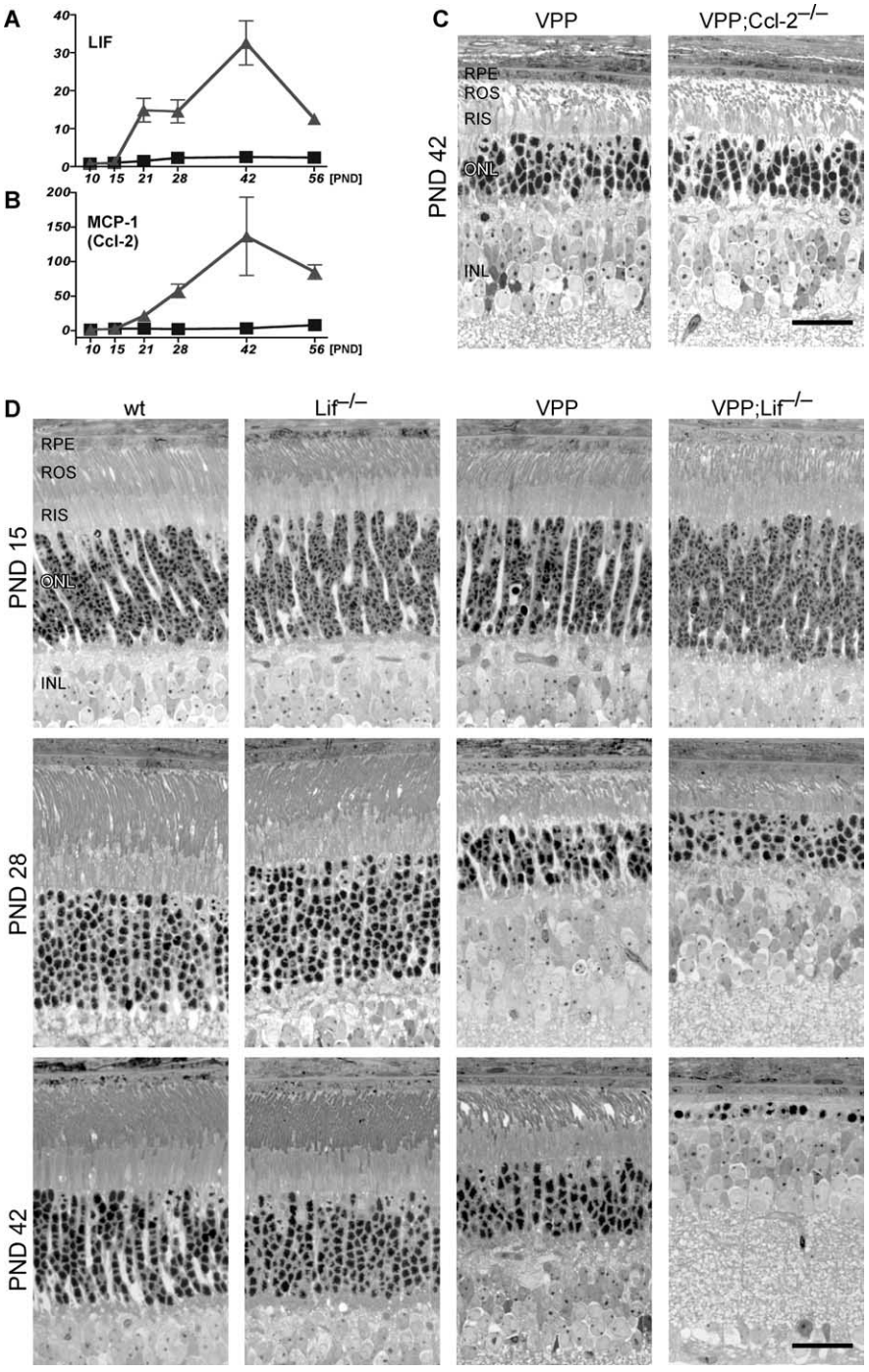

Figure 1. Lack of LIF accelerates photoreceptor degeneration in the VPP retina. ***A***, ***B***, Retinas from wt (squares) or VPP (triangles) mice were isolated at different postnatal days (PND) as indicated. Gene expression of LIF (***A***) and MCP-1 (Ccl-2) (***B***) was analyzed by real-time PCR and normalized to β-actin expression. Expression of both factors was strongly induced in VPP mice starting around PND 15, concomitantly with the onset of photoreceptor degeneration. Shown are the mean mRNA levels ($\pm$SD) of three independent retinas per time point and strain ($n = 3$) relative to the levels of wild-type (wt) at PND 10 which was set to 1. ***C***, Retinal morphology of VPP (left) and VPP;Ccl-2$^{-/-}$ mice (right) at PND 42. Lack of Ccl-2 did not influence the degeneration as reflected by the indistinguishable retinal morphologies. Both genotypes retained 5–6 rows of photoreceptor nuclei in the ONL compared with the 10–12 rows in wild-type retinas (***D***). ***D***, Retinal morphology of wild-type (wt), Lif$^{-/-}$, VPP and VPP;Lif$^{-/-}$ mice was analyzed at PND 15, PND 28 and PND 42 as indicated. Retinal morphology was similar in wt and Lif$^{-/-}$ at all ages tested. Retinas of VPP mice developed normally until the age of 15 d. As expected (Samardzija et al., 2006b), many VPP photoreceptors degenerated until PND 28 before the degeneration slowed down. Photoreceptors of VPP;Lif$^{-/-}$ mice displayed a similar degeneration until PND 28 but had a much more severe progression thereafter as seen by the single row of photoreceptors remaining at PND 42. Shown are representative panels of at least three independent retinas. RPE, Retinal pigment epithelium; ROS, rod outer segments; RIS, rod inner segments; ONL, outer nuclear layer; INL, inner nuclear layer. Scale bars, 25 μm.

rinsed 1x in PBS, washed 3x in PBS (5 min each) and blocked in 20% HINGS at RT for 1 h. The respective secondary antibodies were applied in 5% HINGS at RT for 1 h. Slides were rinsed in PBS, washed 3 $\times$ in PBS (5 min each) and mounted.

Western blotting. Retinas were homogenized by sonication in 100 mM Tris/HCl, pH 8.0, and analyzed for protein content using Bradford reagent. Standard SDS-PAGE (12%) and Western blotting of 40 μg of total retinal extracts were performed. For immunodetection, the following antibodies were used: anti-STAT3 (#9132 Cell Signaling Technology), anti-Akt (#9272, Cell Signaling Technology), anti-gp130 (sc-656, Santa Cruz), anti-GFAP (G-3893, Sigma), anti-CRALBP (gift from John Saari, University of Washington, Seattle, WA), anti-β-actin (sc-1616, Santa Cruz Biotechnology), anti-phospho-STAT3$_{Tyr705}$ (#9131, Cell Signaling Technology), anti-phospho-Akt$_{Tyr473}$ (#9271, Cell Signaling Technology). Blots were incubated overnight at 4°C with primary antibodies followed by a one hour incubation at RT with HRP-conjugated secondary antibodies. Immunoreactivity was visualized using the Western Lightning Chemiluminescence reagent (Perkin-Elmer).

RNA isolation, cDNA synthesis, and real-time PCR. Retinas were removed through a slit in the cornea and snap frozen in liquid nitrogen. Total retinal RNA was prepared using the RNeasy RNA isolation kit (Qiagen) including a DNase treatment to digest residual genomic DNA. One microgram of total RNA were used for reverse transcription using oligo(dT) and M-MLV reverse transcriptase (Promega). cDNAs from individual animals were amplified in duplicates with respective primer pairs (Table 1) in a Light-Cycler instrument 480 (Roche Diagnostics AG) using SYBR Green I Master Mix (Roche Diagnostics AG). mRNA levels were normalized to β-actin and relative gene expression was calculated using the value of one (out of three) wild-type probe as calibrator. For statistical analysis we used ANOVA with Tukey's multiple comparison test (where more than two conditions were compared), ANOVA with Dunnett's multiple comparison test (where several conditions were compared with a control) or a one-tailed *t* test for the comparison of the treatment in *Lif*$^{-/-}$ animals, respectively. *p* values of <0.05 were considered statistically significant.

Results

Lack of LIF accelerates photoreceptor degeneration in a model of retinitis pigmentosa

The degenerating retina of VPP mice induces the expression of several factors connected to an inflammatory or immune response like LIF (Fig. 1*A*) (Samardzija et al., 2006a), monocyte chemoattractant protein-1 (MCP-1) (Fig. 1*B*), Casp-1, interleukin-1β (IL-1β) (Samardzija et al., 2006c), complement component 1qα (C1qα) (Rohrer et al., 2007) and comple-

13768 • J. Neurosci., December 17, 2008 • 28(51):13765–13774

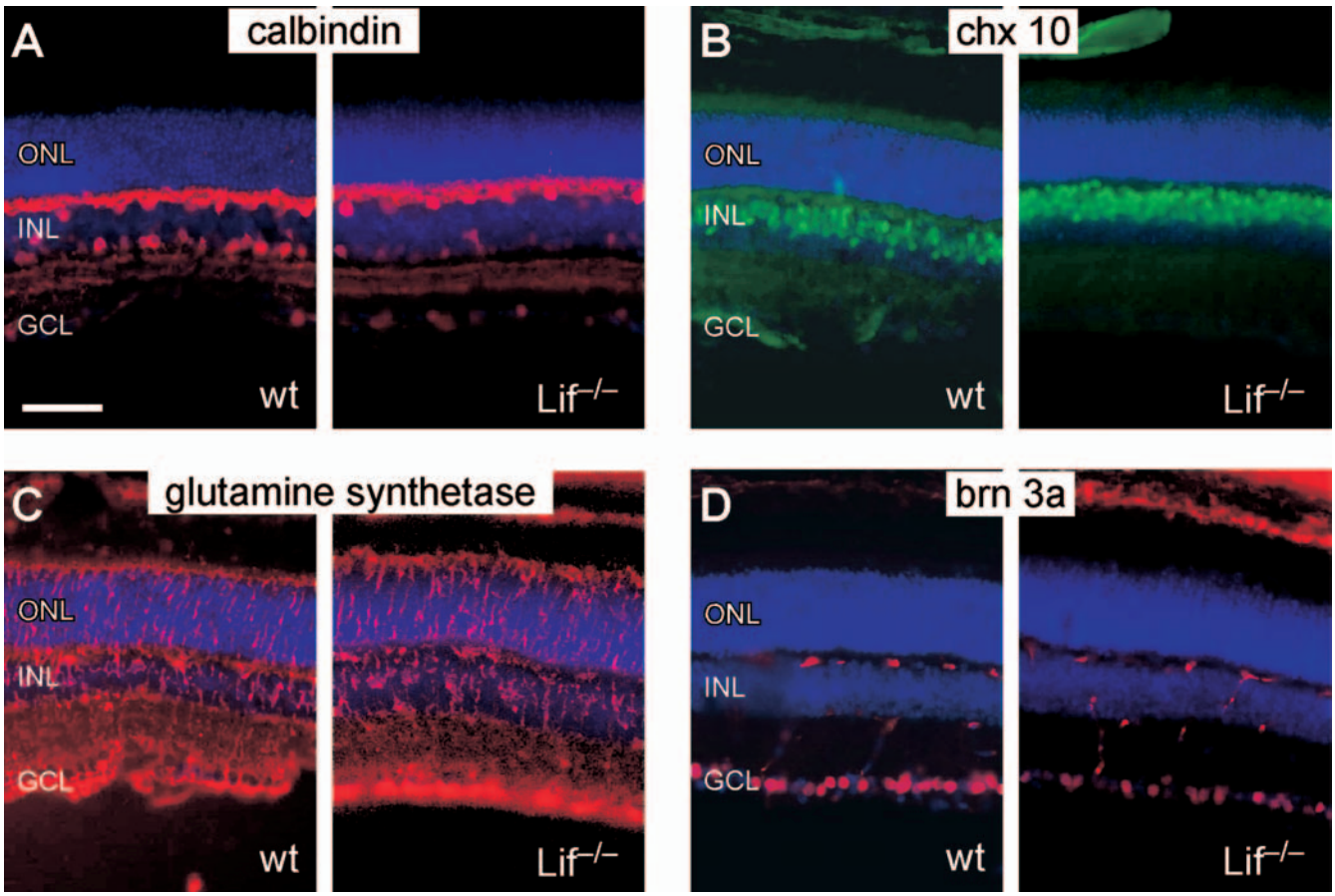

Figure 2. ***A–D***, Lif $^{-/-}$ retinas are similar to wild-type. Retinas of 28-day-old wild-type (wt) and Lif $^{-/-}$ mice, respectively, were stained with antibodies specific for horizontal cells (calbindin, ***A***), bipolar cells (CHX10, ***B***), Muller glia cells (glutamine synthetase, ***C***) and ganglion cells (Brn3a, ***D***). Staining patterns did not differ between wild-type and mutant retinas. GCL, Ganglion cell layer. Other abbreviations as in Figure 1. Scale bar, 50 μm.

ment factor H (CFH, data not shown). To analyze their potential role in the physiology or pathophysiology of the retina, we genetically inhibited MCP-1 and LIF signaling. For this purpose, we generated double mutant mice expressing the VPP transgene on a null background for either the MCP-1 chemokine (*Ccl-2*$^{-/-}$) or the LIF cytokine (*Lif*$^{-/-}$), respectively. Even though MCP-1 was upregulated >100-fold in the VPP retina, lack of functional MCP-1 did not noticeably influence the course of the disease process (Fig. 1*C*). In contrast, genetic ablation of LIF strongly accelerated retinal degeneration and the death of photoreceptors in VPP mice (Fig. 1*D*). Whereas retinas of VPP mice showed the expected slow degeneration with ~6 rows of photoreceptor cells left at PND 42, retinas of VPP mice lacking LIF showed a severely accelerated degeneration with only one row of visual cells remaining 42 d after birth (Fig. 1*D*). Onset and first phase of the degeneration was similar to VPP mice as suggested by the normal retinal appearance at PND 15 and by the only slightly reduced number of photoreceptor nuclei at PND 28.

Although LIF has been implicated in retinal development (Elliott et al., 2006) and lack of LIF was recently reported to increase microvessel density in the retina (Kubota et al., 2008), retinal morphology of *Lif*$^{-/-}$ mice was similar to wild-type mice at all ages tested. Retinal cell layers were well established and distribution of rods and cones was inconspicuous (Fig. 1*D*). In addition, immunofluorescence stainings with antibodies specific for horizontal cells (anti-calbindin), bipolar cells (anti-CHX10), Muller cells (anti-glutamine synthetase) and ganglion cells (anti-Brn3a) resulted in similar staining patterns in wild-type and knock-out mice (Fig. 2). Normal retinal architecture of *Lif*$^{-/-}$ mice is further supported by the equal numbers of retinal ganglion cells in wt and LIF knock-out animals (additional file 1). In addition, retinal function of *Lif*$^{-/-}$ mice was comparable to wild-type animals (data not shown).

Photoreceptor injury induces LIF expression in a subset of Muller glia cells

We used *in situ* hybridization to localize the cells expressing LIF cytokine in response to photoreceptor injury. Whereas most cells did not show enhanced signal intensity compared with controls, few scattered cells were strongly positive for LIF expression in the INL of VPP mice at PND 28 (Fig. 3*A–C*). A very similar expression pattern was also found in retinas of wild-type mice at 12 h after exposure to damaging light (Fig. 3*D–F*,*G*,*J*). This suggests that the same subset of cells might be responsible for LIF upregulation in both models of retinal degeneration. Hybridization of wild-type control retinas with antisense probe did not result in such a staining pattern (Fig. 3*F*) demonstrating that the signal was specific for degenerating retinas. To identify the retinal cell type expressing LIF, we combined *in situ* hybridization with immunofluorescence using antibodies specific for individual retinal cell types. Whereas the *in situ* LIF signal did not colocalize with calbindin (horizontal cells), calretinin (amacrine cells), disabled-3 (type 2 amacrine cells), PKC-β (cone bipolar cells) or Iba-1 (microglia cells) (additional file 2), it labeled a subset of

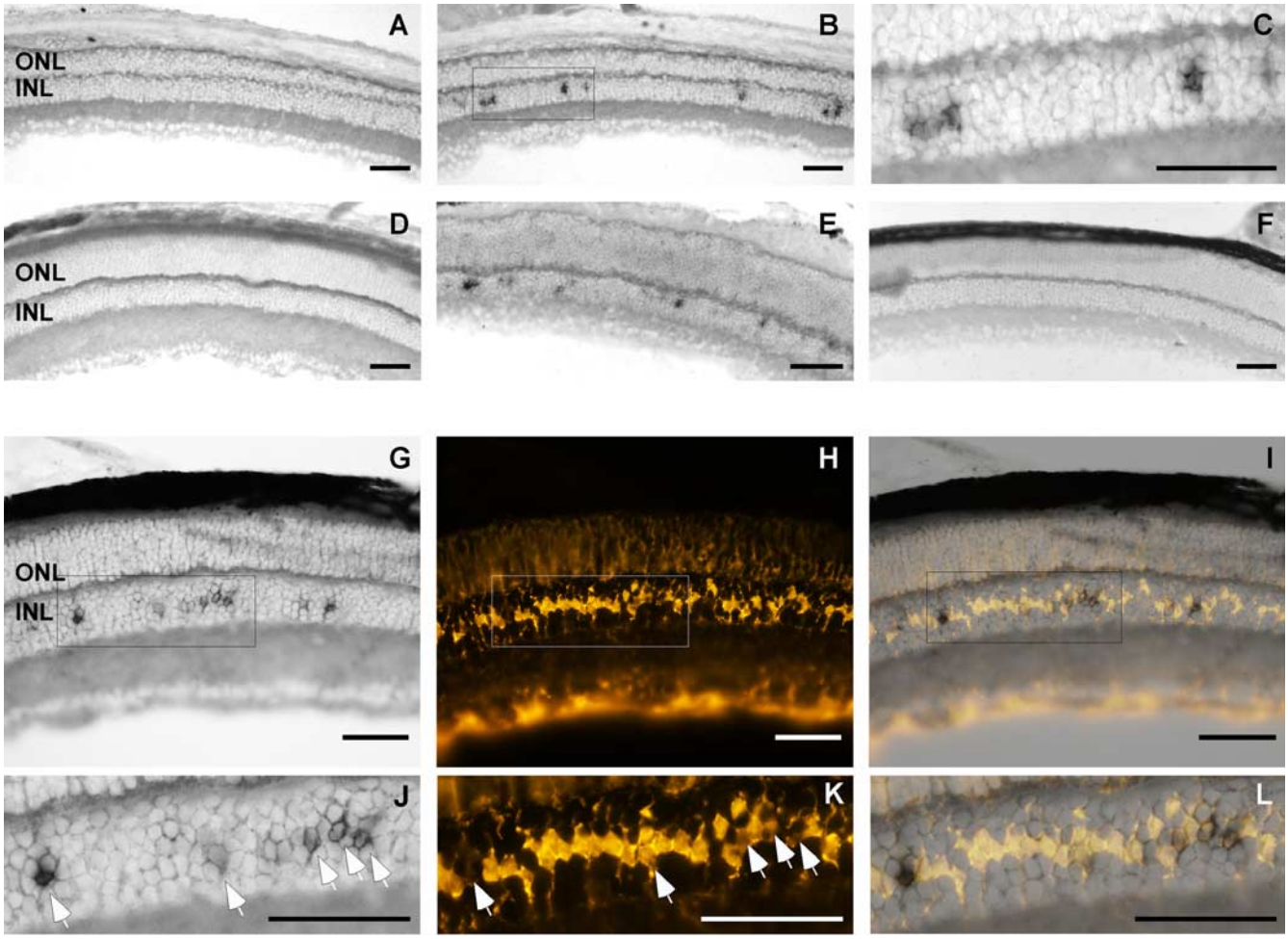

Figure 3. The degenerating retina induces LIF expression in a subset of Muller glia cells. ***A–F***, *In situ* hybridization localizes LIF-expressing cells in the INL. Retinal sections of 28-day-old VPP mice (***A–C***), of wild-type BALB/c mice 12 h after light exposure (***D***, ***E***), or of untreated wild-type mice (***F***) were hybridized with LIF sense (***A***, ***D***) or LIF antisense (***B***, ***C***, ***E***, ***F***) riboprobes. ***C***, Higher magnification of boxed area in ***B***. LIF antisense probes specifically stained scattered cells in the INL in retinas undergoing photoreceptor degeneration (***B***, ***E***) but not in a healthy retina (***F***). ***G–L***, Combined *in situ* and immunofluorescence stainings identified LIF-expressing cells as a subset of Muller glias. Retinal sections of wild-type 129S6/SvEvTac mice 12 h after light exposure were hybridized with LIF antisense riboprobes (***G***, ***J***) and anti-glutamine synthetase antibodies (***H***, ***K***). The merged pictures (***I***, ***L***) identified LIF-expressing cells as a subset of Muller glia cells. ***J–L***, Higher magnifications of boxed area in ***G***. Arrows, cells positive for LIF and GS. Abbreviations as in Figure 1. Scale bars, 50 μm.

cells which stained positive for glutamine synthetase (GS) (Fig. 3*G–L*). This clearly demonstrates that a subset of Muller glia cells upregulated LIF in response to retinal stress. It is interesting to note that the intensity of the GS staining correlated inversely with the intensity of the LIF signal (Fig. 3*J*,*K*).

Lack of LIF prevents activation of Muller glia cells and blocks phosphorylation of STAT3

Muller cell activation is one of the most common hallmarks in a degenerating retina. In virtually all cases studied, retinal Muller cells increase expression of glial fibrillary acid protein (GFAP) in response to a degenerative process (Lewis and Fisher, 2003; Bringmann et al., 2006). This has also been observed in the VPP mouse retina (Fig. 4) (Samardzija et al., 2006a). In contrast to VPP mice on a LIF wild-type background, increased expression of GFAP was completely abolished in retinas of *VPP;Lif*$^{-/-}$ (Fig. 4). The similar expression levels of cellular retinaldehyde-binding protein (CRALBP) (Fig. 4) and the immunofluorescence staining for glutamine synthetase (GS) (Fig. 2), both Muller cell markers, show that the missing glial response was not due to a generally reduced presence of Muller cells in LIF knock-out animals.

Similarly to GFAP in Muller cells, phosphorylation of the anti-apoptotic STAT3 protein has been commonly observed during degenerative processes in the retina (Mechoulam and Pierce, 2005; Samardzija et al., 2006a; Yang et al., 2007; Ueki et al., 2008). As for the increased GFAP expression, phosphorylation of STAT3 was completely blocked in retinas of *VPP;Lif*$^{-/-}$ mice (Fig. 4). Since STAT3 protein was expressed at normal levels (Fig. 4) and the enzymatic machinery to phosphorylate STAT3 was intact in the *Lif*$^{-/-}$ retina (see below), a block of upstream signaling events in the absence of LIF cytokine must account for the lack of STAT3 phosphorylation and the missing Muller cell activation in the double transgenic animals.

Akt, another kinase implicated in retinal degeneration and cell survival (Johnson et al., 2005; Jomary et al., 2006) was slightly activated in degenerating VPP retinas as evidenced by the small increase in phosphorylation observed by Western blotting (Fig. 4). Similar to STAT3, the absence of LIF prevented increased phosphorylation of Akt in response to the degeneration in the *VPP;Lif*$^{-/-}$ retina.

LIF is required for proper signaling in the stressed retina

Recently, Rattner and Nathans (2005) identified photoreceptor-derived Edn2 as a potential signaling molecule regulating a Muller glia cell response to light-mediated injury. Similar to the light-

damaged retina (data not shown), the VPP retina strongly upregulated expression of Edn2 (Fig. 5*A*). Basal expression of Edn2 seemed to depend largely on LIF since Edn2 expression was reduced to 2% of wild-type levels in *Lif*$^{-/-}$ mouse retinas. In VPP mice lacking LIF (*VPP;Lif*$^{-/-}$ double mutants), Edn2 expression was not upregulated and remained at the low basal levels observed in the *Lif*$^{-/-}$ retina, despite the accelerated retinal degeneration in the double mutant mice. Edn1 and Ednrb were expressed at similar levels in all mouse strains tested.

In the injured retina of the VPP mouse, GFAP was induced on the mRNA (Fig. 5*B*) and protein (Fig. 4) levels. Similar to Edn2, however, GFAP expression was strongly reduced in retinas of mice lacking LIF (11% of wt) (Fig. 5*B*) and in contrast to VPP mice (2.7-fold elevated mRNA levels) no increased expression of GFAP was detectable in retinas of double mutant mice which is in line with our protein expression data (Fig. 4). LIF influenced also expression of Casp-1 since basal mRNA levels of this protease were reduced by a factor of 2 in retinas of *Lif*$^{-/-}$ mice (Fig. 5*B*). Similar to Edn2 and GFAP, Casp-1 expression was activated in VPP retinas but not in *VPP;Lif*$^{-/-}$ double mutant mice. Expression of other stress related genes like *Smad1* (data not shown) and *Mcl1* (Fig. 5*B*) were not affected by the lack of LIF and/or the presence of the VPP transgene (Fig. 5*B*).

FGF2 is often implicated in a paracrine pathway of photoreceptor neuroprotection in various models of degeneration (Wen et al., 1995; Gao and Hollyfield, 1996; Joly et al., 2007) and is thought to be produced in an attempt to protect cells in unfavorable conditions. As such, FGF2, was also strongly upregulated in the VPP retina (10.2-fold, Fig. 5*C*). Strikingly, however, VPP retinas lacking LIF completely failed to induce FGF2 expression which remained at the same low basal level (38% of wt) as observed in *Lif*$^{-/-}$ single mutant mice (43% of wt). Expression of other neurotrophic factors like BDNF, GDNF and CNTF remained at basal levels in the different strains with a slight upregulation of CNTF in the double transgenic retina (1.7-fold induction, Fig. 5*C*). Similarly, expression of the anti-apoptotic genes survivin and Bcl-2, both may be regulated in a STAT3 dependent manner (Kim et al., 2006; Weerasinghe et al., 2007) remained at basal levels in the retinas of all strains tested. Thus, the lack of FGF2 induction might have been the main reason for the accelerated photoreceptor degeneration in the VPP mouse lacking LIF.

Retinal degeneration in the VPP mouse not only induced phosphorylation of STAT3 (Fig. 4) but also STAT3 gene expression (1.9-fold) and the expression of at least two additional members of the Jak/STAT signaling pathway (Jak3, 2.6-fold and SOCS3, 3.4-fold). Again, lack of LIF in *VPP;Lif*$^{-/-}$ mice completely blocked activation of this signaling cascade (Fig. 5*D*).

In summary, all genes (Edn2, GFAP, Casp-1, FGF2, STAT3, Jak3, SOCS3) or proteins (pSTAT3, p-Akt, GFAP), which were activated in response to VPP-mediated retinal degeneration showed basal expression in the absence of LIF. This strongly suggests an essential and early role of LIF in the retinal response to photoreceptor injury.

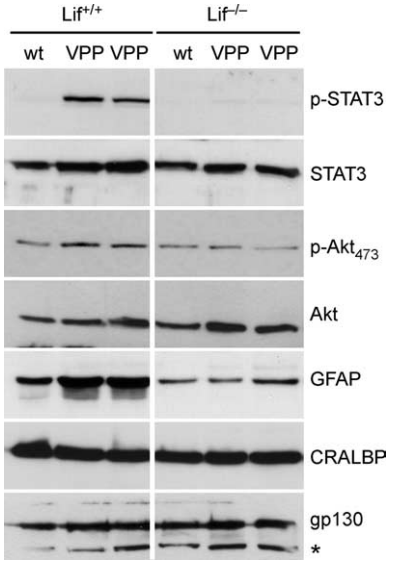

Figure 4. Lack of LIF prevents activation of STAT3, Akt and GFAP. Total retinal extracts of wt, VPP, Lif$^{-/-}$ and VPP;Lif$^{-/-}$ retinas of 28-day-old mice were tested by Western blotting using specific antibodies as indicated. The VPP transgene on a LIF wild-type background (left) induced a strong phosphorylation of STAT3, a weak activation of Akt and a robust upregulation of GFAP. Retinas of VPP mice on a LIF knock-out background (right) did not show any signs of STAT3 phosphorylation and did not increase expression of phospho-Akt and GFP. *Nonspecific signal.

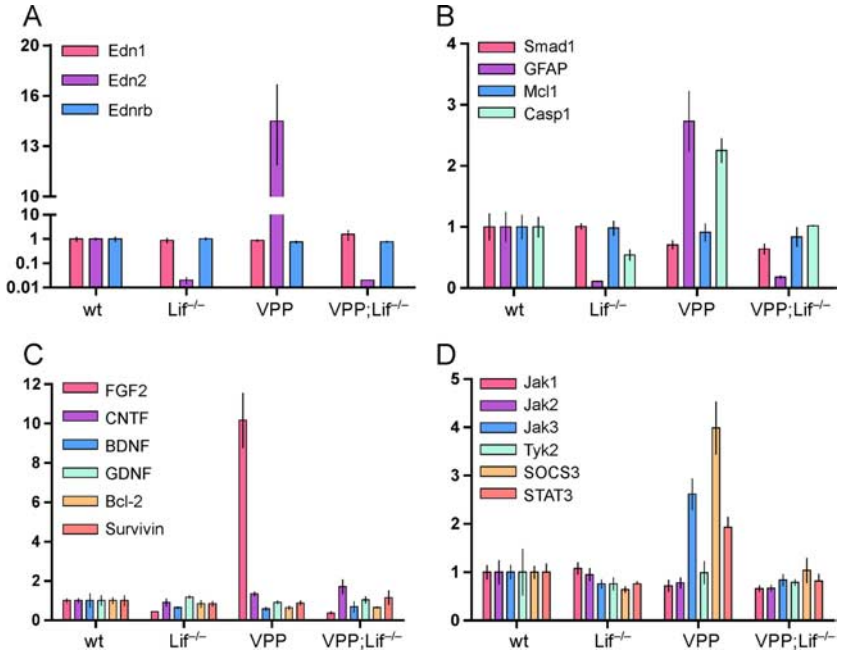

Figure 5. Lack of LIF prevents induction of a genomic response to retinal injury. Total retinal RNA was prepared from 28-day-old wt, VPP, Lif$^{-/-}$ and VPP;Lif$^{-/-}$ mice. cDNA from 3 independent retinas per genotype was amplified in duplicates by real-time PCR. One wild-type sample served as calibrator and the mean of all wild-type samples was set to 1 for each gene amplified. Shown are means ± SD of endothelin-related genes (***A***), stress-related genes (***B***), growth and survival factors (***C***), and of genes relevant for the Jak/STAT signaling pathway (***D***) relative to wild-type levels. Lack of LIF caused very low basal expression levels of Edn2, GFAP and FGF2. In the presence of LIF, VPP-mediated retinal degeneration induced expression of Edn2, GFAP, Casp-1, FGF2, Jak3, SOCS3 and STAT3. The absence of LIF prevented induction of all of these genes in the VPP retina and expression levels remained at similar low levels as in Lif$^{-/-}$ single mutant mice.

Signaling can be restored by the application of rLIF

The missing activation of gene expression and protein phosphorylation in *Lif*$^{-/-}$ mice could be specifically caused by the absence of LIF cytokine or by a general defect in the knock-out animals. To discriminate between these possibilities, we analyzed gene

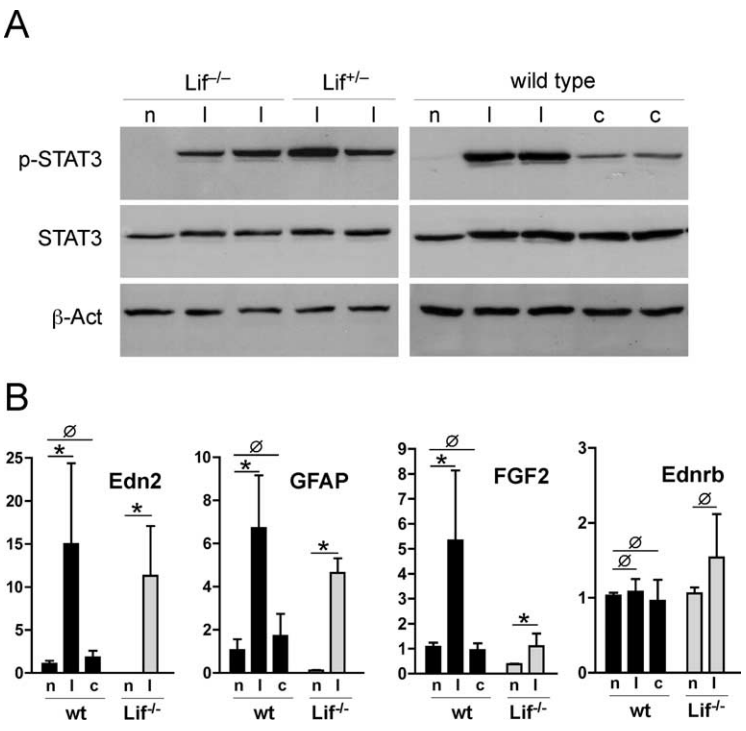

Figure 6. ***A***, ***B***, Injection of rLIF restores signaling in Lif $^{-/-}$ mice. A total of 1 μl (10 ng) of rLIF (l) or of vehicle control (PBS) (c) was injected intravitreally and levels of proteins or mRNAs were analyzed after 24 h by Western blotting (***A***) or by real-time PCR (***B***). ***A***, Injection of rLIF induced phosphorylation of STAT3 in wild-type, Lif $^{+/-}$ and Lif $^{-/-}$ mice. Control PBS injections showed only a minor response. ***B***, Gene expression of noninjected mice (n) or of mice at 24 h after injection of rLIF (l) or vehicle (PBS) (c) in wild-type (black bars) or Lif $^{-/-}$ mice (gray bars). Shown are means $\pm$ SD of $n = 3$–4 per genotype and treatment. Levels in noninjected wild-type animals were set to 1. $^{*}p < 0.05$; $^{\varnothing}p > 0.05$. n, Noninjected; l, rLIF-injected; c, vehicle-injected.

expression after intravitreal injection of rLIF into wild-type and *Lif*$^{-/-}$ mice. rLIF induced phosphorylation of STAT3 similarly in all mice tested (Fig. 6*A*) and strongly activated gene expression of Edn2, GFAP and FGF2 in both wild-type and *Lif*$^{-/-}$ retinas (Fig. 6*B*). Although FGF2 mRNA levels in *Lif*$^{-/-}$ retinas treated with rLIF injections did not reach levels of treated wild-type retinas, induction over nontreated retinas was nevertheless similar (5-fold in wild-type and threefold in Lif$^{-/-}$ retinas) in the two mouse strains. It is interesting to note that rLIF induced expression of Edn2 14-fold in wild-type retinas and >3200-fold in *Lif*$^{-/-}$ animals resulting in similar expression levels in the two animals after rLIF application. Control injections of carrier (PBS) resulted only in a subtle response with low levels of STAT3 phosphorylation (Fig. 6*A*) but not in a significant alteration of gene expression (Fig. 6*B*). These data show that the molecular equipment required to transduce LIF-mediated signaling was present and functional in *Lif*$^{-/-}$ retinas. This suggests that lack of gene activation was a specific consequence of the absence of LIF.

Activation of Ednrb induces the molecular response and protects photoreceptors

The receptor for Edn2 has been found to be expressed on Muller cells and potentially astrocytes in the mouse retina (Rattner and Nathans, 2005). To test whether direct stimulation of Ednrb might be able to activate the molecular response to injury we injected the Ednrb agonist BQ-3020 into the vitreous of wild-type and *Lif*$^{-/-}$ mice (Fig. 7). BQ-3020 efficiently induced expression of FGF2, Edn2 and LIF in wild-type retinas. In contrast, the Ednrb agonist failed to significantly induce FGF2 in *Lif*$^{-/-}$ mice and caused only a 70-fold increase of Edn2 expression in the knock-outs compared with the 3200-fold increase after rLIF application (Fig. 6*B*). This supports our conclusion that the signaling system can efficiently be activated only in the presence of LIF. Note that the strong upregulation of LIF in wt mice may have further supported the production of Edn2 by a positive feed forward loop resulting in a signal amplification which was only possible in wild-type but not *Lif*$^{-/-}$ animals.

Modulation of Ednrb activation was directly relevant for photoreceptor survival. Application of the Ednrb agonist resulted in a strong tendency toward protection of photoreceptors against light damage (Fig. 7*D*), whereas injection of an Ednrb antagonist (BQ-788) into eyes of VPP mice significantly increased retinal cell death (Fig. 7*E*).

LIF-induced signaling and Muller cell activation may act through rod photoreceptor cells

To investigate a potential role of photoreceptors for the signaling mechanisms induced by LIF expression, we injected rLIF into the vitreous of mice which are almost devoid of photoreceptors [3-month-old rd1 (Bowes et al., 1990)] or which have a cone-only retina [*Nrl*$^{-/-}$ (Mears et al., 2001)]. Most importantly, although expression of genes was induced upon injections, the response did not differ between rLIF and PBS-injected retinas in these two mouse strains which both lack rod photoreceptors (Fig. 8*A–F*), in contrast to injections into wild-type mice (Fig. 6*B*). This strongly suggests that a specific LIF-mediated retinal response requires rod photoreceptors.

However, it is interesting to note that basal gene expression and the response to injections differed between rd1 and *Nrl*$^{-/-}$ retinas in several points. (1) Basal expression of Edn2 in the aged rd1 mouse was >1300-fold reduced (7×10^{-4} relative to wt, Fig. 8*A*) which is comparable to the low levels of rod specific Gnat1 (rod transducin) mRNA (1×10^{-4} relative to wt) (Fig. 8*F*). This suggests that Edn2 is mainly expressed in photoreceptor cells. Since these cells are no longer present in rd1 mice, Edn2 expression levels are strongly reduced. Since the cone retinas of *Nrl*$^{-/-}$ mice showed only fivefold reduced levels of Edn2 mRNA (Fig. 8*A*) Edn2 may be expressed by both rods and cones in a wild-type retina. (2) Injections (rLIF and PBS) induced expression of GFAP much stronger in the rd1 mouse retina than in the *Nrl*$^{-/-}$ retina (Fig. 8*B*). (3) Basal levels of FGF2 mRNA were higher in the *Nrl*$^{-/-}$ retina (Fig. 8*C*). (4) The mRNA for Ednrb was increased in rd1 (and *Nrl*$^{-/-}$) retinas (Fig. 8*D*) compared with wild-type. This suggests that the receptor for Edn2 is expressed mainly in cells different from photoreceptors which is in line with the findings from Rattner and Nathans (2005). (5) LIF-R mRNA was reduced only sixfold in the rd1 mouse and 2.5-fold in the *Nrl*$^{-/-}$ mouse (Fig. 8*E*) suggesting that also cells apart from photoreceptors may express the receptor for LIF.

Discussion

Cells and tissues are equipped with endogenous protective mechanisms to cope with photoreceptor injury. Knowledge of these mech-

anisms may allow a targeted and sustained activation of intrinsic molecular pathways which could protect cells against death in a variety of degenerative diseases. Protection against cell death may ensure functionality of the tissue which is especially important in tissues depending on quiescent post-mitotic cells like brain and retina. Here we show that the retina contains a LIF-controlled signaling system which apparently aims at the maintenance of the viability of injured photoreceptors. Activation of the system involves at least photoreceptors and Muller glia cells. The absence of LIF completely blocks this endogenous defense pathway, prevents activation of Muller glia cells in response to a stress situation and keeps several signaling and survival factors at basal expression levels. This results in a drastically accelerated degeneration of visual cells.

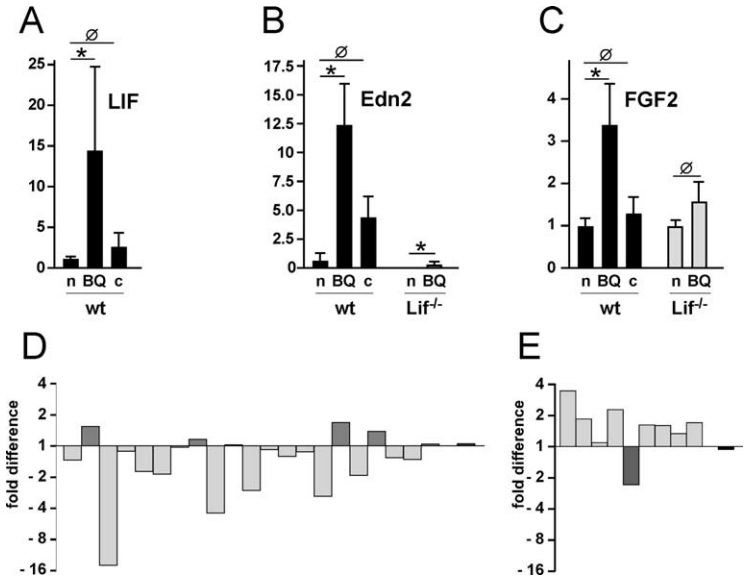

Figure 7. Modulation of Ednrb signaling influences cell survival. ***A–C***, A total of 1 μl (1 μg/μl) of BQ-3020 (BQ) or of vehicle control (H_2O) (c) was injected intravitreally into wild-type (wt) or Lif $^{-/-}$ mice as indicated. Noninjected mice (n) served as controls. Gene expression was analyzed 24 h after injection by real-time PCR on cDNA derived from total retinal RNA. $n = 3$ per treatment. ***D***, Cell death after light exposure in retinas pretreated with BQ-3020. The left eye of each wild-type mouse was injected with BQ-3020 and the right eye with vehicle (sham). Each bar represents the fold difference in cell death between compound and sham treated eyes of a single mouse. The last bar shows the result in a wild-type mouse not exposed to light. Of the 21 mice analyzed, BQ-3020 treated retinas of 15 animals were less severely affected by the light exposure than the contralateral sham treated retinas. This resulted in a strong tendency toward protection by the activation of Ednrb ($p = 0.0536$; paired Student's t test). ***E***, Cell death in retinas of VPP mice treated with BQ-788, an Ednrb antagonist. The left eye of each mouse was injected with BQ-788 and the right eyes with vehicle (sham). Analysis was 2 d after injection. Each bar represents the fold difference in cell death between compound and sham treated eyes of individual VPP mice. The last bar shows the result in a wild-type mouse to test potential toxicity of the compound. Of the 9 mice analyzed, BQ-788 treated retinas of 8 animals were more severely affected by the VPP mediated degeneration than the contralateral sham treated retinas. This resulted in a significantly lower survival of photoreceptors after the inhibition of Ednrb signaling ($p = 0.0351$; paired Student's t test). $^*p < 0.05$; $^{\varnothing}p > 0.05$. n, Noninjected; BQ, BQ-3020-injected; c, vehicle-injected.

Retinal response to injury

Rattner and Nathans (2005) recently proposed a specific retinal response to injury which involves the production and secretion of Edn2 by injured photoreceptors leading to the activation of Muller glia cells via Ednrb and to an increased expression of FGF2. FGF2 is a potent neurotrophic factor that is upregulated in various situations of retinal stress (Gao and Hollyfield, 1996; Hackett et al., 1997; Grimm et al., 2002) and that can protect retinal cells against various insults (Unoki and LaVail, 1994; Liu et al., 1998; Yamada et al., 2001; Schuettauf et al., 2004; O'Driscoll et al., 2007, 2008).

Intriguingly, this response seems not to be initiated by the damaged photoreceptors themselves but rather by a specific subset of Muller glia cells which react with the expression of LIF to photoreceptor injury (Fig. 3). What sets the LIF-expressing Muller cells apart from other Muller cells needs to be investigated. Our combined *in situ* and immunofluorescence stainings suggest that cells expressing high levels of LIF have reduced GS levels. Whether this is an artificial observation due to the staining procedure needs to be analyzed but it is interesting that GS might be down regulated in pathological situations possibly through the action of FGF2 (Kruchkova et al., 2001).

The presence of LIF is required to express Edn2 to normal levels and to induce it in the stressed retina. Since Ednrb is expressed by Muller cells (which also express LIF), Edn2 signaling may induce a positive feed forward loop resulting in an increased stimulation LIF production. This is supported by the strong stimulation of LIF expression after injection of the Ednrb agonist BQ-3020 in wild-type retinas (Fig. 7). In addition to LIF, BQ-3020 application also induced Edn2 and FGF2 expression suggesting that the full response is inducible through activation of Ednrb. Indeed, activation of Ednrb protected cells against light damage and antagonizing the receptor increased cell death in the VPP mouse (Fig. 7). This demonstrates a direct relevance of the LIF-dependent Edn2 signaling for photoreceptor survival and tissue integrity. The existence of a LIF-dependent positive feed forward loop is further supported by the reduced molecular response in retinas of *Lif*$^{-/-}$ mice after BQ-3020 application (Fig. 7).

Since LIF-R and gp130, the two receptor subunits required for LIF binding are ubiquitously expressed in the retina including photoreceptors (Ueki et al., 2008) LIF may directly target visual cells to increase Edn2 production. This notion is supported by our observation that injection of rLIF into eyes of mice without photoreceptors (aged rd1 mice) did not provoke a similar strong response (Fig. 8).

In the presence of increased LIF, the transcription factor STAT3 is strongly phosphorylated and expression of the receptor kinase Jak3 is induced. STAT3 is a downstream mediator of gp130 signaling (Ernst and Jenkins, 2004) and is able to upregulate Jak3 expression (Mangan et al., 2004). In the absence of LIF, STAT3 protein is not activated and expression of Jak3 is not elevated suggesting that LIF may indeed signal through STAT3/Jak3. Since lack of LIF also prevents upregulation of Edn2 expression, the regulation of these molecules may be correlated and directly or indirectly be coordinated by LIF-mediated stimulation of LIF-R.

Similarly to Edn2, STAT3, Jak3 and GFAP, induction of the survival factor FGF2 depends on LIF. It has been shown that injection of rLIF protects the retina against a toxic insult (Ueki et al., 2008), that injection of rLIF upregulates endogenous FGF2 in the retina (Fig. 6), that increased expression of endogenous FGF2 protects against retinal degeneration (O'Driscoll et al., 2008) and that lack of FGF2 activation correlates with accelerated photore-

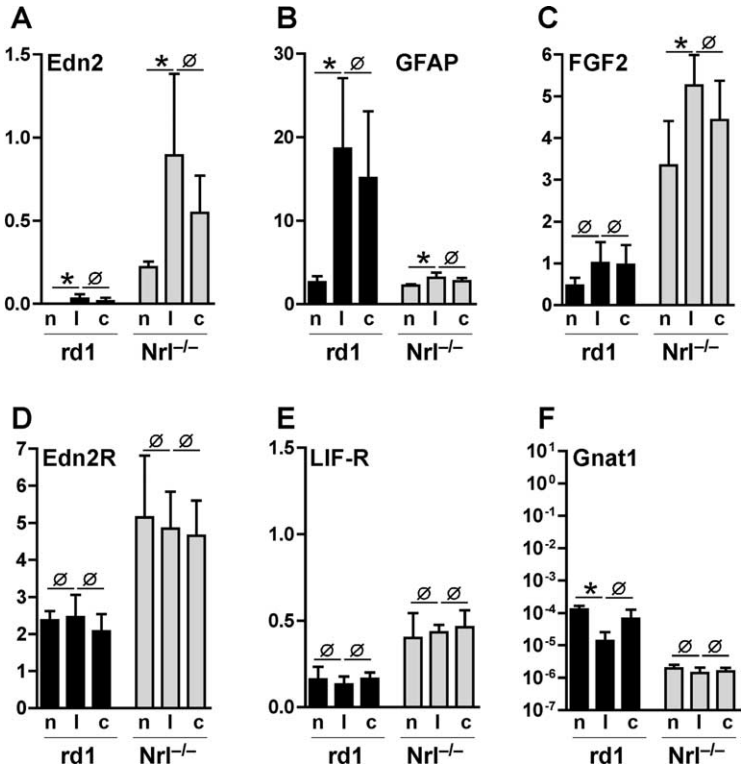

Figure 8. LIF-mediated signaling involves rod photoreceptors. One microliter (10 ng) of rLIF (l) or of vehicle control (PBS) (c) was injected intravitreally into rd1 or Nrl $^{-/-}$ mice as indicated and relative gene expression of Edn2 (***A***), GFAP (***B***), FGF2 (***C***), Ednrb (***D***) LIF-R (***E***), and Gnat1 (***F***) was tested by real-time PCR on cDNA derived from total retinal RNA. Values were expressed relative to RNA levels of untreated wild-type retinas (set to 1, data not shown). Note the logarithmic scale for Gnat1. Shown are means ± SD of $n = 6$ (rd1) or $n = 4$ (Nrl $^{-/-}$) per treatment. *$p < 0.05$; $^{\varnothing}p > 0.05$. n, Noninjected; l, rLIF-injected; c, PBS-injected.

ceptor death (Figs. 1, 5). Thus, is seems highly likely that FGF2 is a major factor in the LIF-controlled protective mechanism. Since independent studies have reported expression of FGF2 by Muller cells (Walsh et al., 2001) and by photoreceptors (Rattner and Nathans, 2005), respectively, regulation of FGF2 expression by LIF needs further detailed investigation.

Together, our results show that LIF is not only essential but also sufficient to serve as the molecular switch to activate an endogenous protective response which may depend on the production of the survival factor FGF2.

Rod photoreceptors are required for a specific LIF-mediated response

Injection of rLIF specifically induced expression of Edn2, GFAP and FGF2 (Fig. 6). Since similar injections in the absence of rod photoreceptors did not cause a significantly different response from control injections (Fig. 8), our results suggest that rod photoreceptors play an essential and specific role in the LIF response pathway. The strong but not exclusive production of Edn2 in rod photoreceptors is demonstrated by the 1300-fold reduced basal Edn2 levels in rd1 compared with wild-type mice. Since rd1 mice at this age (3 months) retain some photoreceptors, mostly cones, in the far peripheral retina (data not shown) and since the all-cone retinas of *Nrl*$^{-/-}$ mice show only fivefold reduced levels of Edn2 mRNA (Fig. 8), cones might also express Edn2 which can be stimulated by retinal injury, although not in a LIF specific way. This conclusion is supported by the lack of significant Edn2 induction in the 661W cone cell line after rLIF application *in vitro* (data not shown).

One of the most common response to retinal injury is the upregulation of the intermediate filament protein GFAP in Muller glia cells (Sarthy and Fu, 1989; Lewis and Fisher, 2003; Nakazawa et al., 2007). This is also evident during the degenerative process in the retina of the VPP mouse (Fig. 4). As for Edn2 and FGF2, expression and upregulation of GFAP depends on the presence of LIF (Figs. 4, 5). The missing induction of GFAP expression in *VPP;Lif*$^{-/-}$ mice suggests that photoreceptor degeneration cannot activate Muller cells and/or astrocytes in the absence of LIF. Injection of rLIF was sufficient to increase expression of GFAP (Fig. 6) but the upregulation was only specific in the presence of rod photoreceptors (Fig. 8). Thus, LIF may not directly target glial cells but may stimulate Muller cells through production of Edn2 in rod photoreceptors.

An endogenous, LIF-mediated neuroprotective response in the retina

Based on our data and on published results (Rattner and Nathans, 2005), we suggest a model pathway which may be used by retinal cells to protect tissue integrity and to preserve photoreceptor function in the presence of damaging stress like excessive light exposure or gene mutations. We propose that a subset of Muller glia cells senses photoreceptor damage and reacts with the upregulation of LIF. Only in the presence of increased LIF, photoreceptors induce expression of Edn2 which may then signal back to Muller glia cells. This may cause a gliosis-like reaction and the stimulation of GFAP expression. Concomitantly, the survival factor FGF2 is produced in Muller cells and/or photoreceptors aiming at the protection of visual cells from further damage (additional file 3). Whether Edn2 expression occurs in healthy or already damaged photoreceptors is currently unknown. Although it was shown that Edn2 is mainly produced in the region affected by a toxic insult (Rattner and Nathans, 2005), the specific response observed after intravitreal injection of rLIF in wild-type animals suggests that also healthy photoreceptors can activate this response pathway. It is thus probable that Edn2 production is a general response of photoreceptors to increased local concentrations of LIF.

Our work establishes LIF as the key molecule in the induction of an endogenous molecular pathway aiming at the protection of photoreceptor cells *in vivo*. This pathway may be part of a tissue defense system which increases the survival of visual cells in situations of environmental or mutational stress. Even though the endogenous potency of the system may not be sufficient to secure the viability of the cells over an extended period of time (photoreceptors in the VPP mouse die eventually), an artificial increase of its efficacy may nevertheless offer the opportunity to significantly prolong the lifespan of visual cells in human patients.

References

Bowes C, Li T, Danciger M, Baxter LC, Applebury ML, Farber DB (1990) Retinal degeneration in the rd mouse is caused by a defect in the beta subunit of rod cGMP-phosphodiesterase. Nature 347:677–680.

Bringmann A, Pannicke T, Grosche J, Francke M, Wiedemann P, Skatchkov SN, Osborne NN, Reichenbach A (2006) Muller cells in the healthy and diseased retina. Prog Retin Eye Res 25:397–424.

Elliott J, Cayouette M, Gravel C (2006) The CNTF/LIF signaling pathway

regulates developmental programmed cell death and differentiation of rod precursor cells in the mouse retina in vivo. Dev Biol 300:583–598.

Ernst M, Jenkins BJ (2004) Acquiring signalling specificity from the cytokine receptor gp130. Trends Genet 20:23–32.

Escary JL, Perreau J, Duménil D, Ezine S, Brûlet P (1993) Leukaemia inhibitory factor is necessary for maintenance of haematopoietic stem cells and thymocyte stimulation. Nature 363:361–364.

Gao H, Hollyfield JG (1996) Basic fibroblast growth factor: increased gene expression in inherited and light-induced photoreceptor degeneration. Exp Eye Res 62:181–189.

Grimm C, Wenzel A, Groszer M, Mayser H, Seeliger M, Samardzija M, Bauer C, Gassmann M, Remé CE (2002) HIF-1-induced erythropoietin in the hypoxic retina protects against light-induced retinal degeneration. Nat Med 8:718–724.

Grimm C, Wenzel A, Stanescu D, Samardzija M, Hotop S, Groszer M, Naash M, Gassmann M, Remé C (2004) Constitutive overexpression of human erythropoietin protects the mouse retina against induced but not inherited retinal degeneration. J Neurosci 24:5651–5658.

Hackett SF, Schoenfeld CL, Freund J, Gottsch JD, Bhargave S, Campochiaro PA (1997) Neurotrophic factors, cytokines and stress increase expression of basic fibroblast growth factor in retinal pigmented epithelial cells. Exp Eye Res 64:865–873.

Hafezi F, Abegg M, Grimm C, Wenzel A, Munz K, Stürmer J, Farber DB, Remé CE (1998) Retinal degeneration in the rd mouse in the absence of c-fos. Invest Ophthalmol Vis Sci 39:2239–2244.

Johnson LE, van Veen T, Ekström PA (2005) Differential Akt activation in the photoreceptors of normal and rd1 mice. Cell Tissue Res 320:213–222.

Joly S, Pernet V, Chemtob S, Di Polo A, Lachapelle P (2007) Neuroprotection in the juvenile rat model of light-induced retinopathy: evidence suggesting a role for FGF-2 and CNTF. Invest Ophthalmol Vis Sci 48:2311–2320.

Jomary C, Cullen J, Jones SE (2006) Inactivation of the Akt survival pathway during photoreceptor apoptosis in the retinal degeneration mouse. Invest Ophthalmol Vis Sci 47:1620–1629.

Kamphuis W, Dijk F, Bergen AA (2007) Ischemic preconditioning alters the pattern of gene expression changes in response to full retinal ischemia. Mol Vis 13:1892–1901.

Kim KW, Mutter RW, Cao C, Albert JM, Shinohara ET, Sekhar KR, Lu B (2006) Inhibition of signal transducer and activator of transcription 3 activity results in down-regulation of Survivin following irradiation. Mol Cancer Ther 5:2659–2665.

Kruchkova Y, Ben-Dror I, Herschkovitz A, David M, Yayon A, Vardimon L (2001) Basic fibroblast growth factor: a potential inhibitor of glutamine synthetase expression in injured neural tissue. J Neurochem 77:1641–1649.

Kubota Y, Hirashima M, Kishi K, Stewart CL, Suda T (2008) Leukemia inhibitory factor regulates microvessel density by modulating oxygen-dependent VEGF expression in mice. J Clin Invest 118:2393–2403.

Lewis GP, Fisher SK (2003) Up-regulation of glial fibrillary acidic protein in response to retinal injury: its potential role in glial remodeling and a comparison to vimentin expression. Int Rev Cytol 230:263–290.

Liu C, Peng M, Laties AM, Wen R (1998) Preconditioning with bright light evokes a protective response against light damage in the rat retina. J Neurosci 18:1337–1344.

Mangan JK, Rane SG, Kang AD, Amanullah A, Wong BC, Reddy EP (2004) Mechanisms associated with IL-6-induced up-regulation of Jak3 and its role in monocytic differentiation. Blood 103:4093–4101.

Mears AJ, Kondo M, Swain PK, Takada Y, Bush RA, Saunders TL, Sieving PA, Swaroop A (2001) Nrl is required for rod photoreceptor development. Nat Genet 29:447–452.

Mechoulam H, Pierce EA (2005) Expression and activation of STAT3 in ischemia-induced retinopathy. Invest Ophthalmol Vis Sci 46:4409–4416.

Naash M, Hollyfield JG, al-Ubaidi MR, Baehr W (1993) Simulation of human autosomal dominant retinitis pigmentosa in transgenic mice expressing a mutated murine opsin gene. Proc Natl Acad Sci U S A 90:5499–5503.

Nakazawa T, Takeda M, Lewis GP, Cho KS, Jiao J, Wilhelmsson U, Fisher SK, Pekny M, Chen DF, Miller JW (2007) Attenuated glial reactions and photoreceptor degeneration after retinal detachment in mice deficient in glial fibrillary acidic protein and vimentin. Invest Ophthalmol Vis Sci 48:2760–2768.

O'Driscoll C, Wallace D, Cotter TG (2007) bFGF promotes photoreceptor cell survival in vitro by PKA-mediated inactivation of glycogen synthase kinase 3beta and CREB-dependent Bcl-2 up-regulation. J Neurochem 103:860–870.

O'Driscoll C, O'Connor J, O'Brien CJ, Cotter TG (2008) Basic fibroblast growth factor-induced protection from light damage in the mouse retina in vivo. J Neurochem 105:524–536.

Rattner A, Nathans J (2005) The genomic response to retinal disease and injury: evidence for endothelin signaling from photoreceptors to glia. J Neurosci 25:4540–4549.

Remé CE, Grimm C, Hafezi F, Marti A, Wenzel A (1998) Apoptotic cell death in retinal degenerations. Prog Retin Eye Res 17:443–464.

Rohrer B, Demos C, Frigg R, Grimm C (2007) Classical complement activation and acquired immune response pathways are not essential for retinal degeneration in the rd1 mouse. Exp Eye Res 84:82–91.

Samardzija M, Wenzel A, Aufenberg S, Thiersch M, Remé C, Grimm C (2006a) Differential role of Jak-STAT signaling in retinal degenerations. FASEB J 20:2411–2413.

Samardzija M, Wenzel A, Naash M, Remé CE, Grimm C (2006b) Rpe65 as a modifier gene for inherited retinal degeneration. Eur J Neurosci 23:1028–1034.

Samardzija M, Wenzel A, Thiersch M, Frigg R, Remé C, Grimm C (2006c) Caspase-1 ablation protects photoreceptors in a model of autosomal dominant retinitis pigmentosa. Invest Ophthalmol Vis Sci 47:5181–5190.

Sarthy PV, Fu M (1989) Transcriptional activation of an intermediate filament protein gene in mice with retinal dystrophy. DNA 8:437–446.

Schuettauf F, Vorwerk C, Naskar R, Orlin A, Quinto K, Zurakowski D, Dejneka NS, Klein RL, Meyer EM, Bennett J (2004) Adeno-associated viruses containing bFGF or BDNF are neuroprotective against excitotoxicity. Curr Eye Res 29:379–386.

Thiersch M, Raffelsberger W, Frigg R, Samardzija M, Wenzel A, Poch O, Grimm C (2008) Analysis of the retinal gene expression profile after hypoxic preconditioning identifies candidate genes for neuroprotection. BMC Genomics 9:73.

Ueki Y, Wang J, Chollangi S, Ash JD (2008) STAT3 activation in photoreceptors by leukemia inhibitory factor is associated with protection from light damage. J Neurochem 105:784–796.

Unoki K, LaVail MM (1994) Protection of the rat retina from ischemic injury by brain-derived neurotrophic factor, ciliary neurotrophic factor, and basic fibroblast growth factor. Invest Ophthalmol Vis Sci 35:907–915.

Walsh N, Valter K, Stone J (2001) Cellular and subcellular patterns of expression of bFGF and CNTF in the normal and light stressed adult rat retina. Exp Eye Res 72:495–501.

Weerasinghe P, Garcia GE, Zhu Q, Yuan P, Feng L, Mao L, Jing N (2007) Inhibition of Stat3 activation and tumor growth suppression of non-small cell lung cancer by G-quartet oligonucleotides. Int J Oncol 31:129–136.

Wen R, Song Y, Cheng T, Matthes MT, Yasumura D, LaVail MM, Steinberg RH (1995) Injury-induced upregulation of bFGF and CNTF mRNAS in the rat retina. J Neurosci 15:7377–7385.

Yamada H, Yamada E, Ando A, Esumi N, Bora N, Saikia J, Sung CH, Zack DJ, Campochiaro PA (2001) Fibroblast growth factor-2 decreases hyperoxia-induced photoreceptor cell death in mice. Am J Pathol 159:1113–1120.

Yang Z, Quigley HA, Pease ME, Yang Y, Qian J, Valenta D, Zack DJ (2007) Changes in gene expression in experimental glaucoma and optic nerve transection: the equilibrium between protective and detrimental mechanisms. Invest Ophthalmol Vis Sci 48:5539–5548.

Zhu Y, Zhang Y, Ojwang BA, Brantley MA Jr, Gidday JM (2007) Long-term tolerance to retinal ischemia by repetitive hypoxic preconditioning: role of HIF-1alpha and heme oxygenase-1. Invest Ophthalmol Vis Sci 48:1735–1743.

Znoiko SL, Rohrer B, Lu K, Lohr HR, Crouch RK, Ma JX (2005) Downregulation of cone-specific gene expression and degeneration of cone photoreceptors in the Rpe65−/− mouse at early ages. Invest Ophthalmol Vis Sci 46:1473–1479.

6.6 Nonessential Role of β3 and β5 Integrin Subunits for Efficient Clearance of Cellular Debris after Light-Induced Photoreceptor Degeneration.

Sandrine Joly[1], Marijana Samardzija[1], Andreas Wenzel[1,2], **Markus Thiersch[1]**, and Christian Grimm[1]

[1]Laboratory for Retinal Cell Biology, Department Ophthalmology, Center for Integrative Human Physiology (CIHP) and Neuroscience Center Zurich (ZNZ), University Hospital, Zurich, Switzerland
[2]Novartis Schweiz AG, Bern, Switzerland

Published in IOVS, Vol. 50, No. 3, 1423–1432 (2009)

6.6.1 Author contribution

Design:	SJ, MS, AW and CG
Experiments:	SJ, MS, and **MT** (real time PCR)
Interpretation:	SJ, MS, AW, **MT** and CG
Manuscript:	SJ and CG
Manuscript Correction:	SJ, MS, **MT** and CG

6.6.2 Summary

The integrins $\alpha v\beta 5$ and $\alpha v\beta 3$ are involved in phagocytotic processes of a physiological normal retina. In this paper we addressed their role in the removal of cellular debris after light-induced photoreceptor apoptosis. We employed $\beta 3^{-/-}$, $\beta 5^{-/-}$ and $\beta 3^{-/-}/\beta 5^{-/-}$ mice, which exhibited a normal retinal morphology. After exposure to cytotoxic levels of white light, mutant and double mutant mice showed a pattern of progressive retinal degeneration similar to wild type controls. Further, we observed no differences in macrophage recruitment between $\beta 3^{-/-}$, $\beta 5^{-/-}$ and $\beta 3^{-/-}/\beta 5^{-/-}$ mice and wild type mice and electron microscopy revealed no disturbed clearance of photoreceptor debris. A molecular marker for lysosomal activity in RPE cells is cathepsin D (catD), which is an enzyme involved in the digestion of photoreceptor outer segments. We analyzed protein levels of the pro-form pro-cathepsin (pro-catD) and mature catD in light exposed wild type and in $\beta 5^{-/-}$ mice. Both mouse strains expressed pro-catD and cat-D

with a slight tendency of elevated mature cat-D levels in wild type mice. The tyrosine kinase receptor MerTK is localized on the apical surface as well as on microvilli of RPE cells and requires the β5 integrin for activation. MerTK mRNA levels were induced after light exposure in $\beta5^{-/-}$ mice but not in illuminated wild type animals, suggesting a potential compensatory mechanism in β5 integrin ablated mice. Focal Adhesion Kinase (FAK) is phosphorylated (pFAK) and thereby activated after light exposure in retinas of wild type mice. However, illumination of $\beta5^{-/-}$ mice caused no accumulation of pFAK suggesting a direct role of FAK in β5 integrin mediated phagocytosis. To test whether phagocytic cells might compensate for the lack of β3 and/or β5, we analyzed retinal gene expression of the monocyte chemoattractant protein-1 (MCP-1), which is involved in macrophage recruitment. Retinal MCP-1 gene expression was strongly induced 6 h after light exposure in all employed models (wild type, $\beta3^{-/-}$, $\beta5^{-/-}$ and $\beta3^{-/-}/\beta5^{-/-}$ double mutant mice) with a rapid return to normal or even below normal expression levels in $\beta5^{-/-}$ mice. The strong activation of MCP-1 in all models and the recruitment of macrophages supported our hypothesis that invading phagocytic cells can compensate for the lack of integrins. In an attempt to confirm this theory, we employed double mutant mice lacking MCP-1 and β5 integrin ($Ccl2^{-/-}/\beta5^{-/-}$) and we exposed them to light. However, illuminated double mutant mice showed neither a difference in the progress of retinal degeneration nor a disturbed macrophage invasion when compared to wild type or $Ccl2^{-/-}$ mice. This indicated that MCP-1 was not involved in macrophage recruitment after photoreceptor injury. Finally, we analyzed the mRNA expression pattern of the chemokine fractalkine (CX3CL1) and four other chemokines (CCL4, CCL5, CCL12 and CCL9), which belong to the same family as MCP-1. CCL4, CCL5 and CCL12 were induced 6 h after light exposure in all analyzed models (wild type, $\beta3^{-/-}$, $\beta5^{-/-}$, $Ccl2^{-/-}/\beta5^{-/-}$ and $\beta3^{-/-}/\beta5^{-/-}$ mice). Especially CCL4 was 3.5 to 4 times stronger induced in $\beta3^{-/-}$, $\beta5^{-/-}$, and $\beta3^{-/-}/\beta5^{-/-}$ mice compared to wild type or $Ccl2^{-/-}/\beta5^{-/-}$. However, whether these molecules are able to substitute β3 integrin and/or β5 integrin remains to be analyzed. Our results clearly show that β3 and β5 integrins are not essential for the clearance of photoreceptor debris after light exposure.

6.6.3 Manuscript

Nonessential Role of β3 and β5 Integrin Subunits for Efficient Clearance of Cellular Debris after Light-Induced Photoreceptor Degeneration

Sandrine Joly,[1] *Marijana Samardzija,*[1] *Andreas Wenzel,*[1,2] *Markus Thiersch,*[1] *and Christian Grimm*[1]

Purpose. During light-induced photoreceptor degeneration, large amounts of cellular debris are formed that must be cleared from the subretinal space. The integrins αvβ5 and αvβ3 are involved in the normal physiological process of phagocytosis in the retina. This study was conducted to investigate the question of whether the lack of β5 and/or β3 integrin subunits might influence the course of retinal degeneration and/or clearance of photoreceptor debris induced by acute exposure to light.

Methods. Wild-type, $\beta5^{-/-}$ and $\beta3^{-/-}$ single-knockout, and $\beta3^{-/-}/\beta5^{-/-}$ $Ccl2^{-/-}/\beta5^{-/-}$ double-knockout mice were exposed to 13,000 lux of white light for 2 hours to induce severe photoreceptor degeneration. Real-time PCR and Western blot analysis were used to analyze gene and protein expression, light- and electron microscopy to judge retinal morphology, and immunofluorescence to study retinal distribution of proteins.

Results. Individual or combined deletion of β3 and β5 integrin subunits did not affect the pattern of photoreceptor cell loss or the clearance of photoreceptor debris in mice compared with that in wild-type mice. Invading macrophages may contribute to efficient phagocytosis. However, ablation of the MCP-1 gene did not prevent macrophage recruitment. Several chemokines in addition to MCP-1 were induced after light-induced damage that may have compensated for the deletion of MCP-1.

Conclusions. Acute clearance of a large amount of cellular debris from the subretinal space involves invading macrophages and does not depend on β3 and β5 integrins. (*Invest Ophthalmol Vis Sci.* 2009;50:1423–1432) DOI:10.1167/iovs.08-2432

Age-related macular degeneration (AMD) is one of the most common retinal diseases that affect people older than 60 years.[1] Lipofuscin, a major correlate for the development of AMD, is generated during ageing by the incomplete decomposition of phagocytosed material from photoreceptor outer segments (POS) in the retinal pigment epithelium (RPE).[2] Efficient and complete phagocytosis is therefore necessary to ensure the integrity of a healthy retina. Various receptors on the membrane surface of the phagocyte and the phagocytic substrates mediate phagocytosis.[3] In the retina, these molecules include CD36, MerTK, and integrin receptors. On the apical membrane of the RPE layer, the CD36 scavenger receptor participates in particle recognition and regulates the internalization process of shed POS.[4–6] After POS binding to the RPE, the tyrosine kinase receptor Mer (MerTK), also present on the apical surface of RPE cells,[7] is indirectly activated via phosphorylation by focal adhesion kinase (FAK).[8] MerTK phosphorylation in turn activates the second messenger inositol 1,4,5-trisphosphate (InsP3), which initializes POS internalization and degradation.[8,9] The αvβ5 integrin receptor localizes similarly to the apical membrane of the RPE and is thought to participate in POS binding.[4,10–12] Moreover, the β5 integrin subunit and MerTK cooperate via FAK activation in the initialization step of phagocytosis.[8,11] On the other hand, αvβ3 vitronectin receptor has a crucial role in the recognition of apoptotic neutrophils and lymphocytes by blood-derived macrophages.[13] Since macrophages invade the lesioned retina and the β3 integrin complex is also found in the RPE,[14] β3 integrin may also be involved in the clearance of retinal debris.

AMD can be divided into two developmental stages: (1) the early stage is characterized by the presence of deposits called drusen[15] and the loss of photoreceptor and RPE cells leading to the development of geographic atrophy[16]; and (2) the hallmark of late AMD is choroidal neovascularization with retinal hemorrhages and increased degeneration of visual cells and the RPE.[17] Several mouse models show AMD-like features during ageing: ELOVL4 (elongation of very long-chain fatty acid) mutant transgenic mice accumulate lipofuscin and show progressive photoreceptor degeneration[18]; $Sod1^{-/-}$ (Cu, Zn-superoxide dismutase) mutant mice develop drusen, choroidal neovascularization, and RPE dysfunction[19]; the $ABCR^{-/-}$ mouse shows an enhanced accumulation of A2E, one of the most important and potentially devastating components of lipofuscin[20]; and the *mcd/mcd* mice with a mutated form of cathepsin D (catD), a lysosomal enzyme responsible for opsin degradation, accumulate phagocytosed photoreceptor material in the RPE, leading to the formation of deposits.[21] Based on defects of the phagocytic mechanism, three additional mouse models have been described: (1) ageing retinas of β5 integrin knockout mice ($\beta5^{-/-}$) display functional and histologic alterations linked to lipofuscin deposits and impairment of phagocytosis[22]; (2) apoptotic debris accumulate in the subretinal space of mice with a blocked β3 integrin receptor[23]; (3) accumulation of lipofuscin, formation of drusen, photoreceptor atrophy, and neovascularization have been reported in mice lacking monocyte chemoattractant protein (MCP)-1 (or CCL2).[24]

Since disturbed phagocytosis seems to be a major feature in retinal disease, we studied the role of β3 and β5 integrin subunits in the clearance of photoreceptor debris generated by exposure to high levels of visible light. Our data demonstrate that the individual or combined deletion of β3 and β5 integrin

From the [1]Laboratory for Retinal Cell Biology, Department of Ophthalmology, Center for Integrative Human Physiology (CIHP), University of Zürich, Zürich, Switzerland; and [2]Novartis Schweiz AG, Bern, Switzerland.

Supported by Swiss National Science Foundation Grant 3100A0-105793 and by the Vontobel Foundation.

Submitted for publication June 13, 2008; revised September 30, 2008; accepted January 14, 2009.

Disclosure: **S. Joly**, None; **M. Samardzija**, None; **A. Wenzel**, None; **M. Thiersch**, None; **C. Grimm**, None

The publication costs of this article were defrayed in part by page charge payment. This article must therefore be marked "*advertisement*" in accordance with 18 U.S.C. §1734 solely to indicate this fact.

Corresponding author: Sandrine Joly, Lab for Retinal Cell Biology, Department of Ophthalmology, University of Zürich, Frauenklinikstrasse 24, Zürich, Switzerland; sandrine.joly@usz.ch.

subunits does not lead to an accumulation of photoreceptor outer segments or to a delayed clearance of cell debris in the model of acute light-induced damage. Both macrophages and RPE cells efficiently cleared the subretinal space in mice independent of the presence or absence of β3 and/or β5 integrin subunits. Alternative receptors such as MerTK may compensate for the lack of integrin receptors. Additional deletion of MCP-1 did not influence phagocytosis or the recruitment of macrophages to the site of retinal injury. Gene expression studies show that additional chemokines are strongly induced after retinal injury and may thus account for macrophage attraction in the absence of MCP-1.

Materials and Methods

Animals and Exposure to Light

All procedures were conducted in accordance with the ARVO Statement for the use of Animals in Ophthalmic and Vision Research and with the regulations of the Veterinary Authority of Zurich. All animals were raised in cyclic light (12 hours light and 12 hours dark; 60 lux at cage level) and were homozygous for the $Rpe65_{450Leu}$ variant.[25] β3 ($\beta3^{-/-}$) and β5 ($\beta5^{-/-}$) knockout mice (generously provided by Richard O. Hynes, MIT, Cambridge, MA), $Ccl2^{-/-}$ mutant mice (Jackson Laboratory, Bar Harbor, ME), and corresponding wild-type mice (all on a mixed 129/B6 background) were maintained at the University Hospital Zurich. Double-mutant mice ($\beta3^{-/-}/\beta5^{-/-}$ and $Ccl2^{-/-}/\beta5^{-/-}$) were generated by classic breeding schemes.

Adult (8–10 weeks of age) wild-type and mutant mice were dark adapted for 12 hours, and their pupils were dilated with 1% Cyclopentolate (Cyclogyl; Alcon, Cham, Switzerland) and 5% phenylephrine (Ciba Vision, Niederwangen, Switzerland) 30 minutes before exposure to 13,000 lux of white light for 2 hours. Mice were killed at different time points ($n = 3$ for each group) after light offset and the retinas or eyes prepared.

RNA Preparation and Semiquantitative RT-PCR Analysis

Retinas were removed through a slit in the cornea and immediately frozen in liquid nitrogen. The rest of the eye (eye cup) was isolated and also frozen in liquid nitrogen. Total RNA was prepared with an RNA isolation kit (RNeasy; Qiagen, Hilden, Germany), including a digestion of the residual genomic DNA by DNase treatment. Identical amounts of RNA were used for reverse transcription using oligo(dT) and M-MLV reverse transcriptase (Promega, Madison, WI). cDNA amplifications were performed with primer pairs designed to span large intronic sequences or cover exon–intron boundaries (Table 1). Gene expression was analyzed by real-time PCR using a polymerase ready mix (LightCycler 480 SYBR Green I Master Mix; Roche Diagnostics, Indianapolis, IN) in a thermocycler (LightCycler Roche Diagnostics). For relative quantification of gene expression, mRNA levels were normalized to β-actin by using the comparative threshold cycle ($\Delta\Delta^{CT}$) method, and relative values were calculated with a respective control sample used for calibration. For the chemokine amplifications, cDNAs from three different mice were pooled and amplified in duplicate.

Light and Electron Microscopy

Eyes were fixed in 2.5% glutaraldehyde in 0.1 M cacodylate buffer (pH 7.3) at 4°C overnight. For each eye, the superior and inferior retina was prepared, washed in cacodylate buffer, incubated in osmium tetroxide for 1 hour, dehydrated in a series of increasing ethanol concentrations, and embedded in Epon 812. Semithin cross sections of 700 nm in thickness were prepared from the lower central retina, which was the most affected region in our light-induced damage model and counterstained with toluidine blue for light microscopy ($n = 3$ for each group), and 50-nm ultrathin sections were cut for electron microscopy analysis.

Immunohistochemistry

Mice were perfused transcardially with 4% paraformaldehyde (PFA) in 0.1 M phosphate buffer (PB; pH 7.4). After isolation of the eyes and removal of cornea and lens, the remaining ocular tissue was immersed for 2 hours in 4% PFA followed by cryoprotection in 30% sucrose in PBS (pH 7.4) at 4°C. The eyes were then embedded in tissue-freezing medium and frozen in a 2-methylbutane bath cooled by liquid nitrogen. Retinal sections (12 μm thick) were blocked in 3% normal goat serum and 0.3% Triton X-100 in 0.1 M PBS (pH 7.4) for 1 hour at room temperature. The sections were then incubated overnight, at 4°C, in the blocking solution containing one of the following primary antibodies: rabbit polyclonal anti-Mer (generous gift from Greg Lemke, Salk Institute for Biological Studies, La Jolla, CA), guinea pig anti-RPE65, and rat monoclonal anti-F4/80 (BMA Biomedicals, Augst, Switzerland). After they were washed with PBS, the slides were incubated with the appropriate secondary antibody coupled to Cy2 or Cy3 fluorescence for 1 hour at room temperature and mounted with anti-fade medium (10% Mowiol 4-88; vol/vol; Calbiochem, San Diego, CA), in 100 mM Tris (pH 8.5), 25% glycerol (wt/vol) and 0.1% 1,4-diazabicyclo [2.2.2] octane (DABCO). Immunofluorescent stainings were analyzed with a digital microscope (Axiovision; Carl Zeiss Meditec, Inc., Dublin, CA).

Western Blot Analysis

Retinas or eye cups ($n = 3$ per group) were homogenized in 100 mM Tris/HCl (pH 8.0) and protein content was analyzed by using the Bradford reagent. Equivalent amounts of proteins were resolved by electrophoresis on sodium dodecyl sulfate–polyacrylamide gels and transferred to nitrocellulose membranes. Membranes were blocked in 5% milk (Bio-Rad, Hercules, CA) in TBST (10 mM Tris/HCl [pH 8.0], 150 mM NaCl, and 0.05% Tween-20) for 1 hour at room temperature before they were incubated overnight at 4°C in 5% milk (in TBST) containing one of the following primary antibodies: anti-phospho-FAK_{Tyr397} (cat. No. 44-624G; Biosource, Camarillo, CA), anti-FAK (cat No. 610087; BD Transduction Laboratory, Lexington, KY), anti-phospho-$Stat3_{Tyr705}$ (cat. No. 9131; Cell Signaling, Beverly, MA), anti-Stat3 (cat. No. 9132; Cell Signaling, Beverly, MA), anti-cathepsin D (generous gift from Tom Cotter, University College Cork, Ireland), and anti-actin (cat. No. sc-1616; Santa Cruz Biotechnology, Santa Cruz, CA). After they were washed, the blots were incubated at room temperature for 1 hour with HRP-conjugated secondary antibodies. Immunoreactivity was visualized with chemiluminescence detection (Western Lightning Chemiluminescence Reagent Plus kit; Perkin Elmer, Boston, MA). Densitometry analysis was performed with NIH software and by normalizing the band intensities to β-actin values.

Table 1. Primer Pairs for Semiquantitative RT-PCR

Genes	Upstream	Downstream	Product Size (bp)
β-Actin	CAACGGCTCCGGCATGTGC	CTCTTGCTCTGGGCCTCG	153
MCP-1	GGCTCAGCCAGATGCAGTTA	CTGCTGCTGGTGATCCTCTT	108
MerTK	GAGGACTGCTTGGATGAACTGTA	AGGTGGGTCGATCCAAGG	73
CCL4	CAAGCCAGCTGTGGTATTC	AGCTGCTCAGTTCAACTCC	109
CCL5	GCTCCAATCTTGCAGTCGT	CTAGAGCAAGCGATGACAGG	165
CCL9	CAACTGCTCTTGGAATCTGG	AGGCAGCAATCTGAAGAGTC	136
CCL12	CCTCAGGTATTGGCTGGAC	GACACTGGCTGCTTGTGATT	124
CX3CL1	CCGCGTTCTTCCATTTGT	CTGTGCTGTGTCGTCTCCA	175

IOVS, March 2009, Vol. 50, No. 3

RESULTS

Effect of Lack of β3 and/or β5 Integrin Subunits on Photoreceptor Degeneration and the Clearance of Cellular Debris from the Subretinal Space

To determine whether phagocytosis or clearance of photoreceptor debris generated by acute photoreceptor degeneration were affected by the deletion of β3 and β5 integrin subunits, we examined retinal histology after exposure to bright light (Fig. 1). In wild-type mice, exposure to light induced cell death in a large number of photoreceptor cells. As early as 6 hours after light offset, the retinas displayed disorganized and disrupted POS compared with nonexposed control retinas (Fig. 1A). As photoreceptor degeneration progressed, typical pyknotic nuclei with condensed chromatin appeared in the outer nuclear layer after 1 day. After 5 days, the photoreceptor layer

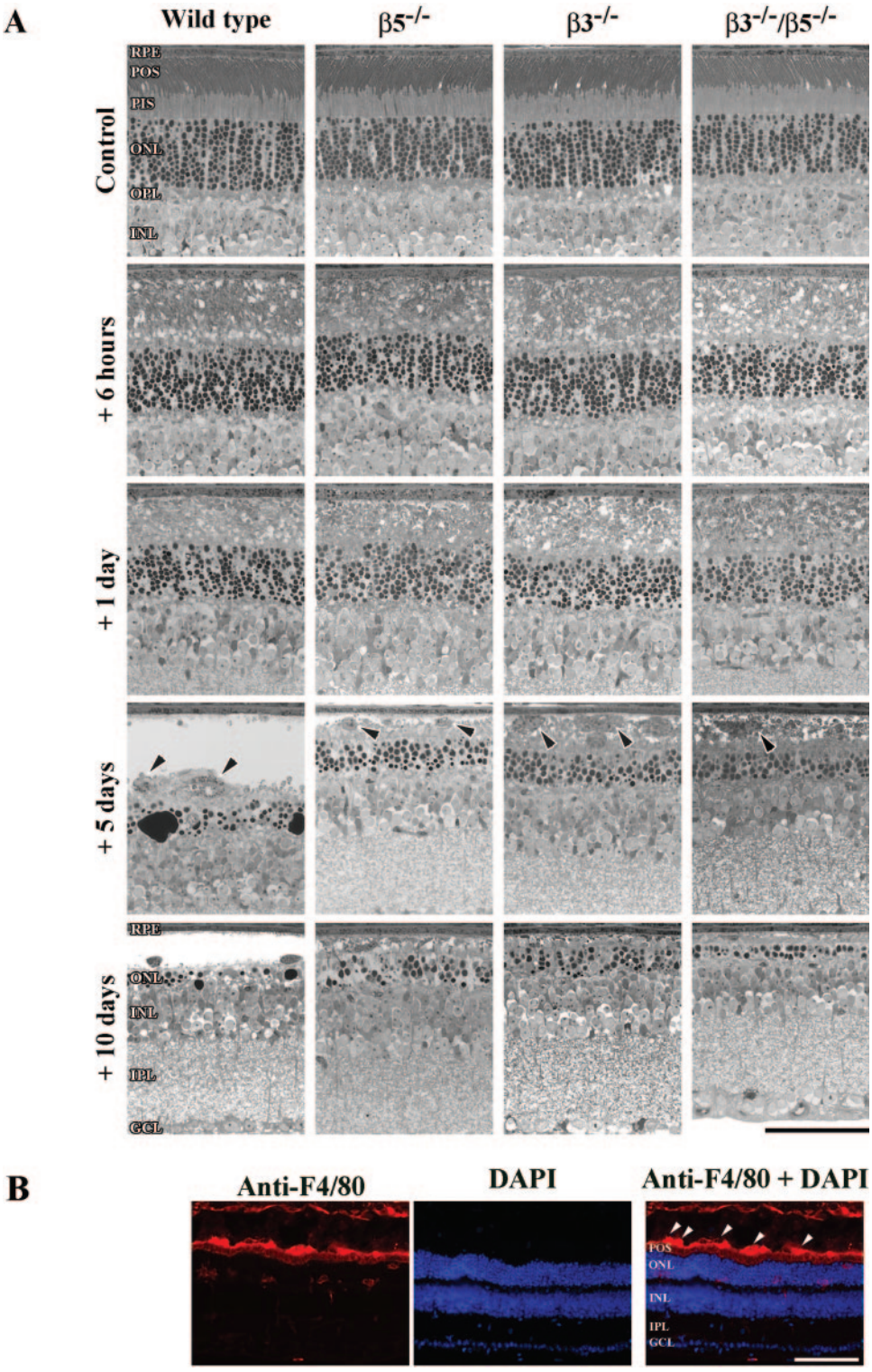

FIGURE 1. Acute clearance of photoreceptor debris from the subretinal space did not depend on β3 and β5 integrins. (**A**) Representative photomicrographs of retinas of wild-type, $\beta5^{-/-}$, $\beta3^{-/-}$, and $\beta3^{-/-}/\beta5^{-/-}$ mutant mice as indicated. Control mice were reared in a normal cyclic light environment (12 hours dark; 12 hours light) and not exposed to light. For light-induced damage, the mice were exposed to 13,000 lux for 2 hours and were killed after 6 hours, 1 day, 5 days, or 10 days, as indicated. Strong vesiculation and degradation of POS was detected already at 6 hours after light offset in all strains. The subretinal space of all strains was invaded by macrophages after 5 days (*arrowheads*). At 10 days, the photoreceptor layer (POS, PIS, and ONL) almost completely disappeared in all groups tested. (**B**) Activated macrophages, detected by the monoclonal antibody anti-F4/80, infiltrated the subretinal space of wild-type mice 3 days after exposure to light (*arrowheads*). Nuclei were stained with DAPI. RPE, retinal pigment epithelium; POS, photoreceptor outer segments; PIS, photoreceptor inner segments; ONL, outer nuclear layer; OPL, outer plexiform layer; INL, inner nuclear layer; IPL, inner plexiform layer; GCL, ganglion cell layer. Scale bar: (**A**) 50 μm; (**B**) 100 μm.

was severely degraded, whereas many macrophages colonized the subretinal space in the injured region of the retina (Fig. 1A, 1B, arrowheads). Recruitment of macrophages and their invasion of the outer retina have already been documented after light-induced damage[26,27] and in a model of chemical-induced injury.[28] Nonexposed (control) $\beta3^{-/-}$, $\beta5^{-/-}$, and $\beta3^{-/-}/\beta5^{-/-}$ mutant mice exhibited normal retinal morphology. The same pattern of light-induced photoreceptor degeneration and macrophage invasion was observed in single $\beta5^{-/-}$ and $\beta3^{-/-}$ mutants, as well as in $\beta3^{-/-}/\beta5^{-/-}$ double-mutant mice (Fig. 1). Although $\beta5$ is involved in phagocytosis and the clearance of photoreceptor tips during the physiological process of photoreceptor shedding[14] and $\beta3$ may be relevant for phagocytosis by macrophages[14,29] and/or RPE,[14] our data show that a lack of these integrin subunits, individual or combined, did not influence efficient clearance of the large amount of photoreceptor debris generated by acute exposure to light.

Moreover, evaluation of the RPE and the subretinal space in the region of photoreceptor degeneration by electron microscopy did not reveal any accumulation of photoreceptor debris (Fig. 2A). At 6 hours after exposure to light, the time of severe POS damage (Fig. 1), distorted outer segments showed strong vesiculation in all mice (Fig. 2A, middle row, arrows) instead of the regular stacks of disks apposed to the RPE in control mice (Fig. 2A, top row). In addition, POS material was observed in RPE cells suggesting ongoing phagocytosis in all the mouse strains (Fig. 2A, middle row, arrowheads). After 10 days, most of the debris in the RPE was digested, and cells of the RPE appeared normal in all the mouse strains. We did not observe accumulation of POS debris in the RPE or in the subretinal space (Fig. 2A, bottom row).

As a molecular measure of phagocytosis, protein levels of pro-cathepsin D (pro-catD) and mature cathepsin D (mature catD) were determined by Western blot analysis in eye cups of wild-type and of $\beta5^{-/-}$ mice (Fig. 2B). CatD is one of the key enzymes involved in lysosomal digestion of POS.[21,30] Levels of the pro form were comparable in the two mouse strains and seemed to increase slightly with time after exposure to light. Mature catD was also present in both mice with a slight tendency of higher levels 1 to 5 days after exposure in wild-type mice. Levels in the knockout mice remained constant throughout the period of analysis.

In conclusion, our results suggest that the time course for the clearance of photoreceptor debris from the subretinal space after acute exposure to light was not severely disturbed by the deletion of $\beta3$ and of $\beta5$ integrins. In addition, the presence of similar catD protein levels in the two mouse strains suggests no major differences in the lysosomal activity of the RPE. However, subtle differences may still exist as may be suspected in light of the minor increase in the levels of mature catD (Fig. 2B) in wild-type mice.

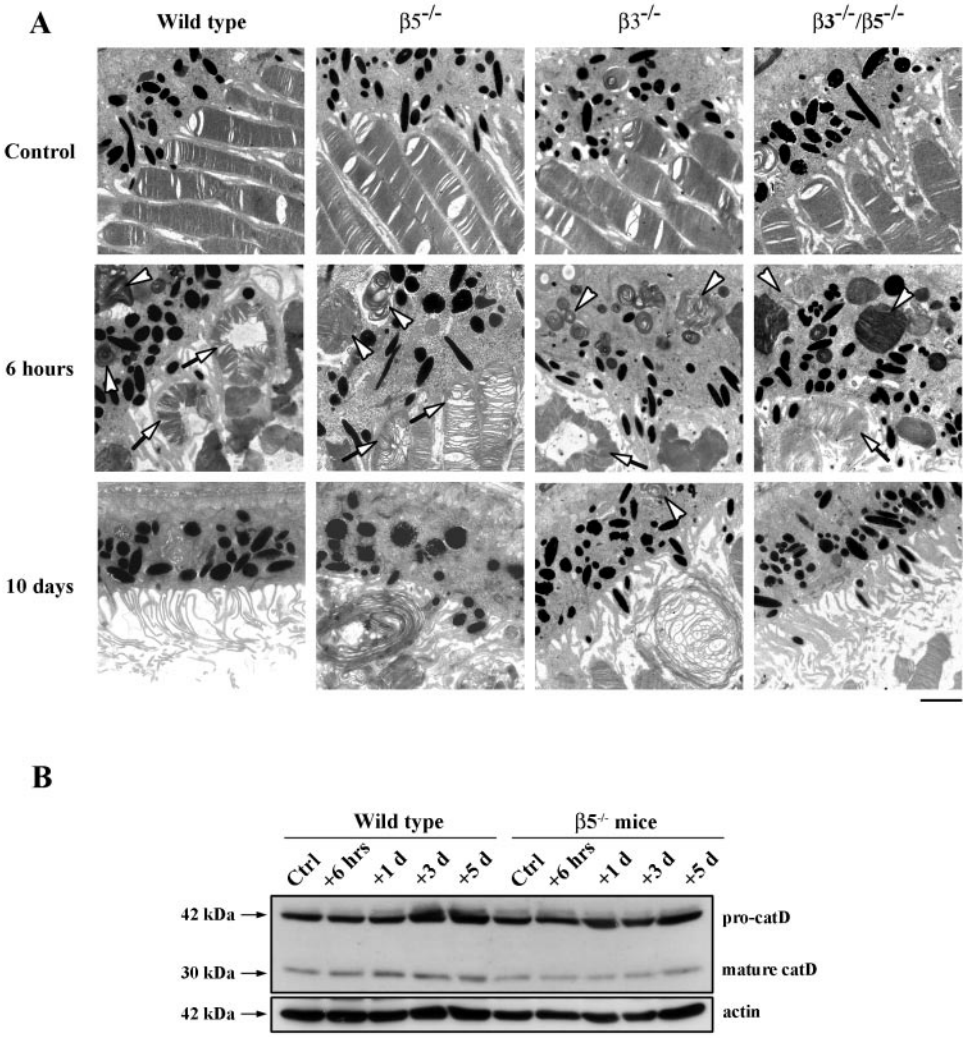

FIGURE 2. Lack of $\beta5$ and/or $\beta3$ integrins did not lead to an accumulation of photoreceptor debris after light-induced damage. (**A**) A normal ultrastructure of the RPE and POS was detected by electron microscopy in unexposed (control) wild-type, $\beta5^{-/-}$, $\beta3^{-/-}$ and $\beta3^{-/-}/\beta5^{-/-}$ mice. Six hours after exposure to light, the POS showed severe vesiculation (*arrows*), and still undigested POS were present within the RPE of all strains tested (*arrowheads*). At 10 days after exposure, no abnormal debris accumulation was detected in the RPE or the subretinal space of all mice tested. Scale bar: 2 μm. (**B**) Western blot for the pro and mature form of cathepsin D in the RPE at different time points after exposure to light as indicated. Retinas of nonexposed mice served as the control (Ctrl). Equal amounts of protein extracts from the RPE of three animals were pooled and tested for the levels of cathepsin D. Actin served as loading control.

Participation of Alternative Receptors in the Removal of Damaged Photoreceptors

A variety of membrane receptors localized on the surface of phagocytes can contribute to the elimination of apoptotic or damaged cells.[3] Among them, the tyrosine kinase receptor Mer is present on the apical surface of the RPE membrane (Fig. 3A) and on the microvilli of RPE cells[7] and thus is a salient candidate for retinal phagocytosis.[8] Since activation of MerTK protein needs the β5 integrin,[22] we first analyzed gene expression of MerTK in eye cups of the wild-type and $\beta5^{-/-}$ animals. Although the lack of β5 downregulated basal expression levels of MerTK to 43% of wild-type (not shown), exposure to light induced the expression of MerTK in eye cups of the $\beta5^{-/-}$ but not in the wild-type animals (Fig. 3B). The increased expression of MerTK in the $\beta5^{-/-}$ animals did not detectably alter the localization of the protein (data not shown). Altogether, these results suggest that RPE cells may compensate for the absence of β5 integrin by the upregulation of molecules such as MerTK to efficiently clear the subretinal space from photoreceptor debris.

Role of Integrin β5 in the Activation of Focal Adhesion Kinase after Light-Induced Damage

It has been demonstrated in vitro that phospho-FAK_{Tyr397} is activated 2 to 3 hours after challenging RPE-J cells with photoreceptor outer segments.[8] Thus, we examined phospho-FAK_{Tyr397} levels in eye cups of the wild-type mice and of the $\beta5^{-/-}$ mice (Figs. 4A–D). Light-induced damage slightly activated FAK in the RPE of the wild-type mice (Figs. 4A, 4B). In contrast, FAK was not upregulated in the RPE of the $\beta5^{-/-}$ mice (Figs. 4C, 4D) supporting a direct role of FAK in β5-mediated phagocytosis.[8] Nevertheless, a comparable increase in retinal phospho-$Stat3_{Tyr705}$ 6 hours after exposure to light showed that the retinas of both wild-type and $\beta5^{-/-}$ mice had experienced similar levels of retinal stress (Fig. 4E).

Upregulation of MCP-1 after Exposure to Light in the Retinas of All Mice

The presence of macrophages in the subretinal space of wild-type but also of the $\beta3^{-/-}$ and $\beta5^{-/-}$ mice (Fig. 1) led us to consider the possibility that these phagocytic cells compensate for a potential phagocytic defect in mice deficient of β3 and/or β5 integrins. MCP-1 (or CCL-2) has already been identified as an important factor for monocyte/macrophage recruitment in pathologic conditions such as experimental autoimmune encephalomyelitis (EAE)[31] and atherosclerosis.[32] Ablation of the MCP-1 gene also decreases microglial activation in the thalamus[33] whereas in the retina, MCP-1 deficiency may result in the formation of drusen-like deposits and other retinal features similar to AMD.[24]

MCP-1 gene expression was highly induced in the neuronal retina at 6 hours after acute exposure to light in the wild-type mice as well as in the single- and double-integrin knockout mice (Fig. 5). Of note, gene expression returned to basal or even dropped below basal levels faster in the mice lacking β5 integrin, but not in those with deleted β3 integrin. The strong activation of MCP-1 combined with the presence of macrophages in the subretinal space of retinas exposed to light supports the hypothesis that invading phagocytic cells compensated for integrin deficiency.

To address the role of MCP-1 in macrophage attraction and thus in the clearance of photoreceptor debris in the retina after light-induced damage, we generated double-mutant mice lacking both MCP-1 and β5 integrin ($Ccl\text{-}2^{-/-}/\beta5^{-/-}$). However, the time course of light-induced photoreceptor degeneration in these double-mutant mice was similar to that in the wild-type and single $Ccl2^{-/-}$ mice (Fig. 6A). In addition, phagocytic

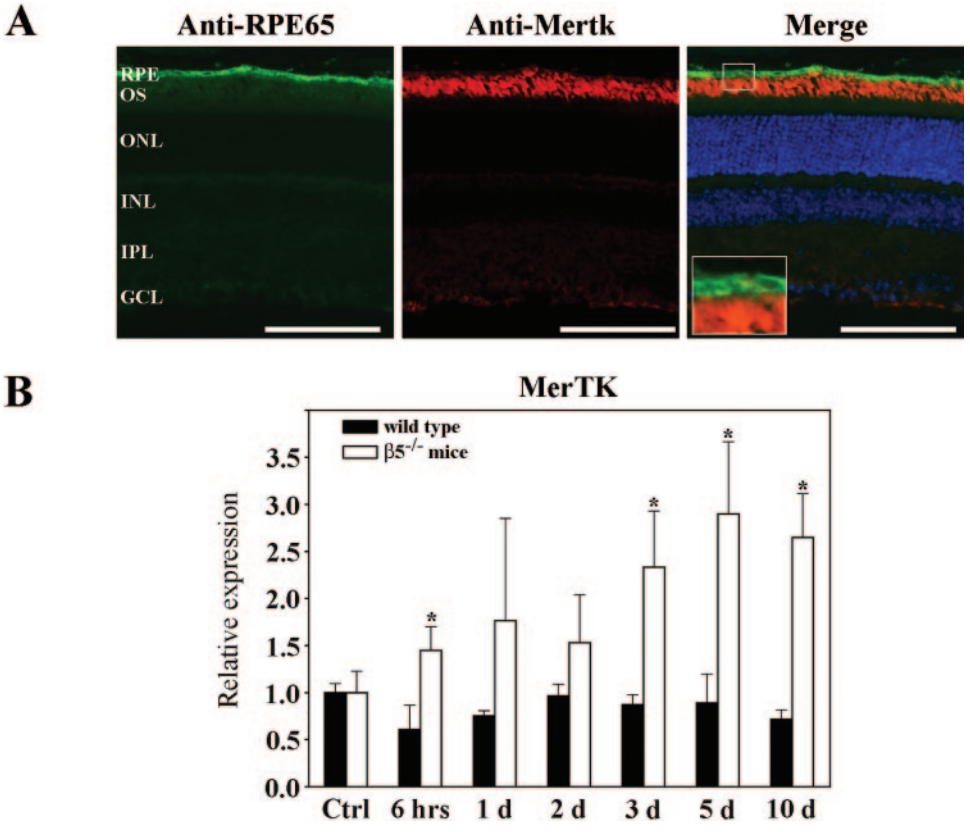

FIGURE 3. Expression of MerTK was increased in the eye cup of β5 knockout mice after exposure to light. (**A**) Localization of MerTK receptor in unexposed wild-type retinas was tested by immunofluorescence using normal fluorescence microscopy. RPE65 specifically localized to the RPE layer (*green*), whereas MerTK staining (*red*) was on the apical surface of RPE cells and on microvilli, as reported by others.[7] Nuclei have been stained with DAPI. Scale bar: 100 μm; *inset*, 33.3 μm. (**B**) Gene expression of MerTK in eye cups of wild-type and $\beta5^{-/-}$ mice as indicated. Expression was analyzed in nonexposed eye cups (Ctrl) or at different time points after exposure to light as indicated. Values were normalized to β-actin, and levels in control eye cups were set to 1 for each strain analyzed. Statistical analysis was performed with the unpaired Student's *t*-test (*$P < 0.05$) to compare MerTK retinal levels between wild-type and $\beta5^{-/-}$ mice. Amplification reactions were performed in triplicate and the results are shown as the mean ± SD ($n = 3$).

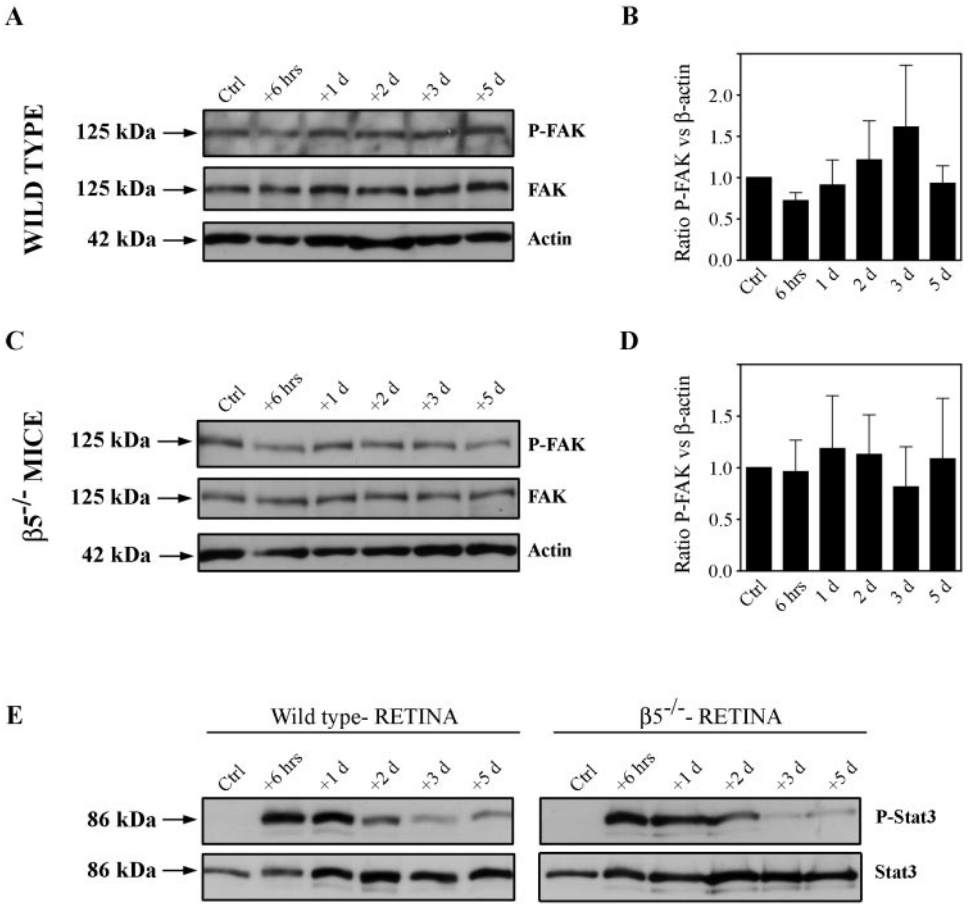

FIGURE 4. Analysis of phospho-FAK and phospho-Stat3 protein levels after exposure to light. (**A–D**) Levels of phospho-FAK$_{Tyr397}$ and total FAK protein in the eye cups of wild-type (**A**) and $\beta5^{-/-}$ mice (**C**). For protein quantifications (**B**, **D**), phospho-FAK levels were normalized to β-actin. Shown are the mean ± SEM of three independent experiments. (**E**) Levels of phospho-Stat3 protein in retinas of wild-type (*left*) and $\beta5^{-/-}$ mice (*right*). Animals were killed at the indicated time points after light offset. Ctrl: nonexposed mice. Shown are representative blots from three independent experiments.

cells appeared in the subretinal space after 5 days in all mice and by 10 days, most of the debris was cleared (Fig. 6A). It has been reported that the absence of MCP-1 is protective in a model of retinal detachment.[34] We noticed that the retinas of the Ccl-2$^{-/-}$ mice seemed to retain more photoreceptor nuclei at 5 and 10 days after exposure to light, suggesting that the absence of MCP-1 may render the retinas also less susceptible to light (Fig. 6A). However, the biochemical quantification of apoptosis did not result in a significantly different rate of cell death between the strains (data not shown).

The identity of these phagocytic cells as macrophages was verified by staining for F4/80, a specific marker for activated macrophages.[35] Three days after light offset, retinas from the Ccl2$^{-/-}$/$\beta5^{-/-}$ mice displayed F4-80-positive cells, showing that activated macrophages invaded the subretinal space of the lesioned area (Fig. 6B). These results suggest that recruitment of macrophages to injured photoreceptors does not depend on functional MCP-1 protein.

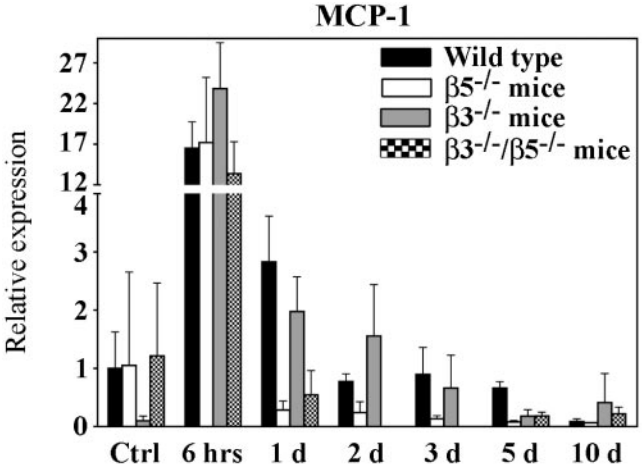

FIGURE 5. MCP-1 gene expression was strongly upregulated 6 hours after light offset in all strains. MCP-1 RNA levels were determined in retinas of wild-type, $\beta5^{-/-}$, $\beta3^{-/-}$, and $\beta3^{-/-}$ /$\beta5^{-/-}$ mice which were or were not (Ctrl) exposed to light. Analysis after exposure was at time points as indicated. Expression is shown relative to levels of control wild-type mice. Amplifications were performed in triplicates (mean ± SD; $n = 3$) and were normalized to actin values.

Role of Induced Expression of Chemokines in Macrophage Recruitment after Light-Induced Stress

Since MCP-1 was not crucial for macrophage recruitment, we hypothesized that other chemokines[36] might be able to compensate for the lack of MCP-1 and may thus be involved in the activation and attraction of macrophages. To test this possibility, we analyzed the expression of five different chemokines after exposure to light in retinas of wild-type and single- and double-knockout mice. The tested chemokines are members of the same CC chemokine family as MCP-1 except fractalkine (CX3CL1) that belongs to the CX3C family.[37] At 6 hours after light offset, CCL4 (also called MIP-1β, Fig. 7A), CCL5 (or RANTES, Fig. 7B), and CCL12 (or MCP-5, Fig. 7C) were highly induced in the neuronal retina in all mouse strains tested. Except for the Ccl2$^{-/-}$/$\beta5^{-/-}$ mutant mice in which levels were close to those of the wild-type, the $\beta3^{-/-}$, $\beta5^{-/-}$, and $\beta3^{-/-}$/$\beta5^{-/-}$ mice presented a 3.5- to 4-fold CCL4 mRNA

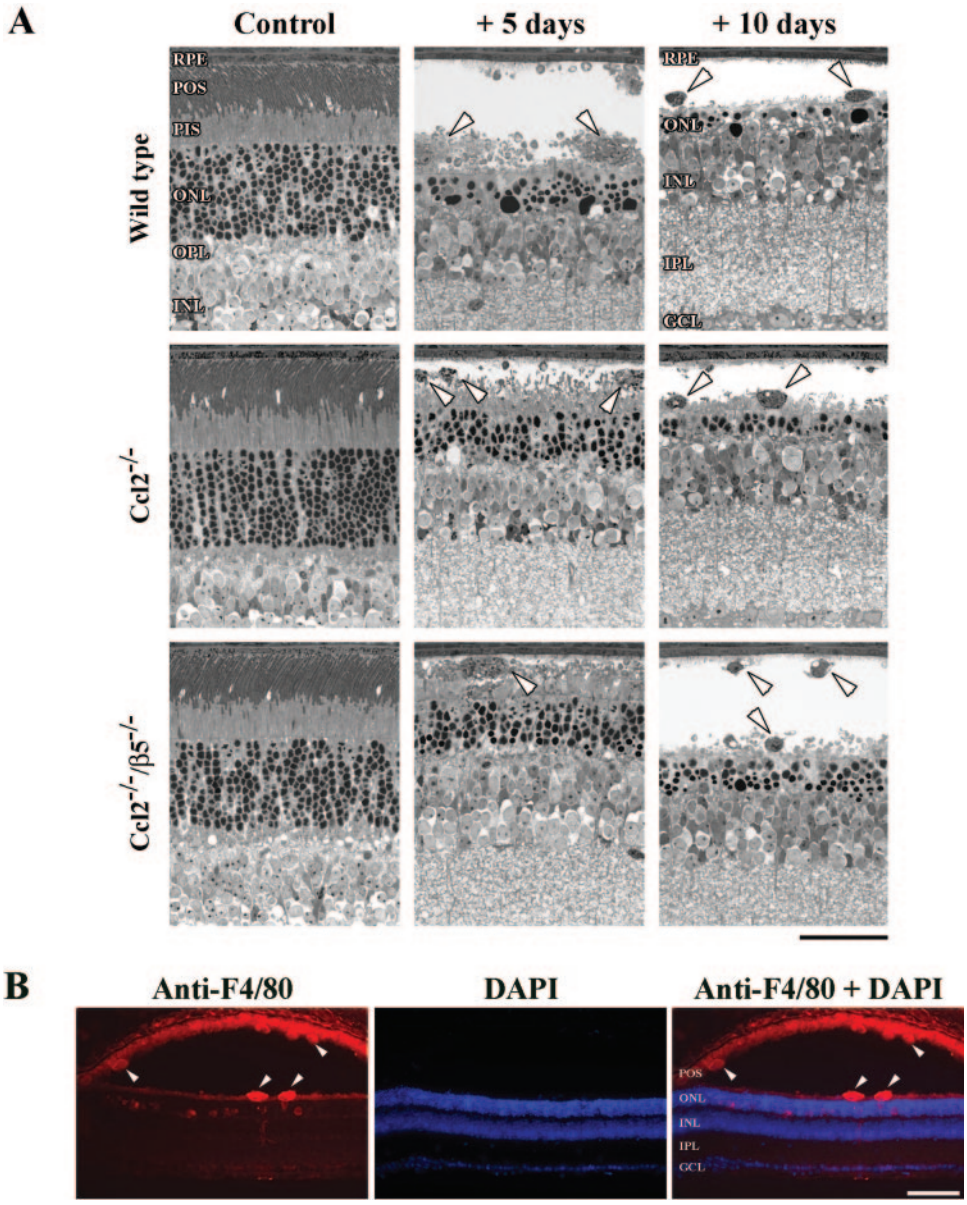

FIGURE 6. Lack of MCP-1 did not prevent infiltration of the subretinal space by macrophages after light-induced stress. (**A**) Representative photomicrographs of retinas from wild-type, $Ccl2^{-/-}$, and $Ccl2^{-/-}/\beta5^{-/-}$ mice not exposed to light (Control) showed regular morphology in all animals. At 5 and 10 days after exposure to light, the subretinal space of all mice was infiltrated by phagocytic cells (*arrowheads*) (**B**) Activated macrophages, detected by the monoclonal antibody anti-F4/80, infiltrated the subretinal space of $Ccl2^{-/-}/\beta5^{-/-}$ knockout mice 3 days after exposure to light (*arrowheads*). Nuclei were stained with DAPI. Layer abbreviations are as in Figure 1. Scale bar: (**A**) 50 μm; (**B**) 100 μm.

superinduction (over wild-type) after 6 hours (Fig. 7A). Whereas CCL4 and CCL12 mRNA levels steadily declined after the initial peak of expression, the levels of CCL5 mRNA remained high or increased even further at 2 and 3 days after exposure. In contrast, expression of CCL9 (or MIP-1γ, Fig. 7D) was regulated with different kinetics and to different levels. The mRNA levels increased later after exposure and stayed slightly elevated for up to 10 days. Of interest, mice lacking β3 or MCP-1 (with or without simultaneous lack of β5) but not those lacking only β5 exhibited increased CCL9 expression after 5 and 10 days compared with the wild-type. Expression of CX3CL1 mRNA (Fig. 7E) was not affected by the light treatment. Our data show that some chemokines were overexpressed early after exposure to light (CCL4, CCL5, and CCL12), whereas others demonstrated a delayed increase (CCL9) or were not differentially regulated at all (CX3CL1). The increased expression of some of the tested chemokines may significantly influence the migration and the recruitment of macrophages to the injured photoreceptors and may thus substitute for MCP-1 in the $Ccl2^{-/-}$ knockout mouse.

DISCUSSION

The β3 and β5 integrins were reported to have crucial roles in particle recognition/internalization[4] and in the binding of shed POS,[11,14] respectively, under physiological conditions. However, both types of integrins were not essential for the clearance of the subretinal space from debris generated after light-induced photoreceptor degeneration. The increased expression of alternate receptors present on the RPE membrane such as MerTK suggests the existence of mechanisms that can compensate for the lack of β5 and/or β3 integrins in acute situations such as light-induced damage. An important part of such mechanisms may be invading macrophages that are attracted and activated by the action of several chemokines. Since the deletion of MCP-1 ($Ccl2^{-/-}$) did not dramatically reduce macrophage infiltration, our results suggest a functional redundancy among chemokines in the retina. Expression of chemokines other than MCP-1 seems to be sufficient to attract a large number of macrophages to support efficient clearance of photoreceptor debris after

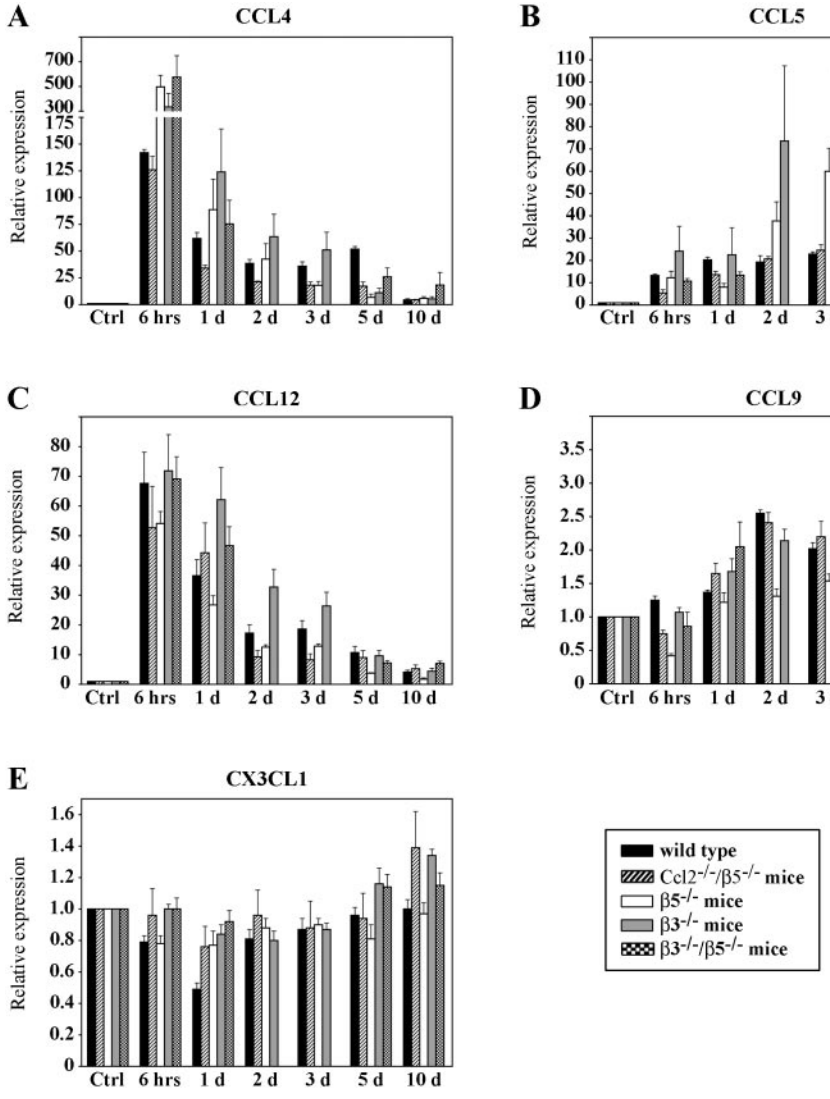

FIGURE 7. Specific regulation of chemokine expression after exposure to light. Relative RNA levels of CCL4 (**A**), CCL5 (**B**), CCL12 (**C**), CCL9 (**D**), and CX3CL1 (**E**) in retinas of wild-type, $Ccl2^{-/-}/\beta5^{-/-}$, $\beta5^{-/-}$, $\beta3^{-/-}$, and $\beta3^{-/-}/\beta5^{-/-}$ mice at various time points after exposure to light as indicated. For each strain, expression is shown relative to the levels of nonexposed mice that were set to 1. Pooled RNA of three different mice was amplified in duplicates. Results are expressed as the mean ± SD and are normalized to actin values.

light-induced damage, even in the absence of β3 and/or β5 integrin.

Similarity of Physiological Phagocytosis and Clearance of Large Amounts of Photoreceptor Debris Generated by Acute Exposure to Light

The β5 integrin receptor, localized on the apical surface of the RPE, is known to be crucial for recognition and binding of POS to the RPE membrane during physiological phagocytosis of shed photoreceptor tips.[14] It has been reported that loss of β5 integrin leads to a desynchronization of retinal phagocytosis and that during ageing, it induced retinal features similar to human AMD including decreased retinal function.[22] These functional defects were associated with morphologic impairments such as vesicular autofluorescent storage bodies and inclusion bodies in the RPE of 12-months-old $\beta5^{-/-}$ mice. In contrast, our results did not show any dysfunction in the clearance of cellular debris after acute exposure to light. This disparity may be due to the age of animals used and/or to the level of cellular stress. Whereas β5 integrin seems to be crucial for the daily task of phagocytosing shed photoreceptor segments, β5 may be dispensable in pathologic situations in which a large amount of cellular debris is generated (as after light-induced damage). The overload of material may trigger additional and β5-independent mechanisms to ensure an efficient clearing of the subretinal space. An important and integral part of such mechanisms may be the recruitment of macrophages—the classic phagocytes—to the lesion site. Thus, lack of β5 may cause more severe alterations in situations where macrophages are not recruited (as in the daily phagocytosis of shed POS) and may be less deleterious in acute situations where additional clearing mechanisms are activated.

Role of the MerTK Receptor in the Removal of Debris after Light-Induced Photoreceptor Degeneration

In vitro blockade of β5 integrin receptor with specific antibodies resulted in an 84% decrease in the uptake of photoreceptor outer segments after 2 hours, but only a 19% decrease after 5 hours,[14] suggesting that RPE cells can activate alternative routes of phagocytosis if the normal pathway has acutely been inactivated.

Many receptors are localized on the apical membrane of the RPE such as MerTK[7] and CD36.[4–6] MerTK is a tyrosine kinase that plays a critical role in the engulfment and clearance of apoptotic cells.[38] It has been demonstrated recently that MerTK cooperates with β5 integrin via FAK phosphorylation.[39,40] Another study reported that initial activation of MerTK by Gas6 ligand (growth arrest-specific gene 6) leads to phosphorylation of FAK and to a secondary activation of the β5

receptor, suggesting bidirectional interactions between MerTK and β5.[41]

Our data show that total MerTK gene expression was significantly induced in eye cups after exposure to light in $\beta5^{-/-}$ deficient mice but not in wild-type mice (Fig. 3D), suggesting that this receptor may contribute to the removal of photoreceptor debris in the absence of β5 integrin. Moreover, MerTK receptor is also expressed at the surface of macrophages,[42] which could be relevant as we observed a massive invasion of macrophages to the subretinal lesion site (Figs. 1, 6). Whether MerTK stimulates an intracellular signaling pathway in the absence of β5 integrin remains to be determined.

Involvement of Chemokines Other Than MCP-1 in Attracting and Recruiting Macrophages to the Injured Photoreceptors

Chemokines are chemotactic cytokines involved in a variety of physiological activities. They are also considered to be important mediators of pathologic responses such as leukocyte recruitment and activation, viral infections, neurodegenerative diseases,[43] tumor progression[44] and angiogenesis.[45] So far, 50 chemokines and 20 chemokine receptors have been identified indicating the existence of redundant mechanisms since each chemokine has specificity for more than one receptor and each receptor can be activated by a range of chemokines.[37]

MCP-1 has been shown to attract monocytes, activated T-cells, and natural killer cells, but not leukocytes.[46] MCP-1 is the ligand for CCR2 receptor, but it can also act via the alternative receptor CCR11.[47] Investigators in several studies have reported that MCP-1 knockout mice present a reduction in the number of recruited macrophages[24] after retinal detachment[34] and in a model of experimental autoimmune encephalomyelitis (EAE).[31] After acute light-induced damage, however, single $Ccl2^{-/-}$ and double $Ccl2^{-/-}/\beta5^{-/-}$ mouse retinas displayed many activated macrophages in the subretinal space, suggesting that MCP-1 was dispensable for the attraction of these cells to the site of injury (Fig. 6). The strong induction of other chemokines suggests that other chemotactic factors can replace MCP-1 function (Fig. 7). This is consistent with other studies that have reported such redundant mechanisms in vitro[48] and in vivo,[49] where a correlation between MCP-1, CCL3, CCL4, and CCL5 mRNA levels and the intensity of inflammation was found in autoimmune anterior uveitis associated with EAE.

In summary, our data show that β5 and/or β3 integrins do not have an essential role in the clearance of cellular debris from the subretinal space after photoreceptor degeneration induced by acute exposure to light. This finding suggests that phagocytic mechanisms during normal physiological processes such as phagocytosis of shed outer segments differ from mechanisms that are activated in situations of acute overload of cellular debris.

Acknowledgments

The authors thank Coni Imsand, Philipp Huber, and Hedwig Wariwoda for excellent technical assistance.

References

1. Fine SL, Berger JW, Maguire MG, Ho AC. Age-related macular degeneration. *N Engl J Med.* 2000;342:483–492.
2. de Jong PT. Age-related macular degeneration. *N Engl J Med.* 2006;355:1474–1485.
3. Lauber K, Blumenthal SG, Waibel M, Wesselborg S. Clearance of apoptotic cells: getting rid of the corpses. *Mol Cell.* 2004;14:277–287.
4. Finnemann SC, Silverstein RL. Differential roles of CD36 and alphavbeta5 integrin in photoreceptor phagocytosis by the retinal pigment epithelium. *J Exp Med.* 2001;194:1289–1298.
5. Ryeom SW, Sparrow JR, Silverstein RL. CD36 participates in the phagocytosis of rod outer segments by retinal pigment epithelium. *J Cell Sci.* 1996;109:387–395.
6. Sparrow JR, Ryeom SW, Abumrad NA, Ibrahimi A, Silverstein RL. CD36 expression is altered in retinal pigment epithelial cells of the RCS rat. *Exp Eye Res.* 1997;64:45–56.
7. Prasad D, Rothlin CV, Burrola P, et al. TAM receptor function in the retinal pigment epithelium. *Mol Cell Neurosci.* 2006;33:96–108.
8. Finnemann SC. Focal adhesion kinase signaling promotes phagocytosis of integrin-bound photoreceptors. *EMBO J.* 2003;22:4143–4154.
9. Strauss O. The retinal pigment epithelium in visual function. *Physiol Rev.* 2005;85:845–881.
10. Finnemann SC, Leung LW, Rodriguez-Boulan E. The lipofuscin component A2E selectively inhibits phagolysosomal degradation of photoreceptor phospholipid by the retinal pigment epithelium. *Proc Natl Acad Sci U S A.* 2002;99:3842–3847.
11. Finnemann SC. Role of alphavbeta5 integrin in regulating phagocytosis by the retinal pigment epithelium. *Adv Exp Med Biol.* 2003;533:337–342.
12. Miceli MV, Newsome DA, Tate DJ Jr. Vitronectin is responsible for serum-stimulated uptake of rod outer segments by cultured retinal pigment epithelial cells. *Invest Ophthalmol Vis Sci.* 1997;38:1588–1597.
13. Savill J, Dransfield I, Hogg N, Haslett C. Vitronectin receptor-mediated phagocytosis of cells undergoing apoptosis. *Nature.* 1990;343:170–173.
14. Finnemann SC, Bonilha VL, Marmorstein AD, Rodriguez-Boulan E. Phagocytosis of rod outer segments by retinal pigment epithelial cells requires alpha(v)beta5 integrin for binding but not for internalization. *Proc Natl Acad Sci U S A.* 1997;94:12932–12937.
15. Sarks SH, Arnold JJ, Killingsworth MC, Sarks JP. Early drusen formation in the normal and aging eye and their relation to age related maculopathy: a clinicopathological study. *Br J Ophthalmol.* 1999;83:358–368.
16. Curcio CA, Medeiros NE, Millican CL. Photoreceptor loss in age-related macular degeneration. *Invest Ophthalmol Vis Sci.* 1996;37:1236–1249.
17. Maguire MG. In: Berger JW, Fine SL, Maguire MG, eds. *Age-Related Macular Degeneration*. St. Louis: Mosby; 1999:17–30.
18. Karan G, Lillo C, Yang Z, et al. Lipofuscin accumulation, abnormal electrophysiology, and photoreceptor degeneration in mutant ELOVL4 transgenic mice: a model for macular degeneration. *Proc Natl Acad Sci U S A.* 2005;102:4164–4169.
19. Imamura Y, Noda S, Hashizume K, et al. Drusen, choroidal neovascularization, and retinal pigment epithelium dysfunction in SOD1-deficient mice: a model of age-related macular degeneration. *Proc Natl Acad Sci U S A.* 2006;103:11282–11287.
20. Mata NL, Tzekov RT, Liu X, Weng J, Birch DG, Travis GH. Delayed dark-adaptation and lipofuscin accumulation in $abcr^{+/-}$ mice: implications for involvement of ABCR in age-related macular degeneration. *Invest Ophthalmol Vis Sci.* 2001;42:1685–1690.
21. Rakoczy PE, Zhang D, Robertson T, et al. Progressive age-related changes similar to age-related macular degeneration in a transgenic mouse model. *Am J Pathol.* 2002;161:1515–1524.
22. Nandrot EF, Kim Y, Brodie SE, Huang X, Sheppard D, Finnemann SC. Loss of synchronized retinal phagocytosis and age-related blindness in mice lacking alphavbeta5 integrin. *J Exp Med.* 2004;200:1539–1545.
23. Hisatomi T, Sakamoto T, Sonoda KH, et al. Clearance of apoptotic photoreceptors: elimination of apoptotic debris into the subretinal space and macrophage-mediated phagocytosis via phosphatidylserine receptor and integrin alphavbeta3. *Am J Pathol.* 2003;162:1869–1879.
24. Ambati J, Anand A, Fernandez S, et al. An animal model of age-related macular degeneration in senescent Ccl-2- or Ccr-2-deficient mice. *Nat Med.* 2003;9:1390–1397.
25. Wenzel A, Grimm C, Samardzija M, Reme CE. The genetic modifier Rpe65Leu(450): effect on light damage susceptibility in c-Fos-deficient mice. *Invest Ophthalmol Vis Sci.* 2003;44:2798–2802.

26. Hoppeler T, Hendrickson P, Dietrich C, Reme C. Morphology and time-course of defined photochemical lesions in the rabbit retina. *Curr Eye Res.* 1988;7:849–860.
27. Gordon WC, Casey DM, Lukiw WJ, Bazan NG. DNA damage and repair in light-induced photoreceptor degeneration. *Invest Ophthalmol Vis Sci.* 2002;43:3511–3521.
28. Kaneko H, Nishiguchi KM, Nakamura M, Kachi S, Terasaki H. Characteristics of bone marrow-derived microglia in the normal and injured retina. *Invest Ophthalmol Vis Sci.* 2008;49:4162–4168.
29. Fadok VA, Savill JS, Haslett C, et al. Different populations of macrophages use either the vitronectin receptor or the phosphatidylserine receptor to recognize and remove apoptotic cells. *J Immunol.* 1992;149:4029–4035.
30. Rakoczy PE, Lai CM, Baines M, Di Grandi S, Fitton JH, Constable IJ. Modulation of cathepsin D activity in retinal pigment epithelial cells. *Biochem J.* 1997;324:935–940.
31. Huang DR, Wang J, Kivisakk P, Rollins BJ, Ransohoff RM. Absence of monocyte chemoattractant protein 1 in mice leads to decreased local macrophage recruitment and antigen-specific T helper cell type 1 immune response in experimental autoimmune encephalomyelitis. *J Exp Med.* 2001;193:713–726.
32. Braunersreuther V, Mach F, Steffens S. The specific role of chemokines in atherosclerosis. *Thromb Haemost.* 2007;97:714–721.
33. Muessel MJ, Klein RM, Wilson AM, Berman NE. Ablation of the chemokine monocyte chemoattractant protein-1 delays retrograde neuronal degeneration, attenuates microglial activation, and alters expression of cell death molecules. *Brain Res Mol Brain Res.* 2002;103:12–27.
34. Nakazawa T, Hisatomi T, Nakazawa C, et al. Monocyte chemoattractant protein 1 mediates retinal detachment-induced photoreceptor apoptosis. *Proc Natl Acad Sci U S A.* 2007;104:2425–2430.
35. Austyn JM, Gordon S. F4/80, a monoclonal antibody directed specifically against the mouse macrophage. *Eur J Immunol.* 1981;11:805–815.
36. Bajetto A, Bonavia R, Barbero S, Florio T, Schettini G. Chemokines and their receptors in the central nervous system. *Front Neuroendocrinol.* 2001;22:147–184.
37. Savarin-Vuaillat C, Ransohoff RM. Chemokines and chemokine receptors in neurological disease: raise, retain, or reduce? *Neurotherapeutics.* 2007;4:590–601.
38. Scott RS, McMahon EJ, Pop SM, et al. Phagocytosis and clearance of apoptotic cells is mediated by MER. *Nature.* 2001;411:207–211.
39. Finnemann SC, Nandrot EF. MerTK activation during RPE phagocytosis in vivo requires alphaVbeta5 integrin. *Adv Exp Med Biol.* 2006;572:499–503.
40. Nandrot EF, Finnemann S. Roles of integrin receptors in the daily phagocytosis of photoreceptor outer segment fragments by the RPE. In: Williams DS, ed. *Photoreceptor Cell Biology and Inherited Retinal Degenerations.* Mountain View, CA: World Scientific Publishing Co.; 2004:371–395. *Recent Advances in Human Biology*; vol. 10
41. Wu Y, Singh S, Georgescu MM, Birge RB. A role for Mer tyrosine kinase in alphavbeta5 integrin-mediated phagocytosis of apoptotic cells. *J Cell Sci.* 2005;118:539–553.
42. Seitz HM, Camenisch TD, Lemke G, Earp HS, Matsushima GK. Macrophages and dendritic cells use different Axl/Mertk/Tyro3 receptors in clearance of apoptotic cells. *J Immunol.* 2007;178:5635–5642.
43. Cartier L, Hartley O, Dubois-Dauphin M, Krause KH. Chemokine receptors in the central nervous system: role in brain inflammation and neurodegenerative diseases. *Brain Res Brain Res Rev.* 2005;48:16–42.
44. O'Hayre M, Salanga CL, Handel TM, Allen SJ. Chemokines and cancer: migration, intracellular signalling and intercellular communication in the microenvironment. *Biochem J.* 2008;409:635–649.
45. Yoshida S, Yoshida A, Ishibashi T, Elner SG, Elner VM. Role of MCP-1 and MIP-1alpha in retinal neovascularization during postischemic inflammation in a mouse model of retinal neovascularization. *J Leukoc Biol.* 2003;73:137–144.
46. Luster AD. Chemokines-chemotactic cytokines that mediate inflammation. *N Engl J Med.* 1998;338:436–445.
47. Schweickart VL, Epp A, Raport CJ, Gray PW. CCR11 is a functional receptor for the monocyte chemoattractant protein family of chemokines. *J Biol Chem.* 2000;275:9550–9556.
48. Lu B, Rutledge BJ, Gu L, et al. Abnormalities in monocyte recruitment and cytokine expression in monocyte chemoattractant protein 1-deficient mice. *J Exp Med.* 1998;187:601–608.
49. Adamus G, Manczak M, Machnicki M. Expression of CC chemokines and their receptors in the eye in autoimmune anterior uveitis associated with EAE. *Invest Ophthalmol Vis Sci.* 2001;42:2894–2903.

6.7 In Conditions of Limited Chromophore Supply Rods Entrap 11-*cis*-retinal Leading to Loss of Cone Function and Cell Death

Marijana Samardzija[1], Naoyuki Tanimoto[2], Corinne Kostic[3], Susanne Beck[2], Vitus Oberhauser[4], Sandrine Joly[1], **Markus Thiersch[1]**, Edda Fahl[2], Yvan Arsenijevic[3], Johannes von Lintig[4], Andreas Wenzel[1,5], Mathias Seeliger[2] and Christian Grimm[1]

[1]Laboratory for Retinal Cell Biology, Department Ophthalmology, University of Zurich
[2]Ocular Neurodegeneration Research Group, Institute for Ophthalmic Research, University of Tuebingen
[3]Unit of Gene Therapy and Stem Cell Biology, Jules Gonin Eye Hospital, University of Lausanne
[4]Institute of Biology I, Animal Physiology and Neurobiology, University of Freiburg
[5]Novartis Schweiz AG, Bern, Switzerland

Published in Human Molecular Genetics, Vol. 18, No. 7, 1266–1275 (2009)

6.7.1 Author contribution

Design:	MS, YA, JvL, AW, MSe and CG
Experiments:	MS, NT, CK, SB, VO, SJ, **MT** (assisted in establishing different mouse strains, histology) and EF
Interpretation:	MS, CK, SJ, **MT**, JvL, MSe, AW and CG
Manuscript:	MS, MSe, AW and CG
Manuscript Correction:	MS, SJ, **MT**, AW, MSe and CG

6.7.2 Summary

In the previous paper, we showed that R91W mice have low protein expression levels of RPE65, reduced 11-*cis*-retinal restoration and an impaired visual function. Here we focused on cone function and cone pathophysiology in these mice. We showed that the mRNA expression pattern of specific cone markers was reduced in R91W mice beginning with 2 weeks of age. We observed moderately reduced

expression levels of the general cone marker cone-transducin (Gnat2), a mild reduction of the green cone opsin marker (Mwl) and a strong reduction of the blue cone opsin marker (Swl). Further, we quantified the number of cones and their spatial distribution by immunohistochemistry in 4 to 40 week old R91W mice in relation to wild type controls. In general, the dorsal retina was less affected than the ventral retina. The number MWL and SWL cones declined rapidly, reaching the minima between 32 and 40 weeks of age. Gnat2 positive cells vanished in the ventral retina already in 16-week-old R91W mice and in the dorsal retina in 32-week-old mutant mice. To visualize the morphological consequences, we employed cone-specific GFP (coGFP) expressing transgenic mice. We generated double mutant R91W/coGFP mice and analyzed GFP positive cells with scanning laser ophthalmoscopy (SLO) to follow cone degeneration in individual animals *in vivo*. Our results were compared to wild type controls as well as to Rpe65$^{-/-}$/coGFP mice and showed that both RPE65 mutant strains start to lose the GFP signal at 6 weeks of age in the ventral retina. However, the loss of the GFP signal was more gradual in R91W/coGFP mice. In order to analyze the implication of 11-*cis*-retinal deficiency on cone opsin trafficking and on cone structural integrity we analyzed retinal morphology in 4-week-old R91W, Rpe65$^{-/-}$, Rpe65$^{-/-}$/rho$^{-/-}$, R19W/Rho$^{-/-}$, and Rho$^{-/-}$ mice in comparison to age-matched wild type mice. Rho$^{-/-}$ mice lack rhodopsin and do not form rod outer segments. R91W and Rpe65$^{-/-}$ mice showed shorter and less densely packed outer segments – the first evidence of retinal degeneration. All animals on Rho$^{-/-}$ background had similar retinal morphology. Further, R91W and Rpe65$^{-/-}$ mice exhibited mislocalized cone opsin, which was corrected in R19W/Rho$^{-/-}$ double mutant mice but not in Rpe65$^{-/-}$/Rho$^{-/-}$ double mutant mice. R19W/Rho$^{-/-}$ mice have low levels of 11-*cis*-retinal but due to the absence of rod outer segments and rhodopsin the chromophore is exclusively available for cones. Rpe65$^{-/-}$/Rho$^{-/-}$ mice have no 11-*cis*-retinal and the mislocalization of cone opsin persists in these animals. Therefore we concluded, that 11-*cis*-retinal was required to correctly localize cone opsin in R19W/Rho$^{-/-}$ mice and that rods and cone might compete for the uptake of 11-*cis*-retinal. To test this hypothesis, we measured photopic (rod and cone function) and scotopic (cone function) ERG in R91W mice on either Rho$^{-/-}$, Gnat1a$^{-/-}$ or Gnat1a$^{-/-}$/Rho$^{-/-}$ background. The results indicated, that residual functionality in R91W single mutant mice depends on rod function in photopic and even in scotopic conditions. The ERG response was abolished in R91W mice with an ablation of rod function (Gnat1a$^{-/-}$ background) but with normal photoreceptor outer segment formation. In contrast, we observed that R91W on Rho$^{-/-}$ background had no rod outer segments but showed an ERG response, which was caused by cones. Rods outnumber cones by 95% and our

results show that rods take up the majority of 11-*cis*-retinal. Under these conditions only rods can generate ERG responses (in scotopic and uncommonly also in photopic conditions). In the absence of rod outer segments 11-*cis*-retinal is available for cones leading to a near-normal cone response in the ERG. That confirmed our hypothesis that rods and cones compete for the binding of 11-*cis*-retinal and that rods entrap 11-*cis*-retinal under conditions of limited chromophore supply leading to cone opsin mislocalization and cone degeneration.

6.7.3 Manuscript

Human Molecular Genetics, 2009, Vol. 18, No. 7 **1266–1275**
doi:10.1093/hmg/ddp026
Advance Access published on January 15, 2009

In conditions of limited chromophore supply rods entrap 11-*cis*-retinal leading to loss of cone function and cell death

Marijana Samardzija[1,*], Naoyuki Tanimoto[2,†], Corinne Kostic[3,†], Susanne Beck[2], Vitus Oberhauser[4], Sandrine Joly[1], Markus Thiersch[1], Edda Fahl[2], Yvan Arsenijevic[3], Johannes von Lintig[4,‡], Andreas Wenzel[1,¶], Mathias W. Seeliger[2] and Christian Grimm[1]

[1]Laboratory for Retinal Cell Biology, Department of Ophthalmology, University of Zurich, Frauenklinikstr. 24, CH-8091 Zurich, Switzerland, [2]Ocular Neurodegeneration Research Group, Centre for Ophthalmology, Institute for Ophthalmic Research, University of Tuebingen, Schleichstrasse 4/3, D-72076 Tuebingen, Germany, [3]Unit of Gene Therapy and Stem Cell Biology, Jules Gonin Eye Hospital, University of Lausanne, 15 Avenue de France, CH-1004 Lausanne, Switzerland and [4]Institute of Biology I, Animal Physiology and Neurobiology, University of Freiburg, Hauptstr. 1, D-79104 Freiburg, Germany

Received December 9, 2008; Revised and Accepted January 13, 2009

RPE65 is a retinoid isomerase required for the production of 11-*cis*-retinal, the chromophore of both cone and rod visual pigments. We recently established an R91W knock-in mouse strain as homologous animal model for patients afflicted by this mutation in RPE65. These mice have impaired vision and can only synthesize minute amounts of 11-*cis*-retinal. Here, we investigated the consequences of this chromophore insufficiency on cone function and pathophysiology. We found that the R91W mutation caused cone opsin mislocalization and progressive geographic cone atrophy. Remnant visual function was mostly mediated by rods. Ablation of rod opsin corrected the localization of cone opsin and improved cone retinal function. Thus, our analyses indicate that under conditions of limited chromophore supply rods and cones compete for 11-*cis*-retinal that derives from regeneration pathway(s) which are reliant on RPE65. Due to their higher number and the instability of cone opsin, rods are privileged under this condition while cones suffer chromophore deficiency and degenerate. These findings reinforce the notion that in patients any effective gene therapy with RPE65 needs to target the cone-rich macula directly to locally restore the cones' chromophore supply outside the reach of rods.

INTRODUCTION

Vertebrate retinas have two types of photoreceptor cells mediating vision—rods and cones. Rods are exquisitely sensitive to light but cones are more critical for daytime vision, acuity and color discrimination. Despite this functional specialization, cone and rod visual pigments use the same chromophore (11-*cis*-retinal) to capture light. The retinal pigment epithelium protein of 65 kDa (RPE65) was shown to be a retinoid isomerase essential for the synthesis of 11-*cis*-retinal. RPE65 is catalyzing the conversion of all-*trans*-retinyl esters to 11-*cis*-retinol (1–3) and mutations in this enzyme cause blindness in humans (OMIM 180069) (4–6). Pathogenic mutations are found in different regions of the *RPE65* gene where they may cause RPE65-deficiency or affect protein structure, modulate docking of binding protein partners and/or influence catalytic activity (3,7).

Studies on different animal models with *RPE65* mutations indicated that the cause and timeframe of cell death is different for cones and rods. In animals with no RPE65, e.g. no

*To whom correspondence should be addressed. Tel: +41 442553872; Fax: +41 442554385; Email: marijana.samardzija@usz.uzh.ch
†These authors contributed equally to this work.
‡Present address: Department of Pharmacology, School of Medicine, Case Western Reserve University, Cleveland, OH 44106-4965, USA.
¶Present address: Novartis Pharma Schweiz AG, Monbijoustrasse 118, CH-3007 Bern, Switzerland.

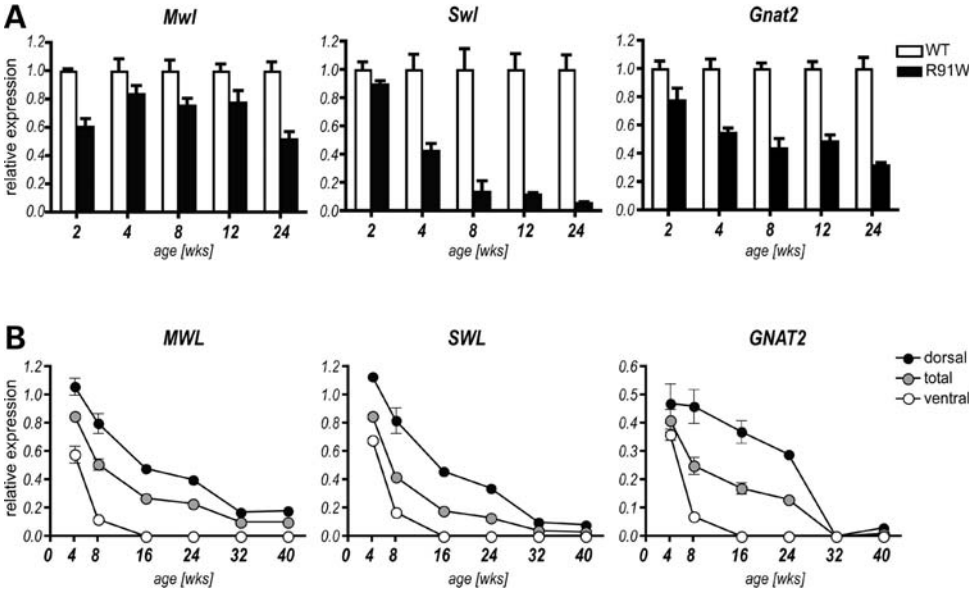

Figure 1. Geographical distribution and temporal cone loss caused by the R91W mutation. (**A**) Relative mRNA levels of cone markers as indicated. Expression was determined in retinas of wild-type and R91W mice at 4, 8, 12 and 24 weeks of age by real-time PCR. Average mRNA levels ± SD (black bars) are expressed relatively to age-matched wild-type controls, which were set to 1 (white bars). RNA isolated from three independent retinas per time-point and genotype was amplified in triplicates. (**B**) Cones were quantified by counting the number of MWL-, SWL- or GNAT2-positive outer segments in dorso-ventrally oriented retinal sections cut trough the optic nerve. Graphs represent values relative to 4-week-old R91W (set to 1) for a given cone-marker and region of the retina (mean ± SEM). An age-dependent decrease of cone marker labeling was observed resulting in an almost complete absence of cones at 32 weeks of age. GNAT2, cone-specific transducin α-subunit; MWL, middle wavelength cone opsin; SWL, short wavelength cone opsin.

11-*cis*-retinal production, rod cell death is proposed to result from constant activation of the phototransduction cascade by unliganded opsin (8). Even though this 'death signal' is present from birth, substantial degeneration occurs only late. Cones, however, appear to be more sensitive to chromophore deficiency. Patients with mutations in *RPE65* show cone photoreceptor loss early in life (9) and in Rpe65$^{-/-}$ animals, most of the cones degenerate within few weeks after birth (10).

In mouse models, early interventions, such as *Rpe65* gene replacement or retinoid supplementation therapy, rescue cone function and preserve cones against degeneration (10–13). The beneficial effect for cones has been directly attributed to 11-*cis*-retinal since it stabilizes cone opsin and promotes proper cone opsin trafficking from the inner to the outer segments (14,15). Thus, while rods are quite resistant to chromophore deficiency, cones are more vulnerable and degenerate earlier. This observation is clinically relevant and of special importance for choosing the treatment window to further improve the outcome of human trials using RPE65 gene therapy (16–19).

Studies addressing cone function and degeneration have been mainly conducted in RPE65 null animals (20–22) that lack the visual chromophore. Current literature, however, indicates that more than 50% of *RPE65* mutations in patients are missense mutations. Recently, we generated a mouse model carrying the R91W mutation in RPE65 (23), which is the most common missense mutation found in patients (24). As these patients retain useful vision at younger ages (25), it was suggested that the mutant RPE65 protein has some capability to produce 11-*cis*-retinal. In R91W mutant mice, we showed that—though strongly reduced—RPE65 protein levels enable visual function superior to that found in RPE65 null mutants. Indeed, small but detectable amounts of 11-*cis*-retinal exist in the eyes of this mouse mutant. Thus, R91W mutant mice represent a unique animal model to analyze the consequences of very limited 11-*cis*-retinal supply for retinal function and integrity.

Here, we focused on the consequences of this phenotype for cone structure and function. We analyzed the time course and characteristics of cone degeneration. Our analysis provides evidence that in R91W mutants rods and cones compete for 11-*cis*-retinal and that cone degeneration is caused by 11-*cis*-retinal insufficiency. Our data reinforce the notion that both photoreceptor types depend on RPE65 for chromophore supply.

RESULTS

Cone loss

Previous studies in Rpe65$^{-/-}$ mice have shown that cone markers are reduced very early during and after postnatal development (10). RPE65 gene delivery (12,13) or administration of 9- or 11-*cis*-retinal (10,11) prevents the downregulation of cone-specific gene expression. Recently, we have shown that 5–10% of normal 11-*cis*-retinal levels can be produced by a hypomorphic RPE65 protein carrying the R91W amino acid substitution (23). Here, we sought to analyze the influence of these limited amounts of 11-*cis*-retinal on the structural and functional integrity of cones.

To approach this question, we examined the mRNA levels of cone-specific markers in 2-, 4-, 8-, 12- and 24-week-old R91W and corresponding wild-type animals (Fig. 1A). All of the tested cone markers {cone opsins [middle wavelength

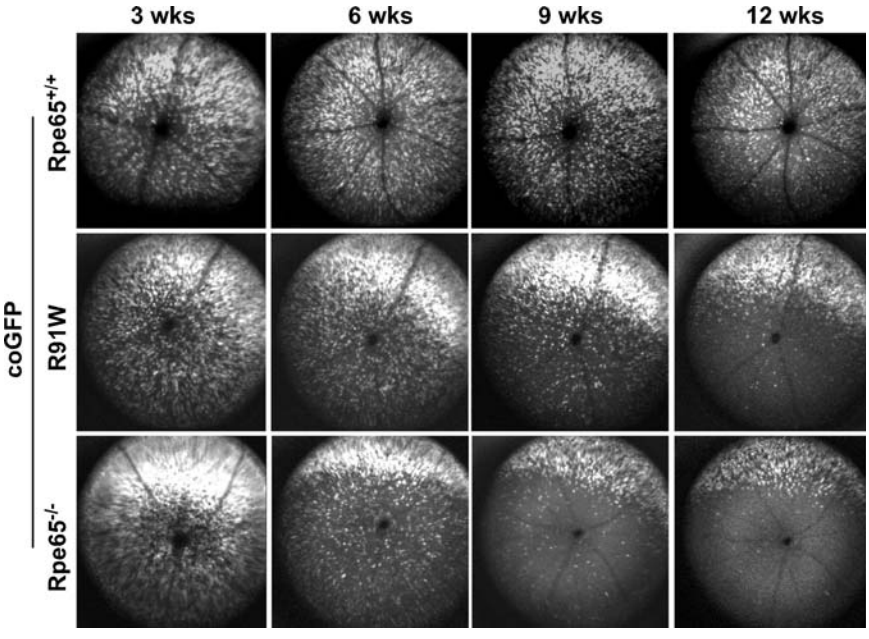

Figure 2. Cone loss in different Rpe65-related genetic backgrounds monitored *in vivo*. Fundus autofluorescence in transgenic mouse lines expressing GFP under the control of a cone opsin promotor (coGFP) monitored by scanning laser ophthalmoscope. Mice were on different *Rpe65* genetic backgrounds (R91W, $Rpe65^{-/-}$ and $Rpe65^{+/+}$) as indicated and fluorescence was monitored every 3 weeks until 12 weeks of age in individual animals. Shown is the temporal cone loss of one representative mouse per genotype. coGFP transgenic mice on a wild-type *Rpe65* background served as controls ($Rpe65^{+/+}$). Note the accelerated loss of GFP-positive cells from the ventral retina in $Rpe65^{-/-}$ animals.

(Mwl), short wavelength (Swl)] and cone-specific transducin α-subunit (Gnat2)} were transcriptionally downregulated as early as at 2 weeks of age (Fig. 1A). At 4 weeks, a time-point when the mouse retina can be considered mature, Mwl expression was reduced to 84% and by 24 weeks only 52% of wild-type levels were expressed (Fig. 1A). The Swl marker was even more suppressed: to 43% in 4 weeks and to only 6% in 24-week-old animals (Fig. 1A). Expression of Gnat2 was 55–32% in the period between 4 and 24 weeks of age (Fig. 1A).

We additionally analyzed these cone markers by immunostaining in 4-, 8-, 16-, 24-, 32- and 40-week-old animals and quantified the number of cells positive for MWL, SWL and GNAT2-cone opsin (Fig. 1B). A dorso-ventral gradient of expression for MWL and SWL cones has been described in the mouse retina (26). In order to analyze the spatial localization of cones, we quantified their dorso-ventral distribution in R91W (see Materials and Methods) at different ages. We compared it with 4-week-old wild-type animals, levels of them were set to 1 for dorsal, ventral or total expression, respectively (Fig. 1B). By 4 weeks of age, the most prominent cone loss occurred in the ventral retina of R91W mice. The MWL and SWL opsins were reduced to 58% and 68%, respectively, when compared with age-matched wild-type controls (Fig. 1B). Degeneration continued gradually and by 16 weeks of age the ventral retina of R91W mice was virtually cone-free. The dorsal retina was better preserved at all time-points tested (Fig. 1B). At 4 weeks of age, the amount of MWL- and SWL-positive cells in the dorsal retina was comparable to the respective wild-type control (Fig. 1B). However, at the same time-point, GNAT2 levels were already reduced to 47%. After 32 weeks of age, GNAT2-positive cells were no longer detectable, but some MWL- and SWL-positive cells remained in the retina of R91W mice (Fig. 1B).

The SWL cones seemed to be the most strongly affected cone type. Between 4 and 8 weeks of age, more than 50% of SWL-positive cells were lost in R91W animals. In the same period, MWL dropped only by 40% (Fig. 1B and data not shown). By 24 weeks, only 16% of SWL cones remained in the upper central retina, whereas 27% of the MWL marker was still detectable.

To explore the morphological consequences of *Rpe65* mutations on cone degeneration *in vivo*, we crossed R91W and $Rpe65^{-/-}$ strains to a transgenic mouse line that expresses GFP under the control of a cone opsin promoter (coGFP). Using scanning laser ophthalmoscopy (SLO) to detect GFP-positive cells, we followed cone degeneration in individual animals in the period between 3 and 12 weeks of age (Fig. 2). The loss in GFP signal, which is representative for cone loss, was detectable already at 6 weeks of age in both *Rpe65* mutant mice strains (Fig. 2). The signal started disappearing in the ventral region of both $Rpe65^{-/-}$;coGFP and R91W;coGFP retinas. However, while in $Rpe65^{-/-}$;coGFP mice this polarization was strongly established already at 6 weeks of age, degeneration in R91W;coGFP mice proceeded more gradually (Fig. 2). These data are in line with our immunostaining data showing that the ventral retina in R91W animals was more prone to cone degeneration.

Cone opsin mislocalization

Lack of 11-*cis*-retinal has been implicated in improper cone opsin trafficking, which results in cone degeneration (14,15).

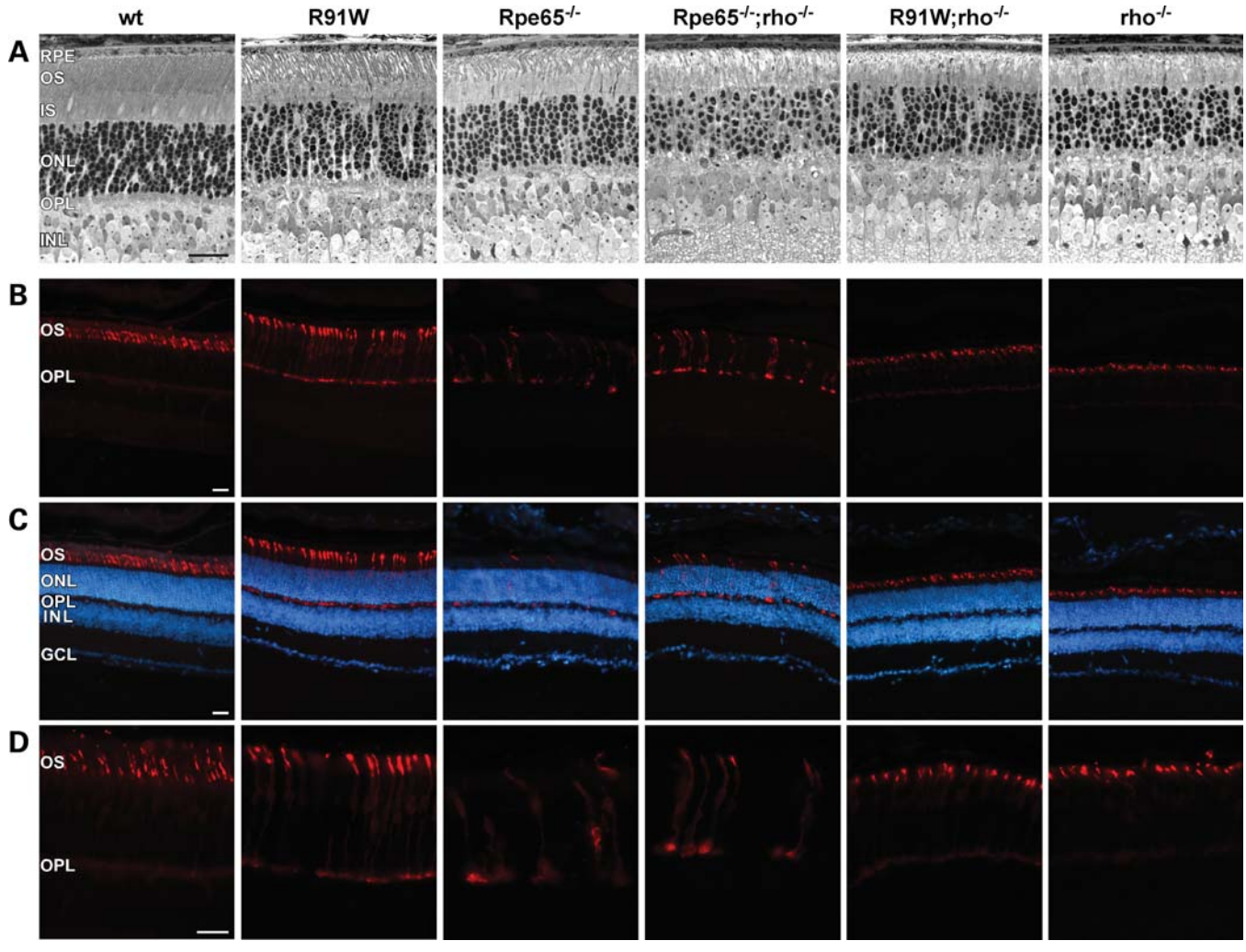

Figure 3. Cone opsin mislocalization in R91W can be corrected by ablation of rod outer segments. Retinas of age-matched 4-week-old mice of indicated genotypes were analyzed. (**A**) Representative light microscopy photographs of retinal morphology. Note the slightly better structural preservation of OS in R91W mice when compared with Rpe65$^{-/-}$ single mutant animals. No gross morphological differences were detected among the three rho$^{-/-}$ mutant mice (Rpe65$^{-/-}$;rho$^{-/-}$, R91W;rho$^{-/-}$ and rho$^{-/-}$, respectively). (**B**–**D**) Immunolocalization of short wavelength (SWL) cone opsin at low (B and C) or higher magnification (D). Nuclei were contrasted with DAPI (C). SWL localized to cone outer segments in all animals. However, in R91W, Rpe65$^{-/-}$ and Rpe65$^{-/-}$;rho$^{-/-}$ mutant mice, SWL mislocalized to synaptic termini in the OPL, to perinuclear regions in the ONL and to cellular protrusions. Ablation of rod OS almost fully corrected cone opsin mislocalization in R91W;rho$^{-/-}$ but not in Rpe65$^{-/-}$;rho$^{-/-}$ mice. RPE, retinal pigment epithelium; OS, outer segments; IS, inner segments; ONL, outer nuclear layer; OPL, outer plexiform layer; INL, inner nuclear layer; GCL, ganglion cell layer. Scale bar: 25 μm.

Here, we analyzed the impact of limited amounts of 11-*cis*-retinal in R91W mice on cone structural integrity.

We compared retinal morphology of six different mouse strains (wt, R91W, Rpe65$^{-/-}$, Rpe65$^{-/-}$;rho$^{-/-}$, R91W;rho$^{-/-}$ and rho$^{-/-}$) at 4 weeks of age by light microscopy (Fig. 3A) and by immunostaining of SWL cone opsin (Fig. 3B–D). As previously reported (23), the first signs of degeneration were already present in 4-week-old R91W and Rpe65$^{-/-}$ animals, visible as shorter and less densely packed photoreceptor outer segments (Fig. 3A). We did not observe major differences in retinal morphology between animals on a rho$^{-/-}$ background (Fig. 3A: Rpe65$^{-/-}$;rho$^{-/-}$, R91W;rho$^{-/-}$ and rho$^{-/-}$). Immunostaining of SWL cone opsin in wild-type mice predominantly stained cone outer segments (Fig. 3B: wt). In R91W animals, however, a strong cone opsin specific signal was detected in synaptic termini of photoreceptors and a weak perinuclear staining was observed as well (Fig. 3B: R91W). In Rpe65$^{-/-}$ animals, the staining pattern was qualitatively similar, but signal intensity was generally lower and a reduced number of cones was observed (Fig. 3B: Rpe65$^{-/-}$).

Using rho$^{-/-}$ animals, we analyzed if structural ablation of rod opsin in R91W would rescue cone opsin mislocalization. This experiment was based on the assumption that 11-*cis*-retinal in R91W;rho$^{-/-}$ mice should be exclusively available to cones. As control we used Rpe65$^{-/-}$;rho$^{-/-}$ animals. Ablation of rod opsin in Rpe65$^{-/-}$ mice had no effect on cone opsin mislocalization (Rpe65$^{-/-}$;rho$^{-/-}$, Fig. 3B). In contrast, in R91W;rho$^{-/-}$ mice cone opsin localization was corrected. It was absent from synaptic termini and was found predominantly in outer segments (Fig. 3B: R91W;rho$^{-/-}$). Immunostaining was almost indistinguishable

to single rho$^{-/-}$ mutants (Fig. 3B: rho$^{-/-}$). To ensure that the rescue effect was indeed mediated by 11-*cis*-retinal, we measured the retinoid content in the eyes by HPLC. The 11-*cis*-retinal and 11-*cis*-retinol content in eyes of 4-week-old R91W;rho$^{-/-}$ animals was 1.3 ± 0.1 pmol and 2.0 ± 0.2 per eye, respectively. No 11-*cis*-retinoids were detected in Rpe65$^{-/-}$;rho$^{-/-}$ double mutants, as reported before (27).

These data show that the rescue of cone opsin misrouting observed in R91W;rho$^{-/-}$ can be attributed to the availability of 11-*cis*-retinal for cones and suggest that cone and rod opsins compete for the chromophore.

Photoreceptor competition for the visual chromophore

Ablation of RPE65 eliminates cone function and remnant minimal visual responses can be attributed to rod function due to the presence of 9-*cis*-retinal forming the visual pigment isorhodopsin (28,29). R91W mice contain similar amounts of 9-*cis*-retinal, but, in contrast to Rpe65$^{-/-}$ mice, they also contain small amounts of 11-*cis*-retinal (23). Accordingly, R91W mice are about 1 log unit more sensitive to light than Rpe65$^{-/-}$ animals under scotopic conditions. The previous functional analysis indicated that electroretinogram (ERG) responses under photopic conditions might originate from both the rod and the cone system (23).

To specifically analyze the source of vision in R91W mutant mice, we abolished rod function by intercrossing R91W knock-in mice with rho$^{-/-}$ and Gnat1a$^{-/-}$ knock-out animals. Rho$^{-/-}$ mice do not develop rod outer segments but initially have a functional cone system (30). Similar to the rho$^{-/-}$ animals, Gnat1a$^{-/-}$ mice have no rod function, but, in contrast, develop normal rod outer segments with regular rod opsin content (31). Functionally, retinas of both mouse strains are considered as pure-cone retinas.

We generated R91W;Gnat1a$^{-/-}$, R91W;rho$^{-/-}$ double mutant and R91W;Gnat1a$^{-/-}$;rho$^{-/-}$ triple mutant mice and compared their function with the previously described wild-type, R91W, rho$^{-/-}$ and Rpe65$^{-/-}$;rho$^{-/-}$ mutant mice (Fig. 4A and B). By the time of analysis all mice were 4-weeks-old.

Dark-adapted ERG intensity series revealed severely depressed responses in R91W mice when compared with wild-type animals (Fig. 4A). As expected, minimal or no responses were detected under the same conditions in rho$^{-/-}$ and all double- or triple mutant animals due to the functional rod ablation (Fig. 4A).

To analyze light-adapted responses, photopic flash intensity series across a 6-log-unit intensity range was recorded in all genotypes (Fig. 4B). Under this condition, R91W and rho$^{-/-}$ revealed very similar threshold sensitivities when compared with wild-type animals (Fig. 4B). Ablation of rod opsin in R91W (R91W;rho$^{-/-}$) caused an additional reduction in sensitivity by 1–1.5 log units (Fig. 4B). However, photoreceptors in R91W;Gnat1a$^{-/-}$ animals lacking rod function but not rod outer segments were much more desensitized than those in R91W;rho$^{-/-}$ animals (Fig. 4B). The severely desensitized response in R91W;Gnat1a$^{-/-}$ was not due to the absence of 11-*cis*-retinal. HPLC analysis of the retinoid content showed that R91W;Gnat1a$^{-/-}$ contained 23.7 ± 1.2 pmol, an amount similar to single mutant R91W animals (23). The mice with the better ERG response (R91W;rho$^{-/-}$) had with 1.3 ± 0.1 pmol per eye an even lower content of 11-*cis*-retinal.

The strongly reduced cone function in R91W;Gnat1a$^{-/-}$ mice thus suggested that in the presence of limited amounts of 11-*cis*-retinal, a substantial cone response can only be generated when rod opsin is absent, as in R91W;rho$^{-/-}$. To prove this principle and to exclude a possible non-specific effect of the Gnat1a$^{-/-}$ knock-out, we generated R91W;rho$^{-/-}$; Gnat1a$^{-/-}$ triple mutant animals. We found no difference in ERG responses between R91W;rho$^{-/-}$ double mutants and R91W;Gnat1a$^{-/-}$;rho$^{-/-}$ triple mutants (Fig. 4B). This suggests that 11-*cis*-retinal in the triple mutants (captured by rod opsin in R91W;Gnat1a$^{-/-}$ animals) was now available for cone opsins, supporting our hypothesis of chromophore competition between rod and cone opsins.

DISCUSSION

We investigated the cone pathophysiology resulting from 11-*cis*-retinal chromophore insufficiency. We show that (i) the R91W mutation causes an early progressive geographic cone atrophy characterized by a ventro-dorsal gradient of degeneration; (ii) cone opsin mislocalization in R91W can be rescued by the ablation of rod opsin; and (iii) ablation of rod opsin increases cone function in R91W mice.

Collectively, our data suggest that rod opsin and cone opsins compete for the available 11-*cis*-retinal. In a situation where only 5–10% of normal 11-*cis*-retinal levels are present (as in R91W knock-in mice), rod opsins seem to entrap almost all available chromophore. Rods may outcompete cones for the following reasons: (i) rods massively outnumber cones; (ii) cones have much higher spontaneous rate of chromophore dissociation (32); and (iii) rods have a larger interface with the RPE—the major chromophore source.

The genetic ablation of rod opsin increases the availability of 11-*cis*-retinal and improves cone structure and function. The functional ablation of rods (Gnat1a$^{-/-}$), however, is not sufficient, which indicates that rod opsin works as a 'chromophore trap' preventing cone function. Our data also suggest that mice do not have an isolated pathway of chromophore delivery specifically reserved for cones, as supply of the chromophore for both rods and cones depends on RPE65.

Cone degeneration

We have shown by RT–PCR, immunofluorescence and by SLO *in vivo* analysis that cone markers were very early reduced in R91W mice. The ventral retina was most affected and was devoid of cones already at 16 weeks of age. It has been shown that the mouse ventral retina is enriched with SWL opsin (26) and SWL cones are reduced particularly early in Rpe65$^{-/-}$ mice (10). Thus, the geographic cone atrophy was qualitatively similar in Rpe65 knock-out and R91W knock-in mice, and in both models, SWL cones were more severely affected than MWL cones. However, in Rpe65 knock-outs, SWL cone opsin loss is more pronounced: Swl RNA is reduced by more than 50% by 2 weeks of age as

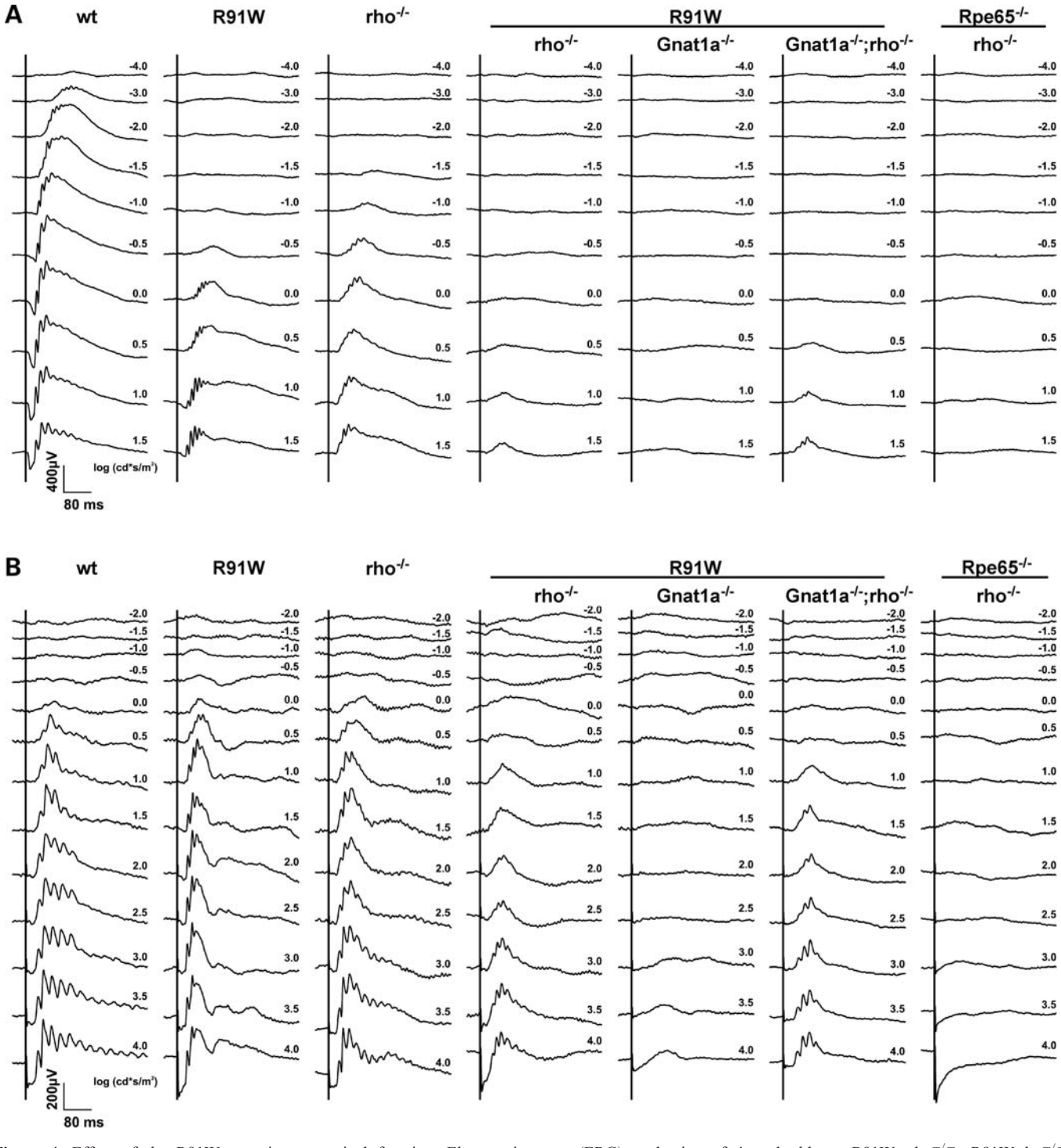

Figure 4. Effect of the R91W mutation on retinal function. Electroretinogram (ERG) evaluation of 4-week-old wt, R91W, rho$^{-/-}$, R91W;rho$^{-/-}$, R91W;Gnat1a$^{-/-}$, R91W;Gnat1a$^{-/-}$; rho$^{-/-}$ and Rpe65$^{-/-}$;rho$^{-/-}$ mice. Single flash ERGs were recorded under dark-adapted (**A,** scotopic) and light-adapted (**B,** photopic) conditions. Additional deletion of rho in R91W and Rpe65$^{-/-}$ enabled the examination of pure cone function in the absence of the rod system. The vertical lines indicate the timing of the light flash. Note that an initial negative deflection in the higher intensity range (above 1.5 log cd*s/m^2) is no retinal electrical response but a flash artifact.

opposed to a reduction of only 10% in R91W knock-in mice (data not shown). We also qualitatively followed cone cell loss in *Rpe65* mutant animals *in vivo* by using coGFP reporter animals monitored by SLO. This method clearly showed that the cone degeneration in R91W animals proceeded more slowly than in Rpe65 knock-out mice. It has to be noted that in coGFP mice the interference with opsin production or the presence of GFP is toxic for cones leading to their death by

1272 Human Molecular Genetics, 2009, Vol. 18, No. 7

about 6 months of age, with some individual variability (data not shown). Thus, the true cone status can probably only be assessed during the first 3–4 months of life in coGFP line and the respective double mutant mice.

By immunofluorescence, we noted a certain discrepancy in the number of GNAT2-positive cells when compared with MWL- and SWL-positive cells. At 4 weeks of age, fewer GNAT2-positive cells were detected than MWL or SWL cone opsin-labeled cells. This discrepancy cannot be explained by lower transcriptional activity since mRNA expression of all three markers was comparably reduced. This may suggest that in degenerating cone cells, GNAT2 is less stable than cone opsins. A similar conclusion has been made in young Lrat$^{-/-}$ and Rpe65$^{-/-}$ mice where posttranslational degradation was accounted as reason for decreased GNAT2 levels (14).

Cone preservation and chromophore competition

An optimal delivery of 11-*cis*-retinal to cones has not only a functional relevance but it is also important for structural maintenance. Recently, Rohrer *et al*. (11) detected cone opsin mislocalization in Rpe65$^{-/-}$ mice, which was corrected upon administration of 11-*cis*-retinal or 9-*cis*-retinal (10). Based on this observation, the authors hypothesized that cones degenerate because of opsin mislocalization as a direct result of 11-*cis*-retinal starvation. Later studies showed, accordingly, that viral *Rpe65* gene delivery to Rpe65$^{-/-}$ mice restores cones (12,13). Finally, 11-*cis*-retinal has been shown to be necessary for proper trafficking of membrane-associated phototransduction components from their synthesis place within the cone inner segment trough the connecting cilium to the outer segment (14,15). Retinas of R91W single mutant mice receive only small [5–10% of wild-type (23)] amounts of 11-*cis*-retinal. Immunostaining data show that cone opsin in R91W animals is mislocalized. This suggests that most of the available 11-*cis*-retinal in R91W animals ends up in rods for reasons explained below. This further suggests that chromophore starvation is the cause for cone degeneration in R91W animals—as for 11-*cis*-retinal deficient animals (Rpe65$^{-/-}$ and Lrat$^{-/-}$). As R91W mice show delayed cone cell death compared with retinas without measurable chromophore, our results suggest that the progression of cone degeneration can be directly attributed to the degree of impairment in the 11-*cis*-retinal supply.

In situations of limited 11-*cis*-retinal delivery to retinas where the vast majority of photoreceptors are rods, the chromophore uptake is presumably based on a 'tyranny of the majority' rule, which favors rods over cones. Additionally, the thermodynamic stability of the rod opsin–11-*cis*-retinal holocomplex and the proximity to the RPE as chromophore source are also favorable for rods. A competition between rods and cones for limited amounts of chromophore has been previously described *in vitro* (33). In our experiments, a competitive chromophore uptake is supported by the fact that even though comparable amounts of 11-*cis*-retinal were found in age-matched R91W single- and R91W;Gnat1a$^{-/-}$ double mutant animals (~25 pmol/retina), the later had only minor ERG responses under photopic conditions. This argues that most 11-*cis*-retinal in R91W is captured by rods and that the retinal function recorded in R91W under photopic conditions is almost completely mediated by the rod system. However, once rod opsin is taken away from the retina (R91W;rho$^{-/-}$), the chromophore becomes available for cones resulting in a corrected opsin targeting and improved cone function.

Biochemical and genetic evidence for a cone-specific visual cycle involving Müller cells and a novel type of all-*trans* to 11-*cis*-retinol isomerase different from RPE65 has been provided by studies in lower vertebrates (34–39). Our findings, however, argue against separate pathways for the regeneration of cone and rod-specific visual pigments in mice. We clearly show that chromophore delivery to both rods and cones strictly depends on functional RPE65. In R91W animals, no other enzyme can compensate for the reduced activity of the mutant RPE65 protein and only the physical ablation of the rod opsin chromophore trap enables cones to incorporate sufficient chromophore to correctly localize opsin to their outer segments. Furthermore, a putative RPE65-independent cone visual cycle involving Müller cells would be expected to be only marginally affected by the presence or absence of rods. The close physical proximity of cones and Müller cells would strongly reduce the ability of rods to compete for the chromophore regenerated and released by Müller cells specifically for cones. Indirect evidence from the current literature further supports the importance of a strong RPE65 activity for proper cone function: the RPE65 protein from the cone-dominated chicken retina is a more efficient enzyme than RPE65 from rod dominated species (40) and the central RPE layer of primates, which localizes to the cone-rich area of the retina, has a higher RPE65 protein expression and activity than the RPE in the peripheral, rod-rich retina (9). The resulting wealthier local chromophore pool in the macular region of the primate retina and the physical absence of competing rods in this area may less strongly affect chromophore delivery to cones in the fovea allowing initial useful central vision by RPE65 patients. Since blue cones are reported to be completely absent from the central fovea (41,42) and instead localize to rod-dominated regions of the human retina, blue cones may be in strong competition with rods for the available chromophore. Except for the macular region, the human retina is comparable to the mouse retina. Our data thus predict that blue cones in RPE65 patients may be more affected than other cone types and may not receive sufficient chromophore for proper function and survival, as proposed recently (43). Indeed, most patients with RPE65 mutations report early difficulties with blue color vision (43,44) supporting our conclusions based on the R91W mouse model.

To our knowledge, this study demonstrates for first time an *in vivo* competition between rods and cones for limited amounts of chromophore and its functional and pathological consequences. Our data suggest that a successful RPE65 gene therapy requires delivery of the functional gene directly to the macular region to supply cones and avoid chromophore 'theft' by rods. The importance of 11-*cis*-retinal supplementation for the cone structural integrity should also be considered in therapies aiming at the inhibition/slowing of the visual cycle and thus at the reduction of available chromophore in the retina. It seems important that the therapeutic value of visual cycle inhibitor compounds should be carefully

Human Molecular Genetics, 2009, Vol. 18, No. 7 1273

Table 1. PCR primers used for genotyping

Genotype	Forward (5′–3′)	Reverse (5′–3′)	Size (bp)
coGFP	CAATTAAGAGATCAGGTAGTGT	AGTTCACCTTGATGCCGTTCTT	641
R91W[a]	GCTGGTCTTGCCTGTATCA	GTCAGAGACAGTGCTGTGTT	998
Rpe65$^{+/+}$	GATGTGGGCCAGGGCTCTTTGAAG	CCCAATAGTCTAGTAATCACAGATG	546
Rpe65$^{-/-}$	GATGTGGGCCAGGGCTCTTTGAAG	GGGAACTTCCTGACTAGGGGAGG	459
Rho$^{+/+}$	TCTCTCATGAGCCTAAAGCT	ATGCCTGGAACCAATCCGAG	470
Rho$^{-/-}$	TCTCTCATGAGCCTAAAGCT	TTCAAGCCCAAGCTTTCGCG	310
Gnat1a$^{+/+}$	TATCCACCAGGACGGGTATTC	GCGGAGTCATTGAGCTGGTAT	387
Gnat1a$^{-/-}$	TATCCACCAGGACGGGTATTC	GGGAACTTCCTGACTAGGGGAGG	273

[a]PCR product was additionally cut with *Taq*I restriction enzyme. Expected fragments: 998 bp for knock-in and 619 bp + 379 bp for wild-type.

evaluated with respect to their specific impact on the cone visual system.

MATERIALS AND METHODS

Mice

All procedures concerning animals were in accordance with the regulations of the Veterinary Authority of Zurich and with the statement of 'The Association for Research in Vision and Ophthalmology' for the use of animals in research. All animals were raised in cyclic light (12:12 h; 60 lux at cage level).

The knock-in mice with an amino acid exchange of Arg by Trp at position 91 in *Rpe65* (R91W) on a 129S6 genetic background are described elsewhere (23). Wild-type (129S6), Rpe65$^{-/-}$ (20), rho$^{-/-}$ (30) and Gnat1a$^{-/-}$ (31) mice were maintained at the animal facility of the University Hospital Zurich. Transgenic coGFP mice, in which GFP expression is driven by 5′ regulatory sequences of the human red pigment (45), were provided by Thomas Hughes, Yale University School of Medicine. The R91W;rho$^{-/-}$, Rpe65$^{-/-}$;rho$^{-/-}$, R91W;Gnat1a$^{-/-}$, R91W;rho$^{-/-}$;Gnat1a$^{-/-}$, R91W;coGFP, Rpe65$^{-/-}$;coGFP double- or triple transgenic mice were generated by classical breeding schemes. Genotyping was performed by PCR on tail genomic DNA using primer pairs indicated in Table 1.

Histology

Animals were sacrificed and the nasal part of the eye was marked for orientation. The enucleated eyes were fixed overnight in 2.5% glutaraldehyde prepared in 0.1 M cacodylate buffer and processed as described previously (46). Semi-thin sections (0.5 μm) of Epon-embedded tissue were prepared from the central retina, counterstained with methylene blue and analyzed using a light microscope (Axiovision, Zeiss, Jena, Germany).

Immunofluorescence and cone quantification

Animals were sacrificed, their eyes were marked nasally, enucleated and perforated at the cornea to allow better penetration of the fixative. After fixation for 1 h in 4% PFA (in PBS), the eyes were cryoprotected in 25% sucrose solution. The eyes were embedded in albumin from hen egg white (Fluka, Buchs, Switzerland) and cut dorsal to ventral through the optic nerve head. Sections (14 μm) were blocked for at least 1 h at room temperature in PBS containing 0.2% Triton X-100 and 10% normal goat serum (Dako, Zug, Switzerland) or 10% normal horse serum (Jackson Immunoresearch, Westgrove, PA, USA). Primary antibodies used were: rabbit anti-GNAT2 (Santa Cruz, CA, USA), goat anti-SWL-opsin (Santa Cruz) and rabbit anti-MWL (Chemicon, Temecula, CA, USA). The immunostaining procedure was as described previously (13).

The most transversal sections, cut through the optic nerve, were chosen to quantify the number of cells positive for GNAT2, MWL and SWL-cone opsins, respectively. The immunoreactive outer segments were counted from periphery to periphery using a BX60 microscope equipped for epifluorescence (Olympus Suisse SA, Aigle, Switzerland) and coupled to the analySIS® 3.0 software (Soft Imaging System). At least four eyes per condition and genotype were analyzed.

RNA isolation and RT–PCR

RNA isolation from retinal tissue and reverse transcription were performed as described previously (46). cDNA quantification was carried out by real-time PCR using the LightCycler 480 Sybr Green I Master kit and a LightCycler 480 instrument (Roche, Mannheim, Germany). cDNAs were amplified with primers for Gnat2, Mwl and Swl (10) and normalized to actin (47). The normalization was done using the comparative threshold cycle method. Relative values were calculated using a suitable calibrator sample. At least three retinas from three different animals were analyzed in triplicates.

Electroretinography

Electroretinograms were recorded binocularly according to previously described procedures (28,48) in anesthetized mice with dilated pupils using a Ganzfeld bowl, DC amplifier, and a PC-based control and recording unit (Multiliner Vision; VIASYS Healthcare GmbH, Hoechberg, Germany). Recordings were obtained in both scotopic (dark-adapted overnight) and photopic (light-adapted 10 min at 30 cd/m^2) conditions.

Single white-flash stimulus intensity ranged from −4 to 1.5 log cd*s/m^2 under scotopic and from −2 to 4 log cd*s/m^2 under photopic conditions, divided into 10 and 13 steps, respectively. For the intensities from 2 to 4 log cd*s/m^2, a

Mecablitz 60CT4 flash gun (Metz, Germany) added to the Ganzfeld bowl was used. Ten responses per intensity were averaged with an inter-stimulus interval of either 5 or 17 s (>1 cd*s/m^2). At least three animals per genotype were analyzed at 4 weeks of age.

In vivo monitoring by SLO

Scanning laser ophthalmoscopy was obtained in dark-adapted GFP-positive mice according to procedures reported previously (49). Mice were anesthetized with ketamine (66.7 mg/kg) and xylazine (11.7 mg/kg) and the pupils were dilated with tropicamide eye drops (Mydriaticum Stulln, Pharma Stulln, Stulln, Germany). SLO was performed with a Heidelberg Retina Angiograph (Heidelberg Engineering), a confocal scanning-laser ophthalmoscope. Laser wavelength used for fundus autofluorescence visualization was 488 nm.

HPLC determination of retinoids

Mice were dark-adapted overnight. All the following steps were carried out under dim red light. Animals were sacrificed, and lens and vitreous were removed from the eye through a slit in the cornea. The rest of the tissue including the retina and eyecup was snap frozen in liquid nitrogen until further analysis. Retinoid extraction and HPLC analysis was performed as described previously (50). Three to six animals per genotype were analyzed.

ACKNOWLEDGEMENTS

We thank Coni Imsand, Philipp Huber and Hedwig Wariwoda for excellent technical assistance.

Conflict of Interest statement. None declared.

FUNDING

This work was supported by the Swiss National Science Foundation (grant numbers 3100A0-105793 and 3100A0-117760), the University of Zurich Forschungskredit and the ProVisu foundation.

REFERENCES

1. Jin, M., Li, S., Moghrabi, W.N., Sun, H. and Travis, G.H. (2005) Rpe65 is the retinoid isomerase in bovine retinal pigment epithelium. *Cell*, **122**, 449–459.
2. Moiseyev, G., Chen, Y., Takahashi, Y., Wu, B.X. and Ma, J.X. (2005) RPE65 is the isomerohydrolase in the retinoid visual cycle. *Proc. Natl Acad. Sci. USA*, **102**, 12413–12418.
3. Redmond, T.M., Poliakov, E., Yu, S., Tsai, J.Y., Lu, Z. and Gentleman, S. (2005) Mutation of key residues of RPE65 abolishes its enzymatic role as isomerohydrolase in the visual cycle. *Proc. Natl Acad. Sci. USA*, **102**, 13658–13663.
4. Marlhens, F., Bareil, C., Griffoin, J.M., Zrenner, E., Amalric, P., Eliaou, C., Liu, S.Y., Harris, E., Redmond, T.M., Arnaud, B. *et al.* (1997) Mutations in RPE65 cause Leber's congenital amaurosis. *Nat. Genet.*, **17**, 139–141.
5. Gu, S.M., Thompson, D.A., Srikumari, C.R., Lorenz, B., Finckh, U., Nicoletti, A., Murthy, K.R., Rathmann, M., Kumaramanickavel, G., Denton, M.J. and Gal, A. (1997) Mutations in RPE65 cause autosomal recessive childhood-onset severe retinal dystrophy. *Nat. Genet.*, **17**, 194–197.
6. Morimura, H., Fishman, G.A., Grover, S.A., Fulton, A.B., Berson, E.L. and Dryja, T.P. (1998) Mutations in the RPE65 gene in patients with autosomal recessive retinitis pigmentosa or leber congenital amaurosis. *Proc. Natl Acad. Sci. USA*, **95**, 3088–3093.
7. Bereta, G., Kiser, P.D., Golczak, M., Sun, W., Heon, E., Saperstein, D.A. and Palczewski, K. (2008) Impact of retinal disease-associated RPE65 mutations on retinoid isomerization. *Biochemistry*, **47**, 9856–9865.
8. Woodruff, M.L., Wang, Z., Chung, H.Y., Redmond, T.M., Fain, G.L. and Lem, J. (2003) Spontaneous activity of opsin apoprotein is a cause of Leber congenital amaurosis. *Nat. Genet.*, **35**, 158–164.
9. Jacobson, S.G., Aleman, T.S., Cideciyan, A.V., Heon, E., Golczak, M., Beltran, W.A., Sumaroka, A., Schwartz, S.B., Roman, A.J., Windsor, E.A. *et al.* (2007) Human cone photoreceptor dependence on RPE65 isomerase. *Proc. Natl Acad. Sci. USA*, **104**, 15123–15128.
10. Znoiko, S.L., Rohrer, B., Lu, K., Lohr, H.R., Crouch, R.K. and Ma, J.X. (2005) Downregulation of cone-specific gene expression and degeneration of cone photoreceptors in the Rpe65-/- mouse at early ages. *Invest. Ophthalmol. Vis. Sci.*, **46**, 1473–1479.
11. Rohrer, B., Lohr, H.R., Humphries, P., Redmond, T.M., Seeliger, M.W. and Crouch, R.K. (2005) Cone opsin mislocalization in Rpe65-/- mice: a defect that can be corrected by 11-*cis* retinal. *Invest. Ophthalmol. Vis. Sci.*, **46**, 3876–3882.
12. Chen, Y., Moiseyev, G., Takahashi, Y. and Ma, J.X. (2006) RPE65 gene delivery restores isomerohydrolase activity and prevents early cone loss in Rpe65−/− mice. *Invest. Ophthalmol. Vis. Sci.*, **47**, 1177–1184.
13. Bemelmans, A.P., Kostic, C., Crippa, S.V., Hauswirth, W.W., Lem, J., Munier, F.L., Seeliger, M.W., Wenzel, A. and Arsenijevic, Y. (2006) Lentiviral gene transfer of RPE65 rescues survival and function of cones in a mouse model of Leber congenital amaurosis. *PLoS Med.*, **3**, e347.
14. Zhang, H., Fan, J., Li, S., Karan, S., Rohrer, B., Palczewski, K., Frederick, J.M., Crouch, R.K. and Baehr, W. (2008) Trafficking of membrane-associated proteins to cone photoreceptor outer segments requires the chromophore 11-*cis*-retinal. *J. Neurosci.*, **28**, 4008–4014.
15. Fan, J., Rohrer, B., Frederick, J.M., Baehr, W. and Crouch, R.K. (2008) Rpe65−/− and lrat−/− mice: comparable models of leber congenital amaurosis. *Invest. Ophthalmol. Vis. Sci.*, **49**, 2384–2389.
16. Bainbridge, J.W., Smith, A.J., Barker, S.S., Robbie, S., Henderson, R., Balaggan, K., Viswanathan, A., Holder, G.E., Stockman, A., Tyler, N. *et al.* (2008) Effect of gene therapy on visual function in Leber's congenital amaurosis. *N. Engl. J. Med.*, **358**, 2231–2239.
17. Maguire, A.M., Simonelli, F., Pierce, E.A., Pugh, E.N.J., Mingozzi, F., Bennicelli, J., Banfi, S., Marshall, K.A., Testa, F., Surace, E.M. *et al.* (2008) Safety and efficacy of gene transfer for Leber's congenital amaurosis. *N. Engl. J. Med.*, **358**, 2240–2248.
18. Hauswirth, W., Aleman, T.S., Kaushal, S., Cideciyan, A.V., Schwartz, S.B., Wang, L., Conlon, T., Boye, S.L., Flotte, T.R., Byrne, B. and Jacobson, S.G. (2008) Treatment of Leber congenital amaurosis due to RPE65 mutations by ocular subretinal injection of adeno-associated virus gene vector: short-term results of a phase I trial. *Hum. Gene Ther.*, **19**, 979–990.
19. Cideciyan, A.V., Aleman, T.S., Boye, S.L., Schwartz, S.B., Kaushal, S., Roman, A.J., Pang, J.J., Sumaroka, A., Windsor, E.A., Wilson, J.M. *et al.* (2008) Human gene therapy for RPE65 isomerase deficiency activates the retinoid cycle of vision but with slow rod kinetics. *Proc. Natl Acad. Sci. USA*, **105**, 15112–15117.
20. Redmond, T.M., Yu, S., Lee, E., Bok, D., Hamasaki, D., Chen, N., Goletz, P., Ma, J.X., Crouch, R.K. and Pfeifer, K. (1998) Rpe65 is necessary for production of 11-*cis*-vitamin A in the retinal visual cycle. *Nat. Genet.*, **20**, 344–351.
21. Aguirre, G.D., Baldwin, V., Pearce-Kelling, S., Narfstrom, K., Ray, K. and Acland, G.M. (1998) Congenital stationary night blindness in the dog: common mutation in the RPE65 gene indicates founder effect. *Mol. Vis.*, **4**, 23.
22. Pang, J.J., Chang, B., Hawes, N.L., Hurd, R.E., Davisson, M.T., Li, J., Noorwez, S.M., Malhotra, R., McDowell, J.H., Kaushal, S. *et al.* (2005) Retinal degeneration 12 (rd12): a new, spontaneously arising mouse model for human Leber congenital amaurosis (LCA). *Mol. Vis.*, **11**, 152–162.
23. Samardzija, M., von Lintig, J., Tanimoto, N., Oberhauser, V., Thiersch, M., Reme, C.E., Seeliger, M., Grimm, C. and Wenzel, A. (2008) R91W

mutation in Rpe65 leads to milder early-onset retinal dystrophy due to the generation of low levels of 11-*cis*-retinal. *Hum. Mol. Genet.*, **17**, 281–292.
24. Thompson, D.A., Gyurus, P., Fleischer, L.L., Bingham, E.L., McHenry, C.L., Apfelstedt-Sylla, E., Zrenner, E., Lorenz, B., Richards, J.E., Jacobson, S.G. *et al.* (2000) Genetics and phenotypes of RPE65 mutations in inherited retinal degeneration. *Invest. Ophthalmol. Vis. Sci.*, **41**, 4293–4299.
25. El Matri, L., Ambresin, A., Schorderet, D.F., Kawasaki, A., Seeliger, M.W., Wenzel, A., Arsenijevic, Y., Borruat, F.X. and Munier, F.L. (2006) Phenotype of three consanguineous Tunisian families with early-onset retinal degeneration caused by an R91W homozygous mutation in the RPE65 gene. *Graefes Arch. Clin. Exp. Ophthalmol.*, **244**, 1104–1112.
26. Applebury, M.L., Antoch, M.P., Baxter, L.C., Chun, L.L., Falk, J.D., Farhangfar, F., Kage, K., Krzystolik, M.G., Lyass, L.A. and Robbins, J.T. (2000) The murine cone photoreceptor: a single cone type expresses both S and M opsins with retinal spatial patterning. *Neuron*, **27**, 513–523.
27. Wenzel, A., von Lintig, J., Oberhauser, V., Tanimoto, N., Grimm, C. and Seeliger, M.W. (2007) RPE65 is essential for the function of cone photoreceptors in NRL-deficient mice. *Invest. Ophthalmol. Vis. Sci.*, **48**, 534–542.
28. Seeliger, M.W., Grimm, C., Stahlberg, F., Friedburg, C., Jaissle, G., Zrenner, E., Guo, H., Reme, C.E., Humphries, P., Hofmann, F. *et al.* (2001) New views on RPE65 deficiency: the rod system is the source of vision in a mouse model of Leber congenital amaurosis. *Nat. Genet.*, **29**, 70–74.
29. Fan, J., Rohrer, B., Moiseyev, G., Ma, J.X. and Crouch, R.K. (2003) Isorhodopsin rather than rhodopsin mediates rod function in RPE65 knock-out mice. *Proc. Natl Acad. Sci. USA*, **100**, 13662–13667.
30. Jaissle, G.B., May, C.A., Reinhard, J., Kohler, K., Fauser, S., Lutjen-Drecoll, E., Zrenner, E. and Seeliger, M.W. (2001) Evaluation of the rhodopsin knockout mouse as a model of pure cone function. *Invest. Ophthalmol. Vis. Sci.*, **42**, 506–513.
31. Calvert, P.D., Krasnoperova, N.V., Lyubarsky, A.L., Isayama, T., Nicolo, M., Kosaras, B., Wong, G., Gannon, K.S., Margolskee, R.F., Sidman, R.L. *et al.* (2000) Phototransduction in transgenic mice after targeted deletion of the rod transducin α-subunit. *Proc. Natl Acad. Sci. USA*, **97**, 13913–13918.
32. Kefalov, V.J., Estevez, M.E., Kono, M., Goletz, P.W., Crouch, R.K., Cornwall, M.C. and Yau, K.W. (2005) Breaking the covalent bond—a pigment property that contributes to desensitization in cones. *Neuron*, **46**, 879–890.
33. Matsumoto, H., Tokunaga, F. and Yoshizawa, T. (1975) Accessibility of the iodopsin chromophore. *Biochim. Biophys. Acta*, **404**, 300–308.
34. Goldstein, E.B. and Wolf, B.M. (1973) Regeneration of the green-rod pigment in the isolated frog retina. *Vision Res.*, **13**, 527–534.
35. Hood, D.C. and Hock, P.A. (1973) Recovery of cone receptor activity in the frog's isolated retina. *Vision Res.*, **13**, 1943–1951.
36. Mata, N.L., Radu, R.A., Clemmons, R.C. and Travis, G.H. (2002) Isomerization and oxidation of vitamin a in cone-dominant retinas: a novel pathway for visual-pigment regeneration in daylight. *Neuron*, **36**, 69–80.
37. Schonthaler, H.B., Lampert, J.M., Isken, A., Rinner, O., Mader, A., Gesemann, M., Oberhauser, V., Golczak, M., Biehlmaier, O., Palczewski, K. *et al.* (2007) Evidence for RPE65-independent vision in the cone-dominated zebrafish retina. *Eur. J. Neurosci.*, **26**, 1940–1949.
38. Fleisch, V.C., Schonthaler, H.B., von Lintig, J. and Neuhauss, S.C. (2008) Subfunctionalization of a retinoid-binding protein provides evidence for two parallel visual cycles in the cone-dominant zebrafish retina. *J. Neurosci.*, **28**, 8208–8216.
39. Mata, N.L., Ruiz, A., Radu, R.A., Bui, T.V. and Travis, G.H. (2005) Chicken retinas contain a retinoid isomerase activity that catalyzes the direct conversion of all-trans-retinol to 11-*cis*-retinol. *Biochemistry*, **44**, 11715–11721.
40. Moiseyev, G., Takahashi, Y., Chen, Y., Kim, S. and Ma, J.X. (2008) RPE65 from cone-dominant chicken is a more efficient isomerohydrolase compared with that from rod-dominant species. *J. Biol. Chem.*, **283**, 8110–8117.
41. Williams, D.R., MacLeod, D.I. and Hayhoe, M.M. (1981) Punctate sensitivity of the blue-sensitive mechanism. *Vision Res.*, **21**, 1357–1375.
42. Curcio, C.A., Allen, K.A., Sloan, K.R., Lerea, C.L., Hurley, J.B., Klock, I.B. and Milam, A.H. (1991) Distribution and morphology of human cone photoreceptors stained with anti-blue opsin. *J. Comp. Neurol.*, **312**, 610–624.
43. Lorenz, B., Poliakov, E., Schambeck, M., Friedburg, C., Preising, M.N. and Redmond, T.M. (2008) A comprehensive clinical and biochemical functional study of a novel RPE65 hypomorphic mutation. *Invest. Ophthalmol. Vis. Sci.*, 5235–5242.
44. Paunescu, K., Wabbels, B., Preising, M.N. and Lorenz, B. (2005) Longitudinal and cross-sectional study of patients with early-onset severe retinal dystrophy associated with RPE65 mutations. *Graefes Arch. Clin. Exp. Ophthalmol.*, **243**, 417–426.
45. Fei, Y. and Hughes, T.E. (2001) Transgenic expression of the jellyfish green fluorescent protein in the cone photoreceptors of the mouse. *Vis. Neurosci.*, **18**, 615–623.
46. Samardzija, M., Wenzel, A., Aufenberg, S., Thiersch, M., Reme, C. and Grimm, C. (2006) Differential role of Jak-STAT signaling in retinal degenerations. *FASEB J.*, **20**, 2411–2413.
47. Samardzija, M., Wenzel, A., Thiersch, M., Frigg, R., Reme, C. and Grimm, C. (2006) Caspase-1 ablation protects photoreceptors in a model of autosomal dominant retinitis pigmentosa. *Invest. Ophthalmol. Vis. Sci.*, **47**, 5181–5190.
48. Tanimoto, N., Muehlfriedel, R.L., Fischer, M.D., Fahl, E., Humphries, P., Biel, M. and Seeliger, M.W. (2009) Vision tests in the mouse: functional phenotyping with electroretinography. *Front. Biosci.*, **14**, 2730–2737.
49. Seeliger, M.W., Beck, S.C., Pereyra-Munoz, N., Dangel, S., Tsai, J.Y., Luhmann, U.F., van de Pavert, S.A., Wijnholds, J., Samardzija, M., Wenzel, A. *et al.* (2005) *In vivo* confocal imaging of the retina in animal models using scanning laser ophthalmoscopy. *Vision Res.*, **45**, 3512–3519.
50. Wenzel, A., Oberhauser, V., Pugh, E.N. Jr, Lamb, T.D., Grimm, C., Samardzija, M., Fahl, E., Seeliger, M.W., Reme, C.E. and von Lintig, J. (2005) The retinal G protein-coupled receptor (RGR) enhances isomerohydrolase activity independent of light. *J. Biol. Chem.*, **280**, 29874–29884.

7 CURRICULUM VITAE

Name	Thiersch	
First name	Markus	
Date of birth	March 25, 1980	
Nationality	German	
Address Office:	Frauenklinikstrasse 24,	
	8091 Zurich, Switzerland	
Private:	Altwiesenstrasse 144,	
	8051 Zurich, Switzerland	
Phone:	Office:	0041/44 255 3872
	Private:	0041/43 321 6232
	Mobil:	0041/78 724 5620
Email:	Office:	markus.thiersch@usz.ch
	Private:	mthiersch@aol.com

Education

October 2004 – present; Ph.D. student in the Lab for Retinal Cell Biology, Department Ophthalmology, University Hospital Zurich; proposed title: “Neuroprotection by Hypoxic Preconditioning and the Role of Hypoxia-Inducible-Factor 1α”

May 2004; Graduated Biochemistry at University of Leipzig, Germany: Diploma thesis at the Centre for Environmental Research UFZ, Leipzig, Germany; title: Mechanisms of *Pseudomonas putida* KT2440 to resist Chlorophenoxy Herbicides

2001 – 2002; student assistant at:
Institute of Biochemistry, University of Leipzig, Germany
Max Planck Institute for Evolutionary Anthropology, Leipzig, Germany
Centre for Environmental Research UFZ, Leipzig, Germany
pe Diagnostik GmbH, Leipzig, Germany

1999 – 2003; study of Biochemistry at University of Leipzig, Germany

Awards

2006; Travel award and speaker at the XIIth International Symposium on Retinal Degeneration 2006 San Carlos de Bariloche, Argentina

Courses

ZNZ (Neuroscience Centre Zurich) Ph.D. program
Statistics for ZNZ researchers; August 2006
Writing research papers for publication; June 2006
LTK Module 1: Introductory course in laboratory animal science; February 2005

Publications

Research Papers

Thiersch, M., Lange, C., Joly, S., Heynen, S., Le, Y.Z., Samardzija, M., Grimm, C. (2009) Retinal neuroprotection by hypoxic preconditioning is independent of HIF-1a expression in photoreceptors. *EJN accepted for publication*

Samardzija, M., Tanimoto, N., Kostic, C., Beck, S., Oberhauser, V., Joly, S., **Thiersch, M.**, Fahl, E., Arsenijevic, Y., von Lintig, J., Wenzel, A., Seeliger, M.W., Grimm, C. (2009) In conditions of limited chromophore supply rods entrap 11-cis-retinal leading to loss of cone function and cell death. *Hum Mol Genet* 18, 2166-2175

Joly S, Samardzija M, Wenzel A, **Thiersch M**, Grimm C. (2009) Nonessential role of beta3 and beta5 integrin subunits for efficient clearance of cellular debris after light-induced photoreceptor degeneration *Invest Ophthalmol Vis Sci* 50, 1423-1432

Joly S, Lange C, **Thiersch M**, Samardzija M, Grimm C. (2008) Leukemia inhibitory factor extends the lifespan of injured photoreceptors in vivo. *J Neurosci* 28, 13765-13774

Thiersch, M., Raffelsberger, W., Frigg, R., Samardzija, M., Wenzel, A., Poch, O., and Grimm, C. (2008) Analysis of the retinal gene expression profile after hypoxic preconditioning identifies candidate genes for neuroprotection. *BMC Genomics* 9, 7

Samardzija, M., von Lintig, J., Tanimoto, N., Oberhauser, V., **Thiersch, M.,** Remé, C. E., Seeliger, M., Grimm, C., and Wenzel, A. (2008) R91W mutation in Rpe65 leads to milder early-onset retinal dystrophy due to the generation of low levels of 11-cis-retinal. *Hum Mol Genet* 17, 281-292

Samardzija, M., Wenzel, A., Aufenberg, S., **Thiersch, M.**, Remé, C., and Grimm, C. (2006) Differential role of Jak-STAT signaling in retinal degenerations. *Faseb J* 20, 2411-2413

Samardzija, M., Wenzel, A., **Thiersch, M.**, Frigg, R., Remé, C., and Grimm, C. (2006) Caspase-1 ablation protects photoreceptors in a model of autosomal dominant retinitis pigmentosa. *Invest Ophthalmol Vis Sci* 47, 5181-5190

Benndorf, D., **Thiersch, M.**, Loffhagen, N., Kunath, C., and Harms, H. (2006) Pseudomonas putida KT2440 responds specifically to chlorophenoxy herbicides and their initial metabolites. *Proteomics* 6, 3319-3329

Book chapters

Thiersch, M., Raffelsberger, W., Frigg, E., Samardzija, M., Blank, P., Poch, O., and Grimm, C. (2008) The hypoxic transcriptome of the retina: identification of factors with potential neuroprotective activity. *Adv Exp Med Biol* 613, 75-85

Grimm, C., Wenzel, A., Samardzija, M., and **Thiersch, M.** (2007) Mechanisms of cell death and neuroprotection in retinal degeneration. *Brain and retina in degenerative diseases of childhood* B. Schmitt et al., Editors., 170-180

Presentations

Oral presentations

Thiersch M., Lange C., Joly S., Samardzija M. and Grimm C. How Hypoxia Can Protect Against Cell Death. Symposium: Enlightened views on life and death of visual cells. A celebratory tribute to Prof. Charlotte Remé, 5-6 June, 2008, Zurich, Switzerland

Thiersch M., Joly S., Samardzija M. and Grimm C. Does Retinal Neuroprotection after Hypoxic Preconditioning Depend on HIF-1α Stabilization? Swiss Eye Research Meeting, February 14-15, 2008, Brunnen Switzerland

Thiersch M., Blank P. and Grimm C. Conditional Knock Out of HIF-1α and the Consequences for Hypoxia Induced Retinal Neuroprotection in a Model of Light induced Retinal Degeneration. 1st Young Researchers Workshop on Vision and Neurodegeneration. 29-30 May 2007 Potsdam, Germany.

Thiersch M., Raffelsberger W., Frigg R., Samardzija M., Wenzel A., Remé C., Poch O. and Grimm C. The Hypoxic Transcriptome: Implications for Neuroprotection. Swiss Retina Meeting, January 16-17, 2007, Brunnen Switzerland

Thiersch M., Raffelsberger W., Frigg R., Samardzija M., Wenzel A., Remé C., Poch O. and Grimm C. Retinal Neuroprotection by Hypoxic Preconditioning: Identification of Possible

Neuroprotective Targets by Analyzing the Hypoxic Transcriptome. XII International Symposium in Retinal Degeneration October 23-28, 2006, San Carlos de Bariloche, Argentina.

Thiersch M., Raffelsberger W., Frigg R., Samardzija M., Wenzel A., Remé C., Poch O. and Grimm C. Retinal Neuroprotection by Hypoxic Preconditioning: Identification of Possible Neuroprotective Targets by Analyzing the Retinal Transcriptome of Hypoxic Preconditioned Mice. 2nd Symposium of the ZIHP (Centre for Integrative Human Physiology), September 22, 2006, Zurich, Switzerland

Thiersch M., Frigg R., Samardzija M., Wenzel A., Remé C. and Grimm C. Retinal Neuroprotection by Hypoxic Preconditioning: Identification of Possible Neuroprotective Targets Using Affymetrix Gene Chip Technology. Swiss Retina Meeting, February 9-10, 2006, Brunnen, Switzerland

Poster presentations

- 4th Pro retina research colloquium Potsdam, March 28 - 29, 2008, Potsdam, Germany
- ARVO Annual Meeting, May 06 - 10, 2007, Fort Lauderdale, Florida, USA
- ZIHP (Centre for Integrative Human Physiology), August 31, 2007, Zurich, Switzerland
- 3rd Pro retina research colloquium Potsdam, March 30 - 31, 2007, Potsdam, Germany
- 6th Day of Clinical Research, March 01 - 02, 2007, University Hospital Zurich, Switzerland
- ZNZ (Neuroscience Centre Zurich) Symposium, October 20, 2006, University of Zurich, Switzerland
- 2nd Pro retina research colloquium Potsdam, March 07 - 08, 2006, Potsdam, Germany
- 5th Day of Clinical Research, March 23 - 24, 2006, University Hospital Zurich, Switzerland

8 ACKNOWLEDGMENT

It is impossible to accomplish such a doctoral thesis alone. I was lucky to meet many new colleagues and friends during the last 5 years who helped me to complete my studies. Sincere thanks to all the people who accompanied me during this time – but particularly to the following people:

The members of my external steering committee Prof. Stephan Neuhauss and Prof. Max Gassmann are kindly acknowledged for reviewing this thesis.

I would like to express my gratitude especially to Prof. Christian Grimm, Prof. Charlotte Remé, Dr. Andreas Wenzel and Dr. Marijana Samardzija, who invited me to work in the lab and who shared their knowledge and experience with me. Christian – my responsible supervisor and internal committee member provided me with a perfect mix of independency (to make my "own mistakes") and supervision (helping me to recognize and to solve problems without losing the focus). However, I am particularly grateful for the support and his understanding during the "times of trouble". Andreas and Charlotte supported me whenever I needed assistance or advice and Marijana introduced me with patience and calmness into the practical aspects of lab-work.
Moreover, I thank all the former and present members of the lab (Sandrine Joly, Christina Lange, Severin Heynen, Corinne Britschgi, Coni Imsand, Hedi Wariwoda, Philipp Huber, Karina Guziewicz, Hao Ren, Rico Frigg, Patricia Blank and Gabi Högger) for their help, support and the friendly lab-atmosphere.

I would like to thank Prof. Max Gassmann & Prof. Randall Johnson, Prof. Pierre Chambon and Prof. Yun Zheng Le who kindly provided the mice we used for the HIF-1α studies.

I kindly acknowledge Dr. Wolfgang Raffelsberger and Prof. Olivier Poch for performing the statistical analyses of our micro-array data and for explaining it in a way we were able to understand it.

I would like to thank all of my friends and especially my dear family – my parents Regina and Andreas and my sister Stephanie – for their unconditional support and for keeping me grounded in hard times.